

Lecture Notes in Electrical Engineering 432

Shoichi Hasegawa

Masashi Konyo

Ki-Uk Kyung

Takuya Nojima

Hiroyuki Kajimoto

Editors

Haptic Interaction

Science, Engineering and Design

 Springer

Lecture Notes in Electrical Engineering

Volume 432

Board of Series editors

Leopoldo Angrisani, Napoli, Italy
Marco Arteaga, Coyoacán, México
Samarjit Chakraborty, München, Germany
Jiming Chen, Hangzhou, P.R. China
Tan Kay Chen, Singapore, Singapore
Rüdiger Dillmann, Karlsruhe, Germany
Haibin Duan, Beijing, China
Gianluigi Ferrari, Parma, Italy
Manuel Ferre, Madrid, Spain
Sandra Hirche, München, Germany
Faryar Jabbari, Irvine, USA
Janusz Kacprzyk, Warsaw, Poland
Alaa Khamis, New Cairo City, Egypt
Torsten Kroeger, Stanford, USA
Tan Cher Ming, Singapore, Singapore
Wolfgang Minker, Ulm, Germany
Pradeep Misra, Dayton, USA
Sebastian Möller, Berlin, Germany
Subhas Mukhopadhyay, Palmerston, New Zealand
Cun-Zheng Ning, Tempe, USA
Toyoaki Nishida, Sakyo-ku, Japan
Bijaya Ketan Panigrahi, New Delhi, India
Federica Pascucci, Roma, Italy
Tariq Samad, Minneapolis, USA
Gan Woon Seng, Nanyang Avenue, Singapore
Germano Veiga, Porto, Portugal
Haitao Wu, Beijing, China
Junjie James Zhang, Charlotte, USA

About this Series

“Lecture Notes in Electrical Engineering (LNEE)” is a book series which reports the latest research and developments in Electrical Engineering, namely:

- Communication, Networks, and Information Theory
- Computer Engineering
- Signal, Image, Speech and Information Processing
- Circuits and Systems
- Bioengineering

LNEE publishes authored monographs and contributed volumes which present cutting edge research information as well as new perspectives on classical fields, while maintaining Springer’s high standards of academic excellence. Also considered for publication are lecture materials, proceedings, and other related materials of exceptionally high quality and interest. The subject matter should be original and timely, reporting the latest research and developments in all areas of electrical engineering.

The audience for the books in LNEE consists of advanced level students, researchers, and industry professionals working at the forefront of their fields. Much like Springer’s other Lecture Notes series, LNEE will be distributed through Springer’s print and electronic publishing channels.

More information about this series at <http://www.springer.com/series/7818>

Shoichi Hasegawa · Masashi Konyo
Ki-Uk Kyung · Takuya Nojima
Hiroyuki Kajimoto
Editors

Haptic Interaction

Science, Engineering and Design

 Springer

Editors

Shoichi Hasegawa
Tokyo Institute of Technology
Yokohama, Kanagawa
Japan

Takuya Nojima
The University of Electro-Communications
Tokyo
Japan

Masashi Konyo
Tohoku University
Sendai, Miyagi
Japan

Hiroyuki Kajimoto
The University of Electro-Communications
Tokyo
Japan

Ki-Uk Kyung
Electronics and Telecommunications
Research Institute
Daejeon
Korea (Republic of)

ISSN 1876-1100 ISSN 1876-1119 (electronic)
Lecture Notes in Electrical Engineering
ISBN 978-981-10-4156-3 ISBN 978-981-10-4157-0 (eBook)
DOI 10.1007/978-981-10-4157-0

Library of Congress Control Number: 2017936447

© Springer Nature Singapore Pte Ltd. 2018

This work is subject to copyright. All rights are reserved by the Publisher, whether the whole or part of the material is concerned, specifically the rights of translation, reprinting, reuse of illustrations, recitation, broadcasting, reproduction on microfilms or in any other physical way, and transmission or information storage and retrieval, electronic adaptation, computer software, or by similar or dissimilar methodology now known or hereafter developed.

The use of general descriptive names, registered names, trademarks, service marks, etc. in this publication does not imply, even in the absence of a specific statement, that such names are exempt from the relevant protective laws and regulations and therefore free for general use.

The publisher, the authors and the editors are safe to assume that the advice and information in this book are believed to be true and accurate at the date of publication. Neither the publisher nor the authors or the editors give a warranty, express or implied, with respect to the material contained herein or for any errors or omissions that may have been made. The publisher remains neutral with regard to jurisdictional claims in published maps and institutional affiliations.

Printed on acid-free paper

This Springer imprint is published by Springer Nature
The registered company is Springer Nature Singapore Pte Ltd.
The registered company address is: 152 Beach Road, #21-01/04 Gateway East, Singapore 189721, Singapore

Preface

Welcome to the proceedings of the second international conference, AsiaHaptics 2016, held in Chiba, Japan, during November 29 through December 1.

AsiaHaptics is a new type of international conference for the haptics fields, featuring interactive presentations with demos. The conference became the place to experience 90 live demonstrations of haptics research.

While the haptics-related research field is huge, this book divided it into six parts.

Part I is composed of eight chapters, treating perception and psychophysics of haptics. They are undoubtedly the basis of the haptics research.

Part II is composed of 23 chapters, treating tactile devices for skin sensation such as vibration, pressure, and temperature, and their rendering methods.

Part III is composed of 18 chapters, treating force feedback devices and rendering methods. Some of them utilized tactile-based illusions so the distinction between tactile devices and force feedback devices is vague.

Part IV is composed of five chapters, treating sensors such as pressure distribution sensor and force sensor, many of which enable novel applications.

Part V is composed of six chapters, treating medical application including surgery simulation and rehabilitation.

Part VI is composed of 24 chapters, treating application of haptics to VR, telepresence, and multimedia, all exploring new application area of haptics.

This book helps not only active haptic researchers, but also general readers to understand what is going on in this interdisciplinary area of science and technology. All papers have accompanied videos available online. Therefore, readers can easily understand the concept of the work with the supplemental videos.

Yokohama, Japan
Sendai, Japan
Daejeon, Korea (Republic of)
Tokyo, Japan
Tokyo, Japan
December 2016

Shoichi Hasegawa
Masashi Konyo
Ki-Uk Kyung
Takuya Nojima
Hiroyuki Kajimoto

Contents

Part I Perception and Psychophysics of Haptics

| | |
|---|----|
| Reconsideration of Ouija Board Motion in Terms of Haptics Illusions (II)—Development of a 1-DoF Linear Rail Device | 3 |
| Takahiro Shitara, Yuriko Nakai, Haruya Uematsu, Vibol Yem, Hiroyuki Kajimoto and Satoshi Saga | |
| Haptic Perception of Macro Texture | 9 |
| Tao Zeng, Wenjing Chen, Nan Li, Liangzong He and Lantao Huang | |
| Natural Human Movements in Geometrically Constrained Haptic Environments | 13 |
| Igor Goncharenko, Mikhail Svinin and Victor Kryssanov | |
| Expression of 2DOF Fingertip Traction with 1DOF Lateral Skin Stretch | 21 |
| Vibol Yem, Mai Shibahara, Katsunari Sato and Hiroyuki Kajimoto | |
| Perceived Hardness by Tapping: The Role of a Secondary Mode of Vibration | 27 |
| Kosuke Higashi, Shogo Okamoto, Hikaru Nagano, Masashi Konyo and Yoji Yamada | |
| Experiments on Two-Handed Localization of Impact Vibrations | 33 |
| Daniel Gongora, Hikaru Nagano, Masashi Konyo and Satoshi Tadokoro | |
| Rubber Hand Illusion Using Tactile Projector | 41 |
| Yuuki Horiuchi, Kazunori Odani, Yasutoshi Makino and Hiroyuki Shinoda | |

| | |
|---|------------|
| Colorful Tactile Stimuli. Association Between Colors and Tactile-Display Stimuli on Russell’s Psychological Plane | 47 |
| Hikaru Hasegawa, Ken Itoh, Shogo Okamoto, Hatem Elfekey and Yoji Yamada | |
| Part II Tactile Devices for Skin Sensation | |
| 3DOF Multitouch Haptic Interface with Movable Touchscreen. | 55 |
| Shun Takanaka, Hiroaki Yano and Hiroo Iwata | |
| A Novel 3RRS Wearable Fingertip Cutaneous Device for Virtual Interaction | 63 |
| Francesco Chinello, Claudio Pacchierotti, Monica Malvezzi and Domenico Prattichizzo | |
| Thermal-Radiation-Based Haptic Display—Calibration and Shape Display | 67 |
| Satoshi Saga | |
| Touching 2D Images Using Haptogram System | 71 |
| Georgios Korres and Mohamad Eid | |
| Hybrid Haptic Texture Rendering Using Kinesthetic and Vibrotactile Feedback | 75 |
| Sunghwan Shin and Seungmoon Choi | |
| Simultaneous Representation of Texture and Geometry on a Flat Touch Surface. | 83 |
| Semin Ryu, Dongbum Pyo, Byung-Kil Han and Dong-Soo Kwon | |
| Ferro-Fluid Based Lightweight and Portable Tactile Display for Persuasive Tactile Cues Including Orientation and Texture | 87 |
| Harsimran Singh, HyeonSeok Seong and Jee-Hwan Ryu | |
| Sole Tactile Display Using Tactile Illusion by Vibration on Toenail | 95 |
| Kensuke Sakai, Taku Hachisu and Yuki Hashimoto | |
| Scalable Architecture for Airborne Ultrasound Tactile Display | 99 |
| Seki Inoue, Yasutoshi Makino and Hiroyuki Shinoda | |
| HapStep: A Novel Method to Sense Footsteps While Remaining Seated Using Longitudinal Friction on the Sole of the Foot. | 105 |
| Ginga Kato, Yoshihiro Kuroda, Kiyoshi Kiyokawa and Haruo Takemura | |
| Initial Progress Toward a Surface Morphable Tactile Interface | 113 |
| Seongcheol Mun, Sungryul Yun, Saekwang Nam, Seung-Koo Park and Ki-Uk Kyung | |

Simulating Texture Sensation of Textiles Using Thermal and Vibro-Tactile Stimulations 115
 Katsunari Sato

Tactile Display Based on Skin-Propagated Vibration. 121
 Yasutoshi Takekawa, Tatsuya Hasegawa, Yoshihiro Tanaka, Kouta Minamizawa and Akihito Sano

High-Quality Texture Display: The Use of Vibrotactile and Variable-Friction Stimuli in Conjunction. 125
 Ken Ito, Shogo Okamoto, Hatem Elfekey and Yoji Yamada

Hybrid Focus Using 70 and 40 kHz Ultrasound in Mid-Air Tactile Display. 131
 Mitsuru Ito, Daisuke Wakuda, Yasutoshi Makino and Hiroyuki Shinoda

Tactile Presentation Using Mechanical and Electrical Stimulation 135
 Vibol Yem, Sugarragchaa Khurelbaatar, Erika Oishi and Hiroyuki Kajimoto

Development of a One-Dimensional Lateral Tactile Display for the Sensation of Texture Using a Speaker Array 143
 Seitaro Kaneko and Hiroyuki Kajimoto

Encountered-Type Visual Haptic Display Using MR Fluid 151
 Hiroki Ohnari, Satoko Abiko and Teppei Tsujita

Whole Hand Interaction with Multi-finger Movement-Based Vibrotactile Stimulation 157
 Shota Iizuka, Hikaru Nagano, Masashi Konyo and Satoshi Tadokoro

Signal and Power Transfer to Actuators Distributed on Conductive Fabric Sheet for Wearable Tactile Display 163
 Yuki Tajima, Akihito Noda and Hiroyuki Shinoda

Multi-electrodes-Based Electrostatic Tactile Display. 171
 Hirobumi Tomita, Satoshi Saga and Hiroyuki Kajimoto

Development of a Sole Pressure Display 175
 Tetsuhiro Okano, Kengo Hiki, Koichi Hirota, Takusya Nojima, Michiteru Kitazaki and Yasushi Ikei

A Design of a New Electro Tactile Beat Module. 181
 Won-Hyeong Park, Sang-Youn Kim, Kunyun Kim and Tae-Heon Yang

| | |
|--|-----|
| Part III Force Feedback Devices and Rendering Methods | |
| Proposal and Implementation of Non-grounded Translational Force and Torque Display Using Two Vibration Speakers | 187 |
| Takeshi Tanabe, Hiroaki Yano and Hiroo Iwata | |
| Engaging Weight Feedback for Bimanual Interaction | 193 |
| Stuart Burmeister, Kimin Kim and Jinah Park | |
| Substituted Force Feedback Using Palm Pressurization for a Handheld Controller | 197 |
| Taku Nakamura, Shota Nemoto, Takumi Ito and Akio Yamamoto | |
| Virtual Two-Finger Haptic Manipulation Method | 201 |
| Alfonso Balandra, Virglio Gruppelaar, Hironori Mitake and Shoichi Hasegawa | |
| Inducing Wrist Twist During Arm Swing by Using Gyro Effect | 205 |
| Hirokazu Miyahara, Yasutoshi Makino and Hiroyuki Shinoda | |
| Passive Haptics: Pulsive Damping Brake for Greater Impulse Perception | 211 |
| Takumu Okada, Shogo Okamoto and Yoji Yamada | |
| Hanger Reflex of the Head and Waist with Translational and Rotational Force Perception | 217 |
| Yuki Kon, Takuto Nakamura, Michi Sato, Takashi Asahi and Hiroyuki Kajimoto | |
| Stable Haptic Feedback Generation During Mid Air Interactions Using Hidden Markov Model Based Motion Synthesis | 225 |
| Dennis Babu, Hikaru Nagano, Masashi Konyo, Ryunosuke Hamada and Satoshi Tadokoro | |
| Relationship Between Force Sensation and Stimulation Parameters in Tendon Electrical Stimulation | 233 |
| Akifumi Takahashi, Kenta Tanabe and Hiroyuki Kajimoto | |
| Force Your Hand—PAM Enabled Wrist Support | 239 |
| Swagata Das, Cassie Lowell and Yuichi Kurita | |
| Unplugged Powered Suit with Pneumatic Gel Muscles | 247 |
| Chetan Thakur, Kazunori Ogawa, Toshio Tsuj and Yuichi Kurita | |
| Prototype Kinesthetic Illusory Device Using Combination of Active and Passive Motion | 253 |
| Hirokazu Minowa, Kentaro Baba and Masamichi Sakaguchi | |
| A Fast Update Approach of a Stiffness Matrix for a Multi-rate Finite Element Deformation Simulation | 257 |
| Ryo Kuriki, Kazuyoshi Tagawa, Hiromi T. Tanaka and Masaru Komori | |

Object Manipulation by Hand with Force Feedback 261
 Shunsuke Fujioka, Takao Uchiyama, Kazuyoshi Tagawa,
 Koichi Hirota, Takuya Nojima, Katsuhito Akahane and Makoto Sato

Visuo-Tactile Interaction with Virtual Objects that Yields Kinetic Effects on Real Objects. 267
 Kyosuke Yamazaki, Keisuke Hasegawa, Yasutoshi Makino
 and Hiroyuki Shinoda

Enhancement of Perceived Force from the Hanger Reflex on Head and Ankle by Adding Vibration 275
 Takuto Nakamura and Hiroyuki Kajimoto

An Immersive Visuo-Haptic VR Environment with Pseudo-haptic Effects on Perceived Stiffness 281
 Daichi Matsumoto, Ya Zhu, Yuya Tanaka, Kyosuke Yamazaki,
 Keisuke Hasegawa, Yasutoshi Makino and Hiroyuki Shinoda

Multi Degree-of-Freedom Successive Stiffness Increment Approach for High Stiffness Haptic Interaction 287
 Harsimran Singh, Aghil Jafari and Jee-Hwan Ryu

Part IV Sensors

A Cooking Support System with Force Visualization Using Force Sensors and an RGB-D Camera 297
 Nobuhiro Totsu, Sho Sakaino and Toshiaki Tsuji

Turning Surfaces into Touch Panels: A Granite-Touch Pad 301
 Hatem Elfekey and Shogo Okamoto

A Finger Sensor for Sharing Visual and Tactile Experience 305
 Haruki Nakamura, Nobuhisa Hanamitsu, Junichi Kanebako
 and Kouta Minamizawa

On a Haptic Phenomenon by Combined Use of the Rubber Artificial Skin Layer with a Strain Gauge and the Tactile Contact Lens 309
 Mitsuhiro Ando, Hiromi Mochiyama, Toshinobu Takei
 and Hideo Fujimoto

Measurement of Stickiness with Pressure Distribution Sensor 315
 Takayuki Kameoka, Akifumi Takahashi, Vibol Yem
 and Hiroyuki Kajimoto

Part V Medical Application

A Wearable Haptic Ring for the Control of Extra Robotic Fingers 323
Irfan Hussain, Giovanni Spagnoletti, Claudio Pacchierotti
and Domenico Prattichizzo

**Relax and Tighten—A Haptics-based Approach to Simulate
Sphincter Tone Assessment** 327
Alejandro Granados, Luc Maréchal, Alastair Barrow, George Petrou,
Christine Norton and Fernando Bello

**Training on Muscle Palpation Using Artificial Muscle Nodule
Models** 335
Kaoru Isogai, Shogo Okamoto, Asuka Noda, Ayumi Matsuzawa
and Yoji Yamada

**Basic Study on Motor Ability Evaluation and Training
System Using Virtual Collision Avoidance** 341
Takuya Makishima, Masaki Orimoto and Masamichi Sakaguchi

**Bimanual Haptic Simulator for Training Hand Palpation
and Lumbar Puncture** 345
James Jose and Rao R. Bhavani

**Prostate Tumor Palpation Simulator Based on Pneumatic and
Augmented Haptics** 353
Aishwari Talhan and Seokhee Jeon

**Part VI Application of Haptics to VR, Telepresence
and Multimedia**

Haptic Directional Instruction System for Sports 361
Ryoichiro Shiraishi, Koya Sato, Yuji Sano and Mai Otsuki

**Tactile Treasure Map: Integrating Allocentric and Egocentric
Information for Tactile Guidance** 369
Mariacarla Memeo, Victor Adriel de Jesus Oliveira, Luciana Nedel,
Anderson Maciel and Luca Brayda

**Motion-Based Augmented Broadcasting System with Haptic
Feedback** 375
Yeongmi Kim, Davud Sadikhov, Kaspar Leuenberger, Beomseuk Choi,
Youngho Jeong, Matthias Harders and Roger Gassert

**Perceiving Physical Attributes of Objects Using
an Electrostatic Tactile Display** 383
Xiaoying Sun, Jian Chen, Guohong Liu and Hui Long

Hapbeat: Tension-Based Wearable Vibroacoustic Device 387
 Yusuke Yamazaki, Hironori Mitake, Minatsu Takekoshi, Yuji Tsukamoto,
 Tetsuaki Baba and Shoichi Hasegawa

**Comparison of Tactile Signals for Collision Avoidance
 on Unmanned Aerial Vehicles** 393
 Stefan Spiss, Yeongmi Kim, Simon Haller and Matthias Harders

Data-Driven Rendering of Anisotropic Haptic Textures 401
 Arsen Abdulali and Seokhee Jeon

**PhysVib: Physically Plausible Vibrotactile Feedback Library to
 Collisions on a Mobile Device** 409
 Gunhyuk Park and Seungmoon Choi

**Towards Universal Haptic Library: Library-Based Haptic Texture
 Assignment Using Image Texture and Perceptual Space** 415
 Waseem Hassan, Arsen Abdulali and Seokhee Jeon

**An Empirical Study of Haptic-Audio Based Online Shopping
 System for the Blind** 419
 Eu Jin Wong, Kian Meng Yap, Jason Alexander and Abhijit Karnik

Character Recognition by Flick Movements Presented on Fingers 425
 Kentaro Yoshida, Koji Tanaka, Keisuke Hasegawa, Yasutoshi Makino
 and Hiroyuki Shinoda

A Tool for Collecting and Designing Haptic Experiences 433
 Mina Shibasaki, Youichi Kamiyama and Kouta Minamizawa

**A Novel Multimodal Tactile Module that Can Provide
 Vibro-Thermal Feedback** 437
 Masashi Nakatani, Katsunari Sato, Kunio Sato, Yuzuru Kawana,
 Daisuke Takai, Kouta Minamizawa and Susumu Tachi

Tactile Perception of Digital Images 445
 Wenzhen Yang, Zhaona Jiang, Xin Huang, Xinli Wu and Zhichao Zhu

**VibGrip++: Haptic Device Allows Feeling the Music
 for Hearing Impaired People** 449
 Junichi Kanebako and Kouta Minamizawa

**A Smart Cushion System with Vibrotactile Feedback
 for Active Posture Correction** 453
 Karlos Ishac and Kenji Suzuki

**HapTONE: Haptic Instrument for Enriched Musical Play
 (II)—System Detail** 461
 Kenta Tanabe, Akifumi Takahashi, Keisuke Hoshino, Daichi Ogawa,
 Taku Hachisu and Hiroyuki Kajimoto

Visual Haptic Interface by Using 2-DOF Indirect Haptic Interface. 467
Takayuki Ishikawa, Hiroaki Yano and Hiroo Iwata

HaptoCloneAR (Haptic-Optical Clone with Augmented Reality) for Mutual Interactions with Midair 3D Floating Image and Superimposed 2D Display. 473
Kentaro Yoshida, Takaaki Kamigaki, Seki Inoue, Keisuke Hasegawa, Yasutoshi Makino and Hiroyuki Shinoda

Haplug: A Haptic Plug for Dynamic VR Interactions 479
Nobuhisa Hanamitsu and Ali Israr

Magnification-Changeable Haptic-Optical Clone 485
Ryota Arai, Yasutoshi Makino and Hiroyuki Shinoda

Computer-Created Interactive 3D Image with Midair Haptic Feedback 491
Yuta Kimura, Yasutoshi Makino and Hiroyuki Shinoda

Mobile HapticAid: Wearable Haptic Augmentation System Using a Mobile Platform 495
Tomosuke Maeda, Keitaro Tsuchiya, Roshan Peiris, Yoshihiro Tanaka and Kouta Minamizawa

Synesthesia Suit. 499
Yukari Konishi, Nobuhisa Hanamitsu, Benjamin Outram, Youichi Kamiyama, Kouta Minamizawa, Ayahiko Sato and Tetsuya Mizuguchi

Part I
Perception and Psychophysics of Haptics

Reconsideration of Ouija Board Motion in Terms of Haptics Illusions (II)—Development of a 1-DoF Linear Rail Device

Takahiro Shitara, Yuriko Nakai, Haruya Uematsu, Vibol Yem,
Hiroyuki Kajimoto and Satoshi Saga

Abstract The Ouija board is a game associated with involuntary motion called ideomotor action. Our goal is to clarify the conditions under which Ouija board motion occurs, comparing visual, force, and vibrotactile cues. In this paper, we demonstrated a newly developed 1-degree of freedom (DoF) Linear Rail Device, which we used to study these ideomotor actions with less friction and inertia.

Keywords Ideomotor action · Pseudo haptics · 1-DoF linear rail device ouiija board

1 Introduction

The Ouija board is a game that can be played by multiple players, using a flat board marked with letters and numbers, and a planchette, which is a small heart-shaped piece. The players place their fingers on the planchette, ask questions, and the piece moves to point at various letters or numbers in response. Several variations can be

T. Shitara (✉) · Y. Nakai · H. Uematsu · V. Yem · H. Kajimoto
The University of Electro-Communications, 1-5-1 Chofugaoka,
Chofu, Tokyo 182-8585, Japan
e-mail: shitara@kaji-lab.jp

Y. Nakai
e-mail: yuriko@kaji-lab.jp

H. Uematsu
e-mail: uematsu@kaji-lab.jp

V. Yem
e-mail: yem@kaji-lab.jp

H. Kajimoto
e-mail: kajimoto@kaji-lab.jp

S. Saga
University of Tsukuba, 1-1-1 Tennodai, Tsukuba, Ibaraki 305-8577, Japan
e-mail: saga@saga-lab.org



Fig. 1 Ouija board (*Kokkuri-san*): a type of ideomotor action

found worldwide, such as *Kokkuri-san* in Japan (Fig. 1). The movement of the game piece is considered to be a type of ideomotor action, which is a psychological phenomenon wherein a person makes movements unconsciously [1].

Typically, the Ouija board involves multiple players, and the movement might result from the “cooperation” of all players. However, no single person thinks that they are responsible, and assume that they are moved by others (including possible spiritual beings). Hence, this phenomenon can be considered as a type of haptic illusion, which induces users’ motion.

In our previous study [2], we showed that visual, force, and vibration cues play roles in this phenomenon. However, the friction and inertia of the device hindered the clear perception of the illusion. In this paper, we demonstrate our new 1-degree of freedom (DoF) device for the study of this phenomenon, which has much smaller friction and inertia.

2 Related Work

Several studies have shown that tactile cues can produce illusory force. Amemiya et al. [3] and Rekimoto [4] realized tractive force presentation with a simple device that uses asymmetric vibration. Skin traction has also been reported [5–8] to be felt as an external force.

While these haptic illusions do not explicitly accompany motion, in ideomotor actions, users assume that the motion is being produced by others. The hanger reflex is similar to this latter situation [9–11]. The typical hanger reflex is an involuntary rotational movement caused by deformation of the skin at particular locations on the head, and users typically comment that their head is being rotated by an external force. The potential cause of this phenomenon is assumed to be shear deformation of the skin [12], which contributes to force sensations [13–15].

In our previous study [2], we hypothesized that there are two necessary conditions for ideomotor actions.

- (1) A mechanism to generate an illusory force; and
- (2) A context that can be interpreted as allowing for the existence of others.

In the case of the Ouija board, this context is achieved explicitly by the existence of the other players, or by a belief in a spiritual being.

In our previous study, we used a fingertip-type haptic device that can create the perception of pulling on the users' fingers. We showed that visual, force, and vibration cues play roles in this phenomenon. However, the device requires improvement to produce a clearer perception of the illusory force. The friction and inertia of the device need to be lowered, and vibration at an arbitrary frequency might enhance the illusion.

3 1-DoF Linear Rail Device

We developed a device that achieves the two conditions (Fig. 2). The device comprises two DC motors (MAXON Inc., 4.5 W, RE16) that pull strings connected to a round planchette that users place their fingers on. The motors can present traction force and vibrotactile stimulation, which are controlled by a microcontroller (mbed NXP LPC1768, ARM Holdings). One motor encoder is used to measure finger position, and a linear rail (LS877, THK CO., LTD.) was used to reduce friction and confine the movement to one dimension.

A visual display is placed on top of the haptic device to present visual information that synchronizes with finger motion (Fig. 3). We presume that vibration and visual stimuli can present illusory force, and an occasional actual force can make users believe that they are really being pulled.

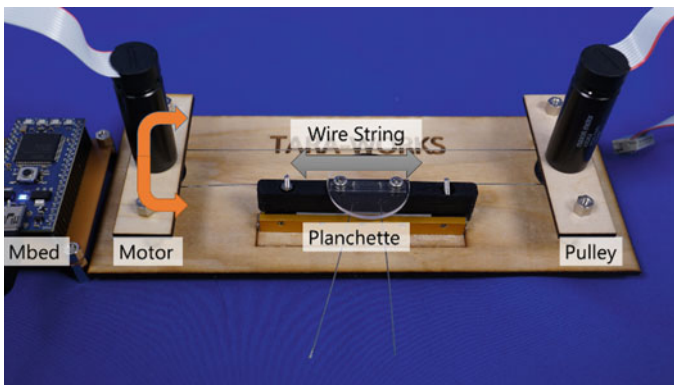


Fig. 2 1-DoF linear rail device

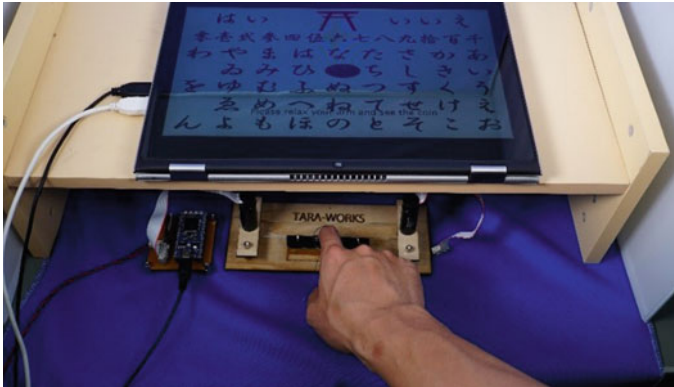


Fig. 3 System setup

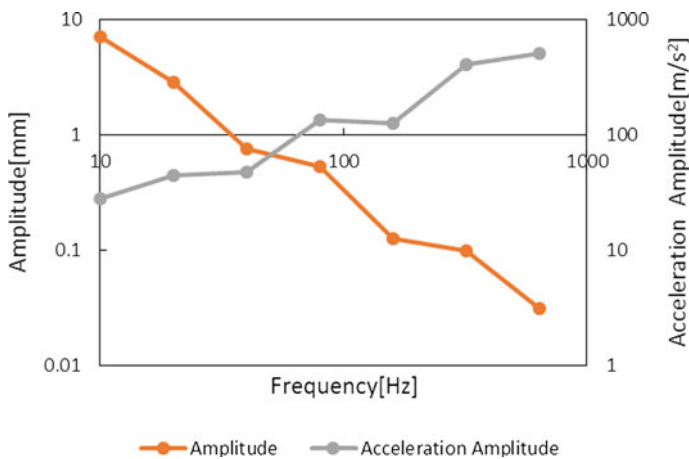


Fig. 4 Frequency characteristics of the device

4 Hardware Evaluation

We conducted a hardware evaluation to determine the frequency characteristics of the device. We measured amplitude and acceleration amplitude with a 10, 20, 40, 80, 160, 320, 640 Hz sinusoidal wave. To see the open-loop characteristics, we did not apply any feedback. The duration of the PWM (Pulse Width Modulation) signal to the motor was changed depending on the sinusoidal wave.

Figure 4 shows the amplitude and acceleration of the recorded data. The acceleration was calculated by multiplying the amplitude with the square of the angular frequency. We observed that the amplitude of the vibration was slightly below 1 mm at 40 Hz, and around 0.1 mm at 160 and 320 Hz, which are well

above the detection threshold of the human hand [16]. As the purpose of presenting vibration in our study was to present tiny cues for finger movement, we can conclude that the system demonstrates sufficient performance.

5 Demonstration

In this demonstration, we use the 1-DoF Linear Rail Device to let participants experience ideomotor action with the Ouija board. The participants place their right index fingers on the planchette, manipulate the planchette freely, and see how the image of the coin moves in synchronization with their fingers.

Next, they are asked to relax their arms and simply look at the coin on the display (Fig. 3). The device presents visual and haptic cues, and uses a novel pseudo-haptic illusion to induce the ideomotor action.

6 Conclusion

In this paper, we developed a new 1-DoF Linear Rail Device that can present force and vibration with low friction and inertia. We presume that vibration and visual stimuli can present illusory force, and an occasional actual force can make users believe that they are really being pulled, and induce unconscious movement in the user.

Acknowledgements This work was supported by JSPS KAKENHI Grant Number JP15H05923 (Grant-in-Aid for Scientific Research on Innovative Areas, “Innovative SHITSUKSAN Science and Technology”).

References

1. Stock, A., Stock, C.: A short history of ideomotor action. *Psychol. Res.* **68**(2–3), 176–188 (2004)
2. Shitara, T., Nakai, Y., Uematsu, H., Yem, V., Kajimoto, H., and Saga, S.: Reconsideration of ouija board motion in terms of haptics illusions. In: *Euro Haptics Conference* (2016)
3. Amemiya, T., Gomi, H.: Distinct pseudo-attraction force sensation by a thumb-sized vibrator that oscillates asymmetrically. *Haptics: neuroscience, devices, modeling, and applications. Lect. Notes Comput. Sci.* **8619**, 88–95 (2014)
4. Rekimoto, J.: Traxion: a tactile interaction device with virtual force sensation. In: *Proceedings of the ACM Symposium of User Interface Software and Technology*, pp. 427–432 (2013)
5. Yem, V., Kuzuoka, H., Yamashita, N., Ohta, S., Takeuchi, Y.: Hand-skill learning using outer-covering haptic display. *Proce. EuroHaptics, Lect. Notes Comput. Sci.* **8618**, 201–207 (2014)

6. Kuniyasu, Y., Sato, M., Fukushima, S., Kajimoto, H.: Transmission of forearm motion by tangential deformation of the skin. In: Proceedings of Augmented Human International Conference (2012)
7. Shull, P., Bark, K., Cutosky, M.: Skin nonlinearities and their effect on user perception for rotational skin stretch. In: Proceedings of the IEEE Haptics Symposium, pp. 77–82 (2010)
8. Kojima, Y., Hashimoto, Y., Kajimoto, H.: Pull-Navi. In: Proceedings of the ACM SIGGRAPH Emerging Technologies Session (2009)
9. Sato, M., Matsue, R., Hashimoto, Y., Kajimoto, H.: Development of a head rotation interface by using hanger reflex. In: Proceedings of the IEEE International Symposium on Robot and Human Interactive Communication, pp. 534–538 (2009)
10. Nakamura, T., Nishimura, N., Sato, M., Kajimoto, H.: Development of a wrist-twisting haptic display using the hanger reflex. In: Proceedings of Advances in Computer Entertainment Technology Conference (2014)
11. Shikata, K., Makino, Y., and Shinoda, H.: Inducing elbow joint flexion by shear deformation of arm skin. In: Proceedings of World Haptics Conference (2015)
12. Sato, M., Nakamura, T., Kajimoto, H.: Movement and pseudo haptics induced by skin lateral deformation in hanger reflex. In: Proceedings of Special Interest Group on Telexistence (in Japanese) (2014)
13. Edin, B.B., Johansson, N.: Skin strain patterns provide kinaesthetic information to the human central nervous system. *J. Physiol.* **487**, 243–251 (1995)
14. Collins, D.F., Prochazka, A.: Movement illusions evoked by ensemble cutaneous input from the dorsum of the human hand. *J. Physiol.* **496**, 857–871 (1996)
15. Ebied, A.M., Kemp, G.J., Frostick, S.P.: The role of cutaneous sensation in the motor function of the hand. *J. Orthop. Res.* **22**, 862–866 (2004)
16. Brisben, A.J., Hsiao, S., Johnson, K.O.: Detection of vibration transmitted through an object grasped in the hand. *J. Neurophysiol.* **81**, 1548–1558 (1999)

Haptic Perception of Macro Texture

Tao Zeng, Wenjing Chen, Nan Li, Liangzong He and Lantao Huang

Abstract The studies of texture perception focused mainly on displaying the textures with interior space gap in the millimeter level and below. We could call this kind of texture “fine texture”. In contrast, the “macro texture” has space gap in centimeters and above, and it is considered as the special texture with tiny texture pattern covered on curved surface. Macro texture contains richer surface information, including both roughness and curvature. This paper introduces a haptic device which could represent sinusoidal macro texture through active and dynamic touch with bare finger.

Keywords Macro texture perception · Haptic device · Curvature perception · Active and dynamic touch

1 Introduction

Haptic texture perception was well studied over the years, and most of the textures to be rendered have their interior space gap in the millimeter and below. We could call them “fine texture”. On contract, the “macro texture” has interior space gap in centimeter and above (Fig. 1a). Form the point of view of geometric properties, the macro texture can be seen as tiny texture pattern (Fig. 1b) covering on curved surface (Fig. 1c). It includes both texture and curvature information.

T. Zeng (✉) · W. Chen · N. Li · L. He · L. Huang
Department of Instrumental and Electrical Engineering, Xiamen University,
Xiamen, China
e-mail: tao.zeng@xmu.edu.cn

T. Zeng
State Key Laboratory of Virtual Reality Technology and Systems, Beihang University,
Beijing, China

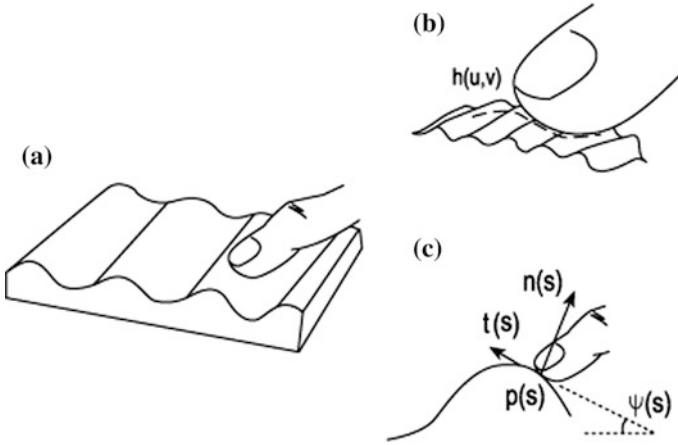


Fig. 1 Haptic perception of macro texture. **a** The finger explores the macro texture; **b** perception of fine texture pattern; **c** perception of curvature

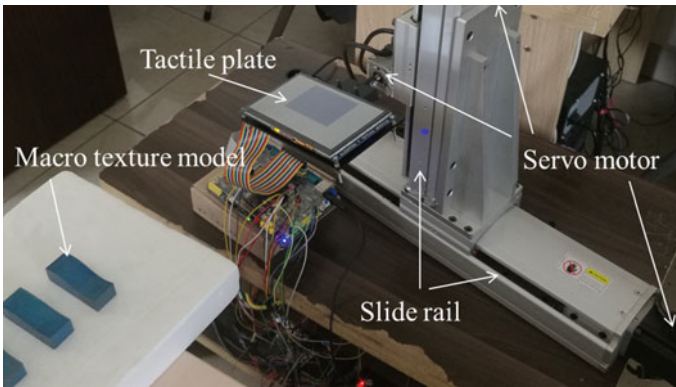


Fig. 2 The haptic device for macro texture perception

2 The Haptic Device and Control Method

The device has three degree of freedom: x-axis, z-axis and rotation about y-axis (Fig. 2). It can independently orient, elevate, and translate the end-effector, making sure that the end-effector is always kept tangential to a virtual macro texture at the contact point during manual exploration to respect the dominant cue for curvature perception [1]. In consideration of the perception of fine texture and curvature simultaneously, the fine texture rendering plate will be used as the end-effector. Its hard and successive surface could display the fine texture based on film squeeze effect, and the curvature based on the reproduction of local contact trajectory. Furthermore, its capacitive touch screen could sensor the position of the finger and

then uses it as the input of the whole control system. This platform can meet the requirement of active and dynamic touch. The finger is free to move forward and backward along the surface of the plate.

Acknowledgements This study was supported by the National Nature Science Foundations of China (No. 61403320), and the open funding project of State Key Laboratory of Virtual Reality Technology and Systems, Beihang University (Grant No. BUAA-VR-15KF-01).

Reference

1. Wijnjtes, M.W.A., Sato, A., Hayward, V., Kappers, A.M.L.: Local surface orientation dominates haptic curvature discrimination. *IEEE Trans. Haptics* **2**(2), 94–102 (2009)

Natural Human Movements in Geometrically Constrained Haptic Environments

Igor Goncharenko, Mikhail Svinin and Victor Kryssanov

Abstract A haptic simulation system with configurable physical constraints for studying skillful human movements is presented. Different curve/surface constraints in 3D can be generated and linked to the system. The system is tested on a variety of tasks performed by human subjects. Theoretical and experimental kinematic profiles are compared for the case of basic rest-to-rest task, namely, line-constrained movement during transport of flexible object. In addition, the demonstration includes also the manipulation of parallel flexible objects, chained objects with elliptical constraint, and a rolling ball manipulation with torque feedbacks applied to the haptic manipulator.

Keywords Motor control • Constrained human movement • Optimality

1 Introduction

It is known that unconstrained rest-to-rest human hand movements can be well predicted by different optimality criteria (e.g., [1, 2]). The knowledge about the optimality criteria is crucial for biological cybernetics, computational neuroscience, robotics rehabilitation, and computer animation. In many practical situations, however, the hand movement is constrained in 3D space and it is not clear what

I. Goncharenko (✉)

3D Incorporated, 2-3-8 Shin-Yokohama, Kanagawa 222-0033, Japan

e-mail: igor@ddd.co.jp

M. Svinin

Faculty of Engineering, Kyushu University, Motoooka 744, Nishi-ku, Fukuoka 819-0395,

Japan

e-mail: svinin@mech.kyushu-u.ac.jp

V. Kryssanov

Graduate School of Information Science and Engineering, Ritsumeikan University,

Nojihigashi 1-1-1, Kusatsu Shiga 525-8577, Japan

e-mail: kvvictor@is.ritsumei.ac.jp

features of human movements, compared with unconstrained movements (such as a bell-shaped hand velocity profile), are preserved. It is also not clear what optimality criteria can satisfactorily capture the features of constrained movements. To find out the most suitable criterion, a wide variety of dynamic environments and spatial constraints imposed on the hand movement should be checked out. Note that it is difficult to implement physical constraints in a re-configurable hardware. However, haptic systems can provide an easy-to-design software solution to the construction of re-configurable environments. In this study, we built a haptic system, which can be extendable for different spatial constraints applied to human hand movement in manipulation of flexible objects. The flexible objects are modeled as multiple mass-springs, connected in sequential, or, parallel way. An analysis based on experiments completed by human subjects with the use of our haptic simulator demonstrates the possibility of a clear discrimination between two prediction criteria, namely, the minimum hand jerk criterion and the minimum object crackle criterion [2]. Also, our preliminary experiments support the applicability of the minimum hand jerk criteria to the prediction of human movements with transporting parallel flexible object (Theoretical derivation of the mathematical models is given in [3].).

2 Haptic System

Our system can support one (for one hand manipulation tasks) or two (for bi-manual operations) point force devices as shown in Fig. 1.

At present, industry-standard SensAble/Geomagic [4] devices are supported. We focused on the efficiency of haptic and simulation loops to achieve real-time capabilities and robust realistic interaction via the point-force devices in constrained VEs. The system has a history unit to record all simulation data: time-dependent parameters, feedbacks, object and hand positions, velocities and accelerations. Recording is performed at a frequency of 100 Hz, sufficient to analyze basic human motions with the average reaction time above 200 ms. To support the addition of a new constraint type, the haptic simulator has the following two features: common way of dynamic simulation and constraint generation method.

2.1 *Dynamic Simulation*

Each new dynamic model is represented by N ordinary differential equations (ODE) system with M time-dependent values:

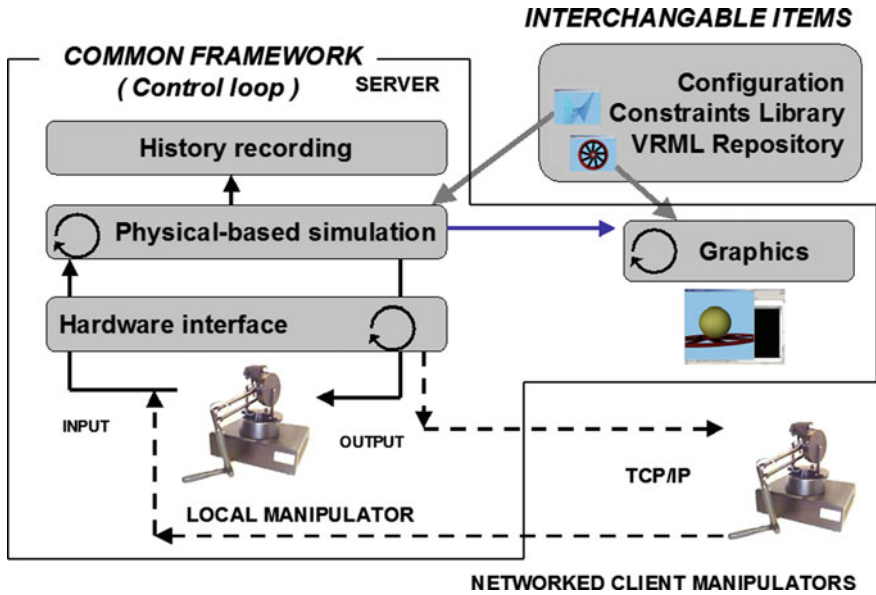


Fig. 1 System architecture

$$dy_i/dt = f_i(y_1, \dots, y_N, c_1(t), \dots, c_M(t)), \quad (1)$$

where y_j ($1 \leq i \leq N$) are the state variables, and parameters $c_j(t)$ ($1 \leq j \leq M$) are feedback force and torque components. The feedback force components are calculated by a spring-damper model using the difference between positions of haptic proxy and driven object. During simulation, system (1) is integrated by the Runge-Kutta 4th-order method for the time step corresponding to the constant cycle of haptic device. Initial condition for integration of system (1) for the rest-to-rest tasks is defined by condition of zero velocity/acceleration of driven object at the start position.

2.2 Constraint Generation

Important cases of constraints for human movement study can be described as parametric analytical curves/surfaces in 3D. For instance, circle in 3D is a constraint for the task of steering wheel (crank) rotation simulation. Such parametric representation has a simple form, and the structure of the right parts in Eq. (1) can also be derived from the parametric representation in analytical form. This procedure of constraint generation is implemented with Mathematica scripts and can be done in semi-automatic manner. There are two basic scripts: one is for one-parametric curves, and the second one is for two-parametric surfaces. Refer to [5] for details of

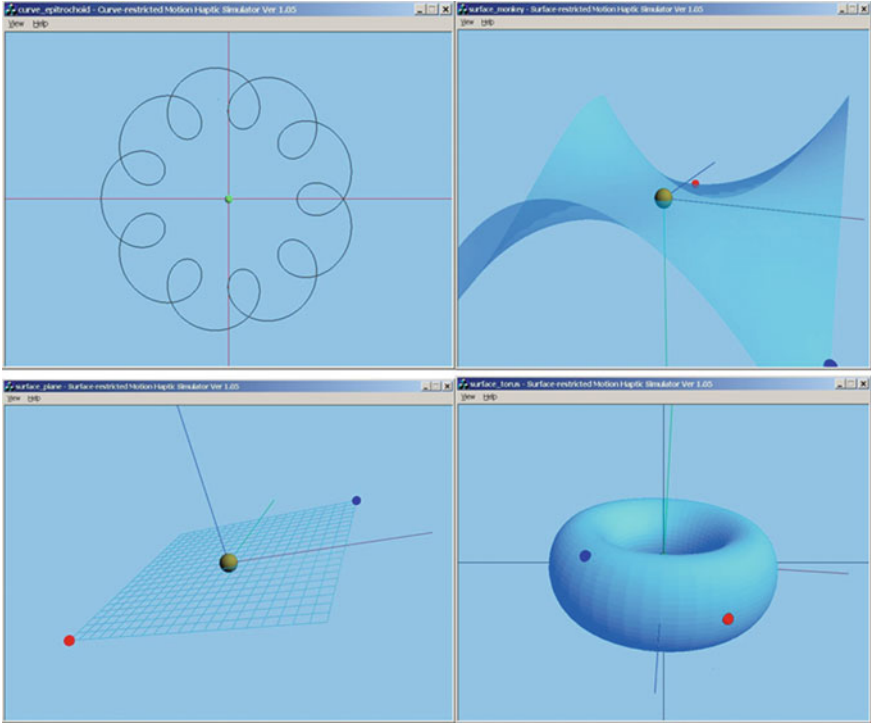


Fig. 2 Examples of curve- and surface-based constraints

constraint generation. In Fig. 2, there are four examples (epitrochoid, monkey saddle, plane, and torus) of constraints generated by the basic scripts. In this figure, the small yellow sphere on the surface can be haptically driven only along the surface.

Besides of the usage of the basic scripts for constraint generation, the structure of the right parts of Eq. (1) can be derived by other methods and linked to the haptic simulator. For instance, rolling ball manipulation included into demonstration is an example of non-holonomic constraint, which was not derived by the basic scripts.

In principle, the geometric constraints in haptic environments can be treated as guiding virtual fixtures [6]. In our research we use force-controlled haptic device (impedance type haptic manipulator). The additional force components in the directions tangential to the constraints are set zero, while those in the normal direction are generated with the use of virtual springs and dampers. The configuration-dependent unit vectors of normal and tangential directions are generated in advance using a Mathematica script. The transitional stiffness and damping matrices in the moving frame, associated with the proxy, are diagonal, with element values providing stability. The rotational stiffness/damping was not used since, in the current version of the haptic simulators, we are dealing only with single point constraints.

3 Case Study: Flexible Object Manipulation

A line constraint in 3D, generated by the basic script, was used in the haptic system to experimentally approve the correct choice between two prediction criteria: minimum hand jerk [2], and minimum object crackle [7]. Both criteria give very similar theoretical hand/object velocity profiles for the task of rest-to-rest flexible object movement, where flexible object is modelled as one mass virtually “connected” with human hand (hand position is defined as the position of haptic proxy) via a spring. When flexible object is modelled by several sequentially connected masses (Fig. 3), the difference between the theoretical profiles predicted by the criteria becomes significant.

The reaching task was formulated for experimenters in such a way so that, initially, all masses were at rest and coincided at the initial point (small left sphere in Fig. 3). Human subjects were instructed to move the 5-mass system to the target point (small right sphere) during designated time $T = 1$ s. All masses should finally be at rest and coincide at the target point. The travel distance was set to 0.2 m. Each mass was set to 0.6 kg and each spring stiffness was set to 600 N/m. As was mentioned in Sect. 2.2, additional guiding forces along the line are zeros, and non-zeros in the directions perpendicular to the line (modelled by springs and dampers).

Tolerances were introduced to count successful reaching trials: position deviation, speed, and time tolerances $\Delta x, \Delta v, \Delta T$ ($\Delta x = \pm 0.006$ m, $\Delta v = \pm 0.006$ m/s, $\Delta T = \pm 0.5$ s) and all masses must obey the tolerances. When a reaching task is successful, haptic interaction is stopped and an audio signal prompts the user to proceed with the next trial.

Five subjects (4 male and one female, all right-handed) participated in the experiment. One subject conducted preliminary experiments to re-define the tolerance set at the subject’s own pace to make experimental results statistically representative and comfortable for the subject. It turned out that the learning of successful movements constituted only 5% of 100 trials for the initial tolerances. The low learning rate is attributed to the relatively narrow time, position, and velocity windows. After setting the tolerances as $\Delta x = \pm 0.012$ m, $\Delta v = \pm 0.012$ m/s, the success rate increased to 17% (200 trials were completed). The

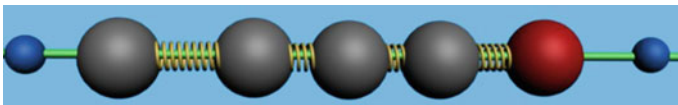


Fig. 3 Flexible object model

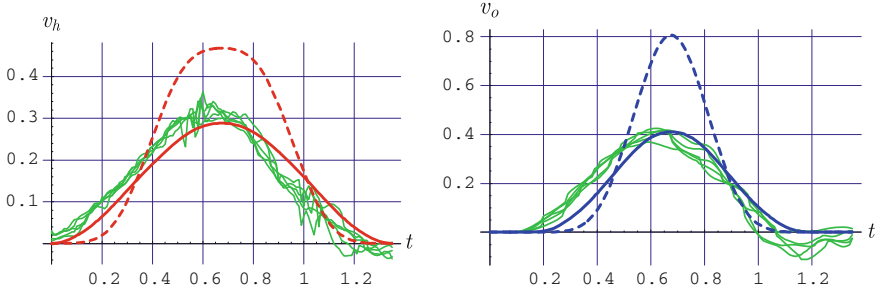


Fig. 4 Hand (*left*) and object (*right*) velocity profiles

average movement time became 1.35 s (maximal 1.49 s, minimal 1.13 s, and standard deviation from average 0.09 s). Finally, the tolerances were set as: $\Delta x = \pm 0.012$ m, $\Delta v = \pm 0.012$ m/s, $T = 1.35 \pm 0.5$ s.

All the subjects successfully caught the movement strategy and demonstrated acceptable success rate. Each subject completed 200 trials, 100 on the first day and 100 on the second day. On the second day, success rates for all five subjects were as follows: 17, 44, 47, 82, 48%. All experimental sets for all subjects demonstrated very similar results in favor of the minimum jerk criterion. Experimental velocity profiles for one of the subject, time-scaled to the subject’s average, are shown in Fig. 4 by thin lines. Hand and object velocity profiles, predicted by minimum hand jerk and minimum object crackle, are shown by thick solid and thick dashed lines, respectively. Note that the last fifth mass’s (left large sphere in Fig. 4) velocity is given as “object velocity.”

Two commonly used integrated measures for sample matching, ME (Mean Error), and VAF (Value Accounted For, %) also demonstrated the favor of the minimum hand jerk criterion.

4 Demonstration

In addition to the line-constrained flexible object manipulation described in Sect. 3, the following demonstrations with constrained dynamics are presented:

- Elliptic constraint: flexible object manipulation
- Line constraint: parallel flexible object manipulation
- Elliptic constraint: chained object manipulation
- Ball-plane constraint: rolling ball balancing task.

Acknowledgments This research was supported in part by MEXT KAKENHI Grant Number JP15K05900.

References

1. Flash, T., Hogan, N.: The coordination of arm movements: an experimentally confirmed mathematical model. *J. Neurosci.* **5**(7), 1688–1703 (1985)
2. Svinin, M., Goncharenko, I., Luo, Z., Hosoe, S.: Reaching movements in dynamic environments: how do we move flexible objects? *IEEE Trans. Robot.* **22**(4), 724–739 (2006)
3. Svinin, M., Goncharenko, I., Lee, H., Yamamoto, M.: Modeling of human-like reaching movements in the manipulation of parallel flexible objects. In: *IEEE/RSJ International Conference on Intelligent Robots and Systems (IROS 2016)* (2016)
4. <http://www.geomagic.com>
5. Goncharenko, I., Svinin, M., Kanou, Y., Hosoe, S.: Predictability of rest-to-rest movements in haptic environments with 3D constraints. *J. Robot. Mechatron.* **18**(4), 458–466 (2006)
6. Li, M., Kapoor, A., Taylor, R.H.: A constrained optimization approach to virtual fixtures. In: *IEEE/RSJ International Conference on Intelligent Robots and Systems (IROS 2005)*, pp. 2924–2929 (2005)
7. Dingwell, J., Mah, C.F., Mussa-Ivaldi, F.: Experimentally confirmed mathematical model for human control of a non-rigid object. *J. Neurophysiol.* **91**, 1158–1170 (2004)

Expression of 2DOF Fingertip Traction with 1DOF Lateral Skin Stretch

Vibol Yem, Mai Shibahara, Katsunari Sato and Hiroyuki Kajimoto

Abstract To reproduce the sensation of rubbing on a surface, we need to laterally stretch the skin of the fingertip with two degrees of freedom (2DOF). Unfortunately, it is difficult to develop a compact 2DOF device for the fingertip because at least two actuators are required. However, if we can perceive the rubbing sensation regardless of the skin stretching direction, a device with 1DOF is sufficient. This study used a lateral skin deforming device with 1DOF, and evaluated the realism of the sensation. We found that even when the direction of skin stretch was opposite or perpendicular to the finger movement, users still perceived it as natural.

Keywords Fingertip · Lateral skin stretch · 1DOF device · Direction

1 Introduction

When we rub the surface of an object with a finger, the frictional force and the associated lateral skin stretch occur on our fingertip skin in the opposite direction of the movement. If we move the finger leftward or forward, our fingertip skin is stretched rightward or backward. Therefore, our skin stretches with two degrees of freedom (2DOF). Several skin stretch devices have been developed to reproduce this sensation [1–4]. However, these devices require at least two actuators to stretch the skin with 2DOF [5], and thus they tend to be large and heavy.

V. Yem (✉) · H. Kajimoto
The University of Electro-Communications, Tokyo, Japan
e-mail: yem@kaji-lab.jp

H. Kajimoto
e-mail: kajimoto@kaji-lab.jp

M. Shibahara · K. Sato
Nara Women's University, Nara, Japan
e-mail: pam_shibahara@cc.nara-wu.ac.jp

K. Sato
e-mail: katsu-sato@cc.nara-wu.ac.jp

In our previous study, we developed a device named FinGAR, which can deform fingertip skin leftward or rightward for presenting various tactile sensations [6]. To make the device compact, we used only one actuator (i.e., 1DOF). During our test, we observed that, even though we can detect the direction of skin deformation when the fingers do not move, we do not notice the direction when we move our fingers.

From the above background, we came up with the hypothesis that, if the direction of lateral skin stretch does not contribute to the realism of the rubbing sensation, we do not need to use several actuators to accurately reproduce skin deformation direction. In this paper, we test this idea with a psychological experiment using part of FinGAR device. The fingertips of the index fingers are deformed to the left or right as users are asked to move their fingers to the left, right, backward or forward, randomly, and score the realism of the sensation.

2 Experiment

2.1 Device

Figure 1 shows the overview of the experimental apparatus, which was originally developed to present both mechanical and electrical stimulation [6]; in this experiment, we removed the electrical stimulation component. An arm that contacts the finger-pad is driven by a DC motor (Maxon 118386) with a 16:1 gear head ratio to deform the skin.

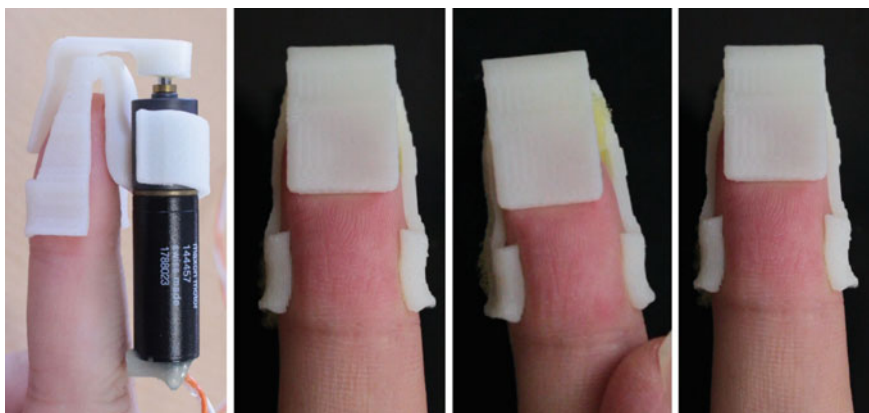


Fig. 1 Overview of wearing the device and skin deformation conditions (from *left* to *right* no stimulus, and skin deforming to the *right* and *left*)

2.2 Design

During the experiment, we asked participants to move their fingers in accordance with a visual marker on a screen. Skin stretch was presented in accordance with the motion of the marker. The stimulus strength of skin deformation s , finger position x and velocity v are expressed by the equations below:

$$s = \frac{s_{th}}{2} \times (1 - \text{Cos}(2\pi ft)), \quad (1)$$

$$x = \frac{p}{2} \times (1 - \text{Cos}(2\pi ft)), \quad (2)$$

$$v = \dot{x} = \pi fp \times \text{Sin}(2\pi ft), \quad (3)$$

where s_{th} is the value at which each participant could clearly detect the direction of skin deformation even when they were moving their finger. p is the tracing distance of the marker (in pixels) and f is the frequency, which represents the speed of the marker. We presented one tracing loop ($0 \leq t \leq 1/f$) for each experimental.

To change the tracing velocity, the *frequency* f was set to three conditions: $f_1 = 1$ Hz (slow), $f_2 = 2$ Hz (medium), and $f_3 = 3$ Hz (fast). There were four conditions for *tracing direction* (*left, right, forward, backward*) and three conditions for *stimulus* (s_{left} , s_{right} , s_{non} (no stimulus for skin deformation)). Each condition was conducted three times, so there were 108 trials ($3 \text{ frequency} \times 4 \text{ tracing direction} \times 3 \text{ stimulus} \times 3 \text{ repeats of each condition}$) for each participant.

2.3 Procedure

Five female volunteers aged 21–24 years participated in this experiment. Four of them were right-handed, and one was left-handed.

Figure 2 shows an overview of the experiment. The GUI on the screen is for guiding the participants during the experiment. They were asked to sit on a chair, wear the device on their index finger of their right hand, and to move a PC mouse (represented by a hand mark on the GUI) following a blue filled target circle. After each trial, they were asked to score the realism of the tracing sensation with a five-stage evaluation (zero to four). A higher score means that the sensation was more realistic.

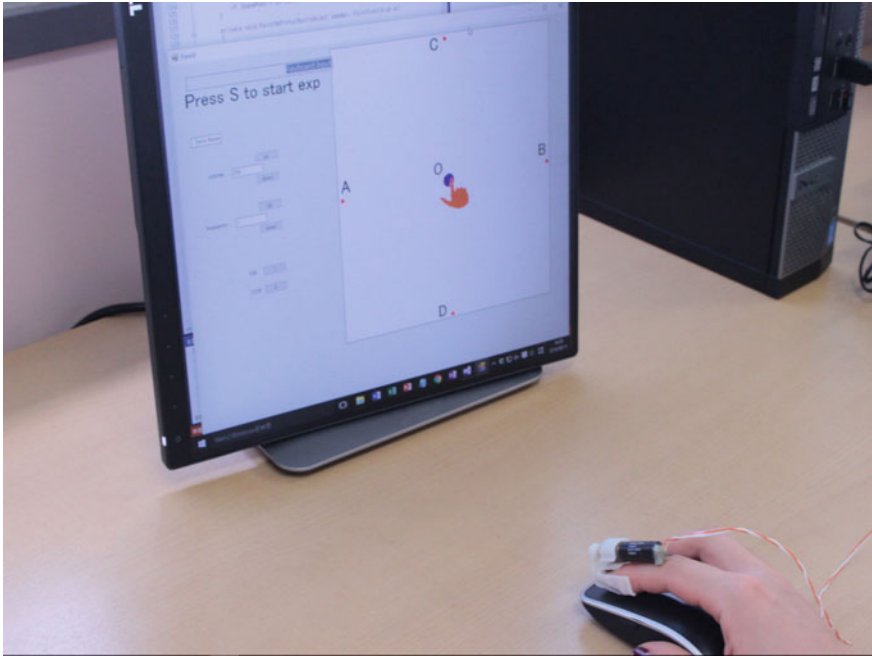


Fig. 2 Overview of the experiment

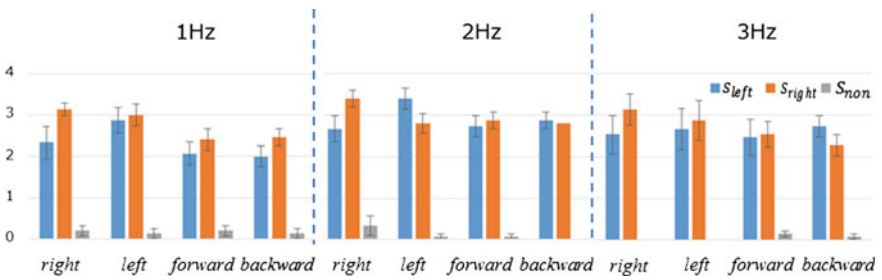


Fig. 3 Scores of realistic sensation for each tracing direction. The left, middle, and right panels show the frequency conditions of 1, 2, and 3 Hz, respectively. Error bars indicate standard deviation

3 Results and Discussion

Figure 3 shows the comparison of three kinds of stimulus for each tracing direction. The results indicated that the average score was over 2.0 for all frequency and tracing direction conditions when the skin deformation stimulus was presented. In contrast, the score almost remained at zero when there was no stimulus.

The results suggest that we can perceive the tracing sensation as realistic while skin stretch is presented regardless of the tracing direction. Therefore, a lateral skin stretch device with 1DOF, such as FinGAR and Gravity Grabber [1], might be sufficient to reproduce a tracing sensation in any movement direction. This result might be an example of the visual dominance over haptics; however, comparing the skin stretch conditions with the no skin stretch condition, the skin stretch greatly contributed to the realism of the situation.

4 Conclusion

This paper described the possibility of presenting 2DOF fingertip traction using only a 1DOF lateral skin stretch device. The experiment showed that we can perceive a realistic sensation of tracing on a surface regardless of the finger's movement direction, when users move their fingers and can see their movements. This result may be a case of visual dominance over haptics, but the skin stretch itself contributed to the realism. The result suggests that a device with 1DOF such as FinGAR or Gravity Grabber might be sufficient for presenting a tracing sensation.

We have planned two steps for future work. First, we will study the effectiveness of the stimulus waveform to make the tracing sensation more realistic. Second, we will combine FinGAR and a virtual reality system to present various kinds of tracing sensations.

Acknowledgements This research is supported by the JST-ACCEL Embodied Media Project.

References

1. Minamizawa, K., Fukamachi, S., Kajimoto, H., et al.: Gravity grabber: wearable haptic display to present virtual mass sensation. In: Proceedings of ACM SIGGRAPH Etech (2007)
2. Bianchi, M., Battaglia, E., Poggiani, M., et al.: A wearable fabric-based display for haptic multi-cue delivery. In: Proceedings of IEEE Haptics Symposium, pp. 277–283 (2016)
3. Imaizumi, A., Okamoto, S., Yamada, Y.: Friction sensation produced by laterally asymmetric vibrotactile stimulus. In: Proceedings of EuroHaptics, Part II, pp. 11–18. Springer (2014)
4. Levesque, V., Hayward, V.: Experimental evidence of lateral skin strain during tactile exploration. In: Proceedings of EuroHaptics (2003)
5. Ho, C., Kim, J., Patil, S., Goldberg, K.: The slip-pad: a haptic display using interleaved belts to simulate lateral and rotational slip. In: Proceedings of IEEE WHC, pp. 189–195 (2015)
6. Yem, V., Okazaki, R., Kajimoto, H.: FinGAR: Combination of electrical and mechanical stimulation for high-fidelity tactile presentation. In: Proceedings of ACM SIGGRAPH Etech (2016)

Perceived Hardness by Tapping: The Role of a Secondary Mode of Vibration

Kosuke Higashi, Shogo Okamoto, Hikaru Nagano, Masashi Konyo and Yoji Yamada

Abstract Humans can discriminate among the hardness of objects by tapping their surfaces. The damped natural vibration caused by tapping and its frequency are known to be the cue for the perception of hardness. This study is an investigation of the characteristics of this perception of hardness, as induced by vibration stimuli including multiple frequency components. We performed a comparative experiment using several damped vibration stimuli, which included either one or two frequency components, and investigated the significance of the secondary vibration mode and the change in its frequency. We found that the presence of the secondary mode significantly enhanced the perceived hardness; however, its frequency had a lesser effect on hardness perception.

Keywords Hardness perception · Tapping · Vibration · Frequency

1 Introduction

Humans use the vibrotactile cue caused by tapping the surface of an object when judging the object hardness [6]. This fact is well known; however, it is astonishing that little is known about the perceptual mechanism responsible for this perception of hardness by tapping. The common understanding among researchers is that vibratory stimulation of higher frequency [3, 7] and larger attenuation [4] leads to greater perceived hardness. As a result, materials with greater rigidity [6] and viscosity loss [4] are felt to be harder.

K. Higashi (✉) · S. Okamoto · Y. Yamada
Graduate School of Engineering, Nagoya University, Nagoya, Japan
e-mail: higashi.kousuke@d.mbox.nagoya-u.ac.jp

H. Nagano · M. Konyo
Graduate School of Information Sciences, Tohoku University, Sendai, Japan

There have been some attempts to simulate the dynamic characteristics of an impulsive contact between a fingertip and an object in terms of either a reaction force and acceleration [1, 2, 5]. Such stimulus mimicking the transient reaction of tapped object enhances the contact realism of objects [5]. Because one of the most significant features of such transient reaction is multiple frequency components of the waveform, it can be assumed that the vibration including higher-frequency component aside from the main component is felt harder than when the vibration merely comprises a single or primary component. However, the hardness perception when the natural vibration caused by tapping the object includes multiple frequency components has not been well studied.

In the present study, we investigated the perceptual roles of individual frequency components in the case of vibrations that include multiple components. Especially, we were interested in the role of the higher frequency component when the vibration consisted of two components, i.e., lower (primary) and higher (secondary) frequency components. We used a customized haptic interface based on a direct-driven DC motor and prepared several natural vibration stimuli. Invited participants compared these stimuli in terms of their perceived hardness, and we then investigated the significance of the frequency of the higher frequency component.

2 Experiment

2.1 Damped Vibration Stimuli

We used a damped vibration stimulus that includes either one or two frequency components. The displacement of the vibration stimulus was determined by

$$x(t) = \begin{cases} x_1(t) \\ x_1(t) + x_2(t) \end{cases} \quad (1)$$

$$x_i(t) = a_i v_i \exp\left(\frac{-t}{\tau_i}\right) \sin(2\pi f_i t) \quad (2)$$

where $x(t)$, v_i , a , τ , and f are the vibration displacement, tapping speed, amplitude per tapping speed, time constant, and frequency of the vibration, respectively. We compared five pairs of stimuli, which are listed in Table 1, by using a paired comparison method. Pair I included a vibration stimulus of 100 Hz and that of 100 and 200 Hz. By making this comparison, we aimed to demonstrate that the presence of the secondary vibration mode could result in the perception of greater hardness. In pairs II and III, we compared vibration stimuli including a single frequency component. Pair II included vibration stimuli of 80 and 100 Hz and pair III included that of 160 and 200 Hz. In each pair, the frequency change was set to 20% decrease from 100 and 200 Hz, respectively. These comparisons would enable us to verify that the higher frequency component is responsible for inducing the perception of greater

Table 1 Frequencies of the vibration stimuli for each stimulus pair

| Stimulus pair | Stimulus 1 | | Stimulus 2 | |
|---------------|------------|------------|------------|------------|
| | f_1 (Hz) | f_2 (Hz) | f_1 (Hz) | f_2 (Hz) |
| I | 100 | – | 100 | 200 |
| II | 80 | – | 100 | – |
| III | 160 | – | 200 | – |
| IV | 80 | 200 | 100 | 200 |
| V | 100 | 160 | 100 | 200 |

hardness. We also compared the answer rates between pairs II and III and investigated the difference of the perceptual reaction against the frequency change in the vicinity of 100 and 200 Hz. In pairs IV and V, we compared vibration stimuli including two frequency components. Pairs IV and V included vibration stimulus made up of 80 and 200 Hz components and 100 and 160 Hz components respectively, and another made up of 100 and 200 Hz components. These comparisons would show whether the 20% frequency change was also effective for hardness perception in the first or secondary mode of multiple-frequency vibration. By comparing the answer rates between pairs IV and V, we investigated the difference of the perceptual reaction against the frequency change between the first and second vibration mode. The time constant of each vibration component was set to $\tau = 0.02$ s. The amplitude of an acceleration per tapping speed of each frequency component was set to 300 s^{-1} so that their max acceleration became equal. When expressed in displacement, the amplitude per tapping speed of the 100 Hz component was $a = 7.6 \times 10^{-4}$ s and that of the 200 Hz component was $a = 1.9 \times 10^{-4}$ s. The amplitude of the 160 Hz component was the same as that of the 200 Hz component to enable us to focus on the effect of the change in frequency.

2.2 Apparatus

We developed the haptic display shown in Fig. 1. The main components of this apparatus are a dial, DC motor (RE40, Maxon motor), current controller (ADS50/10, Maxon motor), and microcomputer (mbedLPC1768, ARM). The participant was able to experience a vibration stimulus by using their fingertip to rotate the dial to a certain angle, which was measured by a rotary encoder installed on the DC motor. The vibration of (1) was presented in the tangential direction of the dial. The tangential displacement of the dial can be described as $x(t) = r\theta(t)$ where r and θ are the radius of the dial and its rotational angle, respectively. The control system employed a feedforward control method operated at 5 kHz.

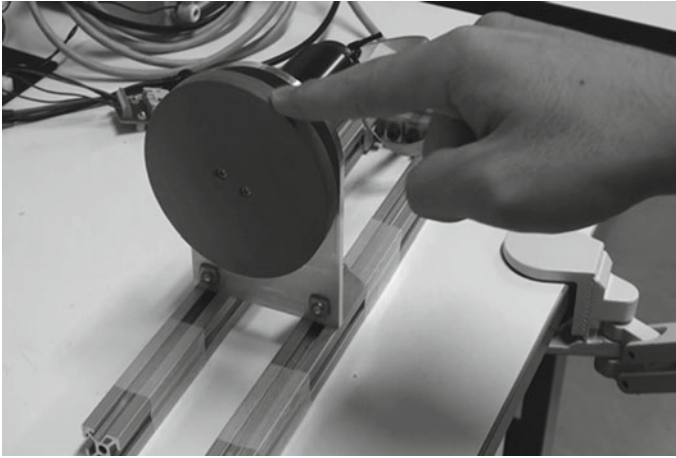


Fig. 1 One degree-of-freedom force display with direct DC motor drive

2.3 Tasks

The participants were five right-handed males in their twenties and thirties. They operated the haptic display and compared the two vibration stimuli presented in pairs. They were able to switch the presented stimulus by using a keyboard and judged which stimulus was felt harder. Each of the five stimulus pairs listed in Table 1 was tested 20 times. In total, 100 comparisons (5 pairs × 20 repetitions) were performed for each participant, and these 100 pairs were presented in randomized order.

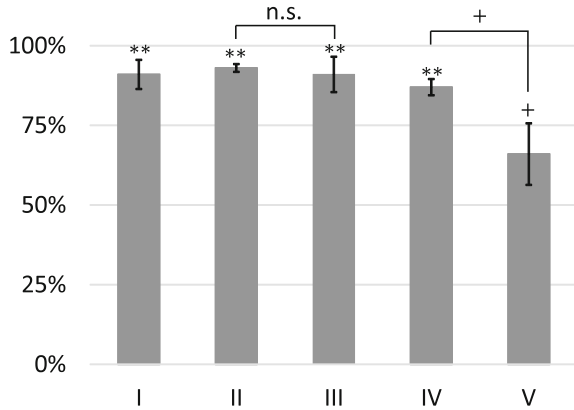
2.4 Results

Table 2 and Fig. 2 show the answer rates at which the stimulus including a higher frequency component was judged to be harder.

Table 2 Probability at which higher frequency components induced greater hardness perception

| Stimulus pair | Participants | | | | | Average |
|---------------|--------------|------|------|------|------|---------|
| | A | B | C | D | E | |
| I | 0.9 | 1.0 | 0.75 | 1.0 | 0.9 | 0.91 |
| II | 0.9 | 0.9 | 0.95 | 0.95 | 0.95 | 0.93 |
| III | 1.0 | 1.0 | 0.7 | 0.95 | 0.9 | 0.91 |
| IV | 0.8 | 0.9 | 0.85 | 0.95 | 0.85 | 0.87 |
| V | 0.7 | 0.85 | 0.65 | 0.8 | 0.3 | 0.66 |

Fig. 2 Answer ratio at which vibration with greater frequency is felt harder. n.s.: not significant, +: $p < 0.1$, **: $p < 0.01$



The *t*-test between the average answer rate of each stimulus pair and a chance level of 0.5 showed that pairs I-IV indicated significant difference ($p < 0.01$) and pair V indicated significant tendency ($p < 0.1$). For pair I, all participants agreed that the stimulus including the secondary mode felt harder than that with only a primary mode. They answered that the stimulus with the higher frequency seemed to be harder for the single-frequency vibration of pairs II and III. By comparing the answer rates of pairs II and III, we could not confirm the significant difference of the perceptual reaction against the frequency change between the vicinity of 100 and 200 Hz. For the vibration including multiple frequency components of pairs IV and V, almost of all participants answered that the stimulus with the higher frequency component was felt harder just like pairs II and III. However, the comparison for pairs IV and V showed that the answer rate of pair V tended to be less than that of pair IV ($p < 0.1$).

3 Discussions

The results for pairs II and III indicate that the 20% frequency changes in the vicinity of 100 and 200 Hz clearly affected the hardness perception. However, comparing the results of pairs IV and V, the frequency change of the secondary mode was less effective than that of the primary mode for all of the participants, even though the frequency of each component was changed just like in pairs II and III. Nonetheless, the presence of the secondary mode is apparently effective as indicated by the answers for pair I. Our experiment indicated that the presence of the secondary mode significantly enhanced our perception of hardness; however, changing its frequency had a lesser effect on the hardness perception than for the vibration with a single-frequency component. This aspect of human hardness perception may lead to a reasonable rendering of object hardness, even if it is difficult to present high-frequency vibrations because of limitations in the hardware or software of haptic interfaces.

4 Conclusions

This study addressed the characteristics of hardness perception by vibration stimuli including multiple frequency components. By comparing five types of stimulus pairs, we investigated the effects of a secondary vibration mode as well as the effect of changing its frequency. The experimental results suggested that the presence of the secondary mode significantly enhanced perceived hardness; however, changing the frequency of this mode was less effective in terms of hardness perception unlike the single-component vibration stimuli.

Acknowledgements This study was partly supported by JSPS Kakenhi (15H05923), and ImPACT (Tough Robotics Challenge).

References

1. Fiene, J.P., Kuchenbecker, K.J.: Shaping event-based haptic transients via an improved understanding of real contact dynamics. *Proc. IEEE World Haptics Conf.* **2007**, 170–175 (2007)
2. Hasegawa, S., Takehana, Y., Balandra, A., Mitake, H., Akahane, K., Sato, M.: Vibration and subsequent collision simulation of finger and object for haptic rendering. In: Auvray, M., Duriez, C. (eds.) *Haptics: Neuroscience, Devices, Modeling, and Applications*. Lecture Notes in Computer Science, vol. 8619, pp. 352–359. Springer (2014)
3. Higashi, K., Okamoto, S., Nagano, H., Yamada, Y.: Effects of mechanical parameters on hardness experienced by damped natural vibration stimulation. In: *Proceedings of IEEE International Conference on Systems, Man, and Cybernetics* pp. 1539–1544 (2015)
4. Higashi, K., Okamoto, S., Yamada, Y.: What is the hardness perceived by tapping? In: Bello, F., Kajimoto, H., Visell, Y. (eds.) *Haptics: Perception, Devices, Control, and Applications*. Lecture Notes in Computer Science, vol. 9774, pp. 3–12. Springer (2016)
5. Kuchenbecker, K.J., Fiene, J., Niemeyer, G.: Improving contact realism through event-based haptic feedback. *IEEE Trans. Vis. Comput. Graph.* **12**(2), 219–230 (2006)
6. LaMotte, R.H.: Softness discrimination with a tool. *J. Neurophysiol.* **83**(4), 1777–1786 (2000)
7. Okamura, A.M., Cutkosky, M.R., Dennerlein, J.T.: Reality-based models for vibration feedback in virtual environments. *IEEE/ASME Trans. Mechatron.* **6**(3), 245–252 (2001)

Experiments on Two-Handed Localization of Impact Vibrations

Daniel Gongora, Hikaru Nagano, Masashi Konyo and Satoshi Tadokoro

Abstract Impact vibration measurements were employed to determine which signal parameters serve as cues to localize impacts on a bar held with both hands. We considered three types of materials: Aluminum, polyoxymethylene (POM) and wood. Impact localization was better when the vibrations obtained from the wood bar were presented to the participants. We observed that to estimate the impact point participants relied primarily on amplitude and duration differences in the vibrations delivered to their hands. When short sine-wave bursts of varying amplitude and duration were used instead of impact vibrations, participants' capacity to localize the impacts improved. The goal of this submission is to further assess this observation with data obtained from the conference attendees.

Keywords Impact vibrations · Bimanual · Localization · Perception

1 Introduction

Consider the scenario depicted in Fig. 1 where a person is holding a bar with both hands. If suddenly something impacts the bar and the only information available are the impact vibrations, can the impact point be estimated? Which signal parameters condition the success in this task?

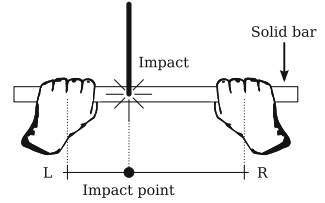
D. Gongora (✉) · H. Nagano · M. Konyo · S. Tadokoro
Graduate School of Information Sciences, Tohoku University,
6-6-01 Aramaki Aza Aoba, Aoba-ku, Sendai-shi, Miyagi 980-8579, Japan
e-mail: daniel@rm.is.tohoku.ac.jp

H. Nagano
e-mail: nagano@rm.is.tohoku.ac.jp

M. Konyo
e-mail: konyo@rm.is.tohoku.ac.jp

S. Tadokoro
e-mail: tadokoro@rm.is.tohoku.ac.jp

Fig. 1 Bimanual impact localization task



Previous studies on single-handed impact perception have demonstrated that impact vibrations influence the perceived impact location [4]. Moreover, it has been shown that people are capable of estimating the impact point [6] and the impact direction [7] using high-frequency vibrotactile cues. Our investigation differs from these studies in that we consider a bimanual impact perception task instead of its single-handed counterpart. Our experiments deal with the interaction between two stimuli presented simultaneously or within a small interval to contralateral regions of the body. [5] illustrated this kind of interaction between primal and subsequent vibrotactile stimuli by establishing a number of conditions under which masking occurs.

In this paper we address the problem of localizing impacts on a bar held with both hands using only vibrotactile feedback. The main contributions are:

- Evidence that suggests people are capable of estimating the impact point using only vibrotactile cues (Sect. 3). We discuss the effects of material type on people’s ability to estimate the impact point.
- Experimental results that explain people’s capacity to estimate the impact point in terms of amplitude and duration differences in the vibrations delivered to the participants’ hands (Sect. 4).

2 Vibration Data Collection

We recorded impact vibrations from aluminum, wood and polyoxymethylene (POM) bars using two vibration sensors attached to the bars by a thin layer of hot-melt adhesive. The bars were 500 mm long, 50 mm wide and 10 mm thick and they were clamped at both ends. We hit the bars twelve times at seven equally-spaced points with an impact hammer equipped with a hard metallic tip to excite the bars in a wide frequency range. Both the impact force and the resulting vibrations were recorded for 50 ms at a sampling rate of 500 kHz. The sensitivities of the vibration sensors and impact hammer are $20 \text{ mV}/(\text{m}/\text{s}^2)$ and $2.3 \text{ mV}/\text{N}$, respectively.

3 Experiment 1: Bimanual Impact Localization

In this section we seek to determine if participants can use impact vibrations delivered to their hands to localize impacts. In addition, we set out to establish the effects of material type on the impact localization task.

3.1 Subjects and Procedure

Seven subjects participated in this study, including one female and six males. All of them had participated in a preliminary study where they were exposed to the same stimuli one week prior to this experiment.

Participants sat down resting their forearms on the arms of the chair. They were instructed to use the string connecting the vibrators to maintain the same hand to hand distance. They waited for the stimulation with their eyes closed and they were asked to point on a touchscreen their impression about the impact point, Fig. 2. Noise-canceling headphones playing pink noise were used to mask auditory cues. A new stimulus was presented about 3 s after participants touched the screen.

3.2 Stimuli

Two Linear Resonant Actuators (Haptuator—Tactile Labs), one for each hand, were enclosed in 3D printed cylinders. The cylinders vibrated parallel to the surface of the skin. They were loosely connected by a polyester sewing thread whose purpose

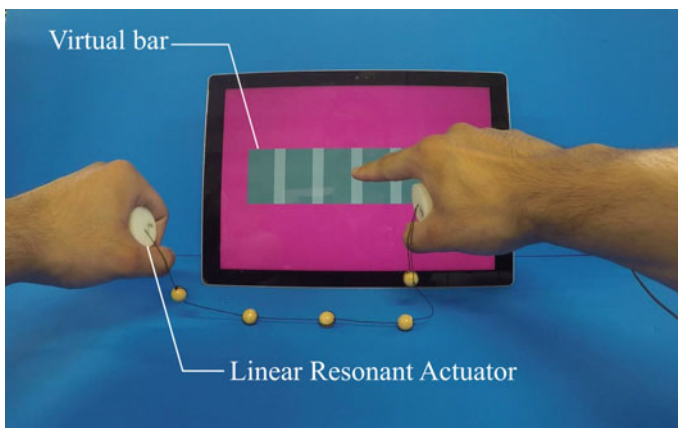


Fig. 2 Experimental set up for delivering vibrations and for recording participants' answers

was to keep a 37 cm hand-to-hand distance. The thread had equally spaced markers for visual reference, Fig. 2.

The average of all twelve impact vibrations at each impact point was used as vibrotactile stimulus. Each of the seven conditions was presented six times. In total, 126 stimuli (3 materials \times 6 repetitions \times 7 conditions) were distributed over the span of three consecutive sessions, each of which lasted no more than 5 minutes. The order of these sessions and that of the conditions in one session were randomly generated for each subject.

3.3 Results

The results of this experiment are summarized in Fig. 3. Impacts on the left side of the bar are expected to be negative while impacts on the right side are expected to be positive. The results for the wood bar do not follow the expected trend. In fact, participants perceived some conditions as their symmetric counterpart. For example, participants associated impacts at R2 with condition L2. This unusual trend is most likely due to asymmetries in the impulse excitation. The impulse obtained from the impact hammer exhibits a similar pattern.

The type of material affected participant’s ability to recognize all impacts points. The information encoded on the impact vibrations of the aluminum bar is useful only for discerning left from right. On the other hand, the impact vibrations of the wood bar carry enough information to enable the participants to make finer judgments about the impact point. Participants could not estimate the impact point reliably using the impact vibrations obtained from the POM bar.

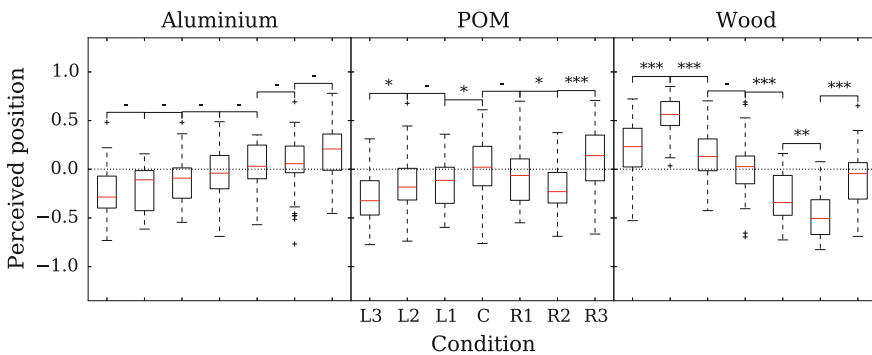


Fig. 3 Left to right Aluminium, POM, and wood collective results of the bimanual impact perception experiment. * $p < 0.05$, ** $p < 0.01$, *** $p < 0.001$

4 Experiment 2: Potential Cues Investigation

We considered three potential cues quantified as the differences in amplitude, duration and delay in the vibrations delivered to the hands of the participants. We measured these cues and then correlated them with the results of the experiment described in Sect. 3. We observed high correlation values for amplitude and duration differences. In this section we evaluate the capacity of participants to estimate the impact point when the impact vibrations are replaced by sine waves varying in amplitude and duration.

4.1 Subjects and Procedure

Four male subjects ranging in age from 20 to 27 served as subjects in this experiment. All of them took part in the previous study. We followed the procedure of the first experiment. The independent variables were the amplitude and duration of the vibrations. In the first experiment we manipulated the amplitude while keeping the duration constant. In the second experiment we controlled the duration and we kept the amplitude constant. All subjects participated in both experiments.

4.2 Stimuli

We used a modulated 250 Hz sine wave as vibrotactile stimulation in this experiment because numerous sites of the human skin are more sensitive to vibrations near this frequency [2, 3]. The envelope $e(t)$ consisted of an exponential attack phase, $1 - e^{-\alpha(t-t_0)}$; a sustain phase; and an exponential release phase, $e^{-\beta(t-t_2)}$.

Vibrations of varying amplitude and duration were produced by adjusting the maximum amplitude and duration of the sustain phase, respectively. The duration of the vibrations was kept below 50 ms in order to replicate the conditions of the first experiment.

4.3 Results and Discussion

The collective results of this experiment are shown in Fig. 4. The horizontal axis of each figure represent the seven conditions corresponding to the seven impact points of the experiment described in Sect. 3. The vertical axis represents the estimated impact point. Given the way this experiment was set up, conditions L3, L2 and L1 should be associated with negative values, whereas conditions R1, R2 and R3 with positive values.

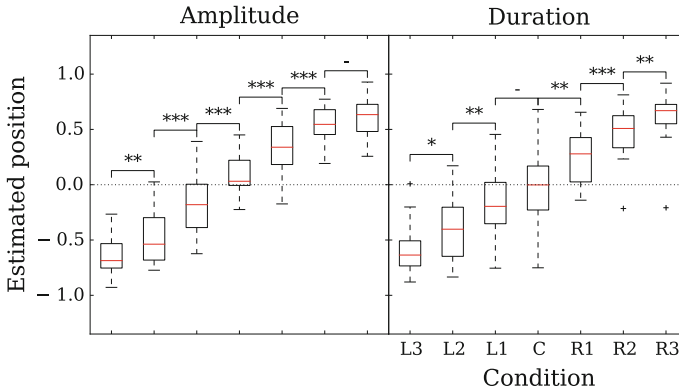


Fig. 4 Combined results of four participants in the cue validation experiment. *Left to right* Results for amplitude and duration cues. $*p < 0.05$, $**p < 0.01$, $***p < 0.001$

The results of this experiment suggest that vibrations differing in either amplitude or duration can be used to represent the impact point on a bar even in the absence of delay. Delay was not considered in this study due to the time characteristics of the propagation of impact vibrations. However when purposefully manipulated, delay can be useful for creating the illusion that vibrations travel from one hand to the other as reported in [10]. Finally, participants' performance in the experiments described in Sects. 3 and 4 is remarkable considering the short duration of the stimuli.

The perceived intensity of vibrations delivered to the skin is influenced by their duration. People are capable of perceiving weaker vibrations if they last longer. This phenomenon was reported in [9] for vibrations whose duration was under 1000 ms. The same effect is observable at different vibration intensity levels and the *enhanced sensitivity* reaches its maximum with 600 ms vibrations [8]. This effect could explain why in our experiments duration differences produced similar results to intensity differences.

Furthermore, in post-experiment discussions, participants indicated that the differences among the two feedback conditions were not evident to them. They thought intensity had been manipulated throughout the experiments. This observation is in agreement with [1] where the manipulation of the duration of short duration vibrations produced changes on the perceived intensity of the vibrations.

5 Conclusion

We studied the perceptual problems associated with a bimanual impact localization task. We first established that participants were capable of estimating the impact point using only vibrotactile cues. Then, we determined that participants used the differences in amplitude and duration in the vibrations delivered to their hands as

primary cues to estimate the contact point. We expect to evaluate these observations with data from the conference attendees. Furthermore, we are currently exploring the use of these findings to improve the response to collisions of a teleoperated robot using vibrotactile feedback.

Acknowledgements This research was partially supported by ImpACT Program “Tough Robotics Challenge”.

References

1. Bochereau, S., Terekhov, A., Hayward, V.: Amplitude and duration interdependence in the perceived intensity of complex tactile signals. In: International Conference on Human Haptic Sensing and Touch Enabled Computer Applications, pp. 93–100. Springer (2014)
2. Choi, S., Kuchenbecker, K.J.: Vibrotactile display: perception, technology, and applications. *Proc. IEEE* **101**(9), 2093–2104 (2013)
3. Jones, L.A., Sarter, N.B.: Tactile displays: guidance for their design and application. *Hum. Factors: J. Hum. Factors Ergon. Soc.* **50**(1), 90–111 (2008)
4. Okazaki, R., Kajimoto, H.: Altering distance perception from hitting with a stick by superimposing vibration to holding hand. In: International Conference on Human Haptic Sensing and Touch Enabled Computer Applications, pp. 112–119. Springer (2014)
5. Sherrick, C.E.: Effects of double simultaneous stimulation of the skin. *Am. J. Psychol.* **77**(1), 42–53 (1964)
6. Sreng, J., Lécuyer, A., Andriot, C.: Using vibration patterns to provide impact position information in haptic manipulation of virtual objects. In: International Conference on Human Haptic Sensing and Touch Enabled Computer Applications, pp. 589–598. Springer (2008)
7. Sreng, J., Lécuyer, A., Andriot, C., Arnaldi, B.: Spatialized haptic rendering: providing impact position information in 6dof haptic simulations using vibrations. In: 2009 IEEE Virtual Reality Conference, pp. 3–9. IEEE (2009)
8. Verrillo, R.T., Smith, R.L.: Effect of stimulus duration on vibrotactile sensation magnitude. *Bull. Psychon. Soc.* **8**(2), 112–114 (1976)
9. Verrillo, R.: Temporal summation in vibrotactile sensitivity. *J. Acoust. Soc. Am.* **37**(5), 843–846 (1965)
10. Zhao, S., Israr, A., Klatzky, R.: Intermanual apparent tactile motion on handheld tablets. In: World Haptics Conference (WHC), 2015 IEEE, pp. 241–247. IEEE (2015)

Rubber Hand Illusion Using Tactile Projector

Yuuki Horiuchi, Kazunori Odani, Yasutoshi Makino
and Hiroyuki Shinoda

Abstract In this paper, we inspect a new rubber hand illusion (RHI) which uses invisible haptic feedback by using an airborne ultrasound tactile display (AUTD). RHI is an illusion that a subject misunderstands the ownership of his/her body. When a subject is given tactile stimulation on his/her hand without visual cues and fake hands visually stimulated at the same time, the subject feels as if the fake rubber hand is his/her real hand. In general, occurrence of RHI is promoted by hiding subject's hand. In this paper, we assume that invisible tactile stimulation by AUTD can make RHI stronger without hiding a real hand. We use a tactile projector system that combines both invisible AUTD stimulus and a visible projected image. We show that this configuration enhances RHI.

Keywords Rubber hand illusion · Airborne ultrasound tactile display

1 Introduction

Rubber hand illusion (RHI) [1, 2] is a well known illusion of ownership of body. This illusion emerges when a subject is given tactile stimulation on his/her hand behind a screen, which prevents them from seeing their own hand, and at the same time fake hand, made of rubber, is visually stimulated by a brush. A Subject feels as if the fake rubber hand is his/her own real hand.

In this study, we assume that hiding subject's own hand is important to prevent them from seeing contact event. Thus RHI without hiding a real hand will be possible when an invisible stimulation is used. Recently, it was confirmed that RHI occurs in the case when a subject can see his/her real hand [3]. RHI with invisible stimulus can make illusionary sensation stronger than this previous study.

Y. Horiuchi (✉) · K. Odani · Y. Makino · H. Shinoda
University of Tokyo, 7-3-1 Hongo, Bunkyo-ku, Tokyo 113-0033, Japan
e-mail: horiuchi@hapis.k.u-tokyo.ac.jp

In this paper, we use airborne ultrasound tactile display (AUTD) for invisible tactile stimulation. In our pilot study, we tried to make haptic sensation with a visual cue of brush strokes. However, the perception of AUTD system was different from the visual cue of brush strokes and RHI was not strongly emerged. In this paper, we use tactile stimulation that does not contradict with visual stimulation. In order to achieve this, we use a tactile projector system to change visual cues freely. This study is important to discuss how the sense of agency changes depending on the tactile and visual stimulus. The results will be applied for controlling artificial limbs efficiently, repairing phantom limb sensations and enhancing tele-existence feeling when a head mounted display is used.

2 Airborne Ultrasound Tactile Display (AUTD)

AUTD is the device that display tactile stimulation in midair [4]. AUTD has 249 speakers and uses converged ultrasound by controlling each phase of transducers to give force feedback. High pressure area is generated about 1 cm diameter at arbitrary position. Figure 1 shows appearance of AUTD.

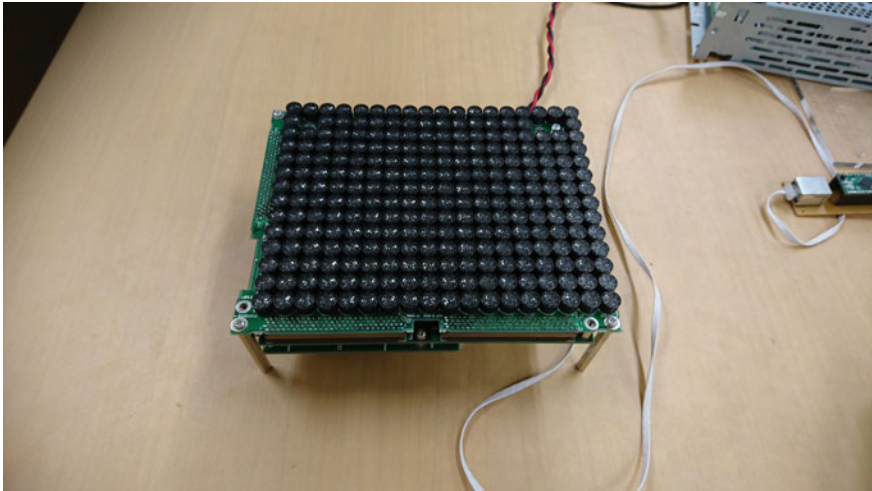


Fig. 1 Airborne ultrasound tactile display (AUTD)

3 Experiment

3.1 Experimental Setting

Figure 2 shows our experimental setting. The subject put his both hands in the workspace. Right fake hand is set in between the both hands. The AUTD and the projector is hanged above the workspace. The invisible tactile stimulus by AUTD can be given on both hands.

3.2 Stimulation in This Experiment

Visual stimulation we use in the study is shown in Fig. 3. Subjects feel tactile stimulation by AUTD, with visual stimulation on the fake hand. In this experiment, we use a shadow of black lizard projected by projector (Sight3D HD-U35) as the visual stimulation.

Figure 4 shows how we combined tactile stimulation and visual stimulation on subjects' hands. Subjects only can see the animated lizard moves on the fake hand. At the same time, subjects feel tactile feedback by AUTD, which cannot be seen.

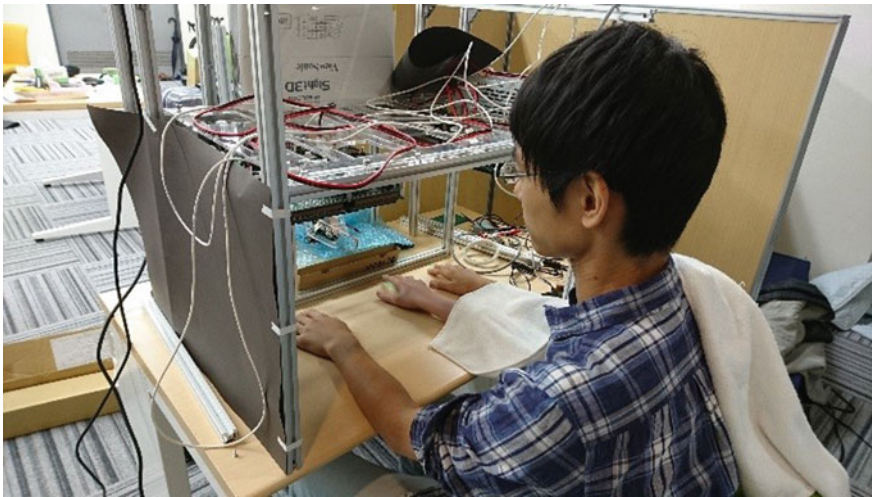


Fig. 2 Experimental setting



Fig. 3 Visual stimulation at subjects' viewpoints. There are a rubber hand and shadow of lizard is visually projected

Fig. 4 Visual stimulation and tactile stimulation

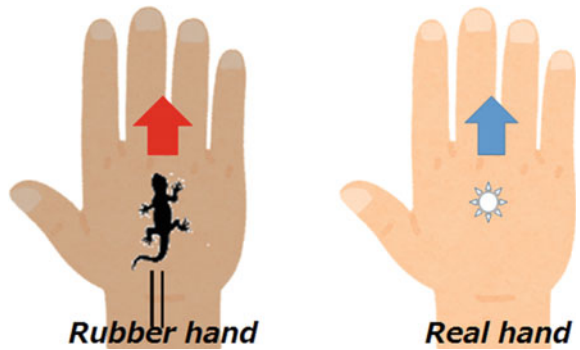


Table 1 Questionnaires

| | |
|----|---|
| S1 | I felt tactile stimulation on the rubber hand |
| S2 | I felt as if the rubber hand was my hand |
| S3 | I felt tactile stimulation on real hand |
| S4 | It no longer felt like my hand belonged to my body |
| S5 | It felt as if I had two right hands |
| S6 | I felt tactile stimulation on both hands at the same time |
| S7 | It felt as if the rubber hand is my real hand |
| S8 | It felt as if my real hand were turning rubber hand |

3.3 Procedure of Experiment

We evaluated how strong RHI occurs by questionnaires which is shown in Table 1. Subjects were asked to score perceived effects by using a ten-point scale ranging from 0 to 9. The score 5 means “I can’t say which side I am on,” and 9 means “I agree this questionnaires strongly.” S1–S2 are questionnaires about ownership of the rubber hand; S3–S4 are questionnaires about ownership of subjects’ own hands; S5–S6 are questionnaires about ownership of both hands; S7–S8 are questionnaires not consist with this illusion.

8 subjects who are twenties participated in the experiment. The all subjects are right handers. We aligned the rubber hand along the real right hand as shown in Fig. 3. In this condition, we displayed tactile stimulation on the real right hand.

In our pilot study, we noticed that RHI occurs stronger after subjects learned the relationship between visual and tactile stimulations. Before the experiment, we displayed shadow of the lizard and tactile stimulation by AUTD at the same time on their left hands to have them understand the relationship. We displayed synchronously and asynchronously tactile and visual stimulation for 1 min, because if we displayed synchronously only, a subject would be upset as it is unexpected stimulation.

After these pre-learning stimulus, we projected shadow of the lizard on the rubber hand and displayed tactile stimulation on subjects’ right hand. For the first 2 min, we displayed asynchronous stimulus. In the asynchronous stimulus, a visual image is not match to a tactile stimulus. The image moves in opposite way. After this stimulation, subjects are asked to answer the questionnaires. This is the “asynchronous condition” in the following results.

After the asynchronous condition, we then give synchronous stimulus. A visual image and a tactile stimulus is displayed for 2 min so that they match in motion. Subjects are asked to answer the questionnaires again. This is the “synchronous condition.”

4 Result

Figure 5 shows the averaged value of questionnaires of 8 subjects and the error-bar means a standard error. Based on the t-test between the asynchronous and synchronous conditions, there are significant differences in S2 and S4 [$p = 0.018$ and $p = 0.043$, respectively]. Even though there are no significant differences, there seems also a differences in S1 and S3 [$p = 0.11$ and $p = 0.39$, respectively].

Ownership of the rubber hand (S2) is stronger in the synchronous condition than the asynchronous one. Ownership of the real hand (S4) is weaker in the synchronous condition. It shows that in the synchronous condition RHI is stronger.

In this experiment, as we displayed asynchronous stimulation and synchronous stimulation in the fixed order, some subjects could not understand how the

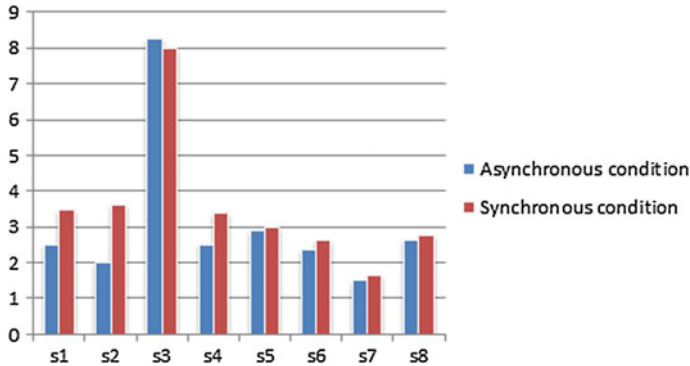


Fig. 5 Result of questionnaires

ownership of their body changed to the rubber hand at the first asynchronous condition. So they answered questionnaires falsely. If the order of stimulation of this experiment is randomized, there will be possibility that difference between both conditions will be more apparent. That is our future work.

5 Conclusion

In this paper, we proposed a new rubber hand illusion(RHI) which used invisible haptic feedback by using an airborne ultrasound tactile display (AUTD). We used a tactile projector system in order to display both invisible tactile stimulus and a visible projected image. Based on our experiment, we showed the following findings. (1) Pre-learning phase was important to enhance RHI intensity. (2) Synchronous condition made stronger RHI than asynchronous condition. These results will be applied for understanding how ownership changes depending on the tactile and visual stimulus.

Acknowledgements This work was partly supported by JSPS KAKENHI 15H05315, 15K12073 and JST ACCEL Embodied Media Project.

References

1. Dalley, S.A., Varol, H.A., Goldfarb, M.: A method for the control of multigrasp myoelectric prosthetic hands. *IEEE Trans. Neural Syst. Rehab. Eng.* **20**(1), 58–67 (2012)
2. Botvinick, M., Cohen, J.: Rubber hands ‘feel’ touch that eyes see. *Nature* **391**, 6699 (1998)
3. Arvid, G., et al.: The illusion of owning a third arm, *PLoS One* (2011)
4. Hoshi, T., Takahashi, M., Iwamoto, T., Shinoda, H.: Noncontact tactile display based on radiation pressure of airborne ultrasound. *IEEE Trans. Haptics* **3**(3), 155–165 (2010)

Colorful Tactile Stimuli. Association Between Colors and Tactile-Display Stimuli on Russell's Psychological Plane

Hikaru Hasegawa, Ken Itoh, Shogo Okamoto, Hatem Elfekey and Yoji Yamada

Abstract Supplementing the presentation of colors with tactile displays has yet to be developed. This study used Russell's affective plane to investigate the association between the rainbow colors and vibrotactile and variable-friction stimuli presented as tactile displays. A user study indicated that high-frequency and rhythmical tactile stimuli that were perceived as arousing were suitable for presenting the warm colors such as red, orange, and yellow. In contrast, low-frequency and slow tactile stimuli that were perceived as less arousing were suitable for the cold colors. Furthermore, unpleasant tactile stimuli that involved fine but strong frictional texture could be linked with purple and with unpleasant psychological images. Our findings indicate that tactile displays can be used to assist the user's perception of hue.

Keywords Hue · Vibrotactile · Friction · Electrostatic

1 Introduction

One of the roles of tactile displays is to compensate or complement visual information; however, the presentation of colors is challenging in this respect. The relationships between temperature stimuli and colors are well known [1–3]. Furthermore, Ludwig and Simner reported psychological relationships between the lightness, chroma, and surface roughness of materials [4]. However, the association between hue and vibrotactile and frictional stimuli has yet to be clarified. Our ultimate goal is to establish a stimulus set for expressing each of the rainbow colors. For this purpose, we associated the tactile-display stimuli with color hues. As described in Sect. 2, we first attempted find associations between color wave-length and the fineness of vibrotactile and frictional stimuli. However, we were unsuccessful because of the discrepancy between psychological images for colors and those for tactile stimuli. We then mapped hue and tactile stimuli via psychological images.

H. Hasegawa (✉) · K. Itoh · S. Okamoto · H. Elfekey · Y. Yamada
Department of Mechanical Science and Engineering, Nagoya University,
Furo-cho, Chikusa-ku, Nagoya, Japan
e-mail: hasegawa.hikaru@c.mbox.nagoya-u.ac.jp

2 Design Principles for Color-Tactile Association

2.1 *Associations Based on Physical Color Elements*

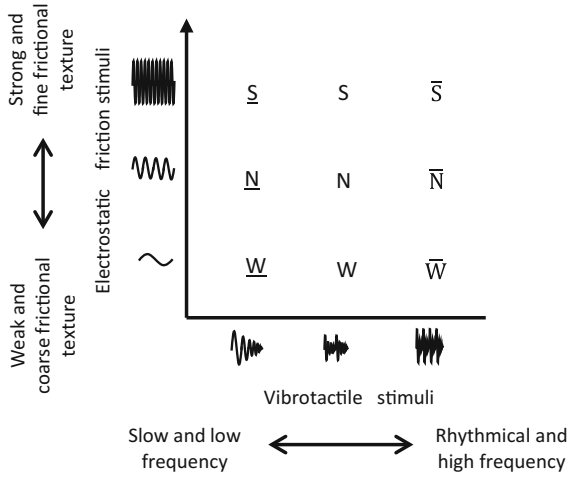
A color is typically decomposed into hue, luminance, and chroma. We considered association of each of these three types of color element with independent tactile stimuli. This idea is supported by findings that texture roughness is correlated with the chroma of a color [4], and a vibrotactile texture display can present textures with various levels of roughness [5]. Furthermore, because hue depends on the frequency of light, intuitive color-tactile associations using vibrotactile stimuli with varying frequencies appear plausible. For example, low-frequency vibrotactile stimuli may correspond to colors such as red and yellow, and high-frequency stimuli may correspond to colors such as blue and purple. We tested such color-tactile associations based on frequency by using a vibrotactile display. Unfortunately, we failed to find frequency-based associations. This was because the impressions provided by colors and vibrotactile stimuli did not match. For example, our impression of warm colors, such as red, orange, and yellow, is energetic. In contrast, low-frequency vibrotactile stimuli that were potentially linked with the warm colors evoked impressions such as calmness and stillness. Hence, the psychological images associated with colors and vibrotactile stimuli are inconsistent, and hue-tactile associations based on frequency may be inconsistent with an intuitive user-experience.

2.2 *Associations Based on Affective Responses*

Colors can be associated with emotions [6]. Furthermore, vibrotactile stimuli can evoke affective responses [7]. These findings led us to use psychological images to connect tactile stimuli and colors. We adopted Russell's psychological plane [8], which is a two-dimensional plane composed of arousal and pleasantness axes. We designed nine tactile stimuli that mapped on Russell's psychological plane, using the vibrotactile and frictional stimuli to present stimuli that varied along arousal and pleasantness axes, respectively (Fig. 1).

Based on prior reports [7], we used attenuating sinusoidal vibrotactile stimuli, and generated different stimuli by changing the frequency of the sinusoidal wave and the tempo of additional signal periodicities, as shown in Fig. 1. High frequency and rhythmical vibrotactile stimuli were arousing, and low frequency and slow vibrotactile stimuli were sleepy. We used the electrostatic friction display to present stimuli that varied along the pleasant-unpleasant axis. We switched friction on and off with switching frequencies of 30–100 Hz, with larger magnitudes for the faster-switching frequencies. Strong and high-frequency friction stimuli were intended to evoke unpleasant user experiences, whereas weak and low-frequency stimuli were intended to be relatively pleasant.

Fig. 1 Nine types of tactile stimuli using vibrotactile and electrostatic friction components. *S*, *N*, and *W* indicate the level of frictional stimuli. *Underline* and *overline* indicate the level of vibrotactile stimuli



3 Experimental System: Tactile Display for Vibrotactile and Electrostatic Frictional Stimuli

We used a tactile display that could present vibrotactile and variable-friction stimuli. The same equipment has been used in another study by the authors [9]. The whole system was computer-controlled at 1 kHz. As shown in Fig. 2, the vibrotactile stimuli were produced by four voice coil actuators (X-1741, Neomax Engineering Co. Ltd., Japan), each of which was located at each corner of the top panel. The four actuators were synchronously driven by a current amplifier (ADS 50/5, Maxon motor, Switzerland) and delivered mechanical vibratory stimuli to the finger pad on the top panel. The frictional stimuli were produced via the electrostatic force induced by the voltage between an aluminum pad and an ITO panel. An insulator (Kimotect PA8X, KIMOTO Co. Ltd., Japan) was located between the ITO panel and aluminum pad. The induced voltage was operated by a high-fidelity voltage amplifier (HJOPS-1B20, Matsusada Precision Inc., Japan).

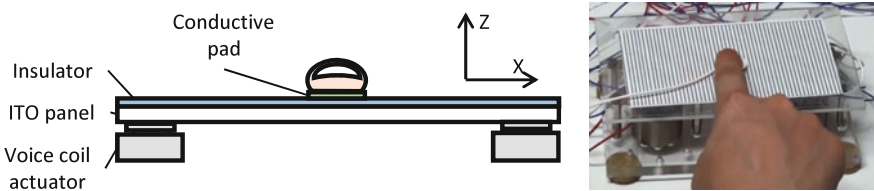


Fig. 2 Tactile texture display for the presentation of vibrotactile and variable-friction stimuli. *Left* Schematic side-view. *Right* Photo of apparatus

4 Experiment

We performed two experiments to investigate the association between colors and psychological images and between the tactile stimuli noted above and psychological images. Three student volunteers who were unaware of the objectives of the study participated in the two experiments in a counterbalanced manner.

In experiment 1, the participant experienced each of the nine types of tactile stimuli and mapped each stimulus on Russell’s psychological plane which was drawn on a sheet of paper. The participant moved their finger on the panel and experienced the tactile stimulus as long as they wanted, but typically each trial lasted several seconds. From this experiment, we assessed whether the designed tactile stimuli were clearly located within Russell’s psychological plane. The nine types of stimuli were presented in randomized order.

In experiment 2, the participants placed each of the rainbow colors, namely red, orange, yellow, green, blue, indigo, and purple, on Russell’s psychological plane. Each color was tested only once for each participant. We did not show printed colors to the participant; he/she imagined each color.

5 Results

Figure 3 shows the results of experiment 1. The tactile stimuli generally differed in their psychological, affective components. Specifically, stimulus \bar{S} was perceived to be arousing, and stimulus \underline{W} was perceived to be less arousing for every participant. Meanwhile, the responses toward S , \underline{S} , \underline{N} , and \bar{W} were inconsistent among the participants.

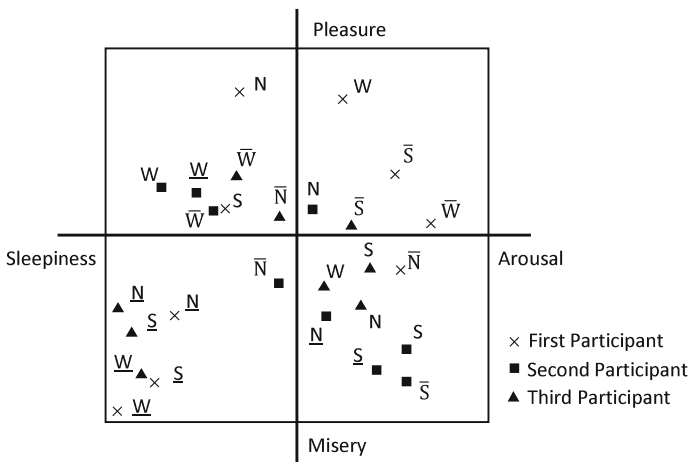


Fig. 3 Tactile stimuli placed on Russell’s psychological plane

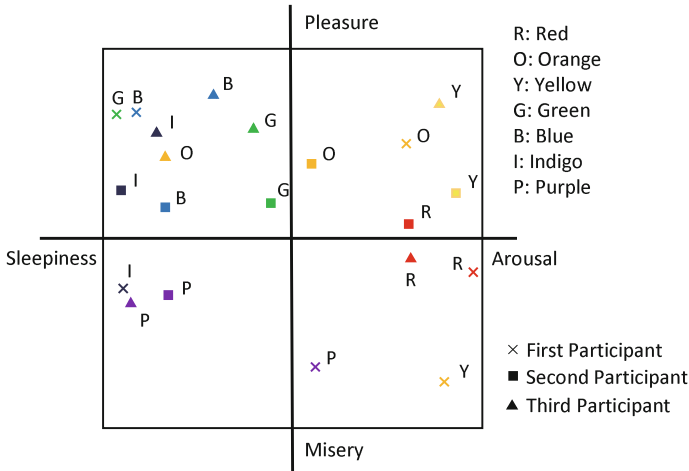


Fig. 4 Colors placed on Russell’s psychological plane

Figure 4 shows the results of experiment 2. Note that locations of red, yellow, blue, and indigo only differed slightly among individuals along the arousal-sleepiness axis. Similarly, red, orange, green, and blue only differed slightly among individuals along the pleasure-misery axis. Moreover, most of the colors were assigned to the positive side of the pleasure-misery axis except for purple, which seems to be an unpleasant color. We also note that the warm colors were considered arousing, and the cold colors were placed in less arousing areas of the space.

6 Discussion and Conclusions

According to experiment 2, individual differences in the psychological associations of colors are small. This indicates that it is possible to present a hue supported by tactile sensory input if we control the arousal and pleasantness of the tactile stimuli. In particular, the warm colors are likely to be consistent with arousing stimuli, and the cold colors are likely to be presented by less arousing stimuli. Among the tactile stimuli tested above, \bar{S} and \underline{W} may be effective for pairing with the warm and cold colors, respectively.

We also note that changing the pleasantness of stimuli is not appropriate for presenting them in conjunction with colors. This is because all rainbow colors except for purple are associated with pleasant or neutral perceptions. Only purple has the possibility of being presented with unpleasant stimuli, such as \underline{S} or \underline{N} in our study.

To summarize, before the current study, no attempts had been made to find associations between the hue of colors and vibrotactile or variable-friction stimuli. We found that a frequency modulation approach, in which high-frequency tactile

stimuli were matched with colors with short wave lengths, was not intuitive for users. Instead, we considered affective responses toward colors and tactile stimuli. Consequently, we found that warm colors can be linked with rhythmical and high-frequency tactile stimuli that evoke arousing responses. Furthermore, cold colors can be linked with slow and low-frequency stimuli that evoke less arousing responses. Since most of the rainbow colors mapped onto positive or neutral regions along the pleasure-misery axis, pleasantness may not be effectively used to classify the colors. Nonetheless, purple can be associated with unpleasant stimuli, namely strong and fine frictional stimuli such as S and N. Because the number of participants was small, we cannot conclusively propose associations between color and tactile stimuli; however, this study highlighted that such associations may exist.

Acknowledgements This study was in part supported by JSPS Kakenhi (15H-05923) and SCOPE (142106003).

References

1. Tinker, M.A.: Effect of stimulus-texture upon apparent warmth and affective value of colors. *Am. J. Psychol.* **51**, 532–535 (1938)
2. Wright, B.: The influence of hue, lightness, and saturation on apparent warmth and weight. *Am. J. Psychol.* **75**, 232–241 (1962)
3. Ho, H.-N., Van Doorn, G.H., Kawabe, T., Watanabe, J., Spence, C.: Colour-temperature correspondences: when reactions to thermal stimuli are influenced by colour. *PLoS One* **9**(3) (2014)
4. Ludwig, V.U., Simner, J.: What colour does that feel? Tactile visual mapping and the development of crossmodality. *Cortex* **49**, 1089–1099 (2013)
5. Asano, Shuhei, Okamoto, Shogo, Yamada, Yoji: Toward quality texture display: vibrotactile stimuli to modify material roughness sensations. *Adv. Robot.* **28**(16), 1079–1089 (2014)
6. Ou, L.-C., Luo, R., Woodcock, A., Wright, A.: A study of colour emotion and colour preference. Part I. Colour emotions for single colours. *Color Res. Appl.* **29**, 232–240 (2004)
7. Schneider, O.S., Seifi, H., Kashani, S., Chun, M., MacLean, K.E.: Hapturk: crowdsourcing affective ratings for vibrotactile icons. In: *Proceedings of ACM CHI Conference on Human Factors in Computing Systems*, pp. 3248–3260 (2016)
8. Russell, J.A.: A circumplex model of affect. *J. Personal. Soc. Psychol.* **39**(6), 1161–1178 (1980)
9. Ito, K., Okamoto, S., Elfekey, H., Yamada, Y.: High-quality texture displays: the use of vibrotactile and variable-friction stimuli in conjunction. In: *Proceedings of AsiaHaptics*. Springer (2016)

Part II
Tactile Devices for Skin Sensation

3DOF Multitouch Haptic Interface with Movable Touchscreen

Shun Takanaka, Hiroaki Yano and Hiroo Iwata

Abstract This paper reports on the development of a multitouch haptic interface equipped with a movable touchscreen. When the relative position of two of a user's fingertips is fixed on a touchscreen, the fingers can be considered a hand-shaped rigid object. In such situations, a reaction force can be exerted on each finger using a three degrees of freedom (3DOF) haptic interface. In this study, a prototype 3DOF haptic interface system comprising a touchscreen, a 6-axis force sensor, an X-Y stage, and a capstan drive system was developed. The developed system estimates the input force from fingers using sensor data and each finger's position. Further, the system generates reaction forces from virtual objects to the user's fingertips by controlling the static frictional force between each of the user's fingertips and the screen. The system enables users to perceive the shape of two-dimensional virtual objects displayed on the screen and translate/rotate them with their fingers. Moreover, users can deform elastic virtual objects, and feel their rigidity.

Keywords Virtual reality · Haptic interface · Shearing force · Multitouch

1 Introduction

In daily life, we touch real objects with our fingers, and perceive their properties such as shape and rigidity. Further, by moving such objects, rotating them, and deforming them, we achieve a task goal. Touch panel interfaces are widely spreading as a tool for handling virtual objects on the screen in a real-world manner. However, while we can access information intuitively with these interfaces, pointing to a specific place on the screen precisely and perceiving the properties of the information is difficult because the information is hidden by the user's finger. The incorporation of haptic information can be useful in overcoming this issue. In particular, multi-finger interaction with haptic sensation is effective because we not

S. Takanaka (✉) · H. Yano · H. Iwata
University of Tsukuba 1-1-1, Tennodai, Tsukuba, Ibaraki 305-8577, Japan
e-mail: takanaka@vrlab.esys.tsukuba.ac.jp

only trace objects' surfaces, but also move and rotate them intuitively with our bare fingers. Moreover, it is preferable to handle virtual objects that have various sizes with bare fingers.

Various touch panel interfaces with haptic sensation have been developed. For example, Nakamura and Yamamoto [1] developed an electrostatic passive haptic interface. By using transparent electrostatic devices and controlling their electrostatic friction, users can touch virtual objects on the screen with multi-fingers. On the other hand, because users have to touch the display through devices, the user cannot touch the screen directly. Norieda and Sato [2] and Roudaut et al. [3] developed haptic touchscreens with equipment attached to the screens. However, although their developed touchscreens can generate an active reaction force to the bare hand from a virtual environment, users cannot push or drag a virtual object from one end to the other end of the screen in one movement. Moreover, it is difficult to generate haptic sensation on some fingertips using their proposed mechanisms. Further, because their systems only display a virtual space the same size as the screen, users can only touch virtual objects that are smaller than the screen. Sinclair et al. [4] developed TouchMover 2.0, which can generate a reaction force from 3D virtual objects in a single dimension perpendicular to the screen plane; it cannot generate a reaction force in the in-plane direction. Roudaut et al. [3] also developed longRangeOuija, a moving-display system that can generate a reaction force to only one fingertip in the in-plane direction via the screen. It is clear that no moving-display system can generate a reaction force to several fingertips via the screen.

If we assume that the relative position of the fingertips is fixed on a touchscreen, the fingers can be considered a hand-shaped rigid object, as shown in Fig. 1. In such situations, the operation of a virtual object with multi-fingers can be simplified, and movement of the hand-shaped rigid object in translational and rotational directions can be controlled by using a three degrees of freedom (3DOF) haptic interface.

In this study, we developed a haptic interface system with 3DOF actuators. When the fingers encounter virtual objects, the system generates a reaction force to the fingertips via the screen by controlling the velocity of the screen. A prototype

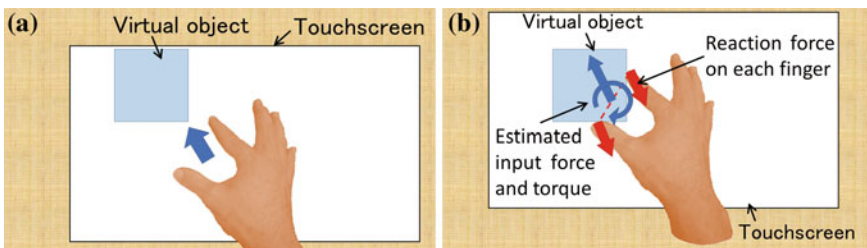


Fig. 1 System concept. **a** When the hand moves toward a virtual object, the touchscreen moves with the fingers. **b** When the fingers hit an object, the screen moves backward and a reaction force is exerted on each finger

system was implemented and its effectiveness evaluated through a performance evaluation experiment.

2 System Configuration

2.1 Hardware Configuration

The prototype system was constructed using an X-Y stage, a capstan drive system, a 6-axis force sensor (PFS055YA251U6, Leptrino Inc.), and a touchscreen (Surface Pro2, Microsoft), as shown in Figs. 2 and 3. The applied forces from a user's fingertips are measured with a force sensor placed under the center of the screen, so as to detect the shearing force applied by the user on the screen. The touchscreen is placed on top of this system and detects the positions of the fingers on the screen. An image of the virtual environment based on the position of the screen in the real world is displayed on the screen. The image of an object on the screen remains stationary in the real world until the user exerts a shearing force on the object. When the user touches a virtual object with his/her bare hand on the screen, a reaction force is generated by controlling the velocity of the end effector of the X-Y stage and the angle of the touchscreen. When the user touches the screen, but touches no virtual object, the screen moves along with the user's fingers. The three actuators used to move the touchscreen are MSMD5AZP1S, made by Panasonic. The sliders of the X-Y stage are RCS2-SA7C-N-8-200-SP, made by IAI, and can

Fig. 2 System configuration

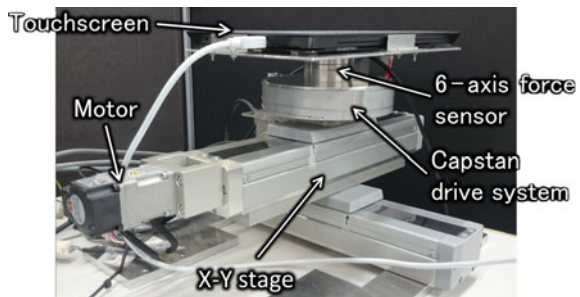


Fig. 3 Overview of the prototype system



move over a range of approximately 206 mm, respectively. The prototype system is an admittance haptic interface that is usually controlled using motion equations in torque control mode. However, we controlled the actuators simply by using the velocity control mode, because it is difficult to control actuators stably with the touch sensor and Windows 7, which both have a low update frequency. In addition, the maximum static frictional force on each finger is approximately 15 N, as the velocity of the touchscreen is zero. In the case where the intensity of the shearing force of a finger is more than 15 N, the finger is likely to have slipped, and it becomes difficult to control the intensity. Therefore, a gel sheet with slightly higher static friction is attached to the screen to fix the relative position of the user's fingertips. However, the user can change hand posture by touching a different place on the screen again, because the user's fingers are not fixed on the screen.

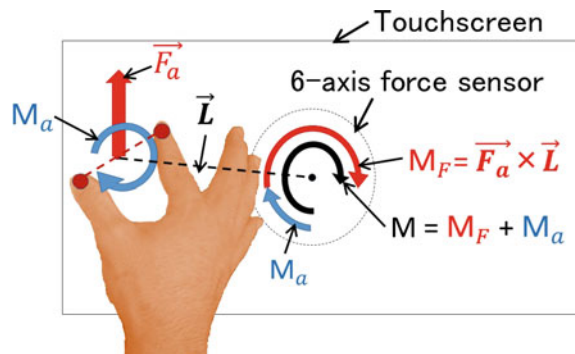
2.2 Software Configuration

Because the force sensor and actuators are situated under the center of the screen, the basic software calculates the applied force and the moment from the fingers, and controls the velocity of each motor. From these pieces of information, the input and output force of each finger can be measured and controlled.

To calculate the force and moment, when a force is exerted on the screen through two of the user's fingertips, the translational force on the screen, F_a , is equal to the translational force F measured by the force sensor. In addition, the moment M_a is calculated using the moment M measured by the force sensor, F_a , and the vector L , which is the displacement of the midpoint of the fingers from the center of the screen, as shown in Fig. 4.

In addition, a translational velocity ∇ and the angular velocity of the screen, ω , are controlled using the X-Y stage and the capstan drive system. To generate an angular velocity at the midpoint of the fingers on the screen, ω_f , the screen's angular velocity ω is set to ω_f . Moreover, to generate the translational velocity of a

Fig. 4 Estimated moment from the user's fingers



finger or the midpoint of fingers on the screen, $\overrightarrow{V_f}$, not only the translational velocity but also the angular velocity ω_f should be considered, because the finger/midpoint of the fingers must be maintained when the angular velocity ω_f is nonzero, and the translational velocity $\overrightarrow{V_f}$ is zero. The translational velocity ∇ is calculated as follows:

$$\omega = \omega_f \quad (1)$$

$$\nabla = \overrightarrow{V_f} + \mathcal{L} \cdot \omega_f \quad (2)$$

3 Haptic Rendering Method

To calculate the direction and magnitude of the reaction force at the finger/midpoint of the fingertips, the resultant forces of the force applied by the user and the force exerted by the screen are considered. The translational velocity $\overrightarrow{V_f}$ and angular velocity ω_f of the fingers are controlled using the X-Y stage and capstan drive system to generate a reaction force on each finger.

By moving the screen in the direction of the user's intention, the static frictional forces exerted on the fingertips can be relieved and the fingers can move freely in the virtual environment. The finger/midpoint of the fingers moves with translational velocity $\overrightarrow{V_f}$ and angular velocity ω_f in the case where no virtual object is being touched as follows:

$$\overrightarrow{V_f} = C * \overrightarrow{F_a} \quad (3)$$

$$\omega_f = C_R * M_a \quad (4)$$

where C and C_R signify the constant of proportionality.

In the case where a virtual object is being touched with one finger, the screen moves along with translational velocity $\overrightarrow{V_f}$ to present the reaction force $\overrightarrow{F_r}$ on the fingertip. This force is calculated based on some properties of the virtual object such as rigidity, friction, and weight.

$$\overrightarrow{V_f} = C * (\overrightarrow{F_a} - \overrightarrow{F_r}) \quad (5)$$

Further, in the case where the virtual object is being touched with two fingers, the screen is moved based on Eq. (5), and rotated around the midpoint of the fingers, as depicted in Fig. 5, using reaction moment M_r caused by $\overrightarrow{F_r}$.

$$\omega_f = C_R * (M_a - M_r) \quad (6)$$

Thus, by controlling the velocity of the screen based on Eqs. (1), (2), (5), and (6), users can feel a reaction force/reaction forces while touching the virtual object.

4 Evaluation Using an Elastic Virtual Object

In previous study [5], we confirmed that our system can present rigid virtual objects. Hence, in this study, we conducted our evaluation test with an elastic virtual object. Specifically, we generated a reaction force from a virtual elastic object containing a virtual rigid cylinder under the surface, as shown in Fig. 5 (left). The virtual object was created to imitate a palpation as in the case when a bone at the back of the hand is touched. The elastic object was defined as a polygon model. Each vertex of each polygon was connected with a spring and damper to each other. In addition, each vertex was connected to the initial position of each vertex with a spring and damper. The object could be deformed by a subject, but was restored, if it remained untouched.

In this experiment, a subject touched the object with his index finger (finger 1) and middle finger (finger 2) using the system. Figure 6 shows a typical example of the time series variation of the reaction force of the two fingers when the subject touched the virtual object from his body, as shown in the Fig. 5 (right). The fingers touched the object's surface at time t1. The reaction force exerted on each fingertip increased gradually after time t1 because the fingers pushed the virtual elastic object. Then, the reaction force increased rapidly after time t2 and t4, respectively, because each finger encountered the virtual rigid cylinder, and exerted a strong force to go over the rigid object. Furthermore, the reaction force decreased at time t3 and t5, respectively, because each finger was completely over the virtual cylinder. Subsequently, because the subject continued to deform the object, each reaction force continued to increase. The actual reaction force of each finger was not equal to each target reaction force calculated based on input force, position of each finger, and the properties of the virtual object because the subject continued to

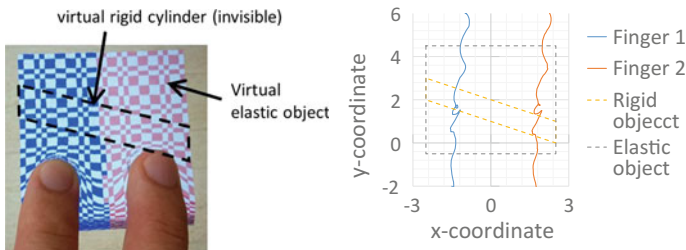


Fig. 5 Overview of the virtual object (left), and trajectories of two fingers (right)

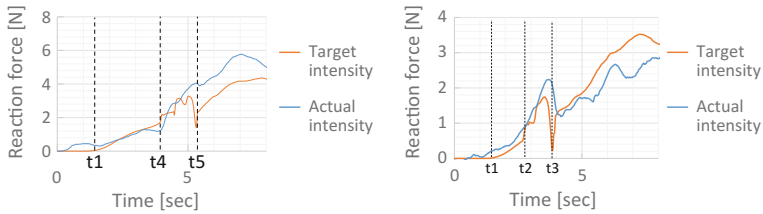


Fig. 6 Time series variation of the force of finger 1 (*left figure*) and that of finger 2 (*right figure*) while touching the virtual object

twist his hand strongly despite going over the rigid object at that time. From the results, we confirmed that the system can generate a reaction force from the virtual object on each fingertip.

5 Conclusion

This paper reported on the development of a visual-haptic interface system. The developed system enables users to feel a haptic sensation from rigid and elastic virtual objects on the fingertips by moving the screen with three actuators. The developed system can be applied to shape design tasks such as intuitive deformation, cutting, and assembly. Moreover, it can be applied in the field of medical training. For example, a user can perceive the stiffness of a virtual organ displayed on the screen by touching it with palpation-like movements, and simulate the surgery. In addition, this system can present horizontal vibration; thus, it can be used to present some texture of virtual objects. We plan to implement such sensations in addition to the reaction force.

References

1. Nakamura, T., Yamamoto, A.: Multi-finger electrostatic passive haptic feedback on a visual display. In: Proceeding of World Haptics Conference 2013, pp. 37–42. IEEE (2013)
2. Norieda, S., Sato, M.: A new haptic touch panel display with optimum control approach. In: Proceedings of IPSJ Interaction 2012 (2012)
3. Roudaut, A., Rau, A., Sterz, C., Plauth, M., Lopes, P., Baudisch, P.: Gesture output: eyes-free output using a force feedback touch surface. In: Proceedings of CHI 2013 (2013)
4. Sinclair, M., Pahud, M., Benko, H.: TouchMover 2.0 - 3D touchscreen with force feedback and haptic texture. In: Proceedings of Haptics Symposium 2014 (2014)
5. Takanaka, S., Yano, H., Iwata, H.: Multitouch haptic interface with movable touch screen. In: Proceedings of SIGGRAPH Asia 2015 (2015)

A Novel 3RRS Wearable Fingertip Cutaneous Device for Virtual Interaction

Francesco Chinello, Claudio Pacchierotti, Monica Malvezzi
and Domenico Prattichizzo

Abstract We present a novel 3RRS wearable fingertip device. It is composed of a static upper body and a mobile end-effector. The upper body is located on the nail side of the finger, supporting three small servo motors, and the mobile end-effector is in contact with the finger pulp. The two parts are connected by three articulated legs, actuated by the motors. The end-effector can move toward the users fingertip and rotate it to simulate contacts with arbitrarily-oriented surfaces. Moreover, a vibrotactile motor placed below the end-effector conveys vibrations to the fingertip. The axes of the two revolute joints of each leg are parallel, so that it constitutes a 2-DoF planar articulated mechanism, constraining the motion of the center of each spherical joint on a plane fixed with respect to the upper body. The mobile end-effector has therefore 3-DoF with respect to the body. The proposed device weights 25 g for 355048 mm dimensions.

Keywords Haptic interfaces · Wearable haptics · Cutaneous devices · Fingertip devices

1 Introduction

Wearable haptic devices are recently gaining great popularity among researchers. Such interfaces will indeed enable natural forms of communication between the wearer and the environment. Humans will be free to move and interact with the surrounding world while being provided with rich and unobtrusive haptic information.

In this respect, fingertip cutaneous technologies have shown promising results. Prattichizzo et al. [5] presented a wearable cable-driven 3-degrees-of-freedom (3-DoF) cutaneous device for the fingertip. It consists of two parts: one is located on the back of the fingertip, supporting three DC motors, and the other one is placed

F. Chinello (✉) · C. Pacchierotti · M. Malvezzi · D. Prattichizzo
Department of Information Engineering and Mathematics, University of Siena, Siena, Italy
e-mail: francesco.chinello@iit.it

F. Chinello · C. Pacchierotti · M. Malvezzi · D. Prattichizzo
Department of Advanced Robotics, Istituto Italiano di Tecnologia, Genova, Italy

in contact with the volar surface of the fingertip. The two parts are connected by three cables, actuated by the motors. The mobile platform can press into the user's fingertip and re-angle to simulate contacts with slanted surfaces. Three force sensors placed on the platform measure the contact force at the fingertip. The maximum force applicable is 1.5 N and the device weights as little as 30 g.

More recently, Tsetserukou et al. [7] presented a 2-DoF wearable fingertip display composed of a five-bar linkage system. Two DC motors, placed on the back of the finger, actuate the linkage mechanism. When the two motors spin in the same direction, the linkage system applies shear stimuli at the finger pulp; when the two motors spin in different directions, the linkage system applies normal stimuli at the finger pulp.

2 3RRS Wearable Device

This paper presents a novel 3RRS wearable fingertip device. It is composed of a static upper body and a mobile end-effector. The upper body (F in Fig. 1) is located on the nail side of the finger, supporting three small servo motors (C), and the mobile end-effector (E) is in contact with the finger pulp. The two parts are connected by three articulated legs (A), actuated by the motors. The end-effector can move toward the user's fingertip and rotate it to simulate contacts with arbitrarily-oriented surfaces. A piezoresistive sensor (D) can also measure the force applied by the mobile platform to the fingertip. Finally, a clamp (B) enables the user to easily fasten the device on the finger.

Each leg, connecting the end-effector to the upper body, is composed of two rigid links connected to each other, the body, and the end-effector, according to a RRS (Revolute-Revolute-Spherical) kinematic chain.

Specifically, three spherical (S) joints connect the distal links of the legs to the end-effector, one revolute (R) joint connects the distal and proximal links of each leg, and another revolute (R) joint connects the proximal link of each leg to the body. The three revolute joints between the proximal links and the body are actuated by the servo motors. In each leg, the axes of the two revolute joints are parallel, so that it constitutes a 2-DoF planar articulated mechanism, constraining the motion of

Fig. 1 The 3RRS thimble

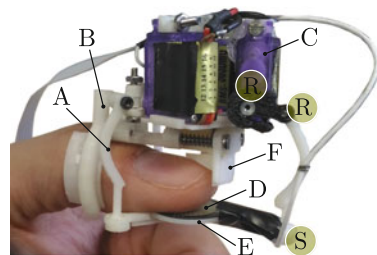


Table 1 3RRS thimble features

| | |
|-----------------------|----------------|
| Controller | Atmega 328 |
| Power | 4.8–6.0 V |
| Roll range | $\pm 25^\circ$ |
| Pitch range | $\pm 25^\circ$ |
| Vertical displacement | 15 mm |
| Normal force | Up to 24 N |

the center of each spherical joint on a plane fixed w.r.t. the body. The mobile end-effector has therefore 3-DoF w.r.t. the body. The proposed device weights 25 g for $35 \times 50 \times 48$ mm dimensions. A preliminary version was presented in [1].

With respect to the cable-driven fingertip devices presented in [2–6], this device solves the indeterminacy due to the underactuation of the platform.

This mechanical structure decouples position and force control problems, simplifying the control structure with respect to the solution proposed in [5].

The operative parameters of our device are summarized in Table 1.

Acknowledgements The research has received founding from European Union’s Horizon 2020 Research and Innovation Programme, Grant Agreement No. 688857 (SoftPro) and from the European Union Seventh Framework Programme FP7/2007–2013, Grant Agreement No. 601165 (WEARHAP).

References

1. Chinello, F., Malvezzi, M., Pacchierotti, C., Prattichizzo, D.: Design and development of a 3rrs wearable fingertip cutaneous device. In: Proceedings of IEEE/ASME International Conference on Advanced Intelligent Mechatronics. pp. 293–298 (2015)
2. Meli, L., Scheggi, S., Pacchierotti, C., Prattichizzo, D.: Wearable haptics and hand tracking via an rgb-d camera for immersive tactile experiences. In: Proceedings of ACM Special Interest Group on Computer Graphics and Interactive Techniques Conference (2014)
3. Pacchierotti, C., Meli, L., Chinello, F., Malvezzi, M., Prattichizzo, D.: Cutaneous haptic feedback to ensure the stability of robotic teleoperation systems. *Int. J. Robot. Res.* (2015) (In Press)
4. Pacchierotti, C., Prattichizzo, D., Kuchenbecker, K.J.: Cutaneous feedback of fingertip deformation and vibration for palpation in robotic surgery. *IEEE Trans. Biomed. Eng.* **63**, 278–287 (2016)
5. Prattichizzo, D., Chinello, F., Pacchierotti, C., Malvezzi, M.: Towards wearability in fingertip haptics: a 3-dof wearable device for cutaneous force feedback. *IEEE Trans. Haptics* **6**(4), 506–516 (2013)
6. Prattichizzo, D., Pacchierotti, C., Rosati, G.: Cutaneous force feedback as a sensory subtraction technique in haptics. *IEEE Trans. Haptics* **5**(4), 289–300 (2012)
7. Tsetserukou, D., Hosokawa, S., Terashima, K.: Linktouch: a wearable haptic device with five-bar linkage mechanism for presentation of two-dof force feedback at the fingerpad. In: Proceedings of IEEE Haptics Symposium (HAPTICS), pp. 307–312 (2014)

Thermal-Radiation-Based Haptic Display—Calibration and Shape Display

Satoshi Saga

Abstract When a human places his hands over a source of heat, his hands become warm owing to thermal radiation. In this research, we employ spatially controlled thermal radiation to display a virtual shape. At a temperature near the nociceptive temperature, a person will tend to avoid a heated region. Using this space, our proposed system displays the virtual shape-like region. In this paper, we describe the proposed radiation system and calibration method.

Keywords Thermal radiation · Haptic display · Calibration

1 Introduction

In recent years, touchscreen interfaces have become popular worldwide. As the distribution of smartphones, expectation for tactile/haptic technology increases. However, haptic based deformable interaction against object are very much limited to complex haptic devices.

Haptic interaction with objects, e.g. sculpting with clay, is a fundamental creative activity. However, haptic display in mid-air will realize unconstrained creative interaction with a virtual object. For example, Hoshi et al. and Long et al. [1, 2] employed an ultrasonic phased array to produce responsive force feedback in mid-air.

Here we propose another method to realize haptic-like display system in mid-air by employing thermal-radiation. Thermal radiation transfers heat in mid-air. By controlling this radiation, we can use heat to display a nociceptive spatial region to a user (Fig. 1 (Left)).

S. Saga (✉)

Faculty of Engineering, Information and Systems, University of Tsukuba,

Tennodai 1-1-1, Tsukuba, Japan

e-mail: saga@saga-lab.org

URL: <http://saga-lab.org/>

© Springer Nature Singapore Pte Ltd. 2018

S. Hasegawa et al. (eds.), *Haptic Interaction*, Lecture Notes

in Electrical Engineering 432, DOI 10.1007/978-981-10-4157-0_11

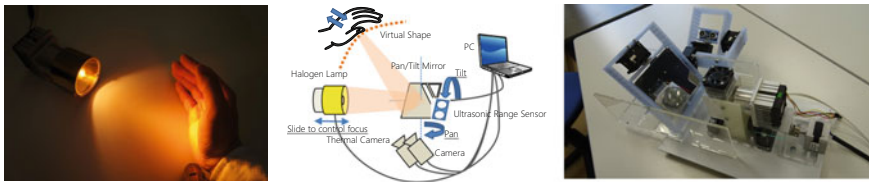


Fig. 1 *Left* Concept image of HeatHapt, *Center* Thermal radiation system, *Right* New system overview, the system is constructed with precise servo motors to calibrate optical systems

2 Calibration Method of Thermal Radiation System

The proposed system has several rotation and image centers, such as an infrared light source, infrared camera center, and ultrasonic emitter/sensor. Thus we have to calibrate the positional relation of the coordinate system precisely (Fig. 1 (Center)).

To evaluate the transformation matrix between the stereo cameras, we have to get several corresponding points on the projected plane [3].

$$\mathbf{m}_c \propto \mathbf{K}_c [\mathbf{R}_{ps} | \mathbf{t}_{ps}] \mathbf{M} \quad (1)$$

$$\propto \mathbf{K}_c [\mathbf{R}_{ps} | \mathbf{t}_{ps}] \mathbf{R}_{cp} \mathbf{K}_p^{-1} \mathbf{m}_p \quad (2)$$

Here, \mathbf{M} is a three dimensional position vector of feature point, \mathbf{m} is a two dimensional position vector which is an intersection of \mathbf{M} and a screen, \mathbf{K} means an internal parameter of a camera, \mathbf{R} and \mathbf{t} is a rotation matrix and translation vector. Each notation, \mathbf{c} , \mathbf{p} and \mathbf{s} , means a coordination of camera, projector (lamp) and screen.

3 Construction of New System

Next, we reconstructed the system to employ precise calibration with the abovementioned method. We employ Dynamixel RX-24F to control several angles precisely. Figure 1 (Right) shows the overview of the new system.

3.1 Calibration Between Light Source and Thermal Camera

With the constructed system we held a calibration with computer vision-based method. First, we scanned the gimbal mirror and projected the light to the screen which is in front of the system. By capturing the scanning thermal images on the screen, we acquired lattice points of the pattern (Fig. 2 (Left)). By employing the lattice points and calculated projection pattern described below, we calibrated the

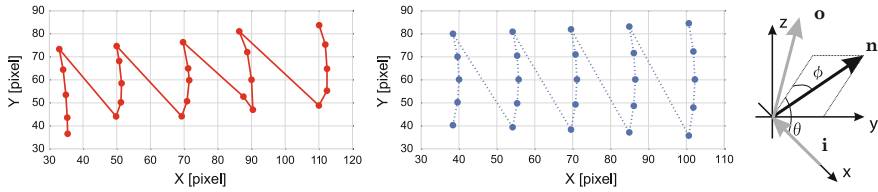


Fig. 2 *Left* Measured lattice, *Center* Projected lattice, *Right* Mirror projection system

position between the thermal camera and the rotating mirror from “SolvePnP” function in OpenCV.

This time we used calculated projection pattern. Normally, the “SolvePnP” function requires squared checker pattern data with the actual size. In our system, the rotation of the mirror creates the distorted checker pattern. Thus we use calculated checker pattern as input by considering the mirror projection system (Fig. 2 (Right), Eq. 4). The acquired projection pattern is shown in Fig. 2 (Center).

$$\mathbf{n} = \begin{pmatrix} \cos \theta \cos \phi \\ \sin \phi \\ \cos \theta \sin \phi \end{pmatrix} \quad (3)$$

$$\mathbf{o} = 2(\mathbf{n} \cdot \mathbf{i})\mathbf{n} - \mathbf{i} \quad (4)$$

4 Conclusion

In this paper, we proposed novel haptic display, which employs thermal sensation characteristic of human and thermal radiation. We described the calibration method of the system by employing stereo vision technique. Further, we calibrated the projection system with the proposed method, and confirmed the method can calculate the relative position and rotation information between thermal camera and light source. In the near future we plan to hold another experiment with precise thermal controlled system, and reveal the better control method to display haptic information with thermal radiation.

Acknowledgements This work was partly supported by JSPS KAKENHI Grant Number 16K00265 (Grant-in-Aid for Scientific Research (C)) and 16H02853 (Grant-in-Aid for Scientific Research (B)).

References

1. Hoshi, T., Takahashi, M., Iwamoto, T., Shinoda, H.: Noncontact tactile display based on radiation pressure of airborne ultrasound. *IEEE Trans. Haptics* **3**(3), 155–165 (2010)
2. Long, B., Seah, S.A., Carter, T., Subramanian, S.: Rendering volumetric haptic shapes in mid-air using ultrasound. *ACM Trans. Graph.* **33**(6), 181:1–181:10 (2014)
3. Zhang, Z.: A flexible new technique for camera calibration. *IEEE Trans. Pattern Anal. Mach. Intell.* **22**(11), 1330–1334 (2000)

Touching 2D Images Using Haptogram System

Georgios Korres and Mohamad Eid

Abstract In this paper, we demonstrate a system to render point-cloud tactile interaction with an aerial still image using a two-dimensional array of ultrasound transducers. The novelty in this demonstration is the ability to control the intensity of the tactile stimulation. The holographic display projects a 2-D image with vertical bars of different colors. Each color corresponds to different intensity of tactile stimulation. The 2-D image pixels are represented as a point-cloud of focal points where the ultrasound array switches between these focal points.

Keywords Ultrasound tactile stimulation · Aerial imaging · Multimodal display

1 Introduction

Aerial imaging is a recent technology that enables displaying 2-D image in mid-air so users can freely interact with it [1]. An LCD display generates an original image, which is then beamed onto an Aerial Imaging Plate (AIP) that reflects the original image into a floating one. Additionally, a two-dimensional array of ultrasound transducers generates perceivable acoustic pressure in mid-air [2, 3]. These two technologies are integrated to create touchable floating images.

G. Korres · M. Eid (✉)

Applied Interactive Multimedia Research Laboratory (AIMlab),
New York University Abu Dhabi, Abu Dhabi, United Arab Emirates
e-mail: mohamad.eid@nyu.edu
URL: <http://wp.nyu.edu/aimlab>

G. Korres
e-mail: george.korres@nyu.edu

2 Demonstration Setup

The demonstration setup is shown in Fig. 1. It consists of three components: a mid-air visual display, an ultrasonic tactile display, and a hand tracker. The mid-air visual display consists of a visual screen located underneath an Aerial Imaging (AI) mirror at 45° so that a floating 2-D image can be displayed on top of the screen. The ultrasound tactile display is a one-tile of the Haptogram system with 10 × 10 ultrasound transducers [4]. The hand tracking device is the commercially available LEAP motion sensor [5]. A link to the demonstration is available here: https://www.youtube.com/watch?v=VwCoM0_h5kE.

Although the concept of an ultrasound array coupled with an Aerial Imaging Display has been previously discussed [6], the Haptogram system extends the concept by controlling the intensity of the focal point. As shown in Fig. 2, the 2-D image pixels are mapped into focal points with corresponding intensities (in this case high intensity for violet and low intensity for green). The Haptogram system controls the acoustic pressure of the focal point in two ways; (1) with pulse width modulation of

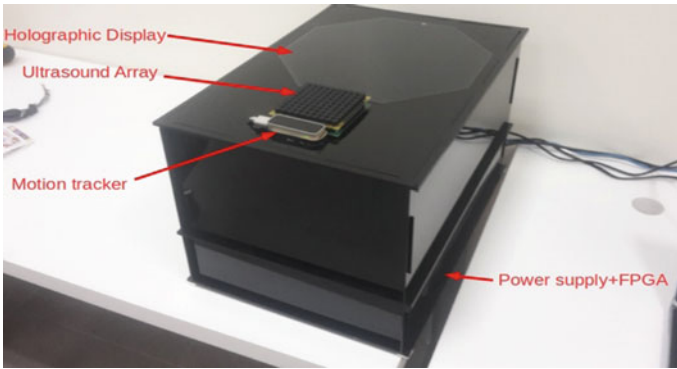


Fig. 1 Haptogram demonstration

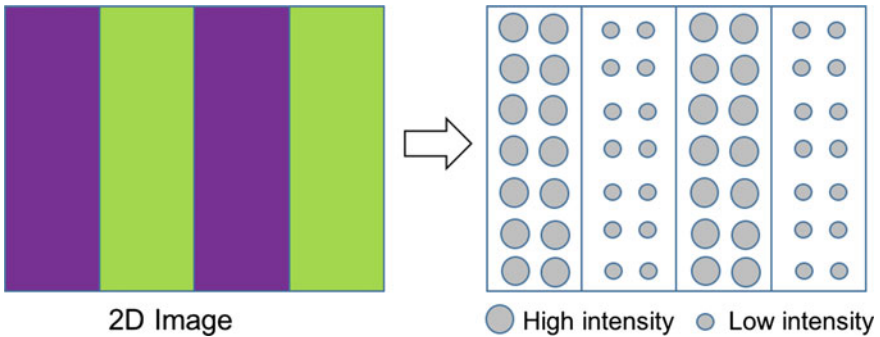


Fig. 2 Controlling stimulation intensity

the transducers' driving signal, and (2) by controlling the modulation frequency of the carrier signal that moderates the perceived intensity of the pressure.

3 Conclusion

In this paper, we present a touchable mid-air 2-D display using focused ultrasound to generate a tactile stimulation and an AI mirror to display holographic 2-D image. Future work includes combining two AI mirrors to provide a full 3-D visual display and using the Haptogram system to display a 3-D tactile object to create a touchable avatar. A potential application scenario is in-car control where a touchable 2-D aerial display could provide the drivers with additional cues so that they can interact with the aerial touch screen as a secondary task (primary task being driving). Other applications include interaction in public restrooms or building secure touch pads.

References

1. Asukanet: Aerial Imagine Displays. <http://www.asukanet.co.jp/> (2008). Accessed 7 July 2016
2. Inoue, S., Makino, Y., Shinoda, H.: Active touch perception produced by airborne ultrasonic haptic hologram. In: World Haptics Conference (WHC), 2015 IEEE, pp. 362–367. IEEE (2015)
3. Long, B., Seah, S.A., Carter, T., Subramanian, S.: Rendering volumetric haptic shapes in mid-air using ultrasound. *ACM Trans. Graph. (TOG)* **33**(6), 181 (2014)
4. Korres, G., Eid, M.: Haptogram: ultrasonic point-cloud tactile stimulation. *IEEE Access* (99), 1–1 (2016)
5. LEAP official website. <http://www.leap.com> (2008). Accessed 7 July 2016
6. Monnai, Y., Hasegawa, K., Fujiwara, M., Yoshino, K., Inoue, S., Shinoda, H.: Haptomime: mid-air haptic interaction with a floating virtual screen. In: Proceedings of the 27th Annual ACM Symposium on User Interface Software and Technology, pp. 663–667. ACM (2014)

Hybrid Haptic Texture Rendering Using Kinesthetic and Vibrotactile Feedback

Sunghwan Shin and Seungmoon Choi

Abstract We present a hybrid haptic texture rendering framework for inhomogeneous texture with high realism. The micro-geometry of a real texture sample is captured using photometric stereo and then rendered using a force feedback device. The vibrational response of the texture is expressed using a neural network-based data-driven model and re-created using a vibration actuator. The former represents the position-dependent geometric property while the latter delivers the invariant aspects including material properties. Our hybrid texture rendering system can improve the realism of virtual haptic texture rendering considerably, although formal verification awaits.

Keywords Haptic texture · Rendering · Photometric stereo · Data-driven model · Inhomogeneous · Synthesis

1 Introduction

Haptic texture is an indispensable haptic property that results from every physical interaction occurring in our daily life. As such, delivering realistic surface texture is one of the most important topics in haptics. Since the very first pioneering Sandpaper system [1], many haptic rendering algorithms and systems have been published. Among them, one notable approach is to use data-driven models to synthesize the textural response in terms of contact acceleration [2–4]. These methods aim to reproduce the vibrational stimulus that occurs in the physical interaction with a real textured surface, and their effectiveness has been well demonstrated for homogeneous texture.

However, it is not straightforward to extend acceleration-based data-driven methods for application to inhomogeneous texture where the texture property depends on

S. Shin (✉) · S. Choi
Pohang University of Science and Technology (POSTECH), Pohang, Republic of Korea
e-mail: scaut11@postech.ac.kr

contact position. In this case, contact acceleration data must be collected and modeled locally at every position, or at least a very dense array of surface points. This implies that an exponentially increasing amount of data is required for modeling.

To solve this problem, we present a hybrid texture rendering method that combines force and vibration feedback both in a data-driven fashion to represent real textured surfaces. Our framework is in agreement with the duplex theory of tactile texture perception [5] tactile texture perception is mediated by vibrational cues for fine texture and by spatial cues for coarse texture. We provide vibration feedback using a neural network-based data-driven model [4], which generates a contact acceleration profile of similar spectral content to the fine textural property of a real sample that is uniform over the surface. Simultaneously, a high-accuracy geometry model of the texture is captured using photometric geometry [6, 7], and corresponding kinesthetic feedback expressing local textural features is also rendered in order to handle the inhomogeneity of the texture. By combining the two texture models, we aim to deliver more realistic and immersive virtual haptic texture to the user.

2 Rendering Hardware

We have augmented a force-feedback device with a voice-coil actuator to deliver both kinesthetic and vibrotactile cues to a user while the user is scanning the textured surface (Fig. 1). As a force-feedback device, Force Dimension Omega.3 is used owing

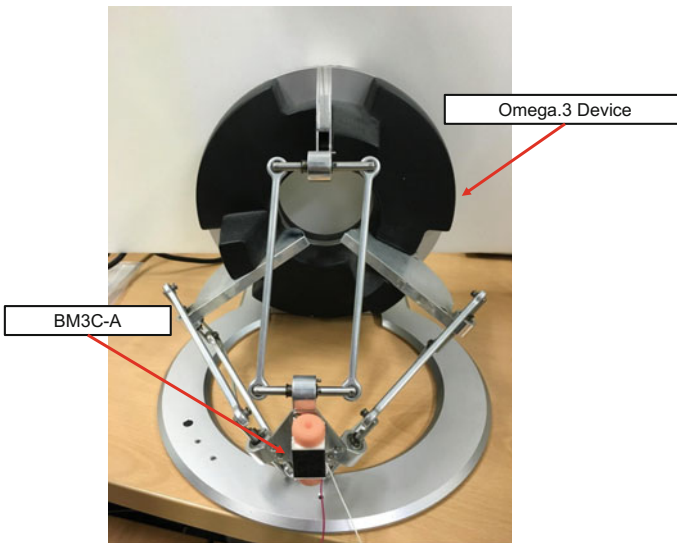


Fig. 1 Our rendering hardware setup. A voice-coil actuator (BM3C-A) is attached at the handle position of a force-feedback device (Omega.3)

to its high structural stiffness and spatial resolution. These features improve the rendering stability of our system, which is a problem in haptic texture rendering using a force-feedback device [8]. Since textural vibration has a wide-band spectrum, we use Haptuator BM3C-A by TactileLabs, Inc. This actuator has an almost flat amplitude response for the frequencies higher than 100 Hz and generates strong vibration sufficient for perception when the actuator is directly coupled to the Omega.3 device.

The tightly coupled structure of our rendering hardware changes the amplitude response of the voice-coil actuator since the relatively heavy force-feedback device acts as a physical inertia and damping component. To guarantee that our actuator always generates the vibration of desired amplitude, we designed a digital filter for the actuator. First, we identified the transfer function of the coupled system by driving the voice-coil actuator using a sinusoidal sweep wave as input and measuring the vibration output using an accelerometer. Then a digital filter was designed based on the inverse of the identified transfer function using MATLAB.

3 Texture Rendering

Our framework uses two texture models to render kinesthetic and vibrotactile feedback for virtual texture (Fig. 2).

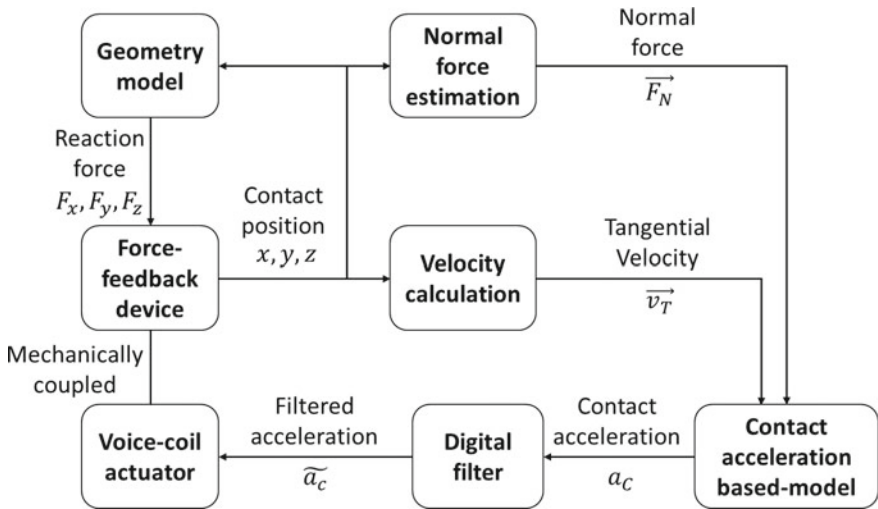


Fig. 2 A diagram of our rendering algorithm. Two texture models render kinesthetic and vibrotactile feedback simultaneously

3.1 Vibration Synthesis

For vibration synthesis, we adopt a data-driven texture rendering approach using contact acceleration data presented in [4]. This method is based on frequency-decomposed neural networks, and it showed comparable modeling accuracy for isotropic texture samples to the best available in the literature.

To produce an appropriate vibration signal to the user, our model requires the user’s scanning velocity and normal force as input variables. The scanning velocity can be directly measured from the force-feedback device. However, the normal force is not, so we estimate it using the penetration depth and the stiffness of a virtual surface on the basis of the force constancy theory (a user provides constant normal force to the surface during lateral scanning [9]). The synthesized signal is filtered and then played back via the voice-coil actuator.

3.2 Force Generation

In parallel, we construct the height map of a texture sample using photometric stereo [6] and calculate the reaction force using the height map for virtual texture rendering. Photometric stereo is an algorithm used in computer vision for estimating the surface normal of objects by taking multiple photos in different lighting conditions. We have designed a lighting apparatus for haptic texture modeling using photometric stereo and demonstrated successful modeling results [7]. Although prior image-based haptic texture modeling methods suffer from low modeling resolution and accuracy, our method using photometric stereo shows high resolution sufficient for modeling and rendering the micro-geometry of tactile texture.

Table 1 Force rendering algorithms used in our software

| | Force direction | Force magnitude |
|---|---|-----------------------------|
| A | $\perp f(x)$ | αd |
| B | $\perp g(x)$ | αd |
| C | $\perp f(x)$ $\parallel f(x)$ | αd $\nabla g(x)$ |
| D | Stick-slip state machine. A in stick, B in slip state | |
| E | Force shading algorithm | |

$f(x)$ nominal surface, $g(x)$ texture surface, d penetration depth

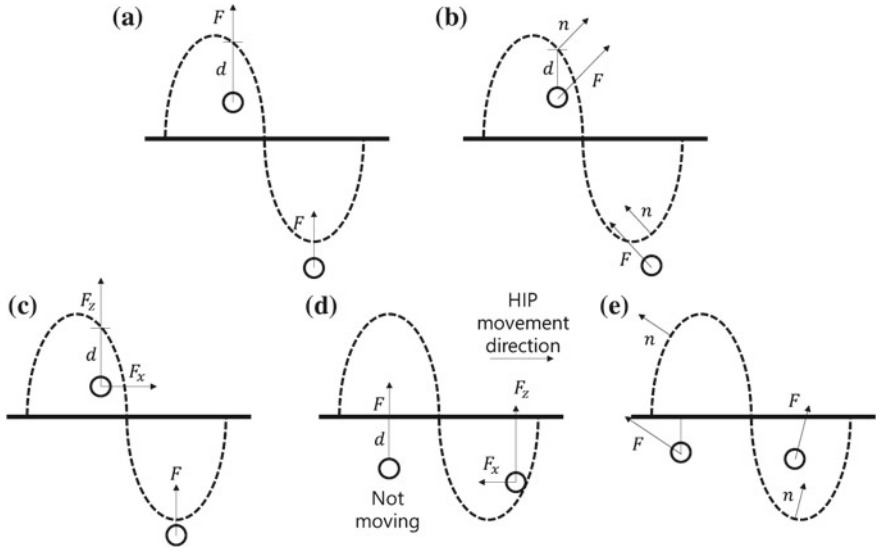


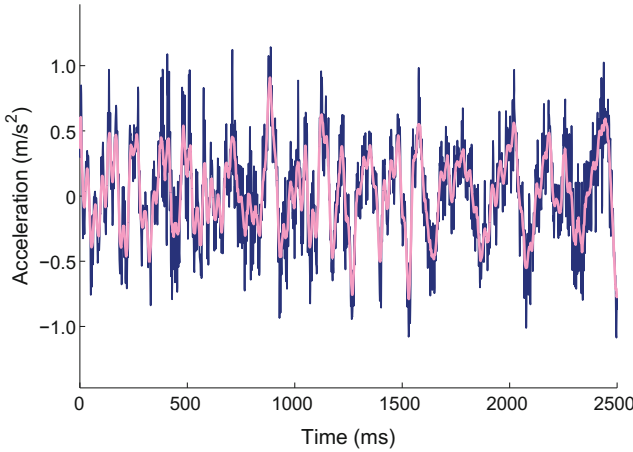
Fig. 3 Schematic diagrams of force rendering algorithms. *Circles* represent the position of the haptic tool in virtual space. *Thick straight lines* represent the nominal surface, and *dashed lines* show textured surfaces. More details on the algorithms are available in [10]

There are many different haptic texture algorithms when the texture model is given as a height map. Among them, we have chosen five methods to compare the effect of force rendering algorithm on perceived texture sensations. The five algorithms are summarized in Table 1 and Fig. 3. All the algorithms are implemented in our demo program, so the audience will be able to experience different sensations resulted from the rendering algorithm only.

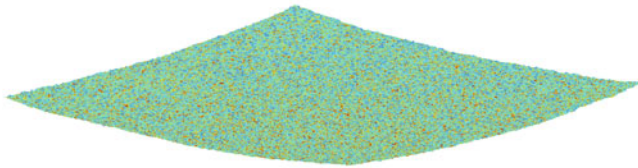
4 Results

In our demonstration, we provide a planar virtual haptic-textured surface to the user to feel using CHAI 3D and our rendering hardware. Figure 4 shows the examples of texture models in our framework. Now our program can render textures of four different materials (a sandpaper, a scrunched paper, a canvas, and a cork board). When rendering rough textures or inhomogeneous textures, our program gives more realistic texture sensations compared to the existing methods.

For future study, we will quantify the improvement in the realism of texture via user study. In the next step, a data-driven friction and visco-elastic model will be integrated into our hybrid texture model to provide holistic texture sensations to the user.



(a) Vibration generated from the data-driven model. Dark navy lines show the original results, and pale pink lines represent the smoothed results using a moving average filter.



(b) The geometry model of a sandpaper sample(color coded)

Fig. 4 The examples of texture models in our framework

Acknowledgements This work was supported in part by the Dual Use Technology Center Program funded by the Ministry of Trade, Industry and Energy and Defense Acquisition Program Administration (12-DU-EE-03), and the Pioneer Research Center Program through the National Research Foundation of Korea funded by the Ministry of Science, ICT and Future Planning (2011-0027994).

References

1. Minsky, M.: Computational Haptics: The Sandpaper System for Synthesizing Texture for a Force-Feedback Display. Massachusetts Institute of Technology (1995)
2. Romano, J., Kuchenbecker, K.: Creating realistic virtual textures from contact acceleration data. *IEEE Trans. Haptics* **5**(2), 109–119 (2012)
3. Culbertson, H., Unwin, J., Goodman, B., Kuchenbecker, K.: Generating haptic texture models from unconstrained tool-surface interactions. In: *IEEE World Haptics Conference*, pp. 295–300. IEEE Press, Korea (2013)
4. Shin, S., Osgouei, R.H., Kim, K.-D., Choi, S.: Data-driven modeling of isotropic haptic textures using frequency-decomposed neural networks. In: *IEEE World Haptics Conference*, pp. 131–138. IEEE Press, Chicago (2015)

5. Hollins, M., Risner, S.: Evidence for the duplex theory of tactile texture perception. *Percept. Psychophys.* **62**(4), 695–705 (2000)
6. Paterson, J., Claus, D., Fitzgibbon, A.: BRDF and geometry capture from extended inhomogeneous samples using flash photography. *Comput. Graph. Forum* **24**(3), 383–391 (2005)
7. Shin, S., Choi, S.: Haptic texture modeling using photometric stereo. In: *IEEE Haptics Symposium*, pp. 366–368. IEEE Press, Philadelphia (2016)
8. Choi, S., Tan, H.Z.: Towards realistic haptic rendering of surface texture. *IEEE Comput. Graph. Appl.* **24**, 40–47 (2004)
9. Choi, S., Walker, L., Tan, H.Z., Crittenden, S., Reifenberger, R.: Force constancy and its effect on haptic perception of virtual surfaces. *ACM Trans. Appl. Percept.* **2**(2), 89–105 (2005)
10. Campion, G.: *The Synthesis of Three Dimensional Haptic Textures*. Springer, London (2011)

Simultaneous Representation of Texture and Geometry on a Flat Touch Surface

Semin Ryu, Dongbum Pyo, Byung-Kil Han and Dong-Soo Kwon

Abstract We propose to combine two types of tactile feedback, electrovibration and mechanical vibration, for haptic interaction on a flat touch surface. This approach would enrich haptic effects for touch screen-based devices by simultaneously providing texture and geometry information.

Keywords Haptic interaction · Touch surface · Electro vibration · Mechanical vibration · Geometry · Texture

1 Introduction

Methods for providing haptic feedback on a touch screen have drawn substantial attention. In particular, vibration-based approaches have been studied in depth, since the mechanoreceptors in human skin are sensitive to frequency-dependent vibrotactile stimuli [1]. Numerous studies have been conducted to determine how to provide mechanical vibration feedback to users interacting with touch screens [2], and have demonstrated that the virtual texture created by vibration motors provides the feel of a real textured surface [3]. Electro vibration-based tactile displays have also been proposed in recent years [4]. By modulating the friction forces between a sliding fingertip and a touch screen, electro vibration can display geometry features, such as bumps [5]. However, most previous research has concentrated on creating

S. Ryu · D. Pyo · B.-K. Han · D.-S. Kwon (✉)
Department of Mechanical Engineering, KAIST, Daejeon, Republic of Korea
e-mail: kwonds@kaist.ac.kr

S. Ryu
e-mail: ryusm@robot.kaist.ac.kr

D. Pyo
e-mail: pyodb@robot.kaist.ac.kr

B.-K. Han
e-mail: hanbk@robot.kaist.ac.kr

only textures or geometry features, although both are equally important in simulating real objects. A few researchers have proposed simultaneous geometry and texture display [6, 7]. In this study, we propose to utilize both mechanical vibration and electrovibration for the simultaneous representation of texture and geometry features.

2 System Implementation

The hardware system was constructed as shown in Fig. 1. Electro-vibration is produced on a 3M Microtouch panel by applying an electrical signal to the connectors. Mechanical vibration, which is originally generated by piezoelectric haptic actuators (resonant frequency of around 150 Hz) attached to the periphery of the panel, is transmitted to the entire panel. During pilot tests, several combinations of the two feedback types were presented to participants. We observed that users are able to independently perceive mechanical vibration and electrovibration when both feedback types are provided simultaneously.

3 Demonstration

We will demonstrate the proposed method using the hardware setup shown in Fig. 1, with some interactive scenarios. In the demonstration, participants will slide their bare finger on the touch screen in order to interact with a set of virtual objects that vary in texture and geometry. Users can feel not only the surface texture of the virtual objects rendered by mechanical vibration (frequency and amplitude modulation), but also object curvatures rendered by electrovibration (amplitude modulation) [7]. For example, users will be able to clearly discriminate between virtual

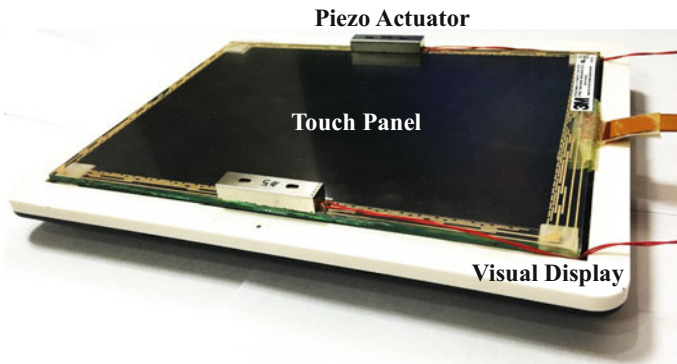


Fig. 1 Hardware setup for providing electrovibration and mechanical vibration

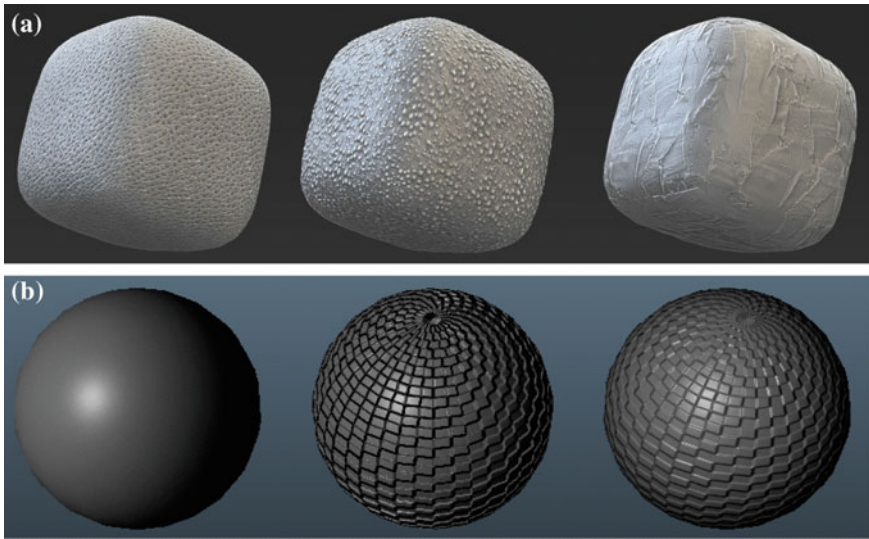


Fig. 2 Examples of demonstration scenarios: **a** cubes with textures, **b** spheres with textures

objects, each of which has different texture (smooth, bumpy, rough, etc.) and shape (cube or sphere), as shown in Fig. 2.

Acknowledgements This work has been supported by the ICT Technology Development of the Research Program of MSIP/IITP [R0711-15-0034, High effective multi-actuators module for Braille smart devices].

References

1. Kaczmarek, K.A., Webster, J.G., Bach-y-Rita, P., Tompkins, W.J.: Electrotactile and vibrotactile displays for sensory substitution systems. *IEEE Trans. Biomed. Eng.* **38**, 1–16 (1991)
2. Chauvelin, C., Sagi, T., Coni, P., André, J.-M., Jauze, C., Lespignet-Najib, V.: Haptics on a touch screen: characterization of perceptual thresholds. *Int. J. Hum.-Comput. Interact.* **30**, 872–881 (2014)
3. Romano, J.M., Kuchenbecker, K.J.: Creating realistic virtual textures from contact acceleration data. *IEEE Trans. Haptics* **5**, 109–119 (2012)
4. Bau, O., Poupyrev, I., Israr, A., Harrison, C.: TeslaTouch: electrovibration for touch surfaces. In: *Proceedings of the 23rd Annual ACM Symposium on User Interface Software and Technology*, pp. 283–292. ACM
5. Kim, S.-C., Israr, A., Poupyrev, I.: Tactile rendering of 3D features on touch surfaces. In: *Proceedings of the 26th Annual ACM Symposium on User Interface Software and Technology*, pp. 531–538. ACM

6. Saga, S., Raskar, R.: Simultaneous geometry and texture display based on lateral force for touchscreen. In: World Haptics Conference (WHC), 2013, pp. 437–442. IEEE (2013)
7. Pyo, D., Ryu, S., Kim, S.-C., Kwon, D.-S.: A new surface display for 3D haptic rendering. In: Auvray, M., Duriez, C. (eds.) Haptics: Neuroscience, Devices, Modeling, and Applications: 9th International Conference, EuroHaptics 2014, Versailles, France, June 24–26, 2014, Proceedings, Part I, pp. 487–495. Springer, Berlin (2014)

Ferro-Fluid Based Lightweight and Portable Tactile Display for Persuasive Tactile Cues Including Orientation and Texture

Harsimran Singh, HyeonSeok Seong and Jee-Hwan Ryu

Abstract This paper proposes a ferro-fluid based tactile display, which is lightweight and portable but yet can replicate convincing contact orientation and texture information. Numerous studies have been conducted to develop a tactile display for providing convincing tactile feedback. However, most of the displays were limited in portability, and restricted to delivering either texture information with vibration cues or contact orientation with force feedback. To the best of our knowledge, the proposed tactile display is the first wearable tactile display which can deliver texture information together with contact orientation, and still be lightweight and portable. New design principle, introducing ferro-fluid, and minimizing moving actuator components with magnet, allows having light weight and compactness to increase portability, and enables providing both contact orientation and texture cues.

Keywords Tactile display · Wearable · Ferro-fluid · Directional cues · Vibrational cues

1 Introduction

In the absence of tactile display, there was a deterioration in performance when perceiving the shape of an object [1]. A surgeon actively palpates the human tissue to check for its mechanical properties such as compliance, viscosity and surface texture, all of which are indications of health of the tissue [2]. Such an information can be provided to the surgeon through a tactile display, the absence of which greatly limits the surgeon's ability to stage the disease adequately. However, compared to kinesthetic feedback, there has been relatively little work done in the area of tactile feedback. Even though a suitable sensing device capable for sensing the mechanical

H. Singh (✉) · H. Seong · J.-H. Ryu
School of Mechanical Engineering, Korea University of Technology and Education,
1600 Chungjeolno, Cheonan, Chungnam, South Korea
e-mail: harsimran@koreatech.ac.kr

J.-H. Ryu
e-mail: jhryu@koreatech.ac.kr

properties of a tissue may be available, the communication of this tactile information cannot be passed onto the surgeon through the rigid handles of the surgical instruments [3]. Thus, there is a need to develop a light weight, compact and wearable tactile display that can replicate convincing contact orientation and texture information to the user. It should be fast actuating and lag free, also have none or as less moving actuators as possible, which would give the user more sense of freedom and less reaction force when wearing something external over finger/s. The use of such a device can sweep across multiple disciplines, including teleoperation and Robotic Minimally Invasive Surgery (RMIS), where the tactile display can be added-on to the master manipulator of the RMIS, thereby combining kinesthetic and tactile information to create the perception that the surgeons fingertip is in direct contact with the patient or the surgical material such as suture.

In the past several decades, much work has been done on developing light weight and wearable tactile displays with the aim of reproducing realistic sensations that a person experiences while interacting with its environment.

The pin arrays typically consists of dense array of skin contactors which move orthogonally to the surface of the skin in an attempt to display the shape of objects via its spatially sampled approximation. Such displays are actuated mostly using electromagnets, piezoelectric crystals, shape memory alloys [4] and pneumatic systems [5]. Vibrational haptic sensation has been one of the most common forms of feedback to the user. Popular vibrating actuators include voice coil motors and piezoelectric materials. It is generally non directional form of tactile feedback which has been an easy solution and is still being vastly used for gaming stations, wearable, virtual reality and smartphones.

Tactile sensation can also be provided using some mechanism that applies two or three dimensional vector force at one or more contact points. Solazzi et al. [6], designed a portable interface for the fingertip for haptic interaction with virtual environments. It could display contact–non contact transition and the local orientation of the virtual surface. However, the overall structure is not that compact and thus imposes limitations on its use as a wearable device.

Most of the tactile displays mentioned above are either limited in terms of portability or restricted to delivering texture information or contact orientation via two/three dimensional vector force. In this paper we present a wearable tactile display that can cue contact point orientation and texture feedback, and still be light weight and compact. To the best of our knowledge, the proposed idea, for the first time incorporates the use of ferro-fluid in a wearable tactile display to provide contact point orientation and texture information.

2 Design of the Tactile Display

Figure 1a shows the proposed schematic design. Neodymium disc magnet is enclosed in a casing together with ferro-fluid, and the casing is attached to the fingertip using velcro. The ferro-fluid gets accumulated on the poles of the neodymium disc magnet.

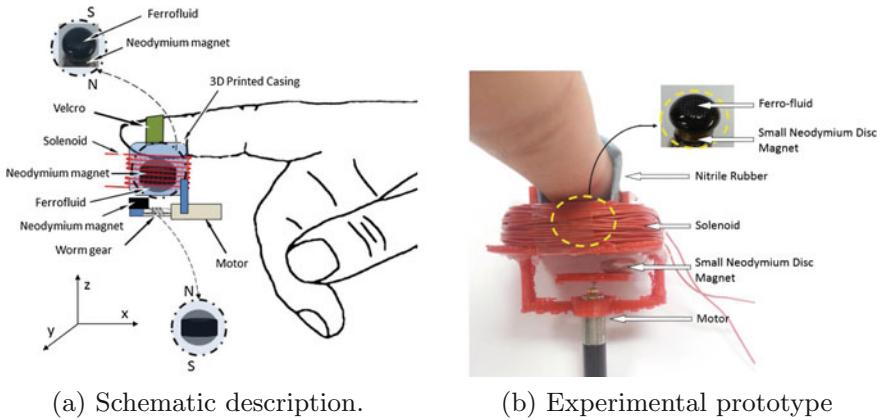


Fig. 1 Schematic and experimental prototype of the proposed ferro-fluid based tactile display

This Neodymium Magnet Enclosed by Ferro-Fluid (NMEF) can apply tangential shear forces to the finger pad by controlling the external magnetic field with the External Neodymium Magnet (ENM) and the solenoid wound around the casing. Because there is no counterbalancing force being applied on the back of the finger and nail, tactile sensation is much enhanced as the applied force can be concentrated to the finger pad.

The ENM and the solenoid work hand in hand to increase or decrease the orientation of the NMEF. The position of the ENM gives the orientation direction to the NMEF and also adds a permanent torque experienced by it. By making a solenoid that has little more magnetic field strength than the ENM, a wide range of orientation angle of the NMEF can be controlled. If there was no ENM, the solenoid would then have to be more powerful to exert the same torque onto the NMEF. This would mean more number of turns and an increase in weight, thus making the tactile display less likely to be wearable.

Our design principle is to have a light and compact structure that can provide fast and lag free actuation. Therefore it is designed to have only one moving actuator, which gives the user more sense of freedom and less reaction force when wearing something external over finger/s. The individual component detail along with its functioning is explained hereafter.

2.1 Enclosure for the Tactile Display

The casing is a thin leak-proof enclosure, which holds the ferro-fluid and neodymium disc magnet and is attached to the base of the human finger via Velcro. The inner shape of the casing is a cuboid whose length and breadth is equal to the radius of the neodymium disc magnet, with a small offset. Under external magnetic fields, such a

tight packing of the magnet in the casing does not allow it to translate on x or y axis, but only to roll, pitch and translate on z axis. To cover the casing where it is attached to the base of the fingertip, nitrile rubber was used due to its excellent stretching capabilities, being inexpensive and easy availability. The shape of the nitrile rubber was concave so that it does not restrict the motion of magnet when it is pushing up on the finger pad and allows its free motion.

2.2 Role of Ferro-Fluid

Ferro-fluids are colloidal suspensions of surfactant-coated magnetic particles, in the order of 10 nm (100 Å) in diameter, in a liquid medium. If a uniform and vertical magnetic field above a critical strength is applied on a ferro-fluid, a pattern of peaks would emerge on the surface when the field strength is above a critical value [7]. The stronger the magnetic field, the larger the spikes. However, the force imposed on the finger with ferro-fluid alone was limited and only impart a faint sensation. If a larger magnet or electromagnet is used, the sensations would be stronger, but then the device would no longer be wearable. Therefore, the ferro-fluid is used here in a different context than stimulating tactile sensations to the human finger. We use ferro-fluid directly on the neodymium disc magnet, so that it gets accumulated on the poles of the magnet. This NMEF keeps its motion stable inside the casing and doesn't allow it to wobble on the external magnetic field's change. It also helps keeping the magnet at the center of the casing and doesn't let it move around in case of no external magnetic field or when the human repositions its finger. Moreover it keeps the inside of the casing lubricated which allows smooth motion of NMEF. Without ferro-fluid, it would be impossible to accurately control the magnet enclosed in the casing using external magnetic fields.

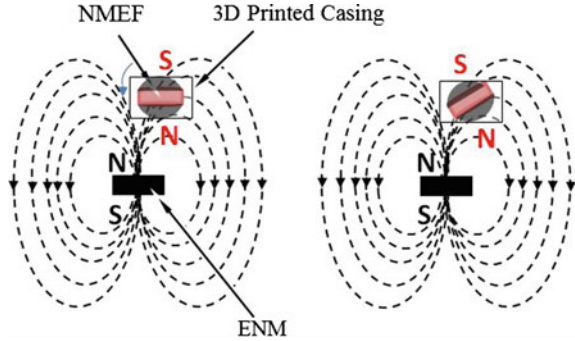
2.3 External Magnetic Field Actuation

External magnetic field is required to actuate the NMEF for delivering orientation and texture feedback to the user. As illustrated in Fig. 1a, two additional actuators were introduced: another similar sized external disc neodymium magnet coupled with a small DC motor; and a solenoid wound around the casing.

External Neodymium Magnet

The External Neodymium Magnet (ENM) is attached to a circular plate fixed at the bottom of the casing. The ENM was installed in such a way that it always repels the NMEF. This magnet was not placed directly below the NMEF but at some offset. Since the NMEF has no translation motion about the x or y axis, it thus tends to flip in the direction of the ENM and tries to align with its magnetic field as shown in Fig. 2. Since the human finger is attached to the casing, so the NMEF will not flip

Fig. 2 Torque experienced by NMEF due to the magnetic field of ENM



completely but rather exert a force onto the finger pad thereby distorting it. Since the NMEF is only allowed to rotate, thus the approximate torque produced is:

$$\tau = mBl \sin \theta \tag{1}$$

where, m is the pole strength of the NMEF, B is the magnetic field of the ENM, l is the height of the NMEF and θ is the angle between the NMEF and the ENM's magnetic field. Since both the magnets are close to each other, we assume that the ENM's magnetic field passing through NMEF is uniform.

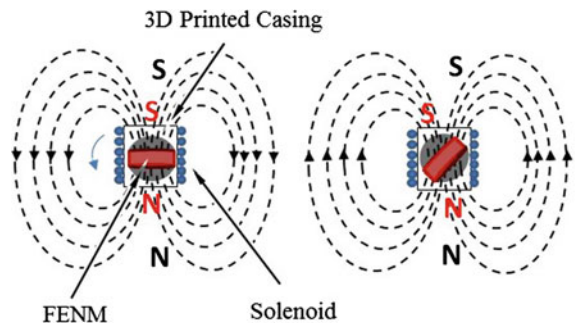
The circular plate on which the ENM is attached is coupled with the motor. The rotation of the circular plate imparts a yaw rotation to the NMEF.

Solenoid

The solenoid wound around the casing, upon excitation generates a magnetic field which runs through the center of the casing, Fig. 3. The strength of this magnetic field is designed to be greater than the ENM and is given by:

$$B = \frac{\mu_0 NI}{L} \tag{2}$$

Fig. 3 Magnetic field of the solenoid **a** decreasing and **b** increasing the orientation angle of the NMEF



where, μ_0 is the permeability of free space, N is the number of turns of the solenoid, I is the current through the solenoid and L is the length of the solenoid. The polarity of this solenoid is either opposite to that of NMEF, in which case the NMEF is held at the centre of the casing, irrespective of the push it's getting from the ENM, or same as the NMEF, in which case it adds on to the torque imposed by the ENM to flip the NMEF.

The excitation strength and frequency of the solenoid controls the vibrations imposed to the NMEF. Calibrating it with proper rendering algorithms can provide texture information to the user along with orientation.

3 Conclusions and Future Works

This paper presents a wearable ferro-fluid based tactile display which is light weight and can display convincing contact orientation and vibrational information. This device uses a neodymium magnet enclosed by ferro-fluid to stimulate the finger pad. It is actuated using external magnetic fields which is controlled using a neodymium magnet, coupled to a small dc motor, and a solenoid. To the best of our knowledge, this is the first wearable tactile display that can replicate both orientation and texture cues. The design structure along with the working principle of the tactile display are presented.

For future research, this work will be extended to design a ferro-fluid based tactile display having no moving actuators. Also a closed loop force control will be implemented that will further increase the accuracy of the device.

Acknowledgements This paper was partially supported by the Industrial Strategic Technology Development Program (10052967) funded by the Ministry of Trade Industry & Energy (MOTIE, Korea), and Intuitive Surgical, Inc.

References

1. Jansson, G., Monaci, L.: Identification of real objects under conditions similar to those in haptic displays: providing spatially distributed information at the contact areas is more important than increasing the number of areas. *Virtual Real.* **9**(4), 243–249 (2006)
2. Okamura, A.M.: Haptic feedback in robot-assisted minimally invasive surgery. *Curr. Opinion Urol.* **19**(1), 102 (2009)
3. Yazdian, S., Doxon, A.J., Johnson, D.E., Tan, H.Z., Provancher, W.: Compliance display using a tilting-plate tactile feedback device. In: *Haptics Symposium (HAPTICS)*, 2014 IEEE, pp. 13–18. IEEE (2014)
4. Velázquez, R., Pissaloux, E.E., Wiertlewski, M.: A compact tactile display for the blind with shape memory alloys. In: *ICRA 2006. Proceedings 2006 IEEE International Conference on Robotics and Automation*, 2006, pp. 3905–3910. IEEE (2006)
5. Moy, G., Wagner, C., Fearing, R.S.: A compliant tactile display for teletaction. In: *ICRA'00. IEEE International Conference on Robotics and Automation*, 2000. Proceedings, vol. 4, pp. 3409–3415. IEEE (2000)

6. Solazzi, M., Frisoli, A., Bergamasco, M.: Design of a cutaneous fingertip display for improving haptic exploration of virtual objects. In: RO-MAN, 2010 IEEE, pp. 1–6 (2010)
7. Rosensweig, R.E.: Ferrohydrodynamics. Courier Corporation (2013)

Sole Tactile Display Using Tactile Illusion by Vibration on Toenail

Kensuke Sakai, Taku Hachisu and Yuki Hashimoto

Abstract We present a novel wearable device for producing tactile sensations to a foot sole while walking. As a method for that, we extended on a tactile illusion in a finger. This illusion can provide tactile sensations in the finger pad when a vibrator is connected to a finger nail and the finger pad is in contact with surface. We applied such kind of tactile illusion to the foot. Following our approach, we developed a prototype of sole tactile display. Our prototype provides two applications. One application is improving the user's motivation of walking by superimposing ground texture. Another application is supporting stable walking by presenting tactile sensations. By combining these applications, user can walk happily and safely.

Keywords Gait stabilization · Ground texture · Nail-mounted tactile display · Sole-tactile sensation

1 Introduction

Haptic sensations at the foot sole are important while walking. Body posture is adjusted according to these haptic sensations, which in turn affects gait [1]. However, because many modern shoes are highly cushioned, haptic sensations at the foot sole are attenuated. This study developed presents a wearable device that produces tactile sensations to the sole while walking. Researches have previously produced vibrations at the foot sole by vibrating a floor [2] and a shoe sole [3]; however, suitable locations for these techniques are limited and vibrators can diminish foot comfort.

K. Sakai (✉) · T. Hachisu · Y. Hashimoto
The University of Tsukuba, 1-1-1, Tennodai, Tsukuba, Ibaraki 305-8573, Japan
e-mail: k_sakai@vrlab.esys.tsukuba.ac.jp

© Springer Nature Singapore Pte Ltd. 2018
S. Hasegawa et al. (eds.), *Haptic Interaction*, Lecture Notes
in Electrical Engineering 432, DOI 10.1007/978-981-10-4157-0_16

2 Method

We extended on a tactile illusion technique developed by Ando et al. [4]: when a vibrator is connected to a fingernail, and the finger pad is in contact with the surface, the user feels vibrations in the finger pad. Application of the illusion to tactile displays does not require a solid barrier (e.g., stimulator) between the touched surface and the user’s skin. We applied such kind of tactile illusion to the toe (Fig. 1), to produce tactile sensations to the foot sole. Compared with direct stimulation of the foot sole, our method has the advantage that it does not reduce foot comfort, because there is no rigid actuator between foot and the ground. Moreover, there is little restriction to movement because the device required for this technique can be light (30 g) and small (150 × 30 mm). In previous research, we confirmed that this technique is effective while walking [5] and has the possibility of supporting human gait [6].

3 Prototype

Figure 2 shows the wearable device prototype. An accelerometer is used to adjust the amplitude of the vibration and detecting the stance phase. A microcontroller outputs a wave signal and an audio amplifier drives the vibrator.

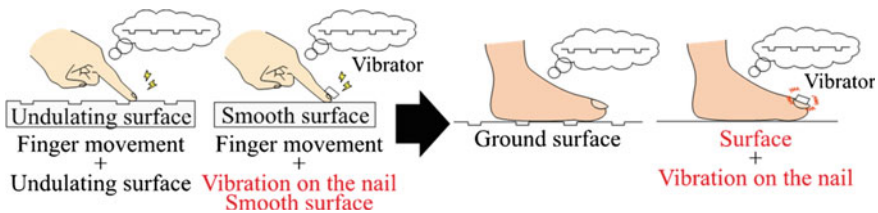


Fig. 1 Tactile illusion from previous research and the proposed method

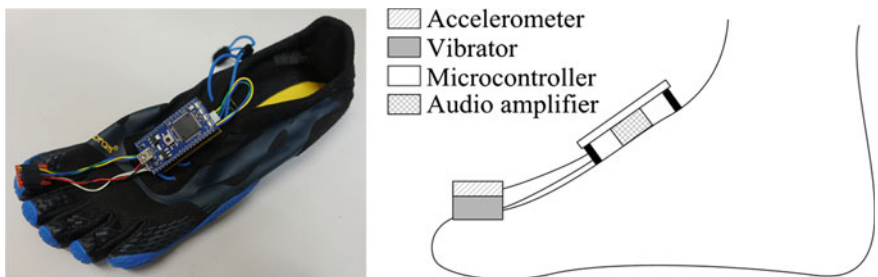


Fig. 2 A wearable device and its configuration

4 Conclusion

This paper describes a wearable device prototype to produce tactile sensations using tactile illusion. The device does not reduce foot comfort and is usable anywhere, enabling fun and safe walking on a daily basis.

References

1. Kavounoudias, A., Roll, R., Roll, J.P.: Foot sole and ankle muscle inputs contribute jointly to human erect posture regulation. *J. Physiol.* **532**(3), 869–878 (2001)
2. Visell, Y., Law, A., Cooperstock, J.R.: Touch is everywhere: floor surfaces as ambient haptic interfaces. *IEEE Trans. Haptics* **2**(3), 148–159 (2009)
3. Ducere, LECHAL. <http://lechal.com/insoles.html>. Accessed 14 Oct 2016
4. Ando, H., Miki, T., Inami, M., Maeda, T.: SmartFinger: nail-mounted tactile display. *ACM SIGGRAPH 2002 Conference Abstracts and Applications*, 78 (2002)
5. Sakai, K., Hashimoto, Y.: Perceptual characteristics of a tactile illusion using toenail-mounted vibration. *ICAT-EGVE 2015*, P10, Poster
6. Sakai, K., Hachisu, T., Hashimoto, Y.: Validity of gait stabilization method by vibration on toenail. *IPSI SIG AAC, 2016-AAC-1* (4), pp. 1–6 (2016) (in Japanese)

Scalable Architecture for Airborne Ultrasound Tactile Display

Seki Inoue, Yasutoshi Makino and Hiroyuki Shinoda

Abstract In this paper, we show a scalable architecture for ultrasound phased array system. The biggest issue here to modularize phased array system is phase synchronization across arrays. Its timing constraint is quite severe because the phase error between arrays directly hits focusing performance. We employ EtherCAT network protocol to achieve scalable precise phase synchronization and effective communication. A new designed phased array unit connects each other in a daisy chain topology with precise timing synchronization, high frame rate, and large capacity communication.

Keywords Ultrasound phased array · Tactile display · Distributed architecture · EtherCAT

1 Introduction

Airborne ultrasonic phased arrays can control acoustic field in the air and it is used in a variety of applications such as super-directive loudspeaker [1], particle levitation [2, 3], and remote tactile display [4]. To obtain wider dynamic range and higher spatial resolution in all direction, it is one of the solutions to place phased arrays as many as possible [5, 6]. Modularizing a phased array system in a unit makes it simplify to wire and install them. However, the biggest issue is to synchronize phases of the phased arrays. For example, when 40 kHz ultrasound is controlled in

S. Inoue (✉) · Y. Makino · H. Shinoda
Graduate School of Information Science and Technology, The University of Tokyo,
Tokyo, Japan
e-mail: seki_inoue@ipc.i.u-tokyo.ac.jp

Y. Makino
e-mail: makino@k.u-tokyo.ac.jp

H. Shinoda
e-mail: shinoda@k.u-tokyo.ac.jp

Y. Makino · H. Shinoda
Graduate School of Frontier Sciences, The University of Tokyo, Chiba, Japan

4 bit phase quantization, the required margin of timing error across transducers is $1.56 \mu\text{s}$, which is very severe condition compared with audio and visual displays. In this paper, we show a new distributed architecture which mainly focuses on large scale tactile display and its implementation.

2 Architecture

The requirements of the phased array unit for 40 kHz frequency are as follows: (1) precise phase synchronization $<1 \mu\text{s}$, (2) high frame rate beyond tactile sense $>11 \text{ kHz}$, (3) distributed computing resources (4) realtime logics for wave form generation and (5) controlled by non-realtime computers.

To achieve both scalability and precise phase synchronization, our strategy is compensating clock drift by communication, rather than relaying global clock source. Relaying signals generated from global clock, which we employed in our legacy system, is simple and effective idea for a small system but propagation delays of wires and receivers/drivers become problem when connecting a large number of units. On the other hand, distributed clocks and its compensation keep precise if the communication jitter is negligible.

Tactile sensation has a wide range of bandwidth, which is from DC to over 500 Hz. Considering the sampling theorem, 11 kHz or higher frame rate is needed.

Computing resources are required to be placed on each units because some applications [7, 8] needs huge amount of computation costs which is non-linear to the number of transducers.

Ultrasonic transducers can be driven by square waves. However, unlike PWM motor control, not only its duty ratio but also its offset time must be controlled, which needs FPGA at the moment. Here, duty ratio results in amplitude of ultrasound and offset time governs phase of ultrasound.

Lastly, considering its ease of usage, a host machine should not require real time operating system.

Based on the above, we employ EtherCAT protocol for the network. EtherCAT is an extension of Ethernet protocol and optimized for large scale realtime fieldbus systems [9]. EtherCAT network consists of a master node and slave nodes. Only one frame is transported in a cyclic period so that it is achievable to maximize bandwidth utilization. It has a built-in feature called "DC" (Distributed Clocks), which achieves clock synchronization with low jitter less than $1 \mu\text{s}$, which is $1/25$ of the period of 40 kHz ultrasound.

Figure 1 shows a block diagram of the proposed architecture. Each units has network co-processor, main processor and RTL (FPGA). With this heterogeneous architecture, high performance computing and precise timing control are achievable. Network processor also manages clock synchronization and pass the clock to RTL directly.

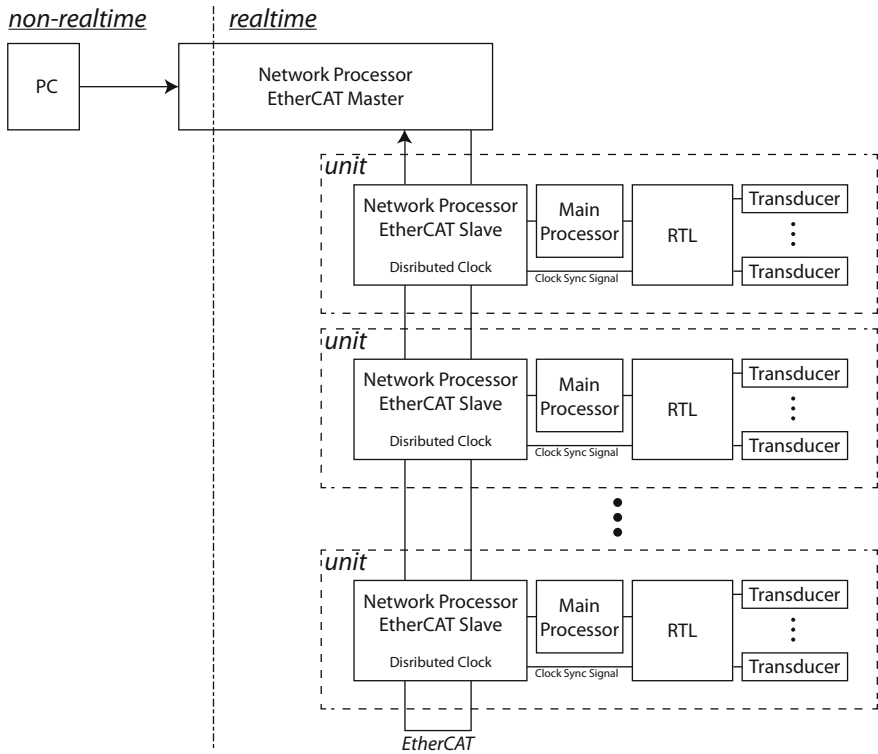


Fig. 1 An architecture for scalable phased array system. Using EtherCAT network, a phase synchronization and a large capacity communication between a large number of units are achieved

3 Implementation

We fabricated a new board which realized the architecture. Figure 2 shows a block diagram of our implementation. Three processors: ARM Cortex-M3, ARM Cortex-R4 and Xilinx Artix7 are mounted and they are connected via dual port random access memories (Tightly Coupled Memory on RZ/T1 and Block RAM on Artix7). M3 is responsible for network and clock synchronization. R4 is used as main multi-purpose processor and calculates phases and amplitude of transducers mounted on the unit. Artix7 generates wave form for transducers, not only that, it can also help R4 for its calculation. Figure 3 shows an overview of the rear of our fabricated board. It has 249 transducers on the front. Only a power supply and two RJ45 cables are needed to run.

We employed Beckhoff TwinCAT3 on Windows 8.1 as EtherCAT master. In this configuration, 11 kHz frame rate was stably achieved. The largest clock jitter between two boards was less than 25 ns when three boards are connected.

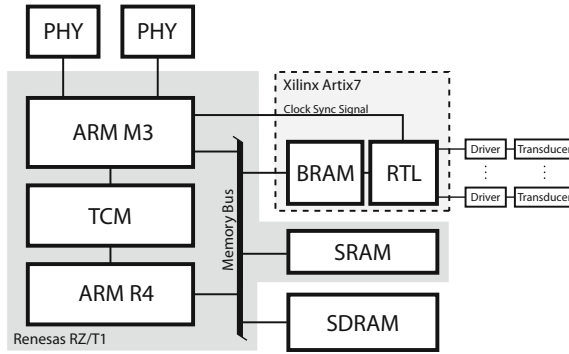


Fig. 2 A block diagram of a phased array unit

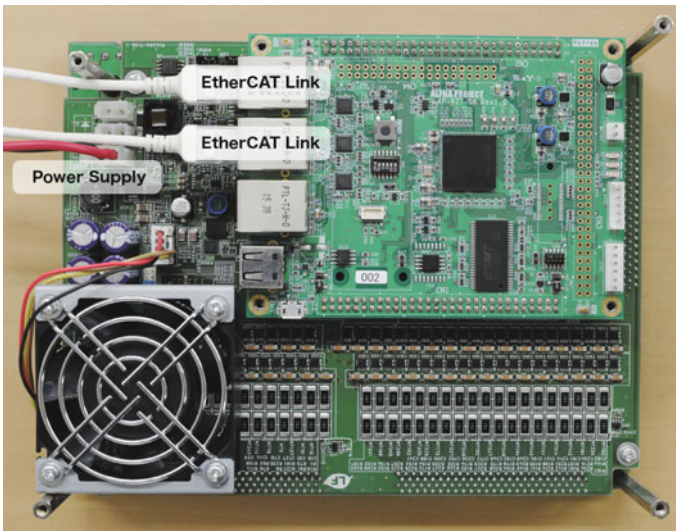


Fig. 3 An overview of an implemented phased array unit

4 Conclusion

In this paper, we have proposed a scalable architecture and its implementation for airborne ultrasound phased array. The unit connects each other with ordinary Ethernet RJ45 cable. Its frame rate is 1 kHz and timing synchronization error across units is less than 1 kHz. In general, tactile displays are desired to be controllable with over 1 kHz frame rate and have many channels with precise timing requirements. We believe this type of architecture is generally helpful for tactile and haptic device implementation.

Acknowledgements This work was supported in part by JSPS Grant-in-Aid for Scientific Research (S) 16H06303, JST ACCEL Embodied Media Project, and JSPS Grant-in-Aid for JSPS Fellows 15J09604. We would like to thank professional members of Shinko Shoji Co., Ltd., Nagano Oki Electric Co., Ltd., and JSL Technology for their technical helps of the system design and implementation.

References

1. Westervelt, P.J.: Parametric acoustic array. *J. Acoust. Soc. Am.* **35**(4), 535–537 (1963). <http://scitation.aip.org/content/asa/journal/jasa/35/4/10.1121/1.1918525>
2. Ochiai, Y., Kumagai, K., Hoshi, T., Rekimoto, J., Hasegawa, S., Hayasaki, Y.: Fairy lights in femtoseconds: aerial and volumetric graphics rendered by focused femtosecond laser combined with computational holographic fields. In: *ACM SIGGRAPH 2015 Emerging Technologies, SIGGRAPH '15*, pp. 10:1–10:1. ACM, New York, NY, USA (2015). <http://doi.acm.org/10.1145/2782782.2792492>
3. Marzo, A., Seah, S.A., Drinkwater, B.W., Sahoo, D.R., Long, B., Subramanian, S.: Holographic acoustic elements for manipulation of levitated objects. *Nat. Commun.* **6**, 8661 EP – (10 2015). doi:[10.1038/ncomms9661](https://doi.org/10.1038/ncomms9661)
4. Hoshi, T., Takahashi, M., Iwamoto, T., Shinoda, H.: Noncontact tactile display based on radiation pressure of airborne ultrasound. *IEEE Trans. Haptics* **3**(3), 155–165 (2010). doi:[10.1109/TOH.2010.4](https://doi.org/10.1109/TOH.2010.4)
5. Hasegawa, K., Shinoda, H.: Aerial display of vibrotactile sensation with high spatial-temporal resolution using large-aperture airborne ultrasound phased array. In: *World Haptics Conference (WHC)*, 2013, pp. 31–36 (2013)
6. Inoue, S., Shinoda, H.: A pinchable aerial virtual sphere by acoustic ultrasound stationary wave. In: *Haptics Symposium (HAPTICS)*, 2014, pp. 89–92. IEEE (2014)
7. Inoue, S., Makino, Y., Shinoda, H.: Active touch perception produced by airborne ultrasonic haptic hologram. In: *World Haptics Conference (WHC)*, 2015, pp. 362–367. IEEE (2015)
8. Long, B., Seah, S.A., Carter, T., Subramanian, S.: Rendering volumetric haptic shapes in mid-air using ultrasound. *ACM Trans. Graph.* **33**(6), 181:1–181:10 (2014). doi:[10.1145/2661229.2661257](https://doi.org/10.1145/2661229.2661257)
9. <https://www.ethercat.org/en/technology.html>

HapStep: A Novel Method to Sense Footsteps While Remaining Seated Using Longitudinal Friction on the Sole of the Foot

Ginga Kato, Yoshihiro Kuroda, Kiyoshi Kiyokawa and Haruo Takemura

Abstract In recent years, a lot of locomotion devices have been developed. However, most locomotion devices require the user to do a walking motion while the user is standing. In this study, we represented the walking sensation while remaining seated by representing the footsteps sensation using longitudinal friction force on the sole of the foot. We developed a haptic device (HapStep) to present the friction force on the sole of the foot and constructed the system that represents the walking sensation in accordance with the motion of the character in the virtual space.

Keywords Virtual reality · Haptic device · Force rendering · Tactile feedback · Walking sensation

1 Introduction

Nowadays, head mounted displays (HMD) begin to spread, and virtual reality (VR) technologies become popular. To improve reality, a lot of researchers try to represent not only visual information but also haptic information.

In such situations, many devices that aim to represent the walking sensation in the virtual space have been developed [1–4]. If we can mimic the walking sensation in the virtual space, the realism of the virtual experience will be improved. Thus, these locomotion devices realize the walking experience in the virtual space by controlling the walking floor to counteract the user's motion. By using these devices, the user can walk unlimitedly in a virtual space. However, conventional locomotion devices require a large scale apparatus. If some external forces are applied to the stance leg when walking in the standing posture, the user will easily lose his balance. Thus,

This work was supported by JSPS KAKENHI Grant Numbers JP15K12082 and JP15K12083.

G. Kato (✉) · Y. Kuroda · K. Kiyokawa · H. Takemura
Graduate School of Information Science and Technologies, Osaka University,
1-5 Yamadaoka, Suita, Osaka 565-0871, Japan
e-mail: katou.ginga@lab.ime.cmc.osaka-u.ac.jp
URL: <http://www.handai.tk>

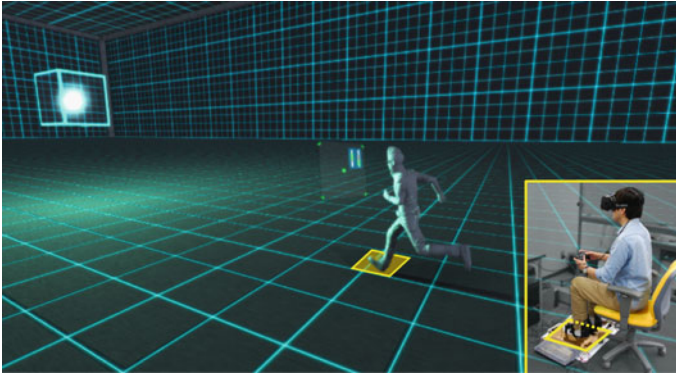


Fig. 1 The system of HapStep

these devices need a large scale apparatus that can support the whole body weight. In addition, there is also a feature that these devices give the user a feeling of fatigue. The tiredness can not be simply said to be a demerit. However, if we can experience the walking without fatigue, long time experience will be possible.

In this study, we aim to represent the walking sensation while the user is remaining seated. We focused on the “footsteps sensation” which occurs when we step forward, and tried to represent the walking sensation by mimicking this footsteps sensation. If we have limited the representation of footsteps sensation, real like walking motion is not required. The apparatus to support the user’s weight is also no longer required, so we can downsize the device. Besides, as mentioned above, the device no longer gives a feeling of fatigue to the user.

We specifically focused on the longitudinal friction force (in following sentence, we call the moving direction of the user “forward”, back direction of the user “backward”) worked on the sole of the foot at the time of footsteps to mimic the footsteps sensation. We developed a haptic device—HapStep to present the longitudinal friction force, and also constructed the system (Fig. 1) in which the user can walk in the virtual space freely and feel the walking sensation.

2 Related Work

To improve reality and immersion of the virtual space, a lot of locomotion devices that represent walking sensation have been developed.

Most of the conventional locomotion devices cancel the user’s walking motion to maintain the user at the neutral position. By maintaining the user’s position, the unlimited walking in a limited space is realized. For example, the device in [1] canceled the walking motion by moving the plates on which each foot is riding alternately utilizing a parallel link mechanism. Parallel link devices can also counteract

the movement in the direction of gravity. Thus, these types of devices can represent various shapes of environments such as stairs. However, the parallel link mechanism is complicated and these devices require a large actuator to support the user's body weight. If the output of motor increases, the bearing power of the parallel link will also become large in theory. However, the size of links cannot be reduced so much in order not to limit the motion of walking movement. The other types of devices that canceled walking movement in the same way as a treadmill have been also developed [2, 3].

If we try to counteract the walking movement as described above, a slip feeling like walking on the slippery floor are also represented to the user. In the real walking, a friction force arises between the sole of the foot and the floor. This friction force acts as the driving force to move the body forward, and human usually feels this friction force through the sole. However, all of the devices described above counteract the work of the driving force. Thus, a user does not feel the driving force, and thus the sensation of friction force is small. Another kind of device in [4] reduces the friction between the shoes and the floor to slide the user's leg to the neutral position when walking. However, this device cannot avoid representing the slip feeling.

There are other studies that focused on the footsteps sensation which occurs when a user steps forward. For example, in [5, 6], the specific vibrations that occur on the sole of the foot when walking on the various types of floors are represented. These vibrations are superimposed on the actual footsteps. Though these devices realized to represent the different floor feeling from the real floor, they did not aim to represent the walking sensation itself.

Most locomotion devices to represent walking sensation counteract the walking movement while the user is standing. Thus, these devices have the feature that the long time experience is difficult due to fatigue. In addition, to support the walking motion, a large prop is required. On the other hand, haptic footstep display [7] tried to represent the walking sensation while remaining seated by mimicking the footsteps sensation. If the walking sensation can be represented while remaining seated, the reality and immersion of the virtual space is improved without giving a burden of walking. Besides, such a device can be operated even in a narrow space. Haptic footstep display represented the footsteps sensation by mimicking the pressure applied to the sole of the foot when walking with a plate mechanism that drives up and down, and realized realistic walking experience. However, to drive the plate up against the weight of the foot, this device requires a strong and big actuator. Besides, this device can not present rapid stimulus such as a collision when a user hits a ground with the foot.

Haptic footstep display mainly focused on the vertical force applied to the sole of the foot when stepping. On the other hand, the force acting as a brake and a driving force to move the body forward is a longitudinal friction force applied to the sole of the foot. We thought this friction force is important to mimic stepping sensation, and decided to utilize this friction to represent walking. When presenting only the friction force, it is not necessary to counteract the weight of the foot, thus the size of device can be reduced.

3 Design

3.1 Measurement of Longitudinal Friction

To represent the walking sensation by mimicking the friction force, we examined the force applied to the sole of the foot when the participants were walking on the treadmill. By using the force sensor (USL06-H5-50N, by Tec Gihan Co., Ltd.), we investigated the longitudinal friction force. Figure 2a shows the measured value of a certain subject, and Fig. 2b shows the outline of the applied force inferred from the result. In Fig. 2b, the orange arrows show the friction force applied to the sole, and the blue arrows show the force inferred that a user applies to the foot. At the beginning of the footstep, [Step-(1)] backward force is applied to the heel side, and then, [Step-(2)] forward force is applied to both of the heel side and thenar side. After them, [Step-(3)] the forward force to the heel side becomes small. Finally, [Step-(4)] large backward force is suddenly applied to the thenar side.

The friction force in step-(1) is inferred as the reaction force against the force to put the foot forward. This force is presumed to act as a brake of the body and stabilize the walking motion. The friction forces in step-(2) and step-(3) are inferred as the reaction force against the backward force to kick out the foot. This reaction force acts as a driving force to move the body forward. As the weight shifts from the heel side to the thenar side, the heel side becomes floating. Thus, in step-(3), the force applied only to the thenar side. As the change of the foot angle, the weight of the body applied not only in a vertical direction but also in a horizontal direction. This is considered the cause of the suddenly change of the force in step-(4). Thus, the force applied by the longitudinal friction force is only the force in step-(1), step-(2), and step-(3).

When we increased the speed of treadmill during the measurement, the forward force applied on both the heel and thenar sides like step-(2) did not appear because of the increase of weight shift speed. On the other hand, except for step-(2), similar forces were applied regardless of the speed.

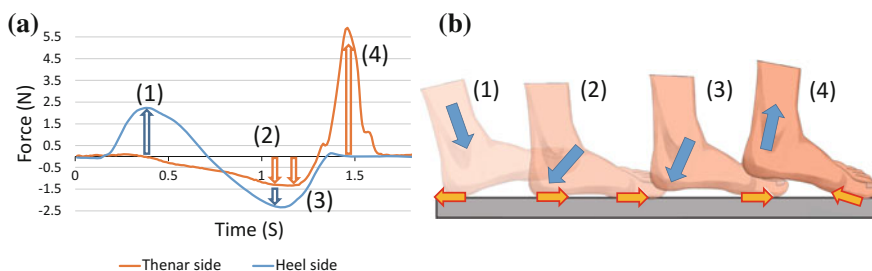


Fig. 2 The measurement results. **a** Shows the result of certain subject and **b** shows the inferred force applied to the foot

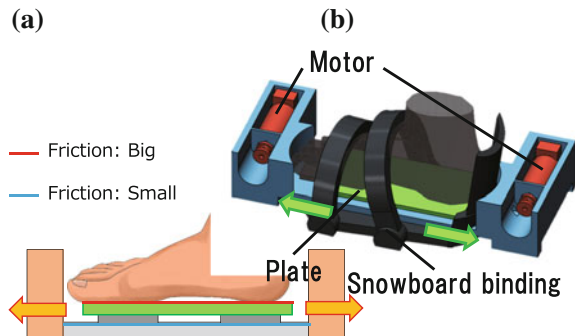
3.2 Design of HapStep

From the measurement result, we found a typical pattern of the temporary change in longitudinal friction force applied to the sole of the foot. If we try to present the vertical force, we have to counteract the weight of the foot. Thus a large mechanism is required. On the other hand, in the case of friction force presentation, we do not have to counteract the weight directly. The presentation of a rapid friction force can be realized with a small mechanism by eliminating the substantial weight of the foot. When the display to present the friction force is grounded, the friction μN applied to the grounded point becomes larger as the normal force N caused by the weight of the foot becomes larger. However, if we reduce the coefficient of dynamic friction μ , the force μN becomes negligibly small.

Thus, we decided to represent the walking sensations by mimicking the longitudinal friction force on the sole of the foot applied at the time of footsteps. Specifically, we present the friction force in the order of “backward”, “forward” to represent the friction force in step-(1), step-(2), and step-(3) measured in the previous section. As we discussed in the previous section, we do not represent the friction force in step-(4), because we think this force is caused by the load due to the body weight. At the time of output, we present backward force firstly in accordance with the timing of the force peak in step-(1). After the first output, we present forward force in accordance with the timing of the force peak in step-(3), because the peak in step-(2) may not be confirmed depending on the walking speed. Output friction force is determined by exponential interpolation based on the obtained friction data in three velocity conditions (1, 2.5, and 4 km/h).

We developed a haptic device—HapStep to realize the friction force presentation. Though the friction force on the thenar side and the heel side are different, to realize a simpler mechanism, we decided to represent the friction force with 1-DOF simple mechanism for now. As shown in Fig. 3a, the plate to put a foot on is placed on a linear rail (SRS12WMUU, by THK CO., LTD.) whose friction is extremely small ($\mu \leq 0.003$, e.g. μ between typical ice and iron is said to be about 0.027). By winding the wire (HARDCORE X8 #6.0, by DUEL CO., Inc.) attached to the plate with a

Fig. 3 The overview of HapStep. **a** Shows the outline of linear rail mechanism and **b** shows the structure of HapStep



motor (RE40 148877, by Maxon Motor AG.), friction force is applied to the sole. By utilizing the small friction rail, the friction μN becomes extremely small, and the longitudinal friction force is directly transferred to the skin. The low friction enables HapStep to present a rapid force. When we measured the friction force presented by HapStep with the same sensor as the previous section, it was confirmed that HapStep can present the rapid force rising up in about 0.07 seconds. When HapStep presented a rapid force, the applied force blurred for a moment at the beginning of the output. However, we think the blur width was enough small not to be noticed by a user. Thus, it can be said that HapStep can present the rapid friction force stably.

In the future works, we will evaluate whether this 1-DOF haptic device can represent realistic footsteps sensation without walking motion through the comparison with the simpler vibration device.

4 Application

If the walking sensation can be represented while remaining seated, various applications will be realized. It becomes possible to represent the walking sensation in narrower space than the space required by the devices that represent walking sensation with a moving floor to cancel the walking movement. Furthermore, long time experience becomes possible since the user is less tired when playing. The user can experience walking sensation in a space at home, and will be immersed to a video game and a movie character by representing walking sensation in accordance with the motion of the characters.

We have constructed the demo system (Fig. 4) as an application of HapStep. We utilize Unity (by Unity Technologies) to construct the virtual space, and the user

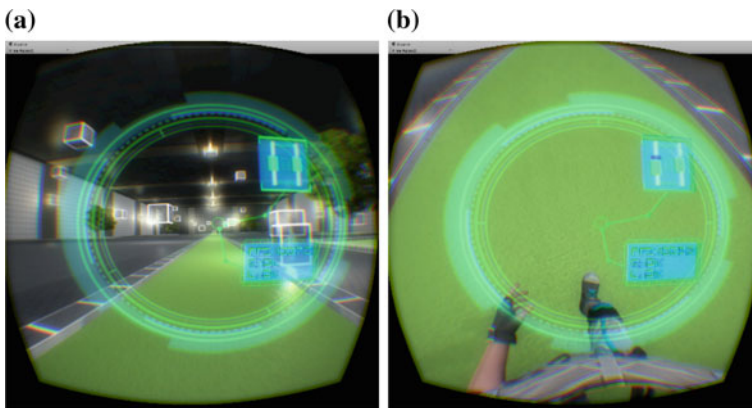


Fig. 4 a The outline of demo system. b According to the walking motion, friction force is presented

can control a virtual character in a space unlimitedly. When the character hits the ground with its foot, the longitudinal friction force is applied to the user in the order of “backward”, “forward” to represent walking sensation. The user wears the HMD and has the character’s point of view. We expect that not only the walking sensation but also the sense of speed can be represented by changing the intervals between each footsteps.

5 Conclusion

In this study, we tried to represent the walking sensation while the user is remaining seated. We developed a novel haptic device—HapStep that represents the footsteps sensation by mimicking the longitudinal friction on the sole of the foot. From the performance evaluation experiment of HapStep, we confirmed that this device can output the friction force stably. Thus, we constructed the system in which footstep sensation is represented according to the visual information. In the future works, we will evaluate the reality of walking sensation represented by HapStep utilizing this system, and investigate whether the representation of the footsteps sensation can express the walking sensation.

References

1. Hiroo, I., Hiroaki, Y., Fumitaka, N.: Gait Master: a versatile locomotion interface for uneven virtual terrain. In: *Proceedings in IEEE Virtual Reality*, pp. 131–137 (2001)
2. Hiroo, I.: Walking about virtual environments on an infinite floor. In: *Proceedings in IEEE Virtual Reality*, pp. 286–293 (1999)
3. John, M.H., Robert, R.C., Xu, Y., Stephen, C.J.: Design specifications for the second generation sarcos treadport locomotion interface. In: *Proceedings in Haptics Symposium*, pp. 1293–1298 (2000)
4. <http://www.virtuix.com/>
5. Rolf, N., Amir, B., Smilen, D., Luca, T., Vincent, H., Stefania, S.: Preliminary experiment combining virtual reality haptic shoes and audio synthesis. In: *Proceedings in EuroHaptics 2010*, pp. 123–129 (2010)
6. Yon, V., Alvin, L., Jeremy, R.C.: Touch is everywhere: floor surfaces as ambient haptic interfaces. In: *Proceedings in IEEE Transactions on Haptics*, vol. 2, no. 3, pp. 148–159 (2009)
7. Ravikrishnan, P.J., Subhransu, K.M., John, F.D., Allison, M.O.: Haptic footstep display. In: *Proceedings in IEEE Haptics Symposium*, pp. 425–430 (2012)

Initial Progress Toward a Surface Morphable Tactile Interface

Seongcheol Mun, Sungryul Yun, Saekwang Nam, Seung-Koo Park and Ki-Uk Kyung

Abstract We demonstrate an initial progress prototype toward a surface morphable tactile interface. The surface is composed of thin film type electro-active material (EAP) and its initial shape is maintained to be a flat membrane. Surface of the membrane is designed to be protrusive by electric field. The height of the protrusion and transition speed of the shape change would be controllable by amplitude and frequency of driving signals.

Keywords Morphable · Tactile · Interface

1 Introduction

We imagine a self-morphing surface which provides adaptive surface physical shape depending on task [1]. For example, the surface of mobile phone is transformed to a keypad shape including physically arranged buttons when a user need to type characters on a touch screen. In order to use physically deformable tactile display on a touch screen device, all components of the tactile display need to be transparent thin films. In this paper, we introduce an initial progress toward a surface morphable interface based on electro-active polymer material.

2 Demonstration

A demonstrator is composed of two buttons with a diameter of 10 and 5 mm respectively (Fig. 1). It maintains flat shape membrane initially and the membrane makes dome shape by electric field. Protrusion of the button is controlled by

S. Mun · S. Yun · S. Nam · S.-K. Park · K.-U. Kyung (✉)
Electronics and Telecommunications Research Institute (ETRI), 218 Gajeong-no,
Yuseong-gu, Daejeon 305-700, Korea
e-mail: kyungku@etri.re.kr

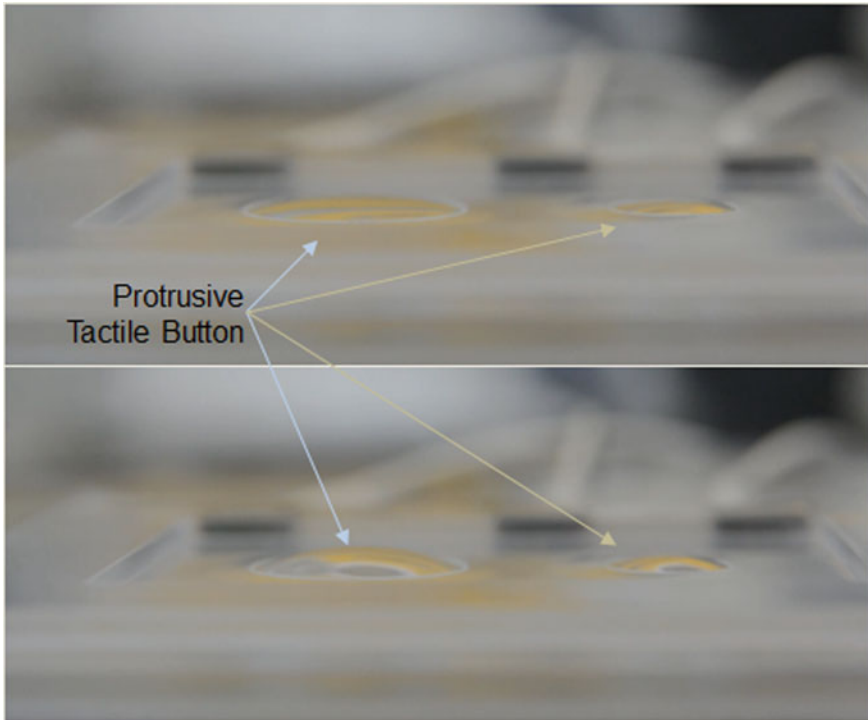


Fig. 1 Morphing tactile button

variation of the electric field. Change of physical shape of the buttons is based on physical transformation of electro-active polymer. This prototype provides very weak output force against finger pressing but it is perceivable. A transparent electro-active polymer coated with compliant transparent electrode layer is used for implementing the button. Total thickness of this prototype is about 1 mm and transparency is 60–80% depending on number of electrode layers. In the demonstration, we vary frequency and amplitude of the protrusion for variation of tactile feeling. This demonstration is at the very beginning stage and we are trying to increase magnitude of output force without loss of transparency.

Reference

1. Kyung, K.U., Lim, J.M., Lim, Y. A. et al.: TAXEL: initial progress toward self-morphing visiohaptic interface. In: IEEE World Haptics 2011, pp. 37–42. IEEE Press, New York (2011)

Simulating Texture Sensation of Textiles Using Thermal and Vibro-Tactile Stimulations

Katsunari Sato

Abstract This study describes the construction of a haptic display that produces thermal and vibro-tactile stimulation to simulate the texture sensation of textiles, which can help online shoppers evaluate products. The results of the sensory evaluation demonstrate that using thermal stimulation in addition to vibro-tactile stimulation improves texture sensation. The current challenges in the development of haptics displays are also discussed.

Keywords Textile • Texture sensation • Thermal display • Vibro-tactile display

1 Introduction

The texture sensation of textiles, which includes sensing properties such as roughness, softness, and coldness [1], plays an important role in evaluating products such as garments. However, there is no way to experience this while selecting and purchasing online products. Haptic devices that simulate the texture of textiles [2–5] are proposed to develop a more advanced online shopping system.

Conventional haptic devices depend on vibro-tactile stimulation to reproduce the roughness or frictional sensation perceived when a human traces the surface of textiles with his/her fingertips [2, 3]. Other studies indicate that thermal stimulation is needed to represent the heat transfer characteristics such as heat conductivity [4] and wet state of textiles [5]. According to these studies, a haptic display utilizing both vibro-tactile and thermal stimulations would provide a more realistic texture sensation of textiles. To design and develop such a haptic display, we investigated the effect of thermal stimulation on vibro-tactile sensation and the differences in sensations produced by the combined stimulation and real textiles.

K. Sato (✉)
Nara Women's University, Nara, Japan
e-mail: Katsu-sato@cc.nara-wu.ac.jp

This study describes the construction of a mouse-type haptic display that produces thermal and vibro-tactile stimulation and compares the sensations produced by the haptic display and real textiles.

2 Thermal and Vibro-Tactile Display

Figure 1 shows the developed haptic display that consists of Peltier elements with thermistors, a vibrator, and a mouse. Four Peltier elements (KSMH029F, KOMATSU KELK Co. Ltd.) apply spatially divided hot and cold stimuli to realize a compact and highly efficient thermal stimulation display [6]. The vibrator is a force reactor (L-type, Alps Electric Co., Ltd.) that produces vibro-tactile stimulation through audio signals. These components are mounted on the left button of the mouse. When users click and drag the left button, they will feel the sensation on their fingers.

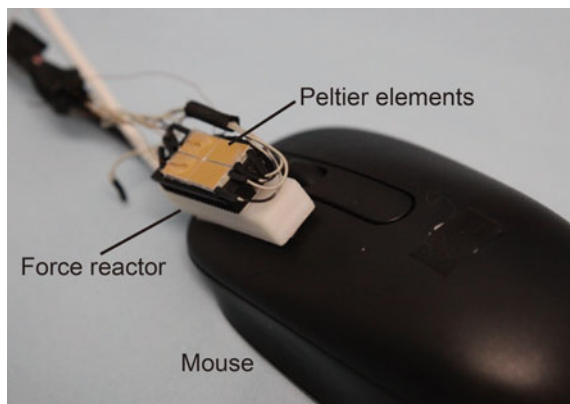
3 Texture Sensation of Textiles

This study uses the semantic differential (SD) method along with factor analysis to evaluate the effect of thermal stimulation and the differences between the sensations produced by haptic display and real textiles.

3.1 Method of Evaluation

The evaluation involved twenty-three and twenty-one female student participants who evaluated real textiles and haptic stimulations, respectively; twenty of them participated in both.

Fig. 1 Thermal and vibro-tactile display on the mouse



Six types of real textiles were used in the evaluation: 1. Cotton broadcloth, 2. Cotton velvet, 3. Silk, 4. Satin, 5. Kanekalon, and 6. Polypropylene twill. The author selected them because these textiles, when touched, produced sensations different from those in the pilot experiment. The textiles were placed on a cooling plate (NCP-2215, Nisshinrika Co., Ltd.) maintained at a surface temperature of 30 °C (n) or 20 °C (c).

The author used audio noise signals identical to those produced when stroking textiles for vibro-tactile stimulation. The signals for vibro-tactile stimulation are denoted by white (W), blue (B), and pink (P) noises to evaluate the effects of the frequency of vibration. Furthermore, two types of thermal stimulations were used: none (n) and approximately 2 °C/s (c) change in skin temperature.

The participants placed their right index finger on a hot plate (NHP-M20, Nisshinrika Co., Ltd.) maintained at a surface temperature of 32 °C for approximately 2 min. Then, they either performed a mouse drag or stroked the textiles to experience sensations produced by the texture. The conditions for stimulation or textile stroking were randomly selected. The process involved moving the finger from left to right at a velocity of 5 cm/s for approximately 2 s. The participants were allowed to repeat the movement. After this, they evaluated their perception using twelve pairs of adjectives (Table 1, [1]) on a scale of minus three to plus three. In the evaluation process, a flat board made of chamaecyparis obtusa was used as the standard texture. The participants evaluated the stimulations and real textiles against the standard. The participants wore eye masks and headphones to eliminate visual and audio effects.

3.2 Results and Discussion

Factor analysis was conducted using a combination of six factors and varimax rotation with all the results from the seven-scaled evaluation. The six factors were labeled “rough,” “cold,” “soft,” “comfort,” “dry,” and “light.” Figures 2, 3 and 4 shows the results plotted using the factor scores on a two-dimensional space. The first and second examples are for rough-cold and dry-light factor spaces, respectively. In each graph, the circular and cross symbols represent the scores of real textiles and stimulation evaluation, respectively. The black and blue dots represent the results obtained with and without temperature change on the finger, respectively. The numbers with “n” or “c” represent the type of textiles (listed in Sect. 3.1) and the type of thermal stimulation. Similarly, the capital letters denote

Table 1 List of adjective pairs for evaluation of sensations [1]

| | | | |
|-----------------|-----------------------|-------------|---------------------|
| Smooth–textured | Scratchy–not scratchy | Hot–cold | Slimy–silky |
| Bumpy–flat | Polish–grainy | Heavy–light | Hard–soft |
| Rough–fine | Coolish–not coolish | Wet–dry | Elastic–not elastic |

Fig. 2 Results of factor analysis in two-dimensional factor space (rough-hot)

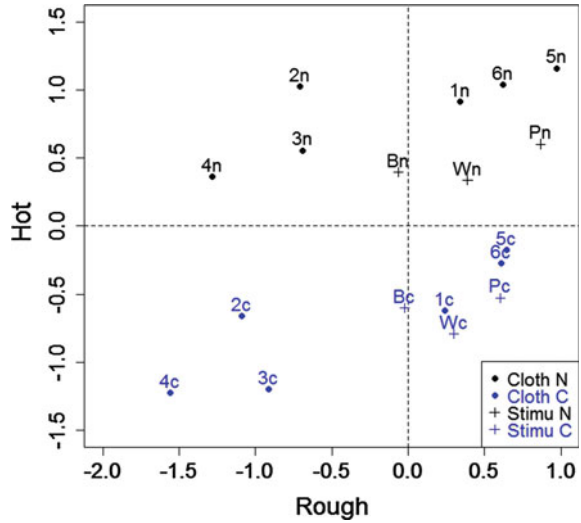
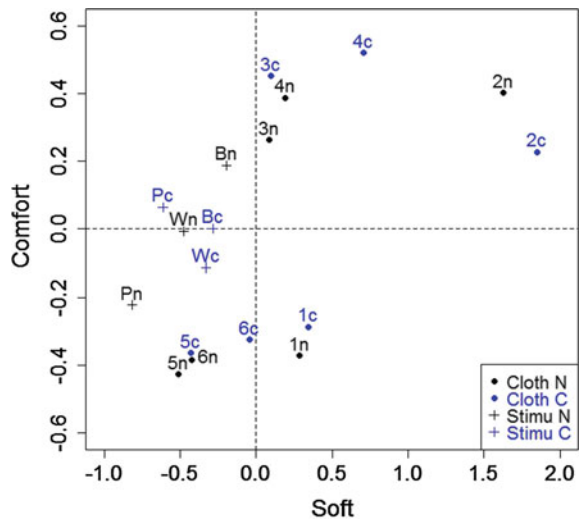


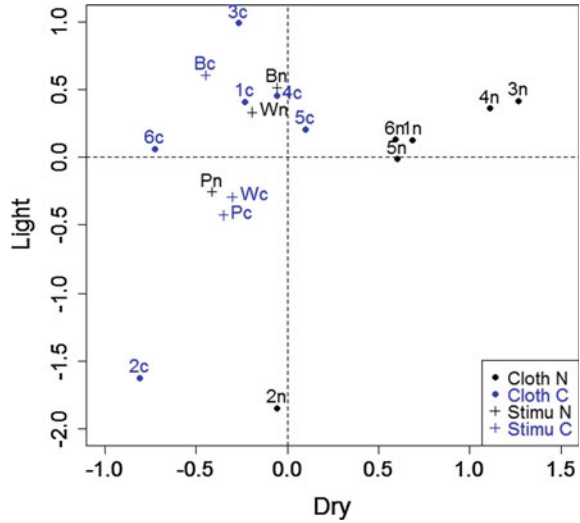
Fig. 3 Results of factor analysis in two-dimensional factor space (soft-comfort)



the vibration conditions. For example, 3c and Pn represent cooled silk and pink noise without thermal stimulation, respectively.

From the results, we can confirm that thermal stimulation can represent changes in the heat sensation of textiles (Fig. 2) but cannot represent changes in dry sensation (Fig. 4). This can be explained based on the findings from previous studies; these studies indicate that both coldness and softness affect the perception of wetness [5]. Therefore, the haptic display must also include stimulations related to softness for representing changes in the dry sensation of textures. Another

Fig. 4 Results of factor analysis in two-dimensional factor space (dry–light)



interesting finding from this study is that the rough sensation seems to be adversely affected by the inclusion of thermal stimulation (Fig. 2). For other factors, no change was noted in the perceived sensation because of thermal stimulation.

With respect to the roughness factor (Fig. 2), the type of vibro-tactile stimulation (frequency of vibration) appears to play a role; a lower frequency of vibration could enhance the rough sensation. However, this still does not provide the range of sensations observed in real textiles, particularly the smoother sensations. This deficiency in texture sensations produced by the stimulation when compared with real textiles is the same as that in other studies [2–4]. Methods for improving the range of sensations produced by the haptic display need to be studied.

4 Conclusion

The results of the sensory evaluation of the stimulation and real textiles show that thermal stimulation along with vibro-tactile stimulation improves the range of texture sensations produced using the haptic display. The results also demonstrate that the range of sensations must be expanded to improve the quality of the haptic display.

Acknowledgements This work is partially supported by JST ACCEL Embodied Media project.

References

1. Shirado, H., Maeno, T.: Modeling of human texture perception for tactile displays and sensors. Proc. World Haptics **2005**, 629–630 (2005)

2. Konyo, M., Tadokoro, S., Takamori, T., Oguro, K.: Artificial tactile feel display using soft gel actuators. *Proc. IEEE ICRA* **200**, 3416–3421 (2000)
3. Messaoud, W.B., BUENO, M.-A., Semail, B.: Textile fabrics' texture: from multi-level feature extraction to tactile simulation. In: *Proceedings of EuroHaptics 2016*, pp. 294–303 (2016)
4. Kurogi, T., Nakayama, M., Sato, K., Kamuro, S., Fernando, C.L., Furukawa, M., Minamizawa, K., Tachi, S.: Haptic transmission system to recognize differences in surface textures of objects for teleexistence. In: *Proceedings of IEEE Virtual Reality 2013*, PO-042, pp. 137–138 (2013)
5. Shibahara, M., Sato, K.: Illusion of wet sensation by controlling temperature and softness of dry cloth. In: *Proceedings of EuroHaptics 2016*, pp. 512–520 (2016)
6. Sato, K., Maeno, T.: Presentation of rapid temperature change using spatially divided hot and cold stimuli. *J. Robot. Mechatron.* **25**(3), 497–505 (2013)

Tactile Display Based on Skin-Propagated Vibration

Yasutoshi Takekawa, Tatsuya Hasegawa, Yoshihiro Tanaka,
Kouta Minamizawa and Akihito Sano

Abstract We have developed a wearable skin vibration sensor that allows users to touch objects directly. The sensor detects skin-propagated vibrations elicited by mechanical interaction between the fingertip and an object. Here, the sensor output includes properties of the user's skin as well as the object. In this paper, texture presentation by using the sensor output is investigated. A simple tactile display is assembled with a vibrator. The experimental result shows that the texture presentation utilizing the inverse function of the transfer function of the sensor output gives more natural feeling as compared with the condition without the signal processing.

Keywords Tactile display · Skin-propagated vibration · Skin properties

1 Introduction

Mechanical stimuli to the skin in tactile displays are often based on simulations and actual measurement data. Culbertson et al. recorded the vibration data with an instrumented tool and created synthetic texture signals in response to user movements [1]. Tanaka et al. developed a wearable skin vibration sensor that allows users to touch objects directly [2]. The sensor detects skin-propagated vibrations elicited by mechanical interaction between the fingertip and an object. The vibration elicited on the skin is one of the important parameters on the evaluation of objects' textures. A simple tactile display can be assembled with a vibrator by using the sensor output. Here, the sensor output includes properties of the user's skin as well as the object.

Y. Takekawa (✉) · T. Hasegawa · Y. Tanaka · A. Sano
Nagoya Institute of Technology, Gokiso-cho, Showa-ku, Nagoya, Japan
e-mail: y.takekawa.161@nitech.jp

Y. Tanaka
e-mail: tanaka.yoshihiro@nitech.ac.jp

Y. Tanaka
JST PRESTO, Kawaguchi, Japan

K. Minamizawa
Keio University Graduate School of Media Design, Hiyoshi, Kohoku-ku, Yokohama, Japan

© Springer Nature Singapore Pte Ltd. 2018
S. Hasegawa et al. (eds.), *Haptic Interaction*, Lecture Notes
in Electrical Engineering 432, DOI 10.1007/978-981-10-4157-0_21

In this paper, texture presentation with a vibrator by using the sensor output is investigated. Conditions of the absence and the presence of the signal processing considering the transfer function of the sensor output are compared in an evaluation of convincing (natural) texture presentation.

2 Experimental Method

We assembled a tactile display system having real-time signal processing shown in Fig. 1. This system consists of the tactile sensor, a vibrator, two amplifiers for the sensor and the vibrator, and an equalizer for signal processing. Frequency response of the fingertip was calculated from the acceleration of the input vibration on the fingertip and the sensor output for sinusoidal sweep vibrations by using a piezo actuator [2]. It includes skin physical properties of the finger pad and physical and electrical properties of the sensor. The transfer function varies among individuals, but its overall tendency is similar. Thus, we used a typical transfer function in this experiment as shown in Fig. 2. The equalizer was set to be similar to the inverse function of that

Fig. 1 Tactile display system and inverse function used for the signal processing to the sensor output

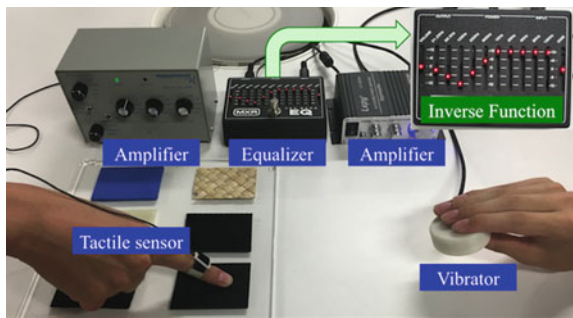
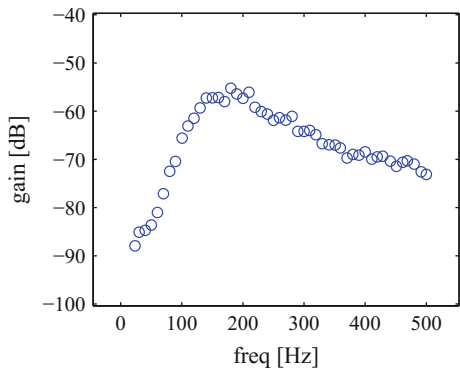


Fig. 2 Typical transfer function from the input vibration on the fingertip to the sensor output



shown in Fig. 2. Subjects were asked to feel two vibrations in the conditions of the absence and the presence of the signal processing of the inverse function, and answer which was more convincing texture presentation.

3 Results and Discussion

The preliminary experimental result showed that many subjects answered the texture presentation utilizing the inverse function is more convincing. It might be perceived as natural. The sensor output includes the skin properties of a finger pad, thus, the vibration in the condition without the signal processing includes two individuals' skin properties. We measured the skin-propagated vibration presented by the vibrator in each condition. The waveform of the power spectral density of the sensor output in the condition with the signal processing tended similar to that when the fingertip touches the actual texture as compared with the condition without the signal processing. For applications, this system has an advantage for simple texture presentation. In future work, we will improve convincing of the feedback and investigate further applications.

References

1. Culbertson, H., Unwin, J., Goodman, B.E., Kuchenbecker, K.J.: Generating haptic texture models from unconstrained tool-surface interactions. In: Proceedings of IEEE World Haptics Conference 2013, pp. 295–300 (2013)
2. Tanaka, Y., Nguyen, D.P., Fukuda, T., Sano, A.: Wearable skin vibration sensor using a PVDF film. In: Proceedings of IEEE World Haptics Conference 2015, pp. 146–151 (2015)

High-Quality Texture Display: The Use of Vibrotactile and Variable-Friction Stimuli in Conjunction

Ken Ito, Shogo Okamoto, Hatem Elfekey and Yoji Yamada

Abstract The sliding of a finger on a material surface results in complex physical interactions. Tactile texture displays have been limited in their ability to capture the aspects of these interactions. As a step forward, we have combined two complementary types of tactile stimuli, vibrotactile and electrostatic, to deliver roughness textures with high realism. These two types of stimuli represent the surface roughness and friction. We then conducted an experiment where participants agreed that the experience of the texture presented by the combined stimuli was more similar to that of an actual specimen than that of textures presented by either type of stimulus. Our experiment indicates that combining vibrotactile and electrostatic friction stimuli, both of these have been studied extensively, results in high-quality tactile contents for surface texture displays.

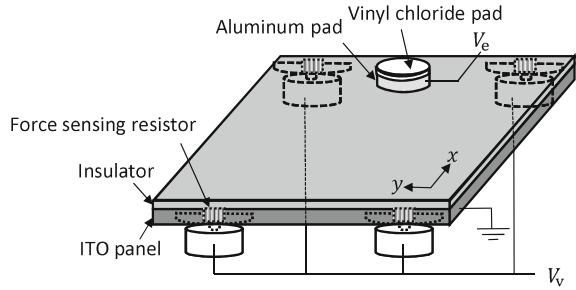
Keywords Tactile display · Vibrotactile · Electrostatic · Texture · Surface texture display · Variable-friction stimulus

1 Introduction

The tactile texture displays are categorized into vibrotactile and variable-friction stimuli [1–4]. Vibrotactile stimuli actively produce mechanical displacements on a fingertip. Variable-friction stimuli induce tactile sensations by controlling the surface friction between a fingertip and a display device. These two types of stimuli are distinct and complementary: For example, vibrotactile stimuli actively provide the tactile sensation, whereas variable-friction stimuli do so passively. In addition, vibrotactile stimuli are good for the presentation of surface roughness [5, 6], whereas friction stimuli are more suited for surfaces where friction is dominant in terms of textural perception [7].

K. Ito (✉) · S. Okamoto · H. Elfekey · Y. Yamada
Mechanical Science and Engineering, Graduate School of Engineering,
Nagoya University, Furo-Cho, Chikusa-ku, Nagoya 464-8603, Japan
e-mail: itou.ken@a.mbox.nagoya-u.ac.jp

Fig. 1 Overall structure of the proposed tactile display with vibrotactile and electrostatic stimuli



These complementary characteristics suggest that a combination of the two types may result in stimuli of higher quality with each type in isolation. An attempt has been made to combine the stimuli [8]; the researchers, however, did not attempt to present the high-quality textures by simultaneously activating the two types of stimuli. Other approach employed a combination of mechanical and electric current stimuli for the purpose of quality tactile displaying [9].

Using vibrotactile and variable-friction stimuli in conjunction, we were able to deliver a roughness texture with a high degree of realism. Real surfaces possess the properties of surface roughness and friction; high-quality virtual surfaces may be realized by using the two types of stimuli simultaneously. This approach can make full use of the two types of stimuli to eliminate the flaws in earlier methods for improving the quality of surface texture displays and vastly improves the quality of virtual tactile textures.

2 Tactile Texture Display Combining Vibrotactile and Electrostatic Stimuli

Figure 1 shows the tactile display developed in this study. Vibrotactile stimuli on the proposed display were produced by four voice coil actuators (X-1741, Neomax Engineering Co. Ltd., Japan), located at each corner of the top panel. The four actuators were synchronously driven by a current amplifier (ADS 50/5, Maxon Motor AG, Switzerland) and produced mechanical vibratory stimuli along the normal to the top panel. The electrostatic stimuli were produced by electrostatic forces induced by a voltage between the aluminum pad and an ITO panel (V_e). An insulator (kimotect PA8X, KIMOTO Co. Ltd., Japan) was fixed on the ITO plate. The voltage V_e was driven by a high-voltage amplifier (HJOPS-1B20, Matsusada Precision Inc., Japan). Four force-sensing resistors (FSR 400 short, Interlink Electronics Inc., USA) were affixed between each voice coil motor and the top plate. The two amplifiers and four resistors were connected to a data acquisition board (TNS-6812, Interface Corporation, Japan). The position of the finger pad was calculated based on the output from the four force-sensing elements. Thus, the display can present the stimulus based

upon the position of the pad. The voltage and current signals were processed at a sampling frequency of 1 kHz.

3 Experimental Procedure

3.1 Tasks

In this experiment, a rank task was applied to assess the performance of the combined texture stimuli. Participants experienced three stimuli: vibrotactile, electrostatic, and vibrotactile plus electrostatic. They compared three types of stimuli with a specimen (shown in Fig. 2), and ranked the three types of stimuli in terms of realism. If a participant ranked a stimulus as first, the stimulus was felt like the specimen the most. Because our display could not distribute stimuli in the contact area, the participants scanned the specimen with a round tip probe, as shown in Fig. 2a. The spatial wavelength of the specimen was 3 mm, and the top of the specimen was 1 mm above the bottom. The participants could experience the specimen and three stimuli as many as they wanted.

3.2 Participants

Six volunteers (all students, non experts, right handed, average age 23) participated in this experiment. They were not informed of the objective of the research.

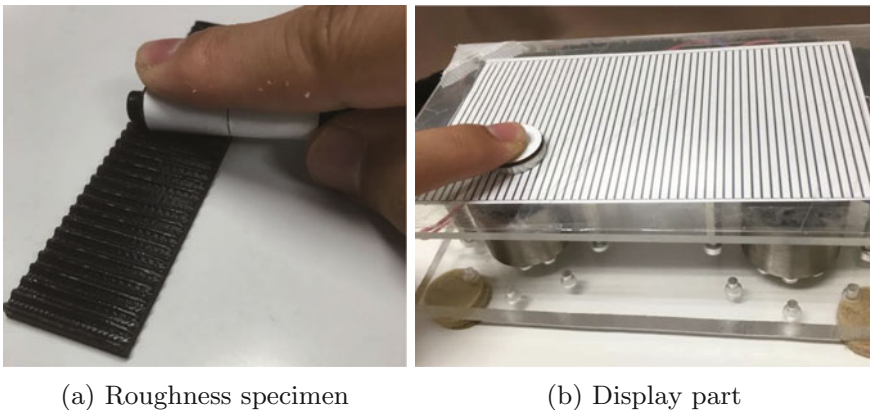


Fig. 2 Roughness specimen to be compared with virtual textures. Participant in the experiment scanned the surface with a round tip probe

3.3 Roughness Texture Stimuli

We used vibrotactile and electrostatic roughness texture stimuli. The presentation algorithm for each stimulus is simple. It has been used in numerous earlier studies. Those studies, however, used only one of the two stimuli (vibrotactile and electrostatic).

The roughness texture stimuli presented a roughness grating scale with a sinusoidal surface asperity, with a spatial period of $\lambda = 3$ mm. The resultant drive force F_v for the vibrotactile actuators was determined by (1), as below:

$$F_v(t) = A \sin 2\pi \frac{x(t)}{\lambda} \quad (1)$$

where $x(t)$ and A are the position of the finger pad and the gain of the force, respectively. The A value were 2.0 and 1.7 N for the vibrotactile and vibrotactile plus electrostatic stimuli conditions, respectively. The voltage instruction to the electrostatic actuator was determined by

$$V_e(t) = B \cos 2\pi \frac{x(t)}{\lambda} \quad (2)$$

where $x(t)$ and B are the position of the finger pad and the voltage gain respectively. The friction force was determined using

$$F_e(t) = \mu(W + kV_e^2(t)) \quad (3)$$

where μ , W , and k are respectively the coefficient of friction between the finger pad and the surface of the panel, the load normal to the panel, and a constant that determine the electrostatic force. k was mainly influenced by the electrode surface area, and the dielectric constant and thickness of the insulator. As a result, the variable-friction force F_e was 0.45–0.89 N for the electrostatic condition when the pressing force W was 1 N. Further, F_e was 0.45–0.79 N for the vibrotactile plus electrostatic condition, with $W = 1$ N. The phases of the stimuli for surface displacement and friction were separated by $\pi/2$ [10, 11]. The force and voltage gains for each stimulus condition were empirically best tuned for each condition such that each texture stimulus was perceived as most similar to the actual roughness specimen shown before the virtual stimulus was presented.

4 Experimental Results

Figure 3 shows the ranks assigned to each stimulus condition by the individual participants. We used the Wilcoxon Rank Sum Test to evaluate two pairs of stimuli; the combined and vibrotactile conditions, and then, the combined and electrostatic

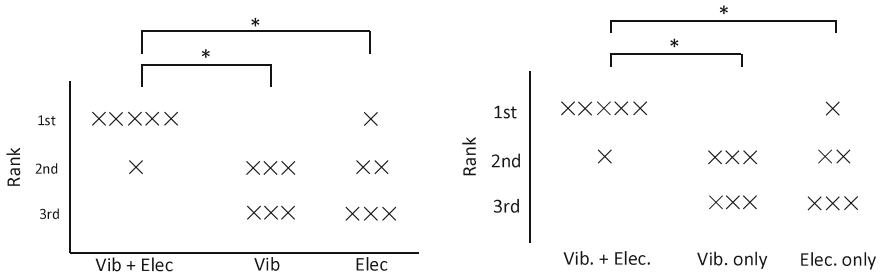


Fig. 3 Experimental result: frequencies of ranks for each stimulus (* indicates $p < 0.05$)

conditions. There were significant differences in two pairs ($p < 0.05$, after Bonferoni correction). These results showed that we could produce high-quality textures by combining Vibrotactile stimuli and electrostatic friction stimuli.

5 Conclusions

We developed a tactile display that can present vibrotactile and variable-friction stimuli to improve the quality of tactile displays. We conclude that the combination of the stimuli results in a more realistic rendering of textures compared to that afforded by vibrotactile and variable-friction stimuli individually.

Acknowledgements This study was in part supported by MEXT Kakenhi (15H05923), SCOPE (142106003).

References

- Asano, S., Okamoto, S., Yamada, Y.: Vibrotactile stimulation to increase and decrease texture roughness. *IEEE Trans. Hum. Mach. Syst.* **45**(3), 393–398 (2015)
- Okamoto, S., Yamada, Y.: Lossy data compression of vibrotactile material-like textures. *IEEE Trans. Haptics* **6**(1), 69–80 (2013)
- Nakamura, T., Yamamoto, A.: A multi-user surface visuo-haptic display using electrostatic friction modulation and capacitive-type position sensing. *IEEE Trans. Haptics* (2016)
- Chubb, E.C., Colgate, J.E., Peshkin, M.A.: ShiverPaD: a glass haptic surface that produces shear force on a bare finger. *IEEE Trans. Haptics* **3**(3), 189–198 (2010)
- Asano, S., Okamoto, S., Yamada, Y.: Toward quality texture display: vibrotactile stimuli to modify material roughness sensations. *Adv. Robot.* **28**(16), 1079–1089 (2014)
- Yamauchi, T., Okamoto, S., Konyo, M., Tadokoro, S.: Real-time remote transmission of multiple tactile properties through master-slave robot system. In: *Proceedings of the 2010 IEEE International Conference on Robotics and Automation*, pp. 1753–1760 (2010)
- Bau, O., Poupyrev, I., Israr, A., Harrison, C.: Teslatouch: electrovibration for touch surfaces. In: *Proceedings of Annual ACM Symposium on User Interface Software and Technology*, pp. 283–292 (2010)

8. Pyo, D., Ryu, S., Kim, S.-C., Kwon, D.-S.: Haptic interaction on a touch surface. In: Lecture notes in Electrical Engineering, vol. 277. Springer (2015)
9. Yem, V., Okazaki, R., Kajimoto, H.: Fingar: combination of electrical and mechanical stimulation for high-fidelity tactile presentation. In: Proceedings of ACM SIGGRAPH Emerging Technologies, pp. 13–14 (2016)
10. Robles-De-La-Torre, G., Hayward, V.: Force can overcome object geometry in the perception of shape through active touch. *Nature* **412**, 445–448 (2001)
11. Fujii, Y., Okamoto, S., Yamada, Y.: Friction model of fingertip sliding over wavy surface for friction-variable tactile feedback panel. *Adv. Robot.* **30** (2016)

Hybrid Focus Using 70 and 40 kHz Ultrasound in Mid-Air Tactile Display

Mitsuru Ito, Daisuke Wakuda, Yasutoshi Makino
and Hiroyuki Shinoda

Abstract We examine haptic sensation by a hybrid focus using 70 and 40 kHz ultrasound. The hybrid focus was generated by 70 and 40 kHz phased array. The spatial resolution of 70 kHz phased array is higher than that of 40 kHz case, instead, the attenuation in the air is large in the 70 kHz case. Therefore, a hybrid system is energy-efficient in which a lower spatial frequency component of force pattern is produced by 40 kHz ultrasound and a higher one is created by 70 kHz. In the preliminary experiment, the subjects touched the hybrid focus and reported the similarity of the sensation to the 70 kHz focus.

Keywords Midair haptics · Tactile display · Airborne ultrasound · Acoustic radiation pressure

M. Ito (✉) · Y. Makino · H. Shinoda

Department of Complexity Science and Engineering, Graduate School of
Frontier Science, The University of Tokyo, 5-1-5 Kashiwanoha, Kashiwa,
Chiba, Japan

e-mail: ito@hapis.k.u-tokyo.ac.jp

URL: <http://www.hapis.k.u-tokyo.ac.jp/>

Y. Makino

e-mail: yasutoshi_makino@k.u-tokyo.ac.jp

H. Shinoda

e-mail: hiroyuki_shinoda@k.u-tokyo.ac.jp

D. Wakuda

Sensing Solution Development Center, Automotive and Industrial Systems
Company, Panasonic Corporation, 1006 Kadoma, Kadoma, Osaka, Japan

e-mail: wakuda_daisuke@jp.panasonic.com

© Springer Nature Singapore Pte Ltd. 2018

S. Hasegawa et al. (eds.), *Haptic Interaction*, Lecture Notes
in Electrical Engineering 432, DOI 10.1007/978-981-10-4157-0_23

1 Introduction

Mid-air haptic display [1] using ultrasound [2, 3] produces tactile sensation to human skins without wearing any devices. But the conventional mid-air haptic device using ultrasound have a significant limitation: its low spatial resolution due to the ultrasound frequency. Since the conventional devices used 40 kHz ultrasound with an 8.5 mm wavelength [2, 4], the focal spot of 40 kHz device was comparable to, or larger than, a finger pad.

The use of 70 kHz ultrasound tried in [5] can improve the spatial resolution by 1.75 times and produce a localized pattern on the finger pad. But a problem of the use of high-frequency ultrasound is the large attenuation in the air. In addition, the efficiency of electro-acoustic conversion is still low, at least in the current device. Therefore, a hybrid system of low-frequency and high-frequency ultrasounds is energy-efficient in which a lower spatial frequency component of force pattern is produced by 40 kHz ultrasound and a higher one is created by 70 kHz.

In this demonstration, we examine haptic sensation by the hybrid focus using 70 and 40 kHz phased array. In the preliminary experiment, the subjects reported they felt a small spot comparable to the 70 kHz case.

2 Acoustic Radiation Pressure in Hybrid Case

The acoustic radiation pressure P (Pa) is proportional to the sound energy density as

$$P = \alpha E = \alpha \frac{p^2}{\rho c^2} \quad (1)$$

where E (J/m^3), p (Pa), ρ (kg/m^3), and c (m/s) denote the sound energy density, sound pressure (effective value), density of the medium, and sound velocity, respectively. α denotes a constant ranging between 1 and 2 depending on the reflection properties of the object surface.

In a hybrid case of ω_1 and ω_2 components, the instantaneous value of the sound pressure is given as

$$p_M(t) = \sqrt{2}p_1(t) \cos(\omega_1 t + \theta_1(t)) + \sqrt{2}p_2(t) \cos(\omega_2 t + \theta_2(t)) \quad (2)$$

Then the radiation pressure proportional to the acoustic energy density is written as

$$P(t) = \frac{\alpha}{\rho c^2} \overline{p_M^2} = \frac{\alpha}{\rho c^2} (p_1^2 + p_2^2) = P_1(t) + P_2(t) \quad (3)$$

under the assumption that the constant α is common to both ω_1 and ω_2 components. We also assumed that the time constants of $p_1(t)$, $p_2(t)$, $\theta_1(t)$, and $\theta_2(t)$ are much

longer than the ultrasound periods, and $\overline{p_M^2}$ shows the temporal average of p_M^2 in a short term comparable to the ultrasound period. $P_1(t)$ and $P_2(t)$ mean the radiation pressure in the case each of the components solely exists.

3 Hybrid Focus

This system is constructed by 70 and 40 kHz phased array. Figure 1 shows the appearance of the phased arrays and the setup for generating hybrid focus. This device generates single focal point along the center axis perpendicular to 70 kHz phased array surface. The focus of 70 and 40 kHz phased array is set at the same

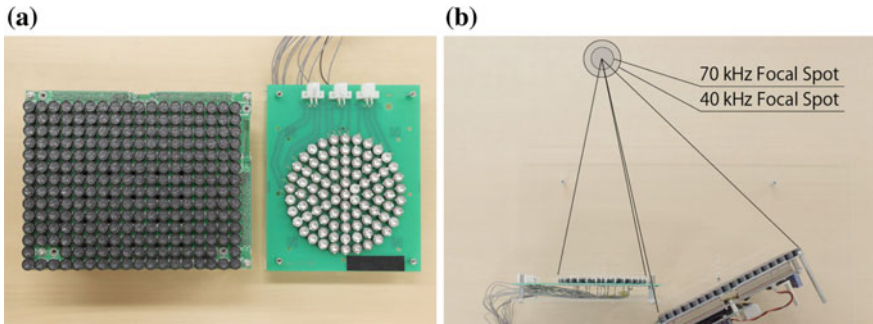
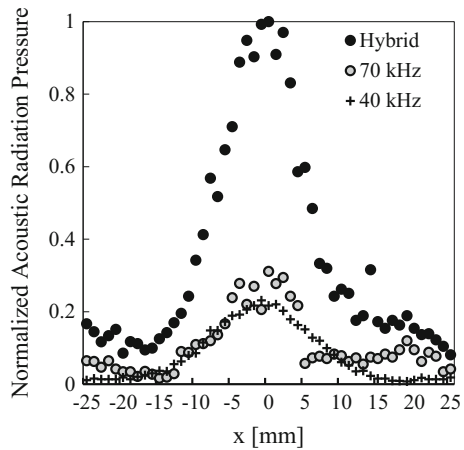


Fig. 1 Photograph of the used phased array. *a* Left 40 kHz phased array, *Right* 70 kHz phased array. *b* Arrangement of 40 and 70 kHz phased array. The angle of 40 kHz phased array is 30° to 70 kHz phased array

Fig. 2 Radiation pressure distribution along the line $y = 0$ parallel to the 70 kHz phased array surface. The focal point was created at $x = 0$ and 300 mm from the 70 kHz phased array surface. “70 kHz” plots show the radiation pressure for the case that only the 70 kHz phased array was turned on



position. We set the focal point to 300 mm from the surface of 70 kHz phased array.

The measured acoustic radiation pressure in the hybrid case is shown in Fig. 2. The measured maximum sound pressure is about 1.5 kPa in the hybrid condition.

Acknowledgements This research was partly supported by JSPS KAKENHI 16H06303 and JST ACCEL Embodied Media Project.

References

1. Sodhi, R., Poupyrev, I., Glisson, M., Israr, A.: AIREAL: interactive tactile experiences in free air. *ACM Trans. Graph.* **32**(4), 134 (2013)
2. Hoshi, T., Takahashi, M., Iwamoto, T., Shinoda, H.: Noncontact tactile display based on radiation pressure of airborne ultrasound. *IEEE Trans. Haptics* **3**(3), 155–165 (2010)
3. Long, B., Seah, S.A., Carter, T., Subramanian, S.: Rendering volumetric haptic shapes in mid-air using ultrasound. *ACM Trans. Graph.* **33**(6), 181 (2014)
4. Hasegawa, K., Shinoda, H.: Aerial display of vibrotactile sensation with high spatial-temporal resolution using large-aperture airborne ultrasound phased array. In: *Proceedings of the IEEE World Haptics Conference*, pp. 31–36 (2013)
5. Ito, M., Wakuda, D., Inoue, S., Makino, Y., Shinoda, H.: high spatial resolution midair tactile display using 70 kHz ultrasound. In: *International Conference on Human Haptic Sensing and Touch Enabled Computer Applications*, pp. 57–67 (2016)

Tactile Presentation Using Mechanical and Electrical Stimulation

Vibol Yem, Sugarragchaa Khurelbaatar, Erika Oishi
and Hiroyuki Kajimoto

Abstract In our study, we developed the FinGAR (Finger Glove for Augmented Reality), which is a tactile display that uses a combination of electrical and mechanical stimulation. The device can selectively stimulate four channels of tactile sensation, based on pressure, low-frequency vibration, high-frequency vibration, and shear stretching, to achieve high-fidelity tactile sensation. The FinGAR was designed to be lightweight, to have a simple mechanism, to be easy to wear, and to ensure that it does not affect natural finger movement. By combining FinGAR with a virtual reality system, users are able to touch and play with virtual objects.

Keywords FinGAR · Electrical stimulation · Mechanical stimulation · Virtual reality · Augmented reality

1 Introduction

Numerous studies have attempted to reproduce tactile sensation via presentation of skin deformation [1], pin matrix pressure [2], vibration [3, 4], or electrostatic force [5]. Each study succeeded in reproducing some degree of tactile feeling, but in a relatively small range. In principle, it may be possible to reproduce any tactile sensation if we could drive the skin with sufficient spatial (up to 1.5 mm at the fingertip) and temporal (0–1 kHz) resolution; however, the skin has a large mass

V. Yem (✉) · S. Khurelbaatar · E. Oishi · H. Kajimoto
The University of Electro-Communications, Chofu, Tokyo 182-8585, Japan
e-mail: yem@kaji-lab.jp

S. Khurelbaatar
e-mail: sura@kaji-lab.jp

E. Oishi
e-mail: oishi@kaji-lab.jp

H. Kajimoto
e-mail: kajimoto@kaji-lab.jp

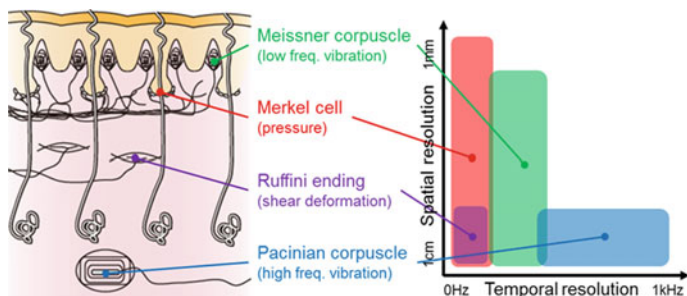


Fig. 1 Mechanoreceptors in skin and their spatiotemporal characteristics

and damping action, and it is difficult to develop the versatile micromachines required for tactile displays.

Tactile information is provided by four types of mechanoreceptors in the skin [6], which respond to four channels of sensation. These mechanoreceptors are Merkel cells for pressure, Meissner's corpuscles for low-frequency vibrations, Pacinian corpuscles for high-frequency vibrations, and Ruffini's endings for shear deformation (see Fig. 1). If we could activate these receptors selectively and combine the four channels, we could then reconstruct any tactile sensation. This is similar to primary (red-green-blue, or RGB) colors in vision, which are based on the physiological existence of three types of cone cells in the retina.

To achieve both selective stimulation and a simple mechanical design, we proposed a combination of electrical and mechanical stimulation and developed a small, lightweight tactile display called FinGAR (Finger Glove for Augmented Reality). Electrical stimulation with an electrode array presents pressure and low-frequency vibrations with spatial resolution, and mechanical stimulation is used to present high-frequency vibrations and skin deformation. We also developed a virtual reality application in which the user can touch and play with objects while receiving tactile sensation on their thumb, index and middle fingers.

Our virtual reality system was exhibited at SIGGRAPH 2016 Emerging Technology and more than 1000 participants experienced our demonstration [7]. This paper describes our system, the presentation algorithm and some noteworthy comments that we obtained from participants during the demonstrations.

2 FinGAR and Virtual Reality Application

The design and a photograph of a hand wearing the device are shown in Fig. 2. The device design is described in detail in [7]. A DC motor (Maxon 118386) with a 16:1 gear head ratio was used to drive an arm that contacts the finger-pad and stretches the skin. The DC motor was also found to serve as a high fidelity vibration unit [8]. The setup can thus provide shear deformation and vibration sensations



Fig. 2 FinGAR and photograph of device when worn on three fingers

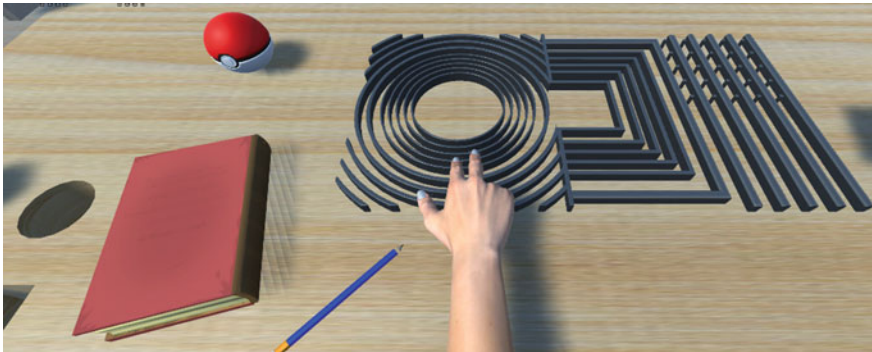


Fig. 3 Virtual objects in touching application

simultaneously. A 4×5 array of electrodes made from a film substrate was attached to the end of the mechanical arm to provide high-resolution pressure and vibration sensations to the finger-pad. Using this combination, we can achieve four-channel stimulation with suitable spatial and temporal resolution.

Figures 3 and 4 show the objects available in the virtual reality application and a view of a user touching and playing with the virtual objects, respectively. Participants wear the device on their thumb, index finger, and middle finger, and hold an optical mouse with their ring finger and pinky finger. The virtual hand is controlled via the mouse. Participants can touch puzzle lines, a pencil, a book cover, a ball, and the edge of a hole by keeping their hand on the mouse and moving it.

To reconstruct the realistic feeling of touching the objects, we designed the following algorithm based on consideration of the finger tracing speed, the contact surface and the roughness of the object.

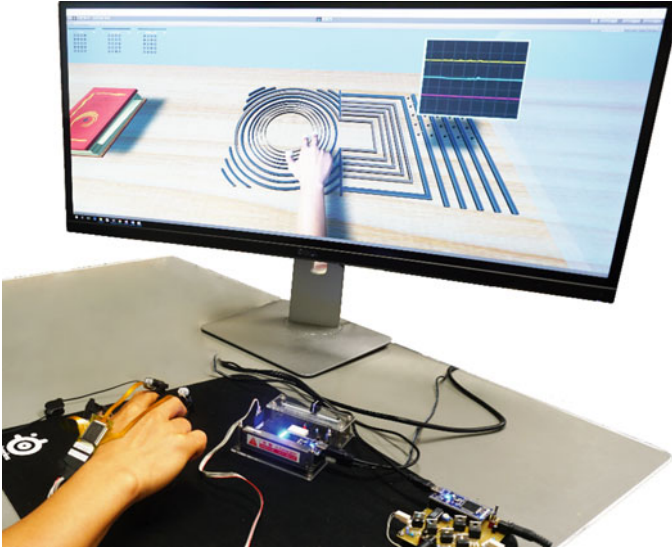


Fig. 4 View of user touching virtual objects

- Mechanical stimulation algorithm

Because the DC motor can be used as a high fidelity vibration unit, our mechanical stimulation setup can provide skin deformation and low- and high-frequency vibration sensations with sufficient temporal resolution. To provide a combination of these sensations, we designed the signal input ($V_{DCinput}$) of the DC motor as follows:

$$V_{DCinput} = \min(k \times Depth_t + A_t(v) \times Tri(2\pi ft), V_{DCinput,max})$$

$$A_t(v) = \min(C \times \sqrt{v}, A_{t,max})$$

where k and C are constants, and $Depth_t$ is the touched object depth at the finger position. Tri , A_t , and f are a triangular waveform function, its amplitude, which depends on the finger velocity v , and frequency, respectively. For stability, the values of $V_{DCinput}$ and A_t were limited to no more than $V_{DCinput,max}$ and $A_{t,max}$, respectively.

The sine waveform is commonly used to present vibration sensations. However, preliminary tests showed that triangular waveforms seem to be better in providing friction and roughness sensations for our device, possibly because it contains natural high-frequency harmonic components. We can change the frequency of triangular waveforms to convey different roughness sensations in a shape. The frequency may be affected by finger velocity, but it was fixed for each material in our current setup.

- Electrical stimulation algorithm

While electrical stimulation can provide pressure and low-frequency vibration sensations by varying the electrical current's polarity [9], we did not use all of its functions in our application. The main purpose of using this stimulation is to provide shape information (e.g., lines, circles, or corners) and the strength of the roughness depends on the shape-tracing speed of the user's finger. We used anodic current because it is safer and easier to adjust its intensity when compared with cathodic current. To convey the shape sensation, only the electrodes within the contact area were stimulated; however, when the contact area increased (e.g., when touching the book cover), some of the electrodes were randomly turned off.

3 Demonstration Results and Discussion

Figure 5 shows our demonstration experience at SIGGRAPH 2016 Emerging Technology. One of the authors stood or sat near the participants to instruct them on how to wear the device and touch objects, and then listened to their comments. More than 1000 people participated in our demonstration and almost all participants were surprised at the realistic sensations stimulated using our device.

The most common comments obtained from the participants are listed below.

- Puzzle lines

The participants perceived the most realistic sensation when touching this structure. They could sense the shape of each line, friction and roughness. Some participants stated that it was made from metal, while others could not determine the material of the lines. To produce a smooth surface sensation, we set the triangular wave frequency to a high value of 150 Hz. The participants could perceive the line shape



Fig. 5 Demonstration experience at SIGGRAPH 2016 Emerging Technology

through electrical stimulation but it was hard for them to feel a corner shape. This may be due to the spatial resolution limitations of the electrode array.

- Pencil

Interestingly, participants sensed the scrolling of a hexagonal pencil when they pushed it with their fingers. In terms of shape touching sensation, however, it seemed to be less realistic. We considered it to be necessary to adjust the contact areas of the electrodes to allow clear perception of each edge of the hexagon.

- Book cover

The participants felt a rough cover made from fabric. The fabric sensation can be produced via electrical stimulation with spatial distribution. The triangular waveform frequency was set at 100 Hz to make the cover feel rougher than the puzzle line.

- Ball

Similar to the pencil, the participants could sense the round shape of the ball. Some said that it was soft while others said that it was smooth. Many participants perceived a sensation of smoothness rather than softness. The triangular waveform frequency was set at 30 Hz.

- Edge of a hole

This seemed less realistic but participants could sense the edge shape.

4 Conclusion

We have developed a new fingertip-type tactile display called FinGAR, in which we combine mechanical and electrical stimulation to provide high-fidelity tactile presentation. FinGAR is small, lightweight, easy to wear, and does not affect natural finger movement. We also developed a virtual reality environment in which users can touch and play with objects such as puzzle lines, a pencil, a book cover, a ball, and the edge of a hole. More than 1000 participants at SIGGRAPH 2016 experienced our system. Based on their comments, we have concluded that our device can present sensations of roughness, friction, fabric texture, and object shape (e.g., puzzle lines, hexagonal pencil, or roundness of a ball).

We have two steps for future work. First, we will use cathodic current for electrical stimulation to present the pressure sensation of gripping or holding objects. Second, to reproduce tactile sensation more realistically, we will conduct psychological experiments to determine how to best combine the mechanical and electrical stimulation.

Acknowledgements This research is supported by the JST-ACCEL Embodied Media Project.

References

1. Minamizawa, K., Fukamachi, S., Kajimoto, H., Kawakami, N., Tachi, S.: Gravity grabber: wearable haptic display to present virtual mass sensation. In: Proceedings of SIGGRAPH Etech (2007)
2. Wall, S.A., Brewster, S.: Sensory substitution using tactile pin arrays: human factors. *Technol. Appl. Signal Process.* **86**, 3674–3695 (2006)
3. Poupyrev, I., Maruyama, S., Rekimoto, J.: Ambient touch: designing tactile interfaces for handheld devices. In: Proceedings of UIST, pp. 51–60 (2002)
4. Yatani, K., Truong, K.N.: SemFeel: A user interface with semantic tactile feedback for mobile touch-screen devices. In: Proceedings of UIST, pp. 111–120 (2009)
5. Bau, O., Poupyrev, I., Israr, A., Harrison, C.: Teslatouch: electro vibration for touch surfaces. In: Proceedings of UIST'10, pp. 283–292 (2010)
6. Jones, L.A., Lederman, S.J.: *Human Hand Function*, 1st edn. Oxford University Press (2006)
7. Yem, V., Okazaki, R., Kajimoto, H.: FinGAR: combination of electrical and mechanical stimulation for high-fidelity tactile presentation. In: Proceedings of SIGGRAPH Etech (2016)
8. Yem, V., Okazaki, R., Kajimoto, H.: Vibrotactile and pseudo force presentation using motor rotational acceleration. In: Proceedings of Haptics Symposium, pp. 47–51 (2016)
9. Kajimoto, H., Kawakami, N., Tachi, S.L.: Electro-tactile display with tactile primary color approach. In: Proceedings of Intelligent Robots and System (2004)

Development of a One-Dimensional Lateral Tactile Display for the Sensation of Texture Using a Speaker Array

Seitaro Kaneko and Hiroyuki Kajimoto

Abstract We report the development of a tactile display made from audio speakers and aluminum plates and having high spatial and temporal resolution. Aluminum plates with thickness of 0.5 mm are attached to audio speakers and aligned at intervals of 1 mm, and skin is deformed perpendicular to the plate direction. The device presents skin deformation with a wide frequency range (10–320 Hz) when a finger is placed on the plates.

Keywords Tactile display · Speaker array · Texture

1 Introduction

Tactile displays that indicate sensations of texture, such as stickiness and smoothness, are subject to ongoing research. To make these sensations more realistic, the relationship between the skin displacement of the finger and the human sensation must be clarified.

There are two steps to developing a tactile display that presents a realistic textured surface. The first step is to record the skin displacement when a finger touches and rubs against objects having rough or smooth textures. The second step is to reproduce the recorded data, or features extracted from the data.

We previously reported a method of observing the horizontal skin displacement of a finger on a textured surface with high spatial resolution [1]. Although the system is in a primary stage of development, it can measure displacement at an interval of 1 mm and a sampling rate of 1 kHz.

S. Kaneko (✉) · H. Kajimoto
University of Electro-Communications, 1-5-1 Chofugaoka,
Chofu, Tokyo 182-8585, Japan
e-mail: seitaro@kaji-lab.jp; kaneko@kaji-lab.jp

H. Kajimoto
e-mail: kajimoto@kaji-lab.jp

The present paper discusses the second step, specifically the hardware needed to reproduce the recorded movement of finger skin on a real textured surface. We report the development of a tactile display having audio speakers and aluminum plates and providing high spatial and temporal resolution. We also discuss the results of a performance evaluation.

2 Related Works

Various studies have presented a texture sensation with a tactile display. Here we summarize studies that have investigated the horizontal displacement of finger skin.

Friction modulation has been used to control the displacement of finger skin by employing ultrasonic vibration of the display surface [2, 3] or an electrostatic force between the object and finger [4]. While these methods can reproduce the friction coefficient, they cannot directly reproduce skin deformation with high spatial resolution.

Pasqueto et al. [5], Wang et al. [6], and Hayward et al. [7] developed a device that horizontally deforms the skin in two dimensions using piezo actuators. The device produces a distributed skin displacement that can express textures, braille, and simple figures. However, its bandwidth is currently limited to 100 Hz, which might not fully express high-frequency components of textures.

3 Device

We applied the following strategy to realize a sufficiently wide bandwidth (250 Hz or more for the Pacinian corpuscle) and high spatial resolution (less than 1.5 mm for the two-point discrimination limen of the fingertip). The contactors were arranged not in a two-dimensional matrix but in a one-dimensional array, and the direction of motion was limited to the direction of the array.

Figures 1 and 2 shows our developed device. Aluminum plates with thickness of 0.5 mm are attached to audio speakers and aligned at intervals of 1 mm, and skin deformation is produced perpendicular to the plates. The device is expected to have a wide bandwidth owing to the use of the audio speakers.

Figures 3 and 4 show details of the device. Each plate is attached to two speakers (AURA SOUND NSW1-205-8A), but the smallest plate is attached to only one speaker. The plates have three shapes: square (shown by the red lines in Fig. 3), rectangular (yellow lines), and diagonal (blue and green lines). Four plates with seven audio speakers constitute a unit, and two units constitute the device with eight outputs.

The device is driven by an eight-channel audio signal output from the audio interface (OCTA-CAPTURE UA-1010, ROLAND) controlled by a personal computer, and audio amplifiers (MUSE SOUND M50).

Fig. 1 Overview of the device

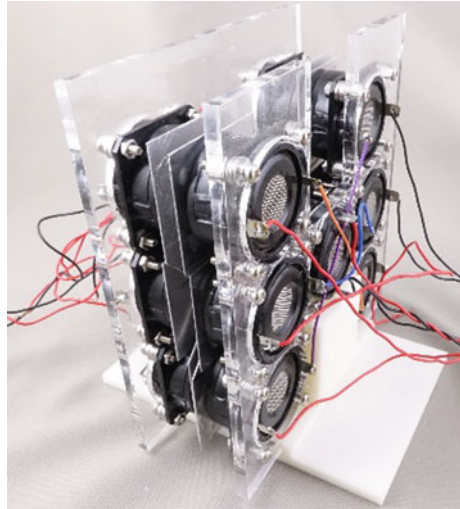
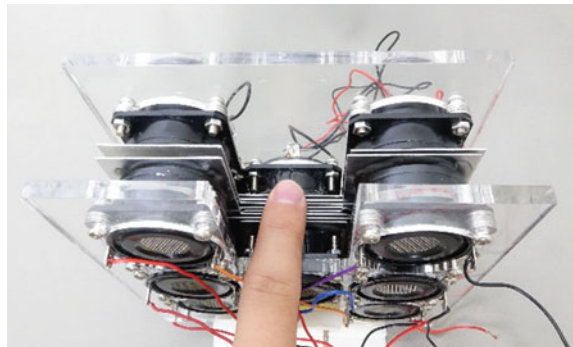


Fig. 2 Top view of the device



4 Performance Evaluation

The frequency characteristics of the device were measured in an experiment.

4.1 Method

Figure 5 shows the overview of the experiment. The vibration of each aluminum plate was measured using a laser range finder (LK-G5000 V, KEYENCE). The input signal was sinusoidal and had a frequency of 10, 20, 40, 80, 160, 320, 640, or 1280 Hz. The sampling rate of the measurement was 10 kHz. We made measurements for two situations: the finger placed and not placed on the plate.

Fig. 3 *Front view of the device*

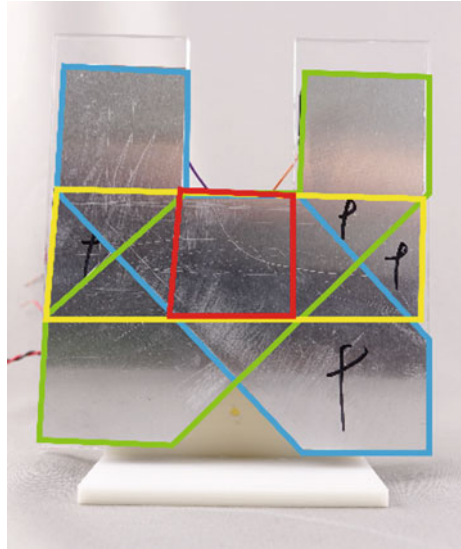
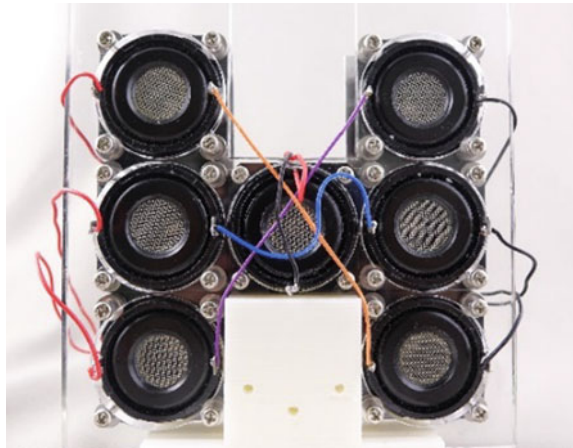


Fig. 4 *Back view of the device*



As the purpose of the experiment was to measure the frequency characteristics of the total system with the personal computer, audio interface, and amplifier, we did not adjust the volume for each frequency. The volume of the personal computer was set to a maximum while the volume of the audio interface and that of the amplifier were set to half-maximum. The waveform was generated using Audacity (<http://www.audacityteam.org>).

4.2 Results

Figure 6 shows the power spectrum of the vibration of a diagonal plate. Figures 7, 8, and 9 show the frequency characteristics of the vibration amplitude for each type of plate when a finger was placed and not placed on the plate.

Fig. 5 Overview of the experiment

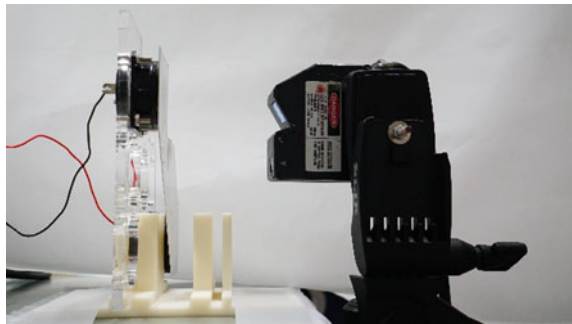


Fig. 6 Spectrum of the diagonal plate

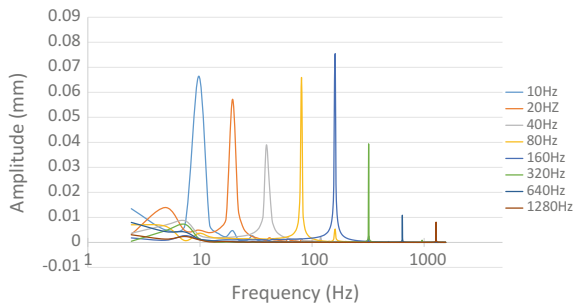


Fig. 7 Frequency characteristics of the square plate

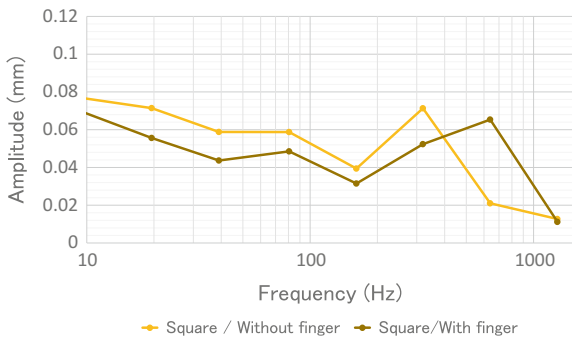


Fig. 8 Frequency characteristics of the rectangular plate

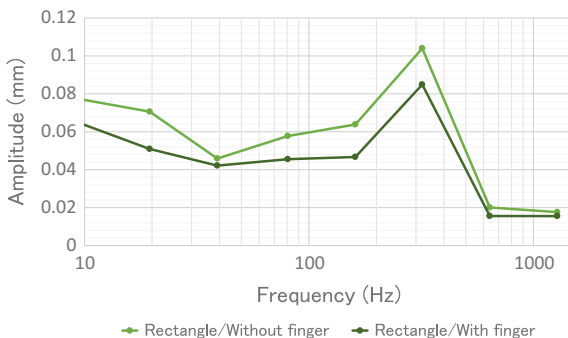
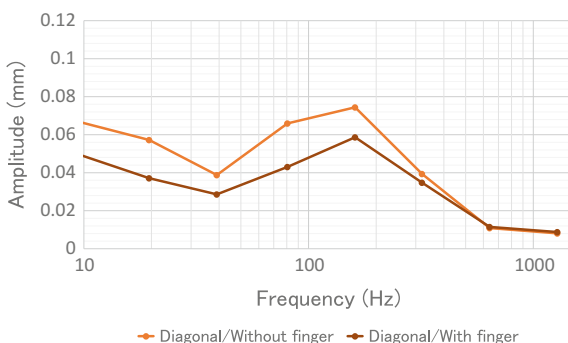


Fig. 9 Frequency characteristics of the diagonal plate



4.3 Discussion

In the output power spectrum, a peak corresponding to the input frequency was mostly observed while some harmonics were observed owing to distortion. The power of these harmonics was around 1/16 of that of the base frequency.

Comparing the cases with and without a finger placed on the plate, we observed that the output amplitude reduced to about 80% when the finger was placed on the plate, which might not be a negligible reduction but can be compensated easily because there was no strong frequency dependency.

For frequencies at and above 640 Hz, the amplitude was greatly reduced. In other words, the system can present a 320-Hz vibration, which meets our requirement. At 320 Hz, there was a difference among the spectra of the different types of plates, and there was a peak at 320 Hz for the rectangular plate. These individual characteristics should be compensated for.

5 Conclusion

We developed a device that reproduces lateral deformation of finger skin. The device has aluminum plates driven by audio speakers. We showed that the device is able to present a skin deformation with a wide frequency range (10–320 Hz) when a finger is placed on the plates.

Our future work will include the compensation of frequency characteristics for each type of plate, and reproduce the skin deformation for each texture recorded by our previously developed recording system.

Acknowledgements This work was supported by JSPS KAKENHI under grant number JP15H05923 (Grant-in-Aid for Scientific Research on Innovative Areas, “Innovative SHITSUKAN Science and Technology”).

References

1. Kaneko, S., Kajimoto, H.: Method of observing finger skin displacement on a textured surface using index matching. In: *Haptics: Perception, Devices, Control, and Applications: 10th International Conference, EuroHaptics 2016, London, UK, 4–7 July 2016, Proceedings, Part II*, pp. 147–155. Springer International Publishing (2016)
2. Biet, M., Giraud, F., Lemaire-Semail, B.: Squeeze film effect for the design of an ultrasonic tactile plate. *IEEE Trans. Ultrason. Ferroelectr. Freq. Control* **12**(54), 2678–2688 (2007)
3. Winfield, L., Glassmire, J., Colgate, J.E., Peshkin, M.: T-PaD: tactile pattern display through variable friction reduction. In: *Second Joint EuroHaptics Conference and Symposium on Haptic Interfaces for Virtual Environment and Teleoperator Systems (WHC’07)*, pp. 421–426 (2007)
4. Poupyrev, I., Israr, A., Bau, C.H.O.: TeslaTouch: electrovibration for touch surfaces. In: *Proceedings of 23rd Annual ACM symposium on User Interface Software and Technology (UIST’10)*, New York, USA, pp. 283–292 (2010)
5. Pasquero, J., Levesque, V., Hayward, V., Legault, M.: Display of virtual braille dots by lateral skin deformation: a pilot study. In: *Proceedings of Eurohaptics 2004, Munich, Germany*, pp. 96–103 (2004)
6. Wang, Q., Hayward, V.: Compact, portable, modular, high-performance, distributed tactile transducer device based on lateral skin deformation. In: *Proceedings of 2006 14th Symposium on Haptic Interfaces for Virtual Environment and Teleoperator Systems* (2006)
7. Levesque, V., Pasquero, J., Hayward, V.: Braille display by lateral skin deformation with the STReSS2 tactile transducer. In: *Second Joint EuroHaptics Conference and Symposium on Haptic Interfaces for Virtual Environment and Teleoperator Systems (WHC’07)*, Tukuba, pp. 115–120 (2007)
8. Kandel, E.R., Schwartz, J.H., Jessell, T.M.: *Principles of Neural Science*, 4th edn. McGraw-Hill, New York (2000)

Encountered-Type Visual Haptic Display Using MR Fluid

Hiroki Ohnari, Satoko Abiko and Teppei Tsujita

Abstract This paper proposes a visual haptic display with an encountered-type haptic interface using MR (Magneto-Rheological) fluid. The proposed system can display arbitrary force by controlling the magnitude of yield stress of MR fluid and provide realistic visualization by displaying computer graphics images on the container of MR fluid directly. An operator can feel resistance force by putting instruments in the MR fluid container and can sense reality by virtue of the visual display on the MR fluid container. This type of system would be useful for surgical simulator since an operator can freely move and easily change the instruments as in real operation. In the demonstration, one of fundamental brain surgery operations, cutting arachnoid trabecular, is considered as an application.

Keywords Haptic interface • MR fluid • Visual haptic display • Surgical simulator

1 Introduction

Surgical simulator using haptic interface and computer graphics images is a new technology to support surgeons for training operational technique and for executing preoperative planning of difficult surgery [1]. However, existing surgical simulators require mechanical attachment between surgical instruments and haptic interface. This loses a sense of reality because an operator needs to attach/detach the instruments that is not in real operation [2, 3]. An encountered-type haptic interface using MR (Magneto-Rheological) fluid is one solution to solve this problem [4]

H. Ohnari · S. Abiko (✉)

Department of Electrical Engineering, Shibaura Institute of Technology,
3-7-4, Koto-ku, Tokyo 135-8579, Japan
e-mail: abiko@shibaura-it.ac.jp

T. Tsujita

Department of Mechanical Engineering, National Defense Academy of Japan,
1-10-20, Hashirimizu, Yokosuka, Kanagawa 239-8686, Japan

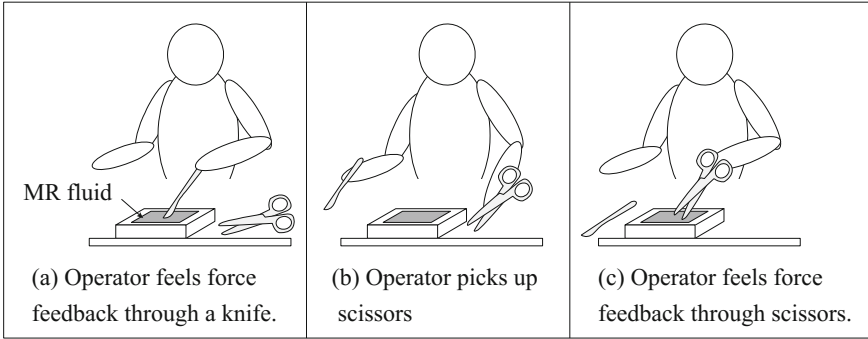


Fig. 1 Cutting force display using MR fluid [4]

(Fig. 1). In the previous research, the design and development of the haptic interface using MR fluid itself was focused on and a method to visualize virtual reality was not deeply considered. Therefore, the point of view did not coincide with an operational point.

This paper proposes a visual haptic display with an encountered-type haptic interface using MR fluid. In the proposed system, the point of view coincides with an operational point, which further improves sense of reality.

2 Fundamental Concept of Force Display Using MR Fluid

Figure 2 shows conceptual scheme for displaying cutting force of soft tissue using MR fluid. As shown in Fig. 2, the cutting the chains of magnetizable particles by knife provides resistance force to an operator. The magnitude of the resistance force can be controlled by changing external magnetic field. In practice, the MR fluid can only provide viscosity. Therefore, servo mechanism was combined with the MR fluid container to demonstrate both stiffness and viscosity of the biological tissue in the previous study [4], and force feedback control was developed for accurate

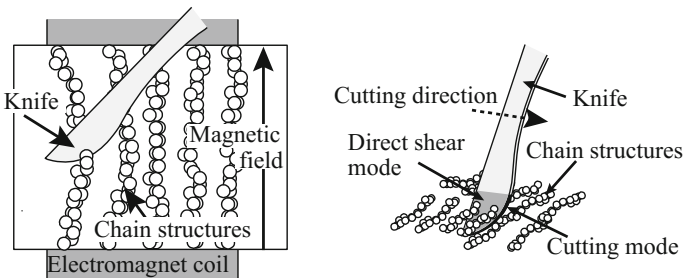


Fig. 2 Concept for displaying cutting force of soft tissue using MR fluid [4]

replication of the biological characteristics [5]. Finally, the haptic interface using MR fluid can display cutting force of biological tissue.

3 Encountered-Type Visual Haptic Display

This section describes an encountered-type visual haptic display using MR fluid. Figure 3 shows system configuration. The system mainly consists of numerical simulation, the haptic interface using MR fluid, a motion capture system and a projector. It projects a computer graphics to the screen on the haptic device directly. Because of the direct projection, the point of view and the operational point are perfectly consistent and the system provides more realistic operational situation. The motion capture system is used to measure the position and orientation of the surgical instrument, and then the magnitude of the resistance force of MR fluid is controlled depending on the tip position of the instrument.

4 Demonstration

In this paper, cutting arachnoid trabecular is assumed to demonstrate. The arachnoid trabecular exists under the cranial bone to support cerebral parenchyma as shown in Fig. 4. In the brain surgery, the cutting arachnoid trabecular is absolutely necessary as a fundamental surgical operation for opening a cerebral fissure. In the demonstration, deformation of the arachnoid trabecular and the resistance force to the operator are exaggerated in order to easily understand the concept of our proposed system. Figure 5 shows the computer graphics directly projected on the haptic device and Fig. 6 shows the demonstration of visual haptic display. When the operator is cutting the arachnoid trabecular, the resistance force to the operator

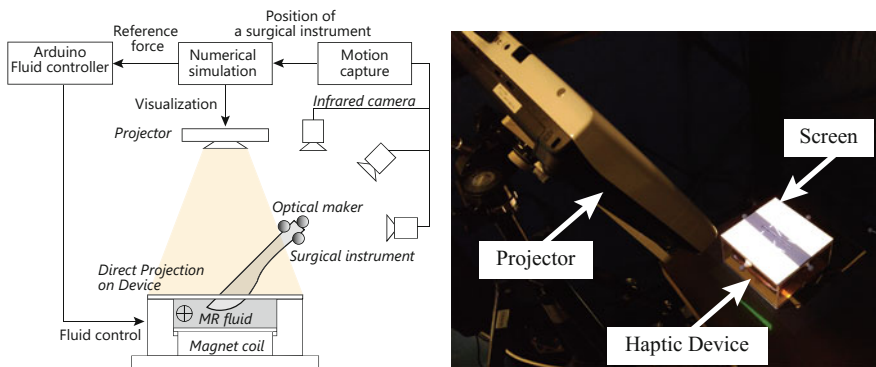


Fig. 3 System configuration

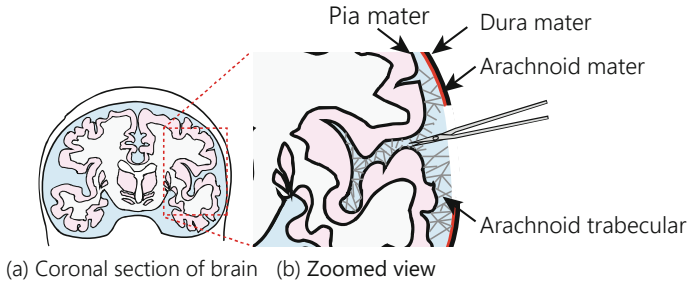


Fig. 4 Overview of the cutting of arachnoid trabecular

Fig. 5 Projected graphics

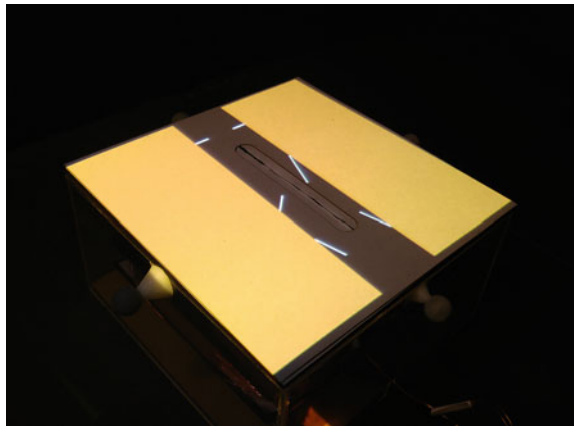
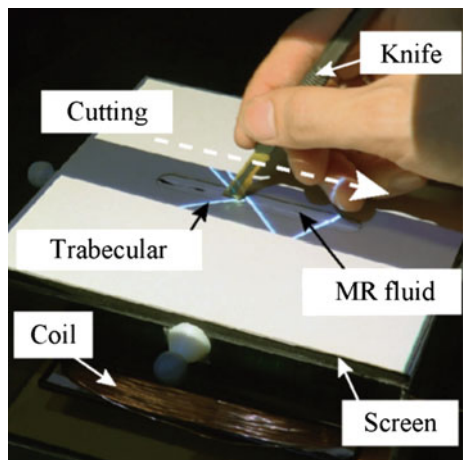


Fig. 6 Visual haptic display demonstration



becomes large due to the controlled current. Just after cutting the arachnoid trabecular, the operator does not feel large resistance force because the current is controlled to zero.

5 Conclusions

This paper proposed an encountered-type visual haptic display using MR fluid. The haptic interface using MR fluid is a novel solution for surgical simulator. This paper proposed direct projection on the haptic device using MR fluid to further improve the sense of reality. Because of the direct projection, the point of view of the operator and the operational point are perfectly coincidence and the operator can feel more realistic operational situation. The demonstration showed the exaggerated simulation of the cutting arachnoid trabecular.

Acknowledgements This work was supported by JSPS Grant-in-Aid for Scientific Research (B) JP16H04309 and JSPS Grant-in-Aid for Young Scientists (A) JP24686029.

References

1. Satava, R.M.: Virtual reality surgical simulator. *Surg. Endosc.* **7**(3), 203–205 (1993)
2. Moody, L., Baber, C., Arvanitis, T.N.: The role of haptic feedback in the training and assessment of surgeons using a virtual environment. In: *Proceedings of EuroHaptics 2001*, pp. 170–173 (2001)
3. Takagi, Y., et al.: Development of haptic interface for a brain surgery simulator. In: *Proceedings of the 2010 JSME Conference on Robotics and Mechatronics*, 1A1-C09 (2010) (in Japanese)
4. Tsujita, T., et al.: Design and evaluation of an encountered-type haptic interface using MR fluid for surgical simulators. *Adv. Robot. (AR)* **27**(7), 525–540 (2013)
5. Kameyama, T., et al.: Displaying cutting force of soft tissue using MR fluid for surgical simulators. In: *Proceedings of the 2014 IEEE Haptics Symposium (Haptics)*, pp. 283–288 (2014)

Whole Hand Interaction with Multi-finger Movement-Based Vibrotactile Stimulation

Shota Iizuka, Hikaru Nagano, Masashi Konyo and Satoshi Tadokoro

Abstract Humans usually use their multiple fingers for several types of whole hand touch interaction such as stroking and grasping. During whole hand interaction, multiple fingers show respective velocity behaviors, which may lead to respective vibrating phenomena. For realistic haptic rendering of fine roughness of surfaces during multi-finger interaction, we proposed a multi-finger vibrotactile rendering method using velocities of multi-fingers. For each finger, a virtual fine rough surface is represented by a sinusoidal vibratory stimulus based on velocity of the corresponding finger and a touched material. We demonstrate the proposed method through two types of application with a multi-finger vibrotactile wearable display. In a first demonstration, a subject touches a virtual surface in a computational 3-D environment and perceives fine roughness of it. In a second demonstration, a subject touches a real surface and perceives augmented fine roughness of the surface on which vibrotactile stimulation is superimposed to modulate the fine roughness of the real surface.

Keywords Vibrotactile display · Multi-finger interaction · Wearable haptics · Texture rendering · Haptic VR/AR

1 Introduction

Humans perform whole hand interaction such as stroking, grasping, and tapping by controlling multiple fingers. During whole hand interaction, humans perceive textures through lateral motions across surfaces by multiple fingers. Multiple fingers

S. Iizuka (✉) · H. Nagano · M. Konyo · S. Tadokoro
Graduate School of Information Sciences, Tohoku University, Sendai, Japan
e-mail: iizuka.shota@rm.is.tohoku.ac.jp

H. Nagano
e-mail: nagano@rm.is.tohoku.ac.jp

M. Konyo
e-mail: konyo@rm.is.tohoku.ac.jp

S. Tadokoro
e-mail: tadokoro@rm.is.tohoku.ac.jp

© Springer Nature Singapore Pte Ltd. 2018
S. Hasegawa et al. (eds.), *Haptic Interaction*, Lecture Notes
in Electrical Engineering 432, DOI 10.1007/978-981-10-4157-0_27

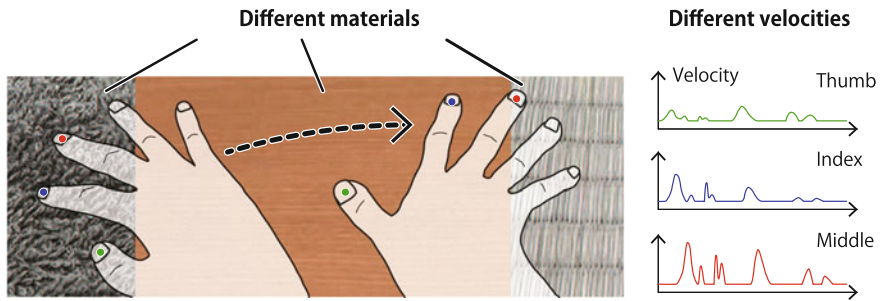
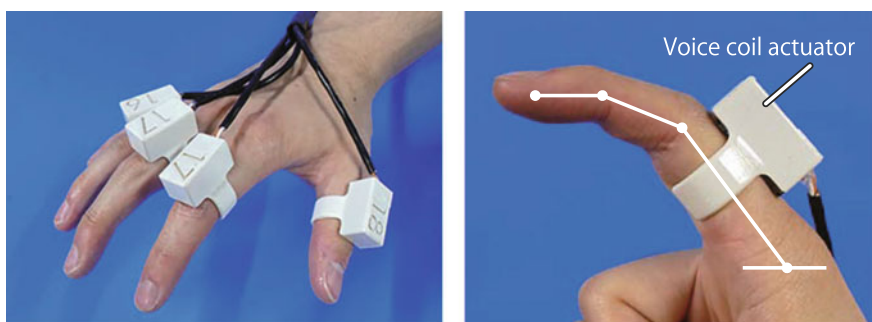


Fig. 1 Whole hand interaction and perception depend on fingers' movements and material characteristics

not only cooperate with each other but also move independently as shown in Fig. 1. Such a difference may lead to high-quality texture perception because of integration of information from multiple fingers [1]. In addition, texture perception depends on the characteristics of materials (Fig. 1). Therefore, for a realistic whole hand haptic interaction, this paper propose a multi-finger texture display consisting of multiple vibratory components, in which vibrotactile stimulation is modulated according to respective fingers' movement and surface characteristics.

2 Apparatus: Multi-finger Vibrotactile Display

We proposed a whole hand texture display consisting of multiple vibratory components as shown in Fig. 2a, b. Figure 2a shows that four vibratory components are



(a) Four vibratory displays for representing multiple vibrotactile stimuli during whole hand interaction

(b) One vibratory component attached to a finger

Fig. 2 Wearable vibratory displays for whole hand interaction

attached to thumb, index, middle, and ring fingers for generating multiple vibrotactile stimuli. We assume that, as shown in Fig. 2b, vibration by each vibrator isolates from those of other vibrators because a finger likes a cantilever and therefore a vibration seems easily transmitted to a finger tip. In addition, the display is open-fingered, which allows us to touch real environment and realizes a haptic augmented reality system such as modifying haptic textures of real materials of object surfaces [2, 3].

3 Method: Vibrotactile Rendering of Fine Roughness Synchronizing with Finger Movement

Humans perceive several aspects of surfaces by touching them [4]. In this paper, we focus on the fine roughness perception of textured surfaces. In order to represent the fine rough textures, we used the vibrotactile stimulation assuming a wavy surface as shown in Fig. 3. This method have been proposed for the representation of surface roughness of several surfaces such as cloths and papers in virtual environments [5, 6].

A vibrotactile stimulation is generated by a voice coil actuator mounted on a finger. A input voltage $V_{act}(t)$ is modulated according to a finger velocity $v(t)$ and a spatial frequency of a wavy surface f as follows:

$$v(t) = \sqrt{\dot{x}(t)^2 + \dot{y}(t)^2} \quad (1)$$

$$V_{act}(t) = A \sin(2\pi f v(t)) \quad (2)$$

where A is a voltage amplitude. We used several values of f to represent several types of roughness perception according to materials. Vibrotactile stimuli are modulated for respective fingers based on a movement and a touched material of each finger.

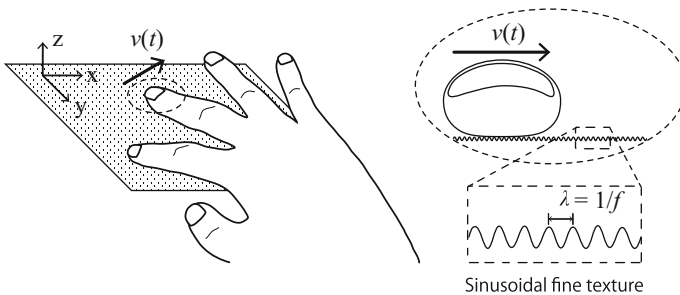


Fig. 3 Fine roughness texture using sinusoidal vibrotactile stimulation

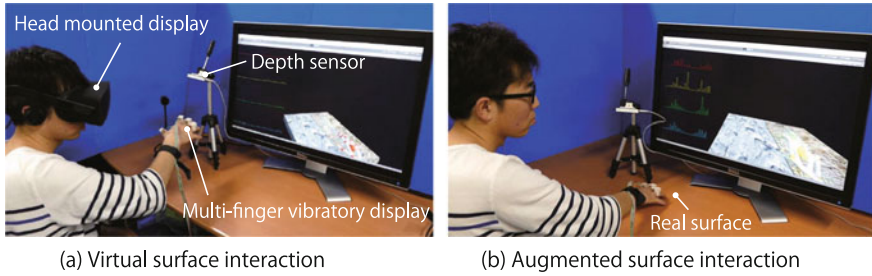


Fig. 4 Whole hand interaction with multi-finger vibrotactile stimulation

4 Application: Whole Hand Interaction with Multi-finger Vibrotactile Stimulation

We demonstrate two types of whole hand interaction with multi-finger vibrotactile stimuli as shown in Fig. 4a, b.

4.1 VR-Based Haptic Interaction: Virtual Rough Surface

A first demonstration provides the VR-based whole hand interaction in which a subject touches a virtual surface and feels the fine roughness of it through a whole hand vibrotactile display and a head mounted display (Rift, Oculus VR, Inc.). Vibrotactile stimuli are generated based on multi-fingers' velocities. Each finger velocity is calculated from hand movement captured by a depth sensor (Leap Motion, Leap Motion, Inc.).

4.2 AR-Based Haptic Interaction: Augmented Rough Surface

A second demonstration is the AR-based whole hand interaction. In this demonstration, a subject perceives the roughness of a touched surface on which vibrotactile stimulation is superimposed. As with the first demonstration, multi-finger vibrotactile stimulation is generated based on velocities of respective fingers.

5 Conclusion

For realistic haptic rendering during whole hand interaction, we proposed the multi-finger vibrotactile rendering method. To represent the fine roughness of textured

surfaces, the vibratory stimuli are modulated based on measured respective fingers' velocities and touched materials. We demonstrated the proposed method with the multi-finger vibrotactile wearable display through the two types of application. In the first demonstration, subjects touch virtual surfaces and perceive the fine roughness of them. In the second demonstration, subjects perceive the fine roughness of a real surface on which vibrotactile stimuli are superimposed.

Acknowledgements This work was partially supported by ImPACT Program "Tough Robotics Challenge."

References

1. Klatzky, R.L., Loomis, J.M., Lederman, S.J., Wake, H., Fujita, N.: Haptic identification of objects and their depictions. *Percept. Psychophys.* **54**(2), 170–178 (1993)
2. Bau, O., Poupyrev, I.: Revel: tactile feedback technology for augmented reality. *ACM Trans. Graph. (TOG)* **31**(4), 89 (2012)
3. Asano, S., Okamoto, S., Yamada, Y.: Vibrotactile stimulation to increase and decrease texture roughness. *IEEE Trans. Hum.-Mach. Syst.* **45**(3), 393–398 (2015)
4. Okamoto, S., Nagano, H., Yamada, Y.: Psychophysical dimensions of tactile perception of textures. *IEEE Trans. Haptics* **6**(1), 81–93 (2013)
5. Okamura, A.M., Dennerlein, J.T., Howe, R.D.: Vibration feedback models for virtual environments. In: *IEEE International Conference on Robotics and Automation*, 1998. Proceedings, vol. 1, pp. 674–679. IEEE (1998)
6. Konyo, M., Tadokoro, S., Yoshida, A., Saiwaki, N.: A tactile synthesis method using multiple frequency vibrations for representing virtual touch. In: *2005 IEEE/RSJ International Conference on Intelligent Robots and Systems*, pp. 3965–3971. IEEE (2005)

Signal and Power Transfer to Actuators Distributed on Conductive Fabric Sheet for Wearable Tactile Display

Yuki Tajima, Akihito Noda and Hiroyuki Shinoda

Abstract We propose a scheme to implement a wearable tactile display with distributed actuators using a “two-dimensional signal transmission sheet (2DST sheet)”. This device provides tactile feedback by driving actuators placed on 2DST sheet. We can drive these actuators without individual wiring from a driver circuit to each actuator. Physical mounting and electrical connection of actuators are integrated into a single action, i.e., sticking a “pin badge connector” into the 2DST sheet. In this paper, we present a 2DST-based power transfer system capable of supplying electricity selectively to each actuator placed on the 2DST sheet and of controlling each power.

Keywords Haptics · Haptic suit · Two-dimensional signal transmission sheet

1 Introduction

Wearable multi-actuator tactile displays have been researched and developed actively. For example, “Haptic suit” such as Teslasuit [1] or Null Space VR [2], that provide tactile feedback on wide area of body by use of multiple (16–64) actuators, were released a few years ago. Most recently, Synesthesia Suit [3] and HALUX [4] were presented at SIGGRAPH 2016. Wearable tactile displays with a lot of actuators will provide richer tactile feedback. Implementation of such a large number of actuators, especially individual wiring to each actuator, is a critical issue.

Y. Tajima (✉) · A. Noda · H. Shinoda
The University of Tokyo, 5-1-5 Kashiwanoha, Kashiwa-shi,
Chiba 277-8561, Japan
e-mail: tajima@hapis.k.u-tokyo.ac.jp

A. Noda
e-mail: Akihito_Noda@ipc.i.u-tokyo.ac.jp

H. Shinoda
e-mail: Hiroyuki_Shinoda@k.u-tokyo.ac.jp

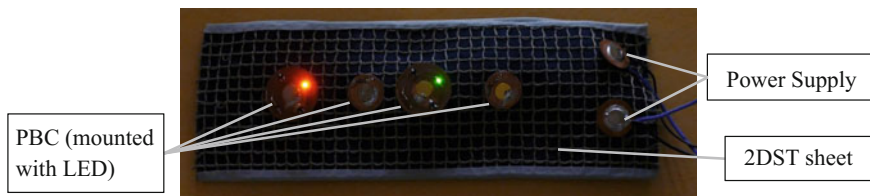


Fig. 1 Demonstration device. LEDs are turned on selectively by inputting alternative current

We propose to use “two-dimensional signal transmission sheet (2DST sheet)” in order to simplify the implementation of such a wearable tactile display. 2DST sheet is a physical medium to conduct electric signal and power in a 2-D plane. In the proposed scheme, multiple actuators can be attached to a single piece of 2DST sheet with a special “pin badge connector (PBC),” similar to a connector proposed by Akita et al. [5]. Just by sticking the needle of a PBC into a 2DST sheet from one side and attaching the catch on the other side, electrical connections are established on both sides. Physical mounting and electrical connection of actuators are integrated into this single action. In this scheme, individual wires for each actuator are eliminated and they can be attached at arbitrary positions on the sheet. In our demonstration video, we selectively turn on/off LEDs which are implemented on 2DST sheet by using this scheme (Fig. 1). In this paper, we describe the way to supply electricity to actuators placed on 2DST sheet, and control them.

2 Proposed Method

2.1 2DST Sheet and Pin Badge Connector

2DST sheet is composed of three layers: a mesh conductive layer, an insulative layer and a solid conductive layer [6] (Fig. 2). Connecting an alternative current (AC) source between the mesh conductive layer and the solid conductive layer, the AC voltage can be extracted at any arbitrary positions of the sheet by using a

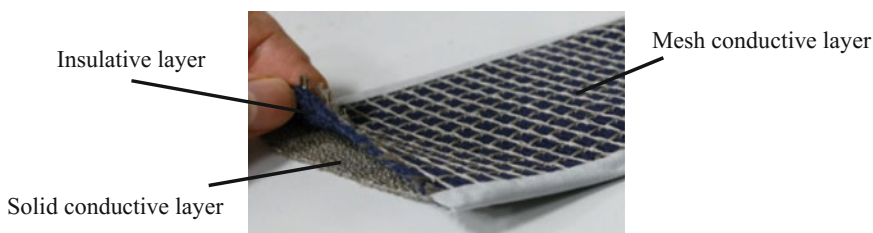


Fig. 2 2DST sheet

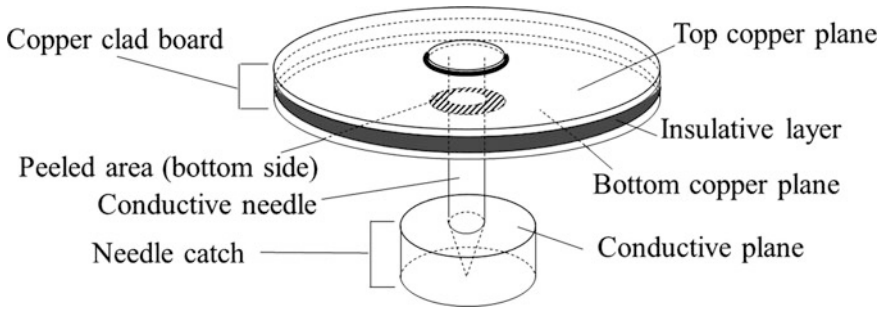


Fig. 3 Schematic of PBC

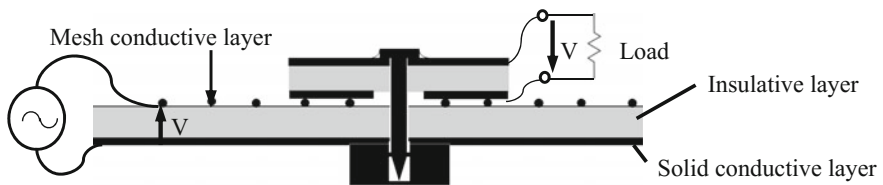


Fig. 4 The voltage supplied on PBC in pinning PBC on the sheet

special PBC shown in Fig. 3. The mesh conductor layer to avoid short-circuit is one of differences from Akita's method [5].

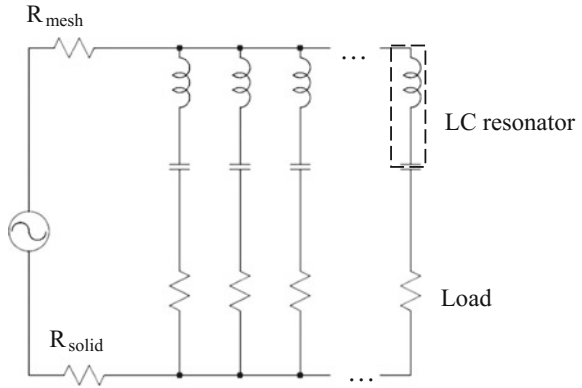
PBC is composed of a copper clad board, a conductive needle and a needle catch. By sticking the needle of a PBC into the sheet from mesh side and attaching the catch to the needle, electrical connections are established between the top copper plane of the PBC and the solid conductive layer of the sheet and between the bottom copper plane and the mesh conductive surface as shown in Fig. 4. To prevent shorting between the bottom copper plane and conductive needle of the PBC, bottom copper plane is partially peeled off around the conductive needle, as shown in Fig. 3.

2.2 Selective Power Transfer and Controlling

For providing spatially patterned tactile stimuli and/or tactile apparent movements, we need to control the actuator's power and drive them selectively. For the former, we can control by changing input AC amplitude. For the latter, we present a frequency domain channel division (FDCD) scheme.

In the FDCD scheme, a different frequency channel is used to transfer power to each of actuators. Channel selection is realized by mounting a LC resonator to each actuator on the PBC. Only when the frequency of AC source matches the LC

Fig. 5 Equivalent circuit for the system



resonance frequency, actuator can be driven with significant power supply. Hence, by connecting AC source with multiple frequency components to the sheet and by turning on/off each frequency component individually, the actuators can be turned on/off selectively.

For quantitative analysis on the system, a simplified equivalent circuit is presented in Fig. 5. In the schematic diagram, the resistances of the mesh conductive layer and the solid conductive layer are represented by R_{mesh} and R_{solid} , respectively. The loads represented with resistor symbols include rectifiers and actuators.

3 Simulation

In this section, selective power transfer capability will be validated through electric circuit simulation.

We assumed that three PBCs are attached on a sheet and that a pure resistive load and a LC resonator are mounted on each PBC. The frequency characteristics are simulated with LTspice IV [7]. This system is represented as an equivalent circuit shown in Fig. 6. In this simulation, we set each resonator's inductance L and capacitance C as shown in Table 1. From a preliminary measurement result, we determined the mesh conductive layer's resistance and the solid conductive layer's resistance as 1.7Ω and 1.1Ω , respectively. Each load is approximated as a 66Ω pure resistance.

Simulated frequency characteristics of the voltage gain, defined as the ratio of the voltage appearing across the load resistor (V_{load}) to the source voltage (V_{source}) are shown in Fig. 7. Resonators 1, 2 and 3 respectively resonate approximately at 26 MHz, 36 MHz and 44 MHz. When one resonator resonates, others are in the off-resonant state and the voltage gain at the same frequency reduces by 25–50 dB, i.e., two to five orders of magnitude less power received. This suggest that these three actuators can be driven selectively by turning on/off each frequency component of AC source individually. The maximum number of channels that can be

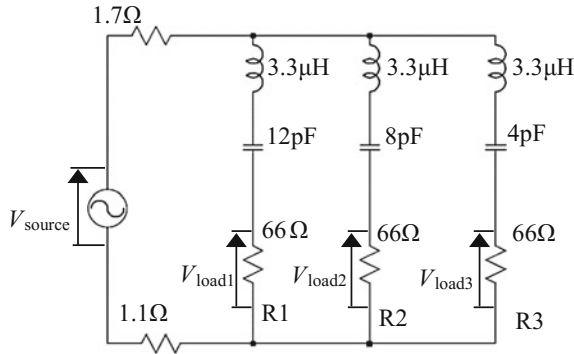
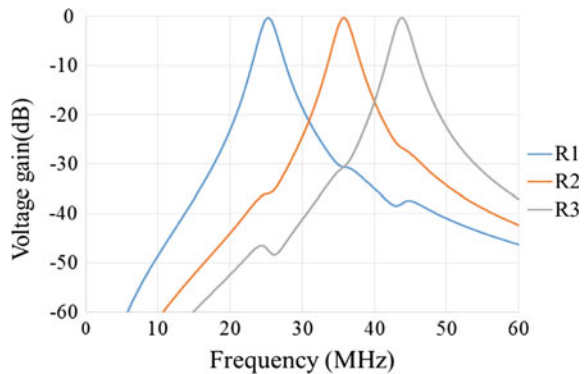


Fig. 6 Equivalent circuit for the simulation

Table 1 LC resonant circuit parameters

| | Inductance (μH) | Capacitance (pF) | Resonance frequency (MHz) |
|------------|------------------------------|------------------|---------------------------|
| Resonator1 | 3.3 | 4 | 43.81 |
| Resonator2 | 3.3 | 6 | 35.77 |
| Resonator3 | 3.3 | 12 | 25.29 |

Fig. 7 Frequency characteristics of the voltage gain evaluated for each resistor



selectively turned on/off with the proposed scheme is proportional to the quality factor (Q -factor) of the LC filters. A filter with higher Q enables to distinguish two signals with smaller difference in frequency and to allocate more channels in a fixed frequency band. The Q -factors of typical chip inductors/capacitors, i.e., the ratio of the reactance to the equivalent series resistance, are about 10–100. Therefore, roughly 10 independent channels can be achieved with the proposed scheme.

4 Experiment

We measured the characteristics of each LC resonator shown in Table 1 by using a vector network analyzer (VNA) as shown in Fig. 8a. The transmission coefficient, or the scattering parameter S_{21} , measured with the VNA represents the square root of the ratio of the power transferred to the load resistance to the available power of the source. An equivalent circuit of the measurement system is shown in Fig. 8b. The measurement result shown in Fig. 9 demonstrates the selective power transfer to each load. The selectivity, i.e., the difference in $|S_{21}|$ between the resonating LC circuit and another off-resonant circuits is 7–17 dB. The degradation in the selectivity compared with the simulation is due to parasitic impedances in each of the actual inductors and capacitors.

The selectivity can be improved by allocating frequency channels more sparsely, and/or increasing the Q -factor of the resonant circuit by increasing the reactance of the inductor and the capacitor.

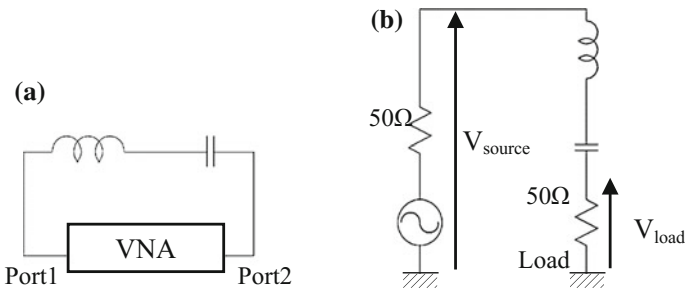
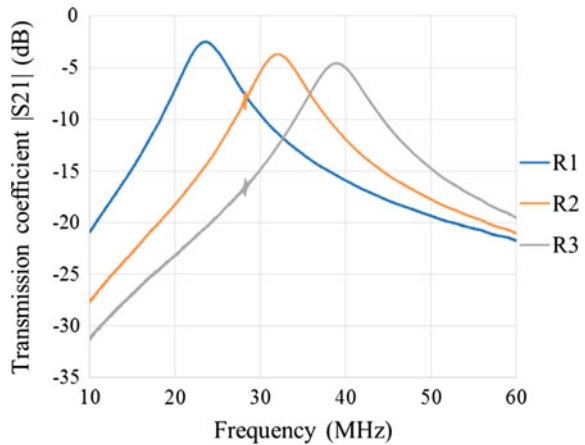


Fig. 8 a Measurement system. b Equivalent circuit for the measurement system

Fig. 9 Transmission coefficient $|S_{21}|$ via resonators



5 Conclusion and Future Works

We proposed a scheme to supply power to multiple distributed actuators on 2DST sheet without individual wiring. In this method, we use 2DST sheet and PBC as transmission medium for supplying power to actuators. Actuators are selectively driven via LC resonators with a unique resonance frequency. By using this method, we can implement actuators to wearable tactile display more easily. Physical mounting and electrical connection are integrated into a single action.

As a future work, we are planning to implement actuators specialized for haptics as Haptuator [8], for example. Haptuator is a voice-coil-based actuator that can operate over a wide-band driving signal. The signal bandwidth required for haptic stimulation is at most 1 kHz and it can be transferred by modulating the carrier signal. For example, modulating a 10-MHz carrier with a 1-kHz baseband signal corresponds to 1/10,000 relative bandwidth, which can be implemented straightforwardly. For this operation, a demodulation circuit corresponding to the modulation scheme (amplitude modulation, frequency modulation, etc.) is required on the receiver side.

Acknowledgements This research was partly supported by JST ACCEL Embodied Media Project and MIC/SCOPE #155103003.

References

1. Teslasuit. <http://teslasuit.io/>. Accessed 20 Oct 2016
2. NullSpace VR. <http://nullspacevr.com/>. Accessed 20 Oct 2016
3. Konishi, Y., Hanamitsu, N., Minamizawa, K., et al.: Synesthesia suit: the full body immersive experience. In: SIGGRAPH Emerging Technologies 2016, Anaheim (2016)
4. Uematsu, H., Ogawa, D., Okazaki, R., Hachisu, T., Kajimoto, H.: HALUX: projection-based interactive skin for digital sports. In: SIGGRAPH Emerging Technologies 2016, Anaheim (2016)
5. Akita, J., Shinmura, T., Toda, M.: Flexible network infrastructure for wearable computing using conductive fabric and its evaluation. In: International Conference on Distributed Computing Systems Workshops 2006, Lisboa, p. 65 (2006)
6. Shinoda, H., Makino, Y., Yamahira, N., Itai, H.: Surface sensor network using inductive signal transmission layer. In: Proceedings of Fourth International Conference Networked Sensing System, Braunschweig, pp. 201–206 (2007)
7. LTspice. <http://www.linear.com/designtools/software/#LTspice>. Accessed 20 Oct 2016
8. Haptuator. <http://tactilelabs.com/products/haptics/haptuator/>. Accessed 20 Oct 2016

Multi-electrodes-Based Electrostatic Tactile Display

Hirobumi Tomita, Satoshi Saga and Hiroyuki Kajimoto

Abstract Haptic interaction with objects, e.g. sculpting with clay, is a fundamental creative activity. To realize such kind of interface with touchscreen, multiple stimulation toward each finger will do. In this research we propose multi-electrode-based electrostatic tactile display and a control method of the charge distribution.

Keywords Haptic display · Electrostatic force · Lateral force

1 Introduction

In recent years, touchscreen interfaces have become popular worldwide. Moreover, popular consumer electronics devices use a dedicated touchscreen as an interface. However, few touchscreens enable reactive tactile signals.

Several researchers have employed vibrations to display texture information. For example, Chubb et al. [1] developed a tactile display that employs a squeeze film to represent the change in friction. The devices provide simple but rich lateral force to the user's finger. However, these devices do not consider the rendering method of geometrical shape.

In our previous research, we propose a method of feeling both large bumps and small textures simultaneously on a screen [2]. By employing the technology, users feel geometry as well as texture information. Because this system was based on a string-based haptic display, the system is only for one finger (Fig. 1).

H. Tomita · S. Saga (✉)
University of Tsukuba, 1-1-1 Tennodai, Tsukuba, Japan
e-mail: saga@saga-lab.org
URL: <http://saga-lab.org/>

H. Tomita
e-mail: tomita@iplab.cs.tsukuba.ac.jp

H. Kajimoto
The University of Electro-Communications, 1-5-1 Chofugaoka, Chofu,
Tokyo 182-8585, Japan
e-mail: kajimoto@kaji-lab.jp
URL: <http://kaji-lab.jp/>

Fig. 1 String-based haptic display

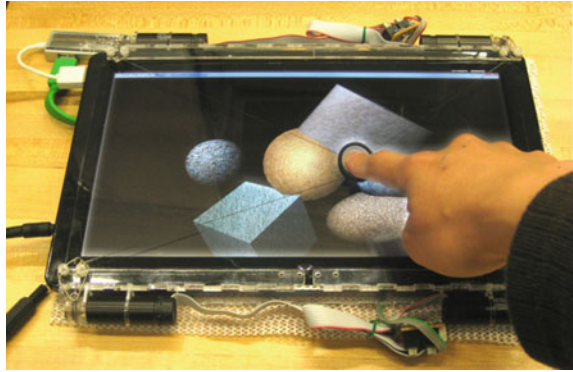
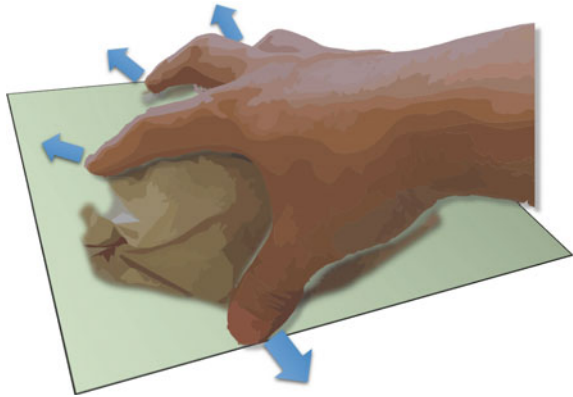


Fig. 2 Virtual grasp on flat screen with electrostatic force



However, our rendering algorithm is easily implemented into other lateral-force-based tactile displays. In recent years other lateral-force-based tactile feedback devices that employ static electric fields have been developed (Senseg, Inc., [3]). By employing the technology, we extend our method to multi-fingered device (Fig. 2).

2 Prototype System

For the first prototype, we use an electrotactile display device (Kajimoto Lab.). The device is designed for direct electrostimulation to fingers. However it outputs 300 V of controlled multiple electrostimulation easily. Based on the device, we design the electrostatic force display. First, we create a single electrode system (Fig. 3). This is made from aluminum foil and 15 μm thicknesses of plastic film. With the electrode, we can generate small vibration to the finger.

Next we use a new electrotactile display system (Kajimoto Lab.) By employing the device, we create multiple electrode system (Fig. 3 (Right)). The electrodes are

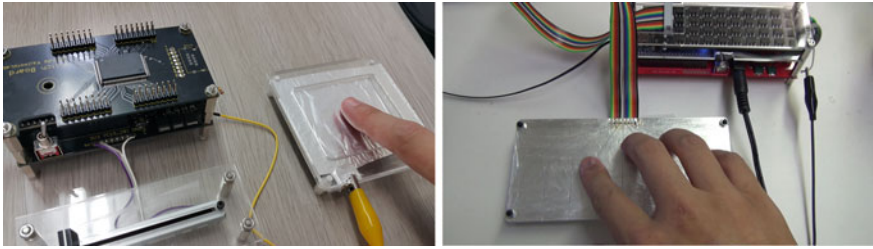


Fig. 3 *Left* Stimulation with single electrode. *Right* Stimulation with multiple electrodes

made from aluminum foil and 15 μm thicknesses of plastic film. With the electrode, we can confirm stronger vibration to the finger compared to 300 V of electrostatic device. In the next session we tested two displaying methods toward multiple electrodes.

3 Two Displaying Method

3.1 Sinusoidal Wave Input

By employing sinusoidal wave input to every electrodes, and by rubbing every electrodes with the fingers, each finger can feel a small bumps [2]. We can confirm that the conventional displaying method can be used to multiple electrodes, too (Fig. 4).

3.2 Rubbing Between Electrodes

By employing scanning input to every electrodes and rubbing the electrodes with a finger, the vibration can be felt far stronger than the sinusoidal input. This result shows that the edge of multiple electrodes can generate stronger output to the rubbing finger.

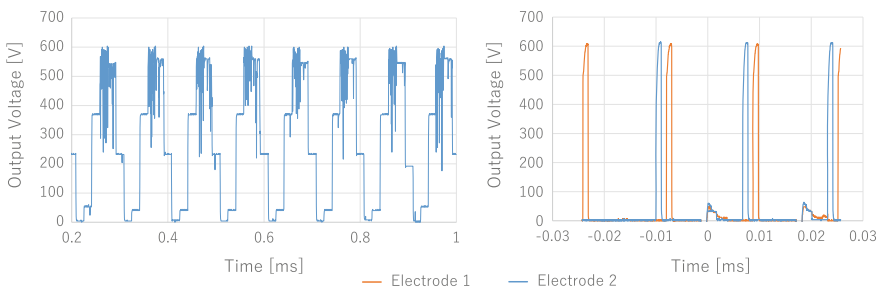


Fig. 4 *Left* Sinusoidal wave input. *Right* Transmitting input

4 Conclusions

In this research, we propose to extend our previous method [2] to multi-fingered device with electrostatic display. First, we test the electrostatic force display with simple devices, and design the multiple electrode system. Second, we test multiple electrodes with 600 V output, and confirm the stronger stimulation. By employing sinusoidal input, we can generate a small bumpy surface. By employing scanning input to the electrodes, we can generate stronger output to the rubbing finger. As a next step, we will hold quantitative experiments with the method and develop better stimulation methods with multiple electrodes.

Acknowledgements This work was partly supported by JSPS KAKENHI Grant Number JP16H 01662 (Grant-in-Aid for Scientific Research on Innovative Areas, “Innovative SHITSUKSAN Science and Technology”).

References

1. Chubb, E.C., Colgate, J.E., Peshkin, M.A.: Shiverpad: a glass haptic surface that produces shear force on a bare finger. *IEEE Trans. Haptics* 189–198 (2010)
2. Saga, S., Raskar, R.: Simultaneous geometry and texture display based on lateral force for touch-screen, pp. 437–442 (2013)
3. Bau, O., Poupyrev, I., Israr, A., Harrison, C.: TeslaTouch: electrovibration for touch surfaces, pp. 283–292. *ACM* (2010)

Development of a Sole Pressure Display

Tetsuhiro Okano, Kengo Hiki, Koichi Hirota, Takusya Nojima,
Michiteru Kitazaki and Yasushi Ikei

Abstract We have developed a haptic device that presents a pressure sensation on the sole of the foot. The device is comprised of an triangular array of 128 air cylinders aligned 10 mm pitch. Each air cylinder is capable of presenting a force of 3.5 N, hence 4 N/cm². The size of the array is approximately 7.5 × 13 cm, which will cover about the half of the foot. Using the device, a preliminary experiment on the characteristics of groping of the foot was performed, and it was observed that the area and direction of the foot affected the accuracy of position recognition.

Keywords Sensation of pressure · Pneumatic device · Groping of foot

T. Okano (✉) · K. Hiki · K. Hirota · T. Nojima
The University of Electro-Communications, 1-5-1 Chofugaoka,
Chofu, Tokyo 182-8585, Japan
e-mail: t.okano@vogue.is.uec.ac.jp

K. Hiki
e-mail: hikikeigo@vogue.is.uec.ac.jp

K. Hirota
e-mail: hirota@vogue.is.uec.ac.jp

T. Nojima
e-mail: nojima@vogue.is.uec.ac.jp

M. Kitazaki
Toyohashi University of Technology, 1-1 Hibarigaoka, Tempaku-Cho,
Toyohashi, Aichi 441-8580, Japan
e-mail: mich@tut.jp

Y. Ikei
Tokyo Metropolitan University, 6-6 Asahigaoka, Hino-Shi,
Tokyo 191-0065, Japan
e-mail: ikei@tmu.ac.jp

1 Background and Purpose

The foot is a part of the human body which we can actively move and touch to obtain haptic information from our environment. This fact suggests that the foot can play a greater role in recognition and manipulation in computer-human interaction.

Most of the haptic researches have focused on hand and fingers. Some studies have focused on the presentation of fine textures on the fingertip; Bliss et al. developed the OPTACON device, which presents tactile patterns using a vibro-tactile display [1]; the research is aimed at assisting blind people by converting a visual image into a tactile pattern. Ikei et al. applied a similar vibro-tactile device, which is called Texture Display, to present textures of virtual objects [2].

Significant research efforts on haptic feedback to the hand have focused on improved performance of object manipulation. Sato and his colleague have made efforts to expand force feedback to multiple fingers of both hands [3, 4]. In addition, there are commercially available devices for hand force feedback [5].

Lederman et al. proposed a taxonomy of the recognition through haptic interaction called exploratory procedure [6]. In a series of studies, they also pointed out the significance of tactile sensation that provides distributed information on the skin surface [7]. Most haptic devices are considered to be lacking in this information because they have relatively small degrees of freedom.

There are other studies that have investigated the presentation of tactile patterns to other parts of body other than the hand. Collins implemented a device called Tactile Television that presents tactile patterns to the back using a 20×20 solenoid array [8]. Kajimoto et al. developed an electro-tactile device with 512 electrodes to present stimulations on the forehead [9]. These studies were aimed at visual-to-tactile conversion for blind people and were not intended to help virtually performing haptic recognition. To the best of our knowledge, there is no research that deals with the haptic exploration of the foot.

This paper describes the development of a prototype system that presents pressure distribution on the back or sole of the foot. The paper also describes the implementation of an experimental system to evaluate the performance of groping by the foot.

2 Pressure Device

The two-point discrimination threshold on the sole is about 10–20 mm [10]. The pneumatic actuator, or air cylinder, was chosen as the actuation mechanism after considering the possible pitch of aligning actuators as well as the intensity of output force. Air cylinders can be easily miniaturized as they have a simple mechanical structure.

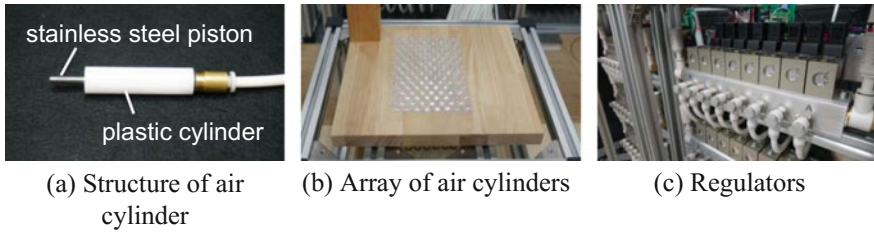


Fig. 1 Pressure device

The device was composed of the control and display components. The display comprised an array of 128 air cylinders. The air cylinder has a stainless steel piston inserted in a plastic cylinder (see Fig. 1a). The diameter of the cylinder is 3 mm and outputs a force of 3.5 N when the air pressure is 0.5 MPa. The air cylinders were aligned in a triangular array with a 10-mm pitch (see Fig. 1b). The size of array was approximately 7.5×13 cm, which covers about the half of the foot.

The air pressure was controlled by electro-pneumatic regulators (see Fig. 1c). The regulator outputs the air whose pressure is controlled by an analog input voltage. The analog voltage was generated by a microcomputer and D/A converters, and as is stated later, the voltage was controlled via a PC through a USB connection. An air compressor was used as the air source; the air was supplied to the regulators through filters and a reservoir tank. The output pressure of the compressor was 0.59–0.78 MPa, which was sufficiently high to present a force of 3.5 N at the air cylinder.

3 Groping System

Groping is considered as the process of recognizing the position and shape of the object on the floor by sliding the foot and sensing the pressure distribution under the foot. In our virtual groping system, the pressure distribution is fed back by the device based on the position of the foot measured by the sensor.

The device was equipped with wheels which enabled horizontal movement. Each actuator generates a force when it is located on the virtual object. The position

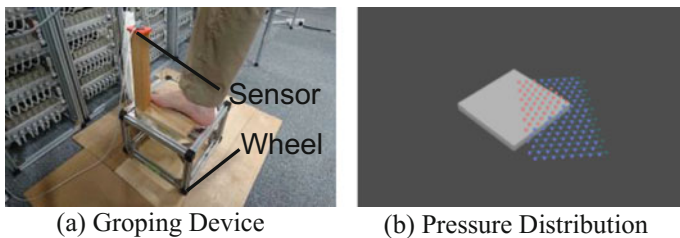


Fig. 2 Groping system

and orientation of the device were measured using a magnetic sensor (Fastrak, Polhemus). Implementation of the Groping Device is shown in Fig. 2. Although, the pressure between the foot and the object needs to be computed by simulating the deformation of the foot caused by the virtual object, in our present system, this process was skipped for the sake of simplicity, and just the pressure distribution was defined. The force produced by each actuator was determined by looking up the pressure distribution.

4 Preliminary Experiment

A preliminary experiment on the accuracy of groping by foot was performed. The subjects were asked to move their foot so that the peak of the pressure distribution (or object center) comes to a specific point (or target point), relying solely on the

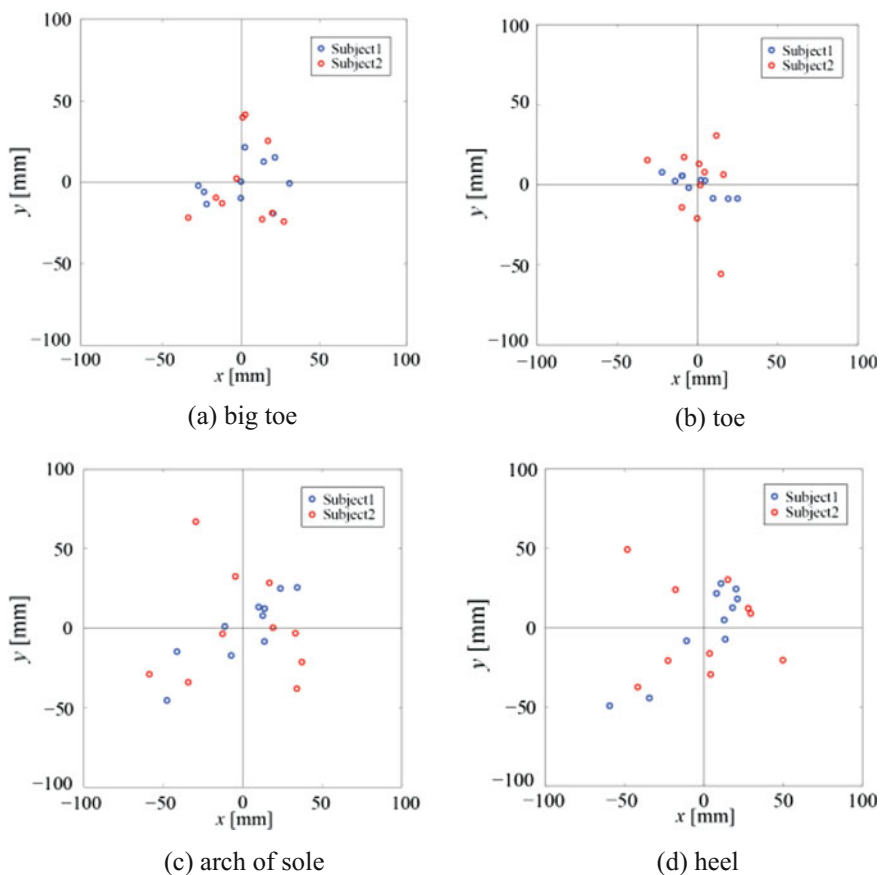


Fig. 3 Distribution of recognized center position

sensation of pressure. The target point is a fixed point in the image of the subject and not explicitly indicated by the experimenter. By measuring the recognized positions of the object center on the foot multiple times, the distribution of the recognized positions around the target point was estimated, and the variance in the recognition of the target point was observed. In our study, the standard deviation was regarded as an index of position recognition accuracy. The number of subjects was 2, and their age was in range of 23–24. The subjects were asked to determine the target point in the area of big toe, toe, arch of foot, and heel (i.e., four conditions), and performed ten groping tasks for each condition. The distribution of the pressure was a sinusoidal convex shape whose radius was 50 mm.

Figure 3 shows the result of the experiment, where the distribution of the center position in the foot coordinate (i.e., x and y directions are right and front, respectively) has been plotted separately depending on the condition. The difference of accuracy depending on the area and direction was observed, although the number of subjects is too small arrive at concrete conclusions. In addition, big toe and toe accuracy was better than that of the arch of sole and heel.

5 Future Work

Further investigation with larger number of subjects is required to provide a more accurate evaluation of position recognition. The alignment of actuators on the device should be reassessed by varying the density of actuators depending on the difference of tactile resolution. This may help in determining the minimum number of actuators required to efficiently cover the sole of the foot.

Acknowledgements This research was supported by JSPS KAKENHI Grant Number JP26240029 and MIC SCOPE Grant Number 141203019.

References

1. Bliss, J.C., Katcher, M.H., Rogers, C.H., Shepard, R.P.: Optical-to-tactile image conversion for the blind. *IEEE Trans. Man-Mach. Syst. MMS* **11**(1), 58–65 (1970)
2. Ikei, Y., Wakamatsu, K., Fukuda, S.: Texture presentation by vibratory tactile display-image based presentation of a tactile texture. In: *Proceedings of VRAIS'97*, pp. 199–205 (1997)
3. Kohno, Y., Walairacht, S., Hasegawa, S., Koike, Y., Sato, M.: Evaluation of two-handed multi-finger haptic device SPIDAR-8. In: *Proceedings of ICAT2001*, pp. 135–140 (2001)
4. Liu, L., Miyake, S., Akahane, K., Sato, M.: Development of string-based multi-finger haptic interface SPIDAR-MF. In: *Proceedings of ICAT2013*, pp. 67–71 (2013)
5. CyberGlove Systems: CyberGlove Systems LLC; in Wikipedia. <http://www.cyberglovesystems.com/> (2015). Accessed 23 Oct 2016
6. Lederman, S.J., Klatzky, R.L.: Extracting object properties by haptic exploration. *Acta Physiol.* **84**, 29–40 (1993)

7. Lederman, S.J., Klatzky, R.L.: Haptic identification of common objects: effects of constraining the manual exploration process. *Percept. Psychophys.* **66**(4), 618–628 (2004)
8. Collins, C.C.: Tactile television: mechanical and electrical image projection. *IEEE Trans. Man-Mach. Syst. MMS* **11**(1), 65–71 (1970)
9. Kajimoto, H., Kanno, Y., Tachi, S.: Forehead electro-tactile display for vision substitution. In: *Proceedings of EuroHaptics 2006*, pp. 75–79 (2006)
10. Weinstein, S.: Intensive and extensive aspects of tactile sensitivity as a function of body part, sex and laterality. In: *The First Int'l Symposium on the Skin Senses*, pp. 223–261 (1968)

A Design of a New Electro Tactile Beat Module

Won-Hyeong Park, Sang-Youn Kim, Kunnyun Kim
and Tae-Heon Yang

Abstract The use of two or more vibration motors in consumer electronic devices can be a solution to haptically simulate a variety of graphical objects. When there is no rendering method to haptically simulate target objects, the manipulation feeling can be missing and the use of motors can be more insecure. One of the several haptic rendering methods is to use beat vibration which is interference pattern between two or more vibrations of slightly different frequencies from two or more vibration motors. However, the strategy of beat vibration brought a new issue for handling multiple vibration motors. This paper presents a new electro tactile beat module which does not need any mechanical vibration motors.

Keywords Electro tactile beat · Beat vibration · Vibrotactile · Haptics · Tactile sensation

1 Introduction

To convey physical haptic stimuli such as vibration, distributed pressure, temperature, hardness, compliance or roughness to humans, a lot of actuators (linear resonant actuators [1], piezoelectric actuators [2, 3], thermal elements [4], solenoids [5], shape memory alloys [6], and ultrasonic/ultrasound actuators [7]) have been developed. Among these actuators, a linear resonant actuator (LRA) is widely used in small consumer electronic devices because of its small size and large vibrational force.

W.-H. Park · S.-Y. Kim

Interaction Laboratory of Advanced Technology Research Center,
Korea University of Technology and Education, Cheonan, South Korea
e-mail: sykim@kut.ac.kr

K. Kim

Korea Electronics Technology Institute, KETI, Sungnam, Republic of Korea

T.-H. Yang (✉)

Center for Mass and Related Quantities, KRISS, Daejeon, Republic of Korea
e-mail: thyang@kriss.re.kr

© Springer Nature Singapore Pte Ltd. 2018

S. Hasegawa et al. (eds.), *Haptic Interaction*, Lecture Notes
in Electrical Engineering 432, DOI 10.1007/978-981-10-4157-0_31

Although the actuator can increase the quality of communication or manipulation, it can hardly express the plentiful haptic feedback. In order to create a variety of tactile sensation in consumer electronic devices, S.Y. Kim proposed a vibrotactile rendering method with two vibration motors (an eccentric motor and a solenoid actuator) and applied it to a mobile racing game [8]. K.U. Kyung developed a Ubi-pen, which provides vibration and distributed pressure, with two vibration motors [9]. S.Y. Kim introduced the concept of traveling vibrotactile wave enabling users to haptically feel the presence of static objects or the motions of dynamic objects [10]. The traveling vibrotactile wave is a vibration flow which originates from one point and gradually propagates to other points. As we described above, tactile feedback can be generated based on a single vibrator or two or more vibrators in many consumer electronic devices. Recently, beat vibration, which is composed of two slightly different frequencies, is used for many haptic applications [11, 12]. However, since this beat vibration can be achieved by interfering two vibration signals having slightly different frequencies, two or more vibrotactile actuators are needed. This paper introduces a new electro tactile beat (ETB) module which can create beat vibrations without any vibrotactile actuators. In the proposed ETB module, two electric fields are applied for creating beat vibration.

2 The Proposed ETB Module

Figure 1a shows a schematic illustration of the proposed electro tactile beat (ETB) module consisting of an upper layer, four connectors, and a lower layer. The two layers are connected to each other via the four connectors having 0.5 mm height. The upper plate having 2 mm thickness is made of acrylic. Electrode (electrode 1) is applied to the beneath of the upper layer by spraying silver nanowire with thickness of 10 μm . The lower layer is made of glass epoxy laminate with thickness of 0.5 mm, and it has two electrodes (electrode 2 and electrode 3, colored in green and yellow, respectively) on the upper surface of the lower layer. The electrode 2 and electrode 3 are made of copper, and they have a form as an

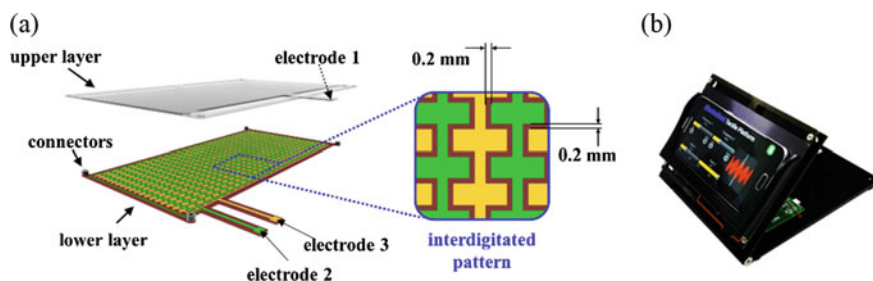


Fig. 1 Proposed ETB module and its platform: **a** structure of the ETB module, **b** fabricated ETB platform

interdigitated pattern with a 0.2 mm gap as shown in the inset image of the Fig. 1a. Let us consider the case in which a ground signal is connected to the electrode 1 (in the upper layer) and two input voltages having slightly different frequencies are applied to the electrode 2 and electrode 3 (in the lower layer), respectively. The input voltages cause two different electric field on the lower layer, and the two electric fields are influenced each other by the small gap (0.2 mm). The influence makes a new electric field, and resulting in an interference pattern like beat phenomenon. The newly created electric field causes electrostatic attraction force between the upper layer and the lower layer. The electrostatic attraction force makes the lower layer vibrates, and the vibration is propagated to the upper layer via the four connectors. Finally, users can feel beat vibrations on the upper layer. Figure 1b shows the fabricated ETB module.

3 Conclusion

In this paper, we proposed the concept of an electro tactile beat module that does not need mechanical actuators. If the proposed module is incorporated into consumer electronic devices, immersive and rich vibrotactile sensations will be provided to users when they interact with their devices.

Acknowledgements This research was supported by the Dual Use Program Cooperation Center (Development of tactile display device for Virtual reality-based flight simulator, 12-DU-EE-03), and also funded by the IT R&D program of Ministry of Trade, Industry and Energy Republic of Korea (Development of Natural Multi-touch/Multi-force Technology based on Cognitive User Experience, 10043388).

References

1. Kweon, S.D., Park, I.O., Son, Y.H., Choi, J., Oh, H.Y.: Linear vibration motor using resonance frequency. U.S. Patent 7,358,633, (2004)
2. Wagner, M., Roosen, A., Oostru, H., Hoppner, R., Moya, M.D.: Novel low voltage piezoactuators for high displacement. *J. Electroceram.* **14**(3), 231–238 (2002)
3. Wood, R.J., Steltz, E., Fearing, R.S.: Optimal energy density piezoelectric bending actuators. *Sens. Actuators A* **119**, 476–88 (2005)
4. Gallo, S., Cucu, L., Thevenaz, N., Sengül, A., Bleuler, H.: Design and control of a novel thermo-tactile multimodal display. In: 2014 IEEE Haptics Symposium (Haptics) (2014)
5. Shakeri, G., Brewster, S.A., Williamson, J., Ng, A.: Evaluating haptic feedback on a steering wheel in a simulated driving scenario. In: Proceedings of the 2016 CHI Conference Extended Abstracts on Human Factors in Computing Systems. ACM (2016)
6. Anderson, W., Eshghinejad, A., Azadegan, R., Cooper, C., Elahinia, M.: A variable stiffness transverse mode shape memory alloy actuator as a minimally invasive organ positioner. *Eur. Phys. J. Spec. Top.* **222**(7), 1503–1518 (2013)

7. Wilson, G., Carter, T., Subramanian, S., Brewster, S.A.: Perception of ultrasonic haptic feedback on the hand: localisation and apparent motion. *Proceedings of the 32nd Annual ACM Conference on Human Factors in Computing Systems*. ACM (2014)
8. Kim, S.Y., Kim, K.Y., Soh, B.S., Yang, G., Kim, S.R.: Vibrotactile rendering for simulating virtual environment in a mobile game. *IEEE Trans. Consum. Electron.* **52**(4), 1340–1347 (2006)
9. Kyung, K.-U., Lee, J.-Y.: Ubi-Pen: a haptic interface with texture and vibrotactile display. *IEEE Comput. Graphics Appl.* **29**(1), 56–64 (2008)
10. Kim, S.-Y., Kim, J.-O., Kim, K.Y.: Traveling vibrotactile wave—a new vibrotactile rendering method for mobile devices. *IEEE Trans. Consum. Electron.* **55**(3), 1032–1038 (2009)
11. Lim, S.-C., Kyung, K.-U., Kwon, D.-S.: Effect of frequency difference on sensitivity of beats perception. *Exp. Brain Res.* **216**(1), 11–19 (2012)
12. Christian, C., Marco, D., Maria, C.: A miniature vibrotactile sensory substitution device for multifingered hand prosthetics. *IEEE Trans. Biomed. Eng.* **59**(2), 400–408 (2012)

Part III
Force Feedback Devices and Rendering
Methods

Proposal and Implementation of Non-grounded Translational Force and Torque Display Using Two Vibration Speakers

Takeshi Tanabe, Hiroaki Yano and Hiroo Iwata

Abstract We here propose a device that can display a translational force and torque using two vibration speakers. Each vibration speaker generates an asymmetric vibration when a sound with an asymmetric amplitude is input. Asymmetric vibrations induce perceived forces that pull or push a user's hand in a particular direction. The user perceives a translational force and/or torque with his/her thumb and index finger based on the direction and amplitude of each speaker's force.

Keywords Non-grounded haptic interface · Vibration speaker · Translational force and torque

1 Introduction

The number of mobile and wearable devices, such as smart phones and smart watches is currently increasing. Non-grounded haptic interfaces have been expected as new display elements for these devices to add the ability to generate haptic sensation. Such devices can generate these sensations in any location because they do not need to be fixed on the ground. Non-grounded haptic interfaces that use the kinesthetic sensory illusion have been proposed. The sensory properties of humans have non-linear characteristics [1]. When a strong stimulus is exerted before a weak stimulus, a user tends to perceive the stronger stimulus and ignore the weak stimulus. Based on this characteristic, Amemiya et al. proposed an interface that is able to induce the sensory illusion using a device that generates a vibration with an asymmetric acceleration [2]. This device consists of a slider-crank mechanism and presents a force in a single direction to the user's hand, despite the vibration of the device.

T. Tanabe (✉) · H. Yano · H. Iwata
University of Tsukuba, 1-1-1 Tennodai, Tsukuba, Ibaraki 305-8577, Japan
e-mail: t_tanabe@vrlab.esys.tsukuba.ac.jp

H. Yano
e-mail: yano@iit.tsukuba.ac.jp

H. Iwata
e-mail: iwata@kz.tsukuba.ac.jp

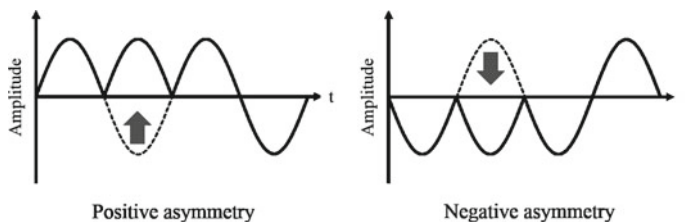


Fig. 1 Asymmetric waves

Similar sensations have been reported to occur using a vibrator. A vibrator can induce the sensation of a force in one direction by generating asymmetric vibrations based on input pulse width modulation (PWM) signals [3, 4]. Yem et al. reported that a DC motor could be used to generate a sense of a torque by inputting asymmetric saw-tooth waves [5]. We also proposed a non-grounded haptic interface that is equipped with a vibration speaker [6]. We confirmed that the vibration speaker generated a perceived force that pulled or pushed a user's hand in a particular direction when an asymmetric amplitude sound signal with a two cycle sine wave that was inverted for a half cycle was input. Figure 1 shows asymmetric waves.

In this paper, we propose a device that can display both a translational force and a torque using two vibration speakers. A user perceives the translational force and/or torque based on two forces exerted on the user's thumb and index finger. This paper describes the basic concept and a prototype system.

2 Basic Concept

Figure 2 shows the basic concept of our proposed method. We propose a device that consists of two vibration speakers (L-ch, R-ch). The two speakers are placed in a side-by-side configuration. When a user holds these between his/her thumb and index finger, each digit primarily perceives the force generated by the adjacent speaker. When the direction of the force exerted by each speaker is controlled, both a translational

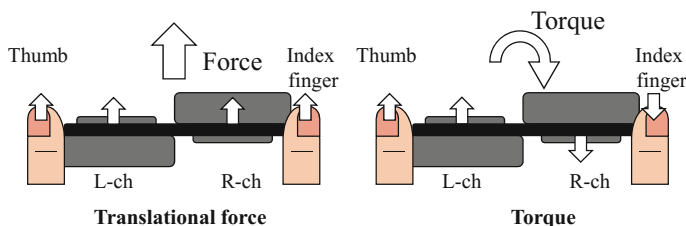


Fig. 2 Basic concept

Table 1 Directions of forces on index finger and thumb

| Thumb | Index finger | Direction of force |
|----------|--------------|--------------------|
| Forward | Forward | Forward |
| Backward | Backward | Backward |
| Forward | Backward | Clockwise |
| Backward | Forward | Counter clockwise |

force and torque can be perceived by the user. If forces with the same direction are presented at the user’s thumb and index finger, the user perceives a translational force in that same direction. In contrast, if forces with opposite directions are presented, the user perceives a torque (Table 1).

3 Prototype System

Figure 3 shows an overview and a dimensional drawing of the prototype device. Each vibration speaker was plugged into a Vibration Transducer Vp2 10 Ω from Acouve Lab ($\phi 43 \times 15$ mm). The asymmetric amplitude signals shown in Fig. 1 were used to provide the haptic sensation. The frequency of the waves were 75 Hz, based on the finding of a previous study that users perceived the strongest force at this frequency [6]. These signals were input through the stereo earphone jack (L-ch, R-ch) of a personal computer (PC). Each signal was amplified with an amplifier circuit using a power amplifier IC (LM386) with a maximum output voltage of ± 4.5 V. Finally, the amplified signal was input to the vibration speaker.

Two vibration speakers were placed on an acrylic plate (3 mm thick). The size of the device was 81.5 (w) \times 43 (h) \times 23 (d) mm, and it had a weight of 77 g. It could be gripped in one hand by a user. The user could perceive a translational force in the front/rear direction and/or a torque around its vertical axis, when gripping the ends of the device as shown in Fig. 3.

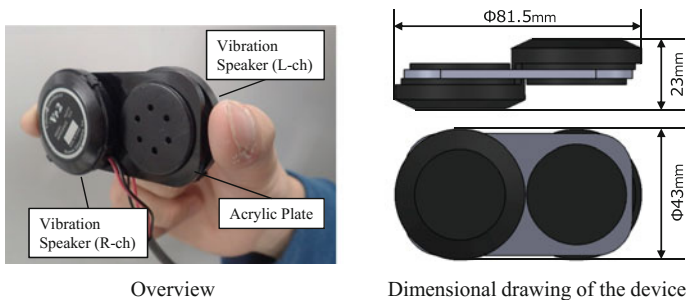
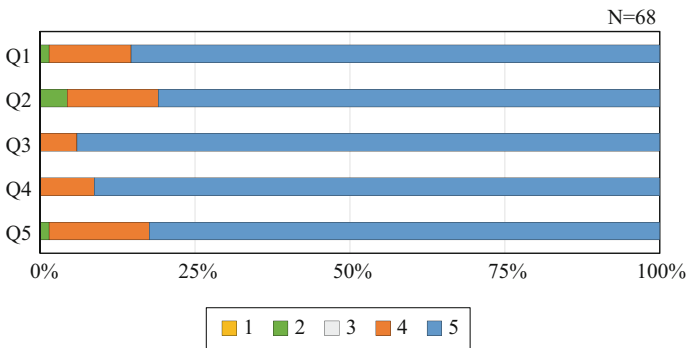


Fig. 3 Developed non-grounded translational force and torque display

Table 2 Questions on the questionnaire

| | |
|----|--|
| Q1 | Did you feel a pulling or pushing force(translational force) toward the front or rear? |
| Q2 | Were you able to identify the direction of the force? |
| Q3 | Did you feel a rotational force (torque)? |
| Q4 | Were you able to identify the direction of the rotational force? |
| Q5 | Were you able to discriminate the translational force from the torque? |

**Fig. 4** Results of questionnaire

4 User Test During Exhibition with Questionnaire

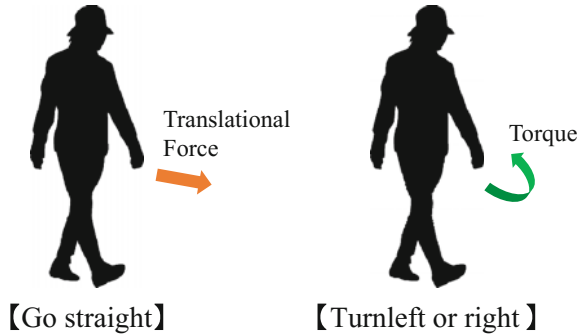
This device was exhibited at the 25th 3D & Virtual Reality Expo on 6/23/2016 [7]. We administered a questionnaire to participants at the exhibition. The five questions of this survey are listed in Table 2. A total of 68 individuals (67 males and 1 female, with an average age of 33.7 years and SD of 10.9 years) participated in the demonstration and were asked to rate each question on a scale of one (strongly disagree) to five (strongly agree). As shown in the results of Fig. 4, 80% of the participants were “strongly agree” to all the questions. This confirmed that the proposed device could present both a translational force and torque.

5 Applications

5.1 Pedestrian Navigation

A pedestrian navigation system could be considered as an application of this device. To provide guidance along a walking route, a system must have the ability to provide information about the walking direction, turning points, and turning directions. A pedestrian navigation system could be achieved by combining our device and a route

Fig. 5 Illustration of pedestrian navigation using our device



guidance system with GPS, which would even provide guidance for a user walking on a dark night. Figure 5 shows an illustration of pedestrian navigation using our device. Currently, the device can lead a user by exerting a translational force when traveling in a straight line. At a crossing, the user can change their walking direction based on the perception of a torque.

5.2 Motion Training System for Sports

Our device could be used as a motion training system for sports by guiding a user’s arm. Our device is not suitable for sports, such as tennis or baseball, which require a ball and/or sport equipment, because the player would need to hold both the device and equipment their in hand. However, it could be used to provide body motion guidance such as for Karate and Tai Chi. This type of motion training system could be achieved by combining a motion capture system and our device. The posture of the user’s arm could be guided by the torque, and the direction that the user should move their arm could be guided by the translational force. Moreover, this system would be more effective when combined with a visual display.

6 Conclusion

We proposed a non-grounded haptic device that can display both a translational force and torque using two vibration speakers. This device was demonstrated in an exhibition, and we asked the participants to fill out a questionnaire. The results demonstrated the effectiveness of the proposed method.

References

1. Stevens, S.: On the psychophysical law. *Psychol. Rev.* **64**(3), 151–181 (1957)
2. Amemiya, T., Ando, H., Maeda, T.: Lead-me interface for a pulling sensation from hand-held devices. *ACM Trans. Appl. Percept.* **5**(3), Article 15, 1–17 (2008)
3. Rekimoto, J.: Traxion: a tactile interaction device with virtual force sensation. In: *Proceedings of ACM Symposium on User Interface Software and Technology*, pp. 427–431 (2013)
4. Amemiya, T., Gomi, H.: Distinct pseudo-attraction force sensation by a thumb-sized vibrator that oscillates asymmetrically. In: *Proceedings of EuroHaptics 2014*, pp. 88–95 (2014)
5. Yem, V., Okazaki, R., Kajimoto, H.: Vibrotactile and pseudo force presentation using motor rotational acceleration. In: *Proceedings of Haptics Symposium 2016*, pp. 47–51 (2016)
6. Tanabe, T., Yano, H., Iwata, H.: Properties of proprioceptive sensation with a vibration speaker-type non-grounded haptic interface. In: *Proceedings of Haptics Symposium 2016*, pp. 21–26 (2016)
7. “- IVR - 25th 3D & Virtual Reality Expo”. <http://www.ivr.jp/en/Home/>. Accessed 23 July 2016

Engaging Weight Feedback for Bimanual Interaction

Stuart Burmeister, Kimin Kim and Jinah Park

Abstract The development of haptic display devices has brought a new level of immersion and realistic fidelity to virtual environments, allowing users to ‘feel’ the virtual world. In this paper, a virtual environment with bimanual haptic feedback for users will be demonstrated, both engaging the user with weight feedback of lifted objects and maintaining the stability of the interaction and simulation when passing objects between hands. Users can then complete a simple speed-training task in a virtual kitchen environment.

Keywords Bimanual · Haptics · Weight feedback · Simulation · Virtual environment

1 Introduction

One of the aims of virtual environments is to give users an engaging experience – where the user is encouraged, through enjoyment and interest, to continuously interact with and explore the environment. The addition of both haptic and visual cues can heighten this through the illusion of senses such as weight [1], creating a more immersive and ‘realistic’ environment, which has been shown to heighten user behaviour [2]. This paper presents a virtual environment that engages the user through bimanual interaction of graspable objects; however, unlike similar work [3], the weight sensation can be ‘passed’ between devices and hands. A simple

S. Burmeister (✉) · K. Kim · J. Park
School of Computing, Korea Advanced Institute of Science
and Technology (KAIST), 291 Daehak-ro, Yuseong-gu, Daejeon 34141,
Republic of Korea
e-mail: montross7@kaist.ac.kr

K. Kim
e-mail: kiminkim@kaist.ac.kr

J. Park
e-mail: jinah@cs.kaist.ac.kr

speed-training task is implemented within the environment, to further guide the user interaction.

2 System

The user interacts within a virtual kitchen environment, consisting of a table, sink, two cutting boards, four coloured plates, and an object that spawns on one of the two cutting boards (Fig. 1). The user can interact with the world through two virtual hands, each virtually coupled with a haptic device to display the forces ‘felt’ by that hand. This includes the weight feedback for when the user is lifting the object, providing a more immersive and engaging experience through the additional feedback.

Each object has a different weight based on its size, and the user feels the weight as they lift the object. Expanding this further to the bimanual setting, the user is able to pass the object between hands, shifting the weight to the alternate hand. In this case, if the weight is ‘passed’ all at once, the sudden shift of force causes jerky and unstable movements, breaking the immersion. To improve stability, the weight is slowly interpolated as the hands come together, sharing the weight equally as the object moves to the alternate hand, and then interpolated again as they separate.

3 Activity

To guide the interaction, a speed-training activity was implemented in the described environment. The user must place the object from the cutting board on the correspondingly coloured plate. The reach of both hands is restricted to one half of the virtual environment, with a small intersecting area, forcing the user to pass the object between hands to reach the entire space. The user is timed as they perform

Fig. 1 User interacting with the virtual environment



the activity, and they are scored based on the number of correct and incorrect placements, with the game ending after 11 correct placements.

Acknowledgements This research was supported by the National Research Foundation of Korea (NRF) grant funded by the Korea government (MSIP) (No. 2010-0028631).

References

1. Hannig, G., Deml, B.: Efficient bimodal haptic weight actuation. In: Kappers, A.M.L., Van Erp, J.B., Bergmann Tiest, W.M., Van Der Helm, F.C. (eds.) EuroHaptics 2010, Part I. LNCS, vol. 6191, pp 3–10. Springer, Heidelberg (2010)
2. Kilteni, K., Bergstrom, I., Slater, M.: Drumming in immersive virtual reality: the body shapes the way we play. *IEEE Trans. Vis. Comput. Graph.* **19**, 597–605 (2013)
3. Talvas, A., Marchal, M., Nicolas, C., Cirio, G., Emily, M., Lécuyer, A.: Novel interactive techniques for bimanual manipulation of 3D objects with two 3DoF haptic interfaces. In: Isokoski, P., Springare, J. (eds.) EuroHaptics 2012, Part I. LNCS, vol. 7282, pp. 552–563. Springer, Heidelberg (2012)

Substituted Force Feedback Using Palm Pressurization for a Handheld Controller

Taku Nakamura, Shota Nemoto, Takumi Ito and Akio Yamamoto

Abstract This paper describes application of force substitution using pressure stimulation on palm to a handheld controller. The prototype controller has two stimulators driven by voice coil motors to press user's both palms separately so that it can represent 2-DoF information, such as force and torque. As a demonstration, a virtual tank operation with first person view was implemented. By providing the pressure stimuli corresponding to the posture of the tank, the user can get intuitive information of the virtual terrain, such as slopes and bumps.

Keywords Force substitution · Ungrounded device · Pressure stimulation

1 Introduction

Haptic feedback for users with ungrounded devices, in a scenario where typical grounded force displays cannot be adopted, has been one of the important challenges in haptic technology. Use of vibration and/or inertia effect is suitable for

Research partially supported by the Center of World Intelligence Project for Nuclear S&T and Human Resource Development by MEXT Japan.

T. Nakamura (✉) · S. Nemoto · T. Ito · A. Yamamoto
The University of Tokyo, Hongo 7-3-1, Bunkyo-Ku, Tokyo 113-8656, Japan
e-mail: taku_nkat@aml.t.u-tokyo.ac.jp

S. Nemoto
e-mail: shota_nemoto@aml.t.u-tokyo.ac.jp

T. Ito
e-mail: takumi_ito@aml.t.u-tokyo.ac.jp

A. Yamamoto
e-mail: akio@aml.t.u-tokyo.ac.jp

S. Nemoto
Hitachi Construction Machinery Co., Ltd, Tokyo, Japan

such devices but has a challenge in representing continuous force; its applications are limited in impulsive force or directional cue rendering. On the other hand, force substitution [1–3], in which kinesthetic sensation is substituted by tactile stimuli, has a potential to represent continuous force, such as reaction force due to load change. In literature, force substitution by using skin stretch successfully provided force and torque feedback on a handheld device [3]. Our research group has focused on pressure stimulations on palms, whose basic concept was introduced in [4]. This work demonstrates operation of a crawler-type vehicle using a handheld controller on which the force substitution is implemented.

2 Demonstration

Figure 1 left shows the prototype controller. The controller has two joysticks to operate a remote/virtual vehicle and two stimulators driven by voice coil motors (Technohands, AVM30-15) to pressurize user's both palms separately. As a result, feedback of the controller could represent 2-DoF information, such as force and torque. In addition, a mechanism for adjusting the angle of the stimulators is installed to absorb individual differences of users' hands. The mechanism can adjust the angle from 0 to 45 degrees and the user can choose suitable angle for the feedback to feel as natural as possible.

As an application scenario, this work adopts remote control of a crawler-type vehicle with first person view. The appearance of the demonstration is shown in Fig. 1 right. A player operates a virtual tank that explores on virtual terrain in a monitor. Each joystick is in charge of driving the crawler on the corresponding side. Each stimulator pushes back the palms to represent external load on the corresponding crawler. The demonstration was implemented by using Unity game engine. The refresh rates of the haptic feedback and visual information were approximately 60 Hz. Since the stimulators only press the hands (and cannot pull), the system can only represent load toward backward direction.

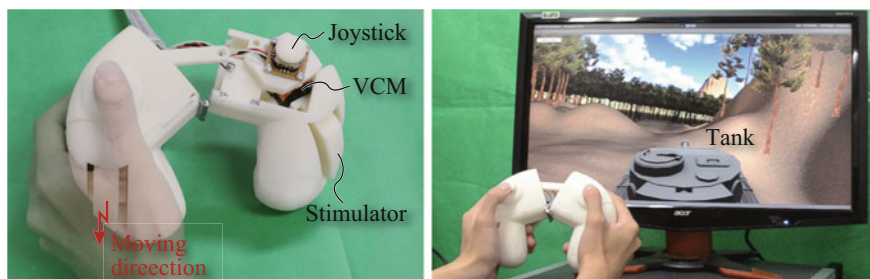


Fig. 1 Prototype controller (*left*) and appearance of demonstration (*right*)

In this particular implementation, the loads on the crawlers were calculated as $K(\sin \theta_p \pm \sin \theta_r)$ where θ_p and θ_r are the pitch and roll angle of the tank respectively, the plus sign is for the left-hand stimulator, and the minus for the right-hand one. When the tank goes up a slope, both stimulators press the user's palms. When one side of the tank rides on a bump, the stimulator on the riding side presses the palm stronger. Although this implementation is not perfectly correct in a physical sense, the controller can provide intuitive information on the interactions between the tank and the terrain.

References

1. Prattichizzo, D., et al.: Using a fingertip tactile device to substitute kinesthetic feedback in haptic interaction. In: EuroHaptics 2010, Part I, pp. 125–130. LNCS 6191 (2010)
2. Quek, Z.F., et al.: Sensory augmentation of stiffness using fingerpad skin stretch. In: Proceedings of IEEE World Haptics Conference 2013, Daejeon (2013)
3. Guinan, A.L., et al.: Discrimination thresholds for communicating rotational inertia and torque using differential skin stretch feedback in virtual environment. In: Proceedings of IEEE Haptics Symposium 2014, pp. 277–282, Houston (2014)
4. Asada, T., et al.: Investigation on substitution of force feedback using pressure stimulation on palm. In: Proceedings of IEEE Haptics Symposium 2016, pp. 389–390, Philadelphia (2016)

Virtual Two-Finger Haptic Manipulation Method

Alfonso Balandra, Virglio Gruppelaar, Hironori Mitake
and Shoichi Hasegawa

Abstract We purposed a novel method for haptic grasping that enables the user to dynamically and naturally control the grasping force between two virtual haptic pointers and the grasped object. This method uses a single haptic interface to control two virtual haptic pointers connected with spring-damper couplings. The user's grasping force is measured with a force sensor, this sensor is placed between the user's fingers and the haptic interface pointer. Then the measured force is introduced into the couplings that connect both pointers. By this means, the user can grab and control the grasping inertia of the grabbed object; enabling a natural and dexterous manipulation.

Keywords Haptic interaction · Two finger haptic interaction · Force sensor

1 Introduction

In our daily life we haptically interact with many objects by using our fingers. In order to steady grasp an object, humans need to use at least two fingers, usually the thumb and index fingers. By having this in mind, we propose a natural method to manipulate a virtual environment (VE) by using two virtual haptic pointers that represent the finger tips of the user. These virtual haptic pointers are connected to each other using a lineal and rotative couplings. To control the movement of both virtual pointers, we directly measured the users' grasping force with a force sensor,

A. Balandra (✉) · V. Gruppelaar · H. Mitake · S. Hasegawa
Tokyo Institute of Technology, 2 Chome-12-1 Ookayama, Meguro, Tokyo, Japan
e-mail: poncho@haselab.net
URL: <http://haselab.net>

V. Gruppelaar
e-mail: virgilio@haselab.net

H. Mitake
e-mail: mitake@haselab.net

S. Hasegawa
e-mail: hase@haselab.net

and then the measured force is directly introduced in to the coupling system causing the pointers to move. This method allows the user to dynamically adjust the grasping force between the pointers and the grasped object.

In contrast, to the commonly used virtual coupling method, that is one of the simplest solutions two manipulate a virtual object, where a push button located on the haptic device grip is used to activate or deactivate a coupling between the haptic avatar and the manipulated object [1]. For simple manipulation tasks this method is enough, but for more complex manipulations this method is not adequate. With this technique, the user do not have to much control on the inertial movement of the object that is grasping, because the user doesn't has the means to dynamically or naturally control the coupling force (grasping force).

2 Related Work

Previous haptic research proposals, about virtual grasping manipulation, were focused concretely on the design proposal of new haptic devices, for two fingers [2, 3] or multiple fingers [4]. These proposals rely on diverse hardware mechanisms to enable a transparent user manipulation, so by a set of different actuators, mechanisms and sensors the user fingers' position and grasping force are measured directly and input into the VE.

In contrast, our proposal is more simple in terms of hardware. Instead on relying on actuators to increase the degrees of freedom (DOF) of the haptic device, we propose to use a touch sensor and attach it to any commercial 6DOF haptic device pointer. By adding a touch sensor the user's finger grasping force can be measured, and then it can be use to move the haptic avatars accordingly to the user's applied force. So, contrary to other proposals that modified the haptic device pointer with extra actuators and sensors to measure the user's finger position, instead we propose to measure the user's applied grasping force on haptic device grip and use it as an input force for moving the virtual coupling system in between the haptic avatars.

On the other hand, we are not proposing any method or mechanism to measure the user's fingers position. Then, the consequence of using only sensors, without adding any extra actuators or mechanisms to the haptic device, to enable virtual grasping, will be an asymmetry between the haptic device display force and the users actions in the VE. [5] In other words, the haptic device asymmetric design, may reduce the grasping transparency because the user's fingers position will not match with the haptic avatars position in the VE. However, we consider that this may not have a great impact on the user's manipulation dexterity.

A similar proposal made by Melder et al. [6], used a set of virtual tools to enable the users two hand manipulation. These tools are then connected to the manipulated object using a set of virtual couplings and rigid frames, allowing a two hand manipulation. Melder also used virtual coupling to enable the VE manipulation, but contrary to our proposal, Melder's work is meant for two hand manipulation so he didn't

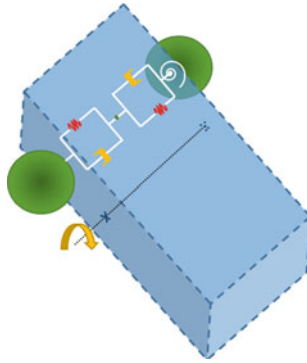


Fig. 1 A diagram of the virtual haptic pointers (*green spheres*) holding a parallelepiped by its parallel faces. Also the diagram shows the lineal spring-damper couplings between the pointers. If the applied force between the couplings is appropriate the object can rotate on its own center of mass (*black dashed line*)

consider the user's grasping force during the object's manipulation. And this may impede the user to have a dexterous control on more delicate manipulation tasks.

3 Description

For the implementation on the hardware side, only a commercial film type force sensor (Flexiforce A201) [7] was used. And on the software side we used two virtual haptic pointers connected with lineal and rotational spring-damper couplings. This coupling system, allow us to calculate the lineal force between the haptic pointers and also the friction between the couplings and the grasped object (see Fig. 1). In addition, the force sensor placed between the user's fingers and the haptic interface pointer, allow us to measure the real grasping force of the user to control the force introduced into the coupling between the virtual haptic pointers. Thereby, the user will be able to naturally and dynamically control the intensity of the grasping force, and by controlling his own grasping force they user will be able to perform specific manipulations on the object, like: gradually slip the object though his fingers or rotate the object on its center of mass while grabbing it.

4 Conclusion

In the demonstration the participants will be able to compare the virtual coupling manipulation method and the two finger grasping method, by manipulating different virtual objects with both methods. So, we expect to demonstrate that, the proposed method can enable a more natural and dexterous haptic operation compared to other manipulation techniques.

This method was developed and proved in Spidar G6 [8], but it could be easily applied on any other commercial haptic interface, like the Novint Falcon [9]. We consider that, the purposed method is versatile enough to be applied on different haptic environments and tasks where the inertial grasping turns to be important, like in medical applications, teleoperation or micromanipulation [10].

References

1. Howard, B.M., Vance, J.M.: Desktop haptic virtual assembly using physically based modelling. *Virtual Reality* **11**(4), 207–215 (2007)
2. Ang, Q.-Z., Horan, B., Najdovski, Z., Nahavandi, S.: Grasping virtual objects with multi-point haptics. In: 2011 IEEE Virtual Reality Conference, pp. 189–190. IEEE (2011)
3. Barbagli, F., Salisbury, K., Devengenzo, R.: Toward virtual manipulation: from one point of contact to four. *Sens.Rev.* **24**(1), 51–59 (2004)
4. Liu, L., Miyake, S., Maruyama, N., Akahane, K., Sato, M.: Development of Two-Handed Multi-finger Haptic Interface SPIDAR-10, pp. 176–183. Springer, Berlin (2014)
5. Barbagli, F., Salisbury, K.: The effect of sensor/actuator asymmetries in haptic interfaces. In: 2003 11th Symposium on Haptic Interfaces for Virtual Environment and Teleoperator Systems, HAPTICS 2003. Proceedings, pp. 140–147. IEEE (2003)
6. Melder, N.: Psychophysical Size Discrimination using Multi-fingered Haptic Interfaces. *Perception*, pp. 274–281 (2004)
7. Ferguson-Pell, M., Haggisawa, S., Bain, D.: Evaluation of a sensor for low interface pressure applications. *Med. Eng. Phys.* **22**(9), 657–663 (2000)
8. Yanlin, L., Murayama, J., Akahane, K., Hasegawa, S., Sato, M.: Development of new force feedback interface for two-handed 6dof manipulation spidarg-g system. In: Proceedings of the 13th Int. Conf. on Artificial reality and Telexistence. pp. 166–172 (2003)
9. Martin, S., Hillier, N.: Characterisation of the novint falcon haptic device for application as a robot manipulator. In: Australasian Conference on Robotics and Automation (ACRA), pp. 291–292. Citeseer (2009)
10. Kamiyama, K., Kojima, M., Horade, M., Mae, Y., Arai, T.: Development of simplified haptic interface for two-finger micro-manipulator. In: 2014 International Symposium on Micro-NanoMechatronics and Human Science (MHS), pp. 1–1. IEEE (2014)

Inducing Wrist Twist During Arm Swing by Using Gyro Effect

Hirokazu Miyahara, Yasutoshi Makino and Hiroyuki Shinoda

Abstract We propose a device that controls arm twist motion by applying rotational force to wrist by gyro effect only while users swing their arms. Gyro moment occurs when an object rotates around two independent axes. In this paper, we use two rotational axes in two different motions to control user's arm twist motion. One is their own arm motion: such as a swing of an arm. And the other one is our device that is mounted on the arm with rotating disks. By using this device, user's wrist voluntarily rotates based on a gyro effect. We used two rotating disks for controlling the amount of gyro moment. For instance, no gyro moment is generated when two disks rotate on the same angular velocity and opposite direction of rotation. In this paper, we show that our prototype system can induce wrist twist as a result of swing down of an arm.

Keywords Gyro effect · Haptic feedback · Wearable device

1 Introduction

In this research, we propose a method for controlling a wrist twist motion in swinging an arm, such as a pitching a ball, by applying rotational force by gyro effect. This method can present actual rotational force to users' wrist only when they swing their arm. By using this method, it is possible to teach wrist rotational motion such as throwing a breaking ball without users' intention of the arm motion by themselves. In order to teach motions unconsciously, many studies are proposed by using tactile or haptic stimulus for direct operation of users' limbs. Hanger reflex

H. Miyahara (✉) · Y. Makino · H. Shinoda
University of Tokyo, 5-1-5, Kashiwano-ha, Kashiwa-shi, Chiba 277-8561, Japan
e-mail: miyahara@hapis.k.u-tokyo.ac.jp

Y. Makino
e-mail: Yasutoshi_Makino@k.u-tokyo.ac.jp

H. Shinoda
e-mail: Hiroyuki_Shinoda@k.u-tokyo.ac.jp

[1] can induce wrist twist as a pseudo force. Users' skin deformation by using two ball effectors [2] can guide the hand motions of translation and rotation along four axes. Shikata et al. proposed a method that induced elbow joint flexion and extension by stretching skin surfaces [3]. These methods are not kinesthetic stimulus but tactile stimulus on skin surface. Chen et al. proposed a method that controls forearm rotation by force of wire tension as external artificial muscles [4]. This method can guide arm rotation by giving external force from a static state. Possessed hand [5] proposed a way to control finger motion by applying electrical stimulus on a forearm.

There are many proposed methods for force presentation by gyro effect. For generating gyro moment, an object must rotate around two independent axes. In general, many methods achieve these rotations of two different axes by rapidly rotating two motors orthogonally attached each other. For example, TorqueScreen [6] can present gyro moment in handheld devices such as smartphones or tablets. Antolini et al. proposed a device which includes two rotational disks using gimbal mechanism for indicating the direction by gyro moment [7]. Yano et al. proposed a method that uses arm motion for generating gyro effect [8]. In our research, we focused on the rotational movement of the arms around the joints in the pitching motion. Our proposed device does not need gimbal mechanism, and includes two rotational disks along same axis. In this paper, we show that users' wrist rotates only when they swing their arm.

2 Proposed System

2.1 Principle

Gyro moment is a force which arises when a rotating object tilts its angle along the perpendicular axis to the rotation axis. The amount of the torque is estimated as follows. Moment of inertia of the disk with radius r , mass m is

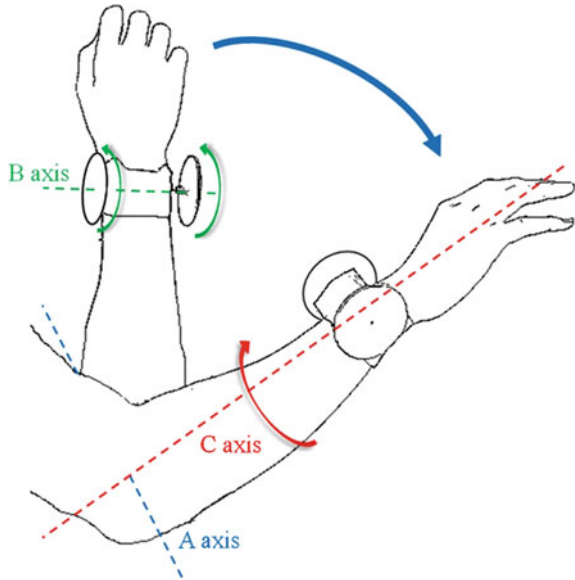
$$I = \frac{1}{2}mr^2 \quad (1)$$

Here we define the angular velocity of a rotating disk ω and Ω is the angular velocity of the vertical axis to the rotation axis of the disk. The gyro moment T is written as

$$T = I\omega \times \Omega = \frac{1}{2}mr^2\omega \times \Omega \quad (2)$$

Figure 1 shows a schematic diagram of the proposed method using gyro moment. Rotational motion of the arm swing occurs along the A-axis. We use a rotational disk along the B-axis so that it becomes perpendicular to the A-axis.

Fig. 1 Schematic illustration of proposed system



When the rotating disks move with the arm swing the motion results in the gyro moment generated along the C-axis, which is perpendicular to both axes. User feels a force to rotate their wrist along the C-axis. When users install two disks on the arm along B-axis as shown in the figure, a total amount of gyro moment is sum of two disks. If the each disk rotates the same angular direction, the total gyro moment is sum of torque generated by two rotational disks, and it causes pronation or supination motion of arm. By contrast, if each rotational direction is opposite with the same amount of angular momentum, the moment applied to the arm becomes cancelled out.

2.2 Prototype

The rotating disks and motors for generating a gyro moment are shown in Fig. 2a. The rotating disk has its radius $r = 30.0$ mm, and its mass $m = 13.2$ g. The rotating disk is a thin cylindrical shape made of a glass epoxy copper-clad laminate substrate, which is usually used for making electric circuits. The rotating disk's moment of inertia is $I = 5.92 \times 10^{-6}$ kg · m², which is calculated by the Eq. (1). The direction and the magnitude of gyro moment are controlled by rotating speed and direction of motors using microcomputer and H-bridge circuits with transistors. Two sets of the rotating disks are mounted on the arm as shown in Fig. 2b. Total mass of the system on the arm including the motors, disks and covering packaging is 337 g.

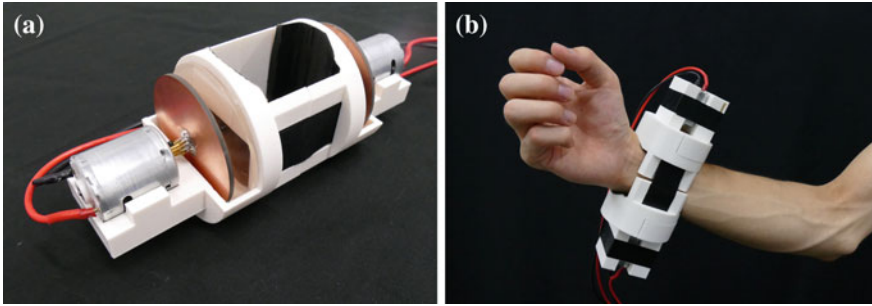


Fig. 2 a Rotational disks and motors, b device mounted on arm

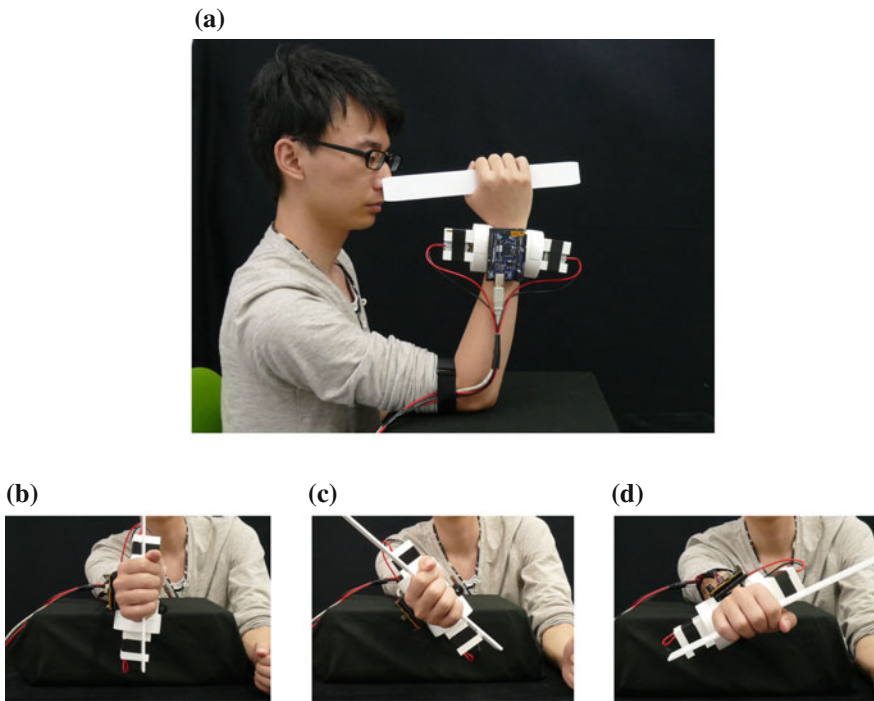


Fig. 3 Wrist twist during swing down the arm, a beginning state, b non-induction, c pronation, d supination

2.3 Demonstration

Figure 3 shows the demonstration system that can induce the rotation of users' wrist during the arm motion. At a beginning state (Fig. 3a), users set their arm perpendicular to the ground. After they swing their arm 90°, wrist doesn't rotate

(Fig. 3b) or rotates in two patterns, pronation (Fig. 3c) or supination (Fig. 3d) direction. By controlling rotational disks velocity independently, the device can present the rotational force feedback of desired direction and strength.

Acknowledgements This work was partly supported by JSPS Grant-in-Aid for Young Scientists (A) 15H05315 and JST ACCEL Embodied Media Project.

References

1. Nakamura, T., Nishimura, N., Sato, M., Kajimoto, H.: Development of a Wrist-Twisting Haptic Display Using the Hanger Reflex. In: Proceedings of 11th Conference on Advances in Computer Entertainment Technology. ACE'14, Article No. 33 (2014)
2. Yem, V., Otsuki, M., Kuzuoka, H.: Development of wearable outer-covering haptic display using ball-effector for hand motion guidance. In: Haptic Interaction, Lecture Notes in Electrical Engineering 277, pp. 85–89 (2015)
3. Shikata, K., Makino, Y., Shinoda, H.: Inducing elbow joint flexion by shear deformation of arm skin. In: Proceedings of IEEE World Haptics Conference on WHC'15, WIP-30 (2015)
4. Chen, C., Chen, Y., Chung, Y., Yu, N.: Motion guidance sleeve: guiding the forearm rotation through external artificial muscles. In: Proceedings of 2016 CHI Conference on Human Factors in Computing Systems. CHI'16, pp. 3272–3276 (2016)
5. Tamaki, E., Miyaki, T., Rekimoto, J.: Possessedhand: technique for controlling human hands using electrical muscles stimuli. In: Proceedings of SIGCHI Conference on Human Factors in Computing Systems. CHI'11, pp. 543–552 (2011)
6. Murer, M., Maurer, B., Huber, H., Huber, H., Aslan, I., Tscheligi, M.: Torquescreen: actuated flywheels for ungrounded kinesthetic feedback in handheld devices. In: Proceedings of 9th ACM International Conference on Tangible, Embedded, and Embodied Interaction. TEI'15, pp. 161–164 (2015)
7. Antolini, M., Bordegoni, M., Cugini, U.: A Haptic Direction Indicator Using the Gyro Effect. In: Proceedings of IEEE World Haptics Conference on WHC'11, pp. 251–256 (2011)
8. Yano, H., Yoshie, M., Iwata, H.: Development of a Non-grounded Haptic Interface Using the Gyro Effect. In: Proceedings of 11th Symposium Haptic Interfaces Virtual Environment and Teleoperator Systems HAPTICS'03, pp. 32–39 (2003)

Passive Haptics: Pulsive Damping Brake for Greater Impulse Perception

Takumu Okada , Shogo Okamoto and Yoji Yamada

Abstract We developed a passive haptic technique, using the brake of a DC motor, to create a greater perception of impulse force. We found that when using the brake of a DC motor, delivering two short pulses immediately prior to the main brake significantly increases the operator's perception of impulse force. This finding was verified during our empirical assessment. In the experiment, all five participants reported that a damping brake with pulsive resistances delivered a larger resistance than that caused by a brake without pulsive changes. Our technique is applicable to passive haptic interfaces, which are inherently safe and energy-efficient.

Keywords Passive haptic interface · Damping brake · Impulse perception

1 Introduction

Passive haptic interfaces, which are inherently safe and energy-conservative, are beneficial for applications that may be used by a number of unspecified users. Thus far, passive haptic interfaces have been investigated by many research groups [1–4]. In contrast to previous studies, the purpose of this study is to induce a large perception of impulsive resistance based on the principles of the passive damping brake of a DC motor and human perception. A large impact is delivered by a large and rapid change of force. Therefore, a physically maximum resistance force is realized by continuously exerting the damping brake force. On the other hand, we focused on the pulsive brake generated by quickly switching the damping brake applied prior to the continuous brake on and off. Our findings revealed that presenting two short pulsive brakes before the continuous brake induces a greater perceived resistance force.

T. Okada (✉) · S. Okamoto · Y. Yamada
Department of Mechanical Science and Engineering, Nagoya University,
Furo-cho, Chikusa-ku, Nagoya, Aichi, Japan
e-mail: okada.takumu@gmail.com

2 Principle

2.1 Damping Brake of DC Motor

We adopted the damping brake of a DC motor to function as the passive element of our haptic interface. This damping brake is generated by the back electromotive force of a short-circuited DC motor. Figure 1 shows a schematic of a computer-controlled short circuit in which R and L are the resistance and inductance of the circuit, respectively. When the DC motor rotates at an angular velocity of $\omega(t)$, on the basis of Kirchhoff's law, the brake torque $\tau(t)$ is determined as follows:

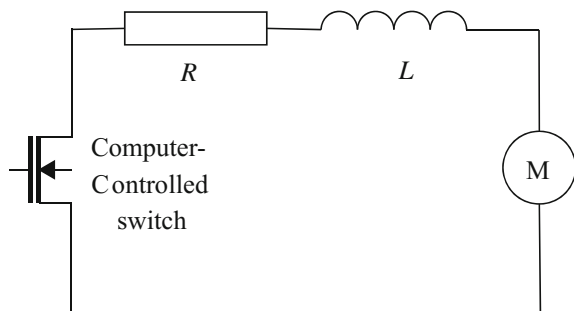
$$\frac{L}{R} \frac{d\tau(t)}{dt} + \tau(t) = -\frac{K^2}{R} \omega(t), \quad (1)$$

where K is the torque constant of the motor. Provided that the inductance L is negligibly small, the brake torque, $\tau(t)$, is proportional to the square of K and the angular velocity, $\omega(t)$. In this scenario, the brake torque is controlled using a switch in the circuit, as shown in Fig. 1.

2.2 Impulsive Resistance Force

One way to illustrate the concept of impulsive resistance force is to consider the physical act of collision. Figure 2 shows the image of a hand, formed into a fist, colliding with an object. The maximum impulse force occurs at the point of contact between the hand and the object. In the same way, an analogous impact can be achieved by the application of a large and rapid brake. The damping brake of the DC motor achieves the most rapid increase of brake torque by continuously applying the maximum brake force. The brake that expresses the largest impulsive resistance is the stepwise brake (see Fig. 2). This brake is realized by switching the short circuit

Fig. 1 Short circuit to control the damping brake of a DC motor



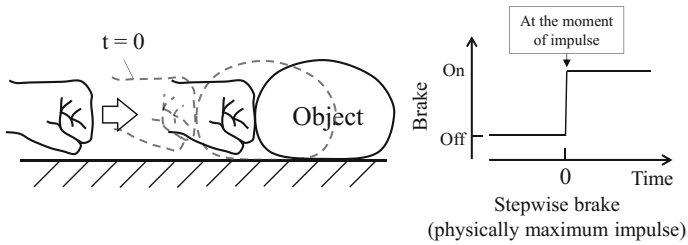


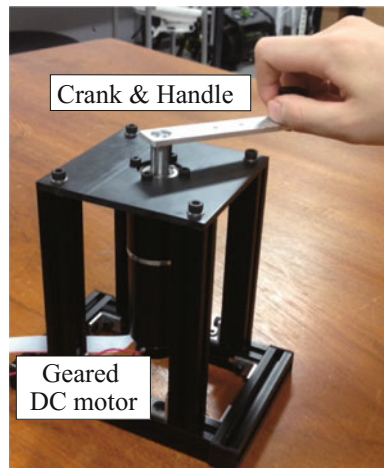
Fig. 2 Impulsive resistance force. *Left* Example of an impulsive resistance caused by a collision between a hand and an object. *Right* Stepwise passive brake which produces the physically largest impulsive force

of the DC motor on at the moment of impact. We aimed to increase the operators perception of braking force above and beyond what was possible by the brake with stepwise brake control.

3 Passive Haptic Interface Based on the Damping Brake of a DC Motor

We designed a passive haptic interface that delivers impulsive resistance forces by using the damping brake of a DC motor as shown in Fig. 3 [5]. The output shaft of the motor (RE-40, Maxon motor, reduction ratio: 12) was connected to a 12 mm long aluminum crank (see Figs. 3 and 5). Participants maneuvered the interface by using the crank. A rotary encoder (Encoder MR Type L, Maxon motor, resultant resolution: 1024 ppr) was installed on the DC motor. A switch of the short circuit

Fig. 3 Passive haptic interface on the basis of the damping brake of the DC motor



was controlled by a microcomputer that operated at 10 kHz. While the switch was on, this device passively presented brake torque to a participant rotating the crank on the above-mentioned principle. A strain-gauge-typed force sensor (USL06-H5, Tec Gihan) without low-pass-filter circuits was used to measure the force at the handle of the crank.

4 Experiment

An experiment was conducted to investigate whether brakes preceded by one or two quick pulses resulted in a larger perceived resistance than that delivered by the stepwise brake. The experimental protocols, including the recruitment procedure of the participants, were approved by the internal review board of the Engineering School, Nagoya University (#15-12).

4.1 *Impulsive Resistance Stimuli*

We compared three types of brakes that delivered impulsive resistance forces. The three types of braking forces were stepwise, one-pulse, and two-pulse stimuli. Figure 4 shows the temporal operation for each type of brake stimulus. The durations of stimuli were unified to be 100 ms, such that the duration did not influence the perceived strength of the brake. The stepwise brake was a continuous brake lasting for 100 ms. As previously mentioned, this brake produced a larger impulsive resistance force than the other types of brake stimuli. The other two stimuli involved one or two short pulses prior to the main brake, which were caused by rapidly controlling the short-circuit. The one-pulse stimulus produced a 5 ms pulse with a 5 ms interval preceding the 90 ms main brake. The two-pulse stimulus had two pulses, each lasting 3 ms with an interval of 3 ms, before the main brake of 88 ms. These pulses were satisfactorily short for the stimuli to be perceived as an impact caused by a collision with an object. We expected that these pulse stimuli would evoke greater sense of impact resistance than that caused by the stepwise brake.

4.2 *Procedure*

Five volunteer students, who were unaware of the objectives of the research, participated in the experiment. During the experiment, the sounds generated by the impact stimulus were muffled by pink noise played through headphones.

In the experiment, the participants were instructed to rank the three types of stimuli on the basis of the strength of the perceived resistance in a forced-choice manner without any duplicated rank on more than two different stimuli. Each of the three types of braking forces was presented when the crank came at an angle of $\pi/2$ rad,

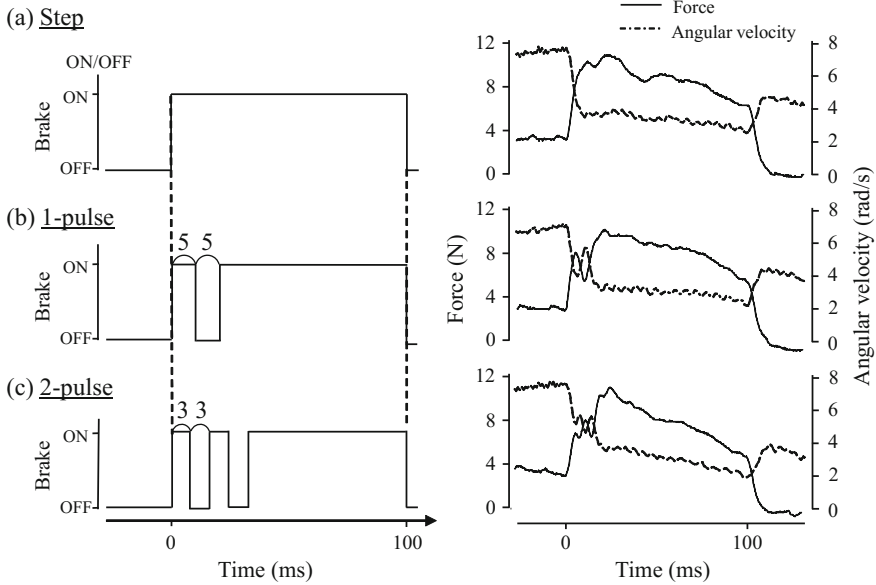
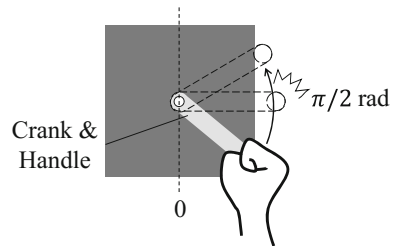


Fig. 4 Three types of braking stimuli. *Left* Control of the brake torque. *Right* Examples of braking forces and angular velocities of the motor. The impulsive resistance stimuli were initiated at $t = 0$ while the participant moved the crank connected to the DC motor

Fig. 5 Experience of impulsive resistance stimuli



as shown in Fig. 5. During the experiment, the participants could freely switch the three types of stimuli by using a keyboard. They were allowed to experience the stimuli repeatedly as many times as they desired by moving the crank back and forth between around 0 rad and $\pi/2$ rad. They were also allowed to rotate the crank at whatever speed was comfortable.

4.3 Results and Discussion

All the five participants ranked the two-pulse stimulus first. As the second largest stimulus, the one-pulse and stepwise stimuli were selected by two and three

participants, respectively. The ranks of the three types of stimuli differed significantly ($p < 0.05$, Friedman test). Subsequently, we conducted pair-wise comparisons by using Wilcoxon's rank sum tests. The ranks for the two-pulse stimulus were significantly different from those of the one-pulse and stepwise stimuli at $p < 0.05$. The two-pulse stimulus produced a larger perceived resistance than the other two types of stimuli. It is interesting that the two pulses preceding the main brake yielded a greater perceived impulsive resistance in spite of the loss of force outputs. This fact implies that the perception of impulsive resistance is not in full agreement with the physical consideration.

5 Conclusion

This study proposed a method for presenting a large impulsive resistance by using a passive haptic interface based on the damping brake of a DC motor. We compared three types of braking stimuli in the experiment. One was a stepwise brake that realized a physically maximum impulsive resistance. Another was a one-pulse stimulus involving a short pulse preceding the main brake. The other one was a two-pulse stimulus that included two pulses before the main brake. All the five participants reported that the two-pulse stimulus delivered the largest resistance. Our method will be easily applicable to many passive haptic interfaces that are inherently safe, and our findings about the human perception of impulsive resistance will improve their abilities.

Acknowledgements This study was in part supported by ImPACT (Tough Robotics Challenge) and JSPS Kakenhi (15H05923).

References

1. Koyama, T., Yamano, I., Takemura, K., Maeno, T.: Multi-fingered exoskeleton haptic device using passive force feedback for dexterous teleoperation. In: Proceedings of IEEE/RSJ International Conference of Intelligent Robotics and Systems, pp. 2229–2234 (2002)
2. Nakamura, T., Yamamoto, A.: A multi-user surface visuo-haptic display using electrostatic friction modulation and capacitive-type position sensing. *IEEE Trans. Haptics* pp. 1–12 (2016)
3. Radulescu, A., Howard, M., Braun, D.J., Vijayakumar, S.: Exploiting variable physical damping in rapid movement tasks. In: Proceedings of IEEE/ASME International Conference on Advanced Intelligent Mechatronics, pp. 141–148 (2012)
4. Srikanth, M., Vasudevan, H., Muniyandi, M.: DC motor damping: a strategy to increase passive stiffness of haptic devices. In: Ferre, M. (ed.) *Haptics: Perception, Devices and Scenarios*, vol. 5024 LNCS, pp. 53–62. Springer (2008)
5. Okada, T., Okamoto, S., Yamada, Y.: Impulsive resistance force generated using pulsive damping brake of DC motor. In: *IEEE International Conference on Systems, Man, and Cybernetics* (2016)

Hanger Reflex of the Head and Waist with Translational and Rotational Force Perception

Yuki Kon, Takuto Nakamura, Michi Sato, Takashi Asahi
and Hiroyuki Kajimoto

Abstract The hanger reflex is a phenomenon in which the head involuntarily rotates when force is applied via a wire hanger placed on the head. The application of pressure to particular points of the head is necessary to induce this phenomenon, which occurs when shear deformation of the skin induces illusory force perception. Because the hanger reflex represents the induction of force and motion using a simple device, and has been found in other body parts such as the wrist, waist, and ankle, it is expected to be useful as an application in haptic interface technology. In this paper, we describe new directions of force associated with the hanger reflex; four translation, and two rotational directions of the head, and four translation and one rotational direction of the waist.

Keywords Hanger reflex · Perceptual force · Haptic display · Skin stretch

Y. Kon (✉) · T. Nakamura · M. Sato · H. Kajimoto
The University of Electro-Communications, 1-5-1 Chofugaoka,
Chofu, Tokyo 182-8585, Japan
e-mail: kon@kaji-lab.jp

T. Nakamura
e-mail: n.takuto@kaji-lab.jp

M. Sato
e-mail: michi@kaji-lab.jp

H. Kajimoto
e-mail: kajimoto@kaji-lab.jp

T. Nakamura
JSPS Research Fellow, Tokyo, Japan

T. Asahi
Department of Neurosurgery, Kanazawa Neurosurgical Hospital,
262-2 Gomachi, Nonoichi, Ishikawa 921-8841, Japan
e-mail: takashi-tym@umin.ac.jp



Fig. 1 Hanger reflex [2]

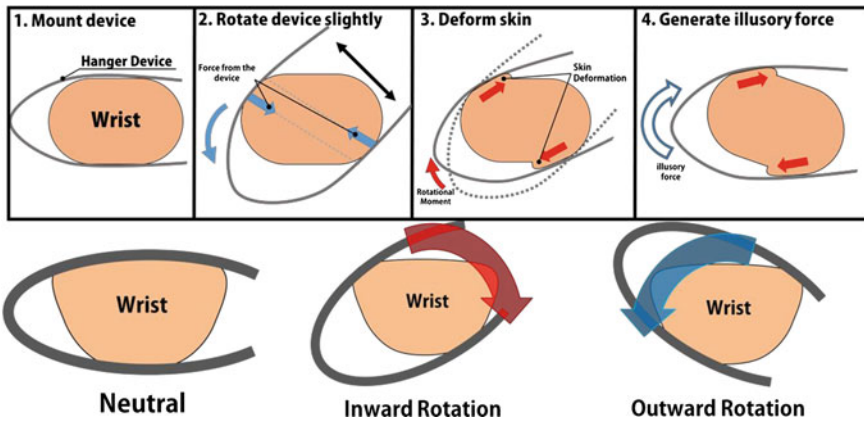


Fig. 2 Mechanism of the hanger reflex device (*wrist*): by changing the orientation of the device, an illusory force can be induced in two directions [10]

1 Introduction

Hanger reflex is a phenomenon in which the head involuntarily rotates when forces are applied in specific locations, such as those created by placing a wire hanger on the head, as shown in Fig. 1 [1, 2]. Sato et al. measured the pressure distribution of the points of contact of the hanger necessary to induce the hanger reflex, and found “sweet spots”, i.e., an optimal position for the hanger. Specifically, they showed that the direction of lateral skin stretch contributes to the direction of the hanger reflex [2, 3], as per the previously observed skin stretch force sensations [4, 5, 6, 7]. Because the hanger reflex represents the induction of force and motion using a simple device, and has also been observed with other parts of the body such as the wrist, waist, and ankle [8, 9, 10, 11], it is expected to have useful application in generating haptic interfaces. Thus, the mechanism and conditions leading to this phenomenon have been previously investigated (Fig. 2). In this paper, we sought to

further examine the hanger reflex with respect to other directions of translation or rotation. To this end, we developed new device enabling to study the whole-body hanger reflex with arbitrary directions of translation and rotation.

2 Device and Preliminary Trials

2.1 Head-Type Hanger Reflex Device

In previous research, the hanger reflex of the head had been confirmed only with respect to the yaw axis (i.e., along the long axis of body parts) [1, 2]. However, as the main cause of the hanger reflex is considered to be the illusory perception of force generated by shear deformation of the skin [3], it is probable that appropriate shear deformation of the skin around other body axes will also generate rotation, and possibly translation as well.

We developed a new elliptical hanger reflex device made of carbon fiber reinforced plastic that is elastic (Fig. 3a-c) [12]. To produce the hanger reflex, the user must rotate the device around their head to produce an appropriate pressure distribution and shear deformation of the skin. We developed three versions of the

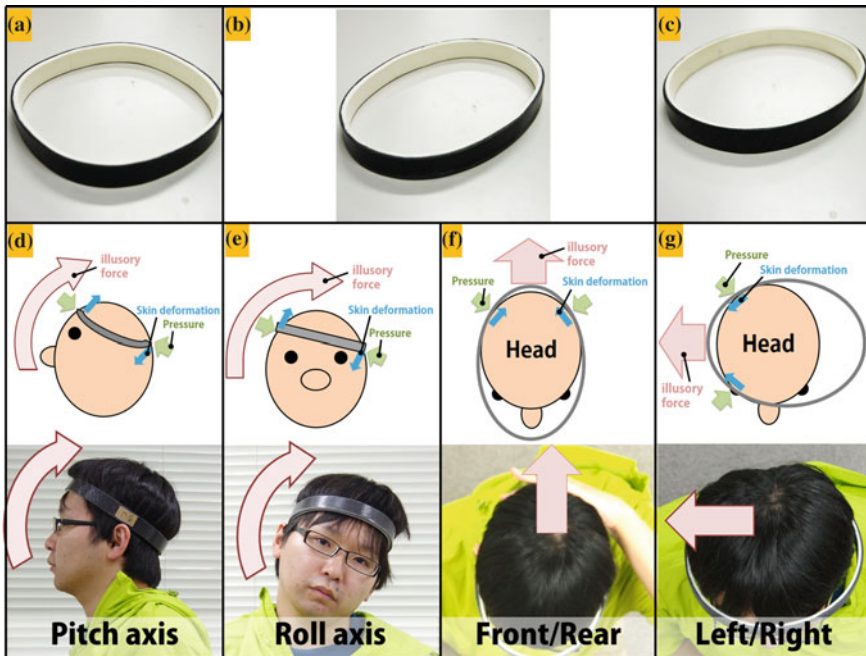


Fig. 3 Head-type hanger reflex (Rotation along the pitch and roll axes, and translation towards the front, rear, left, and right directions)

device to generate different types of skin deformation, as shown in Fig. 3d–g. We confirmed that (1) pressure applied to the upper frontal and lower back regions of the head generated illusory force and rotational motion along the pitch axis (Fig. 3d), and (2) pressure to the upper lateral and lower contralateral regions of the head generated illusory force and rotational motion along the roll axis (Fig. 3e). Furthermore, (3) pressure applied to two back temporal regions generated translational force and movement towards the rear. This was also observed for the front, left and right directions (Fig. 3f, g).

2.2 Waist-Type Hanger Reflex Device

We have found the hanger reflex of the waist, in which the waist rotates along the yaw axis (Fig. 4) [8]. As with the hanger reflex of the head, it is probable that appropriate shear skin deformation will produce rotation along other axes, and possibly translation as well. As body size can vary among individuals, and the device must be relatively large compared with the head-type hanger reflex device, we sought to make a device that was light weight and adjustable.

We developed a new U-shaped hanger reflex device made of stainless steel (SUS304-CSP) (Fig. 5a). The open ends of the device connected via a hook and loop fastener strap, enabling it to fit to any user. The total weight was 400 g. To generate shear deformation of the skin, two contactors made of polyethylene foam and rubber, were placed between the stainless steel frame and the body. The positions of the contactors were adjusted for each case.

To induce translational force, the contactors were attached to the bottom part of the U-shape, where they pinched the body skin (Fig. 5b, c). To induce a rotational force along the pitch axis, the frame was attached along one shoulder, as shown in (Fig. 5d).

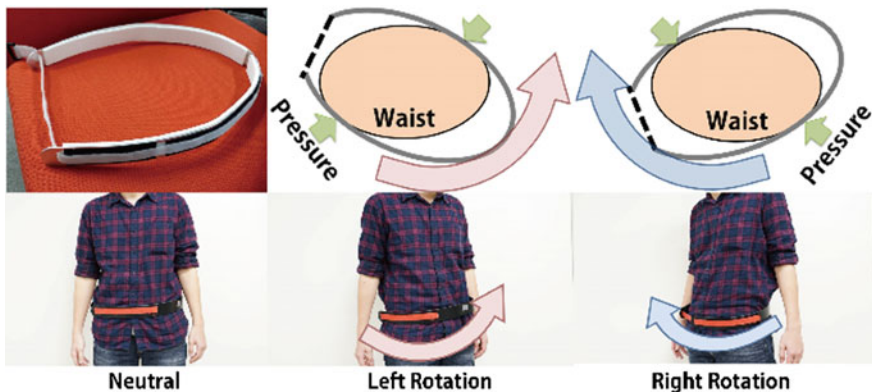


Fig. 4 Waist-type hanger reflex [11]

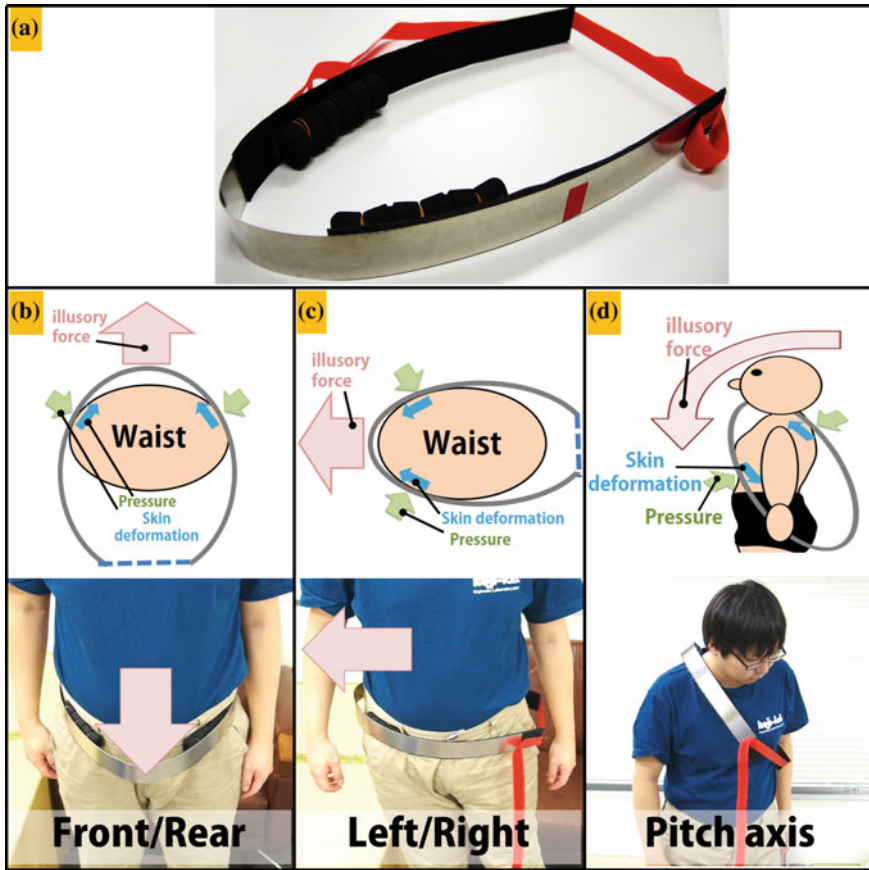


Fig. 5 Waist-type hanger reflex (Rotation along pitch axis and translation to the front, rear, left, and right)

3 User Study

To confirm the reproducibility of this phenomenon, we recruited six participants, all male, aged 21–25 years. They had knowledge of the head-type hanger reflex, but were naïve with respect to the newly developed device. We asked them to attach the device in the various positions described above, and to report the direction of the perceived force. We prepared eight choices (rotation of pitch axis, rotation of roll axis, and translation to the front, rear, left, and right directions) for the head-type device, and six choices (rotation of pitch axis, and translation of front, rear, left and right) for the waist type device. Trials with head type device were conducted first, followed by the waist type device. For each type of device, the mounting conditions were presented in random order. For example, when presenting the head-type

hanger reflex pitch, roll, and translations were presented randomly, and the participants were asked to answer a single perceived force direction for each trial.

For the head-type device, three participants reported the directions of perceived movement as expected. We believe this relatively low rate of correct answers to be due to slip between the device and hairs.

For the waist-type device, four participants reported perceiving force in the expected direction for the translational force to the left, and five participants reported experiencing perceived force in the expected direction for the translational force to the front, rear, and right directions.

Participants did not comment any difficulty in answering easily for any specific body parts, but experimental results showed that perception of the head-type hanger reflex is actually difficult if the rotational and translational conditions are mixed.

4 Conclusion

In this paper, we extended the hanger reflex to additional directions of movement. Specifically, our data indicate that the hanger reflex might be able to induce translational and rotational force illusions in eight directions for the head and six directions for the waist.

As this study is preliminary, we plan to further investigate the detailed conditions leading to the hanger reflex in additional body parts. Additionally, we hope to improve the developed devices, and evaluate them in terms of rate of illusion, strength of illusion, and temporal characteristics such as latency and adaptation. We then hope to further apply the device to the development of whole-body haptic interfaces, for use in the fields of virtual reality, training and rehabilitation.

Acknowledgements This work was supported by JSPS KAKENHI Grant Number JP15K12079.

References

1. Matsue, R., Sato, M., Hashimoto, Y., Kajimoto, H.: Hanger reflex—a reflex motion of a head by temporal pressure for wearable interface. In: *SICE Annual Conference*, pp. 1463–1467 (2008)
2. Sato, M., Matsue, R., Hashimoto, Y., Kajimoto, H.: Development of a head rotation interface by using hanger reflex. In: *The 18th IEEE International Symposium on Robot and Human Interactive Communication*, pp. 534–538 (2009)
3. Sato, M., Nakamura, T., Kajimoto, H.: Movement and pseudo-haptics induced by skin lateral deformation in hanger reflex. In: *SIG TeleXistence 5th Workshop (2014)* (in Japanese)
4. Shull, P., Bark, K., Cutosky, M.: Skin nonlinearities and their effect on user perception for rotational skin stretch. In: *IEEE Haptics Symposium*, pp. 77–82 (2010)
5. Yem, V., Kuzuoka, H., Yamashita, N., Ohta, S., Takeuchi, Y.: Hand-skill learning using outer-covering haptic display, eurohaptics, pp. 201–207 (2014)

6. Kuniyasu, Y., Sato, M., Fukushima, S., Kajimoto, H.: Transmission of forearm motion by tangential deformation of the skin. In: *The 3rd Augmented Human International Conference (2012)*
7. Solazzi, M., Provancher, W.R., Frisoli, A., Bergamasco, M.: Design of a SMA actuated 2-DoF tactile device for displaying tangential skin displacement. In: *IEEE World Haptics Conference*, pp. 31–36 (2011)
8. Nakamura, T., Nishimura, N., Sato, M., Kajimoto, H.: Application of hanger reflex to wrist and waist. In: *IEEE Virtual Reality*, pp. 181–182 (2014)
9. Nakamura, T., Nishimura, N., Sato, M., Kajimoto, H.: Development of a wrist-twisting haptic display using the hanger reflex. In: *The 11th Advances in Computer Entertainment Technology Conference (2014)*
10. Nakamura, T., Nishimura, N., Hachisu, T., Sato, M., Yem, V., Kajimoto, H.: Perceptual Force on the Wrist under the Hanger Reflex and Vibration. In: *EuroHaptics*, pp. 462–471 (2016)
11. Kon, Y., Nakamura, T., Sato, M., Kajimoto, H.: Effect of hanger reflex on walking. In: *IEEE Haptics Symposium*, pp. 313–318 (2016)
12. Asahi, T., Sato, M., Kajimoto, H.: Japan patent JP2500000B, 2014.7.16

Stable Haptic Feedback Generation During Mid Air Interactions Using Hidden Markov Model Based Motion Synthesis

Dennis Babu, Hikaru Nagano, Masashi Konyo, Ryunosuke Hamada and Satoshi Tadokoro

Abstract Generation of stable and realistic haptic feedback in 3 dimensional midair interaction systems has garnered significant research interests recently. But the limitations in the sensing technologies such as unstable tracking, range limitations and occlusions occurred during interactions, along with the motion recognition faults significantly distort motion based haptic feedback. In this paper, a Hidden Markov Model based motion element synthesis for stable haptic feedback generation is proposed. The subjective evaluation experimental results using the proposed model on 3 subjects during a zooming task have shown improvements in user perception of the gestures.

Keywords Gesture interaction · Haptic feedback · Vibrotactile · Hidden Markov model · Mid-air interaction

1 Introduction

Recently virtual reality technology has garnered lot of attention and has been studied actively because of the progress of head mounted displays and motion tracking sensors. Although the methodology and techniques for visual rendering of the virtual world have been developed, the methodology of realistic rendering of haptic

D. Babu (✉) · H. Nagano · M. Konyo · R. Hamada · S. Tadokoro
Human Robot Informatics Lab, Graduate School of Information Sciences,
Tohoku University, Sendai 980-8579, Japan
e-mail: dennis@rm.is.tohoku.ac.jp

H. Nagano
e-mail: nagano@rm.is.tohoku.ac.jp

M. Konyo
e-mail: konyo@rm.is.tohoku.ac.jp

R. Hamada
e-mail: hamada@rm.is.tohoku.ac.jp

S. Tadokoro
e-mail: tadokoro@rm.is.tohoku.ac.jp

interactions in the virtual world is still severely underdeveloped. One of the main technological limitations affecting realistic haptic rendering in midair interactions is noisy and unstable motion data during interactions.

There are several techniques to track position and orientation of human body during midair interactions for haptic feedback generation. While optical tracking systems have been used for precise motion tracking, a more viable option for portable and user friendly haptic interface system is depth cameras such as Kinect (<http://www.microsoft.com>) and Leap Motion Controllers (<http://www.leapmotion.com>). However, subjecting to low precision and stability of the device, depth camera sensors is not satisfactory for precise tracking and subsequent haptic feedback generation. Occlusions of the tracked elements and range limitations of depth tracking infrared sensors deteriorate stable motion tracking and motion based haptic feedback generation. More over as reported in [1], Leap Motion Controllers (LMCs) have uneven sampling frequency which causes discontinuous motion capture data along the time frame with increasing drift as capture duration increases.

While most of the advanced midair haptic feedback technologies uses depth motion sensors for motion sensing no specific research efforts were made to address unstable motion pattern affecting haptic feedback. To address the issue of unstable tracking using depth sensors in [2] the authors use Kalman filter and Particle filter to generate stable motion data from LMC data to control robot motion from human pose data. One of the straight forward approach for haptic rendering from raw data is to apply a low pass or band pass filter [3]. While the approach works well for a master slave system of teleoperation and raw data based haptic feedback systems, the methodology may fail to have the desired effect in unstable motion patterns as there is no definite frequency component differences between unstable and stable motion patterns. More over unlike visual cues haptic feedback has to be selectively rendered based on specified gestures and for specific duration according to user motion avoiding anomalies rather than a continuous generation.

Thus, the recognition of underlying user intentions from erroneous motion patterns is necessary for haptic feedback generation. These recognized gestures may further be utilized to synthesize motion elements for generating stable haptic feedback stimulation rather than using the raw erroneous data patterns. In this work authors propose a method for synthetic motion element synthesis for haptic rendering using Hidden Markov models. The unstable motion patterns are fed to an HMM based gesture recognition algorithm which recognizes the hidden states corresponding to the recognized gesture. Primitive motion elements associated with each states are generated to recreate ideal motion path associated with the gesture. The rest of the paper is organized as follows. Section 2 details the proposed approach and Sect. 3 discusses the experimental set up and procedures. Section 4 elaborates results and finally concludes in Sect. 5.

2 Proposed Approach

HMM based motion synthesis model uses smooth primitive motion patterns stored in look up tables to generate motion elements for haptic feedback control. Multiple HMM models are trained corresponding to different gestures, each varying in the number of states and state transitions. A Viterbi algorithm selects the most suitable HMM state sequence in real time and renders the corresponding primitive elements associated with each state. Even though the detected motion patterns are highly unstable and cluttered the rendered motion sequence for haptic feedback will thus be smooth. Fig. 1 shows the general outline of the proposed approach.

Motion synthesis based haptic feedback generation is a six step process with the initial three steps being unstable motion data acquisition from depth sensor for different gestures for training HMM models with multiple hidden states. Each gesture corresponds to a unique HMM model with unique number of states. Further primitive motion elements are estimated corresponding to each states based on ideal motion data obtained from a stable sensor. These primitive motion elements are stored as look up table and synthesized according to the recognized state as shown in step 4. The synthesized motion data is used for real time haptic rendering control function using a vibrotactile wrist band as shown in steps 5 and 6. The detailed working principle can be referred from Inamura et al. [4]. While in [5] authors used a Mimesis

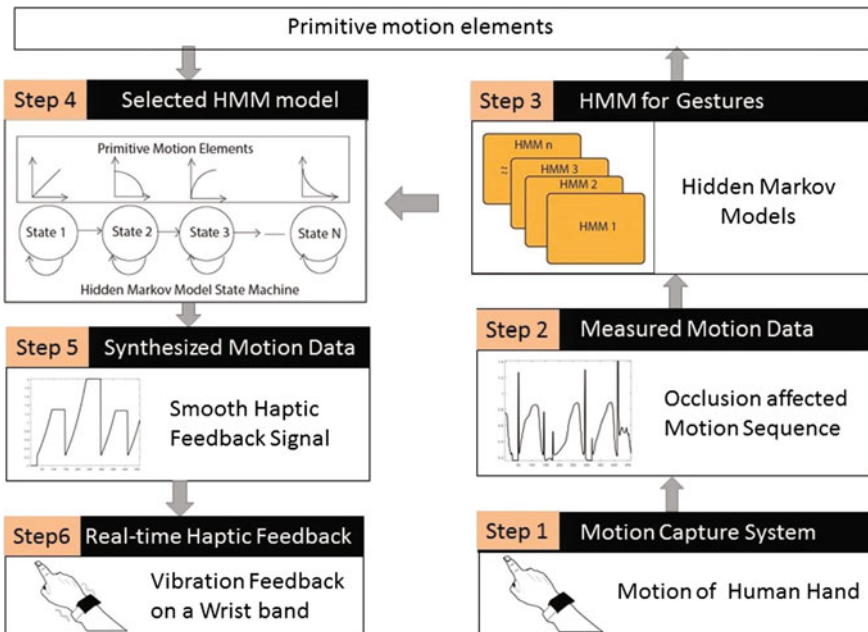


Fig. 1 General outline

loop to recreate human like motion in a humanoid robot, we modify the system for stable and smooth haptic feedback generation.

3 Experiments

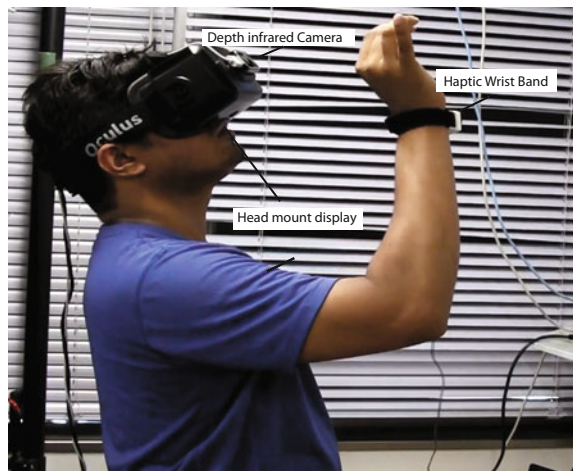
3.1 *Experimental Set Up*

A Leap motion skeletal tracking sensor was used for hand tracking. The sensor was attached to Oculus DK2 head mounted display to ensure mobility of the users during gesture interactions. We used Vibtouch [6] system to generate vibrotactile friction feedback [7] signals. The vibrotactile friction feedback based on the 1 DOF stick-slip model modulates amplitude and frequency of vibration both combinedly and independently to simulate a finger friction during interaction with virtual surface. A haptic wrist band equipped with Haptuator (Tactile Labs, USA) acts as the real time haptic feedback device. The entire experimental set up is shown in Fig. 2

3.2 *Experimental Tasks and Subjects*

A virtual zooming task was selected to evaluate the user perceptions of the HMM synthesized motion sequence with that of raw motion sequences. Subjects were asked to use all the fingers to execute the zoom in and out task. The virtual radius of the zoom circle was used as controlling motion element to generate vibrotactile feedback. Vibrotactile haptic rendering model increases the amplitude and decreases the

Fig. 2 Experimental set up



frequency simultaneously corresponding to increase in zoom radius thereby simulating a vibrotactile friction model [6] during gesture execution.

Three subjects of age range 22–24 well aware of the haptic feedback technology were selected as the subjects. The subjects were asked to compare the synthesized motion sequence based haptic feedback and raw data based haptic feedback using two parameters, smoothness and synchronization of the haptic feedback. Each subjects repeated the tasks 10 times in each cases with each time continuing the task at least 5 times. Subjects then rated the haptic feedback on a scale from 0 to 5 with 5 being the best and vice versa. The external noises were shunted by pink noise via a headset and experimental conditions were altered randomly to avoid biasing.

4 Results and Discussions

Figure 3 shows the measured raw value of the zoom radius and HMM model based synthesized virtual zoom radius during an experiment of Subject 1. As evident from the figure the synthesized radius is very smooth and has no spikes as seen in the case of raw zoom radius. The spikes occurred during the zoom task due to finger tips occlusion in the start phase of zoom out gesture. During this state tracking IR camera is behind the hands and thus cannot track the fingertip positions, causing occlusion. This unwanted spikes may cause cluttered haptic feedback and thereby reducing user experience.

Figures 4 and 5 shows the subjective rating experimentation results of 3 subjects based on smoothness of the feedback and synchronization. As expected the all the subjects had increased perception of the smoothness of the vibrotactile feedback with Subject 3 having significant improvement in rating score. At the same time the synchronization parameter has no significant improvements for all the subjects. This

Fig. 3 Measured and synthesized motion data

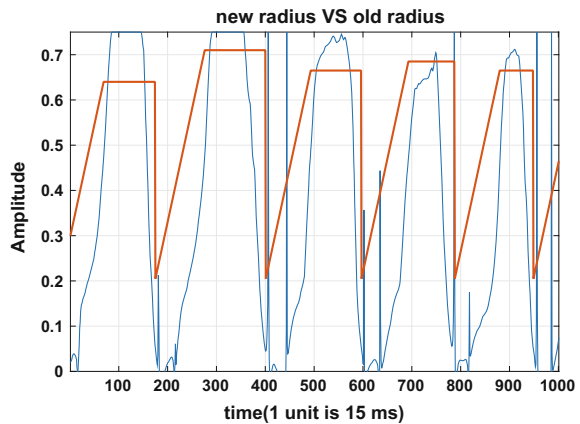


Fig. 4 Synchronization parameter

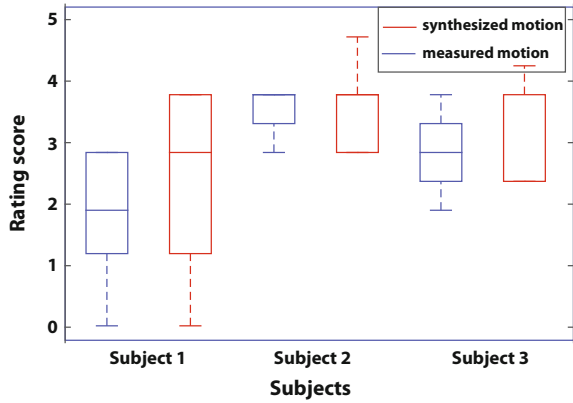
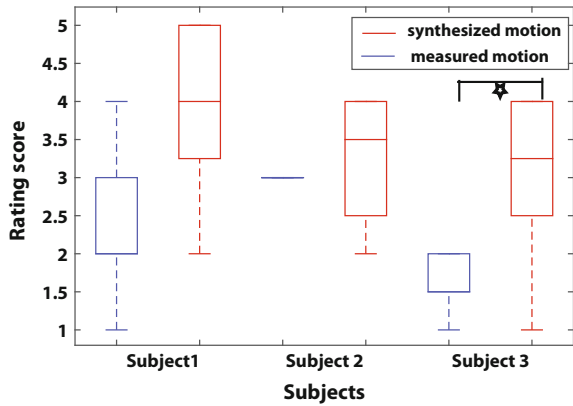


Fig. 5 Smoothness parameter



shows that HMM model has no significant time lag for computation of the real time gesture states and subsequent haptic feedback generation.

5 Conclusion

This paper proposes an HMM based motion synthesis methodology for smooth haptic feedback generation during mid-air interactions. The proposed method was validated through experiments in which subjects compared two types of haptic feedbacks based on the synthesized motion patterns by the proposed method and the raw motion patterns during zooming tasks. The subjective experimental results showed that the smoothness of haptic feedback was improved by the proposed method using HMM model.

Currently authors are working on precise motion synthesis similar to that of actual stable motion data. Authors believe that synthesis of such precise motion elements

may not only help improve user satisfaction, but also help generate “in motion” haptic feedback rather than “after motion” haptic feedback based on current state of the art gesture recognition systems. More over, work is progressing on including more gestures in current framework and increasing the number of participants in experiments to generalize the proposed methodology.

Acknowledgements This work was supported in part from ImPACT Program (Tough Robotics Challenge).

References

1. Guna, J., Jakus, G., Poganik, M., Tomai, S., Sodnik, J.: An analysis of the precision and reliability of the leap motion sensor and its suitability for static and dynamic tracking. *Sensors* **14**(2), 3702–3720 (2014)
2. Du, G., Zhang, P., Liu, X.: Markerless human manipulator interface using leap motion with interval Kalman filter and improved particle filter. *IEEE Trans. Ind. Inf.* **12**(2), 694–704 (2016)
3. Ye, Y., Liu, P.X.: Improving haptic feedback fidelity in wave-variable-based teleoperation orientated to telemedical applications. *IEEE Trans. Instrum. Meas.* **58**(8), 2847–2855 (2009)
4. Inamura, T., Nakamura, Y., Ezaki, H., Toshima, I.: Imitation and primitive symbol acquisition of humanoids by the integrated mimesis loop. In: *IEEE International Conference on Robotics and Automation, 2001. Proceedings 2001 ICRA, vol. 4*, pp. 4208–4213 (2001)
5. Inamura, T., Toshima, I., Nakamura, Y.: Acquisition and embodiment of motion elements in closed mimesis loop. In: *Proceedings of International Conference on Robotics and Automation (ICRA2002)*, pp. 1539–1544 (2002)
6. Tsuchiya, S., Konyo, M., Yamada, H., Yamauchi, T., Okamoto, S., Tadokoro, S., Vib-Touch: virtual active touch interface for handheld devices. In: *RO-MAN: The 18th IEEE International Symposium on Robot and Human Interactive Communication 2009, Toyama*, pp. 12–17 (2009)
7. Tsuchiya, S., Konyo, M., Yamada, H., Yamauchi, T., Okamoto, S., Tadokoro, S.: Virtual Active Touch II: vibrotactile representation of friction and a new approach to surface shape display. In: *2009 IEEE/RSJ International Conference on Intelligent Robots and Systems, St. Louis, MO*, pp. 3184–3189 (2009)

Relationship Between Force Sensation and Stimulation Parameters in Tendon Electrical Stimulation

Akifumi Takahashi, Kenta Tanabe and Hiroyuki Kajimoto

Abstract Most haptic devices have the common problem of requiring a large hardware setup, because they must present actual force. To cope with this issue, we have proposed a method to present force sensation using tendon electrical stimulation. In this paper, we investigated whether it is possible to present force sensation by electrically stimulating the tendon through the skin surface at the wrist. We also investigated the relationship between the amount of sensation and the stimulation parameters. We found that a force sensation can be generated by electrical stimulation to the wrist, and the direction of the force sensation is opposite to the motion elicited by muscle electrical stimulation. We also found that it is possible to control the amount of the sensation by varying both pulse height and pulse frequency.

Keywords Force sensation · Golgi tendon organ · Haptic interface · Ib fiber · Tendon electrical stimulation (TES)

1 Introduction

To improve the sense of immersion in virtual reality, or the operability of telexistence or teleoperation systems, many haptic devices have been developed. However, most of them have the common problem of requiring a large hardware setup to mechanically generate actual force.

If there were a way to directly stimulate receptors related to force, or the sensory nerves extending from those receptors, it would be very energy-efficient, and thus

A. Takahashi (✉) · K. Tanabe · H. Kajimoto
University of Electro-Communications, 1-5-1 Choufugaoka, Choufu,
Tokyo 182-8585, Japan
e-mail: a.takahashi@kaji-lab.jp

K. Tanabe
e-mail: k.tanabe@kaji-lab.jp

H. Kajimoto
e-mail: kajimoto@kaji-lab.jp

dramatically smaller haptic devices could be achieved. There have been many studies on presenting the sense of touch via the electrical stimulation of the nerves extending from tactile receptors [1, 2]. In regard to proprioception sensation, there are also studies that present the sense of gravity or acceleration by galvanic vestibular stimulation [3]. Meanwhile, it is known that motor illusions occur when applying vibrations to the tendon [4–6]. Moreover, it is suggested that electrical stimulation to the tendon (TES) also produces motor illusions [7], which is presumably because of the activity of Golgi tendon organs (GTOs) [8]. Compared with electrical muscle stimulation (EMS), which is also used to present force sensation by stimulating muscles [9–11], TES does not accompany actual body movement. This characteristic is suitable for some situations in which users' motion space is limited, such as in a cockpit.

The goal of this study is to realize a compact force presentation device using TES. In this paper, we investigated whether it is possible to present force sensation via electrical stimuli applied through the skin surface of the wrist, and the relationship between the amount of force sensation and stimulation parameters (i.e., the frequency and height of the current pulse).

2 Experimental Procedure

2.1 Apparatus

Electrical Stimulator: Fig. 1a shows the electrical stimulator. This device controls pulse stimulus pattern and the amount of current from 0 to 25 mA (voltage is up to 300 V) with a micro controller (mbed NCP LPC 1768, NXP Semiconductors). The device has four channels, whose states can change to anode, cathode or isolated from each other through a circuit using photo MOS relays (AQW210S, Panasonic Corporation) (Fig. 1b) on the device. The device realizes bipolar stimulation by changing the target-stimulating electrode; that is, a biphasic pulse train is applied to an electrode (Fig. 1c).

Electrode: Two gel electrodes (1.9 mm × 3.5 mm, Vitrode F-150S, Nihon Kohden Corporation) were installed on the skin at the dorsal part of the left wrist (Fig. 1d).

In preliminary trials, we have confirmed that a force sensation is induced by TES to the wrist and elbow. The direction of the sensation was to the opposite side of the electrodes (i.e., when the electrodes were on the dorsal part, the direction of the perceived force was inward (Fig. 2)). However, an actual movement was not accompanied with TES.

Measurement system for force sensation: We constructed a system to measure force sensation by TES. As shown in Fig. 2, it consists of a spring scale, a pulley, a wristband and string to connect them. The participants were asked to pull the wristband, which was attached to their right arm, until they felt that the force

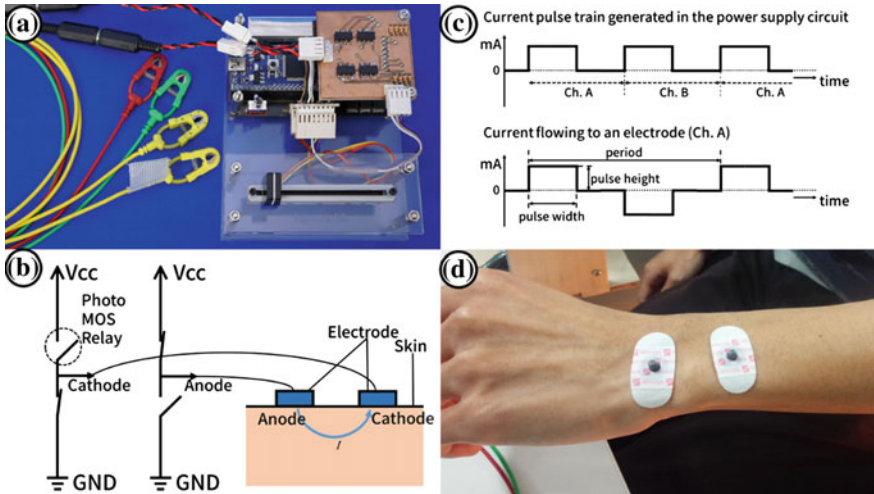


Fig. 1 a Electrical stimulator [2]. b Two Photo MOS relays for one channel to allow a change of the channel state. c Monophasic current pulse train generated in the current control circuit is converted to biphasic pulses by switching the state. d Electrodes on dorsal part of the wrist



Fig. 2 Measurement of perceived force sensation. (Left) Concept image. (Right) Actual system

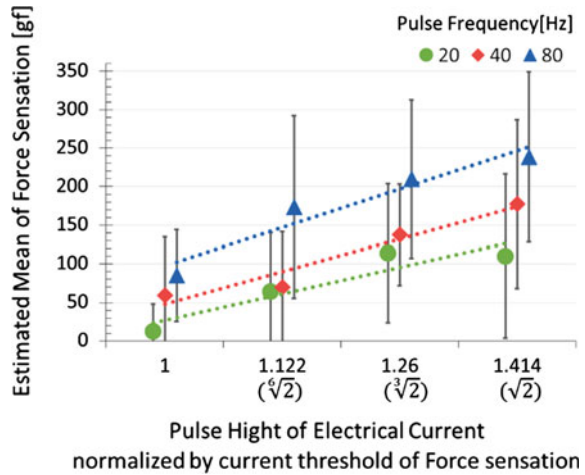
produced by the spring was close to the force sensation produced by TES. Thus, the illusory force was quantified.

We have preliminarily tested the system by presenting actual force to the left arm. Although there were differences between the measured force and actual force, and large variation among individuals, there was also a strong correlation between the two. Thus, we adopted this system in the main experiment.

2.2 Protocol

We applied TES to the left dorsal wrist. First, we obtained each participant's threshold of pulse height such that they barely felt force sensation. Pulse frequency was fixed to 40 Hz.

Fig. 3 Relationship between the amount of force sensation and the electrical current parameters



Then, we investigated the relationship between the amount of force sensation and electrical current parameters. Frequency conditions were 20, 40, or 80 Hz, and pulse height conditions were 1, $\sqrt[6]{2}$, $\sqrt[3]{2}$, or $\sqrt{2}$, relative to the previously obtained threshold. Combination of the conditions gave 12 trials. For each trial, we obtained the amount of perceived force sensation using the measurement system described in 2.1. We recruited eight laboratory members aged 21–24. All were male, and all confirmed that they could feel force the sensation produced by TES.

3 Results

Figure 3 shows the results of the experiment. The vertical axis is the estimated mean of the force sensation. The bars indicate standard deviations. The transverse axis is the pulse height normalized by threshold values. The pattern of the bars represents pulse frequency. We used a two-way ANOVA, and found no interaction. Then, we did a multiple comparison (Tukey HSD test). Regarding frequency, we found significant differences at the 5% level between all frequency pairs. Regarding pulse height, we found a significant difference at the 5% level between almost all pairs except $\sqrt[3]{2}$ and $\sqrt{2}$.

4 Conclusion

We found that TES can induce force sensation, and that the amount of sensation can be controlled by both the pulse height and frequency of the electrical stimulation current. However, frequency is a better way to control the amount of sensation for

the following reasons. First, the possible range of pulse height without pain sensation is small. Second, considering that there was no significant difference between $\sqrt[3]{2}$ and $\sqrt{2}$ in the pulse height condition, there seems to be a saturation, even at $\sqrt{2} = 1.414$ of the threshold current amplitude, which makes control quite difficult. Furthermore, we found that TES has the capacity to present a force sensation of around 250 gf. We must stress that this sensation was not based on muscle electrical stimulation, because if it was caused by muscle contraction, the direction of the force should be to the side of the electrodes (i.e., when the electrodes were on the dorsal part, the direction of perceived force should be outward), but the force that was presented this time was in the opposite direction. Furthermore, actual movement based on muscle contraction was not observed throughout the experiment.

In this experiment, participants are completely passive when presenting sensation. Hence, we will investigate whether the quality of sensation is variable when stimuli are presented interactively. Furthermore, the underlying mechanisms of force sensation must be clarified. Currently, we speculate that it is based on the activity of the Golgi tendon organs (GTOs), but the possibility of force illusion via cutaneous sensation cannot be fully excluded.

If the force sensation is mainly induced by the stimulation to GTOs, the reason why most participants felt the force on their arm to the direction such as Fig. 2 can be described as follows. TES on dorsal part of wrist (Fig. 1d) does not present the information of the muscles' length (since muscle spindle was not stimulated), but present the information of contraction of the dorsal muscles (since GTOs were stimulated). These situation is the same as "isometric contraction", which can be interpreted by that participants as an external force which attempts to move their arms inward, and they are competing against the force.

This hypothesis based on GTOs is supported by some indirect evidence, which was observed in another experiment that showed two patterns of participants; some felt force on their arm, and the others felt on their back of the hand, despite the stimulation is applied on the wrist. It could be explained that the former felt moving the arm was easier than bending their wrist when pseudo isometric contraction occurred. In our future research, we will see if the GTOs are the main factor by observing phenomena related to the GTOs such as the Ib reflection.

Acknowledgements This study was supported by JSPS KAKENHI Grant Number JP25700020.

References

1. Kaczmarek, K.A., Tyler, M.E., and Bach-y-rita, P.: Electrotactile haptic display on the fingertips: Preliminary results. In: Proceedings of the 16th International Conference on IEEE Engineering in Medicine and Biology Society, vol. 2, pp. 940–941. Baltimore, U.S.A (1994)
2. Kajimoto, H.: Electro-tactile display with real-time impedance feedback using pulse width modulation. *Trans. Haptics* 5(2), 184–188 (2012)

3. Taro, M., Hideyuki, A., Maki, S.: Virtual acceleration with galvanic vestibular stimulation in a virtual reality environment. In: Proceedings of IEEE Virtual Reality 2005, pp. 289–290 (2005)
4. Goodwin, G.M., McCloskey, D.I., Mathews, P.B.C.: The contribution of muscle afferents to kinaesthesia shown by vibration induced illusions of movement and by the effects of paralysing joint afferents. *Brain* **95**(4), 707–748 (1972)
5. Eklund, G.: Position sense and state of contraction; the effects of vibration. *J. Neurol. Neurosurg. Psychiatry* **35**, 606–611 (1972)
6. Jones, L.A.: Motor illusions: what do they reveal. *Psychol. Bull.* **103**(1), 72–86 (1988)
7. Gandevia, S.C.: Illusory movements produced by electrical stimulation of low-threshold muscle afferents from the hand. *Brain* **108**(4), 965–981 (1985)
8. Kajimoto, H.: Haptic interface using tendon electrical stimulation. In: Proceedings of the 9th International Conference on Advancement in Computer Entertainment, pp. 513–516 (2012)
9. Tamaki, E., Miyaki, T., Rekimoto, J.: Possessedhand: techniques for controlling human hands using electrical muscles stimuli. In: Proceedings of the 2011 Annual Conference on Human Factors in Computing Systems, pp. 543–552. Vancouver, Canada (2011)
10. Miyamoto, N., Aoyama, K., Furukawa, M., Maeda, T. and Ando, H.: Air tap: The sensation of tapping a rigid object in mid-air. In: Proceedings of Asia Haptics 2014, pp. 285–291 (2014)
11. Lopes, P., Ion, A., Baudisch, P.: Impacto: simulating physical impact by combining tactile stimulation with electrical muscle stimulation. Proceedings of UIST'15. (2015)

Force Your Hand—PAM Enabled Wrist Support

Swagata Das, Cassie Lowell and Yuichi Kurita

Abstract Assisted motions in human body reduce muscular activation and eventually, fatigue. This paper proposes an assistive model for the wrist of a human body enabled with a set of pneumatic actuators that act like artificial muscles for supporting various motions of the user. These motions include flexion, extension, and pronation of the wrist. A series of experiments were carried out in order to verify the effectiveness and efficiency of the glove design by measuring EMG (Electromyography) signals of the concerned muscles, and positive results were obtained.

Keywords Pneumatic artificial muscle (PAM) • Electromyography (EMG) • Wrist support

1 Introduction

Wrist mobility is necessary for humans to perform basic day to day activities, such as eating, dressing, and navigating in buildings. However, joint diseases like arthritis, washerwoman's sprain, and carpal tunnel syndrome cause pain and reduce wrist functionality. Currently 1 in 3 Japanese people over the age of 65 is affected by arthritis [1], and given that Japan has a rapidly aging population, this percentage is likely to increase in the coming years. Additionally, people who often perform repetitive wrist motions (e.g. typing, drawing, sewing, washing clothes, certain sports) are at higher risk of these conditions or other wrist injuries. Gopura and Kiguchi [2] proposed an

S. Das (✉) · Y. Kurita
Graduate School of Engineering, Hiroshima University, 1-4-1 Kagamiyama,
Higashihiroshima City, Hiroshima 739-8527, Japan
e-mail: swagata@bsys.hiroshima-u.ac.jp
URL: <http://www.bsys.hiroshima-u.ac.jp>

Y. Kurita
e-mail: kurita@bsys.hiroshima-u.ac.jp

C. Lowell
Harvard University, Cambridge, MA 02138, USA
e-mail: clowell@college.harvard.edu

exoskeleton robot for wrist motion assist using EMG signals as input information to the controller, and gear drives, and servo-actuators for assistive actuation. The assistive device in [3] is designed for paraplegic patients, in which an algorithm is developed to estimate human intentions related to walking and safely support a patient's walk. Another research uses pneumatic muscles for developing a lower-limb orthosis for the elderly or people suffering from sports injuries, walk or climb stairs [4]. There are various other assistive units developed by researchers with common goals of supporting the elderly or people suffering from muscular injuries. However, no previous work based on soft actuators has been found for assisting human wrist motions.

We have developed a glove-based assistive device that helps reduce the amount of force, a human muscle must exert to execute these motions. The glove utilizes pneumatic artificial muscles (PAMs) and compressed air to push and pull the hand in the desired direction via commands from a microcontroller. The PAM dilates or compresses due to pneumatic driving. During the actuator dilation, a membrane is axially compressed, causing an axial force. The force and motion are straight and inline [5].

The wrist motions considered in designing the glove are flexion, extension, and pronation at present, which can be extended according to desired applications at a later stage. We have chosen these motions for two reasons. First, they are the most commonly used gestures in day to day activities of human beings. Second, extreme conditions of flexion, extension, and even pronation have a high probability of resulting in muscular sprains.

2 Methods

A sequence of experiments was performed according to the procedures detailed below.

2.1 *Intended Motions: Biomechanics*

The main movements defining wrist motion are flexion, extension, and pronation, as demonstrated in Fig. 1. Radial and ulnar deviation do not play a major role in causing muscular fatigue because of a smaller range of motion. Flexion is the movement of the hand towards the forearm. This motion is used for tasks like positioning hands for typing on computers or grasping a vertically oriented light switch and turning it off. The main muscles that produce flexion are flexor carpi radialis (FCR), flexor carpi ulnaris (FCU), and palmaris longus (PL). Extension is the opposite of flexion, where the palm of the hand bends away from the forearm. The responsible muscles are extensor carpi radialis longus and brevis (ECRL, ECRB) and the extensor carpi ulnaris (ECU). Pronation is twisting of the wrist while the elbow and upper arm remain stationary, which alternates the palm from being face up or face down. This

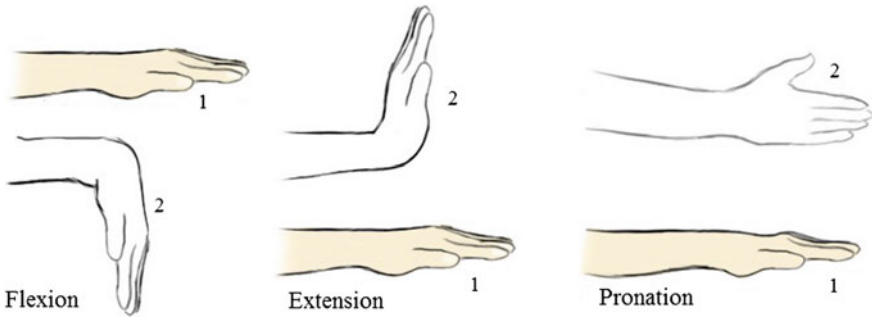


Fig. 1 Wrist movements considered for the glove design

does not take place in the wrist joint but has a large effect on combined hand and wrist functions of daily life. Pronation is a joint effort of the muscles, pronator teres and pronator quadratus [6]. Combination of two or more of these wrist movements can result complex motions of the wrist.

2.2 Glove Design

The initial prototype is designed to be cheap and light-weight, and is built around a commercially available elbow-length glove. Velcro is sewn in the indicated locations (Fig. 2) to provide contact points for the pneumatic artificial muscles (DAIYA industry corporation). These muscles are activated via stretch sensors associated with each actuator. Stretch sensors (YAMAHA corporation) detect the wearer's initial motion and activate the corresponding artificial muscle. This in turn pulls the hand in the desired direction and completes the motion, thus reducing the level of muscle activation.

Flexion is supported by two actuators, which are located on the ventral side of the hand. One end of each actuator is positioned near the palm, on the upper pad. The first flexion actuator attaches just below the little finger, and the second actuator attaches near the base of the index finger. The remaining ends of the two flexion actuators are placed on the ventral side of the hand, near the elbow. The flexion associated stretch sensor is near the dorsal side of the wrist joint, as shown in Fig. 2. The actuator for extension is placed on the dorsal side of the forearm. One end of the actuator is placed near the knuckle of the middle finger, and the other end is centred on the glove near the elbow joint. The stretch sensor used for extension is placed on the ventral side of the wrist joint, aligned towards the thumb. The fourth actuator supports pronation, and is spiralled around the forearm. One end of the actuator is near the ventral side of wrist on the major thumb pad, and the other end is also on the ventral side near the elbow joint. The stretch sensor used for pronation is placed along the wrist joint, just below the thumb, on the inner side of the arm.

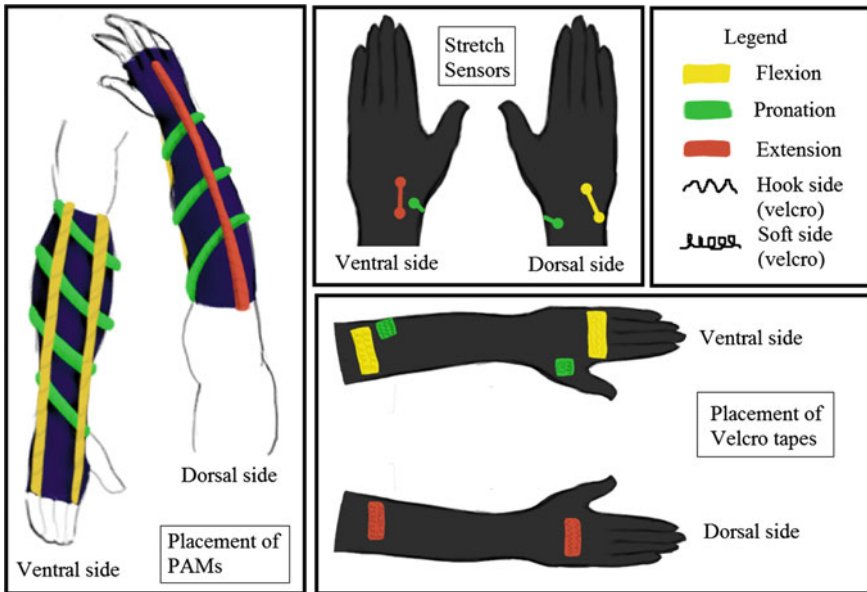


Fig. 2 Components of the glove design: pneumatic artificial muscles (PAMs), stretch sensors, and velcro placement

Stretch sensors give us information about which artificial muscle needs to be activated at which point of time. These sensors change their resistances proportionately to the level of stretching. These values of resistances are then fed to the Arduino Uno board which is programmed to constantly monitor the levels of resistance of each sensor. The Arduino Uno board uses this data to switch the solenoid valves (KOGANEI) on and off, and controls the air pressure connected to the artificial muscles. The pressure to inflate these artificial muscles is generated by a standard air compressor (Meiji).

2.3 *Experimental Testing*

Determining ideal pressure: An ideal pressure for the assistive system will optimize both the required compressor output and the motion-driving force created by the actuators when inflated. Minimizing compressor output reduces the overall resource consumption of the system. However, the compressor and the switch system must still be able to deliver enough air to drive complete actuator inflation and deflation with each cycle.

Due to the lack of precision with traditional, flexible measuring instruments (e.g. soft tape measure), the actuator's diameter change was determined via the stretch sensors. The sensors were wrapped around the actuator and fit snugly at the deflated

state. As the sensor is stretched, its resistance increases. The difference in resistance at the deflated and inflated states was compared for each pressure value.

Efficiency test: In order to prove that the glove actually does reduce the amount of effort required to perform basic wrist movements, we evaluated the glove's performance using electromyography (EMG). The amplitude of the EMG signal correlates directly to muscle activation. As such, a user wearing the wrist support should demonstrate reduced EMG signal strength while performing the same basic wrist actions. Two subjects were asked to perform basic wrist movements while unassisted, as well as while wearing the wrist support, and EMG measurements were taken for both cases.

The tests were carried out under normal laboratory conditions. Two subjects with normal muscular conditions were asked to perform flexion, extension, and pronation with and without the assistive device. These tests were carried out in equal intervals of 5 s normal resting followed by 5 s of action (flexion/extension/pronation), repeating for 25 total seconds in each trial. EMGs for two channels (one channel for ventral side muscles, one channel for dorsal side muscles) were measured in each trial and compared for each case of muscle activation.

3 Results and Discussion

3.1 *Results of Ideal Pressure Test*

Using the aforementioned methods, the ideal operating pressure was determined to be 0.3 MPa. This pressure value consistently inflated and deflated the actuator effectively, maximizing the difference between inflation states without causing operational error. Pressures above 0.5 MPa produced a squealing noise, as if air was leaking out of the actuator, and thus were not tested. Pressures below 0.1 MPa failed to fully inflate the actuators, which in the long term would have limited the actuator's ability to apply force to the wearer's joints.

3.2 *Results of EMG Measurements*

Two subjects were asked to perform flexion, extension, and pronation with and without the assistance of the glove. The EMG channels were chosen such that they could evaluate multiple muscles, simultaneously. Electrodes were placed in positions that could cover the activation of muscles associated to all three motions, thus eliminating the need to change electrode positions for each motion. The first channel could acquire EMG for the following muscles: extensor carpi ulnaris and flexor carpi ulnaris. Channel 2 could acquire muscle activation information of the following muscles, flexor carpi radialis, pronator teres, extensor carpi radialis longus, and brevis.

Fig. 3 EMG response of Subject 1 Channel 1 (Flexion)

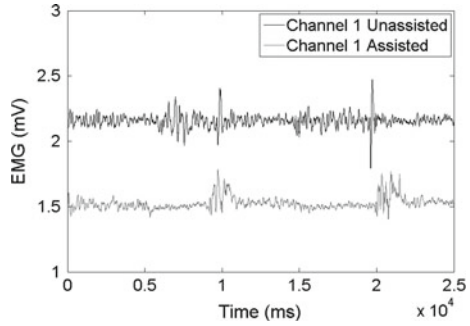
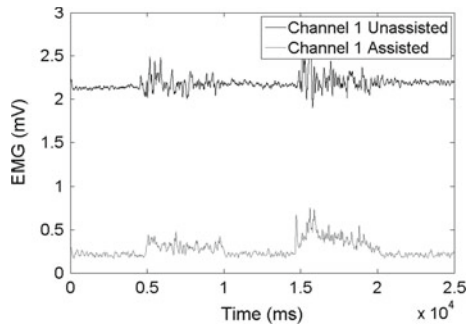


Fig. 4 EMG response of Subject 1 Channel 1 (Extension)



We observed the graphs of EMG for all three types of motions and achieved positive results.

As shown in Fig. 3, subject 1 shows a drastic reduction of muscle activation while wearing the assistive glove. During flexion, the muscle signal was reduced by an average of 31% and 85% for extension (Fig. 4), indicating that the assistive device is extremely effective. In the case of pronation (Figs. 5 and 6), the EMG reduction was 35% in channel 1 and 47% in channel 2. Subject 2 shows a 40% average reduction in channel 1 for flexion, 85% for extension and for pronation, 47% and 57% for channel 1 and 2, respectively.

Fig. 5 EMG response of Subject 1 Channel 1 (Pronation)

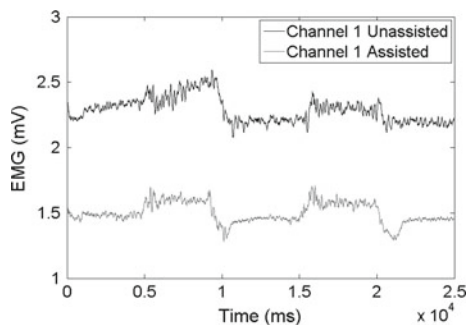
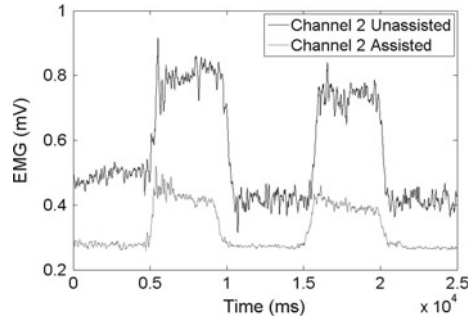


Fig. 6 EMG response of Subject 1 Channel 2 (Pronation)



4 Conclusion

An efficient reduction has been achieved in muscle activation for all three types of wrist motions after putting the assistive glove on, thus proving the effectiveness of the device. However, the EMG measurements can be further improved by more precise EMG measurement considering individual muscles for each of these motions, nevertheless these results would likely corroborate with present findings. This glove can be used by people for ease in day to day activities like sewing, typing, squeezing, etc. Also, it can be used for enhanced performances of throwing (in sports), batting and other similar activities which include wrist motions.

Future works include designing of an improved, sturdier glove with more robust stretch sensors. The presently used stretch sensors need to be calibrated before each trial. Usage of fabric-based sensors can eliminate this step. Until now, only a right hand glove has been designed and implemented. A similar model for the left glove can also be considered, which would simply be a mirror image of the right glove.

References

1. Ibe, H.: Aging in Japan, pp. 1–5. International Longevity Center-USA, New York, NY (2000)
2. Gopura, R.A.R.C., Kiguchi, K.: Development of an exoskeleton robot for human wrist and forearm motion assist. In: 2007 International Conference on Industrial and Information Systems. IEEE (2007)
3. Suzuki, K., et al.: Intention-based walking support for paraplegia patients with Robot Suit HAL. *Adv. Robot.* **21**(12), 1441–1469 (2007)
4. Yeh, T.-J., et al.: Control of McKibben pneumatic muscles for a power-assist, lower-limb orthosis. *Mechatronics* **20**(6), 686–697 (2010)
5. Srosi, J., et al.: Dynamic modeling of a pneumatic muscle actuator with two-direction motion. *Mech. Mach. Theory* **85**, 25–34 (2015)
6. Human Anatomy Lab, University of Colorado. <http://www.colorado.edu/intphys/iphy3415>

Unplugged Powered Suit with Pneumatic Gel Muscles

Chetan Thakur, Kazunori Ogawa, Toshio Tsuj and Yuichi Kurita

Abstract Assistive suits are useful in case of injury or muscle fatigue or due to aging. To support such conditions, we develop the unplugged assistive suit using low air pressure actuated pneumatic artificial muscles (PAMs). In demonstration we show the ability to actuate low power PAMs with the help of a shoe with air pumping capability. Most PAMs require an external source of energy i.e. an electric air compressor to operate, but in our proposed model we use human motions as a tool to generate air pressure which result in assisting motions of a leg in the swing motion by giving sense of assistive feeling to a human. This is also verified by analyzing the experimental results.

Keywords Assistive suit · Pneumatic artificial muscle · Unplugged powered suit

1 Introduction

Due to lack of motivation to walk or exercise in elderly people or people after rehabilitation face difficulty to move around easily and unsatisfactory quality of life. People who continue to exercise after rehabilitation can experience the better quality of life

C. Thakur (✉) · K. Ogawa
Graduate School of Engineering, Hiroshima University, 1-4-1 Kagamiyama,
Higashihiroshima City, Hiroshima 739-8527, Japan
e-mail: chetan@bsys.hiroshima-u.ac.jp
URL: <http://www.bsys.hiroshima-u.ac.jp>

T. Tsuj · Y. Kurita
Institute of Engineering, Hiroshima University, 1-4-1 Kagamiyama,
Higashihiroshima City, Hiroshima 739-8527, Japan
e-mail: tsuji@bsys.hiroshima-u.ac.jp

Y. Kurita
e-mail: kurita@bsys.hiroshima-u.ac.jp

K. Ogawa
Daiya Industries Co. Ltd., 1-4-1 Kagamiyama, Higashihiroshima City,
Hiroshima 739-8527, Japan

and ability to move easily [1]. Assistive suit is the source of external strength for a human being and can be utilized in many situations. Assistive for human motion is needed in situations like rehabilitation, difficult work condition in factories or improve performance in sports [2].

Advantages of pneumatic artificial muscles (PAMs) over other actuators can be found in their light weight, higher strength carrying capacity than active actuators, safe, simple and easy to use [3]. These properties make them a good choice to use in assistive suits and improve person's ability and motivate to experience the better quality of life. Recently pneumatic artificial muscles are being used as actuators for assistive force [4] but the problem is, it can only be actuated with a compress cylinder or air compressor [5]. Use of the compressor is not practical in real life use. Therefore, we need the passive type of pneumatic actuators like a pneumatic gel muscle (PGM). In our experiment, we use the PGM actuators, which can be actuated under very low pressure without the need of the air compressor and can generate the external force to assist in the gait cycle.

In our experiment, we study the effect of the PGMs to support the lower limb during the swing phase of the gait cycle without the need of the air compressor and can be used in everyday use case. We use shoes with pumps that can generate air to actuate the PGMs and observe the change in the lower limb muscle activities using EMG recordings during the experiments.

2 Methods

2.1 Pneumatic Gel Muscle

The PGMs unlike conventional pneumatic artificial muscles can be actuated with very low air pressure for higher strength carrying capacity compared to PAMs. The PGMs consists of an inner tube foamed with flexible gel, outer mesh structure to protect and control contraction and expansion of the PAM (Figs. 1 and 2). One end of the muscle is close and the other end is kept open with a pipe of diameter 4 mm to control air flow. Both the ends are tied firmly to stop air leak from the muscle. The natural length of the PGM is 300 mm, the maximum stretch length is 410 mm and max compressed length is 280 mm.

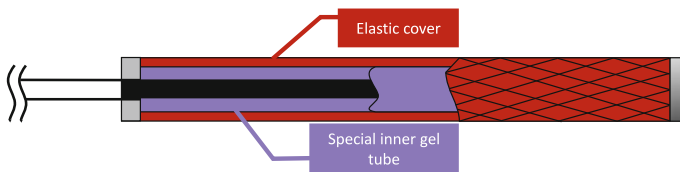


Fig. 1 Without pressure

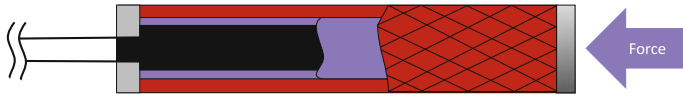
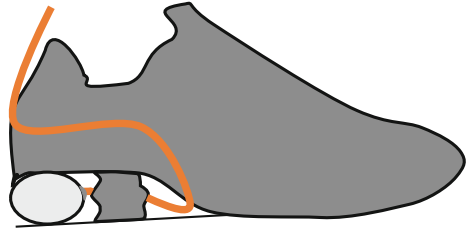


Fig. 2 With pressure

Fig. 3 Swing phase



2.2 Actuating PGM

The objective of our experiment is to build a passive assistive suit using the low power actuated PGM. The PGM is attached between the articulation of the hip and knee of the left leg. To actuate the PGM in our experiment, we use ball pumps as an air source. Two ball pumps are attached to the shoe heel of the contralateral foot i.e. right leg. The Figs. 3 and 4 show the design and working of the shoe in swing and stance phases, respectively. Figure 5 shows the photo of the developed shoe. We decided to take advantage of the dual support phase in the gait cycle as shown in Fig. 6. During this phase the heel strike generates the driving force and actuates the PGM connected to the contralateral leg. This operation helps in reducing muscle activity in the lower limb during the swing phase of the leg where the PGM is connected.

2.3 Experiment

By using PGM, the shoe with the driver pumps and the pipeworks connecting drivers and the PGM, we verify the change in a gait cycle by observing muscle activities

Fig. 4 Stance phase

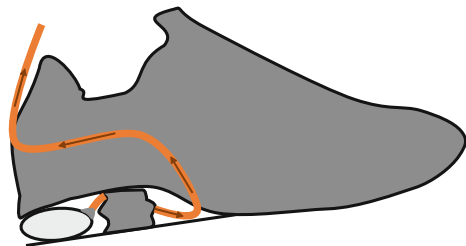




Fig. 5 Driver pump in the shoe

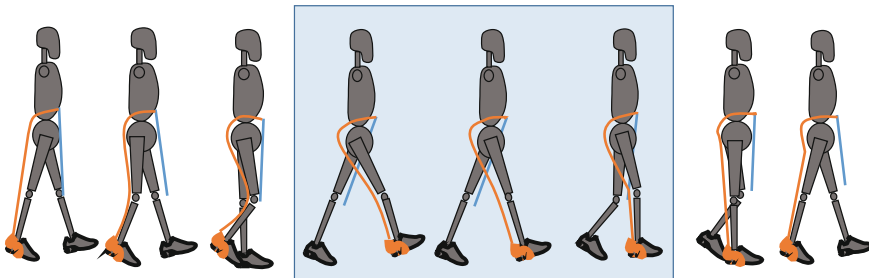


Fig. 6 Dual support phase in a gait cycle

with and without the developed assistive suit. The lower limb muscles such as rectus femoris and soleus are observed during the experiment. During the experiment, the subject was informed about the experiment and EMG measurements. The subject was then provided with the driver shoe and PGM and these were worn by the subject. The subject was then asked to perform a trial with their comfortable speed. The EMG surface electrodes were attached to the muscles under observation. The EMG readings were taken for one gait cycle and the differences were studied.

3 Results and Discussion

Figure 7 shows the result of EMG evaluation of gait cycle with and without assistive suit. The X axis represents muscles studied and Y axis shows EMG voltage output in millivolts (mV). From the bar graph, we can find that the change in the muscle activity in rectus femoris and soleus is 20% and 24% respectively. The use of assistive suit has shown positive effect with reduced muscle activities in rectus femoris and soleus.

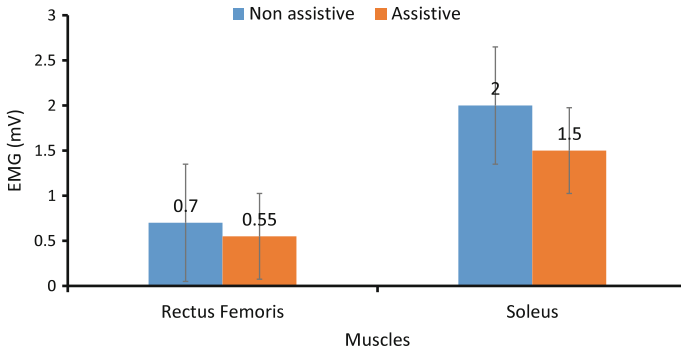


Fig. 7 Experiment results

4 Conclusion

In this study, we developed passive assistive suit using low pressure actuated PGM, air pump based shoe to generate driving force for the PGM. We examined the effect of the assistive suit on the gait cycle with the help of EMG recordings. Our experiment results show that assistive forces are supporting initial swing. Our future work includes to correct the negative effect during walking and explore applications of assistive forces based on the PGM.

References

1. Daz, I., Gil, J.J., Snchez, E.: Lower-limb robotic rehabilitation: literature review and challenges. *J. Robot.* **2011**(i), 1–11 (2011)
2. Suzuki, K., Mito, G., Kawamoto, H., Hasegawa, Y., Sankai, Y.: Intention-based walking support for paraplegia patients with robot suit HAL. *Adv. Robot.* **21**(12), 1441–1469 (2007)
3. Wickramatunge, K.C., Leephakpreeda, T.: Empirical modeling of dynamic behaviors of pneumatic artificial muscle actuators. *ISA Trans.* **52**(6), 825–834 (2013)
4. Daerden, F., Lefeber, D.: Pneumatic artificial muscles: actuators for robotics and automation. *Eur. J. Mech. Eng.* **47**(1), 10–21 (2000)
5. Yeh, T.J., Wu, M.J., Lu, T.J., Wu, F.K., Huang, C.R.: Control of McKibben pneumatic muscles for a power-assist, lower-limb orthosis. *Mechatronics* **20**(6), 686–697 (2010)

Prototype Kinesthetic Illusory Device Using Combination of Active and Passive Motion

Hirokazu Minowa, Kentaro Baba and Masamichi Sakaguchi

Abstract This study investigated a prototype device for inducing kinesthetic illusion. The device is able to convert a low-level movement, for example grasping, into a high level movement in which each finger is experienced as being separately controlled. The key point of the design was to allow a simple action to be experienced as a complex action. The device provides a simple method for inducing kinesthetic illusion.

Keywords Kinesthetic illusion · Sense of agency · Rehabilitation · Finger

1 Introduction

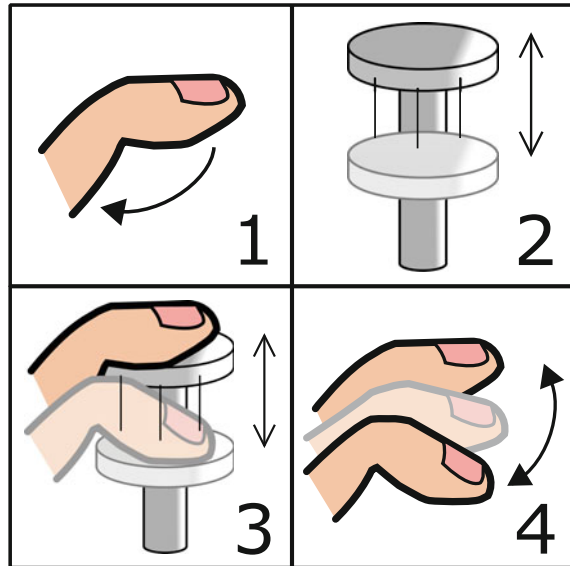
Stroke is a major cause of motor impairment. The number of stroke survivors is increasing as society ages, making the development of efficient motor rehabilitation more urgent. Recent research has focused on the application of kinesthetic illusion [1–3], which has been shown to play an effective role in motor rehabilitation. Our research team has developed a novel kinesthetic illusory rehabilitation system [4], based on the use of synchronized visual and haptic stimuli to induce kinesthetic illusion. In this system, we focused on ensuring that the movement of the fingers in the image matched the real hand position, and provided simultaneous haptic stimuli. After the study was completed, we discovered that the kinesthetic illusion is intensified when complex movement is converted from simple movement by an external force. In the present paper we report the prototype device that we developed.

H. Minowa (✉) · K. Baba · M. Sakaguchi
Nagoya Institute of Technology, Nagoya, Aichi 466-8555, Japan
e-mail: 28413164@stn.nitech.ac.jp
URL: <http://www.vrmech.web.nitech.ac.jp>

K. Baba
e-mail: 27416577@stn.nitech.ac.jp

M. Sakaguchi
e-mail: saka@nitech.ac.jp

Fig. 1 Example of conversion



2 Concept

The conceptual basis of the design is that conversion from simple movements to complex movements creates a sense of agency. In the example shown in Fig. 1, the user is folding his/her finger (1). The device then converts this one-way action into an oscillation (2, 3), giving the user the illusion of controlling the bending and stretching of the finger (4). This is a form of kinesthetic illusion. One difference from conventional kinesthetic illusions is that this illusion requires only a low level voluntary movement, as it combines an active motion and a passive motion. This was discussed in our previous research. As the previous work, we developed a ball-rotation system that is able to induce a kinesthetic illusion using visual and haptic stimuli. Figure 2 shows the system. The device displays a ball-rotation video at the same time as a ball-rotation movement. In addition, holding the balls lightly increases the vividness of the illusion. In this case, the device changes the experience from grasping to ball-rotation. We focused on this conversion process and developed a device that emphasizes this aspect of the illusion.

3 Prototype Device

In this study, we developed a prototype device that converts a simple movement into a complex movement (Fig. 3), by converting a grasping action into the experience of pushing and releasing valves, as if playing a trumpet. Although the user is merely grasping the device, it provides the illusion of controlling the motion of all the fingers.

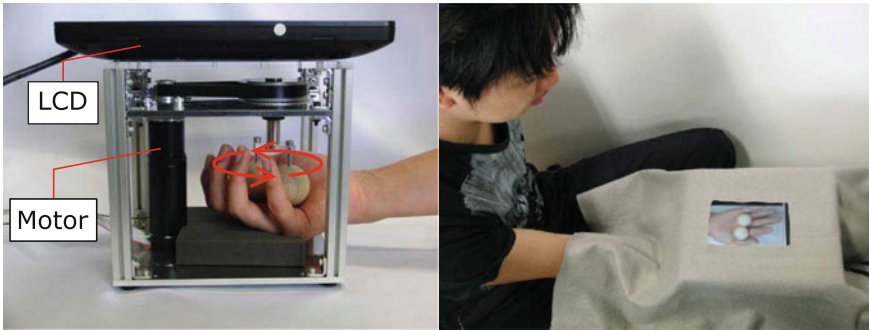


Fig. 2 Ball-rotation system (previous work)

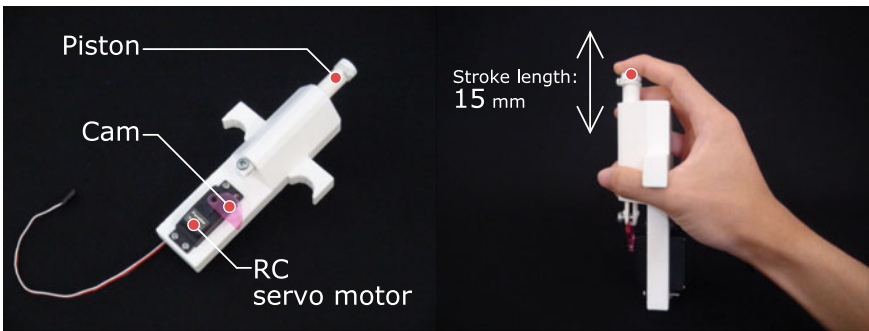


Fig. 3 Prototype device

Acknowledgements This work was supported by JSPS KAKENHI Grant Number JP16H03210.

References

1. Kaneko, F., Yasojima, T., Kizuka, T.: Kinesthetic illusory feeling induced by a finger movement movie effects on corticomotor excitability. *Neuroscience* **149**(4), 976–984 (2007)
2. Aoyama, T., et al.: The effects of kinesthetic illusory sensation induced by a visual stimulus on the corticomotor excitability of the leg muscles. *Neurosci. Lett.* **514**(1), 106–109 (2012)
3. Nojima, I., Mima, T., Kawamata, T.: The effect of visual feedback induced by kinesthetic illusion on motor learning of dexterity movement. *Japan. Phys. Ther. Assoc.* **40**(2), 106–107 (2013)
4. Baba, K., Sakaguchi, M.: Development of ball-rotation system with visual and tactile feedback inducing illusion of motion. In: *SIGGRAPH Asia 2015 Haptic Media and Contents Design*, p. 4 (2015)

A Fast Update Approach of a Stiffness Matrix for a Multi-rate Finite Element Deformation Simulation

Ryo Kuriki, Kazuyoshi Tagawa, Hiromi T. Tanaka
and Masaru Komori

Abstract In this paper, we propose a rapid update approach of a global stiffness matrix for a binary online re-mesh and multi-rate finite element deformation simulation. Our approach enables us to generate realistic and stable reaction force and deformation with quick movement such as stick slip phenomenon. In early evaluative experiments, we can confirm that our approach contributes to the reduction of computational cost of deformation simulation.

Keywords Elastic object · Finite element method · Online re-mesh · Multi-rate · ELL format · GPU/CUDA

1 Introduction

A computationally efficient deformation simulation algorithm for elastic objects contributes to the haptic interaction of surgical training systems, games and so on. However, because a high update rate (about 500 Hz) is required for stable haptic interaction, deformation simulation with high accuracy is especially difficult due to computational cost.

To reduce computational cost of deformation simulation, an online re-mesh method is proposed [1]. In the online re-mesh method, accuracy of deformation simulation is changed locally and dynamically according to the intensity of the

R. Kuriki (✉) · K. Tagawa · H.T. Tanaka
Ritsumeikan University, Kyoto, Japan
e-mail: kuriki@cv.ci.ritsumei.ac.jp

K. Tagawa
e-mail: tagawa@cv.ci.ritsumei.ac.jp

H.T. Tanaka
e-mail: hiromi@cv.ci.ritsumei.ac.jp

M. Komori
Shiga University of Medical Science, Otsu, Japan
e-mail: kom@belle.shiga-med.ac.jp

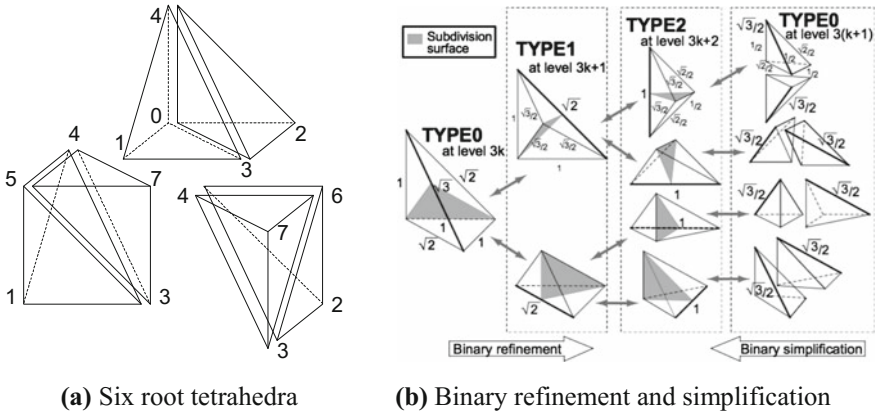


Fig. 1 Tetrahedral adaptive mesh

strain. In addition, Debunne reported that a multi-rate method is also effective in deformation simulation [2]. In the multi-rate method, the time steps of each node is determined adaptively. We previously proposed a binary online re-mesh and multi-rate method [3]. In our proposed approach, an elastic object is represented by a multi-resolution hierarchy of tetrahedral adaptive mesh. In the binary online re-mesh and multi-rate method, first, accuracy of deformation simulation is changed as with the online re-mesh method. Secondary, the time step of each node is changed based on the new accuracy of deformation simulation. Figure 1 shows the tetrahedral adaptive mesh. However, because the approach with the binary online re-mesh and multi-rate method was not implicit integration, our previous approach has a problem with the stability.

2 A Fast Update Approach of a Stiffness Matrix for a Binary Online Re-Mesh and Multi-rate Finite Element Method

To solve above problem, we propose a fast update approach of stiffness matrix for finite element deformation simulation with the binary online re-mesh and multi-rate method on GPU. Figures 2 and 3 show examples of multi-rate deformation simulation of a cube model and ELL format [4] for the binary online re-mesh and multi-rate method where white lines show nonzero values of the sparse matrices. In our approach, a stiffness matrix is stored in ELL format. The advantage of selecting ELL format is that the number of columns of the ELL format is limited to 81 from feature of the tetrahedral adaptive mesh. Besides, local and fast update of a compressed global stiffness matrix is easy, for example, swapping rows. Each row of the stiffness matrix is sorted in ascending order of its time step Δt . The time steps of

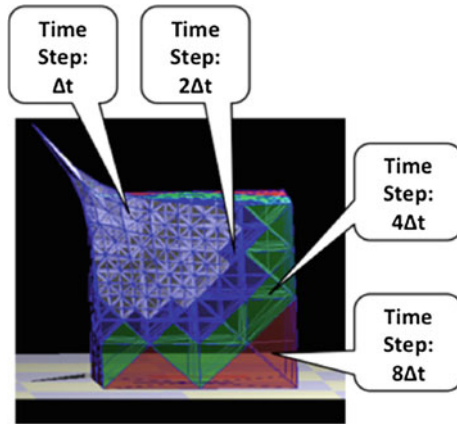


Fig. 2 Binary online re-mesh and multi-rate method

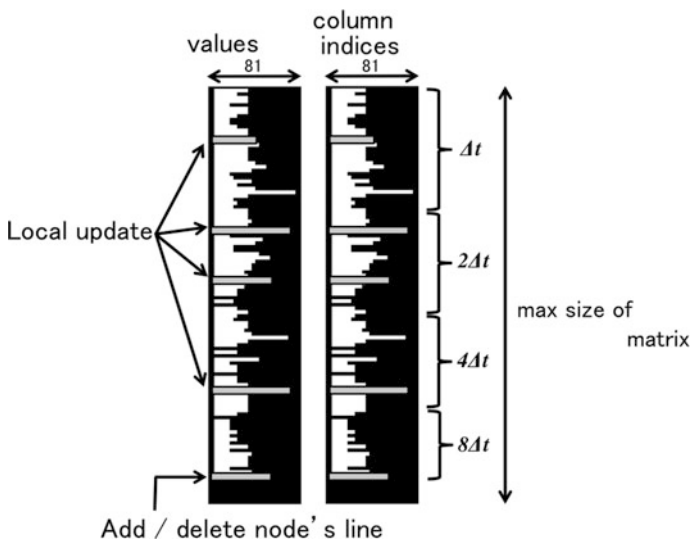


Fig. 3 ELL format for binary online re-mesh and multi-rate method

each node are obtained by truncating its time step satisfying the Courant-Friedrichs-Lewy condition [5] to the nearest N -th power of two that N is natural number. In our approach, based on the time steps of each node, the size of simultaneous equations is varied in each cycle of deformation simulation.

Fig. 4 Example of deformations

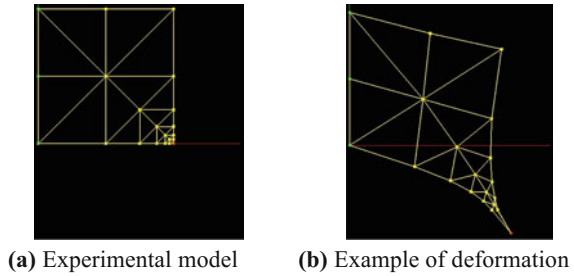


Table 1 Computation time of square model (ms)

| Single-rate model | Multi-rate model |
|-------------------|------------------|
| 0.279 | 0.158 |

3 Evaluation Experiment

As an early evaluative experiment, we compared computation time of a single-rate model, 0.134 (m) on a side of square, with a multi-rate model. The number of nodes and elements are 21 and 24, respectively. In the single-rate model, time steps of all nodes are determined to the minimum time step among all nodes. Biconjugate gradient stabilized method is used as a solver of FEM. In the simulation, the bottom right node was grasped and pulled. The simulation was performed on a PC (CPU: Intel Xeon(R) W3565 3.20 GHz), Memory: 16.0 GB, OS: Windows 10 Enterprise 64 bit, Compiler: Visual Studio 2010, SDK: Open Haptics 3.0).

Figure 4 and Table 1 show the simulation results and computation time. Through the experiment, we confirmed that our approach contributes to the reduction of computational cost of deformation simulation and the stability of deformation simulation.

References

1. Paloc, C., Faraci, A., Bello, F.: Online remeshing for soft tissue simulation in surgical training. *IEEE Comput. Graphics Appl.* **26**, 24–34 (2006)
2. Debonne, G., Desbrun, M., Cani, M.P., et al.: Dynamic real-time deformations using space and time adaptive sampling. In: *Proceedings of ACM SIGGRAPH’01*, pp. 31–36 (2001)
3. Tagawa, K., Sasaki, Y., Tanaka, H.T.: Online re-mesh and multi-rate deformation simulation by GPU for haptic interaction with large scale elastic objects. In: *Proceedings of IEEE Haptics*, pp. 531–538 (2012)
4. Grimes, R., Kincaid, D., Young, D.: *ITPACK 2.0 User’s guide*. Technical Report CNA-150, Center for Numerical Analysis, University of Texas (1979)
5. Courant, R., Friedrichs, K., Lewy, H.: On the partial difference equations of mathematical physics. *IBM J.*, 215–234 (1967)

Object Manipulation by Hand with Force Feedback

**Shunsuke Fujioka, Takao Uchiyama, Kazuyoshi Tagawa,
Koichi Hirota, Takuya Nojima, Katsuhito Akahane
and Makoto Sato**

Abstract This paper describes an implantation of object manipulation with force feedback. A force feedback device SPIDAR-U that is capable of providing independent forces to the thumb and four fingers of a hand was developed. The device was designed to reduce the influence on the magnetic field so that it can be combined with the measurement of hand motion using magnetic sensors. Also, in the simulation of interaction force between the hand model and the virtual object, nonlinearity of elasticity, or force-displacement relationship, was introduced by assuming collision between the bone and the object. A prototype system that integrate the device and the simulation was implemented, and feasibility of our approach was proved.

Keywords Object manipulation • Force feedback device • Hand model

S. Fujioka (✉) · K. Hirota · T. Nojima
The University of Electro-Communications, 1-5-1 Chofugaoka, Chofu,
Tokyo 182-8585, Japan
e-mail: shunsuke_fujioka@vogue.is.uec.ac.jp

K. Hirota
e-mail: hirota@vogue.is.uec.ac.jp

T. Nojima
e-mail: nojima@vogue.is.uec.ac.jp

T. Uchiyama · K. Akahane · M. Sato
Tokyo Institute of Technology, 4259 Nagatsuta-cho, Midori-ku,
Yokohama, Kanagawa 226-8503, Japan
e-mail: kakahane@pi.titech.ac.jp

M. Sato
e-mail: msato@pi.titech.ac.jp

K. Tagawa
Ritsumeikan University, 1-1-1 Noji-higashi, Kusatsu, Shiga 525-8577, Japan
e-mail: tagawa@cv.ci.ritsumei.ac.jp

1 Background and Purpose

Significance of haptic feedback in manipulation tasks has been discussed since the time when the idea of teleoperation was developed [1]. In case of object manipulation in virtual environment, both the simulation of haptic interaction and the haptic feedback device must be performed by the virtual reality system. Most of the investigations on these topics has focused on the interaction using hand.

Some of early researches on the simulation of haptic interaction employed macro model approximating contact [2], and others used deformation model that was localized to the contact area [3]. Recently, because of the advancement of computers, it became possible to simulate deformable whole hand model [4]. The authors also implemented a hand model whose deformation was simulate based on the motion of bones and contact with the object [5], however integration of haptic device with the simulation was remaining as a future work. Also, the necessity of considering the nonlinearity of elasticity has been discussed in many researches. Especially in case of providing force feedback, it is a concern that the linear model may reduce reality.

There are many approaches to the implementation of force feedback device [6], and some devices such as CyberGrasp [7] are commercially available. Recently, the knowledge that the stretch of skin cause the sensation of force is getting attention, and devices based on the knowledge has been developed [8, 9]. However, these devices have relatively fewer and restricted degrees of freedom. Implementation approaches that provide higher degrees of freedom have been investigated in a series researches of SPIDAR. Regarding this device, support of two-handed manipulation [10] and a mechanism avoiding strings to entangle [11] have been proposed. In our implementation, the SPIDAR was employed to provide force feedback to the five fingers of a hand.

This paper will report both integration of force feedback to the simulation of object manipulation and improvement in the algorithm of computing interaction force. A new device, called SPIDAR-U, was developed, and the nonlinearity of elasticity was introduced by computing collision between the bone and the object.

2 Implementation

2.1 Hand Tracking

The hand motion was estimated using magnetic sensors. It is difficult to measure the motion of bones correctly by attaching sensors on the surface of the skin, because the deformation of the skin can cause errors in the measurement. Our approach tried to estimate the angles of the hand joint angles just from the motion of hand nails and the back of the palm (see Fig. 1a).

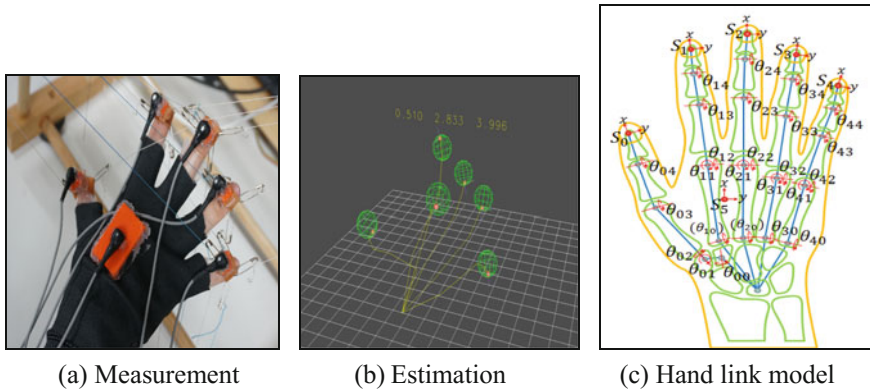


Fig. 1 Implementation of hand tracking system

Nails are connected to the phalanx relatively stiff, hence it is expected that more precise measurement is possible. The back of the palm has relatively large area for mounting the sensor, hence it is expected that the normal vector of the surface and the position of the palm along the normal vector are obtained relatively precisely.

Estimation of hand posture was solved as a problem of inverse kinematics to minimize the error between the real hand and the hand model (see Fig. 1b). Our hand skeleton model has 23 degrees of freedom as shown in Fig. 1c. The steepest descent method was used to seek the joint angles. The average position error at nail sensors was 1.8 mm, and the update rate was 240 Hz.

2.2 Virtual Hand Simulation

The deformation caused by the change of hand posture and contact with the object was simulated, and the force generated by the contact was computed, using a deformable hand model. The model was composed of bones and soft tissue. The soft tissue was defined by a tetrahedral mesh and the deformation of the tissue was simulated by the finite element (FE) method (see Fig. 2).

The position and orientation of bones were determined by the hand tracking computation as described above, and the surface of the bones gave fixed boundary condition on the FE model. Contact with the object at the surface nodes was computed using the penalty method. Our study employed the friction model that has static and kinetic friction states. To mitigate the problem of linear elasticity model as described above, collision between the bone surface and the object was also computed to generate collision force; the friction was not caused in the collision. The shape of the object was defined using Metaball model. Most part of the computation was accelerated by GPUs to realize real time interaction. In our

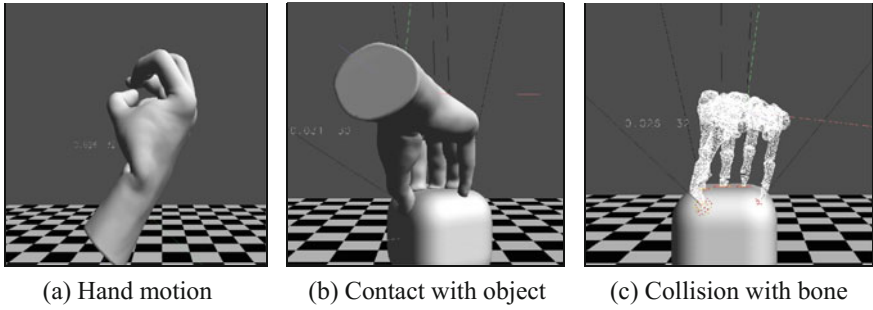


Fig. 2 Simulation of deformation

system, the update rate of the simulation including deformation of object, computation of force, and motion of the object, was approximately 50 Hz.

2.3 Force Feedback

A force feedback device that provides independent force vectors respectively to the thumb and four fingers were developed (see Fig. 3a); the device is referred to as SPIDAR-U.

The force vector on each action point, or fingertip, was controlled by changing the tension of four wires connected to the point. Motors were driven by the amplifier circuit dedicated for the SPIDAR system, and the computation of the wire tension depending the position of action point was performed by AHS library software [12]. The working volume of the device was approximately within 400 mm radius from the center of the volume, and the maximum force in the volume was about 4 N. The device was designed, as stated above, to reduce the influence of the device on the magnetic field that is generated by the magnetic

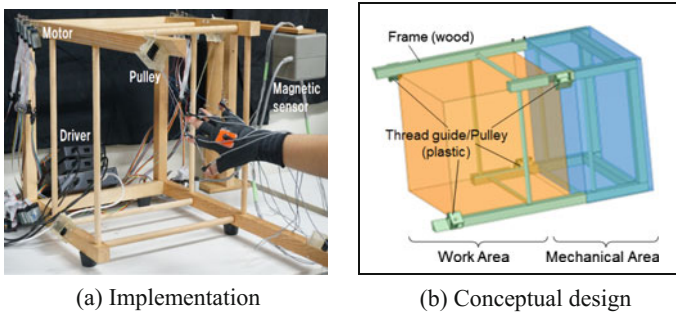


Fig. 3 SPIDAR-U

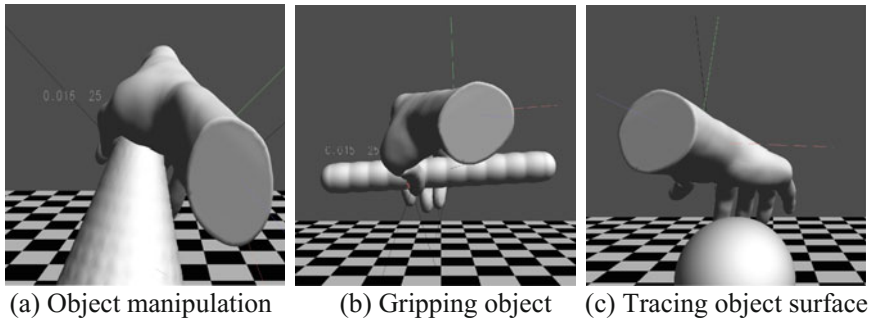


Fig. 4 Object manipulation with finger force feedback

position sensor. The structure of the device was made of wood, and all the mechanical parts leading the wires were made of plastic. Moreover, by taking advantage of wire tension drive, the motors were allocated away from the work area to reduce the effect of the magnetic field caused by the motors (see Fig. 3b).

2.4 Manipulation System

The manipulation system was implemented by integrating the hand tracking, VR hand simulation, and force feedback subsystems. Since these subsystems were running on separate PCs, the manipulation system was composed by connecting them through the network. Through the implementation, feasibility of our approach was confirmed; manipulation of virtual object while feeling the manipulation force was realized, and improvement of stiffness by introduction of bone contact force was empirically confirmed (see Fig. 4).

3 Future Work

The force feedback device must be mechanically improved. A problem found was that wires get entangled each other depending on the posture of the hand. Optimization in the configuration of wires from the viewpoint of possible pose of the hand must be investigated. Another work to be done is to evaluate the reality of manipulation quantitatively to clarify the impact of our system on the improvement of the reality.

Acknowledgements This research was supported by JSPS KAKENHI Grant Number JP16K12474.

References

1. Shimoga, K.B.: A survey of perceptual feedback issues in dexterous telemanipulation. I. Finger force feedback. In: Proceedings of VRAIS'93, pp. 263–270 (1993)
2. Barbagli, F., Frisoli, A., Salisbury, K., Bergamasco, M.: A soft finger proxy model and algorithm. In: Proceedings of the International Symposium on Haptic Interfaces, pp. 9–17 (2004)
3. Ciocarlie, M., Lackner, C., Allen, P.: Soft finger model with adaptive contact geometry for grasping and manipulation tasks. In: Proceedings of World Haptics 2007, pp. 219–224 (2007)
4. Perez, A.G., Cirio, G., Hernandez, F., Garre, C., Otaduy, M.A.: Strain limiting for soft finger contact simulation. In: Proceedings of World Haptics 2013, pp. 79–84 (2013)
5. Hirota, K., Tagawa, K.: Interaction with virtual object using deformable hand. In: Proceedings of VR2016, pp. 49–56 (2016)
6. Burdea, G.: Force and Touch Feedback for Virtual Reality. Wiley-Inter-Science, New York (1996)
7. CyberGlove Systems: <http://www.cyberglovesystems.com/>
8. Minamizawa, K., Kajimoto, H., Kawakami, N., Tachi, S.: A wearable haptic display to present the gravity sensation—preliminary observations and device design. In: Proceedings of World Haptics 2007, pp. 133–138 (2007)
9. Guinan, A.L., Montandon, M.N., Doxon, A.J., Provancher, W.R.: Discrimination thresholds for communicating rotational inertia and torque using differential skin stretch feedback in virtual environments. In Proceedings of Haptics 2014, pp. 277–282 (2014)
10. Kohno, Y., Walairacht, S., Hasegawa, S., Koike, Y., Sato, M.: Evaluation of two-handed multi-finger haptic device SPIDAR-8. In: Proceedings of ICAT2001, pp. 135–140 (2001)
11. Liu, L., Miyake, S., Akahane, K., Sato, M.: Development of string-based multi-finger haptic interface SPIDAR-MF. In: Proceedings of ICAT2013, pp. 67–71 (2013)
12. Sato, M., Isshiki, M., Lin, L., Akahane, K.: Spidar-mouse: a design of open source interface for SPIDAR. In: The Institute of Electronics, Human Communication Group Symposium, pp. 83–88. Asia Graph (2010)

Visuo-Tactile Interaction with Virtual Objects that Yields Kinetic Effects on Real Objects

Kyosuke Yamazaki, Keisuke Hasegawa, Yasutoshi Makino
and Hiroyuki Shinoda

Abstract In this presentation, we describe an HMD-based immersive VR environment which allow us to touch virtual objects and to apply actual kinetic effects on corresponding objects in real world. We utilize foci of airborne ultrasound for generating tactile feedback to users' hands and applying kinetic force to the real objects. Our system offers a new tele-operation system, where bare-handed users can manipulate real objects located away from them with tactile feedback.

Keywords Telexistence · Ultrasound · Tactile feedback · VR

1 Introduction

1.1 *Telexistence with Tactile Feedback*

In the scope of recent VR/AR researches, systems concerning haptic modality as well as conventional audiovisuals have been proposed and demonstrated increasingly. The importance of handling haptic modality in human-computer interaction has become more prominent in the field of Telexistence as well.

Telexistence is a technique that allows its users to virtually exist in a place away from themselves. It consists of a pair of a slave (operated robot) and a master (user). The user's motion is transferred to a remotely connected slave device and let it

K. Yamazaki (✉) · K. Hasegawa · Y. Makino · H. Shinoda
The University of Tokyo, 5-1-5, Kashiwanoha, Kashiwa-shi, Chiba 277-8561, Japan
e-mail: yamazaki@hapis.k.u-tokyo.ac.jp

K. Hasegawa
e-mail: Keisuke_hasegawa@ipc.i.u-tokyo.ac.jp

Y. Makino
e-mail: Yasutoshi_Makino@k.u-tokyo.ac.jp

H. Shinoda
e-mail: Hiroyuki_Shinoda@k.u-tokyo.ac.jp

operate accordingly. Slave devices are embedded with sensors that captures sensory information (vision, audio and/or sense of touch) sent back to the master user offering the sensory feedback. Originating the development of a teleexistence system giving haptic feedback to users [1], the art-of-the state study has succeeded in presenting multi-modal haptic sensations comprising the sense of pressure, vibration, and temperature to users through a robot [2]. Since haptic feedback plays an intrinsic role to facilitate tele-manipulation with improved operability through a robot, haptic teleexistence systems are expected to be efficient for users engaged in operational tasks.

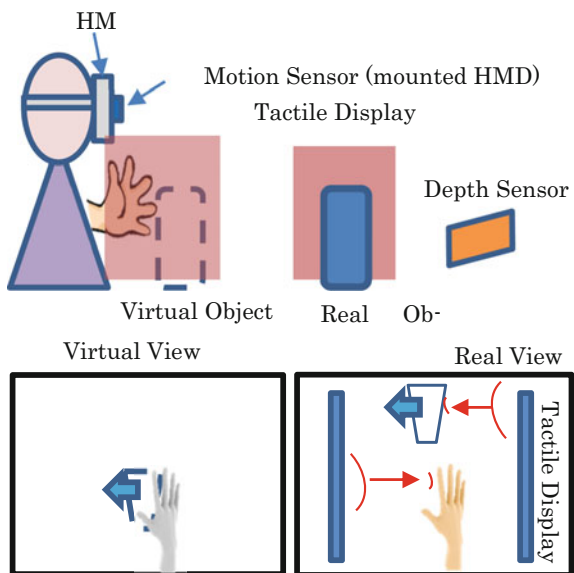
1.2 Our System

As a new form of teleexistence technique, we propose a teleexistence system that gives tactile feedback to a bare-handed user wearing only HMD without a slave robot. The system contains ultrasound transducer arrays (Airborne Ultrasound Tactile Display [3]) in the workspace that generate airborne focused ultrasound causing acoustic radiation pressure presenting the haptic feedback to users and applying kinetic force onto the corresponding real objects apart from the users.

Figure 1 shows overview of proposed system.

In this system, both of real objects and the user's hands are detected by a remote depth and/or motion sensors. Both of the captured bodies are rendered in the same VR space and displayed via HMD. When a user touches objects in the VR space, converged ultrasound irradiates from AUTD to give tactile feedback and move

Fig. 1 Proposed system



objects respectively at the same time so that the user can remotely manipulate the corresponding objects in an intuitive way. The system displaying not real images but objects rendered in VR space, users can see only necessary images without suffering from bad optical condition in real world such as the dark.

Therefore, we expect that the benefits have the user manipulate an object more easily.

In addition, we expect that this system could get rid of suffering from disagreement of spatial awareness between VR and real space, which is one of the problem in tele-manipulation [4], caused by difference of size between the user and the slave robot.

Though the force produced AUTD is weak so that it can move only light objects, the system would be applied to more various and flexible situations other than conventional ones because of the following three reasons. The first one is that proposed system is free from visual interference from a slave robot. Secondly, phased arrays (AUTD) are flat devices so that we can attach them to wall or ceiling, which is equivalent to that we have an actuator embedded in daily environments which virtually appear and disappear as necessary. The third reason is that we only require users to wear just a single HMD, which makes the system convenient and simple. By increasing the number of phased arrays, the force of converged ultrasound and a manipulative range can be improved if necessary [5]. For example, this configuration would be effective in such situations that multiple master users would simultaneously tele-operate since there would be no collision between users in using ultrasound as an actuator instead of rigid robot hands.

1.3 Previous Studies

Makino et al. [6] proposed a novel interactive system named “HaptoClone” that enables real-time interaction with a mid-air 3D optical clone of real objects accompanying tactile feedback. Two users sitting side by side in front of two cabinet-shaped workspaces can see each other’s 3D clone displayed using a pair of micro-mirror array plates named “Aerial Imaging Plate”.

Both workspace is embedded with ultrasound phased arrays on its inner wall. When the user inserts own hand into the cabinet, a depth sensor measures the hand position and calculates if the hand contacts a floating 3D image at the same time.

If the hand touches the cloned image of the object, the phased arrays generates tactile feedback onto the user’s hand and force onto the original object at the other side.

This system realizes mutual interactions and essentially there is in principle no distinction between the slave and the master side. Currently it can’t distance one side from the other since it uses optical system to directly refocus the images.

1.4 Construction in This Paper

In this paper, we describe an implementation of the proposed system and report the preliminary results of experiments that demonstrated the possibility of converged ultrasound moving the objects as it gives tactile feedback to users.

2 System Configuration

2.1 Outline

This system is divided into two sections. One is the visual display system projecting a user's hand and rendered objects. The other is the force generating system presenting tactile feedback and force for objects.

2.2 Image System

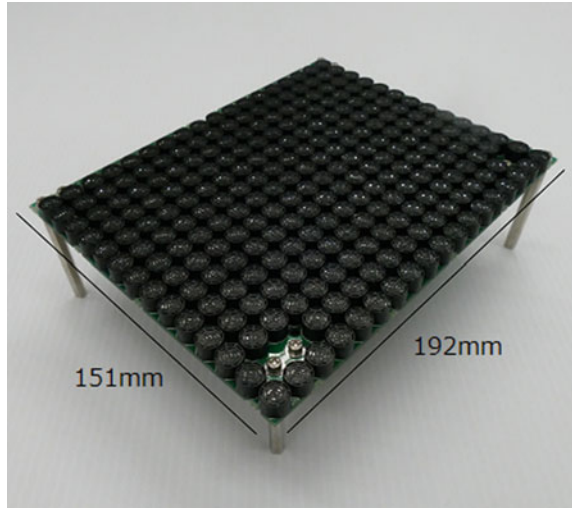
We use a Kinect v2 (Microsoft, Co.) as a depth sensor and a LeapMotion (LeapMotion, Co.) as a hand tracker. Kinect detects not only objects that the users want to handle but also the workspace including objects. For this reason we employ LeapMotion for a robust hand tracking since it gives hand position and posture extracted from its view. Mounted on HMD, it can detect user's hand independently of user's body direction.

The VR space integrating these two data is developed with a game engine "Unity". Unity supports HMD "Oculus rift" and is able to control the phased array described in following next section.

2.3 Force System

We use an aerial ultrasound phased array [5] called "AUTD" as a device generating converged ultrasound (Fig. 2). A total of 249 small ultrasound transducers whose resonant frequency is 40 kHz are arrayed so that they can focus on arbitrary midair position by changing their phases. Applying the AM method to them, various vibrations are presented to skin [7]. Thanks to the nature of ultrasound as waves, the device can focus ultrasound even if its propagation blockage is caused by a small object. It is controlled the COM serial communication via a Microcontroller.

Fig. 2 Arrayed ultrasound transducers



3 Presenting Converged Ultrasound to Objects

Mitsui et al. [7] showed that acoustic radiation pressure from converged ultrasound has the potential to control a light (~ 0.6 g) object two-dimensionally. We likewise verified that the pressure could move two objects as A and B which is heavier (A: 2.6 g B: 26.3 g) than the one used in his study by constructing four-unit arrays (Fig. 3). We observed the behavior of the object when it is placed 22 cm away from the array.

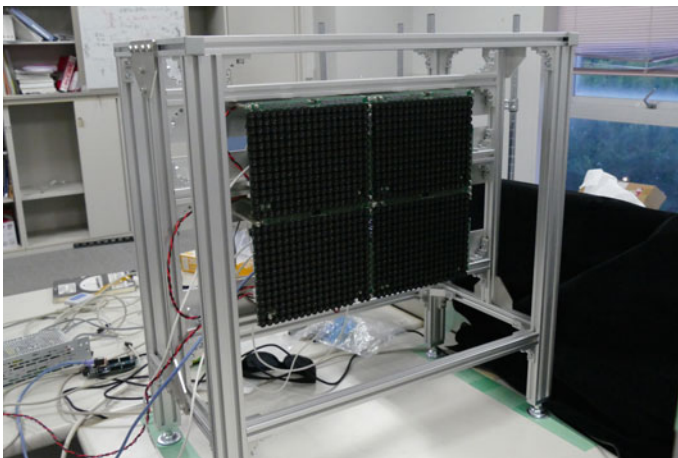


Fig. 3 The array composed of four AUTDs

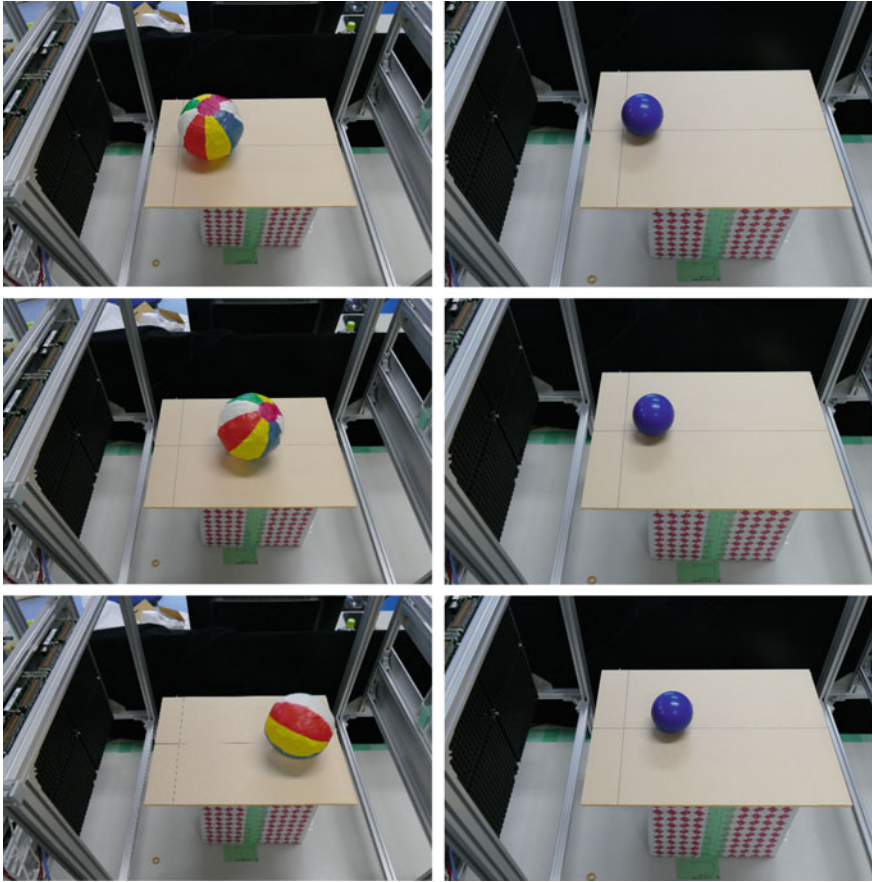


Fig. 4 The movement presenting ultrasound (*Left: A Right: B*)

Figure 4 shows the first three sequential frames of a captured video with its frame rate set to 12 fps, validating that both objects moved. We conclude that the array could handle objects weighing up to around 20 g. We should note that in this verification we used sphere objects which are affected by static friction in a relatively small degree.

In practical cases, multiple devices facing toward different orientations would be required in a workspace so that an object can be pushed from various directions.

4 Conclusions and Future Works

In this paper we proposed a telexistence system which enables users to manipulate objects remotely with tactile feedback and verified that if the converged ultrasound is able to move the two objects (A: 2.6 g B: 26.3 g). And it was found that the ultrasound had the potential to move about 20 g objects two-dimensionally.

After this, we will implement a prototype system which allows users to virtually interact with real objects and evaluate the validity of the proposed system in terms of its usability.

We plan to apply the proposed techniques to practical scenes that conventional telexistence system has not targeted, such as a manipulation in a workspace which is too geometrically complicated for rigid actuators to operate in, or a collective tasks free from mechanical interference caused by other users.

Acknowledgements This research is supported by JSPS KAKENHI 16H06303 and JST ACCEL Embodied Media Project.

References

1. Sato, K., Minamizawa, K., Kawakami, N., Tachi, S.: Haptic telexistence. In: Proceeding of ACM SIGGRAPH 2007 Emerging Technologies Article No. 10 (2007)
2. Fernando, C., Fukuyama, M., Kurogi, T., Kamuro, S., Sato, K., Minamizawa, K., Tachi, S.: Design of TELESAR V for transferring bodily consciousness in telexistence. In: Proceedings of IEEE/RSJ International Conference on Intelligent Robots and Systems, pp. 5112–5118 (2012)
3. Hoshi, T., Takahashi, M., Iwamoto, T., Shinoda, H.: Noncontact tactile display based on radiation pressure of airborne ultrasound. *IEEE Trans. Haptics* **3**(3), 155–165 (2010)
4. Watanabe, K., Kawakami, N., Tachi, S.: An effect of dimensional disagreement between the operator and the slave robot in telexistence master-slave system. *TVRSJ* **14**(3), 391–394 (2009)
5. Hasegawa, K., Shinoda, H.: Aerial display of vibrotactile sensation with high spatial-temporal resolution using large-aperture airborne ultrasound phased array. In: Proceedings of IEEE WHC 2013, pp. 31–36 (2013)
6. Makino, Y., Furuyama, Y., Inoue, S., Shinoda, H.: HaptoClone (Haptic-Optical Clone) for mutual tele-environment by real-time 3D image transfer with midair force feedback. In: Proceedings of ACM CHI, pp. 1980–1990 (2016)
7. Mitsui, Y., Tanaka, K., Inoue, S., Makino, Y., Shinoda, H.: Object manipulation by using airborne ultrasound phased array. In: JSME Conference on Robotics and Mechatronics, No. 16–2, 1A2–14b3 (2016)

Enhancement of Perceived Force from the Hanger Reflex on Head and Ankle by Adding Vibration

Takuto Nakamura and Hiroyuki Kajimoto

Abstract The “Hanger Reflex” is a phenomenon in which a participant involuntarily rotates their head when a wire hanger is attached it, and has also been observed on the wrist and the ankle. Moreover, the force caused by the Hanger Reflex on the wrist is enhanced by adding a vibration stimulus. These phenomena might be potentially useful for the rehabilitation of movement disorders characterized by abnormal posture. In this paper, we generalize this “vibration effect” on the Hanger Reflex by applying vibration to the head and ankle. We developed devices to generate both skin deformation and vibration, and conducted a user study. We observed that all participants perceived the enhancement of the force, and slightly rotated the stimulated parts of the body.

Keywords Hanger reflex · Haptic display · Perceptual illusion · Skin stretch

1 Introduction

In the field of virtual reality and mediated sports training, force feedback plays an important role in improving the immersion of the system and in increasing training efficiency. Force feedback is also effective in medical fields such as rehabilitation, because it can teach correct posture or motion to patients.

However, the widespread use of conventional force feedback devices remains limited, because of issues of size, price, and energy consumption. Conventional devices present a physical force to the user using actuators such as motors. Therefore, whether a device can present a posture to the user or not depends on the

T. Nakamura (✉) · H. Kajimoto

The University of Electro-Communications, 1-5-1 Chofugaoka, Chofu, Tokyo, Japan

e-mail: n.takuto@kaji-lab.jp

H. Kajimoto

e-mail: kajimoto@kaji-lab.jp

T. Nakamura

JSPS, Chiyoda-ku, Japan

performance of the actuator, and high-cost actuators are required to achieve a high-quality experience.

To address these issues, many methods that manipulate the perception of force (i.e. perceptual illusions) have been proposed in recent years [1–5]. These methods induce a perceived force using haptic or visual stimuli, and can be realized by devices with lower sizes, prices, and energy consumption. However, the strength of the force that can be induced by such methods is limited, and it is difficult to use them to present a large motion.

One phenomenon that can induce a large motion is called the Hanger Reflex. In this phenomenon, a participant rotates their head involuntarily when they wear a wire hanger on their head [6, 7]. During this sensory illusion, the participant feels as if their head is being rotated by someone else. Sato et al. [8, 9] confirmed that the deformation of the skin caused by pushing specific points on the head contributes to this phenomenon. The Hanger Reflex on the head has been applied to the treatment of the movement disorder called “cervical dystonia” involving involuntary abnormal head posture [13], and has additionally been observed on the wrist, waist, and ankle [10, 11].

Recently, we reported that a perceptual force caused by the Hanger Reflex on the wrist is enhanced by adding vibration stimulus [12]. Because these phenomena are associated with a specific change in posture with small latency, they are promising avenue for application to the field of virtual reality and sports.

This paper is the generalization of this finding, by adding the vibration stimulus to already known Hanger Reflex sites, particularly the head and ankle. We developed devices to present both skin stretch and vibration, and conducted a user study to confirm the phenomenon.

2 Devices

2.1 *Device for the Head*

In the Hanger Reflex on the head, the “sweet spots” [8], which efficiently induce the Hanger Reflex, are located on the front side of temporal region and the back side of the other temporal region. We prepared an elliptical shape device that is made of CFRP (Carbon Fiber Reinforced Plastics) and deforms elastically [13, 14] (Fig. 1). When the device is worn and rotated slightly, it deforms and presses the head to induce the Hanger Reflex (Fig. 2). To present the vibration stimulus, we placed two vibrators (Vibro-Transducer Vp2, Acouve Laboratory Inc.) on the device, which are driven by the signal generated by a PC and amplified by an audio amplifier (RSDA202, RASTEME SYSTEMS Inc., Niigata, Japan) (Fig. 3).



Fig. 1 The developed device for the head: the device is made of FRP, so it deforms elastically when the user wears it



Fig. 2 Procedure for inducing the Hanger Reflex on the head using the device

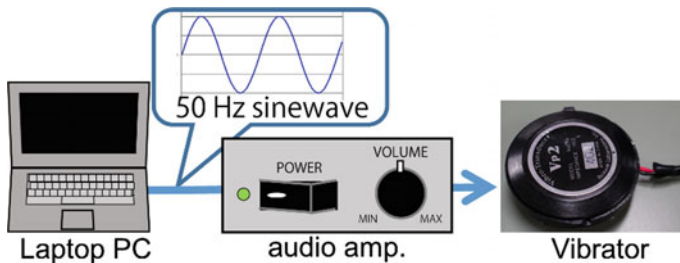


Fig. 3 The system for the hanger device: the laptop PC generates 50 Hz sine wave audio signal and the amplified signal is outputted by the vibrator

2.2 Device for the Ankle

We also prepared a device to produce skin deformation on the ankle and trigger the Hanger Reflex. The device is U-shaped and made of ABS resin (Fig. 4). The wave-shaped part enables the device to bend elastically, and the open part of the device is

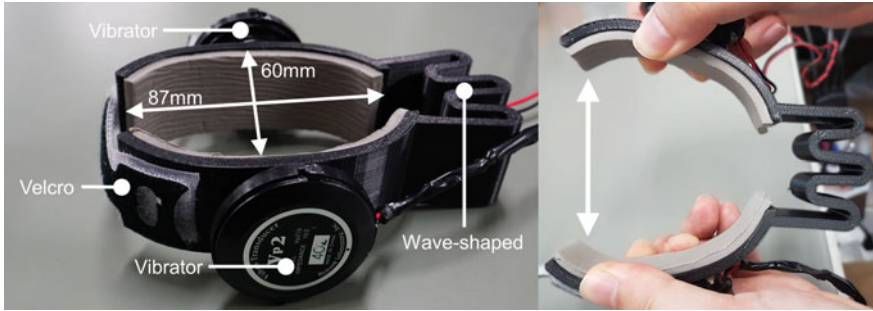


Fig. 4 The developed device for the ankle: the device deforms elastically because of the wave-shaped part



Fig. 5 Procedure to induce the Hanger Reflex on the ankle using the device

fastened by Velcro to induce the Hanger Reflex more strongly (Fig. 5). We also placed two vibrators on the sides of the device, like for the head mounted device.

3 User Study

To confirm that the enhancement of the Hanger Reflex by adding vibration occurs in naïve users, we conducted a user study. We recruited four laboratory members (four males, aged 21–23) who were naïve to this phenomenon. The participants were asked to wear the device and confirm whether the Hanger Reflex occurred, and then the experimenter presented the vibration after the confirmation. The presented vibration was a 50 Hz sinusoidal wave, which has previously been found to be the most effective in the Hanger Reflex on the wrist. We conducted this confirmation because we have previously noticed that the vibration can enhance the Hanger Reflex, but cannot generate it alone. After applying the device, they were interviewed about the changes in perceived force before and after the vibration stimulus was presented.

In case of the head-mounted device, all participants perceived the rotational force caused by the Hanger Reflex. The Hanger Reflex induced by the developed

device generated a strong enough force to rotate their head involuntarily. When we additionally presented the vibration stimulus, all participants reported that they perceived an enhancement of the force. The result was shown not only in their comments, but also in the additional involuntary rotation of the head. We obtained one comment from the participants, which was: “I could oppose the force from the Hanger Reflex alone, but it was difficult to oppose the force from both the Hanger Reflex and the vibration, so I allowed this force to move me.” We observed that some participants rotated their head to near the limit of the range of motion. Also, one participant commented on how the enhancement felt: “By presenting the vibration, I felt as if the Hanger Reflex occurred repeatedly.”

In case of the ankle device, all four participants perceived the rotational force caused by the Hanger Reflex. When we additionally presented the vibration stimulus, all participants reported that they perceived the enhancement of the force. We applied the device to the participants in two postures: sitting, and standing on one foot, the one that was not wearing the device. The participants felt the force more clearly when they were standing on one foot. This result may imply that friction between the leg and the chair occurred and impeded the perception of force from the phenomenon.

Based on the results of the study, we can advance a hypothesis as to why this phenomenon occurs. In the case of the wrist, we propose two candidate reasons. First, the direction of the skin deformation was asymmetric, because we presented a symmetric vibration (sine wave) to the deformed skin, which was generated by the device in advance. Second, the presented vibration was propagated to the muscle spindle and tendon that rotates the wrist, causing hyperextension kinesthesia [15]. Hyperextension kinesthesia is a phenomenon that is caused by presenting a vibration stimulus to the tendon, and induces the feeling of a bending joint without the actual movement of the joint. In this study, the muscles that move the head and ankle are not located around the stimulated area, and it is difficult to conclude that the second candidate relates this phenomenon. Therefore, the first candidate seems more likely: we suggested that skin deformation or skin sensation may relate to why this phenomenon occurs.

4 Conclusion

In this paper, we reported that the force caused by the Hanger Reflex on the head and the ankle is enhanced by adding vibration. We developed devices to induce the Hanger Reflex on the head and the ankle, and placed the vibrators on the devices to present the vibration stimulus. The results confirmed that naïve participants perceive an enhanced force when adding the vibration stimulus to the areas where the Hanger Reflex was induced. It is suggested that the cause of this phenomenon relates to skin deformation or skin sensation, because the muscles that move the head and ankle are not located around the stimulated area.

Acknowledgements This work was supported by JSPS KAKENHI Grant Number JP16J09326

References

1. Minamizawa, K., Prattichizzo, D., Tachi, S.: Simplified design of haptic display by extending one-point kinesthetic feedback to multipoint tactile feedback. In: Proc. of IEEE Haptics Symposium 2010, pp. 257–260 (2010)
2. Amemiya, T., Gomi, H.: Distinct Pseudo-Attraction Force Sensation by Thumb-Sized Vibrator that Oscillates Asymmetrically. In: Proc. of Euro Haptics 2014, pp. 88–95 (2014)
3. Rekimoto, J.: Traxion: a tactile interaction device with virtual force sensation. In: Proc. of 26th ACM Symposium User Interface Software and Tech. (UIST2013), (2013)
4. Kuschel, M., Luca, M.D., Buss, M., Klatzky, R.L.: Combination and integration in the perception of visual-haptic compliance information. *IEEE Trans. on Haptics*, 3, pp. 234–244 (2010)
5. Lécuyer, A.: Simulating haptic feedback using vision: A survey of research and applications of pseudo-haptic feedback. *Presence: Teleop. Vir.*, 18, pp. 39–53 (2009)
6. Matsue, R., Sato, M., Hashimoto, Y., Kajimoto, H.: Hanger reflex: a reflex motion of a head by temporal pressure for wearable interface. In Proc. of *SICE Ann. Conf.* 2008, pp. 1463–1467 (2008)
7. Asahi, T., Sato, M., Kajimoto, H., Koh, M., Kashiwazaki, D., Kuroda, S.: Rate of Hanger Reflex Occurrence: Unexpected Head Rotation on Fronto-temporal Head Compression. *Neurol. Med. Chir.*, 55, pp. 587–591(2015)
8. Sato, M., Matsue, R., Hashimoto, Y., Kajimoto, H.: Development of a head rotation interface by using hanger reflex. In: Proc. of 18th IEEE Int. Symp. Robot Human Interact. Comm. (RO-MAN), pp. 534–538 (2009)
9. Sato, M., Nakamura, T., Kajimoto, H.: Movement and Pseudo-Haptics Induced by Skin Lateral Deformation in Hanger Reflex. In: Proc. of SIG TeleXistence 5th Workshop, (2014) (in Japanese)
10. Nakamura, T., Nishimura, N., Sato, M., Kajimoto, H.: Application of hanger reflex to wrist and waist. In: Proc. of IEEE Virtual Reality (VR) 2014, pp. 181–182 (2014)
11. Kon, Y., Nakamura, T., Sato, M., Kajimoto, H.: Effect of Hanger Reflex on Walking. In: Proc of IEEE Haptics Symposium 2016, pp. 313–318 (2016)
12. Nakamura, T., Nishimura, N., Hachisu, T., Sato, M., Yem, V., Kajimoto, H.: Perceptual Force on the Wrist Unger the Hanger Reflex and Vibration. In: Proc. of Euro Haptics 2016, pp. 462–471 (2016)
13. Asahi, T., Sato, M., Nakamura, T., Kajimoto, H., Oyama, G., Fujii, M., Hayashi, A., Taira, T., Kuroda, S.: Hanger Reflex has Potential to Treat Cervical Dystonia—a Multicenter Clinical Trial with Portable Device Inducing the Hanger Reflex. In: Proc. MDS 18th International Congress of Parkinson’s Disease and Movement Disorders. (2014)
14. Japan Patent Kokai 2014-5552844 (2014.07.16)
15. Goodwin, G.M., McCloskey, D.I., Matthews, P.B.C.: The contribution of muscle afferents to kinesthesia shown by vibration induced illusions of movement and by the effects of paralyzing joint afferents. *Brain*, 95, pp. 705–748 (1972)

An Immersive Visuo-Haptic VR Environment with Pseudo-haptic Effects on Perceived Stiffness

Daichi Matsumoto, Ya Zhu, Yuya Tanaka, Kyosuke Yamazaki, Keisuke Hasegawa, Yasutoshi Makino and Hiroyuki Shinoda

Abstract In this presentation, we describe an immersive visuo-tactile VR system which presents tunable subjective hardness of virtual objects by employing the pseudo-haptic effects. Our system supposes that users put on an HMD and a glove which contains a mechanical structure that presents constraining force to his or her fingers in pinching virtual objects. The system visually displays a re-rendered virtual hand pinching deformed objects with its finger flexion magnified or suppressed graphically, for arousing the pseudo-haptic effect. We expect this method to be effective in creating mobile wearable tactile systems that are correlated to personal VR systems in home applications.

Keywords Pseudo-haptics · Immersive VR

D. Matsumoto (✉) · Y. Zhu · Y. Tanaka · K. Yamazaki ·
K. Hasegawa · Y. Makino · H. Shinoda
The University of Tokyo, 5-1-5, Kashiwanoha, Kashiwa, Chiba 277-8561, Japan
e-mail: matsumoto@hapis.k.u-tokyo.ac.jp

Y. Zhu
e-mail: zhuya@hapis.k.u-tokyo.ac.jp

Y. Tanaka
e-mail: y.tanaka@hapis.k.u-tokyo.ac.jp

K. Yamazaki
e-mail: yamazaki@hapis.k.u-tokyo.ac.jp

K. Hasegawa
e-mail: keisuke_hasegawa@ipc.i.u-tokyo.ac.jp

Y. Makino
e-mail: yasutoshi_makino@k.u-tokyo.ac.jp

H. Shinoda
e-mail: hiroyuki_shinoda@k.u-tokyo.ac.jp

1 Introduction

Researches on immersive VR have become more active than ever since the advent of well-calibrated HMDs such as Oculus rift (Oculus VR, LLC.) [1], which offer a practical platform for personal use with a considerably compact setting. The HMD-based immersive VR is expected to make good applications combined with haptic devices because the view HMD displays is free from visual interference caused by haptic devices.

In this research we aim to construct a personal system which allows mainly home users to experience an immersive VR contents accompanying haptic feedback expressing perceived stiffness of virtually rendered objects. We suppose that the system would not constrain free body movements of users and not be bulky with the aim of its prevalent casual use in future. To this end we exploit the pseudo-haptic effects, which enhance or soften subjective haptic experiences by simultaneously displaying correlated non-haptic (such as video or sound) information to users with haptic stimuli, instead of electrically generating actual external force on users' bodies.

There have been several studies on the pseudo haptic effects, mainly handling the visuo-haptic correlations. By modifying the visual feedback to users according to the expected pseudo haptic effects, users can feel the virtual objects they are in contact with vary in its reacting force [2], shape [3] or mass [4] although there is no actual change in physical interaction in real world. Furthermore, there has been a study reporting that the experimental subjects' perceived hardness of a virtual object presented with active force display is enhanced by simultaneously displaying visual deformation that was visually exaggerated [5]. In our research, we present force sensation passively to users by using the device which only consists of mechanical structures that do not require electric power consumption.

In relation to these examples, we focus on presenting hardness of a virtual object by displaying a re-rendered virtual hand of the user's own holding an elastic virtual object with its finger flexion exaggerated or suppressed. We demonstrate a fabricated system and is currently investigating the condition in displaying a set of stimuli that would elicit the anticipated pseudo-haptics at its best.

2 System Overview and Implementation

Figure 1 shows a whole picture of the fabricated system consisting of HMD, a hand motion sensor and a force-displaying glove. Users see a virtual object and re-rendered his or her own hand via HMD they wear. The position and posture of their hand are captured by the sensor with stereo IR camera (Leap Motion by Leap



Fig. 1 Whole picture of the fabricated system

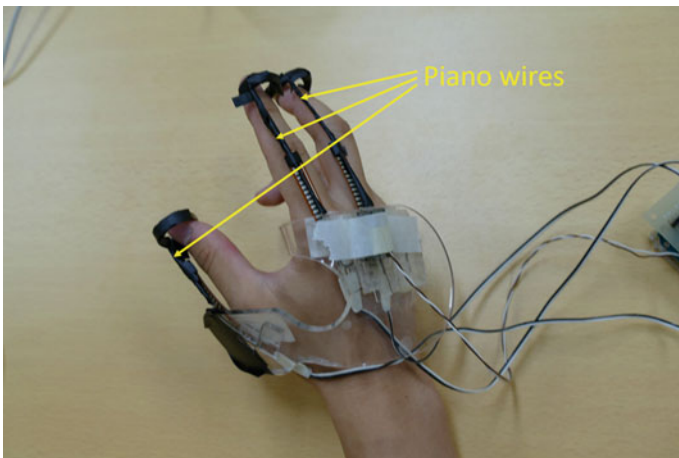


Fig. 2 Picture of the glove users put on to feel reaction force of the virtual objects

Motion, Inc.). The users put on the glove implemented with piano wires that constrain finger movements, making users feel reaction force of the virtual object (Fig. 2). Note that no active electrical components are embedded in the wire and hence the actual reaction force is uncontrollable. The displayed object deforms as the users move their fingers. As stated above, the displayed flexions of users' fingers are processed and the object deformation is directly affected accordingly (Fig. 3). A vibrator is installed on the glove for displaying clicking vibrations representing virtual creaking of the deformed objects.



Fig. 3 Picture of re-rendered virtual hand displayed with its finger flexion unchanged (*top*), magnified (*middle*) and suppressed (*bottom*)

3 Conclusion and Future Works

We expect that the fabricated system can virtually tune subjective hardness of a virtual object held by the users in an immersive VR environment by adjusting displayed virtual images while keeping actual reaction force presented to his or her fingers unchanged. We empirically have found that pinching virtual objects with the device we provided would offer users a haptic experience that is more realistic and conforming to visual feedback than with the bare hands.

In the future, we will evaluate the effect of pseudo-haptics in this system and will investigate a method increasing it.

Acknowledgements This research is supported by JST ACCEL Embodied Media Project.

References

1. Oculus Rift, <https://www.oculus.com/rift/>
2. Lécuyer, A., Burkhardt, J.M., Tan, C.H.: A study of the modification of the speed and size of the cursor for simulating pseudo-haptic bumps and holes. *ACM Trans. Appl. Percept. (TAP)*, **5** (3) (2008)
3. Ban, Y., Kajinami, T., Narumi, T., Tanikawa, T., Hirose, M.: Modifying an identified curved surface shape using pseudo-haptic effect. In: *Proceedings of IEEE Haptics Symposium (HAPTICS2012)*, pp. 211–216 (2012)
4. Narumi, T., Ban, Y., Kajinami, T., Tanikawa, T., Hirose, M.: Augmented perception of satiety: controlling food consumption by changing apparent size of food with augmented reality. In: *Proceedings of ACM CHI*, pp. 109–118 (2012)
5. Sasaki, H., Fujita, K.: Experimental analysis of role of visual information in hardness cognition displayed by force display system and effect of altered visual information. *TVRSJ*, **5**(1) (2000, in Japanese)

Multi Degree-of-Freedom Successive Stiffness Increment Approach for High Stiffness Haptic Interaction

Harsimran Singh, Aghil Jafari and Jee-Hwan Ryu

Abstract In haptic interaction, stability and the object's hardness perception are of great significance. Although numerous studies have been done for stable haptic interaction, however, most of them sacrifice the actual displayed stiffness as a cost of stability. In our recent work, we introduced the Successive Stiffness Increment (SSI) approach whereby the displayed stiffness successively increases with the increase of interaction cycles. It was shown that the haptic interaction was stable and the displayed stiffness was greater than other approaches. This paper extends the SSI approach for multi-DoF haptic interaction. The stiffness increment of the SSI approach depends on the number of interaction cycles which will vary for each axis, therefore, we decouple the interaction by adopting penetration depth-based rendering method using Virtual Proxy (VP). Since the decoupled system has unconstrained end point in the form of moving Virtual Environment (VE), so the boundary conditions are updated in the previously proposed SSI approach at every sample. Phantom Premium 1.5 is used to verify the stability and enhanced displayed stiffness of the proposed approach on a virtual sphere.

Keywords Haptic interaction · Multi-DoF · High stiffness · Impedance device

H. Singh (✉) · A. Jafari · J.-H. Ryu
School of Mechanical Engineering, Korea University of Technology and Education,
1600 Chungjeolno, Chungnam, Cheonan, South Korea
e-mail: harsimran@koreatech.ac.kr

A. Jafari
e-mail: jafari_aghil@kut.ac.kr

J.-H. Ryu
e-mail: jhryu@koreatech.ac.kr

1 Introduction

In haptic interfaces, guaranteeing stability is not a trivial task, and for most cases it is a challenging issue. However, improving the system transparency and enlarging its impedance range can't be overlooked as well. The combination of stability and transparency provides the user with a more realistic feeling of the VE. Eliminating or cutting down the force to stabilize the system distorts the perception of the hardness and stiffness of the VE.

In literature, several approaches have been developed for improving transparency while guaranteeing stability. Among them passivity-based approaches have a major mathematical tool for guaranteeing stable haptic interaction independent of system parameters, and linearity/nonlinearity of the system. Hannaford and Ryu [1] proposed time-domain passivity approach, which uses an adaptive virtual damping to satisfy the passivity constraint and thus making the system stable. Ryu and Yoon [2] proposed a concept which was inspired from graphical interpretation of passivity in a position vs. force graph, to increase the dynamic range of impedance in which a haptic interface can passively interact using passivation method. In energy bounding algorithm [3], the generated energy from the sample and hold is blocked in order to eliminate excessive energy that can make the system unstable. Recently, a less conservative version of force bounding approach was proposed to bound the interaction force such that only the haptic forces passively can be displayed [4]. Recently, Jafari and Ryu [5] proposed a less conservative control approach than passivity approaches for guaranteeing stable haptic interaction inspired from the analogy between virtual environment systems with hysteresis nonlinearity. However, most of the approaches that guarantee stable haptic interaction, either cover a limited range of impedance or sacrifice the actual displayed impedance at the cost of stability.

In [6], we proposed a new approach called Successive Stiffness Increment (SSI) approach to further enlarge the achievable stiffness range by increasing the displayed stiffness with each passing interaction cycle. The haptic interaction starts by displaying a small value of stiffness which later increases close to the desired stiffness of the VE in a couple of cycles. This was achieved by gradually increasing the feedback force with every successive cycle. The proposed approach could guarantee the convergence of the penetration distance and increment of the force feedback with each and every consecutive cycle, and it allowed a much larger stiffness to be displayed compared with any other approach while maintaining interaction stability.

In this paper, we extend the SSI approach for multi-DoF haptic interactions. For multi-DoF haptic interaction, a multi-DoF VP is introduced to decouple the interaction to each axis. However, multi-DoF VP changes the interaction from rigid virtual environment to interaction with moving virtual object. The moving virtual object does not pose a threat to the robustness of haptic interaction as the SSI converges the penetration distance and reduces the generated energy with every passing interaction cycle. To evaluate the performance of multi-DoF SSI approach, experiment was carried on a Phantom Premium 1.5.

2 The SSI Approach for Single-DoF Haptic Interface

In [6], we introduced the concept of Successive Stiffness Increment approach, where the stiffness is slowly increased starting from a low value, with each passing interaction cycle. This was done by breaking down each interaction cycle into pressing and releasing path, as shown in Fig. 1. The force for the pressing path is a function of smaller stiffness (K_p) than the original stiffness of the VE. This value of stiffness may be chosen so as to keep the system stable. Considering that the interaction of haptic probe with the virtual environment is modeled as a simple virtual spring, the force is:

$$f(n) = \begin{cases} K_p x(n) + (F_r - K_p x_r), & \text{for } x(n) \geq 0 \\ 0, & \text{for } x(n) < 0 \end{cases} \quad (1)$$

where, $x(n)$ is the penetration distance, F_r and x_r are the last force and position values of the previous releasing path. It is important to note that all the pressing paths begins from the point where the previous releasing paths ended. In case of first pressing path, F_r and x_r would be 0.

The function for releasing path is:

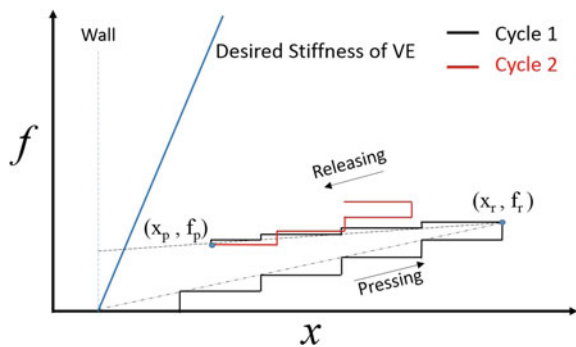
$$f(n) = \begin{cases} K_r x(n) + (F_p - K_r x_p), & \text{for } x(n) \geq 0 \\ 0, & \text{for } x(n) < 0 \end{cases} \quad (2)$$

where, K_r is the stiffness for releasing path which is chosen smaller than the value of K_p . F_p and x_p are the last force and position values of the previous pressing path.

The output energy at the end of every pressing path is:

$$Output = Input + GeneratedEnergy - E_b \quad (3)$$

Fig. 1 Basic principle of the SSI approach



where, $Input$ is the energy during pressing path, E_b is the energy dissipated by the physical damping of the haptic display.

Considering the human operator passive in the range of frequencies of interest in haptics, the consequent pressing path should penetrate the VE until it's input energy is equal to or greater than the output energy of the previous releasing path.

$$Input(n) \geq Output(n - 1) \tag{4}$$

Since the pressing path begins where the previous releasing path ended and because $K_p > K_r$, the penetration distance converges and the force increases after each passing interaction cycle. Also as the system converges, so does the generated energy.

3 Extension of SSI for Multi-DoF Interaction

This section generalizes the SSI approach for multi-DoF haptic interactions. In this paper and in order to calculate the haptic force, we have used a multi-DoF virtual proxy (VP), and it moves along the surface of the VE (see Fig. 2). Once the VP is introduced, the multi-DoF interaction problem can be decoupled into each axis. However, it changes the interaction problem from a rigid VE interaction to a moving virtual object interaction because the proxy is moving along the surface as the haptic interaction point (HIP) moves. The moving virtual objects can be modeled as a system with simple inertia, a spring and a damper in each DoF.

To successively increase the displayed stiffness as close as possible to the desired stiffness, two separate functions for each pressing and releasing paths were defined in [6].

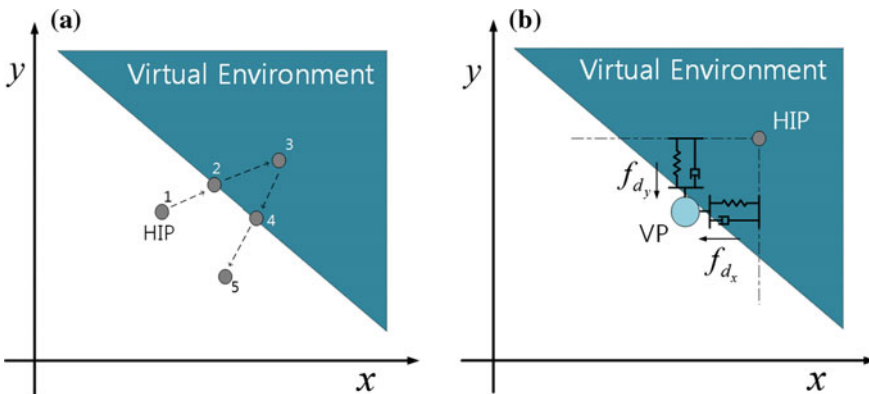


Fig. 2 a An exemplary trajectory of a multi-DoF interaction, and b decoupled representation of the multi-DoF interaction [2]

Pressing Path:

$$f(n) = f_v(n) - \left(\frac{f_v(n) - f(n-1)}{\alpha} \right) \quad (5)$$

where, $f_v(n)$ is the force from the VE and α will determine how steep the pressing path rises. The pressing path does not have to be modified in accordance with the changes in boundary conditions of the VE.

Releasing Path:

After the end of each pressing path, the slope of the line, μ , joining the last position and force values to the boundary of the VE is calculated. This slope was calculated only once per cycle for single-DOF SSI implementation. However, due to multi-DOF changing the VE's boundary, this slope is calculated at every sample during the releasing path. The force during releasing path is a function of this slope.

$$f(n) = f(n-1) + \left(\frac{f_\mu(n) - f(n-1)}{\beta} \right) \quad (6)$$

where, β determines how steep the releasing path is, and,

$$f_\mu(n) = \mu x(n). \quad (7)$$

4 Experimental Evaluation

To demonstrate the performance of the proposed approach, a Phantom Premium 1.5 with a sampling rate of 1 KHz is used. The basic specification of which are: maximum force output 8.5 N, continuous exertable force 1.4 N, physical damping, (bm), selected as 0.0002 Ns/mm. A 3-DoF sphere with its center at origin is simulated which can generate forces along x, y and z-axis. As explained in the previous section, a 3-DoF VP which moves on the surface of the sphere is introduced. The haptic probe penetrates into the sphere's surface while the VP is located on the surface at a minimum possible distance to it. The multi-DoF interaction is decoupled into 3 axis as 3 independent problems, each of which is modeled as a simple virtual spring.

In the multi-DoF scenario, the user randomly moves the haptic probe on the sphere while maintaining contact with it. Figure 3 shows the results for conducting the experiment on a sphere of stiffness 5 N/mm. The position of the haptic probe is shown in Fig. 3a along with the force response of each axis (Fig. 3b, d, f) and its corresponding displayed stiffness (Fig. 3c, e, g). It can be seen that the force response is stable and the displayed stiffness is also close to the desired stiffness of the virtual sphere.

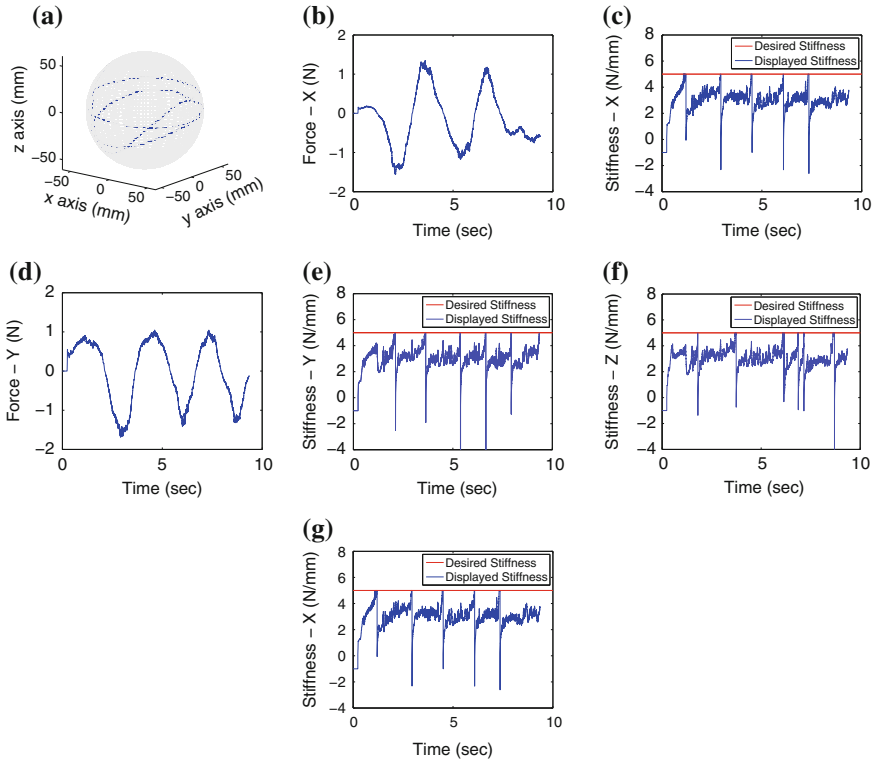


Fig. 3 Experimental results for a virtual sphere of large stiffness (5 N/mm) with the SSI approach. **a** Position, **b** Force response along X-axis, **c** Stiffness along X-axis, **d** Force response along Y-axis, **e** Stiffness along Y-axis, **f** Force response along Z-axis, **g** Stiffness along Z-axis

5 Conclusions and Future Work

This paper extends the SSI approach to multi-DoF haptic interaction. To render multi-DoF virtual object, a multi-DoF VP was introduced which moves along the surface of the virtual object while the haptic probe penetrates inside it. Multi-DoF was decoupled into 3-axis which changes the interaction from rigid wall to moving virtual object. The pressing and releasing path functions described for 1-DoF SSI approach was applied here. The pressing path function was applied without any modifications as it does not depend on the changes in boundary condition of the virtual object. Whereas the releasing path was modified in accordance with moving virtual object. Experimental results of interacting with a high stiffness virtual sphere showed that the proposed approach keeps the haptic interaction stable and also allows for a much larger displayed stiffness to a human operator than any other approach.

Acknowledgements This paper was supported by the Civil-Military Technology Cooperation Program (15-CM-RB-09).

References

1. Hannaford, B., Ryu, J.H.: Time-domain passivity control of haptic interfaces. *IEEE Trans. Robo. Autom.* **18**(1), 1–10 (2002)
2. Ryu, J.H., Yoon, M.Y.: Memory-based passivation approach for stable haptic interaction. *IEEE/ASME Trans. Mechatronics* **19**(4), 1424–1435 (2014)
3. Kim, J.P., Ryu, J.: Energy bounding algorithm based on passivity theorem for stable haptic interaction control. In: *Proceedings of 12th International Symposium on Haptic Interfaces for Virtual Environment and Teleoperator Systems, 2004. HAPTICS '04*, pp. 351–357, March 2004
4. Kim, J.P., Baek, S.Y., Ryu, J.: A force bounding approach for multi-degree-of-freedom haptic interaction. *IEEE/ASME Trans. Mechatronics* **20**(3), 1193–1203 (2015)
5. Jafari, A., Ryu, J.: Input-to-state stable approach to release the conservatism of passivity-based stable haptic interaction. In: *2015 IEEE International Conference on Robotics and Automation (ICRA)*, pp. 285–290, May 2015
6. Singh, H., Jafari, A., Ryu, J.: *Successive stiffness increment approach for high stiffness haptic interaction*, pp. 261–270. Springer International Publishing, Cham (2016)

Part IV

Sensors

A Cooking Support System with Force Visualization Using Force Sensors and an RGB-D Camera

Nobuhiro Totsu, Sho Sakaino and Toshiaki Tsuji

Abstract This paper describes the development of a cooking support system using force sensors and an RGB-D camera. The knife and the cutting board with 6-axis force sensors can detect the external force vector and the position of the exerted force. The proposed force visualization system is supposed to be utilized during cooking.

Keywords Haptic interface · Force sensor · RGB-D camera · Force visualization

1 Introduction

Visualization techniques such as augmented reality have spread to be used in training. Measuring and displaying force information is especially effective. Rehabilitation system is a typical example. Brewer et al. [1] indicated that visual feedback of force influences the subject's perception. In addition to using in rehabilitation, there are some devices for human computer interaction with force visualization. Sugiura et al. [2] developed "FuwaFuwa" which can detect applied pressure and the contact position on a soft material. Tsuji et al. [3] developed a desk-type tactile interface which can detect applied force vector and the contact position on a desk. In these interfaces, users can recognize their applying force and the force information is used for input to a computer. In this paper, the authors developed a new cooking support system with force visualization. The proposed

N. Totsu (✉) · S. Sakaino · T. Tsuji
Graduate School of Science and Engineering, Saitama University,
255 Shimo-okubo, Sakura-ku, Saitama 338-8570, Japan
e-mail: s15mm235@mail.saitama-u.ac.jp

S. Sakaino
e-mail: sakaino@mail.saitama-u.ac.jp

T. Tsuji
e-mail: tsuji@mail.saitama-u.ac.jp

system consists of a knife and a cutting board, which can measure the external force vectors and contact positions. The virtual force vectors are projected on the image shot by an RGB-D camera. Users can see their exerting force while they are cutting foods.

2 Cooking Support System

Figure 1 shows the overview of the cooking support system. 6-axis force sensors are mounted on the knife and the cutting board. By using an RGB-D camera, the markers attached to the knife and the board are recognized and their coordinates are calculated. Therefore, the coordinates of the two sensors can be transformed. If force applied to the board is not fluctuated in a certain time, the system recognizes that a food is placed on the board. Then, the force sensor mounted on the board is calibrated by applying low-pass filter to the sensor and removing the offset values from the sensor values. The RGB-D camera obtains the shape of the food as point cloud data. In this paper, it is assumed that only two points of the contact on a food exist: contact with the knife and a hand. Therefore, the force vectors applied by the knife and the hand are calculated by the two force sensors. The contact position on the knife can be calculated by applying the method of the previous study [3]. The contact position on the hand is calculated as one point of the cloud data. The distance between the point and the line of action of the exerting force is the smallest.

Figure 2 shows the display with force visualization. The subject touches on the board and the virtual force vector is displayed on the contact position in the camera image. Users can confirm their exerting force and contact position.

Fig. 1 System overview

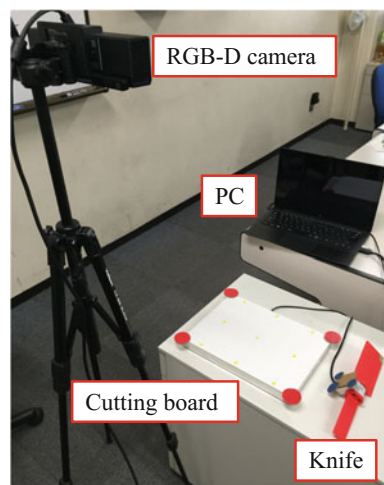


Fig. 2 Force visualization

3 Conclusion

This paper developed the cooking support system which can detect the external force vector and contact position based on the 6-axis force sensors and the RGB-D camera. The proposed system is supposed to be utilized to visualize force information during cooking. In the future, the authors will develop an application for real use and evaluate its utility through experimental verification.

References

1. Brewer, B.R., et al.: Effects of visual feedback distortion for the elderly and the motor-impaired in a robotic rehabilitation environment. In: Proceedings of IEEE International Conference on Robotics and Automation, vol. 2, pp. 2080–2085 (2004)
2. Sugiura, Y., et al.: Detecting shape deformation of soft objects using directional Photoreflectivity measurement. In: Proceedings of the 24th Annual ACM Symposium on User Interface Software and Technology, pp. 509–516 (2011)
3. Tsuji, T., et al.: Developed of a desk-type tactile interface using force sensor. In: Proceedings of the 40th Annual Conference of the IEEE Industrial electronics Society (2014)

Turning Surfaces into Touch Panels: A Granite-Touch Pad

Hatem Elfekey and Shogo Okamoto

Abstract Touch sensing interfaces are used in many human to machine applications with the natural feeling to the touch missing. We propose the use of humantenna touch technique to turn surfaces of natural or artificial conductive or semi-conductive materials into passive touch pads. Because of the conductivity of the human body, AC power lines induce a voltage on the human body which is used as the touch trigger. By the use of electrodes mounted at the edges of the surface, the ratio of voltage detected is used to compute the touch location. Granite touch pad was implemented as an example, and the voltage detected at the electrodes due to various touch locations is presented.

Keywords Humantenna · Granite · Touch pad · Human body

1 Introduction

Touch sensing applications are in ever high demand as touch sensing interfaces are used in most human-machine interfaces. On the other hand, touch pads require special surface that is manufactured for touch sensing. Consequently, the feeling of touch is limited. For example, touching the screen of a smart phone may not feel as rich as touching an actual wall or table top. To enhance the feeling of touch, many haptic feedback technologies have been implemented with the goal of creating artificial sense of surfaces. In this paper, we propose a different approach. We propose turning surfaces into touch pad instead of recreating particular textures via texture displays. As a result, the rich natural texture of surfaces is preserved, while serving as a touch sensing interface.

H. Elfekey (✉) · S. Okamoto
Graduate School of Engineering, Nagoya University,
Furo-cho, Chikusa-ku, Nagoya, Aichi Prefecture, Japan
e-mail: elfekey.hatem.mahmoud@h.mbox.nagoya-u.ac.jp

S. Okamoto
e-mail: okamoto-shogo@mech.nagoya-u.ac.jp

For the aforementioned purpose, many touch technologies are available. Candidates comprise infra-red, camera, acoustic and capacitive technologies. Infra-red based touch sensing technology demands the use of many transmitters and receivers to extract the location of the touch, which may not be preferred for some applications [1]. Although the acoustic pulse recognition (APR) technique use only four microphones and an easy algorithm to precisely locate the touch position, the “touch and hold” feature is unavailable [1, 2]. On the other hand, surface acoustic wave (SAW) touch technology can detect “touch and hold”, yet, the accuracy of the touch detection is dependent on the geometry of the surface [3]. Capacitive touch techniques make use of the capacitance change of the surface due to touch to calculate the position of that touch. Consequently, transmitters and receivers of electrical signals are required to measure the change of capacitance. For example, the user is asked to wear, hold or use a device that acts as the transmitter of an electrical signal [4]. In an earlier study [5], a mat was used as a transmitter of high frequency signals to travel though the human body. When the human touches a surface with four electrodes mounted on the corners, four high frequency currents are detected by the corner electrodes. Depending on the ratios of these currents, the touch location is identified. Such a mat demands additional space and specific installation requirements which are not available for general objects and materials [5].

We propose the use of the induced voltage on the human body from the AC power lines as the touch input, instead of the aforementioned transmitter device. Thus, the proposed touch-sensing technique is passive. Furthermore, the proposed technique turns conductive/semi-conductive surfaces into a touch panel. As a result, materials with desirable mechanical or thermal qualities could be touch sensitive. Also, the geometrical properties of the touch surface does not interfere with touch signals, unless the electrical path between the touch location and the electrode is altered. As proof of concept, a passive granite touch panel is proposed in this paper.

2 Operation Principle

Due to the fact that the human body contains minerals and salts, it exhibits conductive qualities, and hence, is affected by nearby line’s 100/220 V, inducing a potential on the human body [6]. The induced voltage on the human body will be used as the touch trigger for the proposed touch panel.

Granite tiles have relative permittivity range of 5 to 8 F/m [7], hence, it was used to implement a touch floor [8]. However, multiple tiles were used to implement that touch floor. In the present study, using only one tile and four electrodes and a signal conditioning circuit, we implemented a touch pad. The voltage detected at the each corner of the tile has an inverse relation to the distance between the touch location and the respective electrode. Thus, by calculating the ratios of the voltage detected, the touch location is computed.

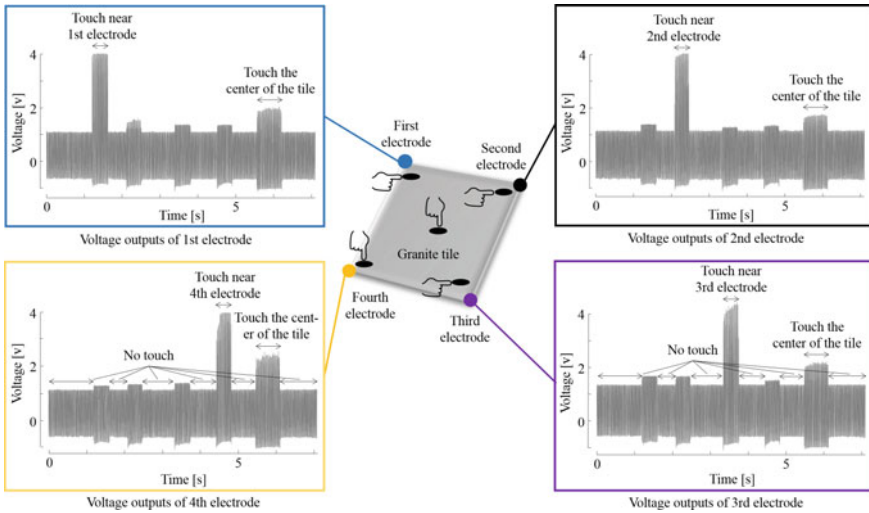


Fig. 1 The voltage detected at the corners of a granite surface while the tile is touched from near the four electrodes and in the middle of the granite tile

3 Experimentation and Results

A regular flat granite tile of 30×30 cm with electrodes mounted on the four corners of the tile was used. A user was asked to touch the granite tile using a bare finger in a typical experimental room. The voltage from the four corners was connected to an oscilloscope for signal evaluation. Figure 1 shows the user touching the tile at specific locations in specified time periods. At time 6 s the user touched the granite tile at the center while at times 1.5, 2.5, 3.5 and 4.5 s the user touched near the first, second, third and fourth electrode receptively. Upon each touch event, a 60 Hz voltage signal was observed at each electrode. The electrode nearest to the touch location received the largest signals. Furthermore, the finger was placed at the center of the tile; the four electrodes received nearly equal level of signals. The voltage of “no touch” received at the four electrodes was significantly smaller than the voltage of touch, as seen in Fig. 1. The above mentioned observation indicates that the location of touch is calculated based on the output of the four electrodes.

4 Conclusion

In this paper, a methodology of turning a regular surface into a passive touch sensing panel was proposed. The system is simple, cost-effective, and of low power, as it is passive.

Acknowledgements This study was in part supported by JSPS Kakenhi (15H05923).

References

1. Walker, G.: *Fundamentals of touch technologies and applications*. Society for information display (2011)
2. Reis, S., et al.: Touchscreen based on acoustic pulse recognition with piezoelectric polymer sensors. In: *IEEE International Symposium on Industrial Electronics*, pp. 516–520. IEEE Press, New York (2010)
3. Ono, M., Shizuki, B., Tanaka, J.: Touch & activate: Adding interactivity to existing objects using active acoustic sensing. In: *Proceedings of the 26th Annual ACM Symposium on User Interface Software and Technology*, pp. 31–40 (2013)
4. Sato, U., Poupyrev, I., Harrison, C.: Touché enhancing touch interaction on humans, screens, liquids, and everyday objects. In: *Proceedings of the 2012 ACM Annual Conference on Human Factors in Computing Systems*, pp. 483–492 (2012)
5. Paradiso, J.A., Hsiao, K., Strickon, J., Lifton, J., Adler, A.: Sensor systems for interactive surfaces. *IBM Sys. J.* **39**, 892–914 (2000)
6. Ma, C.T., et al.: Frequency-bandwidth-tunable powerline notch filter for biopotential acquisition systems. *IEEE Electr. Lett.* **45**, 197–199 (2009)
7. Nigel, J.: *Cassidy: Electrical and Magnetic Properties of Rocks, Soils and Fluids*. In: Jol, H.M. (ed.) *Ground penetrating radar theory and applications*. Elsevier, Amsterdam (2009)
8. Elfekey, H.M., Bastawrous, H.A.: Granite-based touch-sensing floor for machinery safety and exergaming. In: *Proceedings of IEEE 4th Global Conference on Consumer Electronics*, pp. 593–594. IEEE Press, New York (2015)

A Finger Sensor for Sharing Visual and Tactile Experience

Haruki Nakamura, Nobuhisa Hanamitsu, Junichi Kanebako
and Kouta Minamizawa

Abstract In demonstration, we show sharing visual and tactile experience using own finger. In our daily life, we often share our experience, such as seeing or hearing, using own smartphone. However, up still now, touch experience is not possible to share in social network services. Here, we propose a capturing sensor, which is able to capture texture and surface by user's finger, for smartphone device.

Keywords Haptic interface · Haptic experience · TECHTILE

1 Introduction

To sharing experience are our common behaviors in our daily lives. For example, now we often taken by a camera, recorded by smartphone device, and share their experiences through Social Network Service, such as Instagram, SoundCloud or Snapchat. However, up until now, the sharing of corresponding haptic experiences has not been possible. If this haptic experience can be shared, this sensory feedback will be compelling enough and is easy to understand what people are experiences.

In previous researches, we proposed a haptic recording and displaying attachment [1], we called '*a(touch)ment*', and a mobile platform [2], which enables users

H. Nakamura
Tokyo National College of Technology, Tokyo, Japan
e-mail: haruki.nakamura.0321@gmail.com

N. Hanamitsu (✉) · J. Kanebako · K. Minamizawa
Graduate School of Media Design, Keio University, 4-1-1 Hiyoshi, Kohoku,
Yokohama, Kanagawa 223-8526, Japan
e-mail: hanamitsu@kmd.keio.ac.jp

J. Kanebako
e-mail: kanebako@kmd.keio.ac.jp

K. Minamizawa
e-mail: kouta@kmd.keio.ac.jp

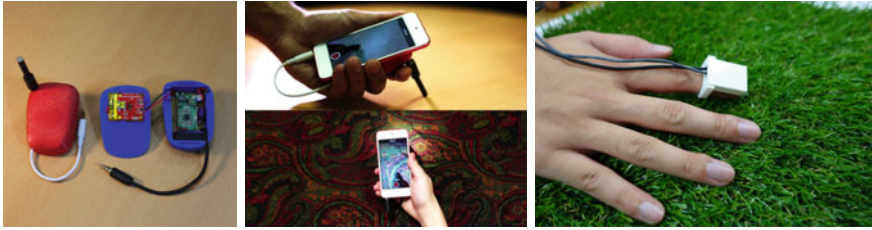


Fig. 1 *A(touch)ment* (left), Capture scene (center), A proposed sensor (right)

to collect and share visuo-tactile experiences. Here we propose a new sensor, as shown Fig. 1 right, for capturing haptic information using ‘*a(touch)ment*’. When user record sense of touch, user attach it to the index finger.

2 Implementation

Okamoto et al. [3] has proposed five psycho-physical dimensions in perceiving tactile textures: roughness/softness/friction/wetness/coldness. Out of these, roughness and friction are the two most useful when capturing surface tactile recognition using a contact sensor. We propose a finger-mounted device, which was integrated acceleration sensor and microphone (Fig. 2). An acceleration sensor is able to capture roughness and low frequency. In addition, a microphone is able to capture low frequency (friction) and a material property (texture) from audio information. To use their features, it is able to capture the texture of special frequency and texture (roughness and friction).

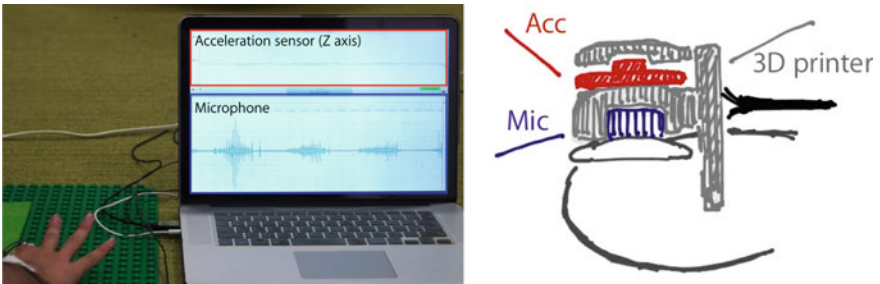


Fig. 2 Appearance of a proposed system

3 Demonstration

In this demonstration, user can record several surface textures using a smartphone device that attached a haptic recording and displaying device, this sensor can put on user's finger and share experience easily in real time through network. Moreover, To combining with this sensor, '*a(touch)ment*' and smartphone device, the recorded haptic experience is able to enhance using filters which was made by acceleration of value and wave form from this sensor and smartphone's sensor.

Acknowledgements This project is supported by JST-ACCEL Embodied Media Project.

References

1. Nakamura, H., Hanamitsu, N., Minamizawa, K.: A(touch)ment: a smartphone extension for instantly sharing visual and tactile experience. In: Proceedings of the 6th Augmented Human International Conference, AH '15, pp. 223–224. Singapore, Mar 2015
2. Hanamitsu, N., Nakamura, H., Nakatani, M., Minamizawa, K.: Twech: a mobile platform to search and share visuo-tactile experiences. In SIGGRAPH Asia 2015 Mobile Graphics and Interactive Applications, SA '15, pp. 10:1–10:3. Kobe, Japan, Nov 2015
3. Okamoto, S., Nagano, H., Yamada, Y.: Psychophysical dimensions of tactile perception of textures. IEEE Trans. Haptics **6**(1), 81–93 (2013)

On a Haptic Phenomenon by Combined Use of the Rubber Artificial Skin Layer with a Strain Gauge and the Tactile Contact Lens

Mitsuhito Ando, Hiromi Mochiyama, Toshinobu Takei
and Hideo Fujimoto

Abstract In this paper, we report a haptic phenomenon observed by combined use of two haptic devices, which are a rubber artificial skin layer with a strain gauge and a tactile contact lens (TCL). The rubber artificial skin layer with a strain gauge is a tactile sensor formed around a finger. The sensor can observe deformation of a finger wearing it by active touch. The TCL is a non-mechatronic touch enhancing device. The TCL makes tactile perception of a surface undulation enhance when the TCL is traced a surface of a tactile target and laid between human skin and the surface traced. We prepare a haptic display using a McKibben rubber pneumatic actuator which is driven according to the sensor output for a demonstration.

Keywords Touch enhancing • Haptic device • Haptic phenomenon • Sensor • Tactile perception

M. Ando (✉) · H. Mochiyama
Department of Intelligent Interaction, Technologies, University of Tsukuba,
Tennoudai 1-1-1, Tsukuba, Ibaraki 305-8573, Japan
e-mail: s1520746@u.tsukuba.ac.jp

H. Mochiyama
e-mail: motiyama@iit.tsukuba.ac.jp
URL: <http://www.frlab.iit.tsukuba.ac.jp/>

T. Takei
Department of Intelligent Machines System Engineering, Faculty of Science and Technology,
Hirosaki University, Bunkyocho 1, Hirosaki, Aomori 036-8560, Japan
e-mail: takei@hirosaki-u.ac.jp

H. Fujimoto
Department of Computer Science and Engineering, Nagoya Institute of Technology (NIT),
Gokiso-Cho, Nagoya, Showa-Ku 466-8555, Japan
e-mail: fujimoto@nitech.ac.jp

1 Introduction

Tactile Contact Lens (here in after we call this TCL) is a non-mechatronic touch enhancing device [1, 2]. While the TCL has a very simple structure (compose of numerous hard pins on a thin flexible sheet), we can feel an amplified surface undulation with this device. The TCL is hoped for not only detection of a surface undulation but also solving haptic perception mechanism in humans.

In this paper, we report a haptic phenomenon observed by combined use of two haptic devices. One of devices is the TCL. Another of device is the rubber artificial skin layer with a strain gauge. The rubber artificial skin layer is a tactile sensor formed around a finger [3]. The sensor can observe deformation of the finger wearing it when the finger touches something actively. The phenomenon is that the TCL enhances a signal from a strain gauge embedded the sensor when a finger wearing the sensor traces undulation surface of the object traced and puts on the TCL. We introduce a haptic display using a McKibben rubber pneumatic actuator which is driven according to the sensor output for a demonstration about the phenomenon.

2 Device

Tactile Contact Lens is a non-mechatronics device. Figure 1 is a pair of a schematic diagram and a photo showing the TCL. The devise has a very simple structure composed of a flexible thin sheet and numerous hard pins on the sheet. The device has an enhancing effect that stimulus of an abnormal part is enhanced when the TCL traces a surface of the object being traced and puts between a finger and the surface traced.

The rubber artificial skin layer is a tactile sensor device that is possible to observe deformations of skin. The sensor is embedded a strain gauge. The sensor has a simple structure Fig. 2 is a pair of a schematic diagram showing components

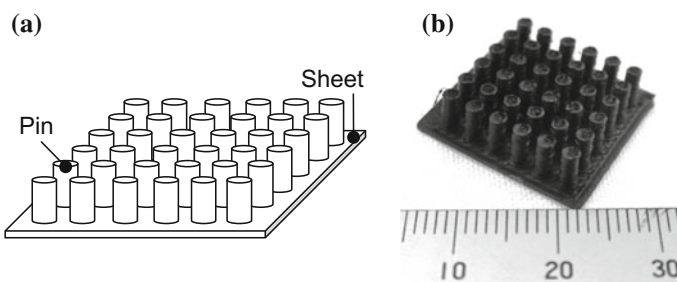


Fig. 1 Tactile contact lens (TCL). **a** Schematic diagram showing components of the TCL **b** Photograph showing the TCL

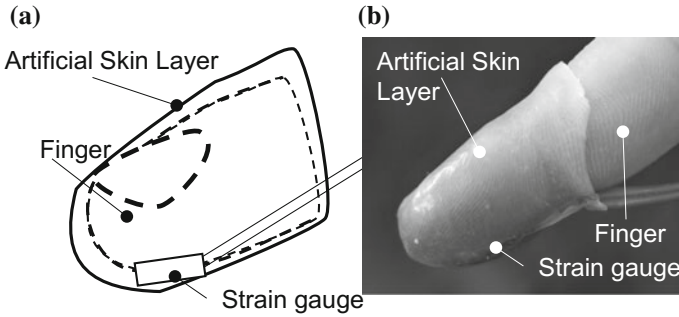


Fig. 2 Rubber artificial skin layer. a Schematic diagram of the sensor. b Photograph of the sensor

of a rubber artificial skin layer with a strain gauge and a photo showing the sensor. The sensor is composed of thin layers of rubbers and a strain gauge.

3 Haptic Phenomenon

The phenomenon is that the TCL enhances a signal from a strain gauge embedded the sensor when a finger wearing the sensor traces undulation surface of the object traced and on the TCL. Figure 3 is a schematic diagram showing a situation that the sensor and the TCL are used. Then the phenomenon is observed in this situation. An experiment is conducted for verification of the phenomenon.

In this experiment, a signals from strain gauge embedded the rubber artificial skin layer is measured when this experimenter's finger wearing the sensor traces an undulation surface of the object traced and puts on the TCL. The traced surface has a sine curve. Figure 4 is a pair of graphs showing the result. It is found the sensor output is enhanced by the TCL. It is possible that we obtain the tangential and normal forces from the signal. In the future work, the possibility is more researched.

Fig. 3 Situation that a finger wearing a rubber artificial skin layer puts on the TCL and traces tactile target

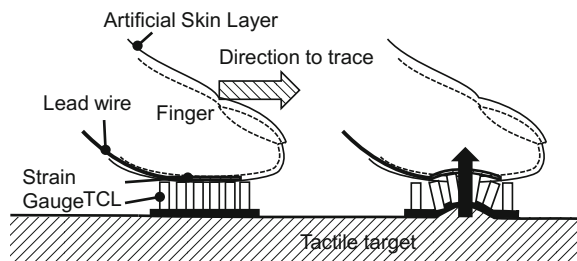
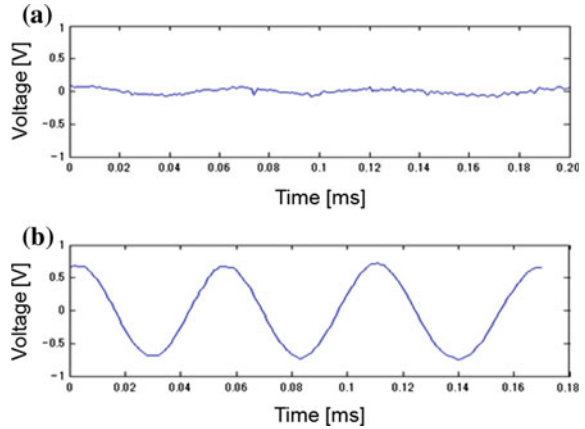


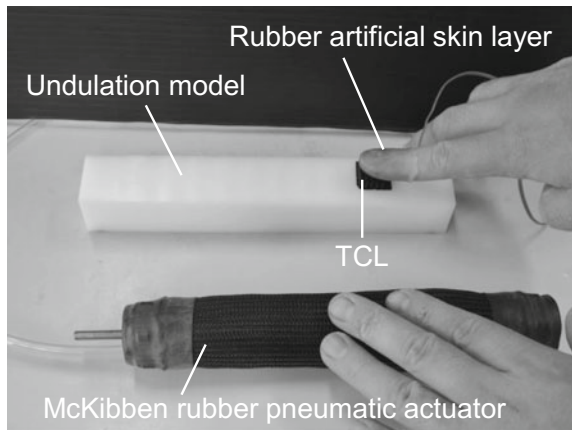
Fig. 4 Comparison in case of the signal when TCL is not used and one when TCL is used. **a** Signal from strain gauges rubber artificial skin layer when TCL is not used. **b** Signal from strain gauges rubber artificial skin layer when TCL is used



4 Haptic Display

We prepare a haptic display using a McKibben rubber pneumatic actuator which is driven according to the sensor output, which is low frequency, for a demonstration as Fig. 5. A tactile impression of an undulation surface is indicated by the haptic display. A solenoid valve is controlled by the sensor output when a finger wearing the sensor and the TCL traced an undulation model whose a cross section is a sine curve. Purpose of the demonstration is making the effect of enhancing the signal plain tactilely by the display.

Fig. 5 Haptic display using a McKibben rubber pneumatic actuator



5 Summary

We introduced haptic devices which are the tactile contact lens and the rubber artificial skin layer. Therefore we report a haptic phenomenon by combined use of the devices. We prepare a haptic display using a McKibben rubber pneumatic actuator which is driven according to the sensor output for a demonstration.

References

1. Sano, A., Mochiyama, H., Takesue, N., Kikuuwe, R., Fujimoto, H.: Touchlens: touch enhancing tool. In: Proceedings of the 1st IEEE Technical Exhibition Based Conference on Robotics and Automation, pp. 71–72, April 2004
2. Kikuuwe, R., Sano, A., Mochiyama, H., Takesue, N., Fujimoto, H.: Enhancing haptic detection of surface undulation. *ACM Trans. Appl. Percept.* **2**(1), 46–67 (2005)
3. Fukuda, K., Mochiyama, H., Takei, T.: Strain-gauge-sandwiched rubber artificial skin layer formed by direct dipping. In: Proceedings of ROBOMECH2015, pp. 2A2-W10 (1)–2A2-W10 (4), May 2015 (in Japanese)

Measurement of Stickiness with Pressure Distribution Sensor

Takayuki Kameoka, Akifumi Takahashi, Vibol Yem
and Hiroyuki Kajimoto

Abstract In this study we developed and evaluated device for the quantitative measurement of stickiness. While typical pressure distribution sensor can measure the pressing force, it cannot measure the tensile force. Hence, we installed a pin array on the sensor, which gives offset pressure to the sensor by its weight. We also show some result of measuring stickiness using natto and baby powder.

Keywords Pressure distribution · Sense of touch · Stickiness · Tactile sensor

1 Introduction

Currently, numerous research on the presentation of human skin sensations are carried out. To reproduce a more realistic sense, measurement of skin deformation distribution and its reproduction is necessary.

Such a measurement has been conducted in several literatures. Levesque et al. [1] measured the horizontal displacement of the finger skin tracing the glass surface. Bicchi et al. [2] captured the change in the contact area of the skin when the finger is in contact with the flexible object. These measurements are closely related to the tactile presentation technique. The measurement of skin horizontal displacement is related to the development of devices that present horizontal displacement [3],

T. Kameoka (✉) · A. Takahashi · V. Yem · H. Kajimoto
The University of Electro-Communications, 1-5-1 Chofugaoka,
Chofu, Tokyo 182-8585, Japan
e-mail: k1413050@edu.cc.uec.ac.jp

A. Takahashi
e-mail: a.takahashi@kaji-lab.jp

V. Yem
e-mail: yem@kaji-lab.jp

H. Kajimoto
e-mail: kajimoto@kaji-lab.jp

and the measurement of the contact area led to the development of a device that presents a flexible feeling by changing the contact area [4].

In this study, we focus on the skin deformation distribution when one feels stickiness. Stickiness (sticky feeling) in the present study refers to a sense that one feels when she/he touches and releases viscous or slimy liquids such as natto (a traditional Japanese food made from soybeans). This stickiness influences the impression of daily good such as, make-up water. Moreover, it is also known as one of the factors of the wet feeling (wetness) of the fabric perception [5, 6]. Hence, the application range is considered large.

One of the factors of the sticky feel is a force, but we mainly focus on the factors of skin sensation. Although the frictional resistance feeling on the display surface is expressed as sticky sensation [7], we deal with the stickiness that is felt when one releases the finger after presses.

Yamaoka et al. [8] observed the relationship between the contact area of an adhesive surface and temporal change of the pressing force, and found that there is a large hysteresis of the contact area. They also create stickiness display based on this finding. However, since the observation was limited to the change of contact area, detailed force distribution during the sticky feel remained unclear, which is necessary for the representation of stickiness sensation by using general pin-matrix type tactile display.

In this study, we build a system to measure the distribution of forces between the adhesive material and the finger skin. This paper describes measurement technique and some results of preliminary experiments.

1.1 Measuring Device

To measure the adhesive strength as a pressure distribution, it is necessary to measure the negative pressure distribution when lifting the skin. However, the general pressure distribution sensors can measure only positive force (push direction).

To solve this issue, we devised a method to insert a pin matrix between the skin and the pressure distribution sensor and apply a preload by the weight of the pin. The actual device is shown in Fig. 1. The device is composed of pin insertion plate made of acryl, spacers, a 10×10 stainless steel pin array, and a pressure distribution sensor (I-SCAN100, Nitta Co., Ltd.). Each pin is arranged on each sensing point of pressure distribution sensor one-to-one, and adds preload to the sensor. By this configuration, adhesive force can be observed by an amount less than the offset force when the finger is raised.

The interval of the sensor elements is 2.54 mm, and the pins were also placed at the same interval. The pin is made of stainless steel, diameter is 2 mm, height is 30 mm, and weight is 0.8 g. If the adhesive force is strong, it is necessary to increase the preload, but it can be achieved easily by changing the length of the pin.

Fig. 1 Measuring device

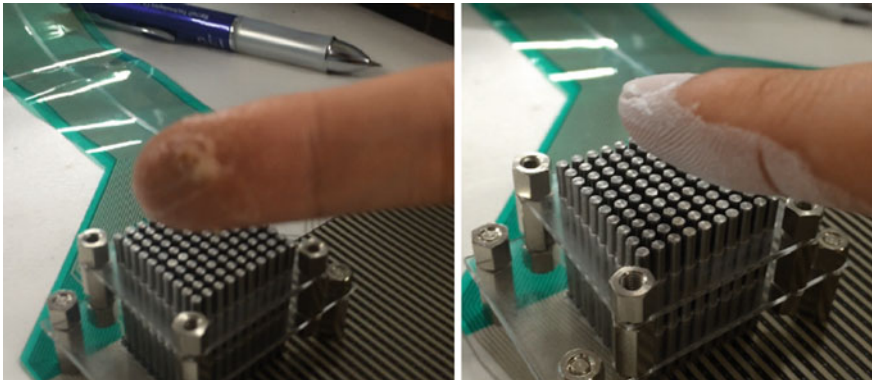
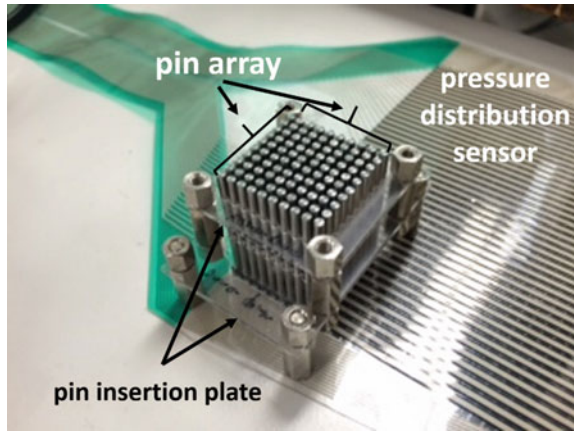


Fig. 2 Natto coating state and baby powder coating state

1.2 Experiment

Adhesive material was painted to the fingertip of the participant, and she/he pressed the fingertip to the pin array surface. When the finger pressure was reached to 0.05 N (maximum value of the sensor this time), she/he was asked to release the fingertip in the vertical direction. The lifting process was done in around 1 s. Measured data was saved as a csv file. In this experiment, we used sthread of natto mixed 100 times (no soy sauce) as the adhesive material, and a baby powder as non-adhesive material (Fig. 2).

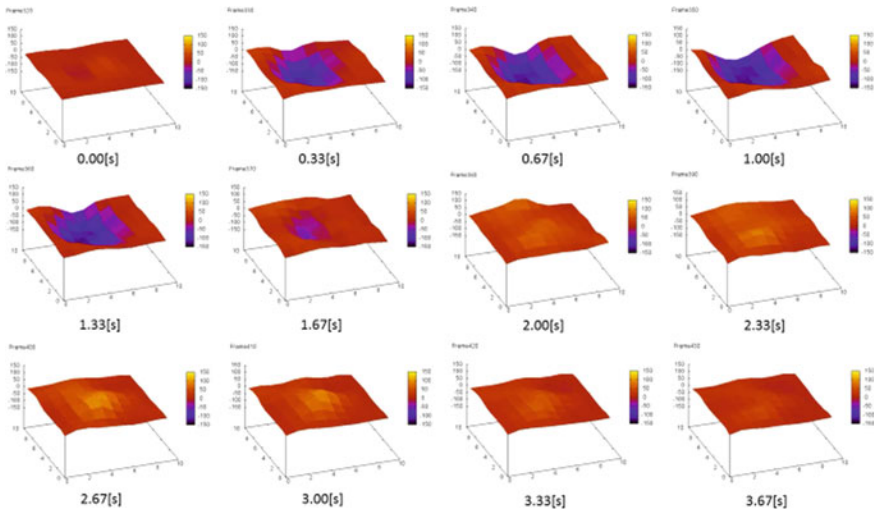


Fig. 3 Pressure distribution change in the case of natto

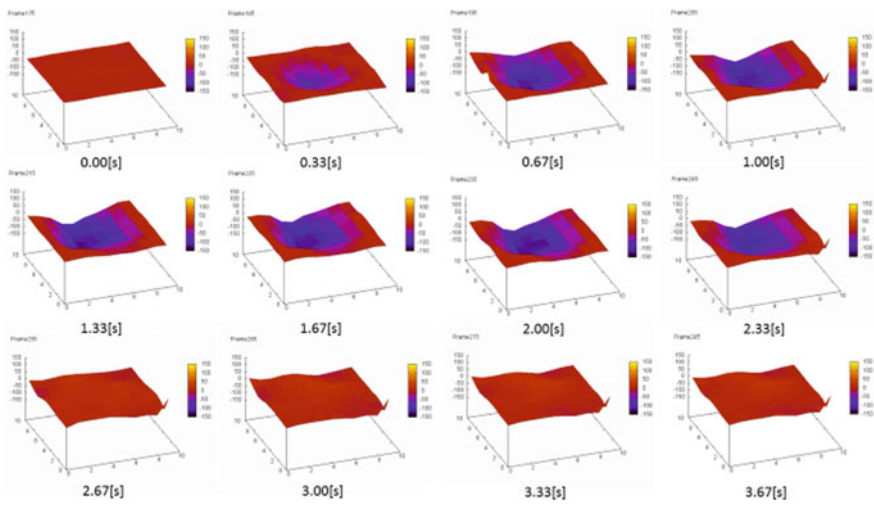


Fig. 4 Pressure distribution change in the case of baby powder

1.3 Experimental Results and Discussion

Figures 3 and 4 shows a change of the pressure distribution of the fingertip measured with natto and baby powder. We subtracted preload from the data, and the pressing force is shown as a negative (vertically downward) value, and the pulling force is shown as a positive (vertical upward) value. We can easily observe that

baby powder did not exhibit pulling force whereas in the case of natto, pulling force was observed.

Looking into more detail of the natto, the pressure distribution of pulling direction (yellow in the figure) was observed from the time the finger was lifted (2.00 s). The pulling force first appeared at two separate locations along the long axis of the finger. Then, the two peaks moved to the center of the finger pad, and eventually converged to one. Afterward, the pulling force gradually decreased, eventually became zero.

2 Conclusion

In this paper, we aimed to quantify sticky feeling of the object surface by observing time change of the pressure distribution on the contact surface.

As typical pressure distribution sensors can measure only the pressing force, we gave preload. It was achieved by a stainless steel pin array on the sensor. The experiment showed clear difference between adhesive and non-adhesive material, and interestingly, we found that pulling force first appear at the edges, and gradually converge to the center.

Our future work includes experiments with various materials, and the development of pin-matrix type tactile display that reproduce force distribution and generate stickiness sensation.

References

1. Levesque, V., Hayward, V.: Experimental evidence of lateral skin strain during tactile exploration. *Eurohaptics*. Ireland (2003)
2. Bicchi, A., Scilingo, E.P., DeRossi, D.: Haptic discrimination of softness in teleoperation: the role of the contact area spread rate. *IEEE Trans. Robot. Autom.* **16**(5), 496–504 (2000)
3. Levesque, V., Pasquero, J., Hayward, V.: Braille display by lateral skin deformation with the STReSS2 tactile transducer. *World haptics* (2007)
4. Fujita, K., Ikeda, Y.: Remote haptic sharing of elastic soft objects Remote haptic sharing of elastic soft objects. *World haptics* (2005)
5. Bergmann, T.W.M., Kusters, N.D., Kappers, A.M.L., Daanen, H.A.M.: Haptic perception of wetness. *Acta Psychol.* **141**(2), 159–163 (2012)
6. Filingeri, D., Fournet, D., Hodder, S., Havenith, G.: Why wet feels wet? a neurophysiological model of human cutaneous wetness sensitivity. *J. Neurophysiol.* Published **112**(6), 1457–1469 (2014)
7. Bau, O., Poupyrev, I., Israr, A., Harrison, C.: Teslatouch: electrovibration for touch surfaces. In: *ACM Symposium on User Interface Software and Technology (ACM UIST)* (2010)
8. Yamaoka, M., Yamamoto, A., Higuchi, T.: Basic analysis of stickiness sensation for tactile displays. Volume 5024 of the series lecture notes in computer science, pp. 427–436 (2008)

Part V
Medical Application

A Wearable Haptic Ring for the Control of Extra Robotic Fingers

Irfan Hussain, Giovanni Spagnoletti, Claudio Pacchierotti
and Domenico Prattichizzo

Abstract This paper presents a wearable haptic ring called “hRing” to control the soft extra robotic finger and to render haptic information to provide cutaneous stimuli. The “hRing” is a novel wearable cutaneous device for the proximal finger phalanx and the extra robotic finger is a device to be used by chronic stroke patients to compensate for the missing hand function of their paretic limb. The hRing consists of two servo motors, a vibro motor, two pairs of push buttons and a belt. The servo motors move the belt placed in contact with the user’s finger skin. When the motors spin in opposite directions, the belt presses into the user’s finger, while when the motors spin in the same direction, the belt applies a shear force to the skin. The soft finger is an underactuated modular robotic finger worn on the paretic forearm by means of an elastic band. The device and the paretic hand/arm act like the two parts of a gripper working together to hold an object. It has been designed to be wearable. Two chronic stroke patients took part in our experimental evaluation on how the proposed integrated robotic system can be used for hand grasping compensation. The hRing enabled the patients to easily control the motion of the robotic finger while being provided the haptic feedback about the status of the grasping action. The patients found the system useful for ADL tasks, the hRing easy to use, and the haptic feedback very informative.

Keywords Wearable haptics · Supernumerary limbs · Grasp compensation · Stroke · Assistive robotics

I. Hussain (✉) · G. Spagnoletti · C. Pacchierotti · D. Prattichizzo
Department of Information Engineering and Mathematics,
University of Siena, Siena, Italy
e-mail: irfan.hussain@unisi.it; irfanmechatronics@gmail.com

I. Hussain · G. Spagnoletti · C. Pacchierotti · D. Prattichizzo
Department of Advanced Robotics, Istituto Italiano di Tecnologia,
Genova, Italy

1 Overview of the System

We propose a novel wearable cutaneous device for the proximal finger phalanx, called “hRing”. It consists of two servo motors, a vibrotactile motor, two pairs of push buttons, and a belt. The servo motors move the belt in contact with the user’s finger skin. When the motors spin in opposite directions, the belt presses into the user’s finger, while when the motors spin in the same direction, the belt applies a shear force to the skin. The device structure is symmetrical and each side features two push buttons, enabling the hRing to be used both on the left and right hand. A preliminary version of this wearable device has been presented in [1]. With respect to the version proposed in [1], the new hRing presented in this work offers enhanced mobility of the finger phalanx, ambidexterity, a vibrotactile motor, and a lighter body structure. In this work, we use the hRing as interface to interact with a novel underactuated soft robotic finger (SRF) and presented in [2] (see Fig. 1). The proposed SRF is an extra robotic finger to be worn on the forearm by means of an elastic band. The robotic device has been devised for compensating hand function in chronic stroke patients to re-gain the grasping capabilities of their paretic hand. The robotic finger and the paretic hand act like the two parts of a gripper, working together to hold an object. The proposed finger device consists of two main parts: a flexible finger and a support base. The flexible finger has a modular structure. The SRF has a single actuator that can flex/extend the whole finger through a tendon. A FSR force sensor is placed at the tip of the robotic finger.

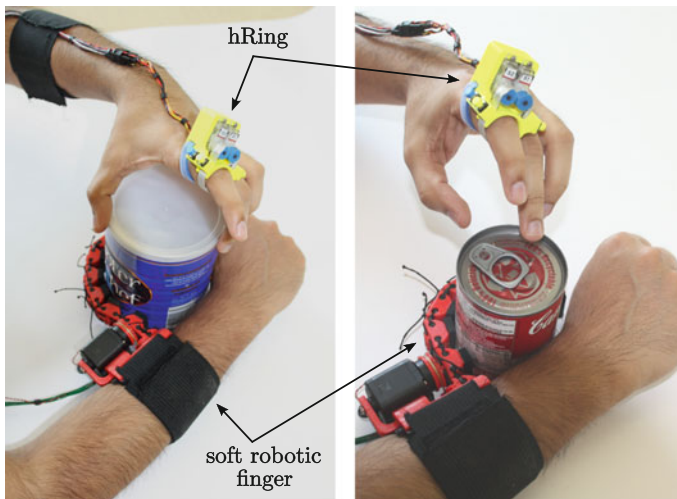


Fig. 1 The integrated system used by a patient in Activities of Daily Living (ADL)

2 Methods and Experiments

Two chronic stroke patients took part to our experimental evaluation on how the proposed integrated robotic system can be used for hand grasping compensation. The subjects were required to wear the robotic finger on their paretic hand and the hRing on the healthy hand index finger (see Fig. 1). The proposed compensatory tool can be used by subjects showing a residual mobility of the arm. Each patient uses the SRF for bimanual tasks typical in Activities of Daily Living (ADL), such as unscrewing a cap of tomato jar, opening a popcorn bag, or opening a can of beans. The hRing interface is used to both control the flexion/extension motion of the robotic finger and to provide the patient with haptic feedback about the forces exerted by the robotic finger on the environment. The patient can press the blue button on the external side of the hRing with the thumb of the same hand to initiates the flexing procedure of the robotic finger. The finger will close until a contact with an object through the FSR mounted on its fingertip is detected. As soon as the contact happens, the robotic finger stops its flexion and the hRing generates a short vibration burst to notify the patient. If the patient presses the blue button again, the finger increases the grasping force on the object. During this process, the hRing belt squeezes the patient's finger proportionally to the grasp force applied by the robotic finger on the environment. When the patient is satisfied with the grasping configuration, he or she can proceed with the task. Finally, pressing the yellow button on the hRing will initiate the opening procedure of the robotic finger. The hRing releases its belt and provides a vibration burst when the opening procedure is completed.

Acknowledgements The research has received founding from European Union's Horizon 2020 Research and Innovation Programme, Grant Agreement No. 688857 (SoftPro) and from the European Union Seventh Framework Programme FP7/2007-2013, Grant Agreement No. 601165 (WEARHAP).

References

1. Pacchierotti, C., Salviotti, G., Hussain, I., Meli, L., Prattichizzo, D.: The hRing: a wearable haptic device to avoid occlusions in hand tracking. In: Proceedings of IEEE Haptics Symposium (HAPTICS) (2016)
2. Hussain, I., Salviotti, G., Spagnoletti, G., Prattichizzo, D.: The soft-sixthfinger: a wearable emg controlled robotic extra-finger for grasp compensation in chronic stroke patients. *IEEE Robot. Autom. Lett.* (2016)

Relax and Tighten—A Haptics-based Approach to Simulate Sphincter Tone Assessment

Alejandro Granados, Luc Maréchal, Alastair Barrow, George Petrou, Christine Norton and Fernando Bello

Abstract Digital Rectal Examination (DRE) is a physical examination performed by clinicians to diagnose anorectal and prostate abnormalities. Amongst these, sphincter tone assessment is a crucial task where a clinician asks the patient to relax or squeeze, whilst measuring its function by the amount of pressure felt on the examining finger. DRE is difficult to learn and current models fail to reproduce the dynamic function of anorectal abnormalities. We propose a haptics-based approach to incorporate sphincter tone into our current simulator by motor-controlled pulling and releasing of cables that are coiled around a silicone model of the sphincters. A range of healthy and abnormal sphincter tone cases can be modelled by controlling the motors symmetrically and asymmetrically.

Keywords Haptics · Sphincter · Diagnosis · Learning · Teaching · Rectal examination

1 Introduction

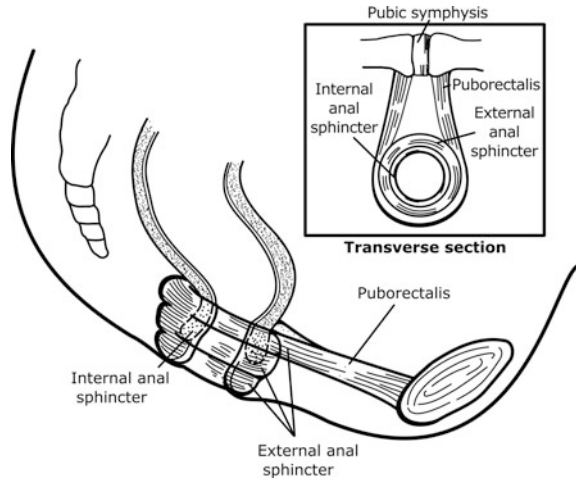
A Digital Rectal Examination (DRE) is an intimate physical examination that forms part of routine assessments of men and women used for diagnostic and treatment purposes related to urinary, colorectal, gynaecological, obstetric and sexual care.

A. Granados (✉) · L. Maréchal · A. Barrow · G. Petrou · F. Bello
SiMMS—Simulation and Modelling in Medicine and Surgery,
Centre for Engagement and Simulation Science, London, UK
e-mail: a.granados@imperial.ac.uk
URL: <http://imperial.ac.uk/simms>

A. Granados · L. Maréchal · A. Barrow · G. Petrou · F. Bello
Department of Surgery and Cancer, Imperial College London Chelsea & Westminster
Hospital, London, UK

C. Norton
Florence Nightingale Faculty of Nursing & Midwifery,
King's College London, London, UK

Fig. 1 Pelvic anatomy relevant to DRE. Diagram of the rectum, anal canal, and surrounding muscles (*adapted from [13]*)



During DRE, the consultant inserts his/her index finger through the anus of the patient to diagnose anorectal [1, 2] and/or male-related prostate [3] abnormalities (Fig. 1a). Due to its unsighted nature, DRE is difficult to learn and teach, assessment is inefficient and feedback is limited. Patient variability is inherent, with opportunities to practice limited and hard to standardize. There is also only vague information as to what constitutes adequate performance. Current teaching models are mostly focused on the prostate [4], failing to reproduce anorectal abnormalities and the dynamic function associated with structures such as sphincter tone. An abnormal anal sphincter may cause faecal incontinence or constipation. Its correct diagnosis is crucial for treatment.

The anal sphincters are composed of several cylindrical layers. The internal anal sphincter, the second innermost layer after the subepithelium, is usually symmetric in thickness, whereas the external anal sphincter, the outermost layer, is a ring-like striated muscle appearing inferiorly with the puborectal muscle superiorly [5]. The puborectalis, a firm soft tissue that forms part of the support of the pelvic floor, together with the pubococcygeus and iliococcygeus, is a U-shaped muscular sling encircling the junction between the rectus and the anus [6] (Fig. 1).

The dynamic function of these muscles is assessed through visual inspection and palpation. During visual inspection, the examiner tests the anal wink (reflex) as part of the assessment of neuromuscular integrity by stroking a cotton pad around the anus [7]. Then, the anal sphincters usually start to relax by applying gentle pressure on the anus, allowing the finger to be advanced into the anal canal. After initial insertion of about 3 cm of the examining finger, the examiner evaluates the puborectalis muscle and the external sphincter by asking the patient to relax, bear down and squeeze [7, 8]. During relaxation, the examiner notices the relaxation of the internal sphincter whilst pushing the puborectalis muscle posteriorly. During strain, the puborectalis muscle moves posteriorly and the internal anal sphincter relaxes

causing the finger to be expelled, whereas during squeeze, the anal sphincters and the puborectalis contract lifting the examining finger towards the umbilicus.

In this paper, we propose a haptics-based mechanism to model the function of the anal sphincters and puborectalis muscles, with the aim of providing a simulation learning environment that allows trainees not only to palpate internal anatomy such as the rectum walls and the prostate, but also to assess the dynamic function of structures such as the anal sphincters.

2 Modelling of Sphincter Tone

We developed a haptics-based simulator that recreates the tissue deformation and touch sensations arising during manual palpation of the rectal wall and prostate for both healthy and pathological cases. Informed by results of our quantitative analysis of DRE [9], the simulator is a combination of a haptic device, a bespoke thimble end effector [10], deformation modelling of MRI-segmented patient-specific anatomy [11] and a custom-made silicon pelvic model (Fig. 2).

We created a representative sphincter model using a 3D printed mould and silicone rubber. It was then mounted behind the anus of our pelvic model. Its external surface consists of two grooves where two cables are coiled and attached to separate motors on either side (Fig. 3).

Our system (Fig. 4) uses E4P optical incremental encoders (US Digital, Vancouver, WA, USA) interfaced with an Arduino Micro microcontroller to measure the rotation of the motors, which pull and release the cables recreating the dynamic function of squeeze and relax of the sphincters, respectively.

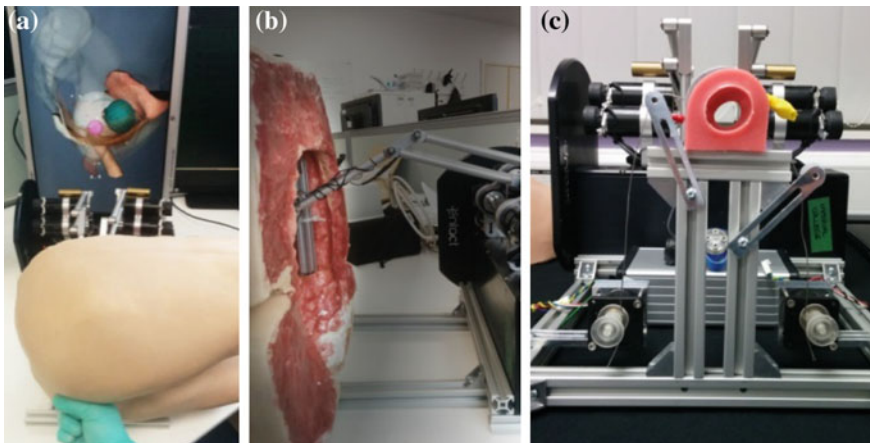


Fig. 2 Haptic-based simulator for training DRE: **a** front, **b** back of pelvic model, and **c** simulator without pelvic model showing the sphincter model and a motor on each side

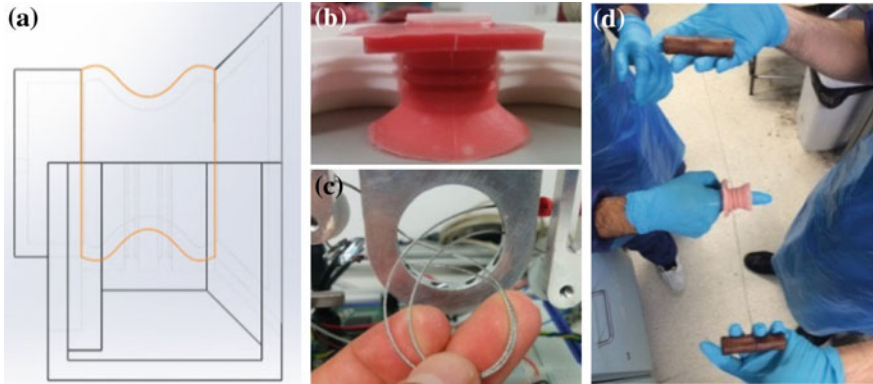


Fig. 3 Modelling of sphincters: **a** mould design, **b** silicone model with external grooves, **c** mounting location of sphincter model with cables coiled, and **d** pulling and releasing principle

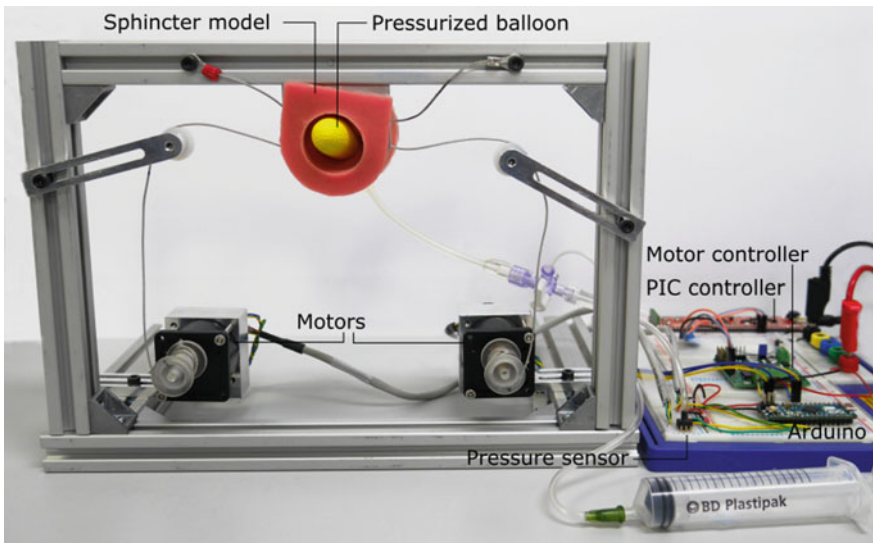


Fig. 4 Experimental setup of the sphincter tone control. The motors are controlled to pull or release the tension on the cable. The inflated balloon positioned inside the sphincter model enables the measurement of the applied pressure exerted by the cables

This mechanism consists of a Maxon A-Max 22 DC motor, a Maxon 900:1 Spur Gearhead (GS38A) and a custom designed capstan. The motors are independently controlled by means of a TRex Jr Motor Controller via serial communication using a PIC controller. The pressure inside a custom made inflated balloon inserted in the sphincter is measured with an ADP5131 pressure sensor (Panasonic Electronic, Osaka, Japan).

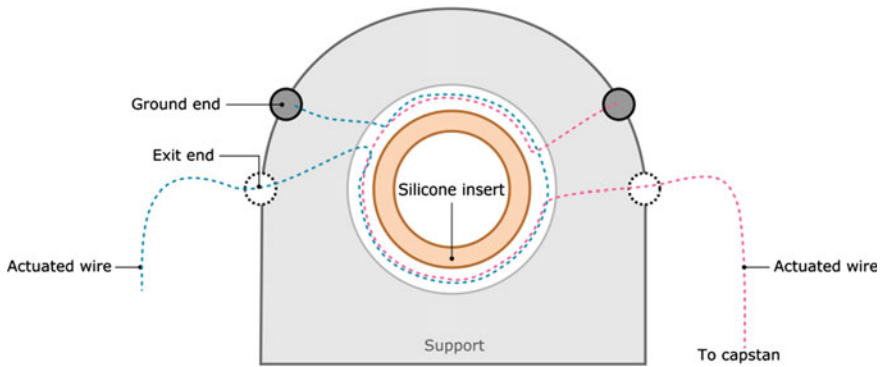


Fig. 5 Schematic diagram of the sphincters mechanism. Actuated wires are grounded at one end, coiled around the silicone model of the sphincters and tied to the capstan at the other end

Multiple threads in C++ are used to control the motors with regards to the encoders output. A range of abnormalities may be modelled by activating the motors asymmetrically.

Key to the design are two independently actuated wires looped around the silicone insert, each grounded at one end and routed via a pulley wheel to the capstan on the gear-motor assembly (Fig. 5). Tightening a cable results in a narrowing of the passage way, whilst at the same time causing a slight rotary effect due to the direction of the wire loop. As the cable is grounded at one end and there is significant friction between cable and silicone, the application of force is non-uniform around the opening and largest approximately opposite to the entry point. By adjusting the exit (grounding) point of the wire, the amount of rotation (twisting) caused and the area of force application surrounding the silicone can be adjusted.

As a single wrap of cable creates a non-uniform force, by offsetting the second cable 180° around the opening, the balance of force application can be independently controlled allowing for the recreation of anomalies whereby one side of the anal sphincter muscles appears stronger than the other. Additional loops of cable could be added with their angle of entry to the sphincter distributed radially around the opening, thus allowing a finer adjustment in the apparent closing force.

At present, the actuation of the motors and their encoder-based control mechanism are independent of the virtual anatomy, since the simulation of squeeze and relax proposed in this paper is not yet related to the virtual deformation of the sphincters or the anal canal, but rather provides an extension of the haptic feedback to other parts of the finger during the examination.

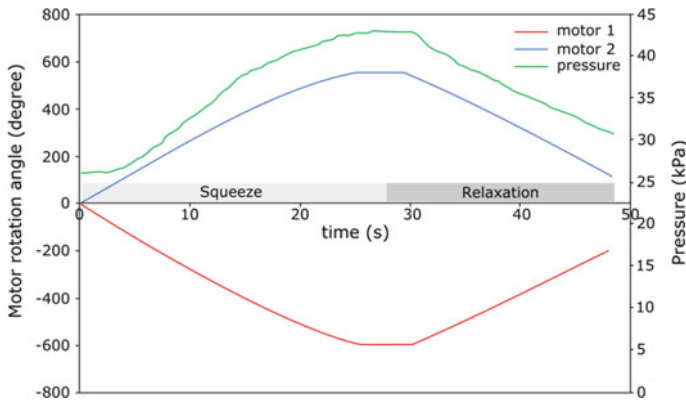


Fig. 6 Motor control and pressure variation inside the sphincter during squeeze and relaxation

3 Experimental Results

The motors were controlled to perform the squeeze and the relaxation of the sphincter. The pressure applied inside the sphincter on the inflated balloon was recorded at the same time (Fig. 6).

The magnitude of pressure between the relax position and the maximum squeeze was about 16 kPa. During relaxation, the cables are unwound removing the application of force. There is no counter force available in our current design to pull the sphincter open. This effect is caused by the silicone gradually resuming its rest shape and by the movement of the finger during palpation. We will investigate whether this effect is not affecting the realism of the simulation in subsequent studies with more clinicians.

4 Conclusion

Anorectal abnormalities and the modelling of the function of anal sphincters and puborectalis muscle structures are commonly underrepresented in current training models. We have extended our simulator system for training and learning DRE by incorporating a haptics-based mechanism to model the function or dysfunction of sphincter tone. In this paper, we present the early key design aspects of our approach. We plan to conduct further experimental studies with clinical experts to accurately model anal wink during visual inspection, as well as the forces exerted on the examining finger during palpation when the patient is asked to relax, strain and squeeze using our proposed mechanism. Experimental studies based on manometry [12] to validate and verify our model and gather further input from clinicians to accurately model sphincter tone and its assessment are also being

considered. This will provide an insight into the reaction forces that are necessary for modelling healthy and abnormal cases using our approach. Lastly, we are working on incorporating an interactive remote control facility that will allow a simulated patient (professional actor playing the role of a patient), or the trainer, to control the sphincter mechanism in order to adequately react to the examination and instruction by the trainee.

Acknowledgements The authors thank Mr. Chi L Wan for his support integrating the PIC microcontroller.

References

1. Bharucha, A.E., Rao, S.S.C.: An update on anorectal disorders for gastroenterologists. *Gastroenterology* **146**, 37–45 (2014)
2. Wong, R.K., Drossman, D.A., Bharacucha, A.E., et al.: The digital rectal examination: a multicenter survey of physician's and students' perceptions and practice patterns. *Am. J. Gastroenterol.* **107**, 1157–1163 (2012)
3. American Cancer Society.: *Prostate Cancer: Early Detection* (2013)
4. Kuroda, Y., Nakao, M., et al.: Interaction model between elastic objects for haptic feedback considering collisions of soft tissue. *Comput. Methods Programs Biomed.* **80**, 216–224 (2005)
5. Dobben, A.C., Felt-Bersma, R.J.F., ten Kate, F.J.W., Stoker, J.: Cross-sectional imaging of the anal sphincter in fecal incontinence. *Am. J. Roentgenol.* **190**, 671–682 (2008)
6. Maldonado, P.A., Wai, C.Y.: Pelvic organ prolapse new concepts in pelvic floor anatomy. *Obstet. Gynecol. Clin. North Am.* **43**, 15–26 (2016)
7. Talley, N.J.: How to do and interpret a rectal examination in gastroenterology. *Am. J. Gastroenterol.* **103**(4), 820–822 (2008)
8. McFarlane, M.J.: The rectal examination. In: Walker, H.K., Hall, W.D., Hurst, J.W., (eds.) *Clinical Methods: The History, Physical, and Laboratory Examinations*, 3rd edn., Chapter 97. Boston, Butterworths (1990)
9. Granados, A., Hald, N., Di Marco, A., et al.: Real-time visualisation and analysis of internal examinations—seeing the unseen. *MICCAI* **8673**, 617–625 (2014)
10. Loisillier, A., Granados, A., Barrow, A., Bello, F.: Thimble end effector for palpation skills training. *Eurohaptics* **9775**, 86–96 (2016)
11. Granados, A., Mayer, E., Norton, C., et al.: Haptics modelling for digital rectal examinations. In: *6th International Symposium, ISBMS Biomedical Simulation*, pp. 40–49 (2014)
12. Orkin, B.A., Sinykin, S.B., Lloyd, P.C.: The digital rectal examination scoring system (DRESS). *Dis. Colon Rectum* **53**(12), 1656–1660 (2010)
13. Madoff, R.D., Williams, J.G., Caushaj, P.F.: Fecal incontinence. *N. Engl. J. Med.* **326**, 1002–1007 (1992)

Training on Muscle Palpation Using Artificial Muscle Nodule Models

Kaoru Isogai, Shogo Okamoto, Asuka Noda, Ayumi Matsuzawa
and Yoji Yamada

Abstract We developed a palpation simulator for training on muscle palpation techniques for myofascial pain syndrome. This simulator consisted of two layers that resemble the hardness of actual human skin-fat and muscle tissues. Furthermore, a muscle nodule model made of urethane rubber was laid in the simulator. Five participants were trained on the palpation technique for localizing the muscle nodule models, using our simulators. After the training session, they localized the muscle nodule models more definitely than before. The proposed muscle nodule palpation simulator may improve manual palpation techniques used for examining myofascial pain syndrome.

Keywords Palpation · Simulator · Muscle nodule · Myofascial pain syndrome

1 Introduction

Many musculoskeletal pains such as neck or back pains are associated with myofascial pain syndrome, which is caused by myofascial trigger points. Myofascial trigger points are hyperirritable spots located at the muscle nodules along the taut bands in the muscle belly [1]. In a clinical setting, myofascial trigger points are localized by palpation. Therefore, the difference in hardness between a muscle nodule and muscle belly is an important objective for the diagnosis of myofascial pain syndrome. However, it is demanding for clinicians to find the slightly hard spots in the muscles, and previous studies have reported that the localization of trigger points by palpation is not reliable [2, 3]. To solve this issue,

K. Isogai (✉) · A. Noda · A. Matsuzawa
Department of Physical Therapy, Tokoha University, Hamamatsu, Japan
e-mail: kisogai@hm.tokoha-u.ac.jp

K. Isogai · S. Okamoto · Y. Yamada
Department of Mechanical Science & Engineering, Nagoya University, Nagoya, Japan

we developed an artificial fat and muscle model for training on palpation for myofascial pain syndrome.

Because the muscles are palpated through the skin and fat tissues, the muscle nodule palpation simulator should also consist of subcutaneous and muscular layers. The hardness of the two layers should resemble that of the actual human skin-fat tissue and muscle tissue, respectively. However, the mechanical characteristics of the human subcutaneous and muscle tissues are nonlinear [4, 5], and the solid model, which is made up of a unique material, cannot represent the mechanical characteristics of human body tissues. Fortunately, a layered rubber structure is known to realize the mechanical characteristics similar to those of human tissues [5, 6]. Therefore, we also adjusted the mechanical characteristics of urethane models by adopting a layered structure with fabric sheets between layers. In this study, we demonstrated that our simulator could improve the palpation technique used for localizing the muscle nodules by physical therapy trainees.

2 Muscle Nodule Palpation Simulator

We developed a urethane rubber model of human gluteal tissue basis on the methods of our previous study [5]. As shown in Fig. 1, the model was cylindrical in shape, with the height and diameter being 70 mm and 120 mm, respectively. The upper layer of the model corresponds to the subcutaneous layer, and its thickness was 12 mm. The lower layer of the model corresponds to the muscle layer, and its thickness was 58 mm. The thickness of skin-fat and muscle layers were comparable to the depth of the human gluteal subcutaneous tissues and muscle tissues. A cotton sheet was laid between the two layers of the skin-fat model and between the skin-fat and muscle layers. Furthermore, the top surface was covered by a stretchable knit sheet. These layered structures achieved nonlinear stress-strain characteristics similar to that of human tissues [5].

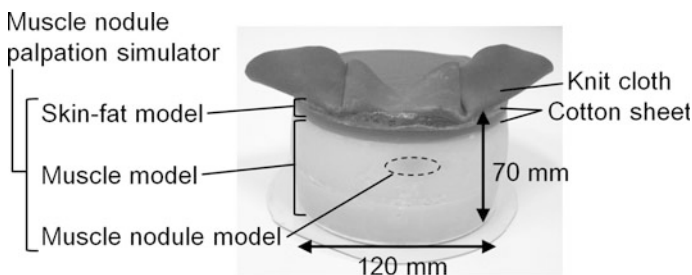


Fig. 1 Urethane—made skin-fat and muscle model for muscle nodule palpation

We embedded a muscle nodule model, which was 31 mm in length, 16 mm in width, and 9 mm in thickness, at 24 mm depth from the surface of the muscle model. The form and burying depth of muscle nodule model were determined based on opinions from clinicians. The nodule model was made of urethane rubber of 405.5 kPa and colored with red ink.

3 Experiment: Training on Muscle Nodule Palpation by Using Artificial Urethane Simulators

Our muscle nodule palpation simulator was intended to aid training on palpation. To confirm the availability, we investigated the effect of the training on localization of the muscle nodule model by using the simulator. This study was conducted with the approval of the internal review board of Tokoha University (Registration no. 2014-015H).

3.1 Stimuli: Artificial Muscle Nodules

As shown in Fig. 2, we developed four types of simulators that differed in terms of the position and direction of muscle nodule models, and one that did not contain a muscle nodule model. Simulator CS contained the muscle nodule model at the position of the circular center. Simulators DRS, DCS, and DSS contained the muscle nodule model at the position 15 mm deviated from the circular center, and the models oriented radial, circumferential, and slant directions, respectively. The participants were blinded to the conditions of the muscle nodule model because all simulators were covered with an opaque knit cloth.

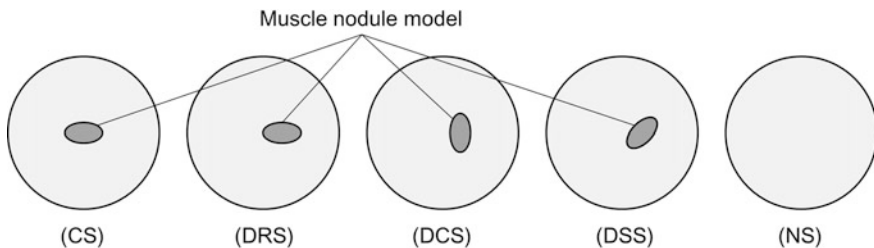


Fig. 2 Positions of muscle nodule models in the urethane models

3.2 Participants

Five physical therapy trainees participated in this experiment. None of them had used the simulators for muscle palpation and they were unaware of the objectives of the present study.

3.3 Procedures

3.3.1 Localization of Nodule Prior to the Training Session

After all the participants were presented a muscle nodule model, they received explanations that some simulators would contain the muscle nodule model within a radius of 30 mm from the circular center at the half depth of the simulator. They were instructed not to lift the simulator and not to peep from the side. Furthermore, they were told not to push the simulator with excessive force, which might cause pain if applied on the actual human body. The participants were allowed to examine each of the four types of simulators—DRS, DCS, DSS, and NS—within 1 min. Simulator CS was not used in the localization task. The simulators were presented in a random order and direction. During each trial, they judged whether the muscle nodule model existed in the simulator. If they judged that the muscle nodule model existed, they placed a paper leaf, which imitated the outer shape of muscle nodule model, on the top surface of the simulator, judging both position and direction. All the participants repeated the procedures mentioned above 20 times, i.e., five repetition for each type of simulator.

3.3.2 Training Session by Using Palpation Simulator

All the participants were trained on palpation using simulator CS to know the sensation experienced by palpating the muscle nodule model for 5 min. They were allowed to lift the simulator and to check the position of the muscle nodule model by looking through the transparent bottom of the simulator. After the training, they were required to freely describe their impressions about the training.

3.3.3 Localization of the Nodule After the Training Session

All participants repeated the same task described in Sect. 3.3.1. Thereafter, they freely described their impressions about the effect of the training session on their judgment.

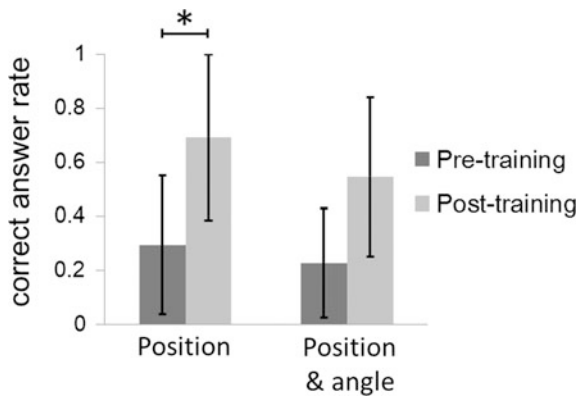
3.4 Analysis

For the trials in which the simulator was perceived to contain the muscle nodule model, we measured the gaps of distance and rotational angle between the silhouettes of the muscle nodule model that was projected to the top surface of the simulator and the paper leaf placed by each participant. We regarded the participants' answers as correct when the distance and angle gaps were smaller than 16 mm and 30°, respectively. We applied Wilcoxon signed rank test on the correct answer ratios for simulators DRS, DCS, and DSS. Note that we excluded the answer for simulator NS, for which the participants mostly responded correctly, from the analysis because they would increase the apparent correct answer ratios.

3.5 Results

Figure 3 shows the mean correct answer ratios for each session and the results of the statistical analysis. The correct answer ratios for the position significantly improved after training. According to the introspective reports provided by the participants after the training session, they could acquire exploratory motion to sense the muscle nodule model deep in the simulator, and they understood the appropriate strength of pressure required to identify the muscle nodule model. Furthermore, in their introspective reports after the post-training session, the effects of the training session were positively recognized. They reported that they could utilize the experiences acquired through the training session.

Fig. 3 Correct answer ratios for a localization task before and after the training session



4 Conclusions

In this study, we demonstrated that the localization techniques for the slightly hard spot in the muscle model had improved after a training session using our palpation simulator. The localization experiments and introspective reports from the trainees suggested the beneficial influences of the knowledge of haptic sensations felt because of nodules in the muscle and exploratory hand motions for effective palpation. The models used in the present study exhibited stress-strain characteristics similar to those of the human gluteal tissues. In addition, these models are believed to be similar to actual human tissues [5]. Clinicians' examination ability for the myofascial pain syndrome may improve by a training program using our simulators.

References

1. Xiaoqiang, Z., Shusheng, T., Qiangmin, H.: Understanding of myofascial trigger points. *Chin. Med. J.* **127**(24), 4271–4277 (2014)
2. Lucas, N., Macaskill, P., Irwig, L., Moran, R., Bogduk, N.: Reliability of physical examination for diagnosis of myofascial trigger points: a systematic review of the literature. *Clin. J. Pain* **25** (1), 80–89 (2009)
3. Myburgh, C., Larsen, A.H., Hartvigsen, J.: A systematic, critical review of manual palpation for identifying myofascial trigger points: evidence and clinical significance. *Arch. Phys. Med. Rehabil.* **89**(6), 1169–1176 (2008)
4. Then, C., Menger, J., Benderoth, G., Alizadeh, M., Vogl, T.J., Hubner, F., Silber, G.: A method for a mechanical characterization of human gluteal tissue. *Technol. Health Care* **15**, 385–398 (2007)
5. Isogai, K., Okamoto, S., Yamada, Y., Ayabe, R., Ohtawa, K.: Skin-fat-muscle urethane model for palpation for muscle disorders, In: *IEEE/SICE International Symposium on System Integration*, pp. 960–964. Nagoya (2015)
6. Aso, M., Yamada, Y., Yoshida, K., Akiyama, Y., Ito, Y.: Evaluation of the mechanical characteristics of human thighs for developing complex dummy tissues, In: *IEEE International Conference on Robotics and Biomimetics*, pp. 1450–1455 (2013)

Basic Study on Motor Ability Evaluation and Training System Using Virtual Collision Avoidance

Takuya Makishima, Masaki Orimoto and Masamichi Sakaguchi

Abstract In this study, we investigated the evaluation or training of motor ability for collision avoidance. This requires prompt recognition of danger, and fast and accurate movement. We developed a prototype measurement system for collision avoidance using VR. In this paper, we describe the characteristics of the system and the results obtained.

Keywords Collision avoidance · Evaluation · Training · Virtual · Motor ability

1 Introduction

A decline in motor ability increases the risk of falling and other accidents. Many approaches have been proposed to the maintenance of motor control for elderly people. Conventional evaluations of the risk of falling have focused on local muscles, balance, or walking [1, 2]. However, alternative approaches have focused on “agility” or the ability to react quickly through body movement when about to fall [3, 4]. In this study, we assumed that this is a more practical approach to reducing accidents such as falling. As it is unacceptable to put the subject in danger by relying on direct touch, we focused on instead on collision avoidance, using Virtual Reality (VR).

In general, people react unconsciously and reflexively to visual stimuli. Avoiding a collision requires early recognition and speed and accuracy of response.

T. Makishima (✉) · M. Orimoto · M. Sakaguchi
Nagoya Institute of Technology, Nagoya, Aichi 466-8555, Japan
e-mail: t.makishima.580@nitech.jp
URL: <http://vrmech.web.nitech.ac.jp>

M. Orimoto
e-mail: 25113037@stn.nitech.ac.jp

M. Sakaguchi
e-mail: saka@nitech.ac.jp

However, these vary from person to person. We assumed that this reflects differences in motor ability, and that this could be used for the evaluation or training of collision avoidance. As the approach of an object is perceived visually, this makes avoidance possible using only visual stimuli, suggesting that unconscious movement can be induced by a virtual image.

In this study, we examine whether or not evaluation or training of motor ability is possible by analyzing collision avoidance. We developed a prototype measurement system for collision avoidance movement, and in this paper we discuss the characteristics of the system and the results obtained.

2 The Measurement System for Collision Avoidance Movement

Figure 1a, b shows the appearance of the system and the VR environment viewed by the user through a head mounted display (HMD).

The system comprises an HMD, camera, PC, and force plate. The subject avoids an object that appears suddenly before the eyes in the virtual image. The avoidance movement is measured by the camera and the force plate. The displacement of the head and the center of pressure (CoP) are recorded. This allows a range of parameters to be acquired, including reaction time, motor time, avoidance speed, avoidance direction, maximum transfer, and body vibration (Fig. 2).

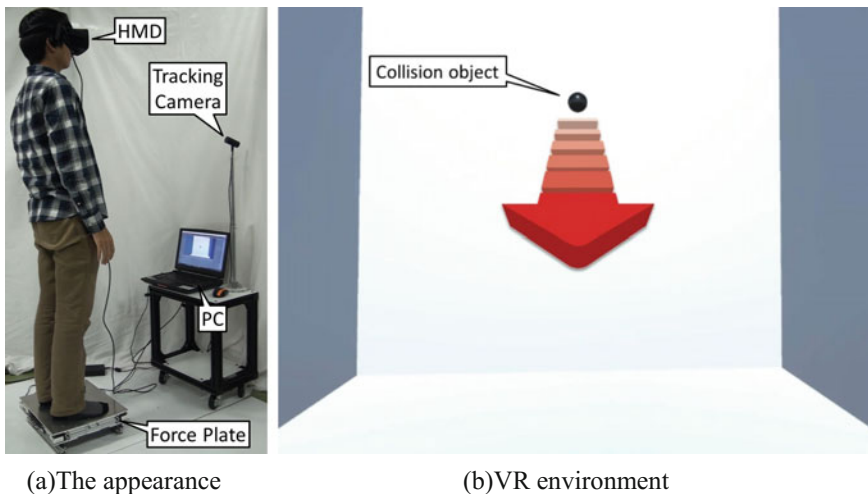


Fig. 1 The measurement system

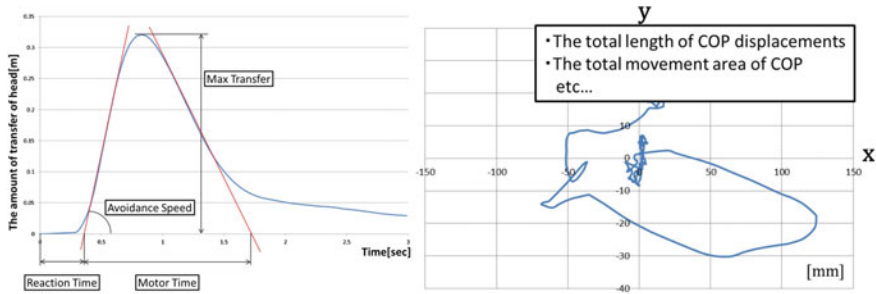


Fig. 2 Examples of obtained result

3 Conclusions

In this study, we suggested the possibility of evaluation or training of motor ability by analyzing collision avoidance, and developed a prototype measurement system. We confirmed that the system was able to capture a range of parameters of the avoidance movement. In future research, we will investigate the types of task that are suitable for motor ability evaluation or training, and will establish methods for addressing them.

Acknowledgements This work was supported by JSPS KAKENHI Grant Number JP16H03210.

References

1. Duncan, P.W., Winter, D.K., et al.: Functional reach: a new clinical measure of balance. *J Gerontol.* **45**(6), 192–197 (1990)
2. Podsiadlo, D., Richardson, S.: The timed “Up & Go”: A test of basic functional mobility for frail elderly persons. *J. Am. Geriatr. Soc.* **39**(2), 142–148 (1991)
3. Berg, W.P., Alessio, H.M., Mills, E.M., et al.: Circumstances and consequences of falls in independent community-dwelling older adults. *Age Ageing* **26**, 261–268 (1997)
4. Muranaga, S., Inou, Y.: Agility of the old aging and physical therapy. *JJ. Phys. Ther.* **16**(9), 725–730 (1999)

Bimanual Haptic Simulator for Training Hand Palpation and Lumbar Puncture

James Jose and Rao R. Bhavani

Abstract This paper addresses a bimanual haptic simulator for training human hand palpation and needle insertion motor skills in lumbar puncture medical procedure using two haptic device for medical students and physicians. This virtual reality environment simulates the human hand palpation and needle puncture with visual and haptic feedback. In this work, we studied lateral haptic model for rendering human hand palpation and layered haptic model for lumbar needle puncture. We have developed a training simulator for detecting the lumbar position and spinal needle insertion skills for lumbar puncture that can be demonstrated as a concept prototype to the medical haptic simulations.

Keywords Bimanual haptics • Medical simulation • Skill training • Lumbar puncture • Hand palpation

1 Introduction

Lumbar puncture (LP) is a procedure whereby a needle of length of 3.5–5 inch is inserted through lumbar vertebral region to the dura at the level of the lumbar spine, in order to either obtain a sample of cerebrospinal fluid (CSF) for diagnostic purposes or to precede injection of drugs. Spinal injection procedures involve injecting medications through a needle placed into a structure or space in the spine. The doctor often uses an injection of colourless, iodine-based contrast and a special type of x-ray to help him or her place the needle in the correct location.

Lumbar spinal needle puncture is a blind process commonly used in the medical field which needs fine motor skills. The main skills involved in the spinal injection

J. Jose (✉) · R.R. Bhavani
AMMACHI Labs, Amrita School of Engineering, Amrita Vishwa Vidyapeetham,
Amrita University, Amritapuri, India
e-mail: josejames@am.amrita.edu

R.R. Bhavani
e-mail: bhavani@amrita.edu

procedure are identifying the lumbar position via hand palpation, control depth and angle of needle insertion using visual and haptic feedback. It is a blind process, in which physicians get the idea of needle insertion depth mainly through haptic feedback. Incorrect techniques or any misplacement of needle puncture to spinal cord resulting from lack of proper training or unskilled supervision creates many complications to patients like cerebral herniation, injury to the spinal cord and nerve roots, dysesthesia (impairment of sensation) etc.

Our previous works are focused on developing computational modelling and training simulation for motor skills in vocational education and training [1–3]. As tactile feedback is very important for physicians for a successful lumbar puncture, this procedure serves as an ideal candidate for the development of a haptic training simulator [4]. R.W. Webster et al. designed a haptic simulation to teach basic suturing for simple wound closure [5]. A. Okamura et al. presents a force model for needle insertion into soft tissue for accurate surgical simulation [6]. Also researchers presents a modeling paradigm for physically based real time rendering of interaction between surgical tools and soft tissues for surgical simulation in multimodal virtual environment [7]. T.R. Coles et al. integrated haptics with augmented reality for training femoral palpation and needle insertion [8]. Related works [9–11] have addressed to develop a force feedback LP simulator, though we tried to develop a bimanual simulator attempt for train both position detection and needle insertion skills in LP.

In this work, we have developed a bimanual haptic simulator for training human hand palpation for detecting the lumbar position and needle insertion motor skills in lumbar puncture medical procedure using two haptic device for medical students and physicians. We studied lateral haptic model for rendering human hand palpation and layered haptic model for lumbar needle puncture. So this simulator offers extensive hands on training to medical students and Physicians for an actual LP procedure on a patient which helps them to learn and train lumbar puncture skills and translates into improved real-world scenarios. Training using haptic simulation will improve safety, quality and education in healthcare.

2 Simulator Setup and Interface

This simulator is comprised of a computer with a simulation visual display connected to two haptic devices as shown in Fig. 1. The haptic devices used in the simulator are Novint Falcon and Phantom Omni/Desktop device from Sensable technology. The haptic device provides force feedback, so users can actually feel the resistant forces on a correct and incorrect trajectory, guides for a better skill learning. Virtual reality simulation interface consists of a virtual human body model, user-steered virtual needle and a hand model. Simulation interface is developed using the open source Chai 3d visuo haptic API.

The main skills involved in the lumbar puncture procedure are identify the lumbar position via hand palpation and control the depth & angle of needle

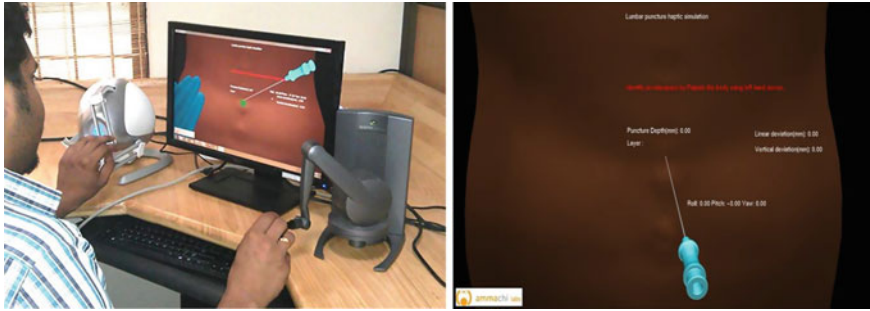


Fig. 1 Simulator setup and interface

insertion using visual & haptic feedback. This training simulator will cover training for all these skills using haptic devices and interactive virtual simulation interface. The human body model with spinal column (from L1 to the sacrum), human hand, and lumbar needle are loaded as three dimensional (3D) file formats in the simulation interface. The models are rendered both in graphics and in haptics for simulation to illustrate how the hand palpated and needle is being inserted. The forces also change when the needle is initially inserted or punctures through the skin. If the needle contacts bone, the student experiences stiffer resistant forces. At each haptic layer, the student feels the surface friction, puncture force, internal friction, and damping. Irrespective of traditional training method, our simulation intelligence track all necessary parameters like depth of insertion, angle of insertion, contacted tissue layer and correct trainees misplaces and mistakes. This learning feature is not available to the student involved in the LP of an actual patient, and may help students improve their technique.

3 System Design and Architecture

The basic design and architecture block diagram of our proposed simulator is shown in Fig. 2. It consist of two haptic devices and a simulation interface. Mainly two LP processes are selected to simulate in this work are Hand palpation & Needle insertion. Two haptic devices acted as both input and output devices to control the simulation interface. Haptic device 1 (Novint Falcon) used to control human hand 3d model and haptic device 2 (Phantom device) used to control the spinal needle 3d model. Selected haptic device 1 is a 3 degrees of freedom (dof) which give only position values to the virtual model and haptic device 2 is a 6 dof which provides position and orientation values to the virtual model. For hand palpation process, human hand 3d model move laterally on human body 3d model by haptic device 1. For needle insertion process, spinal needle model insert on human body model controlling by haptic device 2. Collision detection algorithms detect collisions

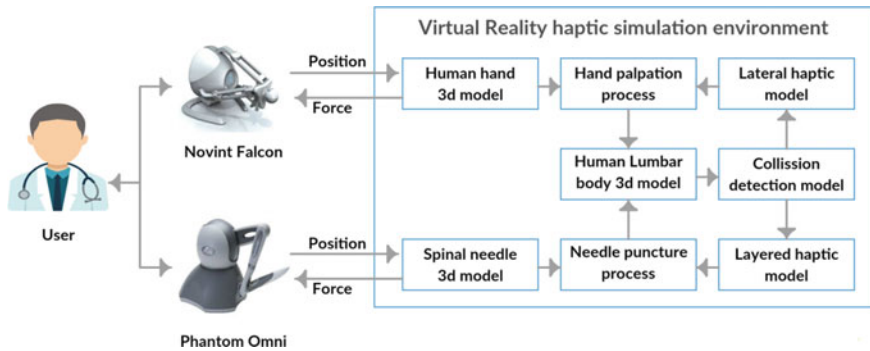


Fig. 2 Simulator block diagram

between human hand—human body surface and needle—human body. When collisions happened, computational models of lateral haptic and layered haptic, render hand palpation and needle insertion force feedbacks.

4 Haptic Models for Hand Palpation and Lumbar Needle Puncture

4.1 Lateral Haptic Model for Hand Palpation

Human haptic interface can provide texture information through vibrations to display visual objects in the screen. But to display geometrical shapes and bump textures more realistic force feedbacks are needed. The use of virtual proxies [12] or god-objects [13] is a common approach for haptic surface rendering, because it allows smooth shaded feedback from unprocessed polygons. Here we using proxy based god-object and haptic volume rendering approach [14] has been adapted to enable haptic feedback for lateral haptic model for hand palpation. Forces acting normal to moving directions of thumb like F_1 , F_2 and F_3 about position P_1 , P_2 and P_3 enables geometrical information as shown in Fig. 3. Collectively these normal forces provide smooth shape feedback by force shading. Our lateral haptic model employs lateral surface force feedback and display bump shapes when moving laterally on a surface.

4.2 Layered Haptic Model for Needle Puncture

Human body lumbar region consist of different layers of tissues from skin to spine as shown in Fig. 4. Each layer has different tissue haptic properties, need different

Fig. 3 Lateral haptic model for hand palpation

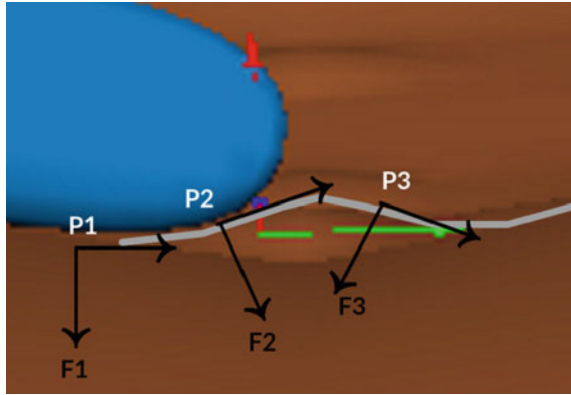
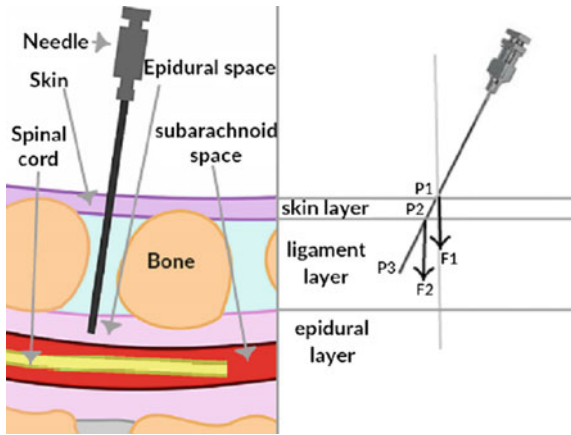


Fig. 4 Lumbar tissue layers and layered haptic model



haptic force feedbacks. So we propose layered haptic model for render needle puncture realistic force feedback as shown in Fig. 4. Each layer is modelled as a thin haptic box with appropriate force vector calculations. The resistant force calculations vary depending upon the material in the layer model, the depth and angle of insertion of the needle [4].

The Layered haptic model renders the forces that affect the needle during the insertion. The forces are calculated depending on needle position, needle orientation and local tissue layer properties. We created haptic layer for corresponding each tissue layer with the material and haptic properties for each layer varying from the other layer. The haptic device display the rendered forces to the user. When the needle tip is inserted through each layer corresponding realistic forces are rendered. So the user can detect the layer transition in needle puncture and get the depth information of puncture. When needle pierced into skin layer the force created is $F1 = -k1*(P2 - P1)$. Similarly needle transit from skin layer to next ligament layer creates force $F2 = -k2*(P3 - P2)$.

5 Conclusion

In this work, we designed and developed a bimanual haptic simulator for training hand palpation to detect lumbar positions and needle insertion skills for lumbar puncture procedures. Also it shows its potential to track all skill parameters and provide feedback and suggestion to trainees which speedup the skill learning curve. Initial work and results with the bimanual haptic LP simulator are encouraging. Irrespective of traditional training method, our Simulation intelligence track all necessary parameters like depth of insertion, angle of insertion, contacted tissue layer and correct trainees misplaces and mistakes by providing real-time feedback. Future work on this simulator includes implementation of a scoring mechanism to measure and track performance of trainees through this simulation and to make the simulator more effective and intelligent.

Acknowledgements We wish to extend our sincere gratitude to Mata Amritanandamayi Devi, Chancellor, Amrita Vishwa Vidyapeetham for being an everlasting source of inspiration for our efforts. We also wholeheartedly thank the wonderful team at AMMACHI Labs for their support and encouragement and for providing constructive criticism and valuable inputs during the various stages of this work.

References

1. Jose, J., Ramesh, S., Akshay, N., Bhavani, R.R.: TryStrokes: Learning on a digital canvas to paint in the real world. In: Global Humanitarian Technology Conference: South Asia Satellite (GHTC-SAS), pp. 68–73. IEEE (2013). doi:[10.1109/GHTC-SAS.2013.6629891](https://doi.org/10.1109/GHTC-SAS.2013.6629891)
2. Jose, J., Unnikrishnan, R., Marshall, D., Bhavani, R.R.: Haptic simulations for training plumbing skills. In: 2014 IEEE International Symposium on Haptic, Audio and Visual Environments and Games (HAVE), pp. 65–70. IEEE (2014)
3. Jose, J., Akshay, N., Bhavani, R.R.: Learning elementary physics through haptic simulations. In: Proceedings of the 2014 International Conference on Interdisciplinary Advances in Applied Computing. ACM (2014)
4. Gorman, P., Krummel, T., Webster, R., Smith, M., Hutchens, D.: A prototype haptic lumbar puncture simulator. In: Studies in Health Technology and Informatics, pp. 106–109 (2000)
5. Webster, R.W., Zimmerman, D.I., Mohler, B.J., Melkonian, M.G., Haluck, R.S.: A prototype haptic suturing simulator. In: Studies in Health Technology and Informatics, pp. 567–569 (2001)
6. Okamura, A.M., Simone, C., O’Leary, M.D.: Force modeling for needle insertion into soft tissue. IEEE Trans. Biomed. Eng. **51**(10), 1707–1716 (2004)
7. De, S., Srinivasan, M.A.: Thin walled models for haptic and graphical rendering of soft tissues in surgical simulations. In: Studies in Health Technology and Informatics, pp. 94–99 (1999)
8. Coles, T.R., John, N.W., Gould, D., Caldwell, D.G.: Integrating haptics with augmented reality in a femoral palpation and needle insertion training simulation. IEEE Trans. Haptics **4**(3), 199–209 (2011)
9. Cleary, K., Lathan, C.: Surgical simulation: research review, computing challenges, and spine biopsy simulator. Parallel Comput. 1–15 (1997)

10. Bostrom, M., Singh, S.K., Wiley, C.W.: Design of an interactive lumbar puncture simulator with tactile feedback. In: IEEE 1993 of Virtual Reality Annual International Symposium, pp. 280–286. IEEE (1993)
11. Farber, M., Hummel, F., Gerloff, C., Handels, H.: Virtual reality simulator for the training of lumbar punctures. *Methods Inf. Med.* **48**(5), 493 (2009)
12. Ruspini, D.C., Kolarov, K., Khatib, O.: The haptic display of complex graphical environments. In: Proceedings of the 24th Annual Conference on Computer Graphics and Interactive Techniques, pp. 345–352. ACM Press/Addison-Wesley Publishing Co (1997)
13. Zilles, C.B., Salisbury, J.K.: A constraint-based god-object method for haptic display. In: Proceedings. 1995 IEEE/RSJ International Conference on Intelligent Robots and Systems 95. ‘Human Robot Interaction and Cooperative Robots’ vol. 3, pp. 146–151. IEEE (1995)
14. Lundin, K., Gudmundsson, B., Ynnerman, A.: General proxy-based haptics for volume visualization. In: World Haptics Conference First Joint EuroHaptics Conference and Symposium on Haptic Interfaces for Virtual Environment and Teleoperator Systems, pp. 557–560. IEEE (2005)

Prostate Tumor Palpation Simulator Based on Pneumatic and Augmented Haptics

Aishwari Talhan and Seokhee Jeon

Abstract In this project, we focus on building a prostate palpation simulator where a practitioner teaches his/herself a process called Digital Rectal Examination (DRE). While conventional mock-up-based training simulators can only provide a fixed number of abnormal conditions, our simulator is capable of creating various prostate abnormalities ranged from a single small tumor to multiple larger tumors, with comparable fidelity and realism. For this, we have developed a new prostate-shaped end-effector that systematically changes the its shape and stiffness using pneumatic and particle jamming techniques with embedded balloon. At current stage, seven pores are embedded in the silicone prostate mock-up, so a medical practitioner can perceive tumors with wide range of stiffness, position, and number.

Keywords Augmented haptic · Medical simulator · Palpation · Pneumatic · Particle jamming

1 Introduction

Medical simulators play an important role in training of the medical students, by providing various medical case that cannot be easily experienced. The medical simulator is useful tool in determining a physician understanding and management of patient complications.

Palpation is one of the clinical diagnosis skills, where medical professionals identify abnormalities by touching and feeling haptic difference between an affected and normal tissue. In particular, the process of the analysis of prostate abnormalities using an index finger palpation through human rectal region is known as Digital Rectal Examination (DRE).

A. Talhan (✉) · S. Jeon

Department of Computer Science and Engineering, Kyung Hee University, 1732,
Deogyong-daero, Giheung-gu, Yongin-si, Gyeonggi-do 17104, Republic of Korea
e-mail: aishwari@khu.ac.kr

S. Jeon

e-mail: jeon@khu.ac.kr

It is reported that, DRE are intimate physical examinations. The prostate cancer is most common cancer and second leading reason of death because of cancer in the United State. There are two kinds of prostate abnormalities: lumpy and hard tissues (tumors). In addition, tumor could be of any shape and size. In this project, we develop a simulator to practice the DRE technique.

2 Methodology

The goal of the work is to develop a haptic interface and rendering algorithm specialized for the training of DRE. Since the main interaction in the DRE process is to insert doctors index finger into the rectal area, a simulator for DRE should provide, for realism, full area contact feedback between the finger and the inner tissue surface of the rectal. On the other hand, the feedback of interest, which is subject to change for flexible simulation of various abnormalities, mainly occurs in very small area, at the doctors fingertip and is generally very subtle. Thus, conventional point-contact-based force feedback haptic interfaces are not suitable for this scenario. As an alternative, this paper presents a haptic augmented reality-based approach empowered by a pneumatic actuation. The peripheral haptic feedback that is not subject to change is supplied by real mannequin mock-up, and the feedback of interest at the trainees fingertip is synthetically generated by a variable haptic property end-effector made of a silicone and embedded pneumatically actuated pores. It has proven that pneumatic approach has the capability to produce natural force feedback [1, 2], and actuator balloons, made up of silicon, can produce the natural skin feeling. In order to independently control the stiffness and size of the pores, we combine the pneumatic pressure control with particle jamming technique where small particle alters the stiffness of the pores when vacuumed. With capability of controlling the size of the pores with pneumatic pressure control and controlling the stiffness of the pores with particle jamming techniques [3], the system can produce lumpy tissues and hard tissues effects. Moreover, a mannequin of the body part presents a physical medium that is similar to a typical patient case and it makes the simulation more realistic [4].

2.1 System Architecture

To achieve above mentioned control, we have designed and developed an architectural model comprising standard pneumatic active and passive components in specialized arrangement as shown in Fig. 1.

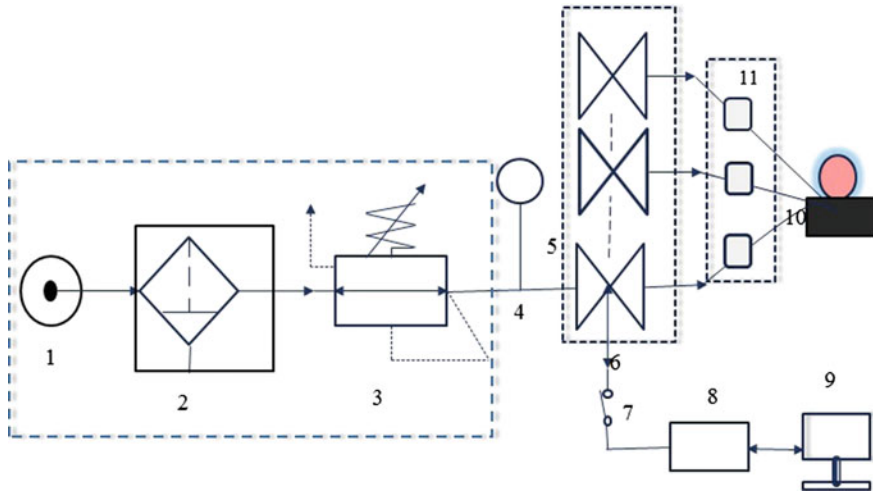


Fig. 1 Illustration of system architecture for the prostate haptic medical simulator. 1 Air source. 2 Filter. 3 Regulator. 4 Gauge. 5 Array of valves. 6 Two-way lines. 7 Switch. 8 DAQ/PLC. 9 Computer. 10 Membrane/prostate with flexible lines. 11 Array of vacuum generator

2.2 End Effector

The core part of our implementation is on the end effector. We developed a new prostate-shaped end effector that systematically changes its shape and stiffness using pneumatic and particle jamming techniques with embedded balloon. The end effector is casted using Eco-Flex 0030 (Smooth-On). The overall layout of the silicon end effector is shown in Fig. 2.

Two layers of pores are arranged, which simulates different depth of the tumors. Upper layer and lower layer has multiple pores that localize the tumor. As mentioned, the stiffness and the size of the tumor are controlled by pneumatic control of each pores.

3 Demonstration

Currently, the silicon prostate mold is designed with seven pores inside. Each of pores is able to provide different seven level of inflation and deflation. In this demonstration, we provide augmented haptic simulator to educate the medical practitioner with better perception of multiple, reconfigurable, and classified scenarios (such as prostatitis, BPH, and cancer) of abnormal conditions with lump, stiff, and deep tumor, of the prostate by performing DRE examination.

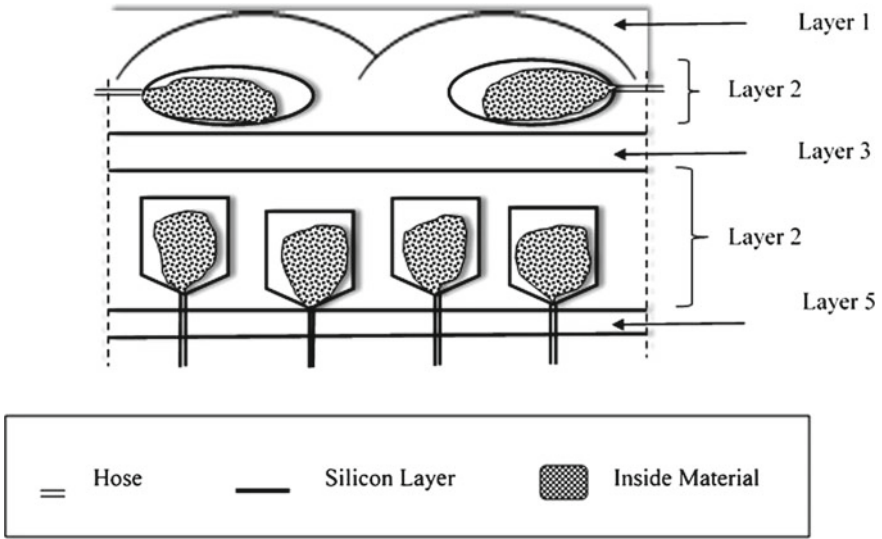


Fig. 2 Illustration of side-view layout of the silicon end effector

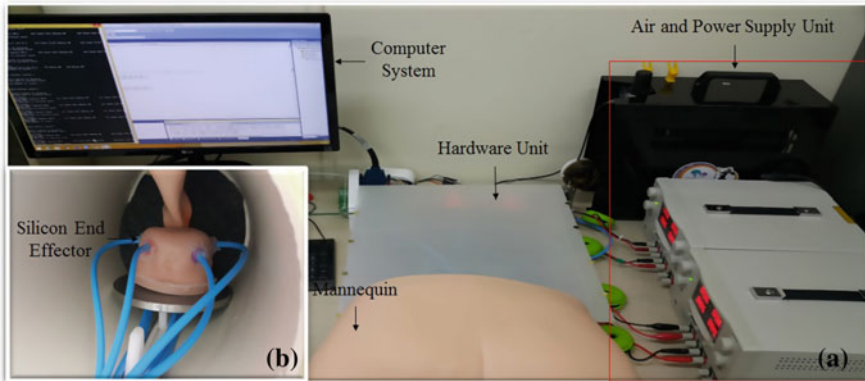


Fig. 3 a Illustration of the overall set-up of the system. b Assembly of end effector within mannequin

The setup of demonstration is shown in Fig. 3. With this setup, participants can experience real-like practice of DRE process with various different symptoms, such as deep stiff tumor or swallow and different sized multiple tumors.

4 Future Work

In this paper, we are intent to demonstrate preliminary study of the prostate tumor palpation simulator. However, in near future we will evaluate the system effectiveness to train the medical practitioner.

Acknowledgements This research was supported by Basic Science Research Program through the NRF of Korea (NRF-2014R1A1A2057100), by Global Frontier Program through NRF of Korea (NRF-2012M3A6A3056074), and by ERC program through NRF of Korea (2011-0030075).

References

1. Kim, Y., Oakley, I., Ryu, J.: Human perception of pneumatic tactile cues. *Adv. Robot.* **22**(8), 807–828 (2008)
2. Li, M., Luo, S., Seneviratne, L.D., Nanayakkara, T., Althoefer, K., Dasgupta, P.: Haptics for multi-fingered palpation. In: 2013 IEEE International Conference on Systems, Man, and Cybernetics. pp. 4184–4189. IEEE (2013)
3. Stanley, A.A., Gwilliam, J.C., Okamura, A.M.: Haptic jamming: a deformable geometry, variable stiffness tactile display using pneumatics and particle jamming. In: World Haptics Conference (WHC), 2013. pp. 25–30. IEEE (2013)
4. Zhu, E., Hadadgar, A., Masiello, I., Zary, N.: Augmented reality in healthcare education: an integrative review. *PeerJ* **2**, e469 (2014)

Part VI
Application of Haptics to VR,
Telepresence and Multimedia

Haptic Directional Instruction System for Sports

Ryoichiro Shiraishi, Koya Sato, Yuji Sano and Mai Otsuki

Abstract We proposed a new haptic instruction system for sports trainings that provides field players with instructed directions. The system consists of a stimulation unit (SU) for a player and an instruction unit (IU) for an instructor. Players wear the SU around their waist, and can recognize instructed directions by vibrations using 13 vibration actuators. The IU sends a direction where the joystick tilts to the SU via wireless communication modules. Preliminary experiments confirmed that the all participants did not feel the slipping away of the SU, and all participants were able to recognize its vibration even though they were running at 5, 10 km/h and standing (0 km/h). However, at 15 km/h, a participant who has a plump body recognized that a little or hardly recognized that at back part. We need to improve the method of providing stimuli at back part. By using the system, instructors and directors can provide the instructed directions to a field player without both any voice and gesture.

Keywords Haptic device · Vibration · Support system · Direction instruction · Superhuman sports

1 Introduction

Indicating directions by voices and gestures to instruct field players how to approach for a ball or other players are often seen in sports. However, in the case that the field player cannot listen the voice or watch the instructor, it is difficult to recognize the instructed direction. Moreover, an instructor says “right” while

R. Shiraishi (✉) · K. Sato · Y. Sano
Program in Empowerment Informatics, School of Integrative and Global Majors,
University of Tsukuba, Tsukuba, Ibaraki, Japan
e-mail: shiraishi_r@golem.kz.tsukuba.ac.jp

M. Otsuki
Faculty of Engineering, Information and Systems, University of Tsukuba,
Tsukuba, Ibaraki, Japan

players are running or playing a game, but the field player cannot understand which direction is correct. Indicating the direction by instructors is important for beginners because they often do not know what should do now/next compared to professional players. To guide correct direction from an instructor to field players, we propose a new system with neither voice nor gesture.

Some researchers have developed haptic devices for teaching directions by using vibrations [1–3], but they have not confirmed yet that these devices can be apply for field players in sports who perform vigorous motions. Therefore, it is necessary to verify the feasibility of haptic devices for teaching directions.

The purpose of this research is to develop a new haptic instruction system, and to confirm that players with the system can recognize instructed directions from the device while they are running.

2 System Overview

Developed haptic system consists of stimulation units (SU) and instruction unit (IU) as shown in Fig. 1a. The SU has microcomputer (The Switch Science mbed HMR1017), wireless communication module (XBee-PRO ZB), geomagnetic sensor (LSM9DS0) and 13 vibration actuators (T.P.C FM34F). The actuators' vibration quantity is 17.6 m/s^2 , which is approximately equal to that of a mobile phone. The SU also has two vibration actuators at back position (actuator no. 7 in Fig. 1a) to make the stimulation stronger because human beings have less sensory organs at back than front and side of the lumbar [4]. The geomagnetic sensor measures the directions of player's trunk. Players in a field wear the SU around the waist as shown in Fig. 1b. The player can adjust the positions of vibration actuators according to the player's body shape. The SU provides field players with vibration sensory stimulations in 12 directions. The instructors, such as coaches and directors of sports team indicate the direction by using the joystick of the IU. The IU can communicate with the SU at least 100 m away. The weight of SU is about 150 g with battery and can be used for at least an hour.

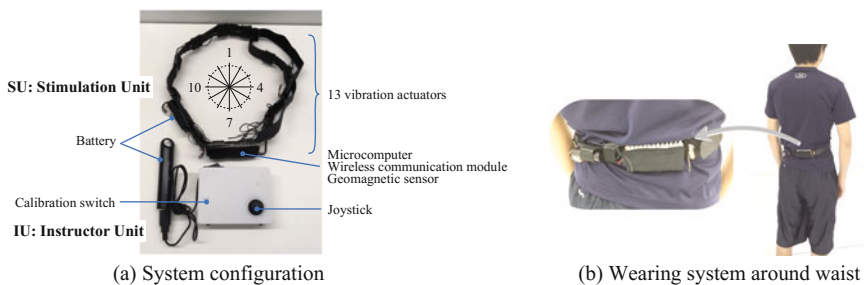


Fig. 1 Developed haptic system

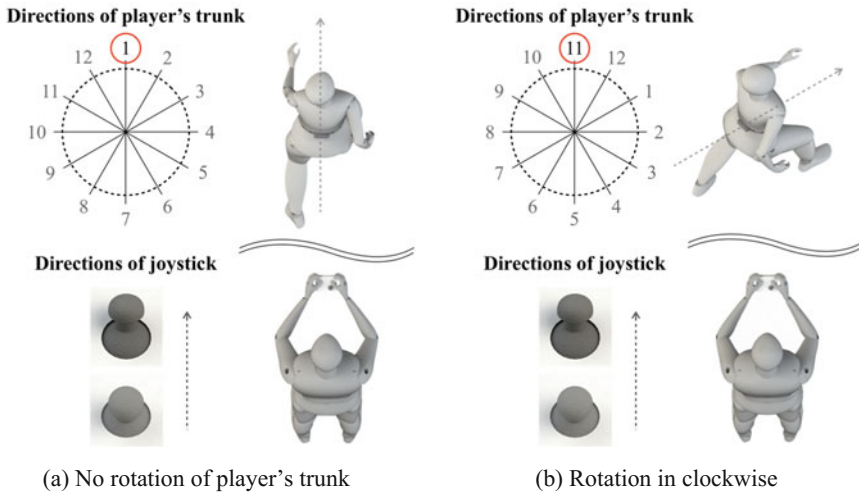


Fig. 2 Relationship between directions of player's trunk and joystick

The directions of player's trunk and the joystick are divided by 12 divisions. The direction of joystick corresponds with that of player's trunk. First, to calibrate both directions, Instructors and players match the direction of their body, then, the instructor with the IU pushes a calibration switch. When the joystick is tilted to the front and the direction of the IU, the front part of vibration actuator; no. 1 is activated (Fig. 2a). In the case that the joystick is tilted to the front and the direction of player's trunk rotates approximately 60° in clockwise, the actuator located at left side of player's body; no. 11 is activated (Fig. 2b). The SU provides field players with the vibration stimulation at the relative direction of instructor.

3 Experiment

We carried out preliminary experiments to confirm that the players with the SU can feel the vibration stimulation and understand the directions while they are running.

In the experiment, we measured gaps between the actual instructed directions and the stimulation positions that players recognized, and we also evaluated the subjective strength of stimulations and the wearabilities of the SU. We applied the system for five participants, and used a treadmill for constant running velocity. The participants wore the SU and ran at 5, 10, 15 km/h and standing (0 km/h). We stimulated 12 directions at random for each participant without any information of starting of the stimulation, and asked participants to answer the position and the strength of stimulations. The position is one of 12 directions, no.1–12, as shown in Fig. 2a, and participants were asked to answer that as quickly as possible.

Table 1 Means of gaps between the actual instructed directions and the stimulation positions

| Velocity (km/h) | Mean | Standard deviation |
|-----------------|------|--------------------|
| 0 | 0.33 | 0.1 |
| 5 | 0.38 | 0.19 |
| 10 | 0.34 | 0.1 |
| 15 | 0.34 | 0.2 |

In addition, they answered the subjective strength of stimulations by 4-grade evaluation (unbearable, high-strength, low-strength, and not at all). To evaluate the wearabilities, we asked them about slipping away of the SU and disturbance of movements by the SU in each velocity. Finally, we asked them whether they felt the phantom vibrations [5] that participants feel the vibration stimulations around their waist after taking off the SU.

From the results of subjective evaluation, the SU did not slip away from the participants' waist and did not prevent their motions and running. All participants recognized the all stimulations at 0, 5, 10 km/h, but at 15 km/h, a participant who has a plump body recognized that a little or hardly recognized that at back part, no. 7. As the comments, three participants concentrated on the stimulations while they are running, and all participants did not recognize phantom vibrations after taking off the SU.

Table 1 shows the means of all gaps between the actual instructed directions and the stimulation positions. There were not differences of the gaps among each velocity.

4 Discussion

We proposed a new haptic directional instruction system to indicate the correct direction from an instructor to field players. We confirmed that the SU had enough wearabilities to apply for sports, and was able to provide the instructed directions using vibration stimulations to players while they were running. However, because the effectiveness was smaller for players who have a plump body than the other players, we need to improve the method of providing stimuli at back part. In addition, developed system can be applied for only one field player. In actual sports, coaches and directors provide instructions to many players. We also need to improve the communication protocols and system's interface in order to change the instructed player at once.

Beginners often do not know what they should do now/next. Proposed system would be effective for them because the system can provide them with the way of approach for a ball and the direction of an opponent player by using haptic stimulation. We need to clarify the effectiveness of the system through actual sports

trainings and games in beginners. Moreover, in this research, we confirmed that participants concentrated on the vibration stimulations from the SU while they were running. However, in a sports game, field players should concentrate on various things, such as position of a ball and other players and combination plays. We also need to confirm that players with the SU can recognize the instructed directions even though they concentrate on their play.

In the future, we plan to apply the system for augmented sports instructions of actual training fields and superhuman sports [6].

Additionally, by using the system, instructors and directors can provide the instructed directions to a field player without both any voice and gesture. Therefore, the system can be applied for not only able-body players but also hearing or visually impaired players. We also plan to apply our system to such players and clarify the effectiveness.

Summary

We proposed a new haptic instruction system for sports trainings that provides field players with instructed directions. The system consists of a stimulation unit (SU) for a player and an instruction unit (IU) for an instructor. The SU has microcomputer, wireless communication module, geomagnetic sensor and 13 vibration actuators. Players wear the SU around their waist, and can recognize instructed directions from the SU. The SU also has two vibration actuators at back position to make the stimulation stronger. The geomagnetic sensor measures the directions of player's trunk. The IU sends a direction where the joystick tilts to the SU via wireless communication modules. The player can adjust the positions of vibration actuators according to the player's body shape. The IU can communicate with the SU at least 100 m away. The weight of SU is about 150 g with battery and can be used for at least an hour. The directions of player's trunk and the joystick are divided by 12 divisions. The SU provides field players with the vibration stimulation at the relative direction of instructor. We carried out preliminary experiments to confirm that the players with the SU can feel the vibration stimulation and understand the directions while they are running. In the experiment, we measured gaps between the actual instructed directions and the stimulation positions that players recognized, and we also evaluated the subjective strength of stimulations and the wearabilities of the SU. As the results, the all participants did not feel the slipping away of the SU, and four-fifth participants were able to recognize its vibration even though they were running. By using the system, instructors and directors can provide the instructed directions to a field player without both any voice and gesture.

Demo Summary

- What the audience will experience with your demo?
 - They will be able to experience to recognize instructed direction from the Stimulation Unit (SU), and to control the wearer by using the Instruction Unit (IU). In addition, they can know the wearabilities of the system if they perform vigorous motions.
If we can bring a treadmill to the conference for running demo, participants can run with the system. Unless we can bring a treadmill, we want enough space for running (e.g. 20 m straight-line distance).
- How many people can participate at one time?
 - Maximum four participants (we will bring two sets of proposed system; two instructors and two players can experience at one time).
- How long is the experience? (It is recommended that the demo experience is less than 3 min)
 - Within 3 min.
- How long will you need for setup?
 - 20 min.
- How many watt is required?
 - 100 W (100 V, 1 A).
- How many people will it take in the booth to explain your demonstration?
 - two or three people.

Keywords: 五個

- Haptic device
- Vibration
- Support system
- Direction instruction
- Superhuman sports

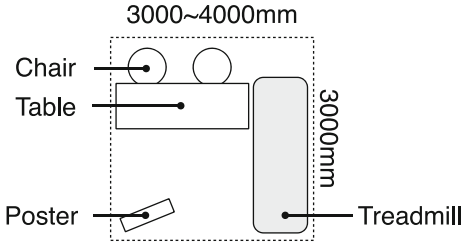
Research Area

- Assistive technology
- Wearable haptic devices

Floor Plan: With a Treadmill

- Layout

Our layout plan is shown in the following figure.



- Dimensions of floor space and height

3 ~ 4 × 3 m (Height: about 2 m).

- Light & Audio

Nothing special.

- Power sources

We need more than 5 plugs and 2000 W.
A treadmill, PC, battery charge of developed system.

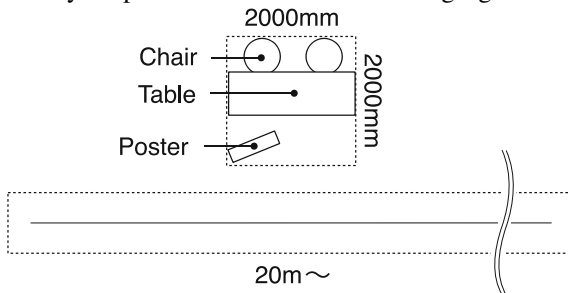
- Equipment

A treadmill: wide * depth * height = 800 * 2300 * 1500 (mm), 180 kg, 100 V, 60 Hz, 15A.

Floor Plan: Without a Treadmill

- Layout

Our layout plan is shown in the following figure.



- Dimensions of floor space and height
2 × 2 m (Height: about 2 m).
And 20 m straight-line distance.
- Light & Audio
Nothing special.
- Power sources
We need more than 3 plugs and 500 W.
PC, battery charge of developed system.
- Equipment
Nothing special.

References

1. Piatetski, E., Lynette, J.: Vibrotactile pattern recognition on the arm and torso. In: First Joint Eurohaptics Conference and Symposium on Haptic Interfaces for Virtual Environment and Teleoperator Systems, pp. 90–95 (2005)
2. Matsuoka, K., Tsuruta, M., Ishii, H., Shimoda, H., Yoshikawa, H.: An experimental study on directional information presentation techniques using vibrotactile stimulation to the head. In: Human Interface Symposium, pp. 139–144 (2006) (in Japanese)
3. Tsukada, K., Yasumura, M.: Activebelt: Belt-type wearable tactile display for directional navigation. In: International Conference on Ubiquitous Computing, pp. 384–399 (2004)
4. Loomis, J.M., Carter, C.C.: Sensitivity to shifts of a point stimulus: an instance of tactile hyperacuity. *Percept. Psychophys.* **24**(6), 487–492 (1978)
5. Rothberg, M.B., Arora, A., Hermann, J., Kleppel, R., St Marie, P., Visintainer, P.: Phantom vibration syndrome among medical staff: a cross sectional survey. *Bmj* **341**, c6914 (2010)
6. Superhuman Sports Society, Official Website. <http://superhuman-sports.org/> (2016). Accessed 29 July 2016

Tactile Treasure Map: Integrating Allocentric and Egocentric Information for Tactile Guidance

Mariacarla Memeo, Victor Adriel de Jesus Oliveira, Luciana Nedel, Anderson Maciel and Luca Brayda

Abstract With interactive maps a person can manage to find the way from one point to another, using an allocentric perspective (e.g. Google Maps), but also looking at a location as from the inside of the map with an egocentric perspective (e.g. Google Street View). Such experience cannot be performed with tactile maps, mostly explored from a top-view. To solve this, we built a system with two different but complementary devices. When coupled, they can provide both allocentric and egocentric spatial information to support the exploration of interactive tactile maps. To show the potential of the system, we built a blind treasure hunt.

Keywords Haptics · Tactile guidance · Spatial coding · Assistive technology · Tactile mouse · Vibrotactile head-mounted display

1 Introduction

Navigation skills involve the ability of localizing yourself and traveling in a space. In addition, it requires updating spatial information related to the environment and efficiently employ such information in emergency cases, such as when a person gets

M. Memeo (✉) · L. Brayda
RBCS, Fondazione Istituto Italiano di Tecnologia (IIT), Genoa, Italy
e-mail: mariacarla.memeo@iit.it

L. Brayda
e-mail: luca.brayda@iit.it

V.A. de Jesus Oliveira · L. Nedel · A. Maciel
INF, Universidade Federal do Rio Grande do Sul (UFRGS), Porto Alegre, Brazil
e-mail: vajoliveira@inf.ufrgs.br

L. Nedel
e-mail: nedel@inf.ufrgs.br

A. Maciel
e-mail: amaciel@inf.ufrgs.br

lost or accesses an interrupted road. The previous knowledge of the navigation path facilitates the reaching of the desired destination. To store data about the itinerary, our brain has to collect and elaborate information on spatial landmarks, on position and orientation of geographical reference points.

This process leads to the creation of a mental schema representing a simplified version of the real itinerary. The creation of mental representations of a map involves spatial reference systems, such as allocentric and egocentric.¹ There is evidence showing that the performance of subjects on different spatial tasks are based on input from both egocentric and allocentric reference frames [1]. However, the preference for using one spatial reference frame over the other, or a combination of different spatial reference frames depends on the participant [3, 4]. The prevalence of one over the other affects the decoding of spatial information [12], but there are no definitive understanding about the adoption of those systems in absence of vision using only haptic modality as it happens for the visually impaired population.

The role of visual experience in the creation of spatial inferential representations is still a debatable topic. Some studies report the superiority of visually impaired people respect to blindfolded sighted subjects [7, 13], while other authors affirm that they actually present impaired performances [9, 10]. One possible reason for this discrepancy is the lack of a method to sequentially verify the use of allocentric and egocentric perspective in the creation of a mental representation of space.

Moreover, visually impaired people encode space mainly through the exploration of tactile maps. The use of printed tactile maps, however, is limited for a number of reasons. For instance, the amount of information that can be presented on a tactile map is limited by its physical dimensions. Moreover, to update the information of the tactile map a new version must be printed. Therefore, there are tactile systems made for blind exploration of virtual environments and maps [5, 8, 11]. Such systems can be used as a learning tool for enhancing orientation and mobility (O&M) training. However, those interactive tactile maps are still mostly explored from a top-view. That hinders the user autonomy for adopting a convenient spatial reference frame.

We propose a new haptic system to provide both egocentric and allocentric cues through the tactile modality. The setup we propose is meant to improve spatial processing in O&M training by providing more information and autonomy to the subject while exploring dynamic tactile maps. In addition, the same setup can be used as a platform to study how each reference frame is applied to understand space during the exploration of tactile maps.

¹Allocentric representation encodes object locations with respect to other objects in a global coordinate system (i.e. top-view perspective). Egocentric representation defines spatial landmarks in relation to the viewer's body in a self-referred coordinate system (i.e. ahead, behind, to the right, to the left respect to viewer's position).

2 A System for Haptic Guidance

Our haptic system is composed by the TAMO3 [6] and a Vibrotactile Head-mounted Display [2] (Fig. 1).

The TAMO3 is a *T*actile *M*ouse sensitive to changes in wrist orientations and providing feedback on three degrees of freedom: height, roll and pitch (Fig. 2). TAMO3 offers a top-view perspective of a virtual map. Users can create a mental map of the explored space by integrating the tactile perception of one finger with the proprioception of the arm.

The vibrotactile HMD is composed by seven electromechanical factors and renders directional cues on the user’s head [2]. It offers a higher resolution on the forehead (such as a “Tactile Fovea”), to ease the detection of objects of interest around the user and to support an egocentric exploration (Fig. 2).

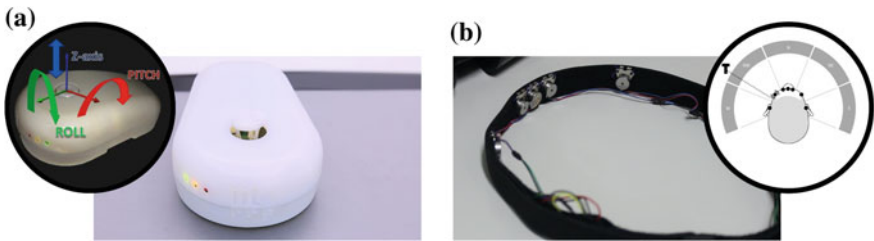


Fig. 1 a Tactile MOUSE 3 (TAMO3), and b a vibrotactile HMD



Fig. 2 Haptic system composed by the Tactile MOUSE 3 (TAMO3), and a vibrotactile HMD. While the TAMO3 supports the exploration of tactile maps from a *top-view*, the vibrotactile HMD provides an *ego-references* directional cue updated as a function of the TAMO3 movement



Fig. 3 The complementary feedbacks of our haptic system: vibrotactile HMD egocentric representation (*right*) and TAMO3 allocentric one (*left*)

In our system, the HMD can provide the direction of an object, but does not provide details about the environment. Additionally, the TAMO3 does not provide directional cues, but provides important cues about the explored area (e.g. shape, dimension, and elevation). Therefore, we hypothesize that only coupling the feedback of both devices, the user can integrate egocentric and allocentric frame systems to perform the task easily and rapidly.

3 Tactile Treasure Hunt

To show how simple it is to use this haptic system, we have built a blind treasure hunt with several treasure boxes hidden inside virtual dips. That simple task can demonstrate how subjects are able to go from a start point to a desired destination just by following the haptic cues provided by the system. Moreover, it will function as a serious game. In this entertaining task, the participants will play as pirates, seeking out for as many treasure boxes as they can in a given time. While the position of the dip is signaled by the vibrotactile HMD, the slope of the terrain can be felt with the TAMO3 (see Fig. 3).

4 Aimed Results

The integrated haptic system provides both egocentric and allocentric cues, in tactile modality. The system should give autonomy to the subject in order to choose when to receive each cue. Even if the use of both cues should made the tactile exploration richer, the subject's autonomy would support the study about the preferences for different reference frames during haptic exploration. Thus, a set of contributions is expected from this setup:

- The integrated haptic system can provide complete support for tactile exploration of virtual maps;

- It should be used to improve O&M training and the acquirement of spatial information;
- The system should provide more autonomy to the user when choosing a convenient reference frame;
- The system should allow the user to perform O&M training remotely (e.g. at home);
- The components of the system can work together and separated, so the HMD can also be used during the actual navigation task to recover the direction of landmarks;
- The system can provide a setup to sequentially verify the use of allocentric and egocentric perspective in the creation of a mental representation of space;
- The system can also be used for different applications, such as the exploration of virtual environments and a virtual desktop application.

Further experiments would allow us to verify the usability of the system and the adoption of reference frames during tactile exploration.

References

1. Cuturi, L.F., Aggias-Vella, E., Campus, C., Parmiggiani, A., Gori, M.: From science to technology: orientation and mobility in blind children and adults. *Neurosci. Biobehav. Rev.* **71**, 240–251 (2016)
2. de Jesus Oliveira, V.A., Nedel, L., Maciel, A., Brayda, L.: Localized magnification in vibrotactile hmds for accurate spatial awareness, pp. 55–64 (2016)
3. Gramann, K., Onton, J., Riccobon, D., Mueller, H.J., Bardins, S., Makeig, S.: Human brain dynamics accompanying use of egocentric and allocentric reference frames during navigation. *J. Cogn. Neurosci.* **22**(12), 2836–2849 (2010)
4. Kappers, A.M.: Haptic space processing-allocentric and egocentric reference frames. *Can. J. Exp. Psychol./Revue canadienne de psychologie expérimentale* **61**(3), 208 (2007)
5. Lécuyer, A., Mobuchon, P., Mégard, C., Perret, J., Andriot, C., Colinot, J.P.: Homere: a multimodal system for visually impaired people to explore virtual environments. In: *Virtual Reality, 2003. Proceedings. IEEE*, pp. 251–258. IEEE (2003)
6. Memeo, M., Brayda, L.: How geometrical descriptors help to build cognitive maps of solid geometry with a 3d of tactile mouse, pp. 75–85 (2016)
7. Memeo, M., Campus, C., Lucagrossi, L., Brayda, L.: Similarity of blind and sighted subjects when constructing maps with small-area tactile displays: performance, behavioral and subjective aspects. In: *Haptics: Neuroscience, Devices, Modeling, and Applications*, pp. 292–300. Springer (2014)
8. Parente, P., Bishop, G.: Bats: the blind audio tactile mapping system. In: *Proceedings of the ACM Southeast Regional Conference*, pp. 132–137. Citeseer (2003)
9. Rieser, J.J., Hill, E.W., Talor, C.R., Bradfield, A., Rosen, S.: Visual experience, visual field size, and the development of nonvisual sensitivity to the spatial structure of outdoor neighborhoods explored by walking. *J. Exp. Psychol.: General* **121**(2), 210 (1992)
10. Ruggiero, G., Ruotolo, F., Iachini, T.: The role of vision in egocentric and allocentric spatial frames of reference. *Cogn. Process.* **10**, 283–285 (2009)
11. Schloerb, D.W., Lahav, O., Desloge, J.G., Srinivasan, M.A.: Blindaid: virtual environment system for self-reliant trip planning and orientation and mobility training. In: *2010 IEEE Haptics Symposium*, pp. 363–370. IEEE (2010)

12. Schmidt, S., Tinti, C., Fantino, M., Mammarella, I.C., Cornoldi, C.: Spatial representations in blind people: the role of strategies and mobility skills. *Acta Psychologica* **142**(1), 43–50 (2013)
13. Tinti, C., Adenzato, M., Tamietto, M., Cornoldi, C.: Visual experience is not necessary for efficient survey spatial cognition: evidence from blindness. *Q. J. Exp. Psychol.* **59**(7), 1306–1328 (2006)

Motion-Based Augmented Broadcasting System with Haptic Feedback

Yeongmi Kim, Davud Sadikhov, Kaspar Leuenberger, Beomseuk Choi,
Youngho Jeong, Matthias Harders and Roger Gassert

Abstract This paper introduces a motion-based augmented broadcasting system enabling haptic, auditory, and visual augmentation of conventional television content. An entertainment use case scenario of the proposed system is presented that comprises haptic feedback for playing along with a TV show using virtual musical instruments. In a preliminary study, the influence of providing haptic feedback as well as visual body skeleton augmentation on the performance in selecting an interactive virtual object in the augmented broadcasting system is examined. While the methods of presentation did not show significant improvements, users clearly favored haptic feedback for interaction.

Keywords Augmented broadcasting · Depth estimation · Motion haptic gloves

Y. Kim (✉)
Department of Mechatronics, MCI, Innsbruck, Austria
e-mail: yeongmi.kim@ci.edu

D. Sadikhov · K. Leuenberger · R. Gassert
ETH Zurich, Zurich, Switzerland
e-mail: d.sadihov@ethz.ch

K. Leuenberger
e-mail: lkaspar@ethz.ch

R. Gassert
e-mail: gassertr@ethz.ch

B. Choi · Y. Jeong
ETRI, Daejeon, Korea
e-mail: bschoi@etri.re.kr

Y. Jeong
e-mail: yhcheong@etri.re.kr

Y. Kim · M. Harders
University of Innsbruck, Innsbruck, Austria
e-mail: matthias.harders@uibk.ac.at

1 Introduction

Augmented Reality (AR) has recently received great attention fueled by today's prevalence of smart phones and novel applications. One possible, but largely unexplored application domain of AR technology is TV broadcasting. Latest television systems allow interactive media control via face, gesture, or voice recognition. However, active interaction with broadcasting content is not yet supported, since conventional broadcasting systems provide only passive audiovisual (AV) streams. To mitigate this lack of interactivity, some attempts have been made to integrate haptic cues into broadcasting systems [1, 3–5]. However, in these cases haptic feedback was only streamed passively without modifying the AV media. Here we present an interactive augmented broadcasting system that aims to provide AV and haptic augmentation based on user's motion input.

When spatially interacting with augmented virtual objects, depth perception is often a concern due to typically encountered distance misestimations [6, 7]. Thus, appropriate feedback is required in order to alleviate such depth estimation errors. In this context, a preliminary study was conducted using the presented system to examine how the selection of interactive objects in augmented broadcasting can be made more efficient.

2 Interactive Augmented Broadcasting System

2.1 *Metadata and Test Platform for Augmented Broadcasting*

An initial augmented broadcasting testbed for mainly AV contents had been proposed in [2], for which the metadata concept of the MPEG-Augmented Reality Application Format (ARAF) was employed. We extend this framework by increasing interactivity and augmenting sensory feedback, specifically including motion-based haptic interaction. In our system, metadata for augmentation consists of time information, an augmentation region, the trajectory of the augmented object, synthesized multi-sensory cues (including haptic cues based on user motions), and environment information. The augmented broadcasting metadata, generated by an authoring server, is multiplexed with the traditional AV content, employing the MPEG-2 transport stream encoder. On a TV set-top box, the augmented broadcasting metadata is obtained by demultiplexing the streamed data (see [2] for details).

2.2 *Motion-Based Input Interface and Motion Haptic Gloves*

A Microsoft Kinect was employed to capture position and orientation of upper body joints of a user, including head, torso, as well as left and right shoulders, elbows,



Fig. 1 Haptic Motion Glove, comprising of 19 vibration motors embedded in a soft layer on the palm, bend sensors on fingers, as well as control/communication/IMU modules attached near the wrist

and hands. These joint data are used to visually depict a simplified upper body skeleton model. Spheres, connected by straight links, represent shoulders, elbows, and hands. Tracking of a user's body allows for active interaction with augmented objects. However, the tracking suffers from lower accuracy when estimating joint angles of the wrist or fingers. Therefore, we developed and included wearable haptic motion gloves to support not only more precise finger interaction, but also to provide augmented haptic feedback. Accurate tracking is achieved utilizing an inertial measurement unit (IMU) module on the wrist and bend sensors attached to each finger. Vibrotactile feedback is rendered to the hand through attached tactors (see Fig. 1). Vibration intensity and duration are controlled independently by a 16-bit PIC microcontroller (PIC24F16KL401). The spatial resolution of vibrotactile feedback was increased by employing haptic illusions, such as the Apparent Tactile Motion phenomenon and the Funneling illusion. With these it was possible to render more fluid motion patterns [4]. The tactile feedback can be generated either initially, at the authoring stage, or in real-time based on a user's motion.

3 Use Case Scenario

The presented components were integrated into an entertainment use case scenario to examine the feasibility of the augmented broadcasting system. An episode of the children's program *Town Musicians of Bremen* produced by the Educational Broadcasting System (EBS, Republic of Korea) was selected as example AV content. The scenario contains three stages with different levels of user involvement and interactivity, as detailed in the following.

Stage 1—Introduction: Initially, four musical instruments, i.e. a drum, castanets, a tambourine, and a triangle, are introduced to the user as AV content. In this stage, pre-authored haptic feedback matching the instrument playing sound is consecutively presented through the haptic gloves, independent of user motion. This introduction

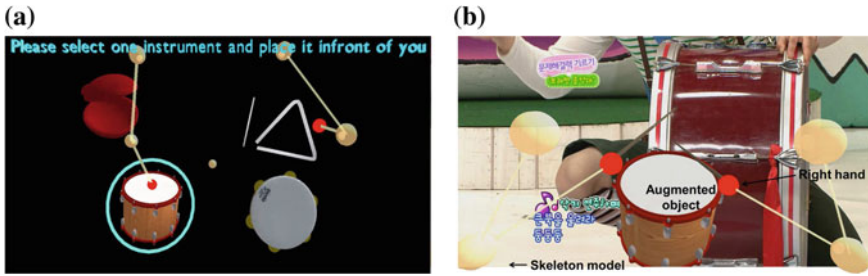


Fig. 2 **a** Interactive selection of an instrument. When a hand collides with an object, a *turquoise circle* appears around that instrument to provide apparent indication of a collision and avoid mis-estimated depth. The user can then select the object by closing the hand. **b** Skeleton model of a user tracked by a Kinect overlaid on the AV content. The *red spheres* represent the hands, the *semi-transparent beige spheres* correspond to the shoulders and elbows

was intended as a passive (but augmented) mode, more akin to conventional TV programs, but with tactile feedback.









Stage 2—Instrument Selection: In this stage, the user can select one of the four instruments (Fig. 2a) to interactively play along with the music in the next stage. To this end, the user has to reach out towards one of the 3D models presented on the TV screen. The Kinect tracks the user's movements, while the joints of the upper body are rendered via spheres. When the hand sphere (red) collides with the bounding box of an instrument model, the user can select it with a grasping movement by closing her hand (i.e. by passing a threshold on the bend sensor outputs). Auditory and haptic feedback is provided to confirm the choice of the user.

Stage 3—Augmented Interaction: After an instrument is selected, the user is able to participate and play along with the music and singing children in the streamed TV show. During this stage, the selected instrument as well as the upper body skeleton is visually overlaid on the screen as shown in Fig. 2b. Also, auditory and haptic content is augmented onto the AV broadcast. Unlike in Stage 1, the latter is now interactive and its behavior is influenced by the user's motion, thus mimicking active participation with the broadcasted program. Table 1 summarizes the sensing methods and the displayed haptic patterns for each instrument. Nevertheless, it should be noted that if a user desires not to receive any augmented haptic, visual or auditory stimuli, he or she can remain in a collision-free state or not select any interactive object, and thus only passively observe the material.

4 A Preliminary Study: The Effect of Augmented Visual and Haptic Feedback on Interactive Object Selection

In initial trials with novice users difficulties were encountered when selecting interactive objects without any visual indication of collision. Since for the time being no stereo rendering is provided, this is likely related to visual misestimation of depth.

Table 1 Sensing method and haptic patterns for each instrument

| Instrument | Sensing | Haptic pattern | Description |
|---|------------------------|---|--|
|  | Motion sensor (Kinect) |  | All motors of a glove are turned on with high intensity for a short period when the drum stick of the corresponding hand collides with the drum |
|  | Bend sensors |  | Vibration motors are activated sequentially to finger tips depending on the bending angle of the fingers |
|  | Accelerometer |  | Two groups of motors (marked in different colors) vibrate in turn with low intensity when the mean magnitude of 3DOF acceleration is above a certain threshold |
|  | Motion sensor (Kinect) |  | Two motors placed on the tip of thumb and index finger of the hand holding the triangle steel rod are activated when collision occurs |

To study this point further, we carried out a preliminary user study, how the visual representation of the user’s upper body skeleton and the provision of haptic feedback during object collision affect object selection performance. Similar to the previously described Stage 2, the experimental task consisted of reaching and grasping a high-lighted virtual 3D drum model. On the screen, four identical instruments were positioned in 3D space, all at the same distance, but translated diagonally from the central viewing axis. Eight healthy, right-handed subjects with mean age of 25.4 years participated in the study. Before the experiment, participants donned the motion glove on the right-hand and were familiarized with the system. For the trials they were positioned about 1.8–2.0 m from the Kinect and TV screen. At the beginning of each trial, subjects had to reach out and touch a cube rendered in the center position between the four drums until it changed color from green to light red to initialize the trial. Then, the cube disappeared and one of four blue spheres above the drums changed its color to red (in a pseudorandom order) to indicate the target. Subjects

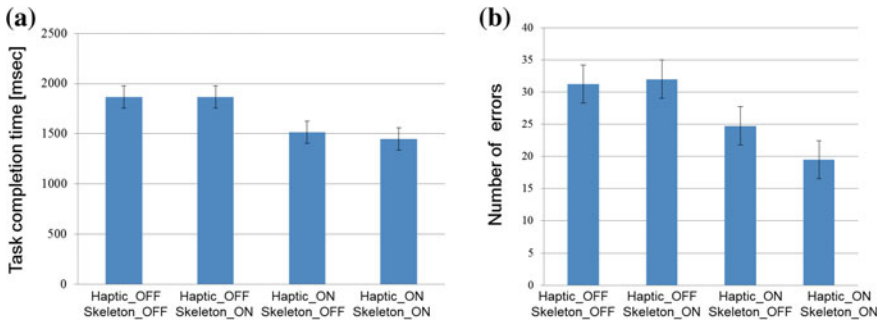


Fig. 3 Experimental results. **a** Mean task completion time, **b** number of accumulated errors during 100 trials per condition. The *error bars* indicate standard error

then had to reach out and select this target by closing their hand. Thereafter, the procedure was repeated.

Two experimental variables (i.e. haptic cues representing collisions and visual display of the upper body skeleton) were combined and tested for each subject. The four experimental conditions were: Haptic_OFF/Skeleton_OFF, Haptic_OFF/Skeleton_ON, Haptic_ON/Skeleton_OFF, Haptic_ON/Skeleton_ON. The five vibration motors on the fingertips were activated during collisions in the Haptic_ON case. Also, instead of visualizing the full skeleton model, a single sphere was depicted to indicate the user interaction point in the Skeleton_OFF condition. After 40 trials were completed in the familiarization phase, a total of 400 trials per subject were collected. At the end, participants were also asked about their preferred modes of feedback. In Fig. 3a, results show a trend of higher task completion times in the Haptic_OFF/Skeleton_OFF, and Haptic_OFF/Skeleton_ON conditions, than in the other two conditions. Similarly, the number of errors was also greater in the former conditions as shown in Fig. 3b. However, a 2×2 within-subjects ANOVA did neither reveal significant interaction ($p > 0.05$) nor significant main effects on task completion time (haptic cues ($p = 0.075$), skeleton display ($p = 0.692$)), or on number of errors (haptic cues ($p = 0.064$), skeleton display ($p = 0.406$)). Still, providing haptic cues led to an improved performance of more than 20% in mean task completion time and error rate. A Wilcoxon Matched Pairs Signed Rank test revealed that the haptic feedback condition was significantly preferred over the no haptic feedback condition by the users ($z = -2.828$, $p < 0.01$). In contrast, the skeleton display did not receive more favorable rankings than the display of the hand interaction point only ($z = -1.414$, $p = 0.157$).

5 Conclusion and Future Work

We have outlined a system enabling a user to both passively perceive haptic content streamed along with AV broadcasts, as well as to actively interact with virtual objects overlaid on the stream along with the AV data. In a preliminary study, the use of a visual upper body skeleton and haptic collision cues were examined to alleviate depth misestimations. However, these modes did not lead to significant improvements of performance. Still, user feedback and results hint at the possibility that haptic cues could still be beneficial, especially for more complex tasks. Several participants commented that they could rely less on visual cues when haptic feedback was provided, thus possibly reducing cognitive load. Finding optimal parameters for different user interactions will be useful when authoring augmented broadcasting content. Further studies incorporating more complex interactions with augmented objects will be carried out in the future to investigate these aspects.

Acknowledgements This work was supported by the ICT R&D program of MSIP/IITP, Rep. of Korea (11921-03001, Development of Beyond Smart TV Technology).

References

1. Cha, J., Ho, Y.S., Kim, Y., Ryu, J., Oakley, I.: A framework for haptic broadcasting. *IEEE MultiMed.* **16**(3), 16–27 (2009)
2. Choi, B., Kim, J., Kim, S., Jeong, Y., Hong, J.W., Lee, W.D.: A metadata design for augmented broadcasting and testbed system implementation. *ETRI J.* **35**(2), 292–300 (2013)
3. Danieau, F., Fleureau, J., Cabec, A., Kerbiriou, P., Guillotel, P., Mollet, N., Christie, M., Lécuyer, A.: Framework for enhancing video viewing experience with haptic effects of motion. In: *Haptics Symposium (HAPTICS)*, 2012 IEEE, pp. 541–546. IEEE (2012)
4. Israr, A., Poupyrev, I.: Exploring surround haptics displays. In: *CHI'10 Extended Abstracts on Human Factors in Computing Systems*, pp. 4171–4176. ACM (2010)
5. Kim, Y., Ryu, C.J., Oakley, I.: Exploring tactile movies: an initial tactile glove design and concept evaluation. *IEEE MultiMed.* **17**(3), 33–43 (2010)
6. Nacéri, A., Chellali, R., Dionnet, F., Toma, S.: Depth perception within virtual environments: comparison between two display technologies. *Int. J. Adv. Intell. Syst.* **3**(1 and 2), 51–64 (2010)
7. Renner, R.S., Velichkovsky, B.M., Helmer, J.R.: The perception of egocentric distances in virtual environments—a review. *ACM Comput. Surv. (CSUR)* **46**(2), 23 (2013)

Perceiving Physical Attributes of Objects Using an Electrostatic Tactile Display

Xiaoying Sun, Jian Chen, Guohong Liu and Hui Long

Abstract Based on the physical principle that the Coulomb force exerted on a finger affects the attractive and frictional felt by the finger sliding through a surface, An electrostatic force tactile approached is proposed, and a related display based on Windows is also developed. With this display, not only the information of static images, including shapes, textures and softness of objects, is perceived realistically, but the contents of dynamic videos are also presented in real-time. Two typical applications referring to the primary education and the auxiliary visually impaired people are exploited to demonstrate the potential practical value of this prototype.

Keywords Tactile representation · Electrostatic tactile · Electro vibration · Touch screen

1 Introduction

Tactile display can perceive the shape, texture and softness of object displayed on multimedia terminal [1], which will improve the interaction between human and virtual world to a new stage with the three dimensional fusion of auditory, visual and tactile [2]. In recent years, tactile display is a hot research topic, and it has great potential in electronic commerce, education, entertainment, as well as visually impaired people applications [3].

Electrostatic force tactile representation is a major research direction of tactile display, and it has obvious characteristics such as real-time, low-power and high-bandwidth. TeslaTouch [4], as the most typical prototype, was designed by Olivier Bau from Disney Research in Pittsburgh [5], and has been successfully applied in

This work is supported by the National Science Foundation of China (Grant 61631010) and the '863' Research Project of China (Grant 2013AA013704).

X. Sun · J. Chen · G. Liu (✉) · H. Long
The College of Communication Engineering, Jilin University,
Changchun 130025, Jilin, China
e-mail: liugh10@mails.jlu.edu.cn

visually impaired people application and navigation. In this study and accompanied video, we demonstrate a novel electrostatic force tactile display prototype, which realistically perceives the different attributes of the objects displayed in images and videos. In addition, eleven Interactive application software, such as the tactile representation experience software, the shape identification software and so on, has been developed to meet the requirement of different applications.

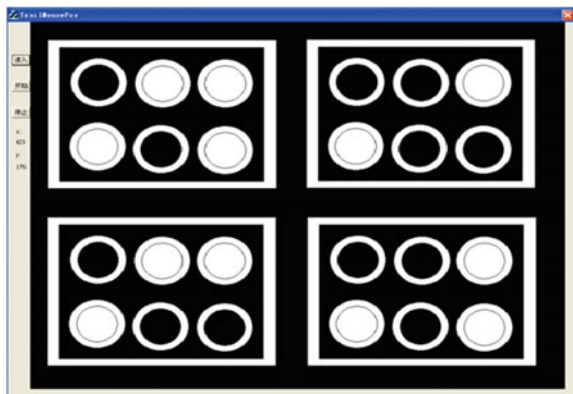
2 Electrostatic Force Tactile Display

The developed electrostatic tactile display based on Windows is shown in Fig. 1, and it consists of a Microsoft Surface, a Microtouch screen, an electrostatic tactile controlling module as well as a finger tracking module. The tactile controlling actuation generates the tactile stimuli signal and loads to the Microtouch screen, then

Fig. 1 Electrostatic force tactile display



Fig. 2 Braille recognition applied in auxiliary visually impaired people



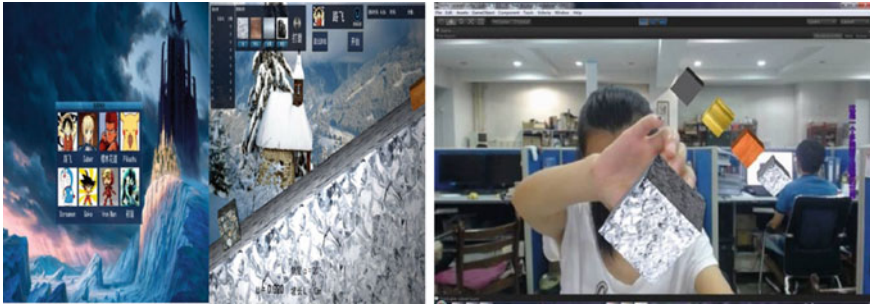


Fig. 3 Friction perception applied in primary education

the related tactile can be provided on the fingertip position. Compared to the previous works, our display makes users perceive multiple tactile by generating different stimuli signals.

3 Two Typical Applications

Braille recognition applied in auxiliary visually impaired people. As shown in Fig. 2, through touching the Braille displaying on the surface, the visually impaired people can obtain the text contents, which establishes an interaction bridge to the virtual world.

Virtual simulation applied in primary education. Referring to abstractive concepts, such as force, electromagnetic fields and thermal, which are invisible, imperceptible but objective, the virtual simulation software has been developed. Take friction perception for example, as shown in Fig. 3, through polishing the interface of different materials, the friction coefficient of the surface can be changed. After releasing the cube, students can obtain their scores. The higher these scores are, the more realistic friction force can be perceived.

References

1. Kaczmarek, K.A., Nammi, K., Agarwal, A.K., et al.: Polarity effect in electrovibration for tactile display. *Biomed. Eng. IEEE Trans.* **53**(10), 2047–2054 (2006)
2. Xia, P., Lopes, A.M., Restivo, M.T.: Virtual reality and haptics for dental surgery: a personal review. *Vis. Comput.* **29**(5), 433–447 (2013)
3. Kim, S.C., Israr, A., Poupyrev, I.: Tactile rendering of 3D features on touch surfaces. In: *Proceedings of the 26th Annual ACM Symposium on User Interface Software and Technology*, pp. 531–538 (2013)

4. Bau, O., Poupyrev, I., Israr, A., Harrison, C.: TeslaTouch.: electrovibration for touch surfaces. In: Proceedings of the 23rd Annual ACM Symposium on User Interface Software and Technology, pp. 283–292 (2010)
5. Bau, O., Poupyrev, I.: REVEL: tactile feedback technology for augmented reality. *ACM Trans. Graph. (TOG)* **89** (2012)

Hapbeat: Tension-Based Wearable Vibroacoustic Device

Yusuke Yamazaki, Hironori Mitake, Minatsu Takekoshi, Yuji Tsukamoto, Tetsuaki Baba and Shoichi Hasegawa

Abstract Hapbeat (Tension-based Wearable Vibroacoustic Device) enhances music appreciation and virtual reality experiences. It is a new type of wearable vibroacoustic device that can transmit a high fidelity acoustic vibration to the body. It consists of two coreless motors and Ultra High Molecular Weight Polyethylene string. The motors generate a vibration in the range of 0–600 Hz and the string transmits this vibration. If compared with other existing device, Hapbeat can generate a powerful low frequency vibration and can transmit vibration to the wide range of the user's body in spite of its compact body.

Keywords Vibroacoustic device · Music listening · Virtual reality · Wearable device · Haptic

1 Introduction

When listening to music, we can feel excitement not only because of the sound that we hear but also the vibrations that we feel in our body. Such a case is attending a live music performance, which can be more exciting than listening to the same music at home. The heightened excitement might be due to a number of factors, such as the sense of unity with other fans and the vibration of the music transmitted through the body. This paper focuses on this vibration, known as acoustic vibration. Acoustic vibration is a phenomenon perceived by our somatosensory system. The joy of listening to music is enhanced by low-frequency vibrations. To simulate such vibrations for the benefit of music listeners, several indoor vibroacoustic devices (some of which are referred to as “body sonic system”) have been developed [1]. Conventional vibroacoustic devices take the form of chairs or beds with transducers that are located along the user's back to enhance the musical experience.

Y. Yamazaki (✉) · H. Mitake · S. Hasegawa
Tokyo Institute of Technology, Tokyo, Japan
e-mail: yus988@haselab.net

M. Takekoshi · Y. Tsukamoto · T. Baba
Tokyo Metropolitan University, Tokyo, Japan

© Springer Nature Singapore Pte Ltd. 2018
S. Hasegawa et al. (eds.), *Haptic Interaction*, Lecture Notes
in Electrical Engineering 432, DOI 10.1007/978-981-10-4157-0_65

In addition, the effects of these vibroacoustic devices relating to relaxation and the suppression of pain are appreciated [2–5] and many dental clinics and relaxation facilities have thus introduced such systems. Similar systems, which transmit sound vibration effects, are used in entertainment facilities such as theme park attractions and 4DX movie theaters. Furthermore, Uematsu et al. developed HALUX to cope with the latency between a driver and vibrators by using a projector [6]. Konishi et al. developed Synesthesia Suit, the full body vibro-tactile suit, to enhance the experience of virtual reality gaming [7]. Despite the effects, vibroacoustic devices are only used in special facilities and are not yet popular in terms of the daily experience of listening to music. This might be explained by the size, cost, and usability of such systems. To cope with the issue, Sakuragi et al. proposed to attach the vibrator on the collarbone and transmit the music vibration via bone conduction [8]. In the previous paper, we proposed a light, wearable and effective vibroacoustic device that contains a string and two motors and can be used as easily as earphones [9]. In this paper, we developed the device in terms of productization; we focused on miniaturization, heat generation, usability, and design. We believe it has the potential to become a new standard tool for music appreciation.

2 Device Description

We propose a new vibroacoustic device (Figs. 1 and 2), namely Hapbeat that includes two motors and a string. The string is worn on the user's body and pulled by two motors (Fig. 1a) whose current is controlled by an audio amplifier. When music signal is detected, the shaft begins to rotate and the rotational directions change quickly. The motors transmit the vibration to the string mounted on a pulley (Fig. 1b) and the user then feels the vibration from the string. The proposed device has two important advantages over vibrators. First, it can transmit the vibration to a wider area of

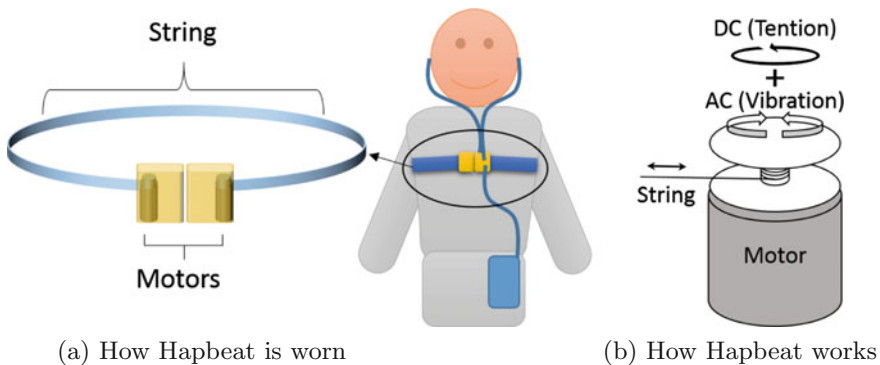
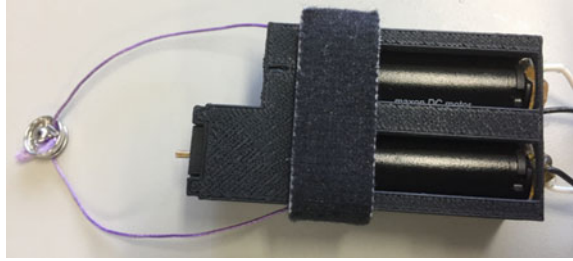


Fig. 1 Image of Hapbeat

Fig. 2 Picture of prototype

the body than conventional vibrators owing to the difference in the contact region between the string and vibrators. While vibrators only contact limited surfaces of the user's body, the string can be worn around the body. Second, DC motors are good at playing low frequencies [10]. Small vibrators are limited in terms of their linear stroke, which in turn limits the amplitude of low-frequency vibration. Meanwhile, motors of any size have no restriction because they can rotate infinitely (Fig. 1b).

2.1 Detailed Description

Motors We use coreless motors. The advantage of coreless motors is responsiveness. It is the most important factor because the direction of rotation is changing rapidly when it plays music vibration especially in high frequency.

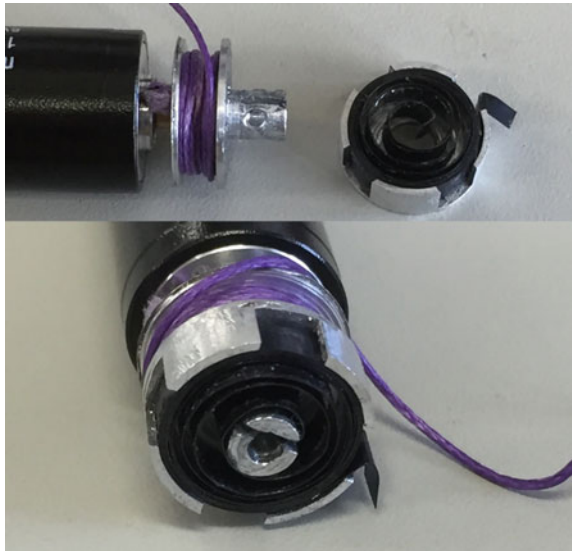
String We use Ultra High Molecular Weight Polyethylene string (Ultra 2 Dyneema No.3, YGK YOZ-AMI Co., Ltd.). The advantages of this material are: its high rigidity, low weight, and low coefficient of friction. These factors are important for transmitting the vibration efficiently and with high fidelity.

Miniaturization In putting into practical use as a wearable device, size and weight should be small as possible. Figure 3 shows the picture of the motors. We chose the motor (Model number 118462, Maxon Moter) which is 13 mm in diameter and 21 g in weight, while the motor used in a previous prototype are 24 mm in diameter and its weight is 71 g. But the heat generation of these motors is a serious problem, consequently that can not be attached to the user's body, and the motors may have a break down caused by overheating. The main factor of the heat generation is direct current used for generating the tension of string by using the motor power. To solve this problem, we used a spiral spring to generate the tension instead of using the motor power (Fig. 4). We tested the differences of the power consumption and the quality of the vibration between the prototypes using the spring (namely NEW) and not (namely Prev.). The power consumption of NEW is 0.59 W and that of Prev. is 2.72 W under the following conditions: we used 100 Hz sinusoidal wave and the active voltage of the audio amplifier output was 1.04 V. To confirm the quality of the vibration of NEW and Prev., we attached an accelerator sensor on the string and checked the wave by using an oscilloscope. Although the shape of the vibration of

Fig. 3 Comparison



Fig. 4 Pulley and spiral spring



Prev. was clear and similar to the wave from the amplifier, we found some noises from that of NEW. Therefore, the quality of the vibration decreases by using the spring. Therefore, we have to verify how the experience is affected by the noises.

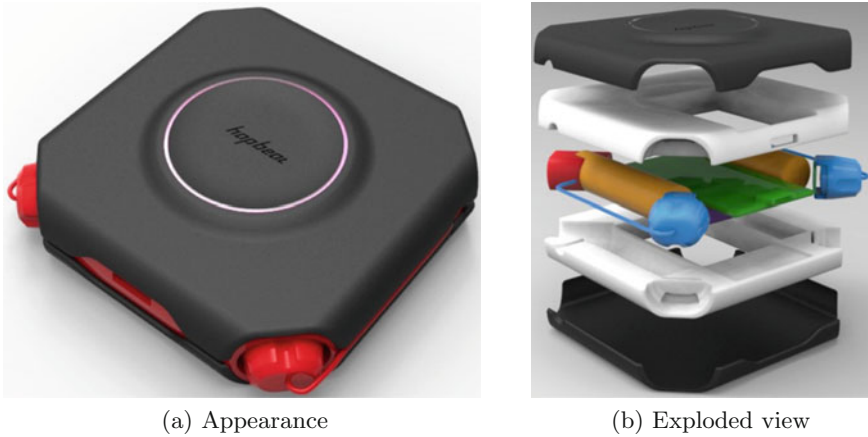


Fig. 5 Design of Hapbeat

Usability To improve an usability, we decided to include following features: a wireless module, a battery, and an amplifier. The previous prototype needed an external power supply and audio amplifier, and it was connected to the audio source with a cable. These factors make the prototype hard to use.

Design Figure 5 shows the idea of the design. To afford a comfortable wear feeling, we formed the edges rounded (Fig. 5a). In the front, we form a ring-shaped mound representing a vibration wave and embed LED. The LED is not only used for illumination but also for an indicator that shows the condition of the device e.g. waiting or playing. The outer case consists of four different parts to simplify its maintenance (Fig. 5b). Also, it can easily dismantled by taking off the screw at the back side of the case.

Acknowledgements This work was supported by JSPS KAKENHI Grant Number JP26280072.

References

1. Komatsu, A.: US Patent 6369312 B1 (2002)
2. Patrick, G.: The effects of vibroacoustic music on symptom reduction. *IEEE Eng. Med. Biol. Mag.* **18**(2), 97–100 (1999)
3. Naghdi, L., Ahonen, H., Macario, P., Bartel, L.: The effect of low-frequency sound stimulation on patients with fibromyalgia: a clinical study. *Pain Res. Manag.* **20**(1), e21–e27 (2015)
4. Kvam, M.H.: The effect of vibroacoustic therapy. *Physiotherapy* **83**(6), 290–295 (1997)
5. Boyd-Brewer, C.: Vibroacoustic therapy: sound vibrations in medicine. *Altern. Complement. Ther.* **9**(5), 257–263 (2003)
6. Uematsu, H., Ogawa, D., Okazaki, R., Hachisu, T., Kajimoto, H.: Halux: projection-based interactive skin for digital sports. In: *ACM SIGGRAPH 2016 Emerging Technologies*, p. 10. ACM (2016)

7. Konishi, Y., Hanamitsu, N., Minamizawa, K., Sato, A., Mizuguchi, T.: Synesthesia suit: the full body immersive experience. In: ACM SIGGRAPH 2016 VR Village, p. 20. ACM (2016)
8. Sakuragi, R., Ikeno, S., Okazaki, R., Kajimoto, H.: Collarbeat: whole body vibrotactile presentation via the collarbone to enrich music listening experience. In: Proceedings of the 25th International Conference on Artificial Reality and Telexistence and 20th Eurographics Symposium on Virtual Environments, pp. 141–146. Citeseer (2015)
9. Yamazaki, Y., Mitake, H., Hasegawa, S.: Tension-based wearable vibroacoustic device for music appreciation. In: International Conference on Human Haptic Sensing and Touch Enabled Computer Applications, pp. 273–283. Springer (2016)
10. Yem, V., Okazaki, R., Kajimoto, H.: Vibrotactile and pseudo force presentation using motor rotational acceleration. In: 2016 IEEE Haptics Symposium (HAPTICS), pp. 47–51. IEEE (2016)

Comparison of Tactile Signals for Collision Avoidance on Unmanned Aerial Vehicles

Stefan Spiss, Yeongmi Kim, Simon Haller and Matthias Harders

Abstract Our recent work focused on the development of intuitive user interfaces for the control of unmanned aerial vehicles, such as quadcopters. Next to intuitive gesture control, a key challenge with remotely operated quadcopters is the display of information about the aircraft surroundings. To this end, we examined the use of rendering tactile stimuli to warn about nearby obstacles. Directional information and distance is encoded via vibrotactile signals from rotating mass motors. Three different methods of delivering the tactile feedback were tested in a user study. Results show that even though participants guided the quadcopter through a maze by tactile stimuli alone, they were, on average, able to avoid full crashes. Further, we found that using sequential signals to indicate obstacles lead to significantly increased numbers of wall contacts.

Keywords Quadcopter · Haptic · Vibrotactile feedback · User interface

1 Introduction

Unmanned aerial vehicles (UAVs) are flight systems that do not carry a pilot, but are, in general, remotely controlled. Due to this, they are often smaller and more efficient. Also, no crew is put in possible danger during flight [1]. A key challenge for an operator is the loss of situational awareness of and knowledge about the surroundings of the aircraft. In most cases, UAVs are equipped with forward facing cameras to provide a video stream to the ground station. However, information about obstacles not in camera view is not readily available, which can be a problem in difficult environ-

S. Spiss (✉) · S. Haller · M. Harders
Department of Computer Science, University of Innsbruck, Innsbruck, Austria
e-mail: stefan.spiss@student.uibk.ac.at

M. Harders
e-mail: matthias.harders@uibk.ac.at

Y. Kim
Department of Mechatronics, MCI, Innsbruck, Austria

ments, for instance in indoor rescue operations. Especially for quadcopters this is of concern due to their omnidirectional maneuverability.

In related work, the use of tactile feedback has been examined for cockpits [10] as well as for waypoint navigation of pedestrians, helicopter pilots, and boat drivers [8]. Using a vibrotactile waist belt led to performance improvement after only short familiarization. A similar application area is the use of tactile feedback for collision prevention and navigation in cars, e.g. [3, 6]. Moreover, related systems have also been employed as electrical travel aids for visually impaired persons to warn about obstacles [4, 5]. Generally, designs often take the form of torso- [9] or belt-type displays [7]. The work closest to ours is by Brandt and Colton [2], who developed a collision avoidance system for quadcopters using a kinesthetic force-feedback device. In this paper, vibrotactile signals are employed for providing directional cues in the horizontal plane. Also, optimal tactile feedback encoding patterns are explored in a user study.

2 System Overview

Quadcopter: We employ the *AR.Drone 2.0* from *Parrot*, shown in Fig. 1 (left). It comprises two cameras (one forward-, one downward-facing), an inertial measurement unit, a pressure sensor, and an ultrasound sensor. The video streams as well as the sensor data are sent over a WiFi network to a PC, using the Parrot SDK. To provide more intuitive control of the quadcopter, we built an intuitive gesture-controlled system, consisting of the MYO bracelet, the Leap Motion controller, and the Oculus Rift. Various head- and hand-gestures allowed the operator to fly the drone in an intuitive manner (see Fig. 1 (middle)). Redundancy in the control signals made the overall system more robust to noisy sensor readings. Nevertheless, the focus of this work is the tactile display of obstacle information, which will be outlined next.

Tactile Feedback Display: A vibratory signaling mechanism was developed to inform users about obstacles around the UAV. The display is comprised of four eccentric rotating mass motors. In the current state, we only encode horizontal directions, i.e. front, back, left, right. The left and right tactors are placed outwards on the



Fig. 1 Quadcopter (*left*), gesture-based control, here with MYO bracelet, Oculus Rift (*middle*), Gazebo drone model, with virtual ultrasound sensors (*right*)



Fig. 2 3D model of tactor holder (*left*), user wearing attached tactors (*right*)

upper arms, the tactor in the back is located in the lower part of the back, and the one in front on the abdomen, below the solar plexus (Fig. 2 (right)). Each motor is placed inside a specially designed holder, shown in Fig. 2 (left); the latter being attached with Velcro to the body. The motors are controlled via pulse-width modulation using an *Atmega328p*. Tactile feedback is rendered according to the distance of obstacles detected in the surrounding of the quadcopter, such supporting the operator in collision awareness and avoidance. Various options for encoding this information via tactile signals exist, wherefore a user study was planned to evaluate the performance. Since an experimental metric would be the number of wall contacts as well as drone crashes, which would potentially damage the quadcopter, we opted for using a simulation of the quadcopter for the experiment. The underlying framework is introduced in the following.

Simulation/Control Framework: For our project, we employ the *Robot Operating System* ROS (<http://www.ros.org/about-ros>)—a framework that can be used for robot development. In order to control the AR.Drone with ROS, the *ardrone_automation* ROS driver (http://wiki.ros.org/ardrone_automation) was used, which is based on the official *AR-Drone SDK 2.0.1* (<http://ardrone2.parrot.com>). For the simulation of the quadcopter the *Gazebo framework* (<http://gazebo.org>) was employed (see Fig. 1 (right) for a depiction), which is a robot simulator that supports ROS. The virtual drone representation is based on the ROS package *tum_simulator* (http://wiki.ros.org/tum_simulator). Note that for the user experiment virtual ultrasound sensors were attached to the outside of the quadcopter model to obtain accurate distance information in the horizontal flight plane. Further, a new ROS node was implemented to render tactile feedback according to detected obstacles.

3 Experiment

3.1 Methods

A user study was conducted to compare the performance of three different tactile obstacle encoding methods, in terms of efficiency and safety. The methods differ in the way information about obstacles is displayed to a participant. For the latter,

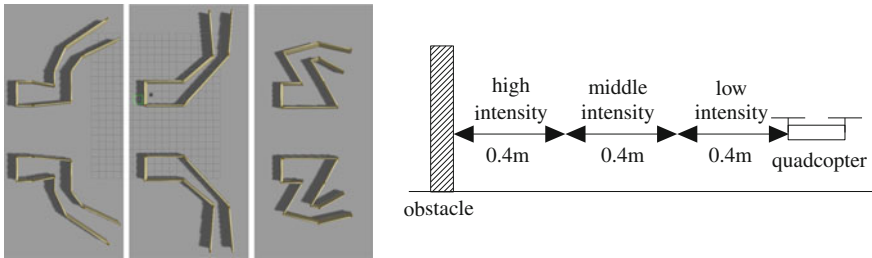


Fig. 3 Mazes used for tactile feedback experiment, each image showing one maze class (*left*), distance intervals used for different tactile intensities (*right*)

obstacle distance is encoded by intensity for three different range intervals, whereas a direction is encoded by activation of one of the tactors. Therefore, it is possible to give warnings for the four distances, left, right, front and back.

In the first method (*nearest only*), only information about the nearest obstacle is displayed. Thus, stimuli due to any other potentially close, but slightly further away obstacles are not generated. The second method (*all simultaneous*) presents feedback for any nearby detected obstacles, on all tactors simultaneously. In this paradigm, up to four tactors may be activated. In the third method (*all alternating*), all detected obstacles are rendered too, however, the corresponding tactile signals are presented sequentially. For the experiment, virtual environments with obstacles (i.e. three different maze classes, consisting of an original maze and its mirrored version) were designed in the Gazebo simulator, as illustrated in Fig. 3 (left). The goal was to navigate these mazes, from a starting position to the finish line. The starting point was always one meter away from the back wall and in the middle of the corridor. The maximum width of all corridors was 3 m, whereas the minimum width was about 1.3 m. The length from start to finish, along the centerline in the corridors, was 17 m in all mazes. As goal line/plane that had to be crossed, the connection between the two ending wall edges was employed. Three intensities of vibratory feedback were applied for encoding equally sized distance intervals. High intensity (~ 2.0 g) was rendered, when an obstacle was closer than 0.4 m, middle intensity (~ 1.3 g) for 0.4–0.8 m, and low intensity (~ 0.8 g) for obstacles at 0.8–1.2 m, respectively (see Fig. 3 (right)), and no signal for larger distances. Thus, when the quadcopter stayed on the centerline in a corridor with maximum width, no feedback was presented. All tactile signals were displayed for 1/6 s, whereas the inter-stimulus interval was set to 1/12 s. Although the simulated quadcopter could be controlled via the developed gesture-based interface, we decided to use an Xbox gamepad controller, to avoid distraction due to the interface. Moreover, the altitude of the quadcopter was fixed. Thus, it was not required to manually start or land the drone.

Ten male participants with a mean age of 23.5 years took part in the experiment. They were mainly recruited at the university and did not receive financial compensation. It was required that all subjects had prior experience with using the gamepad controller, to minimize possible learning effects. All participants were familiarized

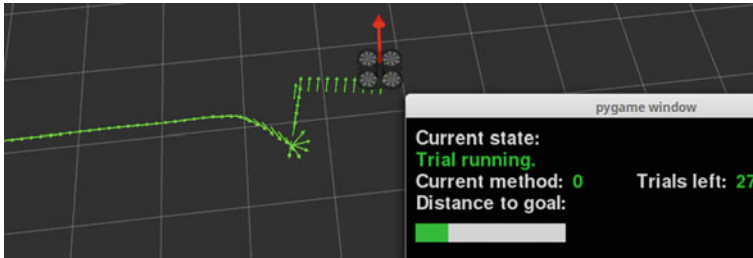


Fig. 4 Visual aid for participants during experiment

with the control and the environment in a training scene. During this, the mazes were visible so that subjects could get used to the quadcopter control, see what is happening when crashing, and to get to know the different feedback methods. Following this, participants had to fly through test training mazes, at least two times per method, under the full experimental condition. For the experiment, subjects were asked to fly through mazes as fast and accurate as possible, while avoiding any crashes. During the experiment the mazes became invisible. However, as visual cues the prior trajectory, as well as the drone forward orientation was shown on a grid (top-down view) (see Fig. 4). On the screen, a box with information on the trial was displayed, showing e.g. the remaining path distance to the goal. Moreover, various events in a trial were encoded with acoustic messages, e.g. the re-/start of a trial or the crash of the drone. The tactile encoding methods and mazes were pseudo-randomly presented, for each method, each maze class three times, resulting in 27 trials per subject. As outcome measurements the number of wall contacts, the time of contact, the travelled distance, the number of crashes, the time of crashes, the trial completion time and the trajectory were captured. Note that real and simulated drones can contact walls without directly crashing. When a (simulated) crash occurs, the quadcopter is reset to a prior position from where the trial can be continued. At the end of an experiment, subjects were asked about their preference of tactile encoding methods using a questionnaire.

3.2 Results

A repeated measures ANOVA revealed that there were significant differences in the number of contacts for the rendering methods ($F(2.0, 18.0) = 7.445$, $p = 0.004$), as well as for the duration of contact ($F(2.0, 18.0) = 8.601$, $p = 0.002$). Post-hoc tests employing Bonferroni correction showed that the *nearest only* method (5.36 ± 1.63 contacts per run) lead to significantly fewer contacts than the *all alternating* method (6.88 ± 1.54 contacts per run), ($p = 0.032$). In Fig. 5 (left), these results are depicted as boxplots. Further, there were significant differences in contact duration between *nearest only* ($p = 0.023$) as well as *all simultaneous* ($p = 0.027$) condition,

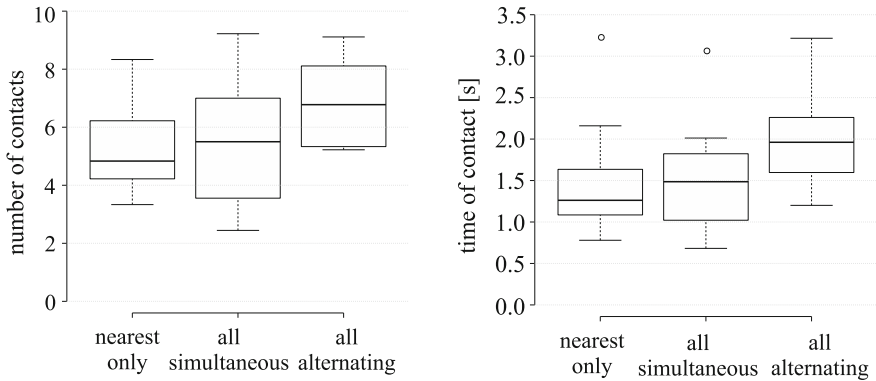


Fig. 5 Number of contacts (*left*), duration of contacts (*right*); with Tukey whiskers for data points at most $1.5 * IQR$ away from first or third quartile

with respect to the *all alternating* method (see Fig. 5 (right)). No significant results were found in other measurements, such as flight time, traveled distance, number of crashes, or time of crashes ($p > 0.05$). The mean number of crashes per flight, for all subjects and methods, was < 0.34 . Moreover, a rank ordered preference for the three coding methods, as specified by the users, was examined via a Friedman test. Results show that there is a significant rank ordered preference ($\chi^2(2) = 8.667$, $p = 0.013$). A post-hoc Nemenyi test indicates that the *all simultaneous* method was clearly preferred over the other two ($p = 0.01$ and $p = 0.037$).

4 Conclusion

In this paper an intuitive interface, comprising tactile feedback devices, for controlling quadcopters was introduced. In order to provide warnings about surrounding obstacles, three different tactile display methods were examined: feedback for only the nearest obstacle, for all detected obstacles simultaneously, and for all obstacles, but sequentially. The results of the user study indicate that the *all alternating* method provides lower performance in contact avoidance than the other two. In addition, the low mean number of crashes per flight of 0.34 shows that a majority of participants was able to control the flight of the quadcopter by tactile feedback only. Overall, it appears recommendable to employ tactile feedback in addition to the video stream shown in the HMD in our setup. In the future, the tactile feedback should be extended to present warnings about obstacles below and above the quadcopter too. Moreover, the tactile feedback system should be tested in reality on an actual quadcopter and not only in a simulator. However, appropriate safety measures have to be taken. Finally, the combination with the HMD and the gesture-based control should be tested too.

References

1. Austin, R.: Unmanned aircraft systems: UAVS design, development and deployment, vol. 54. Wiley (2011)
2. Brandt, A., Colton, M.: Haptic collision avoidance for a remotely operated quadrotor uav in indoor environments. In: Systems Man and Cybernetics, pp. 2724–2731 (2010)
3. Ho, C., Reed, N., Spence, C.: Assessing the effectiveness of “intuitive” vibrotactile warning signals in preventing front-to-rear-end collisions in a driving simulator. *Accident Anal. Prev.* **38**(5), 988–996 (2006)
4. Kim, Y., Harders, M., Gassert, R.: Identification of vibrotactile patterns encoding obstacle distance information. *IEEE Trans. Haptics* **8**(3), 298–305 (2015)
5. Pyun, R., Kim, Y., Wespe, P., Gassert, R., Schneller, S.: Advanced augmented white cane with obstacle height and distance feedback. In: 2013 IEEE International Conference on Rehabilitation Robotics (ICORR), pp. 1–6. IEEE (2013)
6. Scott, J., Gray, R.: A comparison of tactile, visual, and auditory warnings for rear-end collision prevention in simulated driving. *Hum. Factors: J. Hum. Factors Ergon. Soc.* **50**(2), 264–275 (2008)
7. Tsukada, K., Yasumura, M.: Activebelt: belt-type wearable tactile display for directional navigation. In: International Conference on Ubiquitous Computing, pp. 384–399 (2004)
8. Van Erp, J., Van Veen, H., Jansen, C., Dobbins, T.: Waypoint navigation with a vibrotactile waist belt. *ACM Trans. Appl. Percept.* **2**(2), 106–117 (2005)
9. Van Erp, J.B.: Presenting directions with a vibrotactile torso display. *Ergonomics* **48**(3), 302–313 (2005)
10. Van Veen, H.A., Van Erp, J.B.: Tactile information presentation in the cockpit. In: Haptic Human-Computer Interaction, pp. 174–181. Springer (2001)

Data-Driven Rendering of Anisotropic Haptic Textures

Arsen Abdulali and Seokhee Jeon

Abstract It is common to interact with a wide range of surfaces with anisotropic haptic textures in our daily life. However, the rendering techniques were not capable of incorporating the directional grain in a virtual world. In our previous work, we have proposed a data-driven model for anisotropic haptic textures, which stores and interpolates contact vibration patterns. In this paper, we have developed a complementary rendering algorithm. This algorithm has been implemented in form of a cross-platform computing library, and deployed to the tablet-PC-based demonstration setup. A set of eight anisotropic and one isotropic textures is prepared for the demonstration. Two demonstration scenarios have been provided for the realism evaluation.

Keywords Data-driven rendering · Anisotropic texture · RBF networks

1 Introduction and Background

Nowadays, the virtual and real worlds are on the verge of being undistinguishable by human. The immersion into virtual reality is due to high fidelity displays and sophisticated rendering algorithms. Modern rendering algorithms are interactive meaning that they produce feedback accordingly to the physical input of the user. In order to produce a realistic feedback of a touch, the rendering algorithm should consider not only object properties as an input, but the physical input of a user as well.

One of the most complex rendering techniques is haptic texture rendering. The interaction with a surface texture happens either bare-handed [5] or using a tool [2]. In both cases a perceived response changes accordingly to the physical input, such as a stroking velocity and direction, a pushing force, etc.

A. Abdulali · S. Jeon (✉)

Department of Computer Science and Engineering, Kyung Hee University,
Yongin-si 446-701, Republic of Korea
e-mail: jeon@khu.ac.kr

A. Abdulali
e-mail: abdulali@khu.ac.kr

The output response in modern haptic texture rendering algorithms is decided based on the model. The model can be physics based, where the physical process of the touch is simulated, or data-driven, where the model is built based on measurements of real interactions. One of the most successful data-driven model of the haptic texture is evolved in a research group lead by Culbertson et al. [2, 3]. Their model maps the normal force and velocity magnitude of the contact with vibration patterns that are propagated through the tool during tool-surface interaction. These vibration patterns are encoded in autoregressive (AR) coefficients. The rendering application of this model is available in their recent work [3], where they also introduced a library with one-hundreded virtual object surfaces. Since this model is limited to homogenies isotropic textures, a wide range of anisotropic surfaces could not be modeled. Recently, an alternative solution was proposed for modeling of isotropic haptic textures in [6]. Instead of using AR model interpolation, the vibration patterns are stored inside a frequency-decomposed neural network model. This model can be extended to anisotropic texture rendering. However, it is less applicable, since it requires special data collection equipment for the model building. In our recent work [1], we proposed a new approach for modeling anisotropic haptic textures. This method includes two main contributions that makes it possible to build a model of anisotropic haptic texture. First, a new input-space-based segmentation algorithm is developed, which produces stationary acceleration segments with corresponding nearly constant input. Second, a flexible RBFN based model for AR acceleration patterns storage and interpolation is introduced, which makes the increase of the input dimension computationally inexpensive.

In this paper we present a complementary rendering algorithm of anisotropic haptic texture models. This algorithm is developed in form of a cross-platform computing library. Additionally, we built a set of eight anisotropic and one isotropic haptic texture models for performance demonstration of the computing library. We also prepared two demonstration scenarios that will help participants to evaluate the realism of virtual haptic textures.

2 Modeling Procedure

In this section we will provide a brief explanation about the modeling algorithm to define the input of the rendering algorithm. For the complete information about the modeling procedure refer to [1].

2.1 Algorithm Outline

The data-driven model of anisotropic haptic texture maps a two-dimensional velocity vector and normal force of the tool-surface contact with corresponding vibration

patterns that are propagated through the tool. This model is estimated based upon measurements of the real tool-surface contact.

The modeling algorithm of anisotropic haptic textures consists of three stages: *data acquisition and preprocessing*; *data segmentation*; and *model building*.

Data Acquisition and Preprocessing. In this stage, the contact data is acquired during unconstrained tool-surface interaction. The two-dimensional velocity vector is calculated based on the data from a position sensing device. The normal force is captured using a force sensor. The contact vibrations are captured by an accelerometer. The two-dimensional velocity vector and normal force are resampled to the same level of sampling frequency 1000 Hz and low-pass filtered to remove a noise. The acceleration signal is band-pass filtered in a range of 10–1000 Hz to remove a gravity component and noise.

Data Segmentation. The segmentation algorithm partitions the input and output signals into stationary acceleration patterns of contact vibrations having a corresponding nearly constant input. It is assumed that the contact vibration remains stationary if the movement trajectory of the tool remains in a straight line with a nearly constant velocity magnitude and normal force. Hence, the segmentation is performed along the input signals.

The segmentation algorithm is based on a bottom-up technique and consists of two stages. First, the position data is segmented into straight lines, where the line is considered straight if the maximal deviation of position points are below the threshold τ_1 . Similarly, these segments are sub-segmented into signals having a nearly constant velocity magnitude and normal force, where the ratio of the standard deviation to the mean of the velocity magnitude and normal force is limited by the threshold τ_2 .

Model Building. The contact vibration patterns (model output) and corresponding input vectors $\mathbf{u} = \langle v_x, v_y, f_n \rangle$ are provided by segmentation algorithm for a model building, where v_x and v_y are mean values of two velocity components, and f_n is an average normal force of each segment.

The contact vibration patterns are converted to autoregressive (AR) models with a common order. The AR model describes time-varying process in such a way, where the output value depends linearly on its previous outputs. The AR model of each acceleration pattern is represented by m coefficients and the variance, where m is an order of the AR model. Due to the stability issue of the AR model interpolation [4], the AR coefficients are converted to corresponding line spectral frequency (LSF) ones.

Finally, the RBFN model is trained using the set of input vectors and corresponding set of output acceleration patterns, where the output acceleration patterns are represented by LSF coefficients and the variance.

3 Rendering Setup

In this section we will describe a demonstration setup for anisotropic texture rendering algorithm. The setup consist of software and hardware components. The software component is implemented in form of a computing library to make it independent from the hardware. The software architecture of the computing library is depicted in Fig. 1a. The hardware setup that will be used for demonstration is shown in Fig. 1b.

3.1 Software Architecture

The architecture of the rendering software consists of three layers (See Fig. 1a). The upper layer is referred to as interactive layer. This layer computes the input vector \mathbf{u} based on readings from the input device. Additionally, this layer displays response vibrations back to the user. The business logic of the anisotropic haptic texture library is represented by the second layer. This layer is developed in form of a platform independent computing library. The computing library consist of three functional blocks. First block loads the set of haptic texture models into device memory. The second block estimates the LSF (line spectrum frequency) coefficients and the variance by feeding the input vector \mathbf{u} to the RBFN haptic texture model (See Sect. 2.1). The LSF coefficients and the variance are updated inside the buffer in 100 Hz. Meanwhile, the output vibration signal is generated by the third block, which runs on the other computing thread having frequency 2 kHz. The output vibration signal is produced based on buffered LSF coefficients, the variance and m buffered vibration outputs, where m is a number of LSF coefficients. Note also that all functional blocks work in separate computing threads. The frequency of each computing thread can be reset in accordance with user needs.

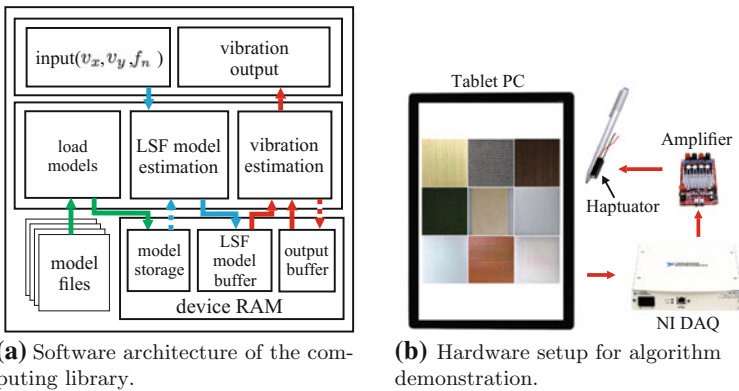


Fig. 1 Hardware for recording and sample set

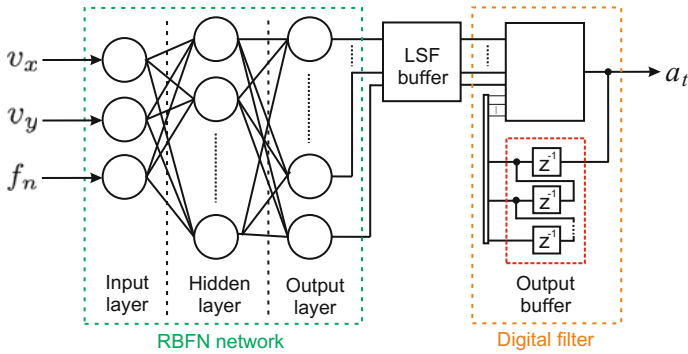


Fig. 2 Model storage and interpolation RBFN architecture

3.2 Vibration Estimation

The set of LSF coefficients and the variance describe the contact vibration pattern for a given vector \mathbf{u} inside the input space of the RBFN haptic texture model (Fig. 2). Therefore, the main task of the RBFN haptic texture model is to provide the mapping of three-dimensional input vector \mathbf{u} with corresponding $(m + 1)$ -dimensional output vector (m LSF coefficients and the variance). This output vector can be calculated using following equation

$$f_i(\mathbf{u}) = \sum_{j=1}^N w_{ij} \phi(\|\mathbf{u} - \mathbf{q}_j\|) + \sum_{k=1}^L d_{ik} g_{ik}(\mathbf{u}), \quad \mathbf{u} \in \mathbf{R}^n \quad (1)$$

where $i = \{1, \dots, m + 1\}$ denotes the index of LSF coefficients and the variance, w_{ij} is a weight constant and \mathbf{q}_j is a center of the radial basis function. The functions $g_k(\mathbf{u})$ ($k = 1, \dots, L$) form a basis of the space \mathbf{P}_p^n of polynomials with degree at most p of n variables.

The output vibration values are calculated using an approach similar to [2]. First, the LSF coefficients are converted to AR ones. Second, the AR coefficients, variance, and m buffered outputs are fed to the transfer function of the Direct Form II digital filter

$$H(z) = \frac{\varepsilon_t}{1 - \sum_{k=1}^p w_k z^{-k}}, \quad (2)$$

where w_k are AR coefficients, ε_t is a random sample from a normal distribution. The output value of the transfer function (See Eq. 2) is the output acceleration value.

3.3 *Hardware Setup and Implementation*

In order to demonstrate the quality of the modeling and rendering algorithms, we designed a tablet-PC-based hardware setup (See Fig. 1b). The tablet PC (Surface Pro 4; Microsoft) was selected as a rendering device. The contact velocity is calculated based on the contact position data from the touch screen of the tablet PC. The normal force of the contact is calculated based on readings from active digital pen (Surface Pen; Microsoft) with a sensing capability of 1024 pressure levels. The output vibrations are displayed using NI DAQ data acquisition device (USB-6251; National Instruments). This output signal is amplified by an analogue amplifier and is displayed using a voice coil actuator (Haptuator Mark II; Tactile Labs).

The set of nine haptic texture models (See Fig. 1b) was built and stored into model files, which are compatible with the rendering application. The same set of samples had been evaluated in a spectral domain in our previous work [1]. This sample set consists of three groups of materials: hard plastic (S1–S3), wood (S7–S9), and fabric (S4–S6). Eight samples have anisotropic texture. The only isotropic sample is S4.

3.4 *Demonstration Protocol*

The audience will have a choice of two demonstration scenarios.

The first demonstration scenario is a simple exploration of virtual and real surfaces. The participant will see a grid of virtual samples on the screen of the tablet PC and a set of corresponding real samples. After exploration of each real-virtual pair, the participant is asked to give a feedback about the realism of rendered textures.

The second demonstration scenario is a matching test of rendered samples. The participant explores a grid of virtual samples, where image textures are hidden. The participant is asked to find a corresponding virtual pair for each real sample. When the participant finishes this task, image textures of samples are displayed and the number of matching pairs can be counted. Similarly, the participant is asked to give a feedback about the realism of rendered textures.

4 Conclusion

In this work we developed a computing library for anisotropic haptic texture rendering. This computing library is deployed on a table-PC-based hardware setup. In order to show the rendering quality to the audience, the set of nine virtual haptic texture models was built and stored into model files. Two demonstration scenario are proposed, which will reveal the realism of the virtual haptic textures.

References

1. Abdulali, A., Jeon, S.: Data-driven modeling of anisotropic haptic textures: data segmentation and interpolation. In: International Conference on Human Haptic Sensing and Touch Enabled Computer Applications, pp. 228–239. Springer (2016)
2. Culbertson, H., Unwin, J., Kuchenbecker, K.: Modeling and rendering realistic textures from unconstrained tool-surface interactions. *IEEE Trans. Haptics* 7(3), 381–393 (2014)
3. Culbertson, H., Delgado, J.J.L., Kuchenbecker, K.J.: One hundred data-driven haptic texture models and open-source methods for rendering on 3d objects. In: 2014 IEEE Haptics Symposium (HAPTICS), pp. 319–325. IEEE (2014)
4. Erkelens, J.S.: Autoregressive modeling for speech coding: estimation, interpolation and quantization. Chapter 4: Spectral Interpolation. TU Delft, Delft University of Technology (1996)
5. Saga, S., Deguchi, K.: Lateral-force-based 2.5-dimensional tactile display for touch screen. In: 2012 IEEE Haptics Symposium (HAPTICS), pp. 15–22. IEEE (2012)
6. Shin, S., Osgouei, R., Kim, K.D., Choi, S.: Data-driven modeling of isotropic haptic textures using frequency-decomposed neural networks. In: World Haptics Conference (WHC), 2015 IEEE, pp. 131–138 (2015)

PhysVib: Physically Plausible Vibrotactile Feedback Library to Collisions on a Mobile Device

Gunhyuk Park and Seungmoon Choi

Abstract This demo presents a mobile application using PhysVib: a software solution on the mobile platform extending an open-source physics engine for automatic vibrotactile feedback upon collision events in a multi-rate rendering architecture. PhysVib runs concurrently with a physics engine at a low update rate and generates vibrotactile feedback commands at a high update rate based on the simulation results of the physics engine using an exponentially-decaying sinusoidal model. We demonstrate an application showing three wall-object pairs with different material properties, and a user interacts with internal objects to feel vibrotactile feedback from collision events.

Keywords Vibrotactile feedback · Automatic generation · Synthesis · Physics engine · Mobile device

1 Introduction

Vibrotactile feedback has been used in interactive applications for a variety of purposes [1], for example, to transmit abstract information, improve task performance, elevate realism, and provide enjoyable experience. Despite its broad utility, designing vibrotactile stimuli is a challenging and time-consuming task and often exacerbated by the lack of suitable authoring software. To solve this problem, there have been many studies to develop graphical authoring tools that support vibrotactile feedback design. Also, automatic conversion of visual content and sound to tactile feedback is an alternative approach [2–5].

It is natural to use physical simulation to provide plausible vibrotactile feedback to diverse physical events in interactive applications at a minimal development cost. A general solution for that is to use a physics engine, which simulates the dynamic behaviors of the objects involved in physical interaction with high accuracy. For instance, PhysX, a real-time physics engine of nVidia, was employed to provide real-

G. Park · S. Choi (✉)

Pohang University of Science and Technology (POSTECH), Pohang, Republic of Korea
e-mail: choism@postech.ac.kr

istic force feedback when collision events occur in a virtual environment [6]. To our knowledge, no such integration efforts have been reported for vibrotactile feedback in spite of its much more frequent uses in interactive applications owing to greater affordability. There have been two previous studies that produce vibrotactile cues using dynamic simulation [7, 8]. However, they do not support a continuous modulation of vibrotactile response synchronized with accurate rigid-body dynamics simulation in general virtual environments since their aim was more for the delivery of abstract meanings.

In this demo, we present a mobile application using PhysVib, which extends a standard open-source 2D physics engine called Box2D in a *multi-rate* rendering architecture. From the collision-related data provided by the physics engine running at a low update rate (e.g., 100 Hz), PhysVib generates vibrotactile feedback commands at a high update rate (e.g., 5 kHz) using the reality-based model [9], which has been widely used for haptic rendering of contact events. Adding only a few material properties to the original data required for dynamics simulation is sufficient for developers to provide compelling vibrotactile feedback and thereby improve the realism of applications.

2 Vibrotactile Feedback Calculation

PhysVib assumes that some of objects are physically connected to the user’s hand, working as “haptic cameras” to the virtual environment based on the general virtual window metaphor. It means that only the collisions associated with haptic cameras trigger vibrotactile feedback. Just as out-of-sight visual objects do not need to be rendered, there are no needs to consider any haptic feedback to the objects that are not linked to the user’s hand. Use of haptic cameras not only preserves the first-person nature of the touch sense, but it also saves the computational load.

A collision between two objects generates an impact force, and it propagates to objects in contact with the collided objects. If two objects of v_1 and v_2 start to collide, the corresponding impact force \mathbf{F}^r between them can be written as

$$\mathbf{F}^r = \mathbf{F}_L^r + \mathbf{F}_A^r, \quad (1)$$

$$\mathbf{F}_L^r = m_1 \Delta \dot{\mathbf{x}}_1 \text{ and } \mathbf{F}_A^r = I_1 \Delta \dot{\theta}_1 \times \frac{\mathbf{l}}{\|\mathbf{l}\|}, \quad (2)$$

where m_1 , $\Delta \dot{\mathbf{x}}_1$, I_1 , $\Delta \dot{\theta}_1$, and \mathbf{l} denote the mass, linear velocity difference, inertia, angular velocity difference of v_1 , and the vector from the contact point to the center of mass of v_1 in Fig. 1. The impact force to v_2 is $-\mathbf{F}^r$. The impact force is propagated to the contacted objects by the principle of action and reaction, and the propagated force moves each object. Note that Box2D automatically calculates \mathbf{x} and θ of all objects in every time step. PhysVib then calculates all F^r s given to each object and integrates them to make a resultant force vector.

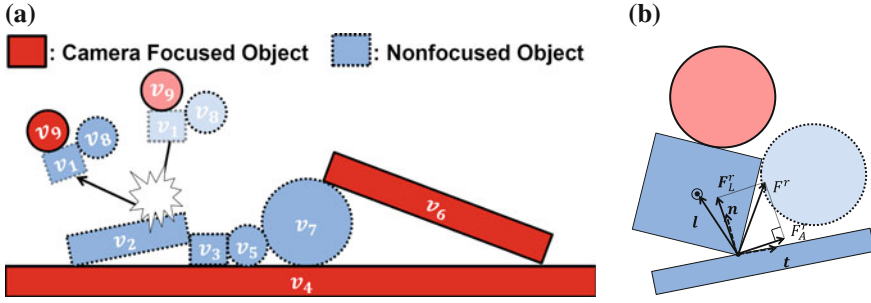


Fig. 1 A collision between two objects in the general environment. **a** A new collision is made between v_1 and v_2 among multiple objects. **b** Impact force \mathbf{F}^r is generated from the collision between v_1 and v_2 . \mathbf{F}_L^r : linear impact force, \mathbf{F}_A^r : angular impact force, \mathbf{n} : surface normal vector, \mathbf{t} : surface tangent vector, and \mathbf{l} : the vector from the contact point to the center of mass of v_1

If a camera-focused object v_c receives a resultant force vector \mathbf{F}_c^r from collisions, PhysVib normalizes corresponding vibration signal’s magnitude A as:

$$A = A^* \frac{\|\mathbf{F}_c^r\|}{m_c + m_h} \quad \text{where} \quad A^* = \frac{1}{2v_{max}} \quad \text{and} \quad m_h = m_{max}. \quad (3)$$

where A^* is a normalization constant, m_c is the mass of v_c , m_h is the mass that represents the effective mass of the user’s hand touching the object, v_{max} is the maximum velocity of objects in the environment and largely depends on the application and user interaction methods. Default value of m_h is the maximum mass of objects in the environment. This normalization step maps a vibration amplitude range on to an environment-independent range (0–1).

PhysVib uses the following exponentially-decaying sinusoidal model for vibrotactile feedback [9]:

$$x(t) = A \sin(2\pi ft) e^{-\tau t}, \quad (4)$$

where $x(t)$ is the vibration signal at time t , A is the *normalized* vibration amplitude determined from the impulse magnitudes computed by the physics engine, and f and τ are the natural frequency and the vibration decay rate of the camera-focused object, respectively. This is a reality-based model that was empirically confirmed from a variety of real objects by measurement [9], and the model was shown to improve the realism of haptic simulation to the great extent [10]. If multiple objects are camera-focused and receives resultant forces, then PhysVib superimposes multiple $x(t)$ signals calculated using Eq. (4). In our user study, users reported that the reality-based model provides more harmonious vibrations to visual scenes than more physically accurate vibrations synthesized from the real contact sound.

In our demonstration, a demo application using PhysVib runs on a commercial smart phone (SAMSUNG SHW-M250S) by attaching an external actuator (TactileLabs Haptuator 2; input range ± 3 V) to the back panel of the phone. This

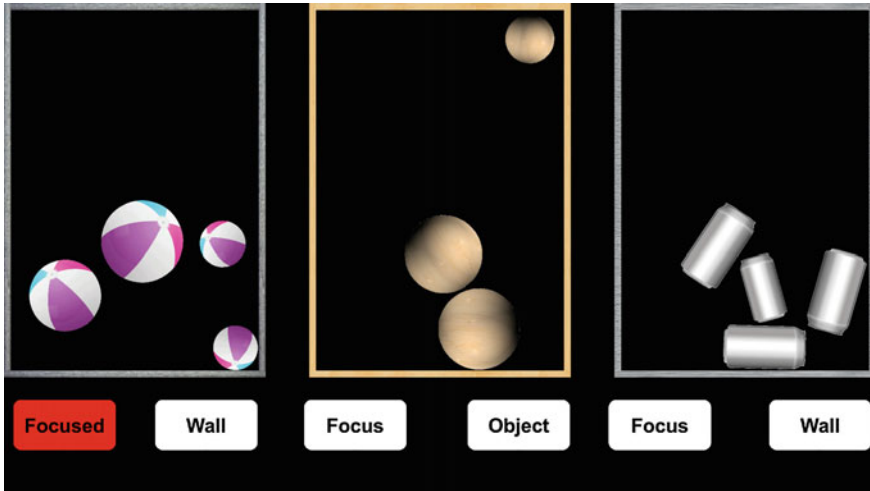


Fig. 2 A screenshot of a demo application using PhysVib

demo application presents three different object pairs of rubber ball–concrete block, wooden sphere–wooden board, and steel can–steel plate (Fig. 2). Users can select which object pair/pairs to be haptically enabled by turning on the focus button into “focused” (colored in red). Also, the focus of haptic cameras can be set on the dynamic objects or the walls. The internal dynamic objects move by tilt motion, and each object can be manipulated by using touch-and-drag.

References

1. Choi, S., Kuchenbecker, K.J.: Vibrotactile display: perception, technology, and applications. In: *Proceedings of IEEE*, no. 9, pp. 2093–2104 (2013)
2. Chang, A., O’Sullivan, C.: Audio-haptic feedback in mobile phones. In: *Proceedings of ACM CHI Extended Abstracts*, pp. 1264–1267 (2005)
3. Hwang, I., Choi, S.: Improved haptic music player with auditory saliency estimation. In: *Lecture Notes in Computer Science (EuroHaptics 2014, Part I)*. LNCS, vol. 8618, pp. 232–240 (2014)
4. Lee, J., Choi, S.: Real-time perception-level translation from audio signals to vibrotactile effects. In: *Proceedings of ACM CHI*, pp. 2567–2576 (2013)
5. Kim, M., Lee, S., Choi, S.: Saliency-driven real-time video-to-tactile translation. *IEEE Trans. Haptics*. 7(3), 394–404 (2014)
6. Chan, L.H., Choi, K.S.: Integrating PhysX and open haptics: efficient force feedback generation using physics engine and haptic devices. In: *Proceedings JCPC*, pp. 853–858 (2009)
7. Sekiguchi, K., Hirota, K., Hirose, M.: Haptic interface using “estimation of box contents” metaphor. In: *Proceedings ICAT*, pp. 197–202 (2003)
8. Williamson, J., Murray-Smith, R., Hughes, S.: Shoogole: excitatory multimodal interaction on mobile devices. In: *Proceedings of ACM CHI*, pp. 121–124 (2007)

9. Okamura, A.M., Cutkosky, M.R., Dennerlein, J.T.: Reality-based models for vibration feedback in virtual environments. *IEEE/ASME Trans. Mechatron.* **6**(3), 245–252 (2001)
10. Kuchenbecker, K.J., Fiene, J., Niemeyer, G.: Improving contact realism through event-based haptic feedback. *IEEE Trans. Vis. Comput. Graph.* **12**(2), 219–230 (2006)

Towards Universal Haptic Library: Library-Based Haptic Texture Assignment Using Image Texture and Perceptual Space

Waseem Hassan, Arsen Abdulali and Seokhee Jeon

Abstract In this study we focused on building a universal haptic texture models library. This library is used to automatically assign haptic texture models to any given surface based on image features. The library is built from one time data-driven modeling of a large number (84) of textured surfaces, which cover most of the daily life haptic interactions. In this demonstration, we will show automatic assignment of haptic texture models to new arbitrary textured surfaces based on their image features, from the universal haptic library of haptic texture models. Afterwards, the automatically assigned haptic model will be rendered.

Keywords Perceptual space • Image feature • Multidimensional scaling • Haptic texture • Image texture

1 Introduction

It is reported that haptic texture has, up to some extent, correlation with image texture [2]. Our hypothesis is to utilize this relationship in the automatic selection of haptic texture models, instead of using pure image based selection. It is well known that two similar looking images can have totally different haptic perception and vice versa. Therefore, it is of utmost importance to cater for the perception aspects of every image and use that knowledge in automatic assignment of haptic texture models. The overall framework required to accomplish this task can be tabulated as follows:

W. Hassan (✉) · A. Abdulali · S. Jeon
Department of Computer Science and Engineering, Kyung Hee University, 1732,
Deogyong-daero, Giheung-gu, Yongin-si, Gyeonggi-do 17104, Republic of Korea
e-mail: waseem.h@khu.ac.kr

A. Abdulali
e-mail: abdulali@khu.ac.kr

S. Jeon
e-mail: jeon@khu.ac.kr

1. One time data driven modeling of texture surfaces to form a library. The range of surfaces should cover most of the daily life haptic interactions.
2. A user study to establish a perceptual space where all the texture surfaces from the library are represented based on their perceptual characteristics of haptic texture.
3. Extract multiple image features of all the texture surfaces.
4. Establish a relationship between haptic perception (step 2) and image features (step 3). Haptic texture models are stored along with the associated image features.
5. Based on the relationship established in step 4, carry out automatic haptic texture model assignment, to newly encountered—outside library—texture surfaces, using the library.
6. Render the assigned model from library as a haptic model for the newly encountered texture surface.

2 Implementation

The universal haptic library was built using 84 real life texture surfaces. The data driven models of all these surfaces were built using the modeling algorithm that is proposed in [1]. Since the library is limited to the isotropic haptic textures, we reduced the input space of the algorithm down to two dimensions, which are the magnitudes of the normal force and the tangent velocity.

3 Demonstration

This demonstration aims at showing the performance of our system for automatic selection and rendering of haptic texture models. As a first step, the image of any textured surface is captured using a camera. This image is then loaded into the algorithm for automatic selection. The algorithm assigns perceptually the closest haptic texture model from the library based on the image features of the new surface. The assigned model is then rendered for the new textured surface. The overall process can be seen in Fig. 1. A small video for this demonstration is available at http://haptics.khu.ac.kr/Universal_Haptic_Library_AsiaHaptics.mp4.

4 Requirements

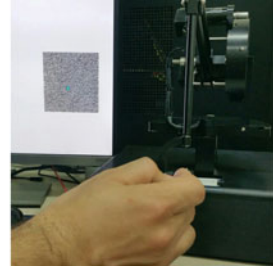
For this demonstration, we would require a table of 6×3 ft (or smaller tables making up the same size). Additionally, availability of at least four electric sockets would be appreciated.



(a) Capturing image of a new textured surface.



(b) Automatic assignment of a haptic model from library.



(c) Rendering the automatically assigned haptic model.

Fig. 1 Illustration of the demonstration process

Acknowledgements This research was supported by Basic Science Research Program through the NRF of Korea (NRF-2014R1A1A2057100), by Global Frontier Program through NRF of Korea (NRF-2012M3A6A3056074), and by ERC program through NRF of Korea (2011-0030075).

References

1. Abdulali, A., Jeon, S.: Data-driven modeling of anisotropic haptic textures: data segmentation and interpolation. In: International Conference on Human Haptic Sensing and Touch Enabled Computer Applications, pp. 228–239. Springer (2016)
2. Wu, J., Song, A., Zou, C.: A novel haptic texture display based on image processing. In: IEEE International Conference on Robotics and Biomimetics, ROBIO 2007, pp. 1315–1320. IEEE (2007)

An Empirical Study of Haptic-Audio Based Online Shopping System for the Blind

Eu Jin Wong, Kian Meng Yap, Jason Alexander and Abhijit Karnik

Abstract The objective of this study was to demonstrate a haptic-audio based system which could enable the blind to shop online independently. The goal was to find out whether a web design with haptic and audio modality, speech recognition and speech synthesizer are usable for shopping and product evaluation. The results showed that an active framed three-section layout design with directed dialogue and cues, along with a haptic-audio enabled browser and a low-cost Falcon device is usable for the blind to navigate, interact, access and haptically evaluate online products; a VoiceXML based shopping cart can enable the blind to interact and verify the cart content; and a voice recognition based payment system can enable them to make online payment.

Keywords Haptics · Audio · Haptic shopping · Web design · Visually impaired

1 Introduction

The client side of the system consists of a haptic-audio enabled browser and the server side consists of product catalogue, shopping cart and payment system which were developed using VoiceXML, H3D, C++ and Python. The product catalogue

E.J. Wong (✉) · K.M. Yap
Faculty of Science and Technology, Sunway University, Subang Jaya,
Selangor, Malaysia
e-mail: 09018359@imail.sunway.edu.my

K.M. Yap
e-mail: kmyap@sunway.edu.my

J. Alexander · A. Karnik
School of Computing and Communications, Lancaster University, Lancashire, UK
e-mail: j.alexander@lancaster.ac.uk

A. Karnik
e-mail: a.karnik@lancaster.ac.uk

has a consistent three-section layout design surrounded by an active frame which surround the display area at the top, bottom, left and right side (Fig. 1). This design allows the blind to easily understand the page overview and layout which in turn helps them to navigate, interact and interpret the content better. The frame is used to warn users that the haptic pointer had reached the edge of the page and to give directional cues to move the pointer to the next option. The top banner section of each page provides an option to exit the page and to display content of another page such as shopping cart. The middle section is used to present the data when an option is selected such as presenting a model for haptic evaluation. The footer section contains options that are related to the data presented in the middle section such as payment option. The system is designed to use the Falcon device [1], speech synthesizer and voice recognition for navigation, interaction and data input. It keeps track on the haptic pointer position in real-time, whenever the pointer hovers over an active portion of the web page, directed dialogue is used to direct user to the next available options. Every product page has an introductory audio message to describe the product. When users select a product, the catalogue will display the product's model. When a model is selected, a virtual 3D model will be rendered for the user to evaluate. To evaluate a model, users use the haptic stylus to trace its dimension and shape, and feel the material texture and firmness. If the user decides to purchase the model after evaluation, he or she can select 'Add To Cart' option to add the model into the cart (Fig. 1).

A total of four products namely chair, sofa, table and miscellaneous are used to provide a wide spectrum of texture, stiffness, size and shape in order to gather a better analysis. H3D API [2] is used to add haptic and audio properties to customize



Fig. 1 Product catalogue

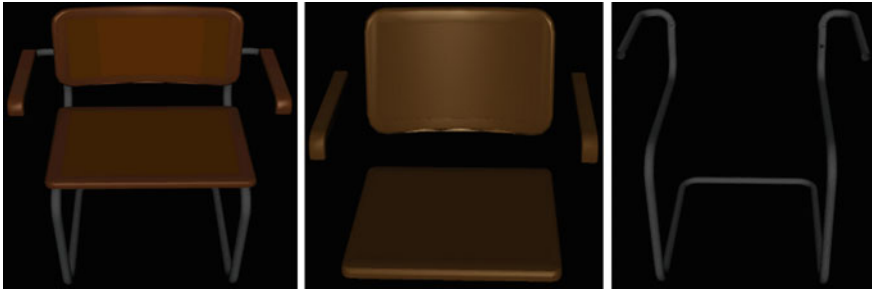


Fig. 2 Different parts of chair model

the X3D scene nodes and fields. H3D API provides the scene definition such as lighting, meshes, textures and friction. Different parts of the model are haptically rendered separately in order to provide the user with a better perception about the model. For example, a chair model (Fig. 2) was rendered in three separate stages, first the complete version of the chair then follow by different parts of the chair.

The shopping cart system (Fig. 3) was developed using XHTML + VoiceXML which is a web mark-up language for developing multimodal applications. Each time an item is added, the system will use cookies and session variable to track product description, price and quantity, and calculate the total amount. When the haptic pointer hovers over the presentation area, audio prompt is used to direct users to issue voice command “Browser Content” or “Click Left Button” on the haptic device in order to start the presentation.



Fig. 3 Shopping cart

The image shows a web form for payment on the IKEA website. The form is titled "Payment" and is set against a background of various furniture items. At the top left is the IKEA logo, and at the top right is a "View Cart" button with a shopping cart icon. The form is divided into three main sections: "Authentication" with fields for "Username" and "Password"; "Personal Information" with fields for "First Name", "Last Name", "Address", "Zip", "City", "State", "Country", "Telephone", "Fax", "EMail", and "Homepage"; and "Credit Card Information" with fields for "Name on Card", "Card Type" (a dropdown menu), "Credit No.", and "Expiry Date". Below the "Credit Card Information" section is a button labeled "VOICE COMMAND TO SUBMIT". At the bottom center of the form is a large, prominent "CANCEL" button. The entire form is enclosed in a brown border.

Fig. 4 Payment form

The payment system (Fig. 4) uses voice recognition and data entry program to fill forms automatically. When the haptic pointer hovers over the form, audio prompt is used to direct the user to issue voice password. If the password is valid, the system retrieves the personal information and parse by a data entry plug-in which will automatically input the data into the fields. Once form is filled, a voice message will direct the user to give the voice command 'Browser Submit' in order to submit the form for processing. If the processing is successful, the system will inform the user via audio message and email.

2 Experimental Study

Fifteen participants, from the Malaysian Association for the Blind [3], between 20 to 55 years old were involved in this study. They have experience in using screen readers and surfing the Internet, however they have no experience in using haptic device. The experiment consists of a series of tasks:

1. Select desire model for product category
2. Haptically evaluate model
3. Add and verify cart content
4. Check-out for Payment

They were required to select models and haptically evaluate them. For dimension evaluation they were required to move the haptic stylus slowly from left to right, front to back and top to bottom, while gauging the model size (in inches). The

ratio of the model to actual product is 1 in.–1.5 ft. For shape evaluation, they had to move the stylus slowly by outlining the model contours in order to perceive its shape. For texture evaluation, they had to applied pressure and move the stylus sideways, backward and forward in order to feel the material. For stiffness evaluation, they had to apply different degree of force to push the stylus downwards into the model surface in order to feel the firmness. After evaluation, they could add models into the shopping cart or verify the cart. Finally, they proceed to check-out and fill-in form for payment.

3 Discussions

The results allow us to draw a number of conclusions. A consistent active framed three-section catalogue design with directed dialogue and directional cues can helps the blind to understand webpage overview, which in turn helps them to navigate, interact and access the content. To avoid getting lost at the edges of the Windows workspace, each page is surrounded by an active frame which is used to give direction when the pointer hovers over it. For haptic evaluation, the complete model and different parts of the model should be rendered separately for a better perception about the model. When rendering the complete model, audio describing the part which the stylus is touching will give users a better understanding of how different parts are connected together. To prevent cognitive overload due to excessive audio information, when rendering individual part, short continuous sound cues is to indicate that the stylus is touching and quiet when not touching the part. For cart presentation, item's details should have short and simple description. Items should be read out one after another with a short pause and a longer pause before presenting the grand total amount Using Cascading Style Sheet to control speaker's volume, stress level, speed and pause duration could improve the clarity of the presentation. Using voice password to automatically fill form can avoid the usage of keyboard and also to relieve users from having to remember form's fields which require considerable amount of time to acquire the skill.

4 Conclusion and Future Work

From the results, the users found the system usable for online shopping as they were able to understand the catalogue layout; able to navigate, interact and access options; able to utilise the shopping cart features; and able to make online payment independently. In term of produce evaluation, they could estimate the model size; feel the different level of material texture and firmness; and could perceive the model shape. We hope that this study could provide a foundation for future investigations into the design of online shopping applications for the blind, so that

they could actively participate in the e-commerce evolution. For future extension, we plan to developed a voice based query to filter and search for products; and to present real-time product information update using HTML5 Server Sent Events.

Acknowledgements Study was supported by Grant—Sunway-Lancaster (Grant No: SGSSL-FST-CSNS-0114-04) at Sunway University, Malaysia.

References

1. Novint Corporation. <http://home.novint.com>. Accessed 4 Aug 2016
2. H3D. <http://www.h3dapi.org>. Accessed 4 Aug 2016
3. MAB. <http://www.mab.org.my>. Accessed 4 Aug 2016

Character Recognition by Flick Movements Presented on Fingers

Kentaro Yoshida, Koji Tanaka, Keisuke Hasegawa, Yasutoshi Makino and Hiroyuki Shinoda

Abstract It is general to recognize informations of languages visually or audibly. But, the recognition of such informations by haptics can be a good way according to the surrounding environment. Moreover, people who lose visual and auditory senses need a character reading method without using such senses. Though the braille is given as an example for character recognition by haptics, learning braille requires a much time and the number of its users who can read braille enough is few. Then, this report proposes a device presenting flick movements onto the fingers for character recognition.

Keywords Haptics · Character recognition · User interface

1 Introduction

Braille is given as an example for character reading by haptic clues. Braille is widely used for presenting symbolic information to visually handicapped people. On the other hand, it needs much learning in a long term, which perhaps results in a low percentage of current braille use [1]. As another example, a sort of tactile displays that presents stimulations representing the image patterns of letters to users' hands is proposed, although its use seems limited within a small number of users [2].

K. Yoshida (✉) · K. Tanaka · Y. Makino · H. Shinoda
Graduate School of Information Science and Technology, The University of Tokyo,
7-3-1 Hongo, Bunkyo-ku, Tokyo 113-0033, Japan
e-mail: yoshida@hapis.k.u-tokyo.ac.jp

Y. Makino
e-mail: yasutoshi_makino@k.u-tokyo.ac.jp

H. Shinoda
e-mail: hiroyuki_shinoda@k.u-tokyo.ac.jp

K. Hasegawa · Y. Makino · H. Shinoda
Graduate School of Frontier Sciences, The University of Tokyo,
5-1-5 Kashiwanoha, Kashiwa-shi, Chiba 277-8561, Japan
e-mail: keisuke_hasegawa@k.u-tokyo.ac.jp

For the establishment of a more intuitive haptic-based symbolic display, we created a device that guides users' hand to trace alphabet trajectories of normal handwriting motion, by which they recognize alphabets they are forced to write [3, 4]. These devices successfully let users tactually read alphabets accurately without long learning in advance. So, it can be said that this method is suitable for person with halfway loss of eyesight or even with normal sight. We expect improvements of the speed and accuracy of this method would enable users to detect sentences longer than a character. In this way, we aim to link haptics to new applications, other than conventional substitute sensing systems.

One intrinsic limitation of the above studies is that the displaying speed would not be faster than actual handwriting. In such a situation that requires fluent text reading, an essential improvement of the method is indispensable. As a new strategy, we noticed "flick input", which is widely used mainly among young Japanese users of smart phones. We briefly describe the Flick input. Users press a 3×4 dial matrix correlated with Japanese letters to the consonant with a finger, and flick to a direction out of several choices for designating the vowel. Flick input goes well with entering Japanese text since individual Japanese letters (Hiragana) denote a pair of a consonant and a vowel. Considering the following two merits in displaying text, we propose a device which presents flick movements on a finger: one is that it is much faster than normal handwriting, and the other is that the presenting position does not change in the flick movements. From the viewpoint of learning, using flick input in daily life might unintentionally reduce necessary learning for the device.

In this paper, we report about a fabricated device which presents flick movements along with the results of experiments using this device. The results indicate the device allowed users to tactually read some sentences and there existed learning effects over a period of hours.

2 Proposed Device

2.1 Outline

The fabricated device is shown in Fig. 1. The device consists of an acrylic jig imitating a smart phone and two-dimensional linear actuator (models EZS3D005-A and EZS6D005-A, Oriental Motor Co., Ltd.) which moves relatively to the jig. Users are supposed to put a finger on an acrylic stage mounted on the tip of the actuators for perceiving flick movements. A vibrator (Forcereactor, Alps Electric Co., Ltd.) is loaded on the stage, so that users can distinguish whether the displayed finger movements correspond to actual flick movements (indicating vowels), or transitions to a letter (indicating consonants) as described in the following. A switch is installed behind the jig, which allows users to control the character presentation.

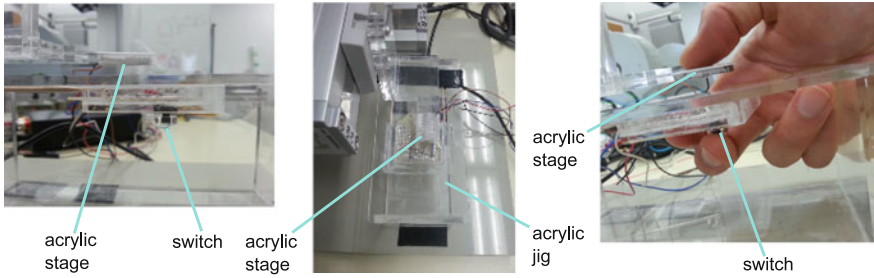


Fig. 1 Proposed device: side view (left figure), top view (middle figure) and an example of how the user holds the device (right figure)

Fig. 2 Presenting flick movements: an example of presenting “e”

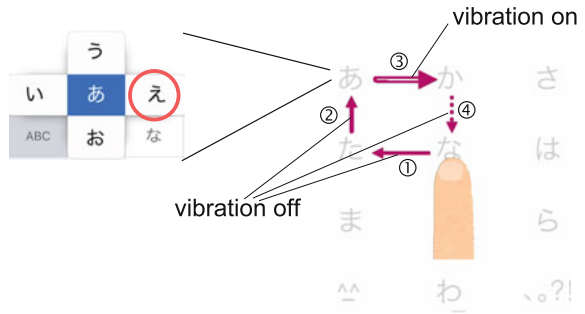


Figure 1 shows an example of how to hold the device. It shows a user’s hand, holding a whole jig with one-hand, putting the thumb on the stage and manipulating the switch with the middle finger, which is just like the way a user holds a smart phone.

The movements of the stage presenting single character of *Hiragana* are concretely as follows. As shown in Fig. 2, we suppose an imaginary character board on the display like actual flick inputs, and the character is presented as movements of a finger on the character dial. First, the initial position of the stage is at the position of “na (な)” located on the center of the character dial in the normal flick input. Second, the stage starts moving to the position of the corresponding consonant. The movement in this step is given as a combination of the lengthwise direction and the lateral direction (not on the diagonals) as shown in Fig. 2. This is because preliminary experiments showed that detection of the moving direction between diagonal movements and the other was a bit difficult. Third, the flick movement, which represents the information of vowels, is presented. For the distinction of this flick movement from previously described one, a vibration is added while moving. At the end of each letter the stage moves back to the initial position. As an example in Fig. 2, the sequence of movements that presents “e (え)” is as follows. The stage moves to upper left which stands for the consonant of “a (あ)” at first. Next, the stage moves to right which stands for the vowel of “e (え)”. Then, the stage goes back to the position of

“na (な)””, the initial position, to prepare the next character. Thus, user re-experiences the flick movements through the moving stage.

In an actual operation, user can control the presenting of characters with a switch. When the switch is pushed to right, the system aborts presenting current character and starts presenting the next one. When the switch is pushed to left, the current character begins to be presented from the beginning again. In either case, user can feel some corresponding patterns of vibrations when the switch is pushed.

2.2 Design

The proposed device consists of three part, a motion presenting part, a switch, and a processing system part.

The processing system includes PC and a microcontroller board (Arduino Mega 2560, product of Arduino). Two-dimensional linear actuator and switch is electronically controlled by the computer via a microcontroller board.

3 Experiment

With the proposed device, we did an experiment as below to give light on users’ recognition and learning speed with the device.

As shown in Fig. 3, each subject performed five sets of tasks with intermittent learning periods that lasted for five minutes between each task. In the tasks, the

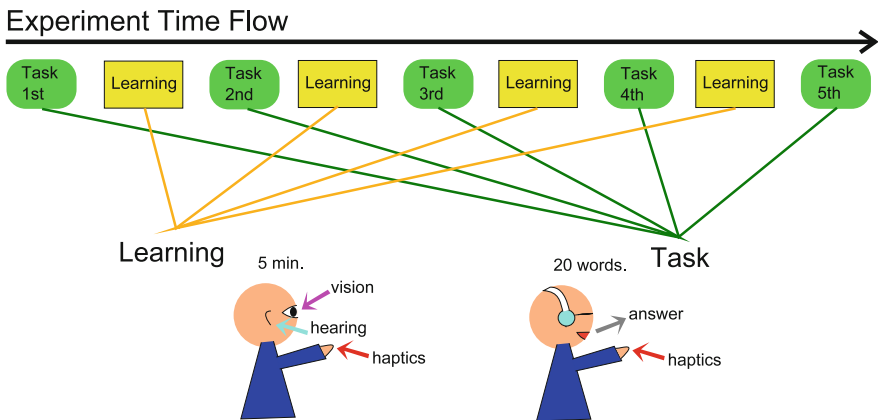


Fig. 3 Procedure of the experiment

subject was presented twenty words or sentences by the device while listening to the white noise through headphones and to close eyes during the task. If the subject understands what words or sentences is presented, then he or she had to answer at once and move on to the next. The subject was allowed to repeat the same presenting until he or she recognizes it. In each task, we got the correct recognition rate of presented twenty words or sentences and the time required for twenty answers. We also checked the transition of answering time on each set of the task. In the learning time, the subject could get information about what was presented by the device not just by haptics but also by visual and auditory senses.

The kinds of characters used in the experiment includes 46 *Hiraganas* and a macron, and the number of characters of individual word or sentence is from two to nine. More than thousand words or sentences are used in each task, and the same words were never presented to the same subject.

4 Result and Discussion

The result of the experiment is shown in Fig. 4. Five subjects participated in the experiment, and those scores are shown in different colors in the graphs. All subjects are sighted, and everyone except Subject 2 always uses the flick input with their smart phones.

The upper graph indicates that almost all subjects could get to recognize presented words at about 80 percent of accuracy. Therefore, it can be said to let users recognize words or sentences through this device. Moreover, the results were improved from 1st trial to 2nd or 3rd trial in the both graphs, so short-term learning can be effective in this method.

The subject 1 in the graphs, who is one of the writer of this paper, showed almost perfect accuracy and the time much faster than other subjects. It is conceivable that the reason is he has been touching this device for a long time. So, this indicates a possibility that other subjects can perform much better scores if they have more time to learn about this device. And surprisingly, these results also show that how subjects get used to the flick input is not a big factor of how the person can recognize words in this method, since the subject 2 who doesn't use flick input in daily life showed the 3rd best scores in the experiment.

On the other hand, the results show great deviation between subjects, and I think the reason is the inflexibility of difficulties. The length and the speed of the flick movements affect the time for presenting one word and also the difficulty to detect it. These parameters were set for the subject 1, one of the writer, to achieve a good score, but it can be too hard for the beginners.

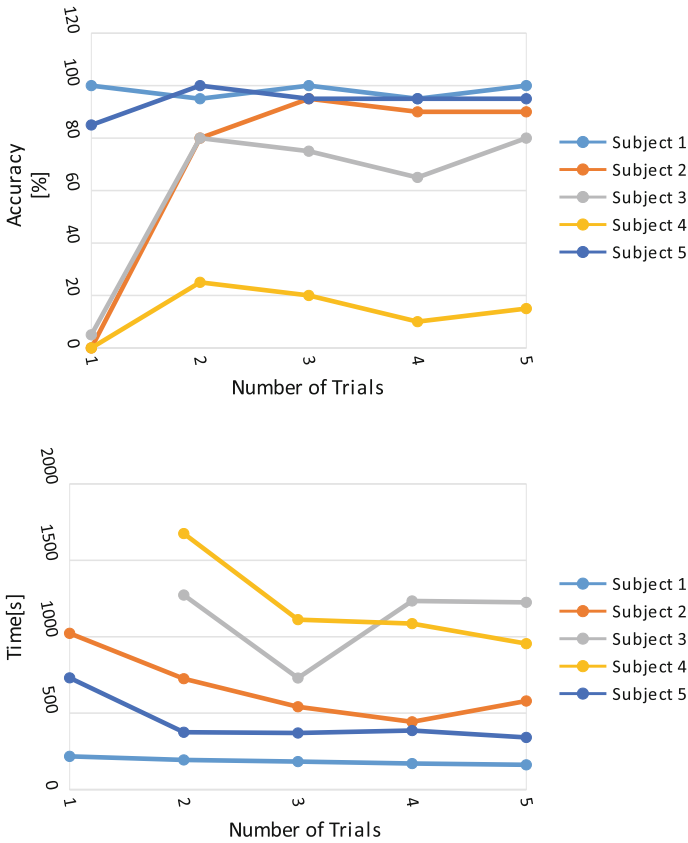


Fig. 4 Results of the Experiment: the accuracy transition (*upper graph*), and the time transition (*lower graph*). The horizontal axis in both graphs represents 1st to 5th trials of the tasks, and the vertical axis represents the accuracy of the trial in the *upper graph*, and the time required for the trial in the *lower graph*. In the *lower graph*, there are two missing points in the 1st trials, but this means that subject 3 and 4 couldn't finish the task without any learnings at the 1st trial

5 Prospect

With the proposed device, we showed that it is possible to recognize words or short sentences by haptics. Nevertheless, there was the variation of results attributable to individual differences, and one subject cannot improve the accuracy till the end in the experiment. So, it is conceivable, as a solution of these problems, to change difficulties according to the accuracy of the user or to learn from easier words and gradually switch them to more difficult ones.

Acknowledgements This research is supported by JSPS KAKENHI 15K12073.

References

1. Social Welfare and War Victims' Relief Bureau, Ministry of Health, Labour and Welfare.:Heisei 18 nen shintai shogaiji sha jittai chosa kekka. (field study about physical obstacle child, person in 2006.)
2. Sueda, O.: Shindo kankaku to shikaku daikou kiki, souon seigyō. (Vibrotactile Sensation and Vision Substitution). vol. 14, No. 3, pp. 138–141 (1990)
3. Hasegawa, K., Sakurai, T., Makino, Y., Shinoda, H.: Character reading via stylus reproducing normal handwriting motion. *IEEE Trans. Haptics* **9**(1), 13–19 (2016)
4. Tanaka, K., Hasegawa, K., Makino, Y., Shinoda, H.: A pocket-size alphabet display with letter trajectories presented to fingers. *Proc. EuroHaptics* **2016**, 472–482 (2016)

A Tool for Collecting and Designing Haptic Experiences

Mina Shibasaki, Youichi Kamiyama and Kouta Minamizawa

Abstract In this study, we have designed the device to collect haptic sensations from the surrounding environments and created objects to experience further. We hold on the workshop to verify the effectiveness of the device. As the result this device showed that children became interested in haptic and stimulated creativity.

Keywords Interaction design · Haptics · TECHTILE

1 Introduction

We humans are surrounded by various haptic sensations, and they always affect us through our skin. When we walk, sit, or eat, we subconsciously handle the haptic information to achieve our daily behaviors. On the other hand, to design new daily objects or experiences while considering haptic sensations, it is important to cultivate the ability to focus consciously on haptic sensations in the world. Previous studies of haptic sensations, Haptica Project [1] held Tactile Workshop to understand and reaffirm the manner of touching the objects. This work refers to how

M. Shibasaki (✉) · Y. Kamiyama · K. Minamizawa
Keio University Graduate School of Media Design, 4-1-1 Hiyoshi, Kōhoku-ku,
Yokohama 223-8526, Japan
e-mail: mina0415@kmd.keio.ac.jp

Y. Kamiyama
e-mail: kamiyama@kmd.keio.ac.jp

K. Minamizawa
e-mail: kouta@kmd.keio.ac.jp

important it is to experience tactile sensation. Heatbeat Picnic [2] aims to pragmatize the intangible “life” and develop the participant’s awareness of their life. And TECHTILE Project [3] aims to create new social value based on the design and expressions through haptics. These approaches indicate that the haptic sensation affects us to feel the connection between human-to-human or human-to-object. Recently, It is being attempts to develop creativity for kids though haptic experience. For example, Yang [4] researches Infants interest in surface and develops various objects for them to explore.

In this research, we collaborated with Miraikan: National Museum of Emerging Science and Innovation, and especially focused on the children, and developed a novel workshop and devices that deliver the experience to get them interested in the haptic sensations in their surrounding world, and exert their creativity to design new products or experiences. We have handled regular workshops in the “Curiosity Field” in Miraikan, which made of several activity areas for the children from toddlers to elementary school age to enjoy experiments and creating, and validated our concept.

2 Concept

Figure 1 illustration is the concept. It will collect haptic sensations from the surrounding environments. We were able to stimulate the children’s haptic creativity Accordingly, we developed device which we called “Haptone” that is based on TECHTILE technology [5] to easily scan the surface of the object and record its haptic sensations. The “Haptone” device consists of haptic microphone, haptic

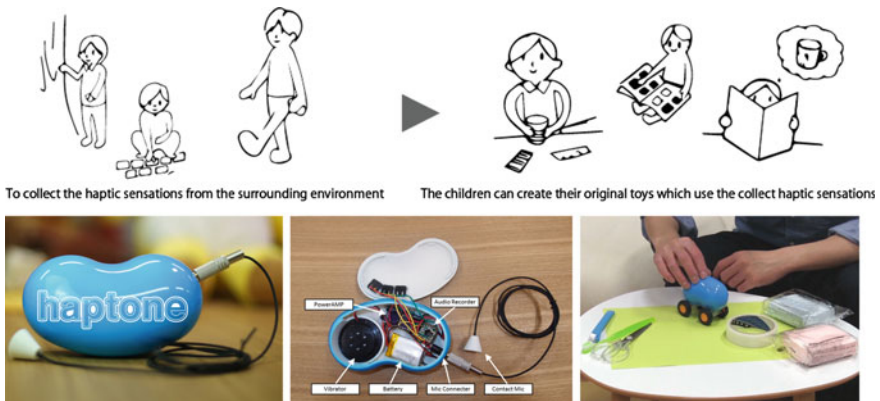


Fig. 1 Concept and Haptone device

recorder, and haptic vibrator, and battery. The collected haptic sensations can be re-played so that the participants can easily compare various haptic sensations that they recorded. The device is portable so that it can also be used out of doors. The shape is designed like a stone or bean so that the children can easily grasp it in their small hands and can easily enjoy haptic sensation.

3 Workshop

The workshop was designed as follows: (1) 10 min for introduction of how to collect and replay the haptic sensations. (2) 15 min for walking around and collecting the haptic sensations from the surrounding field. (3) 5 min for sharing each other the best haptic sensation they collected. (4) 30 min for creating new haptic objects using the collected sensations. (5) 10 min for a presentation and sharing their work.

In the introduction of the workshop, the facilitator asked them to try to express several haptic experiences in words, and then they tried to share the haptic experience using Haptone device in real-time. The participated children from 6 to 12 years old could use the Haptone device without detailed explanation. Then they strolled around the “Curiosity Field” to find various haptic sensations. After selecting the most favorite one, they started to create their own haptic product based on the haptic sensation they felt. As a result, the children could create their original toys, creatures and experiences as shown in Fig. 2. We observed how children behaved in the “Curiosity field” when they walked around with the “Haptone”. Also older children taught younger children how to use this device. They devised ways of collecting haptic sensations. This device provided encouraged communication between children through the toys they made.



Fig. 2 Workshop and works to use device

4 Conclusion

We developed the device to collect haptic sensations and created objects to experience further. This device showed that children became interested in haptic and stimulated children's haptic creativity. "Haptone" shows us that we can be creative using TECHTILE technology.

On other hand, we received many suggestions from children and parents. They deleted haptic data by mistake and forget their haptic recoding. It is better to have multiple storage capabilities.

Future research, we will try to make the device user friendly without any requiring instruction. Children will be able easily use it like a kids building blocks.

Acknowledgements This project is supported by JST-ACCEL Embodied Media Project and JSPS KAKENHI Grant #26700018.

References

1. Suzuki, Y., Suzuki, R.: "Tactile Workshop". In: Tactile Score—A Knowledge Media for Tactile Sense, Springer Briefs in Applied Sciences and Technology, pp. 7–14. Springer (2014)
2. Watanabe, J., Kawaguchi, Y., Sakakura, K., Ando, H.: "Heartbeat Picnic". In: Ars Electronica Cyber Art Exhibition, OK center Linz, Austria (2011)
3. TECHTILE: <http://www.techtile.org/>
4. Yang, J., Otsuka, Y., Kanazawa, S., Yamaguchi, M.K., Motoyoshi, I.: Perception of surface glossiness by infants aged 5 to 8 months. *Perception* **40**(12), 1491–1502 (2011)
5. Minamizawa, K., Kakehi, Y., Nakatani, M., Mihara, S., Tachi, S.: TECHTILE toolkit: a prototyping tool for designing haptic media. In: ACM SIGGRAPH 2012 Emerging Technologies, Los Angeles, Article No. 22 (2012)

A Novel Multimodal Tactile Module that Can Provide Vibro-Thermal Feedback

Masashi Nakatani, Katsunari Sato, Kunio Sato, Yuzuru Kawana, Daisuke Takai, Kouta Minamizawa and Susumu Tachi

Abstract This paper describes a novel tactile module that can provide both vibratory and thermal feedback onto the skin. The module is composed of two different components; miniaturized vibrator and four units of Peltier devices. The dimension of the vibro-thermal tactile feedback device is $16 \times 32 \times 7$ mm, which is small enough for attaching to fingerpad. We describe basic concept of this module, and the state of current prototype including possible applications.

Keywords Tactile display · Thermal feedback · Vibrotactile feedback · Wearable device

Masashi Nakatani, Katsunari Sato, Kunio Sato and Yuzuru Kawana equally contributed to this study.

M. Nakatani · S. Tachi
Institute of Gerontology, University of Tokyo, Tokyo, Japan
e-mail: nakatani@iog.u-tokyo.ac.jp

S. Tachi
e-mail: tachi@iog.u-tokyo.ac.jp

K. Sato (✉)
Nara Women's University, Nara, Japan
e-mail: katsu-sato@cc.nara-wu.ac.jp

K. Sato · Y. Kawana · D. Takai
Alps Electric Co. Ltd., Tokyo, Japan
e-mail: kunio.sato@jp.alps.com

Y. Kawana
e-mail: yuzuru.kawana@jp.alps.com

D. Takai
e-mail: daisuke.takai@jp.alps.com

M. Nakatani · K. Minamizawa
Graduate School of Media Design, Keio University, Tokyo, Japan
e-mail: kouta@kmd.keio.ac.jp

1 Introduction

There are enormous numbers of tactile displays proposed so far. Pin-based tactile display is most studied in analogous to visual displays. This type of tactile display uses multiple contractors that are driven with different actuators [8]. Other tactile displays utilize physical phenomena to induce skin deformation such as electrostatics [14], surface elastic wave [10] or to directly activate sensory afferent by electrocutaneous stimuli [7].

In addition to providing mechanical tactile feedback to provoke tactile sensation, thermal displays also attract attentions recent years [6]. They used water circulation [1], Peltier devices [2], or heaters [5]. The thermal display can not only display thermal cues, but they can also produce tactile perception of material properties [6].

It would be beneficial for the research community to have multimodal tactile displays that can present vibratory and thermal tactile cues simultaneously. Based on recent progress of psychology on vibrotactile and thermaltactile perceptions, it is expected that multimodal tactile display may enhance realistic experience while interacting with presented object. Although multimodal tactile sensors have been proposed [9] and commercially available [4], only a few multimodal tactile displays have been proposed [3]. Considering mobile or wearable computing purposes in the usage of multimodal tactile display, the size of hardware should be taken into account.

Here we developed a small-size tactile module that can provide both vibratory and thermal tactile feedback onto the skin, which is small enough for wearable use. We also evaluated our developed device, and further discussed possible application with the device.

2 Hardware Development

The vibro-thermal tactile unit is composed of two different components: a vibrotactile unit and a thermal tactile unit. We developed these two components separately and then integrated them by closely placed side by side.

Vibrator unit Vibrator unit was developed by miniaturizing previously developed actuator called ForceReactor™ AF series short-vibration feedback device [13]. Since previous actuator was relatively large for mobile device use, so that we developed a prototype that has a smaller dimension. The dimension of current vibrator prototype was $10 \times 3 \times 24$ mm, which was slimmed down comparing with previous one ($7.5 \times 5 \times 35$ mm). The weight is 6 g, which is light enough for integrating with developed thermal tactile unit.

Thermal unit We chose a Peltier device (KSMH029F, KELK Ltd.) as thermal unit for giving tactile feedback. We used four Peltier devices to provide fast thermal feedback as proposed previously [12]. The size of each Peltier device is $6.0 \times 10 \times 1.7$ mm, which is small enough even we used four Peltier devices in tile patterns

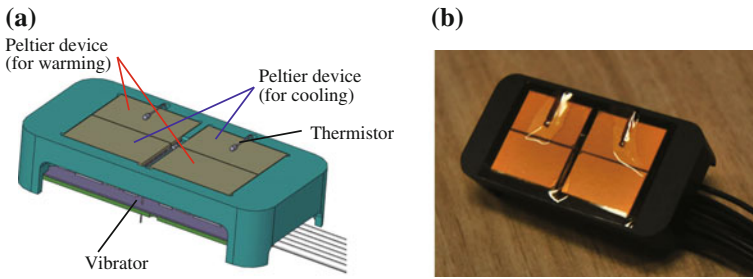


Fig. 1 Schematics (a) and developed (b) vibro-thermal tactile display

as shown in Fig. 1. This configuration enables fast temporal change of temperature, because two of four Peltier devices are used only for cooling and others are used only for warming the skin. The problem of using Peltier devices is that it requires more electricity when one tries to cool down after it is heated, or vice versa. Four-tile configuration can solve this conventional problem and previous study showed that the time to perceive temperature change was improved 36% on average [12].

2.1 Vibro-Thermal Module Assembly

We assembled the vibrator with the thermal unit into one module. Figure 1a is the schematic of the module, and Fig. 1b is the appearance of the developed module. Three thermistors were equipped in order to measure the temperature of warming and cooling Peltier devices including housing base, avoiding too much cooling and warming during thermal feedback. The thermistor between Peltier devices works as a reference point for capturing the temperature of contacting skin. The size of assembled module was $16 \times 7 \times 32$ mm and the weight was 10 g with the housing base.

3 Hardware Evaluation

3.1 Vibratory Characteristics

3.1.1 Hardware

We evaluated frequency response of the developed module. We measured the displacement of the module with a laser displacement sensor (Keyence, LK-H055) from the top of the module. The module was fixed onto the stage with a sponge, in order to

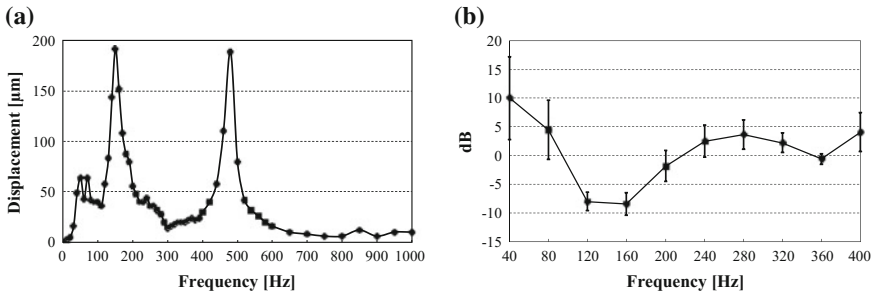


Fig. 2 Frequency response of **a** mechanical vibrator and **b** its equal-loudness contour estimated by human participants

imitate light contact with a finger pad. We observed two resonant frequencies around 150 and 500 Hz as shown in Fig. 2a.

3.1.2 Psychological Characteristics

We also evaluated psychological characteristics of the developed vibrator.

In the experiment, we measured individual difference of vibrotactile sensitivity for different frequencies. We measured equal-loudness contour in this experiment. Participants were asked to adjust the intensity of comparison vibrotactile stimulus to intensity of standard stimulus with a ten-key control pad. We used a 400 Hz of sine wave as standard stimulus. Comparison frequency was one of ten vibrotactile frequencies (40, 80, 120, 160, 200, 240, 280, 320, 360, 400 Hz). Once participants judged adjusted intensity of comparison stimulus is the same as standard stimulus, they terminated one trial and moved on next trial. The order of presented frequency of vibrotactile stimulus was randomized for each participant. Total number of trials were fifty (ten kinds of vibrotactile frequency \times five trials each) and averaged duration for the experiment was about thirty minutes. Five participants attended this experiment.

Figure 2b shows averaged amplitude of tactile stimuli that gave equal perceptual intensity with 400 Hz vibrotactile stimuli. X-axis is the presented vibrotactile frequency and Y-axis is the intensity of stimuli in dB unit that gave equal perceptual intensity.

The data showed apparent lower peak at around 150 Hz, which is due to the resonance of the vibrator. This would be due to the frequency response of vibrator itself which had a steep resonant peak at 150 Hz as shown in Fig. 2a. This data also implies that the frequency response of mechanical stimulator could affect perceptual intensity of vibrotactile stimuli.

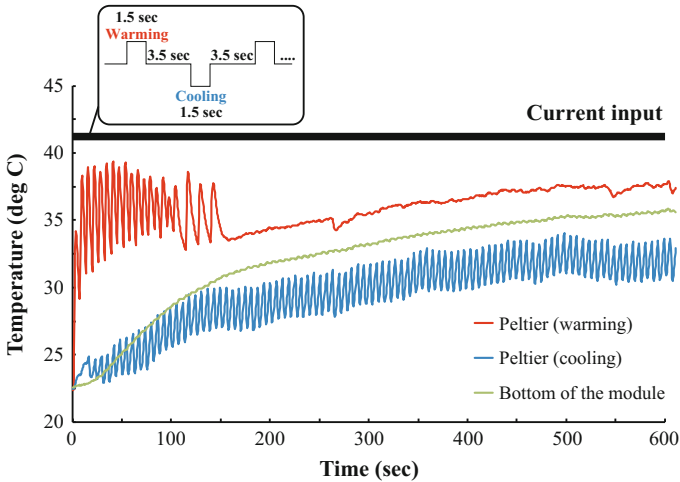


Fig. 3 Temperature profile of termotactile unit in developed module

3.2 Thermal Characteristics

We evaluated thermal characteristic of the developed module. We measured the temperature of warming and cooling Peltier devices using built-in thermistors as indicated in Fig. 1. In addition, we measured the temperature of bottom side of vibrothermal module to observe the trend of heat diffusion in developed module.

In the evaluation experiment, we continuously input current to pairs of warming and cooling Peltier devices respectively in order to alternately increase or decrease their temperature. The duration of applied current was 1.5 s, and the interval between warming and cooling input was 3.5 s. In this experiment, the contact side of warming Peltier devices were always warmed up, and never cooled down by applying current in opposite directions. Similarly, cooling Peltier devices were always cooled down. Once the temperature of module bottom reached at 30 °C, we stopped current input to the Peltier devices. The room temperature was 22 °C, and the sampling rate was 2 Hz in this experiment.

Based on the result shown in Fig. 3, we observed expected increase and decrease of temperature in both warming and cooling Peltier devices, however, we also observed the temperature increasing trend in all thermistors. This was due to the heat diffusion from both warming and cooling Peltier devices. In the beginning of the experiment, the temperature of bottom side of the module increased rapidly until the actuation of warming Peltier devices stopped around 100 s, and kept increasing its temperature slowly. The former temperature increase would be due to the heat diffusion from warming Peltier devices, and the latter would be from bottom side of cooling Peltier devices.

4 Discussion

In this study we developed vibro-thermal tactile display in a small size by assembling small vibrotactile display and four Peltier devices into one module. The size of the module is small (32 mm in maximum length) and light (10 g weight) so that this could be useful for mobile or wearable devices.

Based on the evaluation experiment, the performance of vibrotactile presentation was good in relatively lower frequency bandwidth (120–160 Hz). This may be good characteristics for vibrotactile display, because human has relatively higher sensitivity in this frequency range.

The performance of thermaltactile presentation in the developed module seemed to be equivalent to previous study (Sato et al. [11]). An issue we realized was that we needed to improve the performance of heat exhaustion of the module. This issue is always with thermal tactile displays, however, we plan to overcome this difficulty by using materials that can easily absorb heat from the housing base.

Vibro-thermal tactile display would increase the possibility of presenting material property in tactile modality. As discussed in previous literature, temperature information is highly associated with recognizing materials through skin sensations. Combining with vibrotactile presentation, we may increase the variety of displaying tactile materials using our developed module. In our preliminary trial, we added cooling temperature presentation while watching a cup poured water with vibrotactile feedback. Our participants told that it was realistic tactile experience, or even reported that their finger felt as if it were wet. This may be perceptual illusion or physically wet because of dew formation, and this empirical phenomenon is worth studying in future experiment.

We also realized that we needed to develop a system that can easily edit vibro-thermal tactile stimuli. Currently we controlled vibrotactile and thermaltactile display from different software, but an integrated system for editing tactile stimuli may increase the usability of the module that we developed. This is also an item of the list for future development of this series of study.

Acknowledgements This research was supported by JST-ACCEL Embodied Media project. Authors thank Dr. Hiroyuki Kajimoto for helpful discussion.

References

1. Ho, H.N., Jones, L.A.: Contribution of thermal cues to material discrimination and localization. *Percept. Psychophys.* **68**(1), 118–128. doi:[10.3758/BF03193662](https://doi.org/10.3758/BF03193662)
2. Ho, H.N., Jones, L.A.: Development and evaluation of a thermal display for material identification and discrimination. *ACM Trans. Appl. Percept.* **4**(2) July 2007. doi:[10.1145/1265957.1265962](https://doi.org/10.1145/1265957.1265962)
3. Hribar, V.E., Pawluk, D.T.: A tactile-thermal display for haptic exploration of virtual paintings. In: *The Proceedings of the 13th International ACM SIGACCESS Conference on Computers and Accessibility*. pp. 221–222. *ASSETS '11*, ACM, New York, NY, USA (2011). doi:[10.1145/2049536.2049577](https://doi.org/10.1145/2049536.2049577)

4. Jimenez, M., Fishel, J.: Evaluation of force, vibration and thermal tactile feedback in prosthetic limbs. In: Haptics Symposium (HAPTICS), 2014 IEEE. pp. 437–441, Feb 2014
5. Jones, L., Berris, M.: The psychophysics of temperature perception and thermal-interface design. In: Proceedings of the 10th Symposium on Haptic Interfaces for Virtual Environment and Teleoperator Systems, 2002. HAPTICS 2002, pp. 137–142 (2002)
6. Jones, L.A., Ho, H.: Warm or cool, large or small? the challenge of thermal displays. *IEEE Trans. Haptics* **1**(1), 53–70 (2008). doi:[10.1109/TOH.2008.2](https://doi.org/10.1109/TOH.2008.2)
7. Kajimoto, H., Kawakami, N., Tachi, S., Inami, M.: Smarttouch: electric skin to touch the untouchable. *IEEE Comput. Graph. Appl.* **24**(1), 36–43 (2004)
8. Killebrew, J.H., Bensmaïa, S.J., Dammann, J.F., Denchev, P., Hsiao, S.S., Craig, J.C., Johnson, K.O.: A dense array stimulator to generate arbitrary spatio-temporal tactile stimuli. *J. Neurosci. Methods* **161**(1), 62–74 (2007). <http://www.sciencedirect.com/science/article/pii/S0165027006005073>
9. Kim, J., Lee, M., Shim, H.J., Ghaffari, R., Cho, H.R., Son, D., Jung, Y.H., Soh, M., Choi, C., Jung, S., Chu, K., Jeon, D., Lee, S.T., Kim, J.H., Choi, S.H., Hyeon, T., Kim, D.H.: Article stretchable silicon nanoribbon electronics for skin prosthesis. *Nat. Commun.* **5** (2014)
10. Nara, T., Takasaki, M., Maeda, T., Higuchi, T., Ando, S., Tachi, S.: Surface acoustic wave tactile display. *IEEE Comput. Graph. Appl.* **21**(6), 56–63, Nov 2001. doi:[10.1109/38.963461](https://doi.org/10.1109/38.963461)
11. Sato, K., Maeno, T.: Haptics: Perception, Devices, Mobility, and Communication: International Conference, EuroHaptics 2012, Tampere, Finland, June 13-15, 2012. Proceedings, Part I, chap. Presentation of Sudden Temperature Change Using Spatially Divided Warm and Cool Stimuli, pp. 457–468. Springer, Berlin, Heidelberg (2012)
12. Sato, K., Maeno, T.: Presentation of rapid temperature change using spatially divided hot and cold stimuli. *J. Robot. Mechatron.* **25**(3), 497–505 (6 2013)
13. Wakuda, H., Kawauchi, T.: Bodily sensed vibration generator system 3 Jun 2004. <https://www.google.ch/patents/US20040104625>, uS Patent App. 10/717,070
14. Yamamoto, A., Ishii, T., Higuchi, T.: Electrostatic tactile display for presenting surface roughness sensation. In: 2003 IEEE International Conference on Industrial Technology, vol. 2, pp. 680–684, Dec 2003

Tactile Perception of Digital Images

Wenzhen Yang, Zhaona Jiang, Xin Huang, Xinli Wu
and Zhichao Zhu

Abstract This paper introduces a prototype system of the tactile perception of digital images. The prototype system is comprised of several models, which include automatic image segmentation, texture shape recovery, multi-points interaction, real-time image deformation, and texture tactile rendering. For a common digit image, the prototype system in some extent can automatically recover the texture tactile information from its pixel information.

Keywords Digit image · Tactile perception · Prototype system

1 Introduction

Usually, most of us believe the digital images only can be seen, and cannot be touched [1]. However, the tactile information implied in digital images has many interesting applications for museum exhibitions, game interactions, military training, and the blind education etc. How to discover the tactile information from digit images is a basic scientific problem [2, 3].

W. Yang (✉) · Z. Jiang · X. Huang · X. Wu · Z. Zhu
Virtual Reality Laboratory, Zhejiang Sci-Tech University, 15-348 Room,
Hangzhou 310018, China
e-mail: ywz@zstu.edu.cn
URL: <http://www.wzyang.com>

Z. Jiang
e-mail: 874018809@qq.com

X. Huang
e-mail: 15854286@qq.com

X. Wu
e-mail: wxl@zstu.edu.cn

Z. Zhu
e-mail: zczhu@zstu.edu.cn

We develop a prototype system of the tactile perception of digital images. The prototype system in some extent can automatically recover the tactile information of common digital images.

2 The Models of the Prototype System

The prototype system is comprised of several models, which include automatic image segmentation model, texture shape recovery model, multi-points interaction model, real-time image deformation model, and texture tactile rendering model etc.

Based on the division and merging of image regions, this prototype system achieves the object contours of a digit image, as shown in Fig. 1.

According to the shape from shading algorithm, this prototype system reconstructs the 3D texture shape of a digit image, as shown in Fig. 2.

Furthermore, this prototype system has the real-time image deformation model, multi-points interaction model, and texture tactile rendering model, as shown in Fig. 3, to feedback the tactile information of common digit images.

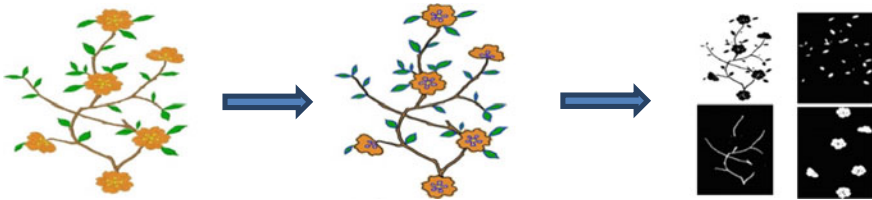


Fig. 1 Automatic image segmentation model



Fig. 2 Texture shape recovery model



Fig. 3 Real-time image deformation, multi-points interaction, and texture tactile rendering model

3 Conclusion

For generating the tactile information of digit images, we explore the efficient acquisition and expression method of the object contours in a digital image, research the recovery and expression method of the tactile texture in a digital image, realize the deformation of a digital image with region character, design the rigid flexible hybrid haptic rendering method, then, develop a prototype system of the tactile perception of digital images.

The prototype system in some extent can automatically recover the tactile information of common digital images, and can be applied in many fields.

References

1. Lareau, D., Lang, J.: Instrument for haptic image exploration. *IEEE Trans. Instrum. Meas.* **63**, 35–45 (2014)
2. Zhang, X., Sourin, A.: Image-inspired haptic interaction. *Comput. Animat. Virtual Worlds* **26**, 311–319 (2015)
3. Rasool, S., Sourin, A.: Image-driven haptic rendering. *Trans. Comput. Sci.* XXIII **8490**, 58–77 (2014)

VibGrip++: Haptic Device Allows Feeling the Music for Hearing Impaired People

Junichi Kanebako and Kouta Minamizawa

Abstract We improved a haptic device called “VibGrip (VG)”. The VG allows feeling the music by vibration for hearing impaired people. This device converts audio signal into vibrations that can be felt with the use of the 5 fingers. With 5 actuators, it is possible to feel the different musical part on each finger. The past version was only providing vibrations. “VibGrip++ (VG+)” has 5 pressure sensors it detects how strong grasping the device. This system allows controlling the intensity of each finger’s vibration and also controlling filter-effect intuitively. With this function, people with hearing impaired can feel the vibration of each musical part more clearly and enjoy in the concert.

Keywords Audio-tactile interfaces · Hearing impaired · Sensory substitution

1 Introduction

There is a wide range of research about sensory substitution including feel the sound by tactile stimuli. For instance, presenting pitch of the sound on the tip of finger like Braille patterns or transferring rhythms through vibrations [1–3]. A tactile vocoder [4] that allows listening to audio with vibration arrays placed on the fingers or a haptic chair [5] used for speech training that allows one to feel the vibration stimulation by sitting on a chair-shaped stool are examples of research that enables sensation by converting sound information into touch information.

We can assume that the vibration information aids a hearing impaired people in terms of providing the missing auditory information. However, the techniques above are difficult to implement in a regular environment because it requires a large scale system and the actuator is expensive so there is a demand for a simpler

J. Kanebako (✉) · K. Minamizawa
Keio University Graduate School of Media Design,
Hiyoshi 4-1-1, Kohoku-ku, Yokohama, Kanagawa 223-8526, Japan
e-mail: kanebako@kmd.keio.ac.jp
URL: <http://embodiedmedia.org/q>

structure and an equipment that can change and transmit audio information into vibration using the regular actuator technique.

We developed hearing device VibGrip [6] it converts audio information into vibrations that can be felt with the use of the 5 fingers. With 5 actuators, it is possible to feel the different musical part on each finger. For example, thumb is mapping for keyboard sounds, forefinger is mapping for vocal sounds and middle finger is mapping for drum sounds. On the other hand, VG has no sensor and it is difficult to control the intensity of vibration. We improved VG by using pressure sensor. The VG+ allows controlling the intensity of each finger's vibration and also controlling filter-effect. With this function, people with hearing impaired can feel the vibration of each musical part more clearly and enjoy in the concert.

2 System Description

The VG+ has piezoelectric actuators mounted on a small housing. The piezoelectric actuators used in this device can generate frequencies between 100 Hz–40 kHz and since it is suitable for producing low frequencies, it is possible to feel the audio information as vibrations. This is done by holding the device in one hand and having all fingers come into contact with the piezoelectric actuator.

The connection of the VG+ with a PC outputs a mono audio signal (5ch) via the audio interface and done using an amplifier. The design concept of the housing includes a third ear on the device which has been set to mimic the shape of an ear which serves as a hearing expansion. In addition, it is easy to hold with a grip shape similar to the ones in a bicycle. There are 5 pressure sensors mounted on the actuator, it detects how strong grasping the device with each finger. In current prototype we used Arduino and pressure sensor: Interlink 402. Figure 1 shows the shape and structure of VG+.

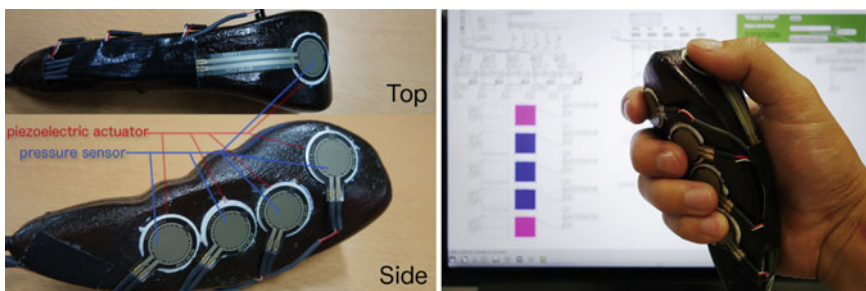


Fig. 1 Structure and shape of VG+

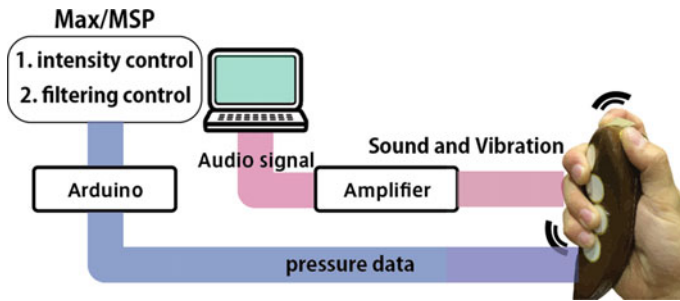


Fig. 2 VG+ system diagram

The integration of the system that we are proposing for this time (Fig. 2). VG+ device works as haptic display and controller. VG+ application consists of two modes. One is controlling the intensity of each finger's vibration, the other is controlling center frequency of low-pass filter. With this application, people with hearing impaired can adjust the vibration more intuitively.

3 Experience

The presenting condition are Audio+Vibration (AV) and vibration (V). In condition V, participant will wear the headphone has noise cancelling function: Bose QC25 to simulate sensorineural hearing loss. At first, participant sits on the chair and grasp the VG+, then system starts automatically plays rock music. They move each finger to control the vibration in mode1: intensity control and mode2: low pass filter control in condition AV. After that, participant try mode1 and 2 in condition V.

Acknowledgements This project is supported by JST-ACCEL Embodied Media Project.

References

- Galvin, K.L., Ginis, J., Cowan, R.S.C., Blamey, P.J., Clark, G.M.: A comparison of a new prototype Tickle Talker with a Tactaid 7. *Aust. N. Z. J. Audiol.* **23**(1), 16–18 (2001)
- Ifukube, T.: From sensory substitute technology to virtual reality research. *Artif. Life Robot.* **2**(4), 145–150 (1998)
- Sasaki, N., Ohtsuka, S., Ishii, K., Harakawa, T.: The development of a music presentation system by two vibrators. In: *Computers Helping People with Special Needs*, pp. 602–605 (2014)
- Ifukube, T.: A neuroscience-based design of intelligent tools for the elderly and disabled. In: *WUAUC 2001 Proceedings of the 2001 EC/NSF Workshop on Universal Accessibility of Ubiquitous Computing: Providing for the Elderly* (2001)

5. Nanayakkara, S., Wyse, L., Taylor, E.A.: The haptic chair as a speech training aid for the deaf. In: OzCHI 2012: Proceedings of the 24th Australian Computer-Human Interaction Conference (2012)
6. Kanebako, J., Kusunoki, F., Inagaki, S., Namatame, M.: Proposal for science learning materials using a “VibGrip”. In: Proceedings of the 12th International Conference on Advances in Computer Entertainment Technology, Article No. 36 (2015)

A Smart Cushion System with Vibrotactile Feedback for Active Posture Correction

Karlos Ishac and Kenji Suzuki

Abstract The developed system provides vibrotactile feedback through a pressure sensory cushion designed to be attachable to a chair in order to encourage users to sit upright. The sensory component of the cushion utilizes an array of 9 low-cost pressure sensors that detect the user's presence and posture. The sensory cushion calibrates to the user's upright posture using a guided setup implemented in a paired smart phone application. When the system detects inappropriate sitting posture such as slouching, vibrotactile feedback is delivered to the user as negative reinforcement. The vibration location is relative to the area in need of immediate posture correction. We conducted an experiment to observe the response of the user's sitting posture to vibrotactile feedback. The experiments demonstrated a classification accuracy of 94.1% during calibration and showed that vibrotactile feedback was effective in encouraging users to sit upright with an increase of 56.7% of time spent seated upright.

Keywords Smart cushion · Vibrotactile feedback · Posture correction · Haptics · Pressure sensing

1 Introduction

Poor posture is linked to lower back pains, headaches and fatigue [1]. Upright sitting posture has many benefits for human health in the prevention of injuries and increase in work productivity. Continuous posture tracking and correction covers many domains including the workplace, biomedical, personal fitness, occupancy monitoring and gaming. In recent years there has also been more behavioral exploration to how sitting posture affects awareness of VDT of worker's activity [2], some works also suggest good posture can improve handwriting ability [3]. The expansion of this domain has lead to several mobile applications to monitor sitting and standing posture [4]. However it is still difficult to realize continuous posture tracking and

K. Ishac (✉) · K. Suzuki
School of Integrative and Global Majors, University of Tsukuba, Tsukuba, Japan
e-mail: karlos@ai.iit.tsukuba.ac.jp

correction on the seat due to limited sensor capabilities on the smart phone. We, therefore, propose a sensory cushion system for active posture correction by using negative vibrotactile training.

Pressure sensing systems have demonstrated accuracy in the detection and tracking of posture in both blind and known studies [5]. It has been demonstrated that haptic feedback was effective in enforcing upright posture and that when haptic feedback was disabled the subjects continued to sit upright [6]. However the placement of sensors in the system is not a good indicator of upright posture since the shoulders and lumbar sides are not accounted for. In our developed system, we aim to accurately detect pressure at much larger locations on the user’s back, including the shoulders, side lumbar and along the spine.

Similar systems such as cushionware [7] attempt to detect sitting posture by using a pressure sensing pillow that the user sits on. Although this can be an indicator of sitting posture, it cannot provide as much pressure resolution as a lumbar support cushion. In our design we utilize a sensory cushion that is placed behind the user’s back.

2 System Overview

2.1 System Components

The smart cushion system is comprised of 9 circular pressure sensors, 4 vibration motors, Bluetooth module, rechargeable circuit and logic circuit. The pressure sensors are arranged in an array of 3 rows and 3 columns as shown in Fig. 1.

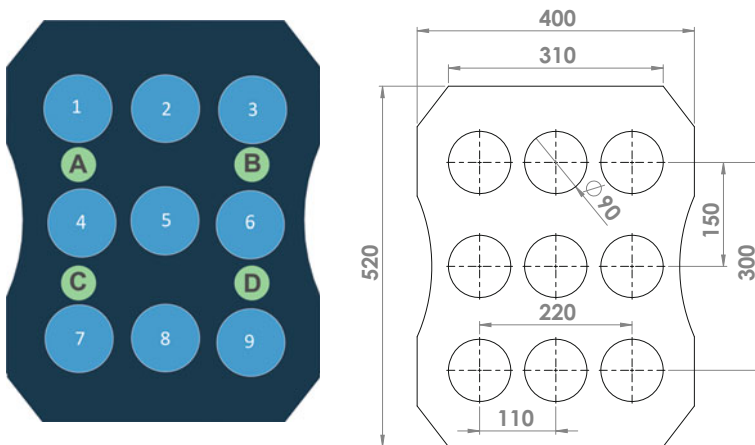


Fig. 1 Smart cushion pressure sensor arrangement ($i = 1 \dots 9$) and vibration motor locations ($j = A \dots D$)

The vibration motors are located at each quadrant on the cushion equidistant from the centre as shown in Fig. 1. This arrangement is to allow the pulsing of individual areas on the back in order to give the user greater understanding of which areas are in need of immediate attention. This is unique to our system as many alternative devices tend to vibrate the entire cushion and can confuse the user.

2.2 Software Model

The system first calibrates the sensors to the user’s upright posture through an app guided calibration routine. Our software scans the snapshot for approximate balance in pressure distribution from the centerline. The templates are constructed by a pilot study that measured sensor activation during different sitting conditions. The app also shows the user real-time feedback of the pressure pads during calibration to allow for correction of imbalances.

2.3 Posture Tracking and Classification

The sensors actively collect data at 200 ms intervals which is then matched to posture templates based on MSE shown in Table 1. Depending on the state detected by template matching, the appropriate vibration motors would activate to alert the user of the area that needs to be corrected.

In order to predict a posture we observe deviations at each sensors, these are represented by ϵ . We denote the calibrated force readings at each pressure sensor f_i where i is in reference to the sensor position shown in Fig. 1 as 1 ... 9. The array $V_i(t = 0)$ refers to the voltage readings at all pressure sensors at the time of calibration given at $t = 0$. The array $V_i(t)$ refers to the instantaneous voltage readings at time t . This is used to compute the mean-squared error at each individual sensor location during continuous posture tracking mode.

$$V_i(t) = [f_1(t) \dots f_9(t)] \tag{1}$$

$$V_i(t = 0) = [f_1(0) \dots f_9(0)] \tag{2}$$

The MSE is denoted by $\epsilon(t)_i$ where ϵ is the computed deviation at time t at sensor i .

$$\epsilon(t)_i = (V_i(t) - V_i(0))^2 > \alpha \tag{3}$$

where α is a constant threshold determined from experimental pilot studies. If the computed error at each individual location is less than the threshold α then we assume that the user is seated in the upright position. If the deviation error at a

Table 1 Haptic feedback model

| γ | S_p | ϵ | Vibration pattern | Action suggested |
|----------|---------------------------|---|-------------------|------------------------------|
| 1 | No user | $\sum_i^{n=9} \epsilon_i > n\alpha$ | No activation | Sit down |
| 2 | Sitting upright | $\sum_i^{n=9} \epsilon_i < \alpha$ | No activation | Maintain upright posture |
| 3 | Upper back no contact | $\epsilon_1, \epsilon_2, \epsilon_3 > \alpha$ | C and D | Sit back in upright posture |
| 3 | Lower back no contact | $\epsilon_7, \epsilon_8, \epsilon_9 > \alpha$ | A and B | Pull back lower back |
| 4 | Slouching forward | $\epsilon_2, \epsilon_5 > \alpha$ | C and D | Sit back in upright posture |
| 5 | User slouching right | $\epsilon_3, \epsilon_6, \epsilon_9 > \alpha$ | A and C | Pull back right side of body |
| 5 | User slouching left | $\epsilon_1, \epsilon_4, \epsilon_7 > \alpha$ | B and D | Pull back left side of body |
| 6 | Right shoulder no contact | $\epsilon_1 > \alpha$ | B | Pull back right shoulder |
| 6 | Left shoulder no contact | $\epsilon_3 > \alpha$ | A | Pull back left shoulder |
| 6 | Right lumbar no contact | $\epsilon_7 > \alpha$ | D | Pull back right lumbar |
| 6 | Left lumbar no contact | $\epsilon_9 > \alpha$ | C | Pull back left lumbar |

particular sensor exceeds the threshold then a reference posture is predicted based on a state lookup table. These states are denoted by $S_{p=1\dots 9}$. The state look-up table also uses a variable γ to perform a priority based search where it will predict the posture on a top-down look-up that ensures the state detected ranges from critical to specific. When the posture is predicted it is displayed on the app and the appropriate motors are pulsed at a frequency of 5 Hz until the user corrects their posture.

3 Experiment and Results

We conducted 2 experiments to verify the accuracy of the classification algorithm and observe changes in time spent seated upright when vibrotactile feedback is enabled (Fig. 2). Both experiments were conducted on 6 subjects (4 male, 2 female) aged 27 ± 3 with a weight of 73 ± 17 kg. Both experiments were filmed and the pressure sensor array data was recorded at 200 ms intervals. Subject consent is obtained before experiments.

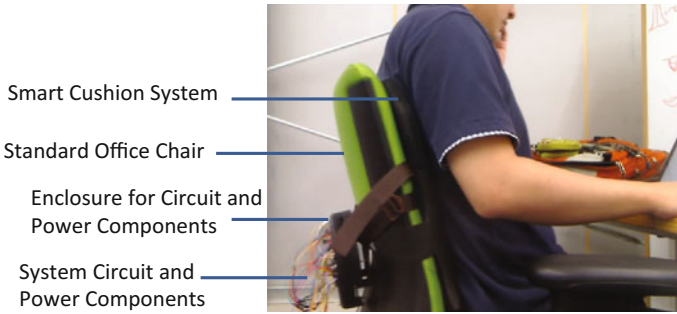
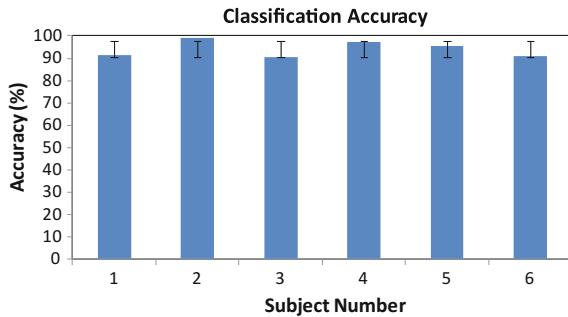


Fig. 2 Experimental setup for performance and response tests

Fig. 3 Classification accuracy of all subjects during calibration



3.1 Performance Test

For the first experiment the user's were asked to sit in an upright position through a guided routine by the experimenter and the smartphone app. Once the upright position is verified by the visualization of sensors on the app and experimenter, a snapshot of the pressure values is taken. After this the user is instructed to sit in a random posture for 5 trials. The posture is template matched and displayed on the app. The percentage of successful classifications during calibration phase is shown in Fig. 3.

3.2 Response Test

After calibration has been validated, the user begins a 2 h study where their posture is actively tracked. During this study the user works normally at their desk using a laptop/PC. In the first hour vibration is disabled and during this phase we only record the data from the pressure sensors. In the second hour vibration is enabled and we observe how the user's respond to the feedback. The percentage of time spent sitting upright and time spent slouching is displayed in Figs. 4 and 5.

Fig. 4 Comparison of time spent seated upright for all users

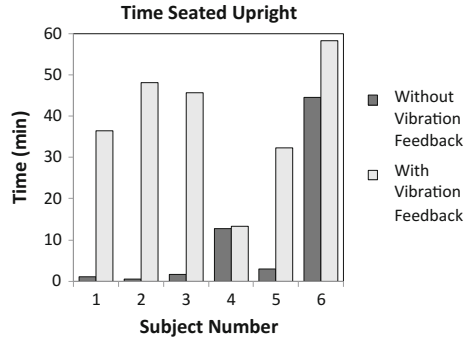
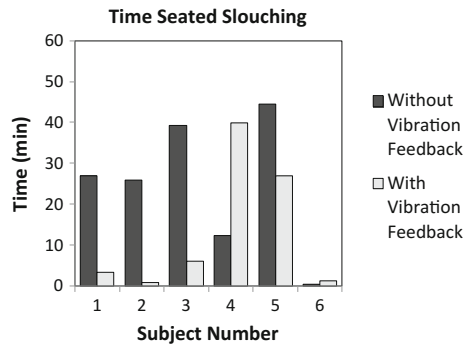


Fig. 5 Comparison of time spent slouching for all users



4 Discussion and Conclusion

In the first experiment, Subjects would attempt to sit in an upright posture by watching the sensor feedback on the screen. 5 out of 6 subjects were able to successfully activate all pressure sensors giving a detection accuracy of 83.3%. Subject 6 was not able to activate the sensors at the shoulders due to their slim build. In future prototypes this can be solved by increasing the sensitivity and contact radius of the pressure sensors.

Overall we observed an average of 94.1% of successful classifications during the calibration phase. In total there were 2.63% of unclassified instances and 3.1% of mismatched instances during the calibration phase. This can be resolved by modifying the variance threshold values for classification.

The results in Fig. 3 show an average increase of 56.7% (outlier excluded) in time spent sitting upright when vibration was enabled. When vibration was disabled, 5 out of 6 subjects showed frequent slouching to the left with little contact at the right shoulder and lumbar. When vibration was enabled, this imbalance was reduced and it was observed that subjects were actively responding to vibration to fix their slouching. Figure 4 shows that 4 out of 6 Subjects experienced a major decrease in time spent slouching when vibration was enabled with an average decrease of 32.8%.

Subject 4 is considered an outlier in the results. It was observed that the subject demonstrated major slouching to the left side, with little contact at the right shoulder. Initially the subject tried to correct his/her posture to stop the vibration, but could not get back into their calibrated position so gave up and withstood the vibration.

In this paper we have presented a low cost device for active encouragement of seated upright posture. The experiments have validated the accuracy of our classification algorithm with a 94.1% of successful classifications during calibration. Our results also demonstrate that vibrotactile feedback is effective in training user's to sit upright with an increase of 56.7% time spent seated upright when vibration was enabled. Overall 4 out of 6 subjects posture was successfully corrected. 1 out of 6 subjects was unable to activate all sensors at the outer regions of the cushion due to their slim build and this can be resolved in the future design and arrangement of the sensors to accommodate a more diverse range of users. 1 out of 6 subjects could not return to their calibrated upright posture, so the vibration feedback was continuous for the majority of the experiment. This is easily resolved by the recalibration of the upright posture. We also envision the implementation of posture regulation levels for our end users where they can manage the strictness of the system in encouraging their upright posture.

We believe the applications of this system can extend to many areas including rehabilitation. In the future we plan to extend this system to include greater functionality such as sitting time regulation and monitoring of other human biosignals.

References

1. Helander, M.G., Zhang, L.: Field studies of comfort and discomfort in sitting. *Ergonomics* **40**(9), 895–915 (1997)
2. Manabe, Y., et al.: Development of perceptual functions as primitive awareness for VDT work environment. In: 2011 3rd International Conference on Awareness Science and Technology (iCAST). IEEE (2011)
3. Wu, Y.-P., Chen, J.-H.: A surveillance system designed for the correction of sitting posture in writing. In: 2012 9th International Conference on Ubiquitous Intelligence and Computing and 9th International Conference on Autonomic and Trusted Computing (UIC/ATC). IEEE (2012)
4. Samiei-Zonouz, R., Memarzadeh-Tehran, H., Rahmani, R.: Smartphone-centric human posture monitoring system. In: 2014 IEEE Canada International Humanitarian Technology Conference (IHTC). IEEE (2014)
5. Kamiya, K., et al.: Sitting posture analysis by pressure sensors. In: 19th International Conference on Pattern Recognition, ICPR 2008. IEEE (2008)
6. Zheng, Y., Morrell, J.B.: A vibrotactile feedback approach to posture guidance. In: 2010 IEEE Haptics Symposium. IEEE (2010)
7. Liang, G., et al.: Cushionware: a practical sitting posture-based interaction system. In: CHI 2014 Extended Abstracts on Human Factors in Computing Systems. ACM (2014)

HapTONE: Haptic Instrument for Enriched Musical Play (II)—System Detail

Kenta Tanabe, Akifumi Takahashi, Keisuke Hoshino, Daichi Ogawa, Taku Hachisu and Hiroyuki Kajimoto

Abstract We developed a novel musical entertainment system ‘HapTONE’ that draws on auditory, tactile, and visual senses. HapTONE presents players with high-fidelity vibrotactile sensations, not only after a key on pressing the keyboard but also during the actual process of pressing the key itself. HapTONE is composed of eight key units that is composed of a vibrator and a distance sensor. This instrument reproduces the touch sensation of a keyboard and stringed, wind, percussion or non-musical instruments. We also developed some applications using HapTONE, which were exhibited at the computer graphics and interactive techniques conference ‘SIGGRAPH 2016’. In this paper, we describe the system details of HapTONE that enable accurate, low-latency feedback and easy expansion.

Keywords Vibrotactile · Musical instrument · Haptics

K. Tanabe (✉) · A. Takahashi · K. Hoshino · D. Ogawa · H. Kajimoto
The University of Electro-Communications, 1-5-1 Chofu-ga-oka,
Chofu, Tokyo 182-8585, Japan
e-mail: k.tanabe@kaji-lab.jp

A. Takahashi
e-mail: a.takahashi@kaji-lab.jp

K. Hoshino
e-mail: hoshi@kaji-lab.jp

D. Ogawa
e-mail: ogawa@kaji-lab.jp

H. Kajimoto
e-mail: kajimoto@kaji-lab.jp

T. Hachisu
University of Tsukuba, 1-1-1 Tennodai, Tsukuba, Ibaraki 305-8577, Japan
e-mail: hachisu@ai.iit.tsukuba.ac.jp

1 Introduction

For centuries, playing musical instruments has been one medium humans have used to entertain themselves. In recent years, electronic instruments have enabled people to play a variety of instruments using just one interface such as a synthesizer to produce various type of audio output. However, haptics are not typically used. One can hear a sound of xylophone or violin when the keys on the keyboard of an electronic piano is pressed, but the touch sensation remains that of a plastic keyboard.

Although several studies on haptic feedback have been linked to music, many of them aimed to enhance the listening experience [1, 2]. However, Hachisu et al. aimed to enhance the playing experience on tablet PCs by using vibrotactile sensations [3], thereby augmenting haptic sensation. For keyboard-type instruments, Marshall and Wanderley [4] added tactile sensations to a piano to create a learning system, and Oboe and De Poli [5] created a virtual keyboard that reproduced the touch sensation of keyboard instruments such as the piano or organ.

Here we report on a system we developed called ‘HapTONE’ that modulates the haptic sensations of a keyboard by presenting the player with different vibrotactile sensations, not only after pressing keys on the keyboard but also during the actual process of pressing the key itself [6]. We also developed applications using HapTONE (percussion, pseudo-string and interactive projection mapping of living creatures using haptics), and exhibited it at the annual computer graphics and interactive techniques conference ‘SIGGRAPH 2016’. In this paper, we describe the system details of HapTONE that enable accurate, low-latency feedback, and easy expansion.

2 System Detail of HapTONE

Main Components of HapTONE

Figure 1 (left) shows the appearance of HapTONE system. It is comprises eight key units, five microcontrollers (mbed NXP LPC1768), four Digital-to-Analog (DA) converters with two outputs (MCP4922, Microchip Technology Inc.), one Analog-to-Digital (AD) converter with eight inputs (MCP3208, Microchip Technology Inc.), and a PC for audio-visual feedback. A key unit is composed of a vibrator (Vp408, Acouve Laboratory) and an optical distance sensor Fig. 1 (right). All units were 3D-printed. The vibrator is driven by an audio amplifier (SA-60, S. M.S.L). The distance sensor is composed of a photo-reflector (TPR-105F, GENIXTEK).

Calibration of Optical Distance Sensor

The voltage output from the optical distance sensor was non-linearly rated with distance. We calibrated sensors by using cubic natural spline interpolation. First, for five distances (measured by height gauge), we obtained voltage data repeated



Fig. 1 HapTONE system (left) and the key unit (right)

10 times and calculated the mean. From these five sampled pairs of distances and voltages, a spline curve was estimated. Then, by using this spline curve, we interpreted sensor values into a linearized 256-step distance value.

Multi-channel, High-Speed Feedback

HapTONE measures the stroke distance of each key at a 1-kHz sampling rate. This provides vibrotactile and auditory sensation not only after pressing the key but also during the actual stroke operation. This gives the sensation of continuous vibration associated with the player's motion such as the vibration of a violin (i.e., stringed instruments). Stroke distance and speed are calculated using these data and are also converted into MIDI data. Then, these data are sent to the PC for audio-visual feedback. The PC presents the auditory feedback, but the vibration waveform model for haptic feedback is programmed in the microcontrollers beforehand, and played by changing some parameters depending on the stroke distance and speed. This structure greatly reduces latency between the user's action and haptic feedback, enabling users to feel not only simple vibration, but also the physical properties of a contact object.

To achieve such a low-latency system, HapTONE adopted a multiprocessors structure (Fig. 2). The five microcontrollers are divided into two groups according to their function: mother and children. Four children microcontrollers control vibrotactile feedback of two keys, and one mother microcontroller sends MIDI and distance data to the PC. The sensor outputs are fed in parallel to mother and children, and stroke distance and speed are calculated at each microcontrollers independently. Mother and children communicate with each other via a serial interface to change instruments. This independence simplifies development and enables high-speed feedback in the case of such a multi-channel situation.

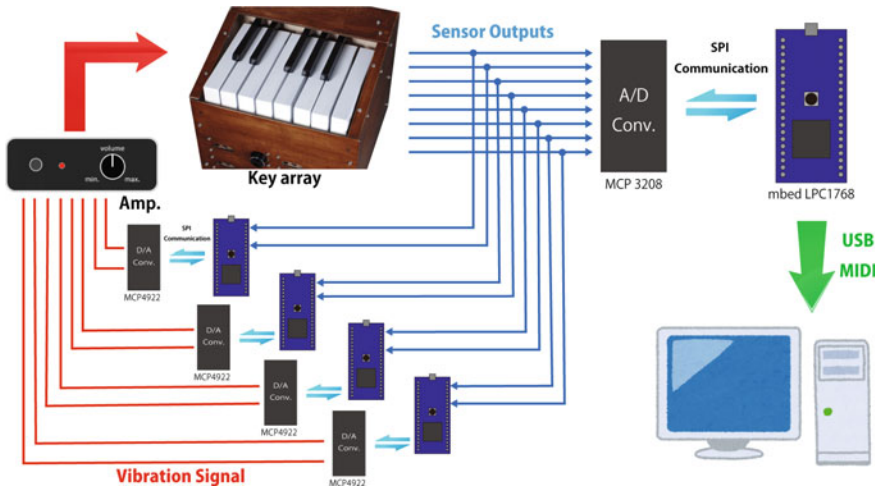


Fig. 2 The overall system of HapTONE

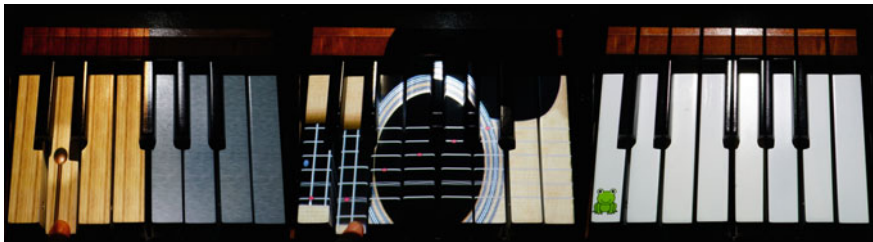


Fig. 3 Applications using HapTONE

3 Exhibit at SIGGRAPH 2016

We developed three applications: percussion, string and living creatures, using interactive projection mapping of animations and haptics (Fig. 3). These applications are briefly described in [6], and were exhibited at SIGGRAPH 2016. Figure 4 is a photograph of our exhibition. Over 1500 people experienced HapTONE, and a majority expressed surprise and appeared impressed by the differences in touch sensations for each application. Children were observed to be especially absorbed in playing with HapTONE, with some playing with the system for >5 min. HapTONE and its combined interactive sound, visual, and tactile sensations appeared to be enjoyed by many people.



Fig. 4 Exhibit in SIGGRAPH '16

4 Conclusion and Future Work

In this paper, we described the system details of a haptic musical instrument device ‘HapTONE’. The calibrated optical distance sensor and the multiprocessors system enabled accurate, low-latency feedback and easy expansion of the system. We also developed three applications using HapTONE, which were exhibited at SIGGRAPH 2016. Our future work will include developing suitable vibration parameters for each musical instrument, and expanding the system to include non-musical instruments such as gaming devices.

Acknowledgements This research is supported by the JST-ACCEL Embodied Media Project.

References

1. Karam, M., Branje, C., Nespola, G., Thompson, N., Russo, A.F., Fels, I.D.: The emoti-chair—An interactive tactile music exhibit. In: Proceeding of SIGCHI Conference on Human Factors in Computing Systems (CHI) 2010 Extended Abstracts, pp. 3369–3074 (2010)
2. Baijal, A., Kim, J., Branje, C., Russo, F., Fels, D.I.: Composing vibrotactile music: a multi-sensory experience with the emoti-chair. In: Proceedings of IEEE Conference on Haptic Symposium (HAPTICS), pp. 509–515 (2012)
3. Hachisu, T., Kajimoto, H.: HACHIStack: dual-layer photo touch sensing for haptic and auditory tapping interaction CHI 2013, pp. 1411–1420 (2013)
4. Marshall, M.T., Wanderley, M.M.: Vibrotactile feedback in digital musical instruments. In: Proceedings of New Interfaces for Musical Expression (NIME06), pp. 226–229 (2006)
5. Oboe, R., De Poli, G.: Multi-instrument virtual keyboard—the MIKEY project. In: Proceedings of New Instruments for Musical Expression (NIME 2002), pp. 1–6 (2002)
6. Ogawa, D., Tanabe, T., Yem, V., Hachisu, T., Kajimoto, H.: HapTONE: haptic instrument for enriched musical play. In: SIGGRAPH 2016 ACM SIGGRAPH 2016 Emerging Technologies Article No. 12 (2016)

Visual Haptic Interface by Using 2-DOF Indirect Haptic Interface

Takayuki Ishikawa, Hiroaki Yano and Hiroo Iwata

Abstract This paper describes development of a visual and haptic feedback interface by using a direct input touch panel display and 2 Degree-of-Freedom (DOF) indirect haptic interface. In this system, a user should wear no gear on his/her fingertip, and can touch the objects with it. The system consists of a display, a motion tracker, and a 2-DOF haptic interface equipped with a force sensor. The systems measure the position of the fingertip of a user and produce an appropriate horizontal force on the thenar eminence (the group of muscles on the palm of the human hand at the base of the thumb) of the user. Through an evaluation test, it was verified that the effectiveness of the system for perceiving the hardness of virtual object at the fingertip.

Keywords Virtual reality · Haptic display · Indirect-haptic feedback · Direct-pointing interface · Thenar eminence

1 Introduction

If a person is able to touch real objects with his/her own bare hand through a haptic interface, he/she may be able to perceive additional rich information about the object. One of the solutions to address this issue is to use an exoskeleton-type haptic interface with special thimbles that do not cover a user's fingertips. Another solution is to have separate input and output regions, e.g., the fingertip is used for input and another region of the hand is used for output. Mohareri et al. [1] proposed an asymmetric force feedback control framework for a tele operated bimanual surgical environment in which force feedback is generated to the other hand of the user to overcome the instability of the direct haptic feedback, which is caused by communication time delays and so on. This technique brings stability to the

T. Ishikawa (✉) · H. Yano · H. Iwata
University of Tsukuba, 1-1-1 Tennodai, Tsukuba, Ibaraki 305-8573, Japan
e-mail: t_ishikawa@vrlab.esys.tsukuba.ac.jp

bimanual tasks of tele operated bimanual surgical systems. However, since there are many single-handed tasks, one-handed haptic feedback is desired.

To overcome the above issues, we proposed an indirect haptic feedback method [2]. We combined a 2-DOF haptic interface with a visual display to enable users to virtually perceive the surface and friction of 3D virtual objects. In this system, as the input method, an indirect input method with an upright visual display was chosen. As another option, an input method with a horizontal display, which enables a user to touch it directly, can also be considered.

By combining an indirect haptic interface and a direct pointing interface, it was assumed that a user's haptic sensation such as feeling of hardness, may be changed, because the visual information near the finger that is used for input changes according to the motion of the fingertips.

In this study, we developed a prototype system that had a touch panel display as a direct input and an indirect haptic interface as output method without any equipment on the fingertip of a user. An experiment to perceive the hardness of virtual elastic objects by using magnitude estimation method was conducted. The perception value of the hardness were changed according to the hardness of the visual model, even though the hardness of the haptic model was the same. At this time, prepared a visual model and the haptic model respectively, the modulus of elasticity of the haptic model was constant.

2 Configuration

In this study, a desktop environment is considered as the main target. In indirect haptic feedback interface, input point and output point are separated. The tip of the index finger is selected as the input point because a fingertip is usually used to touch objects. To avoid encumbering the fingertip motion, the output point is fixed as a point on the hand except on the index finger. Since the thenar eminence, on account of being distant from the fingers, does not restrict finger motion, it was selected as the output point in this study. This output point is convenient for a desktop task such as a pointing task with a mouse interface, because a user can place his/her thenar eminence on the end effector of the indirect haptic interface, leaving his/her finger free to move and point in 3D space. In addition, the finger motion is unrestricted as nothing is attached to the fingertip.

As shown in Fig. 1, a user places his/her thenar eminence on the force sensor. If the user pushes the object with his/her fingertip, the horizontal component of the reaction force is produced on the user's thenar eminence by the 2-DOF haptic interface. Figure 2 shows the prototype of the proposed indirect haptic interface with a direct pointing environment. In this environment, a horizontal display showed a virtual object as a cube.

In order to verify the effectiveness of the system, the position of the fingertip, the velocity of the fingertip, and the force on the thenar eminence were measured, when touching a rigid object, or an elastic object. A typical example of touching them are

Fig. 1 Concept of indirect haptic interface

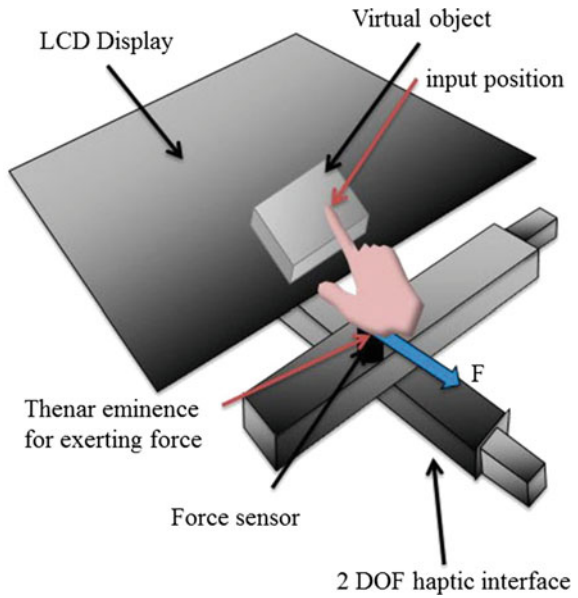
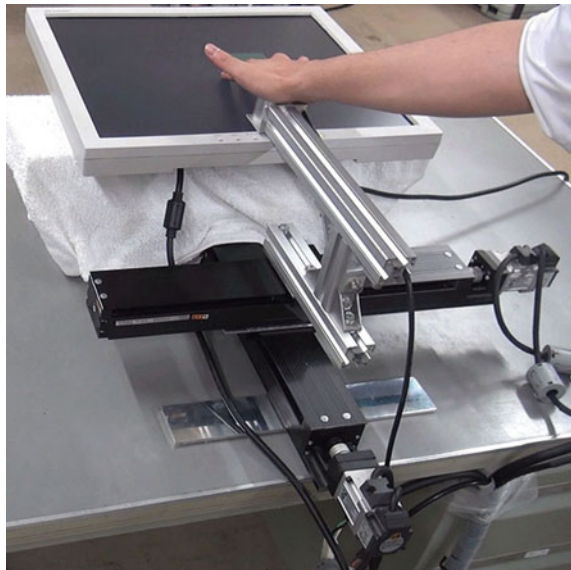


Fig. 2 Prototype of a visual haptic interface



shown in Figs. 3 and 4, respectively. The response time of this system were 0.04, and 0.06 s when touching the rigid object and the elastic object, respectively. As a results, a reaction force from each virtual object can be presented in real time. The user could feel the difference between the rigid and the elastic object.

Fig. 3 Motion during touching a rigid virtual object

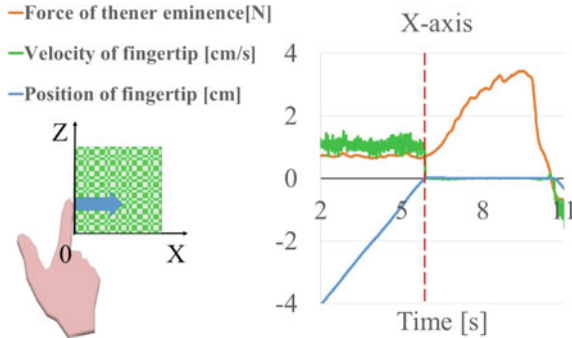
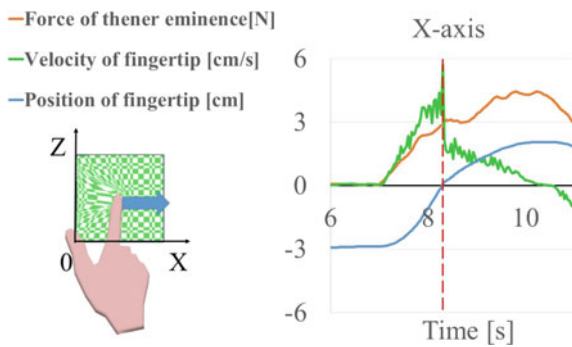


Fig. 4 Motion during touching an elastic virtual object



The system consists of a 24-inch LCD display, a 2-DOF haptic interface equipped with a motion tracker and a force sensor, and a PC for controlling them. The 2-DOF interface is equipped with two linear actuators (KR33, produced by THK). Each actuator has an AC servomotor (MSMD011P1S, produced by Panasonic) and an optical shaft encoder. Their maximum speed is 833 mm/s and maximum force is 200 N. One actuator is placed on top of another actuator, horizontally perpendicular to each other. The size of the operating region of the end effector is 300×300 mm. A motion tracker Flex 13, produced by Optitrack, is used to measure the position of the fingertip. In addition, a force sensor (CFS034CA301, produced by Leptrino) is placed on top of the end effector. Force applied to the thenar eminence is measured by the force sensor. The PC (Windows7 Professional OS, 64-bit CPU, Intel Core i5 650) communicates with the interface through a master control board (HCRTEXsd, produced by Vanguard Systems).

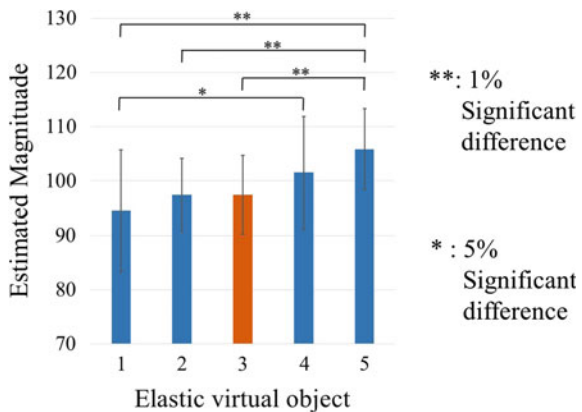
3 Evaluation Test

In hardness perception, basically haptic sensation is dominance compared with other sensations. In the proposed method, visual effect around fingertip which contacts with virtual objects might influence the hardness perception. In this experiment, the subjects touched elastic virtual cubes by using a prototype system. Then, the subjects asked the hardness of the elastic virtual cubes based on a magnitude estimation method. The elastic objects were implemented as a polygon model that has been expressed with the network of springs and dampers. Each vertex of the polygons is connected to its original position with a spring (resilience) and a damper. Therefore, the cube can be deformed, and restore the original shape, when it remained untouched. In addition, since each virtual cube had a visual model, and haptic model, respectively, the cube had hardness of visual model, and that of the haptic model, individually. 5 spring constants of the resilience of the visual models were prepared. The spring constant of the resilience of the haptic model was fixed as same as the middle value of the hardness of the 5 cubes which was as same as the standard stimulus in the visual model.

6 subjects conducted 5 trials in each condition, 25 trials in total, respectively. Each subjects touched a cube which was randomly selected from the 5 cubes, and compared with the standard stimuli. And the subjects answered the hardness of each comparison stimulus, if the hardness of the standard stimuli was 100. Figure 5 shows the experimental results.

The multi-way ANOVA measured a 1% significant difference between cross-sections. Post hoc tests using the Scheffe Multiple Comparison tests revealed significant differences at a 1% significance level (**) in a combination of the visually stiffness 5 and stiffness1, 2, and 3. Also significant difference at 5% significance level (*) was found between stiffness 1 and 4. As a result, it was suggested that visual dominance was observed when changing the elastic modulus of the visual model of the elastic virtual object by using our system, even though the

Fig. 5 Comparison of estimated magnitudes



resilience of the haptic model was fixed in constant. This means the subjects perceived the hardness of touched object at the fingertip, and focused not on the thenar eminence but on the fingertip.

4 Conclusion

In the study, we have developed an indirect haptic interface with a direct pointing environment that it is possible to obtain a sense of touch with virtual objects on his/her bare hand. In experiment of hardness perception of VR objects with the subjects' bare hand by using this system, the visual dominance of hardness perception was observed. At that time, the subjects focused on the contact at the fingertip. This system can be applied for a shape modeling system, and a surgical simulator.

In the future, we plan to optimize the combination of visual and haptic models. Moreover, we plan to develop frictional force rendering method and more complex virtual environment with the system.

References

1. Mohareri, O., Salcudean, Nguan, C.: Asymmetric force feedback control framework for tele-operated robot-assisted surgery. In: Proceedings of ICRA 2013, pp. 5800–5806 (2013)
2. Yano, H., Taniguchi, S., Iwata, H.: Shape and friction recognition of 3D virtual objects by using 2-DOF indirect haptic interface. In: Proceedings of World Haptic Conference 2015, pp. 202–207 (2015)

HaptoCloneAR (Haptic-Optical Clone with Augmented Reality) for Mutual Interactions with Midair 3D Floating Image and Superimposed 2D Display

Kentaro Yoshida, Takaaki Kamigaki, Seki Inoue, Keisuke Hasegawa, Yasutoshi Makino and Hiroyuki Shinoda

Abstract In the previous study, a new interactive system called HaptoClone was proposed. In HaptoClone system, a user can interact with optically copied objects from the adjacent workspace with haptic feedback. In this study, we propose an improved version of the HaptoClone system called HaptoCloneAR, which superimposes a virtual 2D screen on the copied objects by using half-mirrors. The system can display 2 different images independently to each workspace. In this paper, we show a basic configuration of the HaptoCloneAR system. We demonstrate a feasibility of the proposed system with our prototype.

Keywords 3D interaction · Augmented reality (AR) · Tactile display · Telexistence

1 Introduction

In the previous study by Makino et al., they proposed HaptoClone (Haptic-Optical Clone) system, which was a mutual interactive system [1]. This system enables two users sitting side by side interact mutually with each other's cloned 3D volumetric image with haptic feedback. Since the 3D image is cloned optically by using a pair of micro-mirror array plates (MMAPs), the refresh rate of the cloned image is as fast as the speed of lights, and users can see it without wearing any glasses [2]. When

K. Yoshida (✉) · S. Inoue · Y. Makino · H. Shinoda
Graduate School of Information Science and Technology, The University of Tokyo,
7-3-1 Hongo, Bunkyo-ku, Tokyo 113-0033, Japan
e-mail: yoshida@hapis.k.u-tokyo.ac.jp

Y. Makino
e-mail: yasutoshi_makino@k.u-tokyo.ac.jp

H. Shinoda
e-mail: hiroyuki_shinoda@k.u-tokyo.ac.jp

T. Kamigaki · K. Hasegawa · Y. Makino · H. Shinoda
Graduate School of Frontier Sciences, The University of Tokyo,
5-1-5 Kashiwanoha, Kashiwa-shi, Chiba 277-8561, Japan

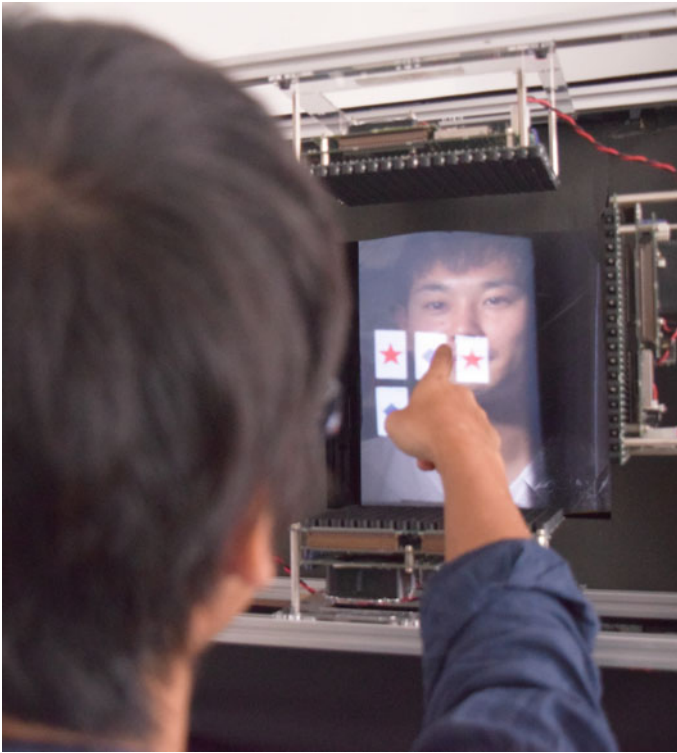


Fig. 1 The picture of using HaptoCloneAR

users or objects touch the cloned image, haptic feedback is also given by using an airborne ultrasound tactile display (AUTD) [3]. AUTD can make converged ultrasound foci to make tactile stimulations in midair by controlling phases of each transducer. The contact positions, where AUTD gives forces, are determined by measuring contact point from depth images by Kinect2 sensors. Since the volumetric image in the HaptoClone system was realized by an optical mirror mechanism, it was difficult to display artificial images onto cloned volumetric images.

In this paper, we propose a new system named HaptoCloneAR (Haptic-Optical Clone with Augmented Reality) that superimposes 2D images onto conventional 3D cloned images. Figure 1 shows a picture of HaptoCloneAR. We present a virtual screen onto the cloned floating image to show a lot of information. Haptic feedback is also given to the virtual 2D screen when a user touches it. With this HaptoCloneAR system, users sitting side by side can interact with each other with touchable 2D information. For example, people can play cards in the virtual field seeing an opponent's face.

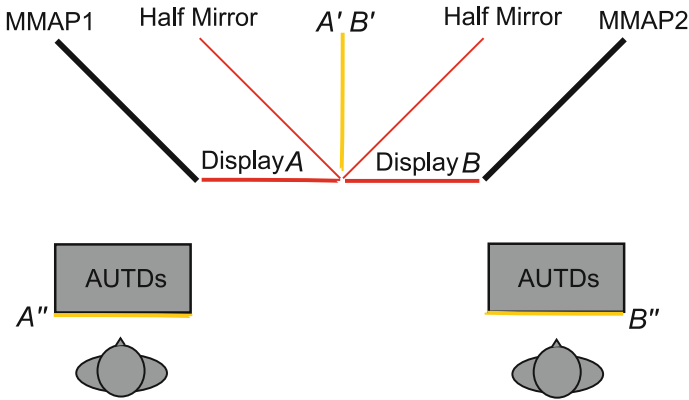


Fig. 2 Configuration of the system: added displays and half mirrors are painted in *red*, and the reconstructed images are painted in *orange*

2 Principle

Figure 2 shows the configuration of HaptoCloneAR. In our proposed system, two half mirrors and two displays, shown in red, are added to the HaptoClone (the previous system). This configuration reconstructs the image of display A to A' by reflection of the half mirror. The reconstructed image at A' is reconstructed at A'' by the MMAP1. Therefore, a user sees the reconstructed image of the display A at A''. In the same way, the image of display B is seen at B'' through half mirror, and MMAP2.

One important characteristic of this configuration is that, two images of the display A and B are reconstructed independently to each workspace. As a result, the system can present different images to each user. This characteristic is suitable for presenting information that should be given to each user independently, such as playing cards.

3 Prototype System

Figure 3 shows the picture of the proposed prototype system. As shown in Fig. 3, half mirrors and displays are installed at the positions explained in Fig. 2. Then, the image from the user's point of view is shown in Fig. 4 (in adjusted light environments). A user can see not only adjacent 3D environments but also superimposed 2D display information. By using measured finger position with Kinect2 sensors, users can touch floating image, as well as the cloned 3D image, by using AUTDs, which is set in front of the users.

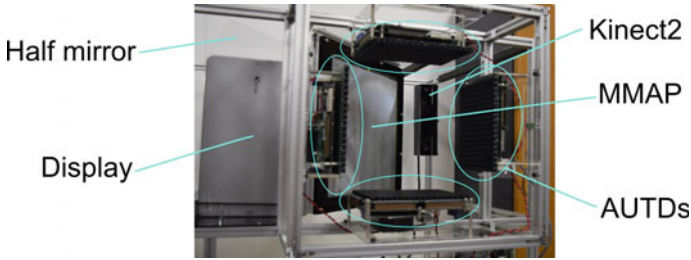


Fig. 3 Whole system of HaptoCloneAR

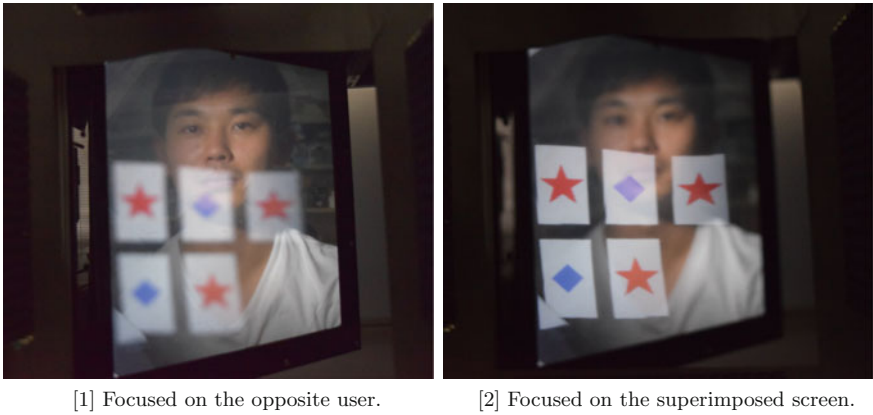


Fig. 4 User's vision: an image of cards is superimposed onto the opposite user's face

4 Conclusion

In this study, we proposed a new interactive system named HaptoCloneAR, which is an improved version of the previous system HaptoClone. In the previous HaptoClone system, users could touch copied objects from the adjacent workspace. In our proposed HaptoCloneAR system, we added 2D displays to superimpose 2D image on 3D floating image. Users can see and touch both of them. This 2D image can be presented independently to each side, which enables the system to show different information for each user. This is very effective when we assume applications that require one-way information such as playing cards. In this paper, we showed the principle of the HaptoCloneAR system and our prototype.

Acknowledgements This research is supported by JSPS KAKENHI 16H06303 and JST ACCEL Embodied Media Project.

References

1. Makino, Y., Furuyama, Y., Inoue, S., Shinoda, H.: HaptoClone (Haptic-Optical Clone) for mutual tele-environment by real-time 3D image transfer with midair force feedback. In: Proceedings of the 2016 CHI Conference on Human Factors in Computing Systems, pp. 1980–1990. San Jose Convention Center, San Jose, CA, USA, 7–12 May 2016
2. Asukanet Co. Ltd.: AI Plateurl. <http://aerialimaging.tv/>
3. Hoshi, T., Takahashi, M., Iwamoto, T., Shinoda, H.: Noncontact tactile display based on radiation pressure of airborne ultrasound. *IEEE Trans. Haptics* **3**(3), 155–165 (2010)

Haplug: A Haptic Plug for Dynamic VR Interactions

Nobuhisa Hanamitsu and Ali Israr

Abstract We demonstrate applications of a new actuator, the Haplug, in dynamic virtual environments. The haplug is a linear voice coil motor packaged between springs in a plug-like casing. Response and bandwidth of the haplug are optimized for haptic interactions, and tuned by the motor inertia and spring stiffness. A pair of haplugs is mounted on the hand-tracking controllers of HTC Vive and renders a variety of haptic feedback, such as, feelings to colors, interactions with objects, surface texture and dynamic object behaviors. The Haptic Plug allows rich control of haptic effects in VR and other interactive settings.

Keywords VR · Haptic handhelds · Dynamic haptics

1 Introduction

Current Virtual Reality (VR) systems feature a head-mounted display (HMD) to render rich and dynamic virtual environments surrounding a user. These systems are further enhanced by hand-tracking controllers that track users actions, gestures and motion in the environment and provide tactile sensations coupled with the audio-visual content. Due to the low-fidelity nature of the embedded actuator, the haptic feedback is limited to homogenous “buzz-like” vibrations. We present another haptic actuator, the *Haptic Plug* or *Haplug* (Hap-lug), which extends the bandwidth of the haptic actuator and renders high-frequency smooth vibrations, low-frequency motional cues as well as mid-frequency flutter sensations. These sensations are coupled with dynamic VR activities and demonstrated in this submission.

In the following section, we illustrate the design of the Haplug and its implementation with the HTC VIVE controller. This is followed by our framework and

N. Hanamitsu (✉) · A. Israr
Disney Research, Pittsburgh, USA
e-mail: nobuhisa.hanamitsu@disneyresearch.com

introduction to applications. Finally, we illustrate the demonstration layout for Asia Haptics.

2 Haptic Plug

The actuator design of Haplug is shown in Fig. 1. On the core of the actuator is a linear voice coil motor (LVCM), whose coil is fastened to a 3D printed casing. A spring of stiffness k_1 is inserted between the coil and the moving mass of inertia M . Another spring of stiffness k_2 is placed before packing the actuator with a cap.

The spring stiffness, casing dimensions, and the moving inertia are optimized for low- to mid- frequency response (resonance peak at ~ 20 Hz). The actuator can play periodic waveforms, pulses and filtered noise, and time controlled patterns. The actuator design is simple, versatile and can be scaled to wide variety of off-the-shelf motors. A 3D adapter is printed to house the actuator and mounts through the center slot of the Vive controllers, as shown in Fig. 1.

The frequency response of the Haplug is adjusted to match with that of the human detection threshold curve, as shown in Fig. 2. This way, the control features of the Haplug are naturally optimized in the dynamic range of haptic perception. Figure 2b shows measured frequency response of the Haplug with preferred spring stiffness. It is observed that the first order approximation of the Haplug follows the human detection threshold curve determined in [1]. However, for accurate modeling, weights of the casing and the moving mass, the orientation as well as the compliance of the hold must be considered in the model.

3 Framework and Applications

A pair of Haptic Plugs is mounted on two Vive hand-tracking controllers. VR environments are developed in Unity 3D using a SteamVR Plugin and haptic effects are channeled through stereo audio channels [2]. The tracked location of the

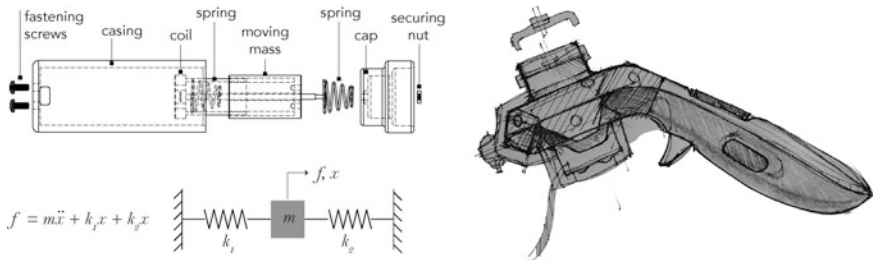


Fig. 1 Dynamical modeling of Haplug and its use with a Vive controller

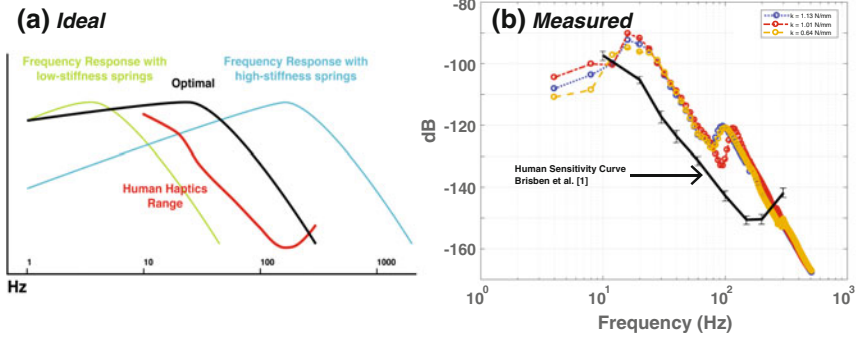


Fig. 2 Frequency response matching of Haplug, and the measured frequency response of the mockup prototype using preferred spring stiffness

end-effector, \mathbf{X} , is compared to the virtual environment, \mathbf{Y} . Based on user interactions, a haptic function $\mathbf{H} = f(\mathbf{X}, \mathbf{Y})$ is defined. In this section, we explore a library of rendered haptic effects and demonstrate in use cases.

3.1 Haptic Effects

The Haptic Plug plays a set of haptic effects. It plays low- to mid- frequency flutter sensations, and high-frequency (>80 Hz) smooth vibrations. Moreover, it plays pull and push sensations as a consequence of pulse inputs. The response time of the actuator is fast (<10 ms) and the feedback is perceivable in the 2–200 Hz range. A set of expressive effects is shown in Fig. 3.

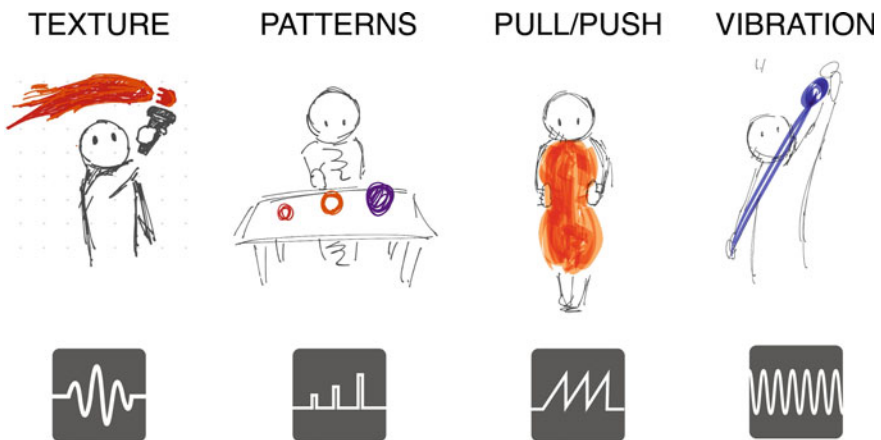


Fig. 3 Applied effects using the Haptic Plugs in VR settings

3.2 Use Cases

Following are some use cases and applications designed and implemented for this demonstration. With these cases, we highlight rich interactions with the Haptic Plug.

3.2.1 Surface Textures

The haplug can render wide variety of surface textures by periodically turning the haptic feedback on and off and/or modulating the perceived intensity of stimulations. A VR experience is designed that consists of three touch surfaces the user interacts with. In one surface, black and white stripes are associated with OFF and ON state of stimulations. By varying hand movements and spatial layout of patterns, attendees will feel varying feedback caused by rapid transitions of the haptic signal. In the second surface, texture of surfaces varied from fine to coarse, therefore rendering smooth to rough textures. In the third surface, users feel textural features of various pavements, landmarks, and regions in the pictures or they interact with an viscoelastic surface.

3.2.2 Feelings to Colors

In another installation, users produce colorful strokes in the surrounding free space. We associate vibration frequency and amplitude to the color's Hue, Chroma and Lightness according the vibration to color mapping in the CIELAB model. The color to vibration mapping is determined using a subjective evaluation study to be published.

3.2.3 Object Manipulation

In this installation, users interact with objects in the environment. In one case attendees handle and drag objects. A "snap" action is highlighted by a brief pulse pushing or pulling the hand, and drag forces are represented by vibration amplitude coupled to the hand motion. Heavier objects render high resistance and therefore higher amplitude, whereas, lighter objects render low resistance and therefore lower amplitude.

3.2.4 Dynamic Object Behaviors

The haplug cannot render static forces, such as the weight of an object. However, transient forces as a result of dynamic interactions with the objects and spaces can

be presented with high fidelity. We modulate and perceptually synchronize the parameters of vibrations with activities and dynamic behaviors of object interactions, where a user interacts with springy, viscous and inertial objects. In one case, the user bounces, throws and juggles balloons in the environments, and in another case, the user switches tools to pop them.

3.2.5 Illusory Movements

We also developed an interactive scenario, where a user balances rolling objects on a wooden slab and feel moving and floating objects between the hands. In another case, the user has super-power capabilities. The effects are made using well-known sensory illusions in touch, such as apparent tactile motion, in which phantom motion and content is produced between the two hands holding Haptic Plugs [3].

4 Demonstration Layout and Presentation

In AsiaHaptics 2016, we will offer a wide variety of applications to highlight use of the Haptic Plug. Attendees will experience virtual environments using HTC VIVE VR system, and coherent haptic feedback will be rendered through instrumented hand tracking controllers. Attendees will go over the list of experiences and provide feedback to the authors for future use and research.

The demo will be accommodated in a typical 2 m by 2 m demonstration space. Only one attendee will go through the VR demonstration that lasts no more than 3 min, however, other attendees can visualize the experience while standing and waiting for their turn. Putting on and taking off the systems are minimized and take roughly 1 min including instructions and introduction. Two organizers will man the booth and participants will receive gifts and postcards reminding them of the project after the conference.

References

1. Brisben, A.J., Hsiao, S.S., Johnson, K.O.: Detection of vibration transmitted through an object grasped in the hand. *J. Neurophysiol.* **81**(4), 1548–1558 (1999)
2. Israr, A., Zhao, S., McIntosh, K., Schwemler, Z., Fritz, A., Mars, J., Bedford, J., Frisson, C., Huerta, I., Kosek, M., Koniaris, B., Mitchell, K.: Stereohaptics: a haptic interaction toolkit for tangible virtual experiences. In: *ACM SIGGRAPH 2016 Studio (SIGGRAPH '16)*, p. 57, Article 13. ACM, New York, NY, USA (2016)
3. Israr, A., Zhao, S., McIntosh, K., Kang, J., Schwemler, Z., Brockmeyer, E., Baskinger, M., Mahler, M.: Po2: augmented haptics for interactive gameplay. In: *ACM SIGGRAPH 2015 Emerging Technologies (SIGGRAPH '15)*, p. 1, Article 21. ACM, New York, NY, USA (2015)

Magnification-Changeable Haptic-Optical Clone

Ryota Arai, Yasutoshi Makino and Hiroyuki Shinoda

Abstract We propose a novel interactive system that optically transfers a scaled 3D image of one side to the other. As conventional Haptic-Optical Clone, users can communicate with each other through the copied floating images with tactile feedback produced by airborne ultrasound tactile displays. Additionally, the system can change the size of the copied images from the real size by using Fresnel lens.

Keywords 3D image · Mid-air tactile feedback · Haptic-optical clone

1 Introduction

In recent years, three-dimensional (3D) images have entered a practical stage, and, even for unaided eyes, high-definition 3D images are possible thanks to recent advancement of light field displays. In interaction with 3D images, artificial haptic feedback is indispensable for identifying what virtual objects the users are touching and manipulating floating 3D objects. In addition, such tactile feedback added to 3D images is effective to heighten the reality in virtual reality (VR) and communication. Repro3D [1] reported that additional tactile sensation increases the real sense of images. HaptoClone [2] realized a human–human communication through a realistic 3D image with a tactile feedback and proved the impact of the haptic feedback.

In this paper, we propose a communication system through scaled 3D image with tactile feedback. In this system like Fig. 1, the user(s) can interact with scaled 3D images of actual human or objects in real time. The goal of the research is to enable such a system where we can communicate with magnified images of small insects, for example. It also enables to equalize the hand sizes between an adult and child who communicate through this system.

R. Arai (✉) · Y. Makino · H. Shinoda
The University of Tokyo, 5-1-5 Kashiwanoha, Kashiwa, Chiba 277-8561, Japan
e-mail: arai@hapis.k.u-tokyo.ac.jp

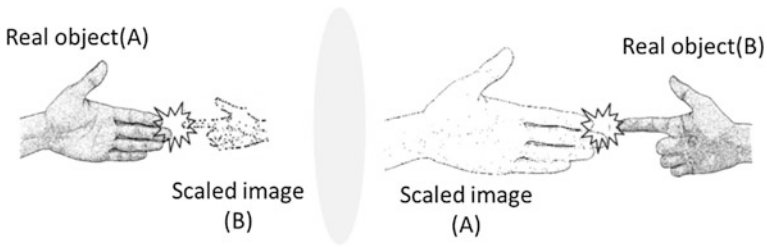


Fig. 1 Schematic illustration

2 Prototype

We show the overall system in Figs. 2 and 3. This system is composed of Fresnel lens and air born tactile display (AUTD). Fresnel lens placed in center makes scaled 3D images to right and left sides. An object of left-side workspace is optically magnified and copied to the right-side workspace and at the same time, an object of right-side is demagnified in the left-side. The AUTD units attached in each workspace give force feedback in midair by concentrating the acoustic energy at the cross-sections of the real object and copied 3D image. The 3D configurations of the real objects in the both workspaces are captured and the cross-sections are calculated by a computer.

2.1 Scaled 3D Images

We use a Fresnel lens to realize such a magnification-changeable interaction. In case of using single lens, inverted images are made for mutual sides. The

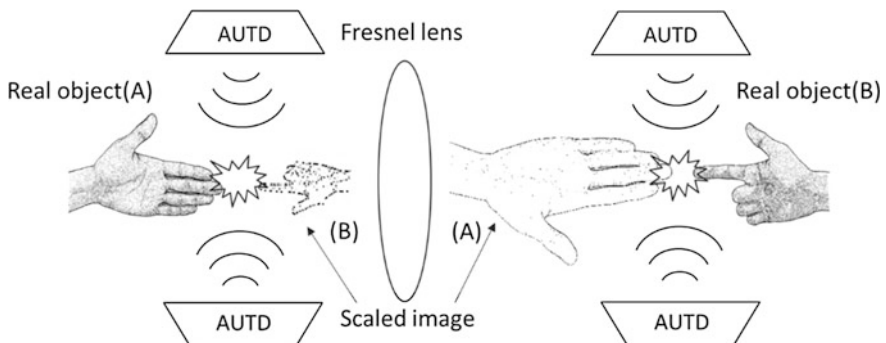


Fig. 2 System overview

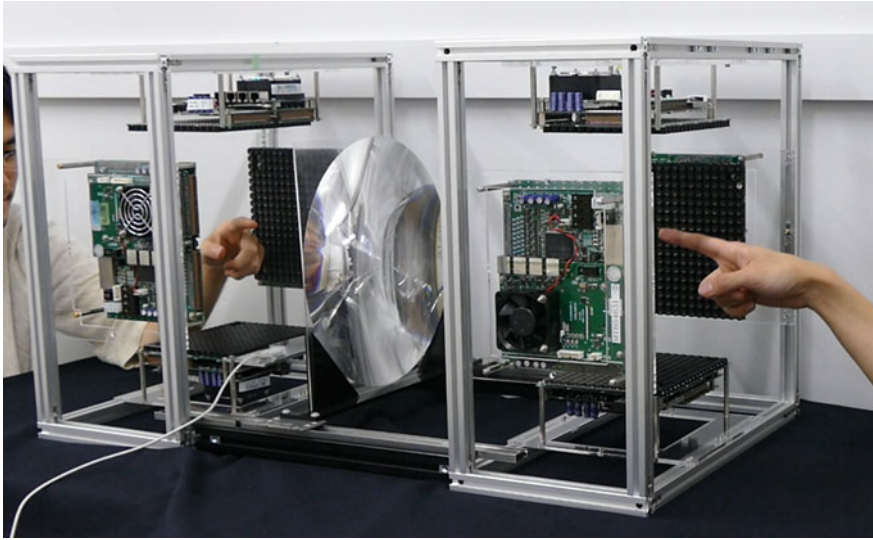


Fig. 3 Proposed system

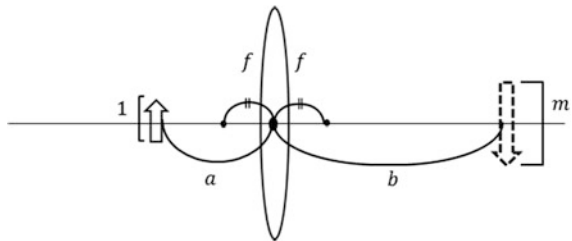
magnification m and positions of the 3D images are obtained from the following formulas (1) and (2). Figure 4 shows the schematic diagram

$$\frac{1}{a} + \frac{1}{b} = \frac{1}{f} \tag{1}$$

$$m = \frac{a}{a-f} \tag{2}$$

The parameter a is the distance between the lens and the object and b is the distance to the 3D image. f and m mean the focal length of the lens and magnification rate of the image, respectively. In this paper, we use a lens of $f = 150 \text{ mm}$ with the lens size of 300 mm^2 . For example, when the object approaches to the lens, the image becomes bigger and moves to a farther position. As a limitation of the workspace position, the object must apart from the lens more than f to form the real image. Figure 5 shows examples of actual scaled images.

Fig. 4 Magnification and positions of the object and real image



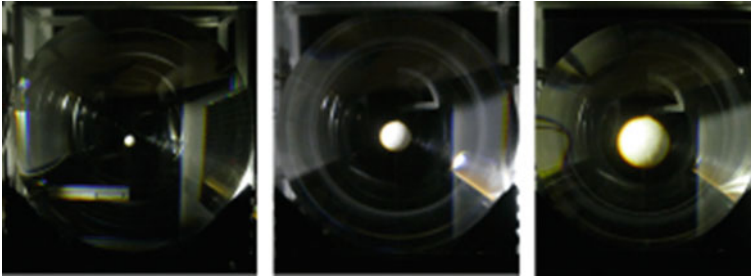
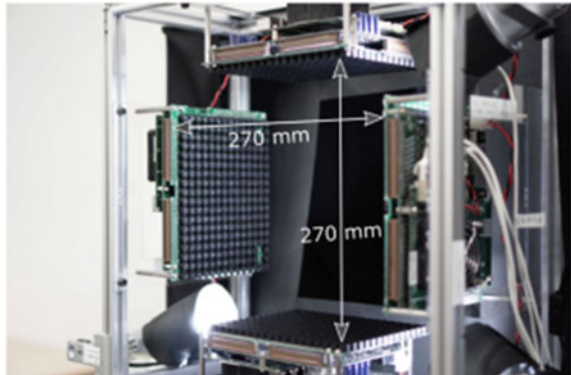


Fig. 5 Actual scaled images in some magnification rate

2.2 *Midair Tactile Feedback*

In this paper, we use airborne ultrasound tactile display (AUTD) proposed by Iwamoto et al. [3]. This device can give force feedback in midair by converging wave. Though some converging methods have been proposed recently, we use the method proposed by Inoue et al. [4], that was used in HaptoClone. The method uses standing waves by surrounding ultrasound transmitters (Fig. 6) and can produce a larger skin deformation than traveling waves. The cross-sections between a real object and 3D image is calculated from a Leap Motion (LM-C01-JP) data in this experiment. In the current system, the applied force (acoustic energy) is the maximum one the system can provide regardless of the magnification ratio.

Fig. 6 Configuration of four AUTD units



Acknowledgements This research was partly supported by JSPS KAKENHI 16H06303 and JST ACCEL Embodied Media Project.

References

1. Yoshida, T., Shimizu, K., Kurogi, T., Kamuro, S., Minamizawa, K., Nii, H., Tachi, S.: RePro3D: full-parallax 3D display with haptic feedback using retro-reflective projection technology. In: 2011 IEEE International Symposium on VR Innovation (ISVRI), pp. 49–54 (2011)
2. Makino, Y., Furuyama, Y., Inoue, S., Shinoda, H.: HaptoClone (haptic-optical clone) for mutual tele-environment by real-time 3D image transfer with midair force feedback. In: Proceedings of the 2016 CHI Conference on Human Factors in Computing Systems, pp. 1980–1990 (2016)
3. Iwamoto, T., Tatezono, M., Shinoda, H.: Non-contact method for producing tactile sensation using airborne ultrasound. In: International Conference on Human Haptic Sensing and Touch Enabled Computer Applications, pp. 504–513. Springer, Berlin (2008)
4. Inoue, S., Makino, Y., Shinoda, H.: Active touch perception produced by airborne ultrasonic haptic hologram. In: World Haptics Conference (WHC), 2015 IEEE, pp. 362–367. IEEE (2015)

Computer-Created Interactive 3D Image with Midair Haptic Feedback

Yuta Kimura, Yasutoshi Makino and Hiroyuki Shinoda

Abstract We created a system that enables a user to touch and interact with 3D images formed by a light source device in mid-air. A user can get the haptic feedback without wearing a special device by using focused airborne ultrasound. The pattern of 3D images of 36864 dots and tactile feedback points are fully programmable and updated at the refresh-rate of 18 Hz. Using this system, we demonstrate the feasibility of handling a 3D virtual object.

Keywords Midair haptics · 3D interaction · Aerial 3D image · Noncontact tactile feedback

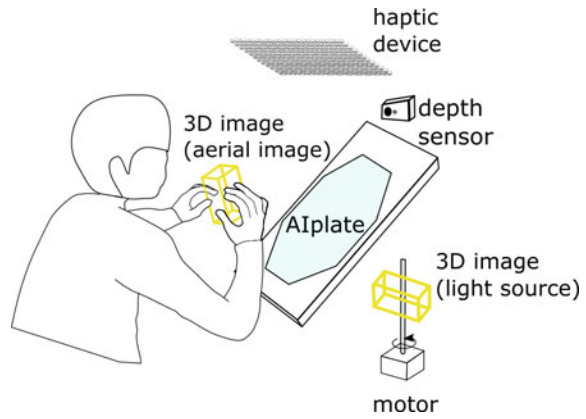
1 Introduction

Recently, two examples of interaction systems through floating images with midair haptic feedback have been demonstrated. One is HaptoMime [1] that enables interaction with a floating 2D image and produces noncontact tactile feedback by using air born tactile display (AUTD [2]). The other example is HaptoClone [3] that produces haptic and optical clone image. In HaptoMime, the interaction was limited in 2D and a midair touch panel was presented. HaptoClone realized 3D interaction through 3D images, but the image was optically produced from a real object. Even before the two examples, we can find systems that enable interaction between user and programmable 3D image with tactile feedback, as RePro3D [4]. However, it needs wearing a special device to obtain haptic feedback. In contrast to these, this research produces programmable 3D image with noncontact tactile feedback. Therefore, the proposed system in this paper produces programmable 3D image with noncontact haptic feedback, which possesses all the three features that it is programmable, 3D, and noncontact. Figure 1 shows schematic of the equipment.

Y. Kimura (✉) · Y. Makino · H. Shinoda
The University of Tokyo, 5-1-5 Kashiwanoha, Kashiwa, Chiba 277-8561, Japan
e-mail: kimura@hapis.k.u-tokyo.ac.jp

© Springer Nature Singapore Pte Ltd. 2018
S. Hasegawa et al. (eds.), *Haptic Interaction*, Lecture Notes
in Electrical Engineering 432, DOI 10.1007/978-981-10-4157-0_82

Fig. 1 System overview



2 System

Figure 2 shows appearance of the system. The system is composed of three elements, a light field display device (3D part), depth sensor (sensor part), and tactile feedback part (AUTD part). First, the 3D part is divided into rotating LED arrays and a micro-mirror array plate named AIP (Aerial Imaging Plate by ASUKANET,

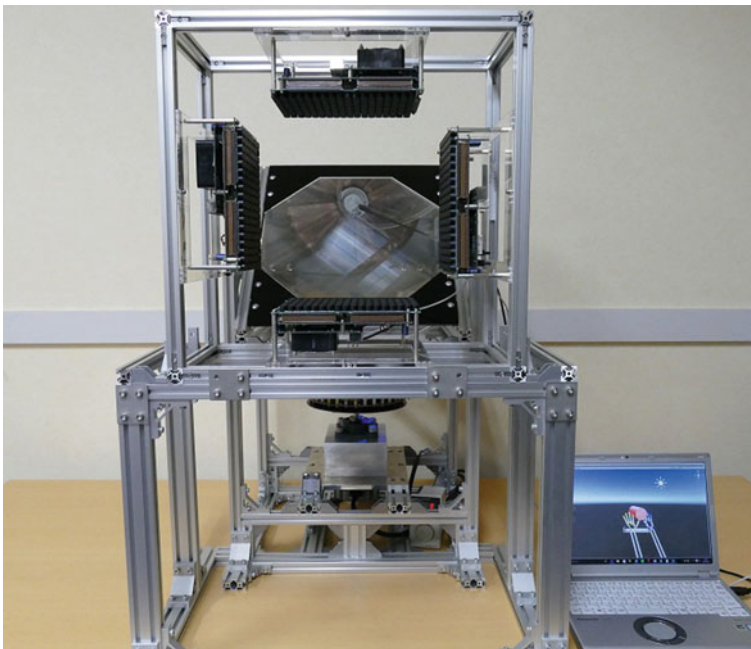


Fig. 2 Photograph of the device

Co., Ltd.). A 3D image is drawn by flashing each LED at an appropriate timing. By reflecting this 3D image to the user's side using AIP, it produces a touchable 3D optical image. In the current specification, the 3D image is created with 36864 dots in a cylindrical region of 48 mm height and 146 mm diameter. The refresh rate of the 3D image is 18 Hz. Second, the sensor part has a role to get the position and posture of the user's hands by a depth sensor. The obtained data is transformed to a simulation model in a game engine, Unity. The model interacts with a virtual object prepared in Unity. By synchronizing this interaction in virtual and real spaces the contact between a user and optical 3D image is produced. Third, the AUTD part creates haptic feedback on the hand by the ultrasonic radiation pressure. The refresh rate of the haptic stimulation is also 18 Hz in the current system.

3 Application and Purpose of the Research

Using this device, a user can handle a computer-created 3D object with touch sensation in real world (Fig. 3). In principle, it will support the 3D design in computer, where the designers can create 3D models intuitively as if they are shaping clays. However, the current device is the first prototype, and there still is a distance to such a practical application. The most considerable problem is the visual image resolution. In the current system, the 3D image is created by only 36,864 dot light sources for a cylindrical region of 48 mm height and 146 mm diameter. Therefore, the purpose of this research is to clarify the condition of contact model and haptic feedback for efficient handling of 3D virtual objects. Important parameters are the threshold between contact and out-of-contact states, friction

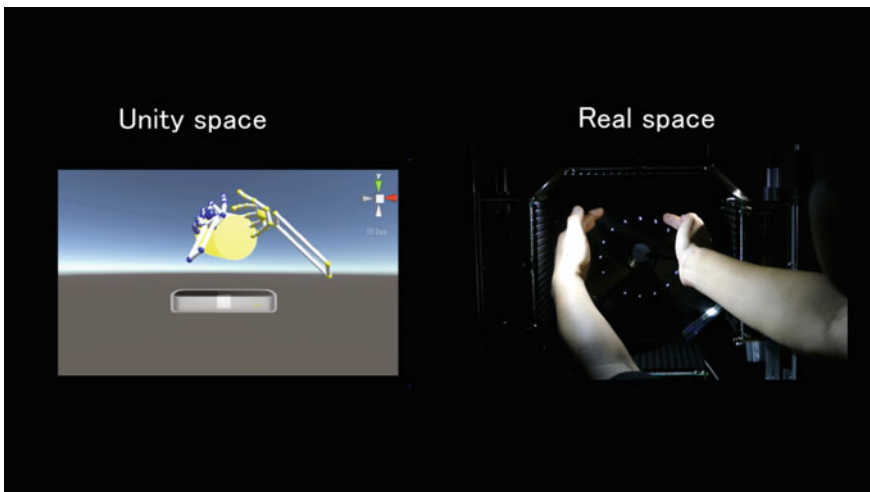


Fig. 3 Virtual object in unity and optical 3D image in real world

coefficient, and dynamics parameters of the virtual object. It is also crucial to examine the problems of optical occlusion and finger penetration through the virtual object surface. In this conference, we perform a demonstration to evaluate the feasibility of 3D-virtual-object handling. Attendees can experience the usability under typical interaction models.

Acknowledgements This research was partly supported by JSPS KAKENHI 16H06303 and JST ACCEL Embodied Media Project.

References

1. Monnai, Y., Hasegawa, K., Fujiwara, M., Inoue, S., Shinoda, H.: HaptoMime: mid-air haptic interactions with a floating virtual screen. In: Proceedings of the 27th ACM User Interface Software and Technology Symposium (UIST2014), pp. 663–667, Hawaii, USA October 5–8, 2014
2. Hoshi, T., Takahashi, M., Iwamoto, T., Shinoda, H.: Noncontact tactile display based on radiation pressure of airborne ultrasound. *IEEE Trans. Haptics* **3**(3), 155–165 (2010)
3. Makino, Y., Furuyama, Y., Inoue, S., Shinoda, H.: HaptoClone (haptic-optical clone) for mutual tele-environment by real-time 3D image transfer with midair force feedback. In: Proceedings of CHI (2016)
4. Yoshida, T., Shimizu, K., Kurogi, T., Kamuro, S., Minamizawa, K., Nii, H., Tachi, S.: RePro3D: fullparallax 3d display with haptic feedback using retro-reflective projection technology. In: Proceedings of the IEEE International Symposium on VR innovation 2011, pp. 49–50, 19–20 March, Singapore

Mobile HapticAid: Wearable Haptic Augmentation System Using a Mobile Platform

Tomosuke Maeda, Keitaro Tsuchiya, Roshan Peiris, Yoshihiro Tanaka and Kouta Minamizawa

Abstract In this paper, we propose mobile HapticAid, a wearable haptic augmentation system which combines a polyvinylidene fluoride (PVDF) skin vibration sensor, a mobile platform such as iOS devices and TECHTILE amplifier. It can enhance haptic perception through a PVDF skin vibration sensor and vibro-tactile feedback. This system is small enough to be portable. The participants will be able to experience the enhancement of touch objects.

Keywords Haptic augmentation · Wearable device · Embodied media

1 Introduction

Technology advancement can enhance human ability. For example, eyeglasses enhance seeing capabilities, and a hearing aid can support or partially fix hearing deficits. Similarly, we developed HapticAid which is haptic augmentation system.

We developed the mobile HapticAid which is small enough to be portable and demonstrate that by augmenting the haptic perception. We aim to restore the haptic

T. Maeda (✉) · K. Tsuchiya · R. Peiris · K. Minamizawa
Graduate School of Media Design, Keio University, 4-1-1 Hiyoshi, Kohoku-ku, Yokohama,
Kanagawa 223-8526, Japan
e-mail: t.maeda@kmd.keio.ac.jp

K. Tsuchiya
e-mail: Tsuchiya.Keitaro@gmail.com

R. Peiris
e-mail: roshan@kmd.keio.ac.jp

K. Minamizawa
e-mail: kouta@kmd.keio.ac.jp

Y. Tanaka
Nagoya Institute of Technology, Gokiso-cho, Showa-ku, Nagoya 466-8555, Japan
e-mail: tanaka.yoshihiro@nitech.ac.jp

Y. Tanaka
JST PRESTO, 4-1-8 Honcho, Kawaguchi, Saitama, Japan

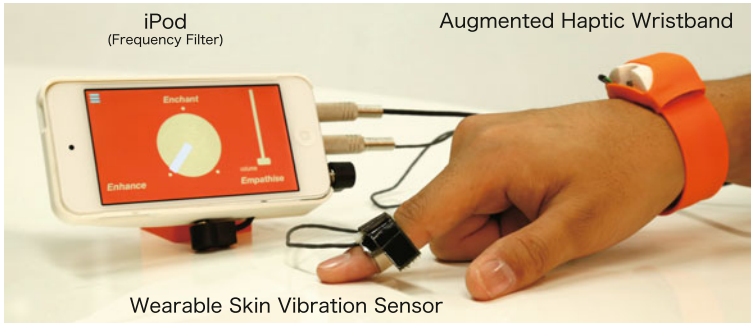


Fig. 1 Mobile HapticAid system

sensation of elder people suffering from diminished touch sensation. In previous studies, Tactile Contact Lens developed by Kikuuwe et al. [2], uses the principle of leverage, thereby enabling the determination perception of irregularities on surfaces. Tanaka et al. [6] developed the system for performing a laparoscopic surgery; it can detect lumps and provide real-time feedback using a tactile display. These studies are over devices. Ando et al. [1] developed the SmartFinger which is used for haptic augmentation for virtual reality. In other approaches, the white noise is represented on hand or the wrist [3, 5].

2 Implementation and Demonstration

We developed the mobile HapticAid, a wearable haptic augmentation system as shown in Fig. 1. The mobile HapticAid consists of three main components: a sensor that acquires the signal of haptic information from the fingertip directly which is skin vibration (Haptic sensor) [7]; a smartphone which can uses digital signal processing and power amplifier [4] for haptic augmentation (Signal processor); and a wrist worn haptic actuator (Augmented haptic wristband) to apply the enhanced haptic sensation.

In the demonstration, the participant will be able to experience the enhancement of touch object using the mobile HapticAid. For example, the participants can experience the actual (amplified) roughness when touching a sheet of paper; experienced touch sensations when using a keyboard and a pen, and touching objects and so on.

Acknowledgements This work is supported by a JST ACCEL Embodied Media Project and JSPS KAKENHI Grant Number 26700018.

References

1. Ando, H., Watanabe, J., Inami, M., Sugimoto, M., Maeda, T.: A fingernail-mounted tactile display for augmented reality systems. *Electron. Commun. Jpn. (Part II: Electronics)* **90**(4), 56–65 (2007)
2. Kikuuwe, R., Sano, A., Mochiyama, H., Takesue, N., Tsunekawa, K., Suzuki, S., Fujimoto, H.: The tactile contact lens. In: *Sensors, 2004. Proceedings of IEEE*, pp. 535–538. IEEE (2004)
3. Lakshminarayanan, K., Lauer, A.W., Ramakrishnan, V., Webster, J.G., Seo, N.J.: Application of vibration to wrist and hand skin affects fingertip tactile sensation. *Physiol. Rep.* **3**(7), e12465 (2015)
4. Minamizawa, K., Kakehi, Y., Nakatani, M., Mihara, S., Tachi, S.: Techtile toolkit: a prototyping tool for designing haptic media. In: *ACM SIGGRAPH 2012 Emerging Technologies*, p. 22. ACM (2012)
5. Seo, N.J., Kosmopoulos, M.L., Enders, L.R., Hur, P.: Effect of remote sensory noise on hand function post stroke. *Front. Hum. Neurosci.* **8** (2014)
6. Tanaka, Y., Nagai, T., Fujiwara, M., Sano, A.: Lump detection with tactile sensing system including haptic bidirectionality. In: *World Automation Congress (WAC), 2014*, pp. 77–82. IEEE (2014)
7. Tanaka, Y., Nguyen, D.P., Fukuda, T., Sano, A.: Wearable skin vibration sensor using a PVDF film. In: *World Haptics Conference (WHC), 2015 IEEE*, pp. 146–151. IEEE (2015)

Synesthesia Suit

**Yukari Konishi, Nobuhisa Hanamitsu, Benjamin Outram,
Youichi Kamiyama, Kouta Minamizawa, Ayahiko Sato
and Tetsuya Mizuguchi**

Abstract The Synesthesia Suit provides immersive embodied experience in Virtual Reality environment with vibrotactile sensations on the whole body. Each vibrotactile actuator provides not a simple vibration but we designed the haptic sensation to match virtual reality contents.

Keywords Haptic suit · Haptic design · Virtual reality · TECHTILE

Y. Konishi (✉) · N. Hanamitsu · B. Outram · Y. Kamiyama · K. Minamizawa ·
T. Mizuguchi

Graduate School of Media Design, Keio University, Minato-ku, Japan
e-mail: y.konishi@kmd.keio.ac.jp

N. Hanamitsu
e-mail: hanamitsu@kmd.keio.ac.jp

B. Outram
e-mail: benjamin.outram@kmd.keio.ac.jp

Y. Kamiyama
e-mail: kamiyama@kmd.keio.ac.jp

K. Minamizawa
e-mail: kouta@kmd.keio.ac.jp

T. Mizuguchi
e-mail: t@mzgc.net

A. Sato
Rhizomatiks co. ltd., Shibuya, Japan
e-mail: ayahiko@rhizomatiks.com

T. Mizuguchi
Enhance Games, Inc., 4-1-1 Hiyoshi, Kohoku-ku, Yokohama-City, Kanagawa 223-8526,
Japan

1 Introduction

We propose a full body haptic suit that provides immersive experience with virtual reality environment. Our system consists of a suit, a haptic controller and designed tactile waves. In this suit, haptic feedback is not simple vibration which are used conventional game controllers, but haptic effects that we designed like sound effects based on TECHTILE [1] technology. We originally developed this suit for the Game “Rez Infinite” that will be released for PlayStation VR.

2 Related Research

There are some researches of multi-channel haptic interface or feedback. Haptic Interface for Immersive Projection Display [2] was one of the suit type haptic interface. Surround Haptics [3] proposed moving tactile strokes using multiple vibrators spaced on a gaming environment. And they also proposed Mango [4] witch was an editor for multi-channel tactile feedback.

3 Proposed System

Synesthesia Suit: As shown in Fig. 1, Synesthesia Suit has 24 tactile channels and provides vibrotactile sensations on the entire body. The suit was designed easy-to-wear and available for everyone regardless body height and size. The voice coil actuators are put on the shoulder, upper arm, lower arm, back of the hand, hip, thigh, knee, shin, instep, stomach and back.

Synesthesia Engine: The control flow is shown in Fig. 2. Synesthesia Engine controls the 24 channels tactile signals actively according to the triggers of game playing or the interaction with the virtual reality environment, while 24 channels control 26 vibrators as there are two vibrators inserted in hip position. And Synesthesia Engine has the library of tactile signals. We made these signals by recording tactile signals or modulating pre-recorded sound effects. The haptic effects inundate the user’s entire body by designing the spatial pattern based on the phantom sensation phenomena.

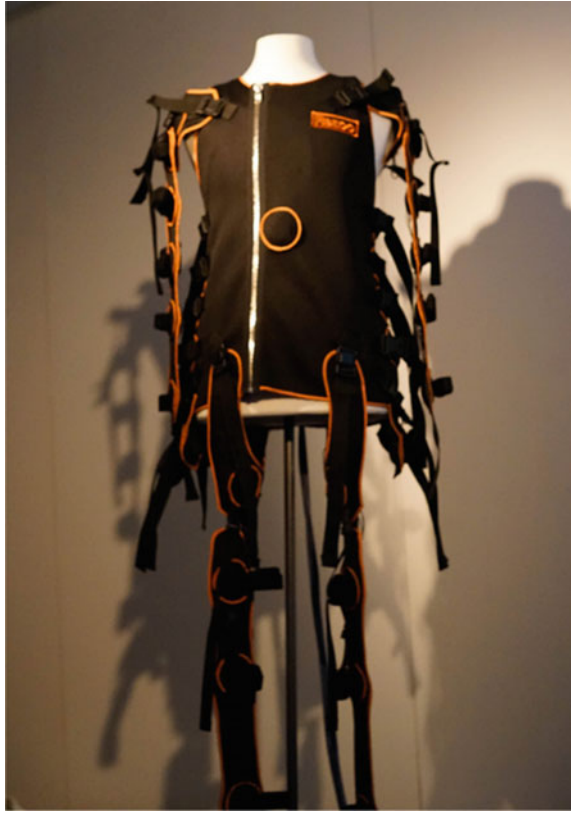


Fig. 1 Suit overview

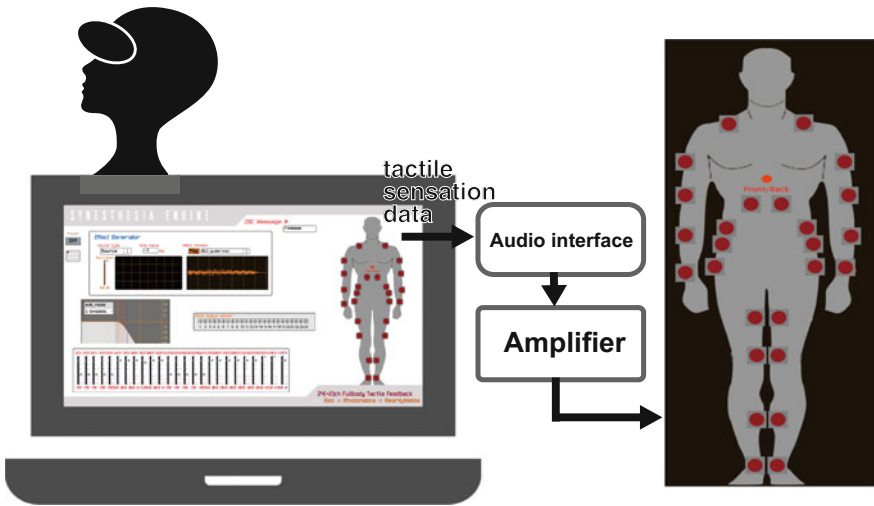


Fig. 2 Control flow

4 Haptic Contents Design

In case of “Rez Infinite”, our concept of the experience of Synesthesia Suit is that the users feel as if they completely dived into the Rez world. Through a lot of discussions with the game creator, we drew out imaginative haptic feelings of Rez world and then designed these as vibrotactile sensation and providing pattern for each part of body. Not only the synesthetic haptic sensation, we also designed the haptics for the game interaction such as locking, shooting, hitting and warping.

We also aim to apply Synesthesia Suit for other virtual reality environments other than PlayStation VR, we made other demonstration using motion capture system. This contents focused on embodied interaction. The user can walk in the virtual reality world and can feel haptic sensation of touching to some objects that has various types of texture, slipping through light wall or diving into the creatures.

5 User Experiences

Our first demonstration of Synesthesia Suit was PlayStation Experience 2015 (Figs. 3 and 4). According to the user experiment, we confirmed that the user could feel as if they dived into the Rez world and enclosed by variety of texture of the sounds. And then they felt that they came back from the another world when they finished the suit experience. And other users said “Reality is far away by vibration and sound, as if I was like floating in the virtual world.” “I was likely not come back from the world of the game.” and so on.



Fig. 3 Demonstration of “Rez Infinite”



Fig. 4 Demonstration of embodied interaction contents

Acknowledgements This work was supported by JST-ACCEL Embodied Media project and technically supported by Mr. 2bit ISHII and Rhizomatiks team. The costume was designed by Mr. Toshihiko Sakurai. “Rez Infinite” was developed by Monstars and Resonair.

References

1. Minamizawa, K., Kakehi, Y., Nakatani, M., Mihara, S., Tachi, S.: Techtile toolkit: a prototyping tool for designing haptic media. In: Proceedings of SIGGRAPH 2012 Emerging Technologies (2012)
2. Yano, H., Kakehi, N., Ogi, T, Hirose, M.: Haptic interface for immersive projection display. In: Proceedings of Human Computer Interaction (HCI'99), vol. 2, pp. 1030–1034 (1999)
3. Israr, A., Kim, S.-C., Stec, J., Poupyrev, I.: Surround haptics: tactile feedback for immersive gaming experiences. In: Proceedings of CHI '12 Extended Abstracts on Human Factors in Computing Systems, pp. 1087–1090 (2012)
4. Oliver, S.S., Israr, A., Karon, E.M.: Tactile animation by direct manipulation of grid displays. In: Proceedings of ACM Symposium on User Interface Software and Technology (ACM UIST) (2015)